

https://dspace.org/

Biocatalytic potetial of degrading enzyme systems belonging to the genus rhodococcus rhodochrous, new approaches towards green chemistry

Govindjee, Varsha Parshotam

2018
https://hdl.handle.net/10539/25927

Downloaded from a DSpace repository. https://dspace.org/

BIOCATALYTIC POTENTIAL OF NITRILE DEGRADING ENZYME SYSTEMS BELONGING TO THE GENUS *RHODOCOCCUS RHODOCHROUS*. NEW APPROACHES TOWARDS GREEN CHEMISTRY.

Varsha Parshotam Govindjee

A Thesis submitted to the Faculty of Chemistry, University of the Witwatersrand, in fulfilment of the requirements for the degree of Doctorate of Philosophy

Johannesburg, March 2018

Declaration

I declare that this Thesis is my own, unaided work. It is being submitted for the Degree of Doctor of Philosophy at the University of the Witwatersrand, Johannesburg. It has not been submitted before for any degree or examination at any other University.

…….

Mrs Varsha Parshotam Govindjee

School of Chemistry, University of the Witwatersrand, Johannesburg 2018

This thesis is submitted after examination and approval by the following supervisors

Supervisor: Professor Dean Brady

…….

Co-Supervisor: Dr. Moira Bode

…….

External Co-Supervisor: Dr. Konanani Rashamuse

School of Chemistry, University of Johannesburg, 27th day of March, 2018

.

Abstract

In an attempt to find more efficient and "greener" catalytic processes towards the synthesis of advanced pharmaceutical intermediates, three bacterial strains, namely *Rhodococcus rhodochrous* ATCC BAA-870, *R. rhodochrous* A29 and *Pimelobacter simplex* A99, were evaluated as nitrile hydrolysing biocatalysts.

R. rhodochrous ATCC BAA-870 showed constitutive expression of a low-molecular weight cobalt containing nitrile hydratase and a highly enantioselective amidase enzyme that were involved in the kinetic resolution of 3-hydroxy-3-aryloxybutanenitrile and 3-hydroxy-3-arylpropanenitrile. The (*R*)-3-hydroxy-3-aryloxybutanamide and (*S*)-3-hydroxy-3-arylpropanamide intermediates were both accumulated with excellent enantioselectivity (>99% ee).

Interestingly, the same cells demonstrated enantioselective resolution of β-substituted aminonitriles to amides through a moderately selective nitrile hydratase enzyme when adjusted to a higher pH. With the substrates 3-amino-3-(4-methoxyphenyl)propanenitrile, and 3-amino-3-*p*-tolylpropanenitrile an enantiomeric purity of the residual nitrile (85% ee and 21% ee respectively) was achieved; while the resultant amide was obtained with 62% ee (3-amino-3-(4-methoxyphenyl)propanamide) and 48% ee (3-amino-3-*p*-tolylpropanenitrile) respectively.

Induction studies demonstrated that both nitrile hydratase and amidase expression in strains A29 and A99 were inducible, with transient expression observed when cultured in the presence of benzonitrile. Furthermore, in a noteworthy discovery, studies on strains ATCC BAA-870, A29 and A99 revealed that the incorporation of 0.5% (v/v) dimethylformamide during cultivation induced nitrilase gene expression. This was evident by the appearance of a new, dominant 40 kDa protein band observed by SDS-PAGE analysis, and confirmed by LCMS-MS sequencing (showing high similarity to Uniprot Q03217). The induced nitrilase in strains A29 and A99 was inhibited by the nitrilase inhibitors benzylamine (61.37% and 79.49%) and benzaldehyde (88.45% and 87.49%) respectively. ATCC BAA-870 cells were however unaffected due to the presence of the alternative nitrile hydratase and amidase system facilitating nitrile hydrolysis.

The induced nitrilases converted 3-cyanopyridine to nicotinic acid, and showed excellent enantioselectivity towards 3-amino-3-phenylpropanenitrile (>99% ee), and moderate enantioselectivity towards 3-amino-3-(4-methoxyphenyl)propanenitrile (40% ee).

Therefore, *Rhodococcal* species are capable of expressing various nitrile hydrolysing enzymes that are enantioselective towards classes of beta-substituted nitrile compounds representative of diverse pharmaceuticals such as beta blockers, statins and peptidomimetics. The activity profile of these versatile microbial biocatalyst can be tailored through induction to yield single enantiomer nitriles, carboxamides or carboxyacids.

Acknowledgements

There are many I have met through the passage of time that have driven me to complete this PhD. Some having done so by their quiet encouragement while others succeeding only by persistence. Baps in his living years tried to convince me of the merit of studying further but I did not heed his advice…though I would like to believe that I have driven to that point having taken the scenic route along the way.

To my husband Shails, thank you. With such ease you seemed to take on the duties of both father and mother to our kids. The personal sacrifices you made in your life paved the way for me to achieve what I have.

To my mother Lalita, who always sacrificed herself for her family. You will always be loved by those around you, even when the words don't fall on your ears as easily as they should.

To my wonderful kids, Niamh and Neharika. You continue to inspire me daily with your boundless energy and curiousity.

To Ba and Bapujee; Mohinee, Harshad, Nana, Jagdish kaka, Mahesh and Neema. Thank you for all you have done and continue to do to build the personalities that develop before me daily.

To my dear friends, Heidi, Babalwa, Joni, Asha and Fritha. I have learnt much from our chats and miss you all. The years and miles may continue to seperate us, but you will always remain in my thoughts. To Mr. Manchidi, thank you for all the wonderful years and the fits of laughter you provided when needed.

To Dean, Moira, Koni, Kgama, Tsepo, Chris, Sibongile, Priyen, Kwezi, Advaita, Ntombi, Ofense, Daria, Kevin, Gugu, Mulalo, Paul, Petrus and Stoyan …Thank you for your guidance through this period.

Finally to my new literary hero, though deceased he may be. It is through books like "Oh, The Places You Will Go" by Dr Seuss, that I have found myself once again acquainted with the truth that has often come knocking on the well walked doors I have passed through in my life…anything can be achieved by hard work and a positive attitude.

“But on you will go though the weather be foul.
On you will go though your enemies prowl.
On you will go though the Hakken-Kraks howl.
Onward up many a frightening creek,
Though your arms may get sore and your sneakers may leak…

“And will you succeed? Yes! You will indeed! (98 and ¾ percent guaranteed).

In your memory and for you Bapujee



This thesis is based on the following papers

Enantioselective hydrolysis of β-hydroxy nitriles using the whole cell biocatalyst *Rhodococcus rhodochrous* ATCC BAA-870

Henok Kinfe, **Varsha Chhiba**, Joni Frederick, M. L. Bode, K. Mathiba, Paul. A. Steenkamp, and Dean Brady

(Journal of Molecular Catalysis B: Enzymatic, 2008)

Enantioselective biocatalytic hydrolysis of β-aminonitriles to β-amino-amides using *Rhodococcus rhodochrous* ATCC BAA-870

Varsha Chhiba, Moira, L. Bode, Kgama Mathiba, Wendy Kwezi, Dean Brady

(Journal of Molecular Catalysis B: Enzymatic, 2012)

Enzymatic stereoselective synthesis of β-amino acids

Varsha Chhiba, Moira Bode, Dean Brady, and Kgama Mathiba

(Cascade Biocatalysis, Chapter 14, pp 297-313)

Hydrolysis of nitriles by soil bacteria: variation with soil origin

O. K. L. Rapheeha, M. P. Roux-van der Merwe, J. Badenhorst, **V. Chhiba,** M. L. Bode, D. Brady

(Journal of Applied Microbiology, 2017)

Dimethylformamide – a novel inducer of nitrilase in *Rhodococcus rhodochrous* and *Pimelobacter simplex*

V. P. Chhiba-Govindjee[1], K. Mathiba[1], C. W. van der Westhuyzen[1], P. Steenkamp[1], J. K. Rashamuse[2,] S. Stoychev[1], M. L. Bode[3] and D. Brady[3]

(Draft Manuscript to be submitted)

Table of Contents

Declaration i
Abstract ii
Acknowledgements iii
Table of Contents vii
Aims ix
Objectives of This Study ix
Chapter Contents ix
Hypothesis xi
Table List xii
Figure List xiii
Common Amino Acid Abbreviations xvii
Preface: Moving South Africa Towards a Global Bio-economy Strategy xviii
Chapter One: Introduction to Green Chemistry 1
1.1 Green Chemistry and Sustainable Chemistry 2
1.2 Cascade Reactions 5
1.2.1 Chemical cascade reactions 5
1.2.2 Biological cascade reactions 6
1.3 Role of Biocatalysis in the Generation of Pharmaceutical Intermediates 8
1.4 Microbes as Chemo-Selective Agents 8
1.5 The Biocatalytic Versatility of Rhodococcus 9
1.6 Enzymes as Chemoselective Agents 11
1.7 Commercial Application for Nitrile Biocatalysts 12
1.8 References 18
Chapter Two: Nitrile Transforming Enzymes. A Literature Review 23
2.1 Nitrile Biocatalysis 24
2.2 Enzymes Involved in Nitrile Conversion 25
2.2.1 Aldoxime Dehydratase (EC 4.99.1.5) 26
2.2.2 Nitrogenase (EC 1.18.6.1) 28
2.2.3 Oxynitrilase (EC 4.1.2.10) 28
2.2.4 Cyanase (EC 4.3.99.1) 29
2.2.5 Nitrilase (EC 3.5.5.1) 30
2.2.6 Nitrile Hydratase (EC 4.2.1.84) 58
References 72
Chapter Three: PAPER I 81
Chapter Four: PAPER II 82

Chapter Five: PAPER III 83
Chapter Six: PAPER IV 84
Chapter Seven: PAPER V (draft manuscript) 85
Chapter Eight: Conclusion 86
Appendix 90
Appendix 1A-1C: ATCC BAA-870 NMR Spectra (DMF induced cells) 91
Appendix 1A: (^{1}H NMR) - Basified Sample Extraction 92
Appendix 1A (^{13}C NMR) - Basified Sample Extraction 93
Appendix 1A (^{1}H NMR) - Acidifed Sample Extraction 94
Appendix 1A- (^{13}C NMR) - Acidified Sample Extraction 95
Appendix 1B - Strain A29 NMR Spectra (DMF-induced cells 96
Appendix 1C - Strain A99 NMR Spectra (DMF-induced cells) 98
Appendix 2: Amidase Docking Studies 100
Appendix 3: 3-CP, Nicotinamide and Nicotinic Acid Standard Curves. 114
Appendix 4: SDS-PAGE Report 115
ATCC BAA-870-SDS-PAGE Report 116
Strain A29- SDS-PAGE Report 122
Strain A99-SDS-PAGE Report 130
Appendix 5A-5C: LCMS-MS Data 137
ATCC BAA 870- LCMS-MS Peptide Data 138
Strain A29- LCMS-MS Peptide Data 140
Strain A99 LCMS-MS Peptide Data 177

Aims

To evaluate nitrile degrading biocatalysts belonging to the genera *Rhodococcus* and *Pimelobacter*, to ascertain their synthetic potential in the production of higher value pharmaceutical intermediates.

Objectives of This Study

1. To apply biocatalysis to provide a synthetic reaction that is in accordance with the principles of Green Chemistry.
2. To explore the application of nitrile biocatalysts in the synthesis of single enantiomer pharmaceutical intermediates, and in particular through the hydrolytic kinetic resolution of beta-substituted nitriles.
3. To apply the biocatalytic cascade of nitrile hydratase and amidase of *R. rhodochrous* ATCC BAA-870 to synthesize carboxylic acids. To assess substrate structure effects (stearic and electronic) on enzyme selectivity profiles displayed by this system when using a range of β-amino and β-hydroxy substituted nitriles. The influence of electron withdrawing or donating substituent groups and their proximity to the nitrile group will be assessed.
4. To assess the role that varied chemical inducers play in directing nitrile hydrolysis in resting cells of *R. rhodochrous*, specifically Strains A29, A99 as well as ATCC BAA 870.
5. To characterize the induced nitrilase in *Rhodococcus rhodochrous* strain A29 and *Pimelobacter simplex* A99.

Chapter Contents

Chapter 1: A brief overview on “Green Chemistry” and Sustainable Chemical Processes is provided in this chapter. The intention here being to address the growing need for novel biological processes for use in the production of both commodity chemicals as well as advanced pharmaceutical agents (APIs).

Chapter 2: This chapter provides a review on known nitrile hydrolyzing biological systems. An extensive review of the current information landscape for both nitrilase and nitrile hydratase enzyme systems are provided. This is followed by an in-depth study into each enzyme reaction mechanism; substrate profiles for each enzyme type; enzyme structure and function correlations; as well as gene expression and transcription regulation.

Paper I: Paper one document’s the kinetic resolution of β-hydroxy substituted aryloxynitriles and aryl propanenitriles using the nitrile hydrolyzing biocatalyst *Rhodococcus rhodochrous* ATCC BAA-870. Contribution to the findings documented in this paper includes but is not limited to substrate synthesis, microbial cultivation and enzyme induction, as well as biocatalytic profiling of *R. rhodochrous* ATCC

BAA-870. Assistance was provided with all research documentation and preparation of the final manuscript.

Finally, amidase substrate docking studies was initiated with assistance provided by Dr Chis van der Westhuyzen (CSIR). This was done to determine the mechanism driving stereoselective conversion of the amide to acid product by the native amidase enzyme in this strain (see **Appendix 2** for substrate docking results done on the amidase produced by ATCC BAA-870).

Paper II: Paper two is an extension of the initial characterization work done using *R. rhodochrous* ATCC BAA-870. Where the initial study looked at producing enantiopure β-adrenergic agents and statin intermediates, Paper II looked at stereoselectively producing peptidomimetic type molecules of pharmaceutical importance. A number of β-substituted nitrile substrates demonstrating an amino substituent at the chiral β-position were evaluated in this study. Contributions to the findings in this paper were provided as principal investigator. All cell cultivation, kinetic resolution work and product purification work was undertaken. Assistance was provided with product profiling by NMR, HRMS analysis and data interpretation. Research documentation and manuscript preparation was completed as well.

Paper III: The book chapter, incorporated in this thesis as Paper 3 is a review outlining current research findings in the area of nitrile biocatalysis. Manuscript preparation was initiated with subsequent editing and formatting assistance provided by Prof D. Brady and Dr. M. Bode.

Paper IV: Paper 4 is a study into the diversity of nitrile degrading microbial systems isolated from various South African natural environments. Isolated strains were biocatalytically profiled by Mrs. Gulston to determine their enantio-selectivity profiles on a range of β-substituted nitriles. Contribution to this paper was provided with enzyme characterization studies that were undertaken.

Paper V: Paper 5 is an in-depth study into the role inducers such as benzonitrile and dimethylformamide play in the regulation of nitrile degrading enzyme gene expression. Two varied *Rhodococcus rhodochrous* species (ATCC BAA-870, strain A29), as well as in *Pimelobacter* simplex (strain A99) were profiled through the course of this study. Induction studies, biocatalytic profiling (using 3-cyanopyridine as substrate), inhibitor studies, protein sequencing by LCMS-MS was completed with analytical support provided by Mr. K. Mathiba. Data interpretation, research documentation and preparation of the final manuscript for publication were completed as well.

Hypothesis

Rhodococci are extremely versatile biological agents capable of hydrolyzing nitrile functionalities with considerable regio- and enantio-selectivity. Cells belonging to this genus show potential for application in "greener" industrial processes.

Table List

Table 1.1: E-factor values in varied production environments 4

Table 1.2: Genomic content of various sequenced *Rhodococci.* 10

Table 1.3: Nitrile hydrolysing microbes and their application in chemical synthesis 12

Table 2.1: Biological characteristics of purified nitrilases…. 36

Table 2.2: *R. rhodochrous* J1 nitrilase catalytic residues..... 44

Table 2.3: Comparison of NitR versus XylS and AraC……..……45

Table 2.4: Characteristics of purified nitrile hydratase enzymes…… 63

Table 2.5: Amino acid residues located at the α and β interface of nitrile hydratase produced by *Pseudonocardia thermophila* JCM3095……..…… 69

Figure List

Figure 1.1: Cascade enzymatic process designs employed in industry.……7

Figure 1.2: Bio-catalytic cascade reaction demonstrating the synergistic action of a ketoreductase, nitrilase and a glucose dehydrogenase enzyme ……...8

Figure 1.3: Ammoxidation of 3-picoline to produce 3-CP (*A*) with subsequent gas-phase oxidation of 3-CP to generate nicotinamide and nicotinic acid (*B*)……..14

Figure 1.4: Biological synthesis of nicotinamide and nicotinic acid using resting cells of *Rhodococcus rhodochrous* ATCC BAA-870 and strain A29, and *Pimelobacter simplex* strain A99……....15

Figure 1.5: Enantioselective Biosynthesis of *R*-(-)-mandelic acid from (*R,S*)- mandelonitrile using a nitrilase enzyme……16

Figure 1.6: Substituted β-amino acids displaying β^2, β^3, and $\beta^{2,3}$ configurations……...17

Figure 2.1: Nitrile metabolic pathways in nature……24

Figure 2.2: Schematic diagram showing the mechanism of action of aldoxime dehydratase enzyme……..25

Figure 2.3: ADH substrate binding site with amino acid interaction in the catalytic site by Ser219 and His320……26

Figure 2.4: Schematic diagram showing the mechanism of action of nitrogenase enzymes…...27

Figure 2.5: Schematic diagram showing the mechanism of action of oxynitrilase enzymes……28

Figure 2.6a: Schematic diagram demonstrating organic and inorganic nitrile hydrolysis using different enzymes systems……29

Figure 2.6b: Proposed nitrilase mechanisms for nitrilase and cyanide hydratase enzymes……30

Figure 2.7: Crystal structure of a hyperthermophilic nitrilase from *Pyrococcus abyssi*……....32

Figure 2.8: Branches of the Nitrilase superfamily……...33

Figure 2.9: Schematic diagram showing the mechanism of action of nitrilase enzymes……...34

Figure 2.10: Schematic diagram showing the proposed nitrilase catalytic mechanism for BNZ and benzamide hydrolysis……38

Figure 2.11: Proposed nitrilase mechanism generating both acid (A) and amide (B) products…..39

Figure 2.12: Dimeric structures of 1ERZ, 1EMS, 1F89 and 1J31 showing the signature αββα-αββα fold……...40

Figure 2.13a: UNIProt KB-Q03217 protein sequence……..41

Figure 2.13b: Molecular representation of *R. rhodochrous* Strain J1 nitrilase…….....42

Figure 2.14: MAFFT protein sequence alignment of *Rhodococcal* nitrilases……...43

Figure 2.15: A comparison of the amino acid sequences of various transcription regulators…….....50

Figure 2.16: Zernike Phase Contrast- TEM image showing GroEL and GroES proteins……52

Figure 2.17: 60 kDa Chaperonin protein sequence alignment……...56

Figure 2.18: Crystal structure of Co-type nitrile hydratase from *Pseudonocardia thermophilia*.....57

Figure 2.19: Self-subunit swapping of LMW-nitrile hydratase enzymes…….58

Figure 2.20: Schematic diagram showing nitrile hydratase and amidase cascade reactions…....61

Figure 2.21: Nitrile hydratase reaction mechanisms…….62

Figure 2.22: Nitrile hydratase α-subunit amino acid sequence alignment……....68

Figure 2.23: Organisation of the nitrile hydratase gene cluster in varied microorganisms…….....70

Abbreviations List

Å	Angstrom
ADH	Aldoxime dehydratase
BNZ	Benzonitrile
CDH	Cyanide dihydratase
CH	Cyanide hydratase
3-CP	3-Cyanopyridine
DMF	Dimethylformamide
DNA	Deoxyribonucleic Acid
E. coli	*Escherichia coli*
Glu-Lys-Cys	Glutamine- Cysteine- Lysine
GroEL	60 kDa Chaperonin
HMW- nitrile hydratase	High Molecular Weight-nitrile hydratase
HPLC	High Performance Liquid Chromatography
HRMS	High Resolution Mass Spectroscopy
kDa	Kilodalton
LCMS-MSMS	Liquid Chromatography Mass Spectroscopy
LMW-nitrile hydratase	Low Molecular Weight-nitrile hydratase
mmol	Millimole
MM	Minimal Media
NAD	Nicotinamide Adenine Dinucleotide
NADP	Nicotinamide Adenine Dinucleotidephosphate
Nitrile hydratase	Nitrile hydratase
*nit*A	Aliphatic Nitrilase Gene Sequence
*nit*R	Aliphatic Nitrilase Positive Regulator Gene Sequence
ORF	Open Reading Frame
PAGE	Polyacrylamide Gel Electrophoresis
P. simplex	*Pimelobacter simplex*
R. erythropolis	*Rhodococcus erythropolis*

R. rhodochrous	*Rhodococcus rhodochrous*
SDS	Sodium Dodecyl Sulphate
SDS-PAGE	Sodium Dodecyl Sulphate Polyacrylamide Gel Electrophoresis
TSB	Tryptone Soy Broth
UPLC-MS	Ultra Performance Liquid Chromatography- Mass Spectroscopy

Common Amino Acid Abbreviations

Glycine	Gly (G)
Alanine	Ala (A)
Valine	Val (V)
Leucine	Leu (L)
Isoleucine	Ile (I)
Methionine	Met (M)
Phenylalanine	Phe (F)
Proline	Pro (P)
Serine	Ser (S)
Threonine	Thr (T)
Cysteine	Cys (C)
Asparagine	Asn (N)
Glutamine	Gln (Q)
Tyrosine	Tyr (Y)
Tryptophan	Trp (W)
Aspartate	Asp (D)
Glutamate	Glu (E)
Histidine	His (H)
Lysine	Lys (K)
Arginine	Arg (R)

Preface: Moving South Africa Towards a Global Bio-economy Strategy

The European Bio-economy Strategy was launched in February 2012 and was created to address issues relating to sustainable biological resource generation and its conversion to vital products and bio-energy. The strategy was signed by several Commission departments and was structured around three pillars: 1) to increase investment into research, innovation and skills development; 2) to reinforce policy interaction and stakeholder engagement; 3) and lastly to enhance markets and overall competitiveness.

The strategy was aimed to provide answers to some of the challenges facing many European countries. These included the depletion of finite energy resources; providing food security for a steadily increasing population; providing palliative care and improving on health treatments for an aging population; and finally counteracting global environmental pressures by reducing institutional carbon emissions and environmental pollution levels.

In the context of the South Africa economy, the national Bio-economy Strategy needs to answer these global challenges but has the added complication of addressing significant socio-economic imbalances that still plague the country. For these reasons economic growth in South Africa must be coupled with poverty reduction and improved quality of life. This can only be achieved by coordinated efforts that span across varied institutions. Academia, science councils and other public/ private institutions need to drive collective research initiatives that stimulate the development of new markets and research avenues as these in turn will drive the economic cogwheels needed to keep the South African economy moving.

Nitrile catalysis is a research area which has functioned to successfully bridge the divide between scientific councils such as the CSIR and academic institutions such as the University of the Witwatersrand. This project has almost two decades of collective research from numerous individuals and still continues to drive innovation in academia. What it needs though is a foothold into industry, a partner willing to commercialise the technology.

It is my hope that the information gathered through this research will assist this process and that the additional years of research insight and sacrifice by numerous researchers will result in the formation of a commercial success story still to come.

Chapter One: Introduction to Green Chemistry

1.1 Green Chemistry and Sustainable Chemistry

The term green chemistry is defined as "**The invention, design and application of chemical products and processes to reduce or to eliminate the use and generation of hazardous substances**" (Anastas and Warner, 1998). A basic strategy to achieve this would have to consider what many schools of economy have coined as the "triple bottom line" philosophy. This requires that an enterprise ensure regard for environmental protection, societal benefit, and market advantage as a whole (J. Elkington). This can only be achieved by the implementation of both sound economic and fundamental scientific principles.

The inclusion of the impact of chemical products and processes in the design of the process allows for a link to be drawn between the potential hazards associated with the process and the eventual performance criteria to be used in measuring the success of a process, while the phrase "use and generation" in the definition takes into account both undesirable substance produced through the process and all other substances employed from start to completion of a process.

The word hazard in this definition is not restricted only to physical hazards such as chemical exposure and carcinogenicity, explosiveness, flammability and corrosiveness of the chemicals used, but also includes global threats such as global warming, stratospheric ozone depletion, resource depletion and possible bioaccumulation. This allows for a broader perspective on the far reaching effects of research and industrial processes and seems philosophically and pragmatically consistent.

New strategies are often being sought out to address the underlying issue of enantio-selective synthesis of chiral molecules as alternatives to traditional asymmetric synthesis or kinetic resolution. However the limitations of chemical synthesis are not easily overcome since fine-tuning non enzymatic catalysts is often a much more complicated process. Biological catalysts on the other hand are often more amenable to catalytic adjustments with a change in the operating pH, temperature, immobilization of the enzyme as well as alteration to the working solvent conditions having considerable effect on the profile of the same biocatalyst. The crux of the matter here though is the absolute requirement for identifying highly selective catalysts that can be employed in the synthesis of small therapeutic compounds of interest, and doing so in a sustainable "greener" manner.

Sustainable biotechnology by definition requires that research processes in the future meet basic requirements deemed necessary but also provide adequately for future generations. This when applied to chemical processes has created the *12 Principles of Green Chemistry*, which sets out guidelines on how chemical synthesis processes should be designed. The 12 principles noted by Anastas and Warner (1998) are as follows:

The 12 Principles of Green Chemistry*

1. Reduce waste production. Waste prevention is always better that subsequent cleaning up.
2. Employ technologies which maximise atomic economy. All synthetic methods employed should be designed to maximize material incorporation in the final product formed.
3. Reduce or eliminate human health and environmental toxicity by using synthetic methodologies that show little or no toxicity to human health of the general environment.
4. Chemical products generated should be designed to preserve efficacy while reducing toxicity.
5. Chemical processes should reduce the amount of auxiliary substances (solvents and separation agents) in the process.
6. The environmental and economic effects of the process undertaken should be minimized.
7. Synthetic methods should be conducted at ambient temperature and pressure to reduce the process carbon footprint.
8. Renewable raw materials or feed stocks should be used rather than employing substrates that can be depleted.
9. Avoid using processes which require product derivatization (adding on of protecting or de-protecting groups).
10. Selective catalytic reagents should be preferentially selected over the use of stoichiometric reagents.
11. Chemical products formed should undergo degradation after use and not persist in the environment, breaking down into innocuous products.
12. Substances used in chemical processes should be chosen carefully to minimize the possibility of chemical accidents, environmental contamination as a result of release or the possibility of explosions and fires.

*Anastas, P. T.; Warner, J. C. Green Chemistry: Theory and Practice, Oxford University Press: New York, 1998, p.30.

Two well recognised measures often used to determine the overall environmental acceptability of a chemical process include the E-factor (the mass ratio of waste generated in relation to the desired product being formed), as well as the atomic efficiency of the reaction/ process (the molecular weight of the product divided by the sum of the molecular weights of all of the other stoichiometric reagents used in the reaction) (Sheldon 2008). A high E-factor value calculated for a particular process means the generation of large amounts of waste material, with an E-factor of zero being preferred. A drawback with regards to E-factor calculations however is that water utilization is not considered.

Other proposed methods for determining the environmental suitability of a process includes the effective mass yield (EMY) which is defined as the percentage of product in relation to all the materials used in the preparation undertaken (Hudlicky *et al.* 1999). The shortcoming of this method of calculation seems to be the exclusion of so-called benign chemical compounds such as sodium chloride, acetic acid and others which many still pose an environmental risk if employed in large enough quantities. Constable *et al.* (2002) proposed the use of mass intensity (MI), which was defined as the total mass used in a particular process divided by the mass of the product. In this particular case MI= E factor + 1.

However most often, the method employed in determining the environmental impact of a process seems to be the E- factor as well as atomic efficiency (atom economy) (Trost 1991; Sheldon 2000; Sheldon 2007).

Different industries generate varied product profiles, with the product tonnage sometimes being offset against a waste production profile that appears to be excessive. Nowhere is this more obvious than in the “Pharmaceutical production” industry environment, where 25-100% of waste is generated relative to product formation levels (Table 1.1).

Table 1.1: E-factor values in varied production environments

Industry Segment	**Product tonnage** [a)]	**kg waste** [b)]**/ kg product**
Oil refining industry	10^6- 10^8	<0.1
Bulk chemicals industry	10^4- 10^6	<1- 5
Fine chemicals industry	10^2- 10^4	5- 50
Pharmaceutical industry	10-10^3	25- 100

a) Represents annual production volume of a product at one site (lower-end) to global production (upper end demonstrated)

b) All other material produced through the reaction process excluding the desired product.

Most chemical processes can be improved through one-pot reactions using cascade reactions, as these would obviate the need for multiple product work ups and reduce the associated yield loss that occurs during each of the individual process steps undertaken.

1.2 Cascade Reactions

Living organisms have biological processes that not only catalyse efficient conversion of simple compounds into complex ones, but do so under ambient reaction temperature and pressure conditions. This is done by cascade reaction systems that shuttle compounds through various metabolic synthesis and degradation pathways, thus creating myriads of different organic compounds along the way. Naturally then, synthetic one-pot reaction systems are attempts at mimicking natural processes that occur in living organisms, with various chemical bonds and stereo-genic centres being formed without the added step of isolating the intermediates. These processes are favoured since yields are improved with an overall concomitant reduction in the waste material being generated.

One-pot reactions are characterised as being a *domino* type reactions which involve two or more sequential bond-forming reactions; or a *tandem* type reaction process, which facilitates the transformation of two or more different catalytic processes at the same time. The combination of enantioselective catalysts and cascade reaction systems allow for the production of complex chiral molecules.

Catalytic cascade reactions therefore allow minimization of time, cost, effort and a reduction of wastage thereby allowing for novel biomimetic processes to reach the levels of molecular complexity needed for the production of biologically active molecules.

1.2.1 Chemical cascade reactions

Synthetic chemistry by definition is the process used to generate desired molecular compositions and therefore as a field, is limitless in scope. Cascade reactions in this field of research involve choreographed reactions where each synthetic step is required to justify its presence in a string of reactions. This needs to be assessed against the backdrop of ecological requirements as stated in the 12 principles of Green chemistry by Anastis and Warner.

Strategies employed towards generating these biologically active compounds, are often forms of art in themselves with some simple; at other times elaborate processes, being concieved and evaluated. The production of endiandric acid is one such cascade reaction product which is derived from linear, achiral polyunsaturated precursors through a sequence of thermally favourable pericyclic reactions.

Endiandric acid A-C was initially discovered and isolated from the Australian tree *Endiandra introrsa* has been shown to demonstrate antibacterial activity against *Bacillus subtilis, Micrococcus luteus, Streptococcus faecalis, Pseudomonas palida* and *Escherichia coli,* with improved activity when compared to the well known and extensively used antibiotic ampicillin (Chouna *et al.* 2009). Endiandric acid has also been used to cure uterine tumours, rubella, female genital infections as well as rheumatism.

1.2.2 Biological cascade reactions

Biocatalytic cascade reactions are often classified as belonging to one of four different groups.

A single substrate molecule being converted to a single product using one or more steps constitutes a *linear type cascade reaction* (Fig 1.1(a)). An important case of these types of reactions is deracemizations in which one enantiomer of a racemic compound is converted to an enantiopure product. Linear cascades are often used to drive reversible reactions to completion when the product of the first reaction is then converted to another product, thereby constantly drawing the reaction out of an equilibrium state.

In *orthogonal cascade reactions* the transformation of a substrate to product includes coupling with other reactions that are needed to regenerate cofactors or co-substrates or remove by-products (Fig 1.1(b)). An example of this process is the conversion of keto acids into *D*-amino acids by the enzyme *D*-amino acid aminotransferase (Galkin *et al.* 1997).

Parallel cascade reactions are processes in which two products are produced from two substrates using two distinct bio-catalytic reactions which are coupled by co-factors or co-substrates (Fig 1.1(d)). A cascade reaction described by Gotor and co-workers employed the use of an alcohol dehydrogenase enzyme and a Baeyer-Villiger monooxygenase enzyme for the production of non-racemic alcohols and sulfoxides (Bisogno *et al.* 2010).

Finally, cyclic cascade reactions using a mixture of substrates are selectively converted into intermediates which in turn are transformed back to the starting material (Fig 1.1(c)). This repetitive process allows for the accumulation of the compound which is left behind during the first transformation. This process is widely used for the chemo-enzymatic deracemization of amino acids, hydroxyl acids as well as amines.

Enzyme initiated cascade reactions may be extended to more than two enzymes (Fig. 1.2), or include non-biological catalysts. Commercial companies such as Merck & Co have employed synthetic sequence technologies in the synthesis of the anti-migraine drug telcagepant (Xu *et al.* 2010). This particular process includes the incorporation of organo-catalysis (using Jorgensen's catalyst) together with a one-pot reaction with three intermediates being produced, with no chromatographic purification needed.

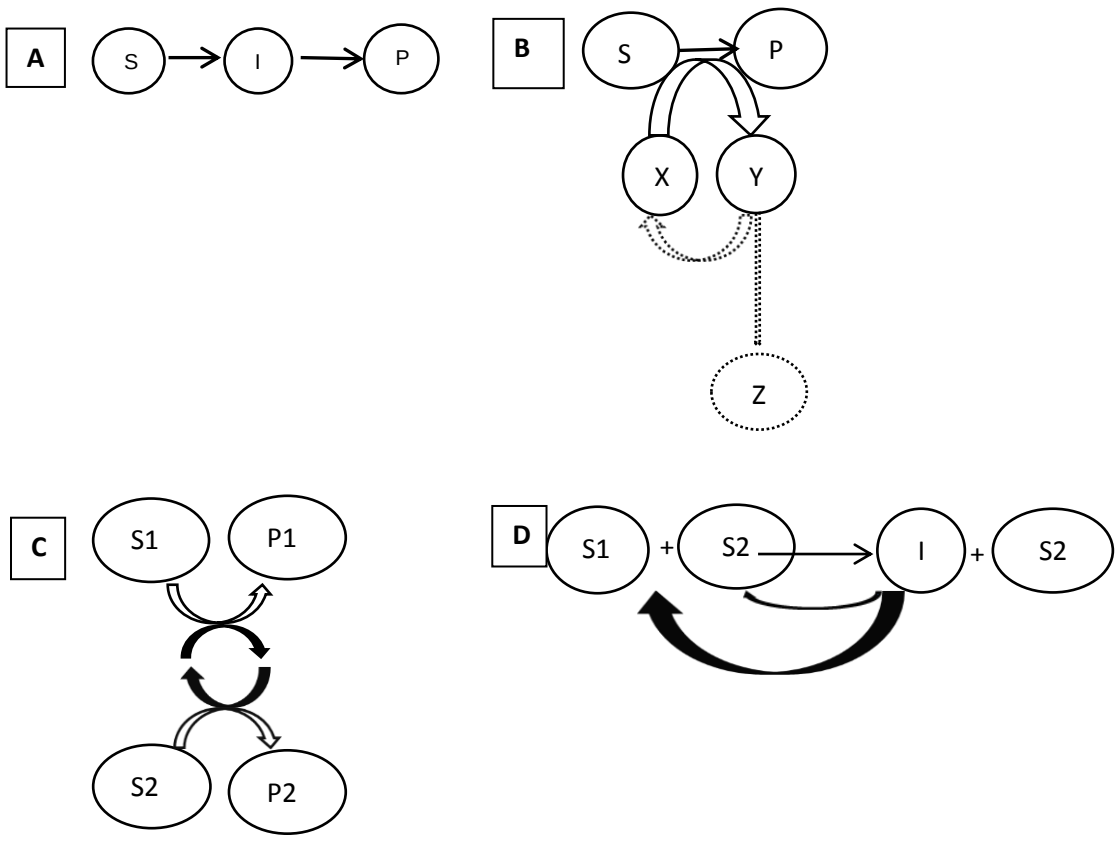


Figure 1.1: Cascade enzymatic process designs employed in industry.

a) Linear cascade; b) orthogonal cascade reactions; c) cyclic cascade reactions; and d) parallel cascade reactions. Image adapted from García-Junceda *et al.* 2015.

Biosynthetic molecules display a great deal of complexity in their structures. This is often the result of a combination of catalytic cascades reactions as well as the use of different substrates. Bio-catalytic enzymes function synergistically to facilitate reaction processes, with certain enzymes requiring the action of specific coenzymes and co-factors for activity. The success of such processes hinges on the involvement of both organocatalysts and other molecular catalysts which are responsible for functional group activation, thus increasing the molecular diversity of the products being synthesized.

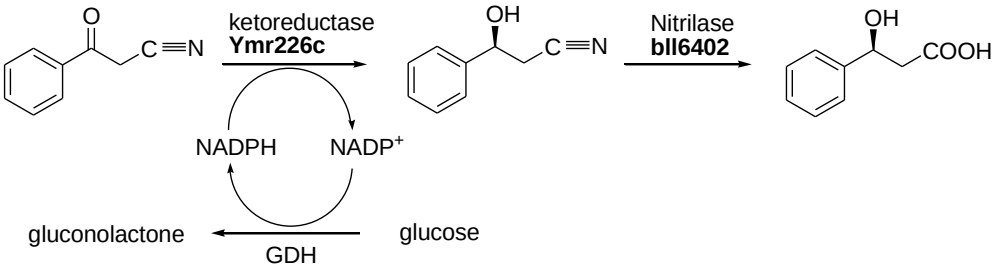


Figure 1.2: Bio-catalytic cascade reaction demonstrating the synergistic action of a ketoreductase, nitrilase and a glucose dehydrogenase enzyme.

1.3 Role of Biocatalysis in the Generation of Pharmaceutical Intermediates

Stereochemistry plays an important role in the pharmaceutical industry with the three-dimensional structure of a compound affecting the manner in which the chemical agent reacts in a chiral environment like the human body. Racemic compounds have paired mirror-image enantiomers that may interact with cell receptors in remarkably different ways. Where a single-enantiomer could have the required pharmacological activity, another could be ineffective or even toxic. The production of enantiopure molecules is therefore crucial with the translated benefits of improved efficacy, predictable pharmacokinetics as well as reduced toxicity in-vivo being of vital importance (Eichelbaum and Gross. 1996)

The synthesis of enantiomerically pure compounds (coined EPC-synthesis) was introduced in the 1980's by Professor Seebach, and included chemical production methods that were used in the preparation of chiral enantiopure compounds (Seebach and Hungerbuhler, 1980). The three main synthetic approaches highlighted include:

1. Resolution of racemic compounds.
2. Synthetic transformation reactions using enantiomerically pure starting material (sometimes referred to as a chiral pool)
3. Stereo-selective reactions that involve an enantiopure reagent as the source of chirality. These are often included in stoichiometric/ catalytic quantities to drive reactions but are not included in the final product themselves.

1.4 Microbes as Chemo-Selective Agents

The production of enantiomerically pure or diastereomerically pure materials can be produced in several ways. A racemic mixture can be resolved by both chemical as well as physical methods. Pro-chiral molecules can be transformed to generate chiral molecules by asymmetric synthesis reactions via the use of chiral reagents or catalysts.

In general, nitrilase, nitrile hydratase (nitrile hydratase) and amidase enzyme systems offer potential for use in the selective conversion of nitriles to their corresponding acid or amide products. These are

particularly useful in the biological synthesis of non-natural amino acids and peptide therapeutic molecules (peptidomimetics).

1.5 The Biocatalytic Versatility of Rhodococcus

The genus *Rhodococcus* is a versatile group of gram positive, *Nocardioform* actinomycetes that are capable of degrading a range of recalcitrant, and sometimes toxic, organic compounds. They have been isolated from diverse environments ranging from terrestrial soil samples to aquatic plant materials (Finnerty, 1992; Warhurst and Fewson, 1994).

The catabolic versatility demonstrated by these cells is attributed to their ability to accumulate diverse catabolic genes, while their robust cell physiology allows them to survive in harsh environmental conditions. *Rhodococcus* cells appear to adopt a strategy of hyper-recombination which is associated with the presence of a large genome (Table 1.2).

Whole genome studies done on *Rhodococcus* sp. RHA1, show that these cells house a 9.7 Mb genome which includes three large linear plasmids ranging from 1100 kb-330 kb in size (Table 1.2). These cells were found to degrade a wide variety of plant derived compounds that are produced in oxygen rich niche environments (McLeod *et al.* 2006).

Other *Rhodococci* such as *R. opacus* M213, which were isolated from fuel contaminated soil samples were found to house many catabolic genes. Some degraded polycyclic aromatic hydrocarbons (PAHs) while others were involved in naphthalene biodegradation (Pathak *et al.* 2016). Strain B4 showed a high level of tolerance to benzene (KEGG database, entry T00882) (Table 1.2).

R. erythropolis M12 and strain PR4 produced novel secondary metabolites with strain M12 degrading 4, 4'-dithiobutyric acid (Khairy *et al.* 2016). Strain PR4 was found to produce unusual heterobacins, while *Rhodococcus* IcdP with its smaller genome size (5.92 Mbp), showed the presence of metabolic genes that were similar to *R. opacus* M213. Many of these genes encoded enzymes required for the degradation of a PAHs and organochlorine pesticides, such as benzo[*a*] pyrine, and indeno [1,2,3-*cd*] pyrene (Qu *et al.* 2015).

R. pyridinivorans SB3094 cells have been found to degrade methyl-ethyl-ketones, and are used in the reticulation of wastewater systems containing high levels of petrochemical hydrocarbon (Dueholm *et al.* 2014).

Finally, *R. equi* 103S is considerably different to the previous strains described above. Being an animal pathogen species, it shows a considerably smaller genome size (5.59 Mbp) in comparison to many other *Rhodococcal* species but this adaption appears to allow for host colonization, thus occupying a specific niche environment.

The ability to utilise different substrates has a physiological basis with a general tolerance to substrates and solvents being a key factor. *Rhodococci* have been found to catalyze regio and stereoselective reactions with many applied to the stereoselective conversion of (*R,S*)-mandelonitrile.

Table 1.2: Genomic content of various sequenced *Rhodococci*.

Organism	**Sequence completion date**	**Reference**	**Chromosome (Mbp)**	**Plasmid (base pairs)**	**Total size (Mbp)**
R. jostii RHA1	2006	McLeod *et al.* 2006	7.8	1 123 075; 442 536; 332 361	9.7
R. opacus B4	2009	KEGG database, Entry number T00882	7.9	558 192; 244 997; 111 160; 4 367; 2773`	7.9
R. erythropolis MI2	2016	Khairy *et al.* 2016	6.45	400000; 350000	7.2
R. erythropolis PR4	2009	Sekine *et al.* 2006	6.5	271 577; 104 014; 3637	6.5
Rhodococcus sp. Strain IcdP1	2015	Qu *et al.* 2015	5.92	-	5.92
R. rhodochrous ATCC BAA 870	2011	To be published	5.7	453 000	5.83
R. pyridinivorans	2014	Dueholm *et al.* 2014	5.2	361397; 2035	5.59
R. equi 103S	2010	Letek *et al.* 2010	5.04	80610	5.04

1.6 Enzymes as Chemoselective Agents

Although chemical methods were previously used in the generation of chiral compounds, biological agents such as enzymes have been increasingly exploited due to their stereoselective “bias” with many biocatalytic reactions possible under ambient temperature and reaction conditions. Enzymes by nature are effective catalytic agents due to their ability to alter substrate planar configuration, making reaction progression towards transition state intermediates energetically favourable.

Most industrial chemical processes focus on classic synthesis, with attention being placed on reducing the number of steps needed to form a desired product. This is done not only to reduce the energy requirements needed and improve the overall techno-economics of the process, but to improve the process efficiency and eliminate waste material generation.

New strategies are often being sought out to address the underlying issues required for enantio-selective synthesis of chiral molecules.Traditional asymmetric synthesis or kinetic resolution is often complicated by the operational limits under which reactions can be done. Biological catalysts on the other hand are often more amenable to catalytic adjustments with a change in the operating pH, temperature, immobilization of the enzyme as well as alteration to the working solvent conditions having considerable effect on the profile of the same biocatalyst. The crux of the matter here though is the absolute requirement for identifying highly selective catalysts that can be employed in the synthesis of small therapeutic compounds of interest, and doing so in a sustainable “greener” manner.

Several well-known industrial and pharmaceutical intermediates can be produced through the transformation of nitriles. These include nicotinic acid, nicotinamide, acrylamide, acrylic acid, and mandelic acid which are useful chiral synthons for the production of enantiopure agricultural and pharmaceutical intermediates (Table 1.3).

New strategies are often being sought out to address the underlying issue of enantio-selective synthesis of chiral molecules as alternatives to traditional asymmetric synthesis or kinetic resolution. However the limitations of chemical synthesis are not easily overcome since fine-tuning non enzymatic catalysts is often a much more complicated process. Biological catalysts on the other hand are often more amenable to catalytic adjustments with a change in the operating pH, temperature, immobilization of the enzyme as well as alteration to the working solvent conditions having considerable effect on the profile of the same biocatalyst.

Table 1.3: Nitrile hydrolysing microbes and their application in chemical synthesis

Microorganism	Biocatalytic process	Reference
Rhodococcus rhodochrous J1	Nicotinic acid synthesis	Almatawah and Cowan. 1999
Rhodococcus rhodochrous LL100-21	*ortho*-, *meta*-, *para*- substituted CH_2CN compounds	Hashimoto. 1984
Rhodococcus rhodochrous ATCC BAA-870	3-hydroxy-4-aryloxybutanenitrile 3-hydroxy-3-arylpropanenitrile	Kinfe *et al.* 2008
Rhodococcus rhodochrous ATCC BAA-870	3-amino-3-*p*-tolylpropanenitrile, 3-amino-3-(4-methoxyphenyl) propanenitrile	Chhiba *et al.* 2013
Rhodococcus sp. AJ270	(*S*)-3-aryl-4-cyanobutyric acid	Kumaran *et al.* 2003
Rhodococcus sp. CCZU10-1	Benzoylformic acid	He *et al.* 2012
Arthrobacter nitroguajacolicus	Acrylic acid synthesis	Shen *et al.* 2009
Agrobacterium radiobacter	*(S)*-ketoprofin, (*S*)-flurbiprofen, (*S*)-fenoprofin	Chen *et al.* 2003
Alcaligenes sp. Nitrilase (transformed and expressed in *E.coli*)	Mandelic acid synthesis	Xue *et al.* 2011 Zhang *et al.* 2010

1.7 Commercial Application for Nitrile Biocatalysts

Nitrile hydratase and or coupled nitrile hydratase/ amidase producing microorganisms are often employed in many commercial biosynthetic processes. Some are used in the biocatalytic hydrolysis of nitriles to generate commercially important products such as nicotinamide (Nagasawa *et al.* 1988); in acrylic acid synthesis using *Rhodococcus ruber* strain AKSH-84 (Kamal *et al.* 2011); for the production of α-hydroxyisobutyric acid from α-hydroxyisobutyronitrile (Bhatia *et al.* 2013); while a nitrile hydratase enzyme produced by *Rhodococcus rhodochrous* J1 is used for the commercial biosynthesis of acrylamide from acrylonitrile (Kobayashi *et al.* 1992; Yamada and Kobayashi, 1996).

1.7.1 Acrylamide Production (Large-scale Commodity Process)

Acrylamide production through enzymatic hydration of acrylonitrile using *Rhodococcus rhodochrous* J1 is still one of the most relevant and well adopted industrial processes used in the production of this multi-tonne scale commodity chemical. Acrylamide is a crucial commodity chemical which finds industrial application as a soil conditioner, coagulator; stock additive in paper processing and sizing; and is used for paint and petroleum product recovery during processing. The estimated market size in 2003 was approximately 206 million pounds per year (Energetics, Inc. 2003).

The conventional chemical method for synthesis makes use of a copper salt catalyst to facilitate hydration of acrylonitrile. However, this process results in higher levels of acrylic acid production relative to acrylamide with multiple by-products such as ethylene cyanohydrin and nitrolotrispropionamide being produced as well.

The first nitrile bioconversions were done at Mitsubishi Rayon in 1985, and involved the use of a nitrile hydratase to generate 30000 tons of acrylamide (Faber 1995). Currently, DiaNitrix as well as Mitsubishi (Japan) and Senmin Pty Ltd. (South Africa) employ nitrile degrading biocatalysts for the production of ~120000 tons of acrylamide per year. These biocatalytic conversion processes have gathered favour both locally and internationally due to their ability to generate high value compounds using greener technologies which are selective. They show reduced energy requirements and are coupled with a considerable reduction in carbon dioxide emission levels, making this process more cost effective.

1.7.2 Acrylic Acid (Large-scale Commodity Process)

Acrylates (which include acrylic acid and its ester products) make up a two billion pound market (Biobased report, 2003) that is used in the preparation of emulsions and polymers that find application in the coating, textiles, paint, and paper and adhesives market. Acrylic acid is produced commercially by aerobic oxidation of propylene or propane (Campbell *et al.* 1970).

The worldwide production scale of acrylic acid reached approximately 2.9 billion pounds in 2002, with Rohm and Haas, BASF, Celanese, Dow and American Acryl being the major producers (Biobased report, 2003). Most of the acrylic acid produced exists in the form of a polymer, with an increase in demand for use in the preparation of super absorbents being the key driver for production. Growth in the acrylic acid market showed an annualized increase of 6.5% until 2000 with over supply and a lower chemical demand driving lower prices thereafter.

1.7.3 Nicotinic Acid Production (Pharmaceutical Application)

Nicotinic acid (also know as niacin or vitamin B3) is often supplemented in the production of animal feedstocks and employed in the production of many pharmaceutical intermediates.

Commercially, 3-picoline which is the starting pyridine base required for the production of nicotinic acid, is generated using the Chichibabin reaction method. In this process a mixture of an aldehyde, ketone and ammonia are reacted in a gas-phase to produce a mixture of pyridine and 3-picoline. The methyl group in 3-picoline is then selectively oxidized to form 3-cyanopyridine (3-CP) with little in the form of undesired side products being formed (Fig. 1.3A)

Subsequent hydrolysis of 3-CP to generate nicotinamide or nicotinic acid can be achieved by using a chemical catalytic process (Fig 1.3) or via a biocatalytic process (Fig. 1.4).

Vanadium is often employed as a catalyst in the gas-phase ammoxidation and oxidation steps, with vanadium oxide often chosen as the preferred metal oxide. Reaction promoters include a range of group 5 and first row transition and alkaline metals, although the mechanism by which these function is not well understood. The physical properties of the catalysts play a crucial role with particle size and shape; pore sizes; surface area; mechanical integrity; and attrition resistance being important for the functioning of the catalyst. However, a limitation of this process relates to further oxidation resulting in the production of high levels of nicotinic acid in the product stream.

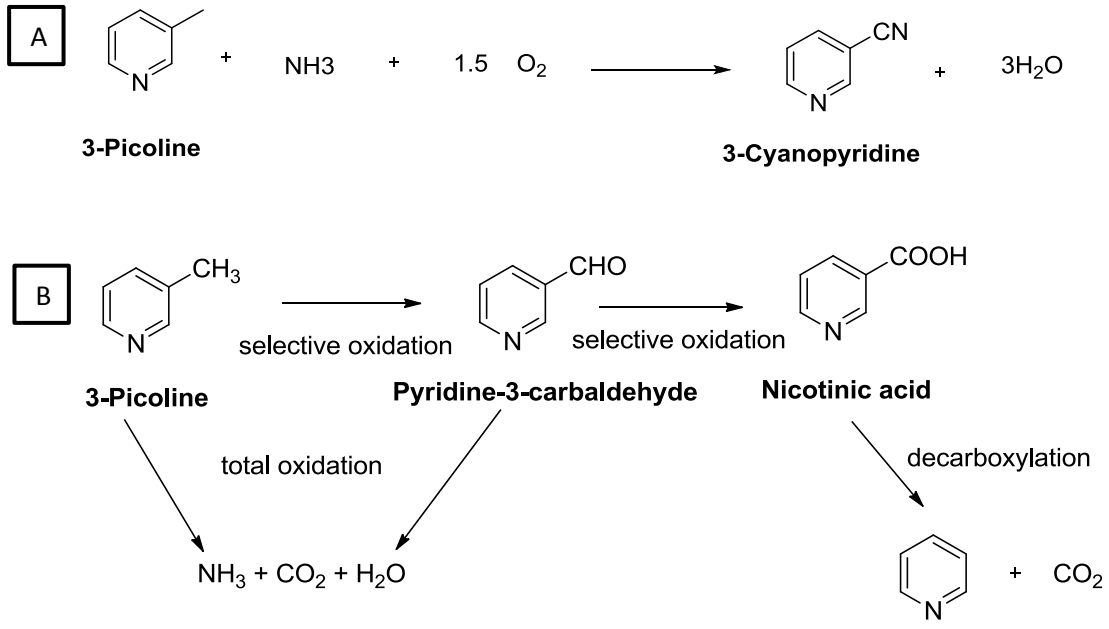


Figure 1.3: Ammoxidation of 3-picoline to produce 3-CP (*A*), with subsequent gas-phase oxidation of 3-CP to generate nicotinamide and nicotinic acid (*B*) (reproduced from R. Chuck, 2005).

However, nitrilase and nitrile hydratase enzymes have been used in the commercial production of both nicotinamide and nicotinic acid (Fig. 1.4). Mathew *et al*. (1988) demonstrated that resting cells of

R. rhodochrous J1 having high benzonitrilase activity catalysed complete conversion of 3-CP to nicotinic acid. Vaughan *et al*. (1989) also showed that cells belonging to the genus *Nocardia rhodochrous* Strain LL 100-21, were capable of producing nicotinic acid from 3-CP, while a thermostable nitrilase produced by *Bacillus pallidus* Strain Dac521 (Almatawah and Cowan. 1999), was shown to catalyse the direct hydrolysis of 3-CP to nicotinic acid with a conversion rate of 76 nmol/ min/ mg dry cell mass.

Nicotinic acid production from 3-CP is not only limited to production by prokaryotic catalytic systems solely, with many fungal nitrilase enzymes have also been studied to determine their potential for use in the biocatalytic conversion of 3-CP to nicotinic acid (Kaplan *et al.* 2006). Ahmad and Moat (1966) studied a number of prototrophs and tryptophan auxotrophs of *Saccharomyces cerevisiae* to determine whether these strains could produce nicotinic acid. Their results indicated that the tryptophan auxotrophs studied utilized tryptophan to synthesise nicotinic acid under aerobic growth conditions.

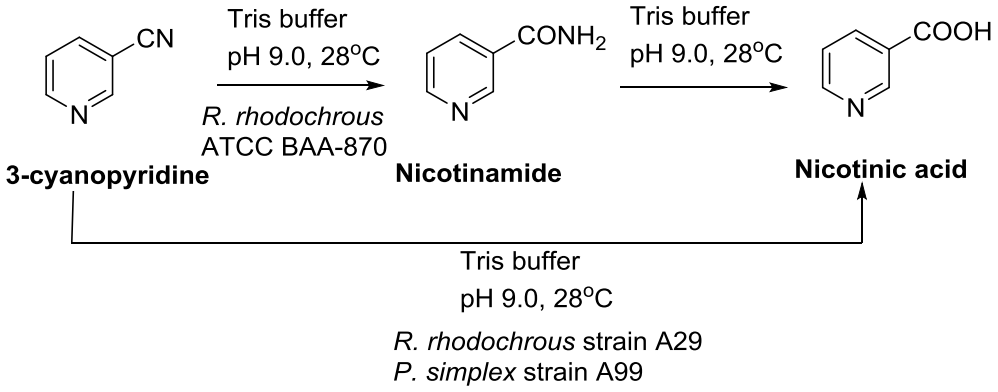


Figure 1.4: Biological synthesis of nicotinamide and nicotinic acid using *Rhodococcus rhodochrous* ATCC BAA-870 and strain A29, and *Pimelobacter simplex* strain A99.

The commercialization of this particular technology by Lonza, China shows the techno-conomic feasibility of using biocatalytic processes to generate not only commodity chemicals but also products generated for animal and human end-use applications as well.

1.7.4 Mandelic Acid (Production of Advanced Pharmaceutical Agents)

The production of *R*-(-)-mandelic acid is of considerable biological importance since it serves as a chiral synthon which can be susbsequently resolved to generate a variety of agricultural and pharmaceutical intermediates (Desantis *et al.* 2002; Gröger, 2001). (*R*)-(-)-Mandelic acid is widely used in the preparation of antibiotics, antiobesity drugs, and antitumor agents, functioning as a chiral resolving agent (Kaul and Banerjee, 2004; Yamamoto *et al.* 1991).

The production of (*R*)-(-)-mandelic acid using an enzymatic route comes with significant advantages such as the non-requirement for co-factor addition; dynamic kinetic resolution with the theoretical possibility of a 100% yield of the (*R*)-enantiomer; as well as a cheaper starting material in the form of a racemate starting feed (Kaul *et al.* 2004).

The enantioselective biocatalytic conversion of racemic mandelonitrile to (*R*)-mandelic acid was first demonstrated by Yamamoto and co-workers using the nitrilase present in the *Alcaligenes faecalis* whole cells tested (Yamamoto *et al.* 1991) (Fig. 1.5). Since then, Kaul and colleagues have achieved this same feat using three different bacteria namely *Pseudomonas putida*, *Microbacterium paraoxydans* and *Microbacterium liquefaciens* producing the required enantiomer with high ee (>93%) (Kaul *et al.* 2004). Similarly, He and colleagues isolated an *Alcaligenes* sp. ECU0401 which showed excellent enantioselective conversion of mandelonitrile to (*R*)-mandelic acid (<99.9%) (He *et al*. 2007).*R*-Mandelic acid is now manufactured at a multi-ton scale.

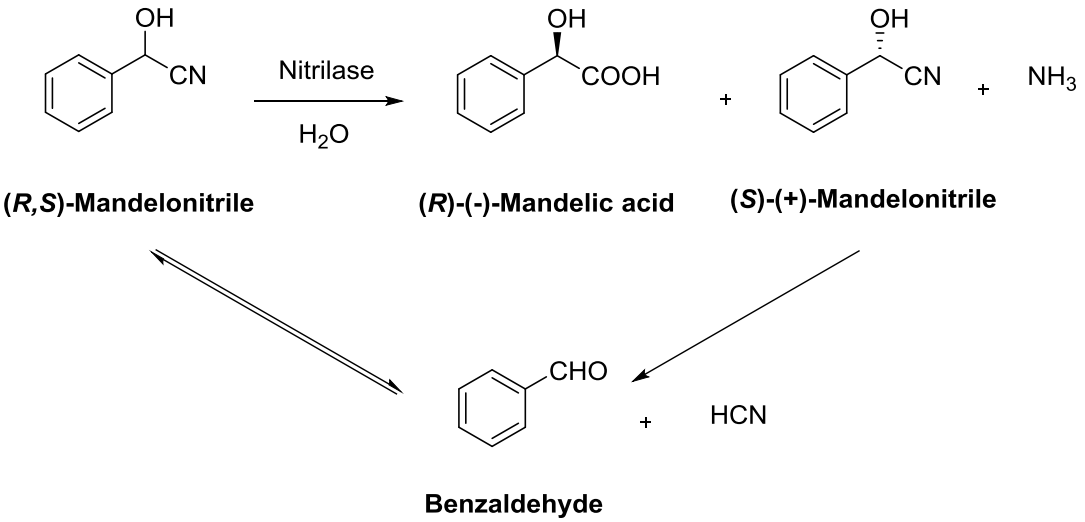


Figure 1.5: Enantioselective biosynthesis of *R*-(-)-mandelic acid from (*R,S*)-mandelonitrile using a nitrilase.

1.7.5 Beta-Substituted APIs

Beta-hydroxy as well as β-amino acid containing structures are often found in compounds of pharmaceutical importance (Hsiao *et al.* 2004; Wolin *et al.* 2004; Zhu *et al.* 2010). Some well-known β-adrenergic agents such as propranolol, alprenolol, metoprolol and fluoxetine are employed for the treatment of cardiac disorders and used to regulate blood pressure in patients suffering from hypertension (Kamal *et al.* 2005). Enantioselective beta-amino acids can serve as precursors for synthesis of a range of biologically active molecules such as the antifungal antibiotic cispentacin (Davies *et al.* 1993). Still others function as treatment agents for use in the management of type 2 diabetes (Steinhuebel *et al.* 2009), while taxol, which has been successfully synthesized by

conformational control (Holton *et al.* 1994) is employed as an anticancer agent in the treatment of ovarian, breast, lung, bladder, melanoma, esophageal as well as other solid tumors.

Many of these therapeutic molecules are required as single-enantiomer formulations with chemical synthesis often unable to sufficiently resolve the racemic starting material employed. Single-enantiomer products have traditionally been generated using either a chemical or chemo-enzymatic processes with a number of chemical synthetic methods employed for the preparation of β^3 amino acids (Lieljeblad and Kanerva, 2006) (Fig. 1.6).

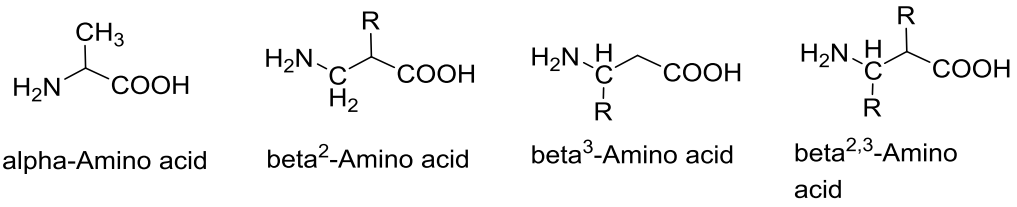


Figure 1.6: Substituted β-amino acids displaying β^2, β^3, and $\beta^{2,3}$ configurations.

Methods commonly employed for the synthesis of β-amino acids rely on a) homologation of existing α-amino acids, b) Thorpe reaction followed by reduction, c) nitrile reduction, d) nitrile hydrolysis as well as stoichiometric use of chemical auxiliaries.

Work done in our labs have shown that stereo-selective nitrile hydrolysis of a number of beta-substituted nitriles substrates is possible (Kinfe *et al*. 2009; Chhiba *et al.* 2012). Cells belonging to the genus *Rhodococcus rhodochrous*, more specifically strain ATCC BAA-870 has provided valuable insight into the stereoselective potential of the nitrile degrading enzymes present in these systems.

The list of commercial applications for nitrile hydrolyzing biocatalysts has still not reached its true potential. Studies done by numerous researchers the world over continue to shed light on the versatility of these enzymes and microorganisms. There are a number of enzymes that hydrolyse both organic and inorganic nitrile sources, thus providing unique catalytic capabilities by a group of extremely versatile biocatalysts. Chapter 2 will attempt to provide an indepth study into the structure, function and mechanism of both nitrilase and nitrile hydratase enzymes.

1.8 References

Ahmad F. and Moat, A. G. Nicotinic acid biosynthesis in prototrophs and tryptophan auxotrops of *Saccharomyces cerevisiae*. (1966). J. Biol. Chem. **241**: 775-780.

Almatawah, Q. A. and. Cowan, D. A. Thermostable nitrilase catalyzed production of nicotinic acid from 3-cyanopyridine. (1999). Enzyme. Microb. Technol. **25**: 718-724.

Anastas, P. T. and Warner, J. C. Green Chemistry: Theory and Practice. Oxford University Press: New York, 1998: 30.

Bhatia, S. K., Mehta, P. K., Bhatia, R. K. and Bhalla, T. C. An isobutyronitrile-induced bienzymatic system of *Alcaligenes* sp. MTCC 10674 and its application in the synthesis of α-hydroxyisobutyric acid. (2013). Bioprocess. Biosyst. Eng. **36**: 613-625.

Bisogno, F. R., Rioz-Martínez, A., Rodríguez, C., Lavandera, I. de-Gonzalo, G., Pazmiño, D. E. T., Fraaije, M. W. and Gotor, V. Oxidoreductases working together: concurrent obtaining of valuable derivatives by employing the PIKAT method. (2010). ChemCatChem. **2**: 946-949.

Campbell, W. E., McDaniel, E. L., Reece, W. H., Williams, J. E. and Young, H. S. Oxidation of propylene to acrylic acid over a catalyst containing oxides of arsenic, niobium, and molybdenum. (1970). Ind. Eng. Chem. Prod. Res. Develop. **3**:325-334.

Chen, C., Chiu, W., Liu, J., Hsu, W. and Wang, W. Structural basis for catalysis and substrate specificity of *Agrobacterium radiobacter* N-carbamoyl-D-amino acid amidohydrolase. (2003). J. Biol.Chem. **278**: 16194-26201.

Chhiba, V., Bode, M. L., Mathiba, K., Kwezi, W. and Brady, D. Enantioselective biocatalytic hydrolysis of β-aminonitriles to β-amino-amides using *Rhodococcus rhodochrous* ATCC BAA-870. (2012). J. Mol. Catal. B- Enzym. **76**: 68-74.

Chouna, J. R., Nkeng-Efouet, P. A., Lenta, B. N., Devkota, K. P., Neumann, B., Stammler, H. –G., Kinbu, S. F. and Sewald, N. Antibacterial endiandric acid derivatives *from Beilschmiedia Anacordioides*. (2009). Phytochemistry. **70**: 684-688.

R. Chuck. Technology development in nicotinate production. (2005). Appl. Cataly. A. **280**: 75-82.

Constable, D. J. C., Curzons, A. D. and Cunningham, V. L. (2002). Metrics to 'Green Chemistry'- Which are the best. Green Chem. **4**: 521-527.

Davies, S. G., Ichihara, O. and I. Walters, I. A. S. An expeditious asymmetric synthesis of (-)-(1R,2S)-Cispentacin. (1993). Synlett. 461-462.

Dueholm, M. S., Albertsen, M., D'Imperio, S., Tale, V. P., Lewis, D., Nielsen, P. H. and Nielsen, J. L. Complete genome of *Rhodococcus pyridinivorans* SB3094, a methyl-ethyl-ketone-degrading bacterium used for bioaugmentation. (2014). Genome. A. **2**: e00525-14.

DeSantis G, Zhu Z, Greenberg W. A., Wong, K., Chaplin, J., Hanson, S. R., Farwell, B., Nicholson, L. W., Rand, C. L., Weiner, D. P., Robertson, D. E. and Burk, M. J. An enzyme library approach to biocatalysis: Development of nitrilases for enantioselective production of carboxylic acid derivatives. (2002). J Am Chem Soc. **124:** 9024–9025.

Eichelbaum, M. and Gross, A. S. Stereochemical aspects of drug action and disposition. (1996). Advances in Drug Research . **28**: 1-64. Academic Press.

Faber, K. (1995). Biotransformations in organic chemistry (2nd edition; Berlin: Springer-Verlag)

Finnerty, W. R. The biology and genetics of the genus *Rhodococcus*. (1992). Annu. Rev. Microbiol. **46**: 193-218.

García- Junceda. E., Lavandera, I., Rother, D. and Schrittweiser, J. H. (Chemo)enzymatic cascades- Nature's synthetic strategy transferred to the laboratory. (2015). J. Mol. Catal. B-Enzym. **114**: 1-6.

Galkin, A., Kulakova, L., Yoshimura, T., Soda, K. and Esaki, N. Synthesis of optically active amino acids from α-keto acids with *Escherichia coli* cells expressing heterologous genes. (1997). Appl. Environ. Microbiol. **63**: 4651-4656.

Gröger H. Enzymatic routes to enantiomerically pure aromatic α-hydroxy carboxylic acids: a further example for the diversity of biocatalysis. (2001). Adv Synth Catal. **343**: 547–558.

He. Y. C., Xu, J. H., Xu, Y., Ouyang, L. M and Pan, J. Biocatalytic synthesis of (*R*)-(-)-mandelic acid from racemic mandelonitrile by a newly isolated nitrilase-producer *Alcaligenes* sp. ECU0401. (2007). Chin. Cheml Lett. **18**: 677-680.

Holton, R. A., Kim, H-B., Somoza, C., Liang, F., Biediger, R. J., Boatman, P. D., Shindo, C. C. Smith., Kim, S., Nadizadeh, H., Suzuki, Y., Tao, C., Vu, P., Tang, S., Zhang, P., Murthi, K. K., Gentile, L. N. and Liu, J. H. First total synthesis of Taxol. 2. Completion of the C and D rings. (1994). J. Am. Chem. Soc. **116**: 1599-1600.

Hsiao Y., Rivera, N. R., Rosner, T., Krska, S. W., Njolito, E., Wang, F., Sun, Y., Armstrong, J. D., Grabowski, E. J. J., Tillyer, R. D., Spindler, F. and Malan, C. (2004). J. Am. Chem. Soc. **126**: 9918-9919.

Hudlicky, T., Frey, D. A., Koroniak, L., Claeboe, C. D., and Brammer Jr, L. E. Towards a 'reagent-free' synthesis. Tandem enzymatic and electrochemical methods for increased mass yield. (1999). Green Chem. **1:** 57-59.

Kamal, A., Khanna, G. B. R., Krishnaji, T., Tekumalla, V. and Ramu, R. New chemoenzymatic pathway for β-adrenergic blcking agents. (2005). Tetrahedron Assymmetry. **16**: 1485-1494.

Kamal, A., Kumar, M. S., Kumar, C. G., Shailk, T. B. Bioconversion of acrylonitrile to acrylic acid by *Rhodococcus ruber* strain AKSH-84. (2011). J. Microbiol. Biochem. **21:** 37-42.

Kaplan, O., Nikolaou, K., Pišvejcová, A. and Martinkova, L. Hydrolysis of nitriles and amides by filamentous fungi. (2006). Enzyme Microb. Technol. **38**: 260-264.

Kaul, P., Banerjee, A., Mayilraj, S. and Banerjee. U. C. Screening for enantioselective nitrilases: kinetic resolution of racemic mandelonitrile to (*R*)-(-)-mandelic acid by new bacterial isolates. (2004). Tetrahedron: Assymmetry. **15**: 207-211.

Khairy, H., Meinert, C., Wübbeler, J. H., Poehlein, A., Daniel, R., Voigt, B., Riedel, K. and Steinbüchel, A. Genome and proteome analysis of *Rhodococcus erythropolis* MI2: Elucidation of the 4,4'- dithiodibutyric acid catabolism. (2016). PLoS ONE. . **11**: e0167539. Doi:10.1371/ journal.pone.0167539.

Kinfe, H. H., Chhiba, V., Bode, M. L., Mathiba, K., Steenkamp, P. A. and Brady, D. Enantioselective hydrolysis of β- hydroxy nitriles using whole cell biocatalyst *Rhodococcus rhodochrous* ATCC BAA-870. (2009). J. Mol. Catal. B-Enzym. **59**: 231-236.

Kobayashi, M., Nagasawa, T. and Yamada, H. Enzymatic synthesis of acrylamide: a success story not yet over. (1992). Trends Biotechnol. **10**: 402-408.

Letek, M., González, P., MacArthur, I., Rodríguez, H., Freeman, T. C., Valero-Rello, A., Blanco, M., Buckley, A., Cherevach, I., Fahey, R., Hapeshi, A., Holdstock, J. Leadon, D., Navas, J., Ocampo, A., Quail, M. A., Sanders, M., Scortti, M. M., Prescott, J. F., Fogarty, U., Meijer, W. M., Parkhill, J., Bentley, S. D., and Vázquez-Boland, J. A. The genome of a pathogenic *Rhodococcus*: Cooptive virulence underpinned by key gene acquisitions. (2010). PLOS Genetics. **6**: 1-17.

Lieljeblad, A. and Kanerva, L. T. Biocatalysis as a profound tool in the preparation of highly enantiopure β-amino acids. (1999). Tetrahedron. **62**: 5831-5854.

Mathew C. D., Nagasawa, T., Kobayashi, M., and Yamada, H. Nitrilase-catalyzed production of nicotinic acid from 3-cyanopyridine in *Rhodococcus rhodochrous* J1. (1988). Appl. Environ. Microbiol. **54:** 1030-1032.

McLeod, M. P., Warren, R. L., Hsiao, W. W., Araki, N., Myhre, M., Fernandes, C., Miyazawa, D., Lillquist, A. L., Wang, D., Dosanjh, M., Hara, H., Petrescu, A., Morin, R. D., Yang, G., Stott, J. M., Schein, J. E., Shin, H., Smailus, D., Siddiqui, A. S., Marra, M. A., Jones, S. J., Holt, R., Brinkman, F. S., Miyauchi, K., Fukuda, M., Davies, J. E., Mohn, W. W., and Eltis, L. D. The complete genome of *Rhodococcus* sp. RHA1 provides insight into a catabolic powerhouse. (2006). Proc. Natl. Acad. Sci. USA. **103**: 15582-15587.

Pathak, A., Chauhan, A., Blom, J., Indest, K. J., Jung, C. M., Stothard, P., Green, S. J. and Ogram, A. Comparative genomics and metabolic analysis reveals peculiar characteristics of *Rhodococococcus opacus* strain M213 particularly for naphthalene degradation. (2016). PLos One. **11**: e0161032.

Qu, J., Miao, L-L., Liu, Y. and Liu. Z-P Complete genome sequence of *Rhodococcus* sp. strain IcdP1 shows catabolic potential. (2015). Genome. A. .**3**: e00711-15.

Seebach, D. and Hungerbuhler, E. Synthesis of enanatiomerically pure compounds (EPC-Synthesis), (1980). Modern Synthetic Methods, Scheffold, R., ED., p 97, Salle and Sauerlander, Frankfurt.

Sekine, M., Tanikawa, S., Omata, S., Saito, M., Fujisawa, T., Tsukatani, N., Tajima, T., Sekiqawa, T., Kosugi, H., Matsuo, Y., Nishiko, R., Imamura, K., Ito, M., Narita, H., Taqo, S., Fujita, N., and S. Harayama. Sequence analysis of the three plasmid harboured in *Rhodococcus erythropolis* strain PR4. (2006). Environ. Microbiol. **8**: 334-346.

R. A. Sheldon. Atom efficiency and catalysis in organic synthesis. (2000). Pure Appl. Chem. **72**: 1233-1246.

R. A. Sheldon. The E factor: fifteen years on. (2007). Green Chem. **9**: 1273-1283.

R. A. Sheldon. E factors, green chemistry and catalysis: An odyssey. (2008). Chem. Commun. 3352-3365.

Shen, M., Zheng, Y. G., Liu, Z. Q. and Shen, Y. C. Production of acrylic acid from acrylonitrile by immobilization of *Arthrobacter nitroguajacolicus* ZJUTB06-99. (2009). J. Microbiol. Biotechnol. **19**: 582-587.

Steinhuebel D., Sun, Y., Matsumura, K., Sayo, N. and Saito, T. Direct asymmetric reductive amination. (2009). J. Am. Chem. Soc. **131**: 11316-11317.

Trost, B. M. The atom economy- a search for synthetic efficiency. (1991). Science. **254**: 1471-1477.

Vaughan, P. A., Knowles, C. J. and Cheetham, P. S. J. Conversion of 3-cyanopyridine to nicotinic acid by *Nocardia rhodochrous* LL100-21. (1989). Enzyme and Microbial Technology. **11**: 815-823.

Warhurst, A. M. and Fewson, C. A. Biotransformations catalysed by the genus *Rhodococcus*. (1994). Crit. Rev. Biotechnol. **14**: 29-73.

Wolin R. L., Santillán, Jr., Barclay, T., Tang, L., Venkatesan, H., Wilson, S., Lee, D. H. and Lovenberg, T. W. Novel glycine transporter type-2 reuptake inhibitors. Part 2: β- and γ amino acid derivatives. (2004). Bioorg. Med. Chem. **12**: 4493-4509.

Qu, J., Miao, L-L., Liu, Y. and Liu, Z-P. Complete genome sequence of *Rhodococcus* sp. strain IcdP1 shows diverse catabolic potential. (2015). Genome announcements. **3**: e00711-00715.

Xu, F., Zacuto, M., Yoshikawa, N., Desmond, R., Hoerner, S., Ioth, T., Journet, M., Humphrey, G. R., Cowden, C., Strotman, N. and Devine, P. Asymmetric synthesis of telcagepant, a CGRP receptor antagonist for the treatment of migraine. (2010). J. Org. Chem. **75**: 7829-7841.

Xue Y-P., Xu, S-Z., Liu, Z-Q. and Zheng, Y-G. Enantioselective biocatalytic hydrolysis of (*R,S*)-mandelonitrile for production of (*R*)-(-)-mandelic acid by a newly isolated mutant strain. (2011). J. Ind. Microbiol. Biotechnol. **38**: 337-345.

Yamada, H and Kobayashi, M. Nitrile hydratase and its application to industrial production of acrylamide. (1996). Biosci. Biotechnol. Biochem. **60**: 1391-1400.

Yamamoto, K. Z., Oishi, K., Fujimashu, I. and Komatsu, K. Production of R-(-)-mandelic acid from mandelonitrile by *Alcaligenes faecalis* ATCC 8750. (1991). Appl. Environ. Microbiol. **57** ; 3028-3032.

Zhang, Z-J., Xu. J-H., He, Y-C., Ouyang, L-M., Liu, Y-Y. and Imanaka, T. Efficient production of (R)-(-) mandelic acid with highly substarte/product tolerant and enantioselective nitrilase of recombinant *Alcaligenes* sp. (2010). Process Biochem. **45**: 887-891.

Zhu, Y., Wu, G., Zhu, X., Ma, Y., Zhao, X., Li, Y., Yuan, Y., Yang, J., Yu, S., Shao, F. and Lei, M. Design, synthesis, biological evaluation, and structure activity relationship (SAR) discussion of dipeptidyl boronate proteasome inhibitors, part II: comprehensive understanding of the SAR of β-amino acid composed of dipeptidyl boronic acids and molecular modelling. (2010). J. Med. Chem, **53**: 8619-8626.

Websites:

Acrylamide Market Research Report 2014-QY Research Reports, accessed 20th October 2017,

http://www.qyresearchreports.net/market-research-report/acrylamide-market-research-reprort-2014-2

J. Elkington, http://www.sustainability .co.uk/sustainability.html

Energetics, Inc. Industrial bioproducts: Today and tomorrow. U. S. Department of Energy, Office of energy efficiency and renewable energy, Office of the biomass program, Washington, D. C. 2003.

Chapter Two: Nitrile Transforming Enzymes. A Literature Review

2.1 Nitrile Biocatalysis

Pre-biotic life is postulated to have commenced with hydrogen cyanide playing a central role in this process (Matthews. 2006). Hydrogen cyanide polymerization is believed to have occurred when cyanide reacted with water, oxygen, and natural salts resulting in the formation of amino acids and nucleic acid precursor molecules. Oro *et al.* (1980) demonstrated in some pioneering experiments that α-amino acids and adenine could be synthesized in an ammonium hydroxide solution. This provided a possible avenue for the emergence of life on our planet.

Nitriles are also produced in nature with more than 2000 plant species produce cyanide during metabolism. Many exist as organic cyanide and nitrile compounds (R-CN) or as inorganic cyanide molecules (HCN).

Naturally produced nitriles are divided into three distinct compound groupings based on their structure: i) Cyanogenic glycosides- the largest group of nitrile containing compounds in nature and are subdivided based on their individual a-glycon moeities as well as their origin of production; ii) Cyanolipids- esters of α-hydroxylated nitrile molecules; and iii) Glucosinolates- produced as a result of phytopathogen resistance.

Many organic nitriles exist as cyanogenic glycosides and have been identified in both terrestrial and marine environments. Here they function as an immediate defence response with the liberation of HCN deterring predation by herbivores. Nitrile compounds in these organisms can also function as nitrogen transportation vehicles, facilitating nitrile catabolism to generate both nitrogen and glucose that feed directly into primary metabolic processes.

Plants such as *Arabidopsis thaliana* produce auxins such as indole-3-acetic acid from the nitrile indole-3-acetonitrile, and cyanolipids that regulate cell growth cycles (Bartling *et al.* 1992).

Lastly, cyanate compounds also occur naturally in nature as a result of urea dissociation and photo-oxidation of cyanide (Hagel *et al.* 1971). They can also be the result of non-enzymatic decomposition of carbomyl phosphate molecules.

The major source of anthropogenic environmental cyanide discharge comes from the petrochemical refining industry; the synthesis of organic chemicals and plastics; during electroplating processes; from gas manufacturing industries; in metal mining and processing industries; and from work done in the aluminium processing sector. The annual release of cyanide into the environment from these industries is believed to be >14 million kg per year.

There is no global accumulation of nitriles, which indicates that there is a natural mechanism for their conversion, and indeed a number of enzymes have been found in nature that is responsible for this.

2.2 Enzymes Involved in Nitrile Conversion

Nitrile catalysis in most organsims proceeds via an enzymatic hydrolysis reaction with the nitrile substrate being converted to the corresponding amide or acid product. This can occur through the action of a nitrilase mediated enzyme which produces an organic acid as a product; or by nitrile hydratase catalysis which generates an amide product with the concomitant production of ammonia (Fig. 2.1).

Inorganic nitriles on the other hand undergo catalytic conversion through the action of other enzymes such as cyanide hydratase, cyanide dihydratase as well as cyanase. Each of these enzymes generates different product streams, with fomamide being produced in the case of cyanide hydratase (Wang *et al.* 1992). Formic acid and ammonium cyanide are produced using cyanide dehydratase (Ingvorsen *et al.* 1991) while carbon dioxide and ammonia is generated by cyanase enzymes (Dorr and Knowles. 1989).

Nitrogenase enzymes produced by a variety of nitrogen-fixing microbes are also capable of reducing nitrile compounds to produce the corresponding hydrocarbon and ammonia as a reaction by-product (Liu *et al.* 1997).

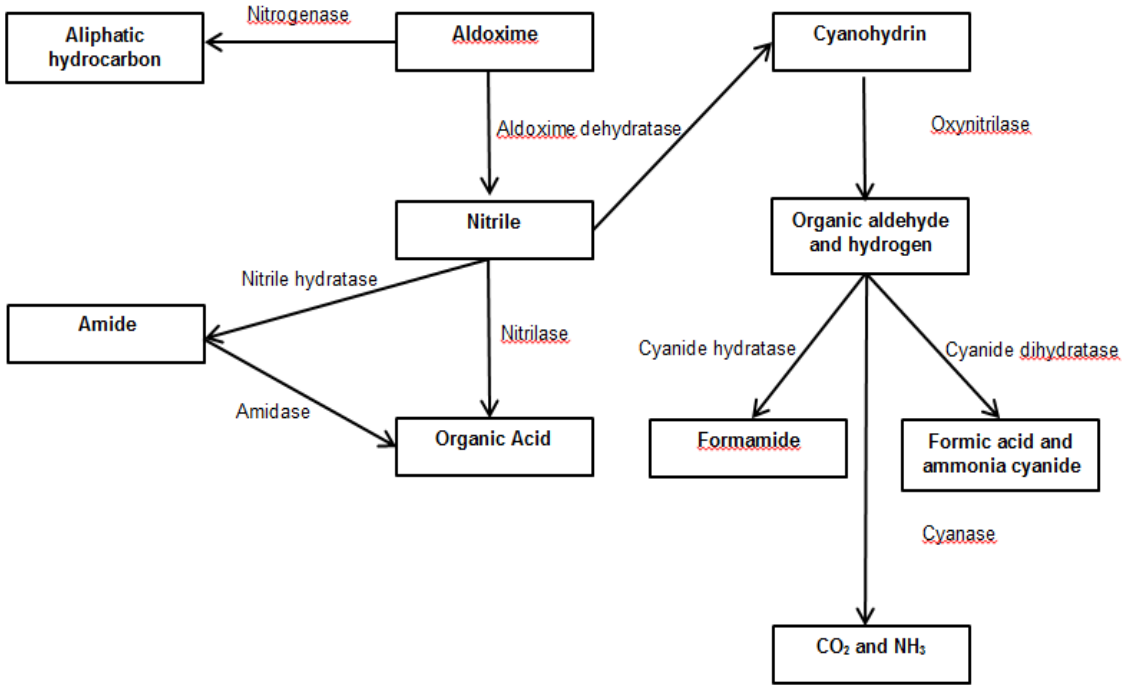


Figure 2.1: Nitrile metabolic pathways in nature (adapted from Banerjee *et al*. 2002).

2.2.1 Aldoxime Dehydratase (EC 4.99.1.5)

Aldoxime dehydratase (ADH) enzymes are non-hydrolytic, heme-containing lyases that catalyse the dehydration of aldoximes to generate nitrile molecules (Fig. 2.2). ADH activity is dependent on the oxidative state of the heme Fe^{2+} ion, with no activity observed when the ferric enzyme contained a Fe^{3+} ion instead.

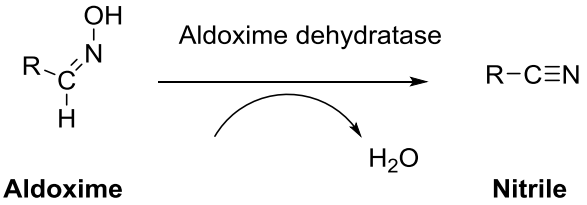


Figure 2.2: Schematic diagram showing the mechanism of action of aldoxime dehydratase enzymes.

Aldoxime compounds are often intermediates in the synthesis of various biologically active compounds. These include compounds produced in plant cells that involve the action of specific cytochrome P450 molecules responsible for the conversion of amino acids to glucosinolate and phytohormone intermediates.

The ability to degrade aldoximes is widespread amongst both $Gram^+$ and $Gram^-$ bacteria and fungi, although activity in yeasts is rare. Kato *et al.* (2000) screened 333 different yeast genera and identified 2 species, *Candida methanolica* TPU 1217 and *Pichia miso* TPU 1306, that demonstrated aldoxime dehydratase activity,

Aldoximes in various bacterial and fungal organisms are converted by heme-containing ADH enzymes that generate nitrile products which are then hydrolyzed by nitrilase, nitrile hydratase as well as amidase enzymes. These nitriles are then converted to their corresponding acid or amide products. Cells cultured in the absence of aldoximes lacked ADH activity suggesting that the enzyme is inducible.

Genetic organizations of aldoxime dehydratase and nitrile converting genes are physically linked with both being located on the same chromosome. This has been confirmed in a *Bacillus* species; a pseudomonad species; in *Rhodocccus*, *Acinetobacter* as well as *Pseudomonas* strains (Kato and Asano, 2006; Kato *et al.* 2004). The close proximity of these genes may be the result of common evolutionary development, enabling genetic inheritances as a unit.

Spectroscopic evaluation of ADH enzymes indicates that a change in the coordination mode of the substrate plays a crucial role in the regulation of the enzyme activity. The oxygen atom of the aldoxime is coordinated to the ferric heme while the nitrogen atom is coordinated to the ferrous heme (Kobayashi *et al.* 2005). Dehydration of the substrate can then proceed but only via an *N*-coordinated substrate, with general acid-base catalysis reaction noted where the histidine functions as a catalytic residue in the distal heme-pocket (Sawai *et al.* 2009).

Crystal structure studies have indicated that the hydrogen bonding between the OH of the aldoxime and the side chains of Ser-219 and His-320 control orientation of the substrate and allow for the elimination of the OH group creating a prefixed site for substrate recognition and binding (Fig. 2.3). Mutagenesis studies have also confirmed the crucial role of Glu143, Arg 178, Ser 219 and His 320 amino acid residues, since alterations here resulted in a 60-90% loss in enzyme activity (Sawai *et al.* 2009).

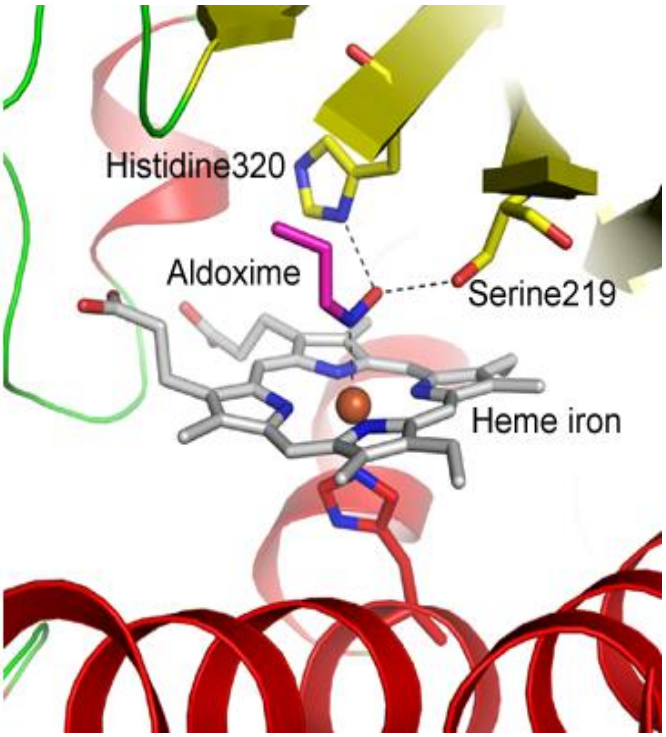


Figure 2.3: ADH substrate binding site with amino acid interaction in the catalytic site by Ser219 and His320.

http://www.spring8.or.jp/en/news_publications/press_release/2009/091109/

The aldoxime substrate is not only bound to the heme iron but also fixed by hydrogen bonds to a serine and histidine residues (219^{th} and 320^{th} residue from the amino terminal of the protein).

ADH enzymes are specifically useful in the environmentally benign synthesis of various nitrile molecules (Sawai *et al.* 2009), with enzyme classification based on substrate preference (some prefering aliphatic while others prefer aromatic-aldoxime substrate molecules). The triple pathway towards generating carboxylic acids from aldoximes via the nitrile is still not employed in any industrial processes due to the inherent stability problems observed in ADH enzyme systems.

2.2.2 Nitrogenase (EC 1.18.6.1)

Nitrogenase enzymes belong to the group of oxido-reductases which catalyse the reduction of nitriles and other molecular nitrogen compounds. These reactions produce ammonia in an ATP driven biocatalytic process (Fig. 2.4).

HCN serves as a substrate for many nitrogenase enzymes and is reduced to methane, ammonia, and methylamine (Fischer *et al.* 2000; Hardy and Knight, 1967; Li *et al.* 1982; Riviera-Ortiz and Burris, 1975). The nitrogenase enzyme produced by *Klebsiella oxytoca* shows parallel accumulation of ammonia from cyanide, indicating that ammonia production could act as an alternate nitrogen source for growth (Kao *et al.* 2003).

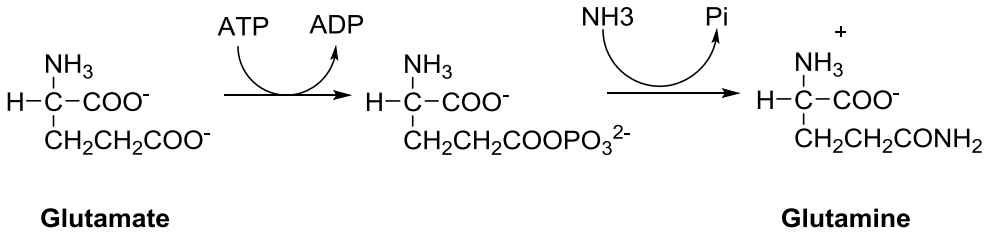


Figure 2.4: Schematic diagram showing the mechanism of action of nitrogenase enzymes.

2.2.3 Oxynitrilase (EC 4.1.2.10)

Most oxynitrilases are flavoprotein enzymes that catalyse reversible condensation of hydrogen cyanide with aldehydes, to produce optically active cyanohydrins (Fig. 2.5). This reaction proceeds through an ordered Uni Bi mechanism.

Oxynitrilases demonstrate several characteristics noted in flavoprotein oxidase enzymes, even though the reactions they catalyse do not involve a net oxidation-reduction process (Massey *et al.* 1966). They appear to resemble reactions that are catalysed by two other flavoproteins, namely *N*-methylglutamate synthetase and glyoxylate carboligase. In the case of *N*-methylglutamate synthetase, the substrate activation occurs via a cyclic oxidation-reduction sequence in which the flavin functions as a typical oxidation-reduction catalyst (Pollock and Hersh, 1973). Another mechanism seems unlikely, although alternate theories suggest that the flavin moiety may participate directly in the catalysis. Charge-transfer interactions between the electron-deficient flavin and the aldehyde substrate could result in the nucleophilic addition of the cyanide moiety.

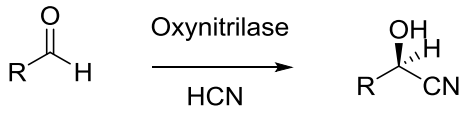


Figure 2.5: Schematic diagram showing the mechanism of action of oxynitrilase enzymes

In terms of their commercial significance, oxynitrilase enzymes are used in the preparation of α-hydroxyketones, α-hydroxyacids, β-amino alcohols as well as amino nitriles and azaridine molecules (Effenberger 1996). Transcyanation using both aromatic and aliphatic aldehydes (-RCOH) has been demonstrated with consistent enantioselectivities for a broad range of aliphatic substrates being noted.

2.2.4 Cyanase (EC 4.3.99.1)

Cyanase enzymes belong to the lyase class of enzymes and are responsible for hydrolysing cyanate in bacteria and plants. This is achieved by catalysing the reaction of cyanate with bicarbonate to generate ammonia and carbon dioxide as products.

$$NCO^- + 3H^+ + HCO_{3-} \longrightarrow NH_4^+ + 2CO_2$$

The *E.coli* cyanase enzyme shows that the catalytic mechanism involves a nucleophilic attack of bicarbonate on cyanate, which produces an anhydride, transition-state intermediate which decarboxylates to produce CO_2 and carbamate (Johnson and Anderson, 1987). The resulting carbamate then undergoes decarboxylation to generate a second carbon dioxide and ammonia by-product.

Cyanase activity in *E. coli* is inducible with expression maintained under control of the *cyn* operon. A constitutive form of the same enzyme has however been reported in cyanobacteria such as *Synechococcus* UTEX625 (Miller and Espie, 1994) as well as *Synchocystis* PCC6803 (Harano *et al.* 1997) where its function may be related to providing CO_2 for photosynthesis.

2.2.5 Nitrilase (EC 3.5.5.1)

Nitrilases belong to the group of hydrolases (EC 3) which catalyze the hydration of nitrile compounds. Members of this family appear in plants, animals and fungi (Brenner 2002). Prokaryotae also appear to have phylogenetically related nitrilase enzymes present in them, indicating that the enzyme family may have emerged prior to separation of plants, animals and fungi into their distinctive evolutionary families (Pace and Brenner, 2001).

The larger nitrilase superfamily contains a group of closely related cyanide hydratase (CH) and cyanide dihydratase (CDH) enzymes which hydrolyze cyanide to formamide, while the later catalyzes the conversion of nitriles to generate formic acid and ammonia.

CH enzymes belong to the group of hydro-lyase enzymes first discovered in the fungal species *Stemphylium loti*, a pathogen of the cyanogen producing plant *Lotus corniculatus* (Fry and Miller, 1972). Cyanide tolerance in this species was found to be the result of enzyme induction after exposure to cyanide. This resulted in the conversion of HCN to formamide in a manner analogous to that demonstrated by nitrile hydratase enzymes (Fig. 2.6a and 2.6b),

CDH enzymes belong to the group of hydrolase enzymes which are responsible for hydrolysis of cyanide, producing formate and ammonia (Fig. 2.6a). Ingvorsen *et al.* (1991) first identified the enzyme in a strain of *Alcaligenes xylosoxidans* subsp. *denitrificans* DF3. Since then many other bacteria have been found that demonstrate the same activity including organisms such as *Bacillus pumilis* C1 (Meyers *et al.* 1993), *P. fluorescens* NCIMB 11764 (Kunz *et al.* 1994) and *P. stutzeri* AK61 (Watanabe *et al.* 1998).

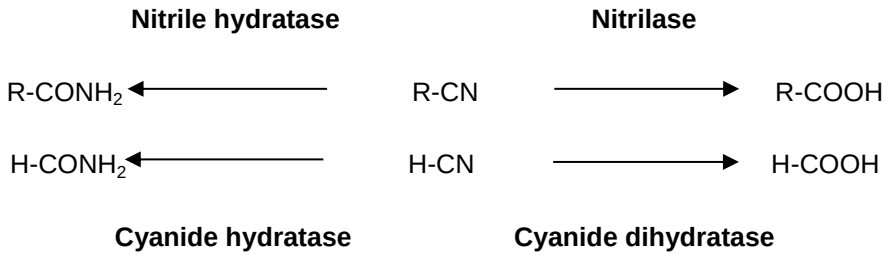


Figure 2.6a: Schematic diagram demonstrating organic versus inorganic nitrile hydrolysis using different enzymes.

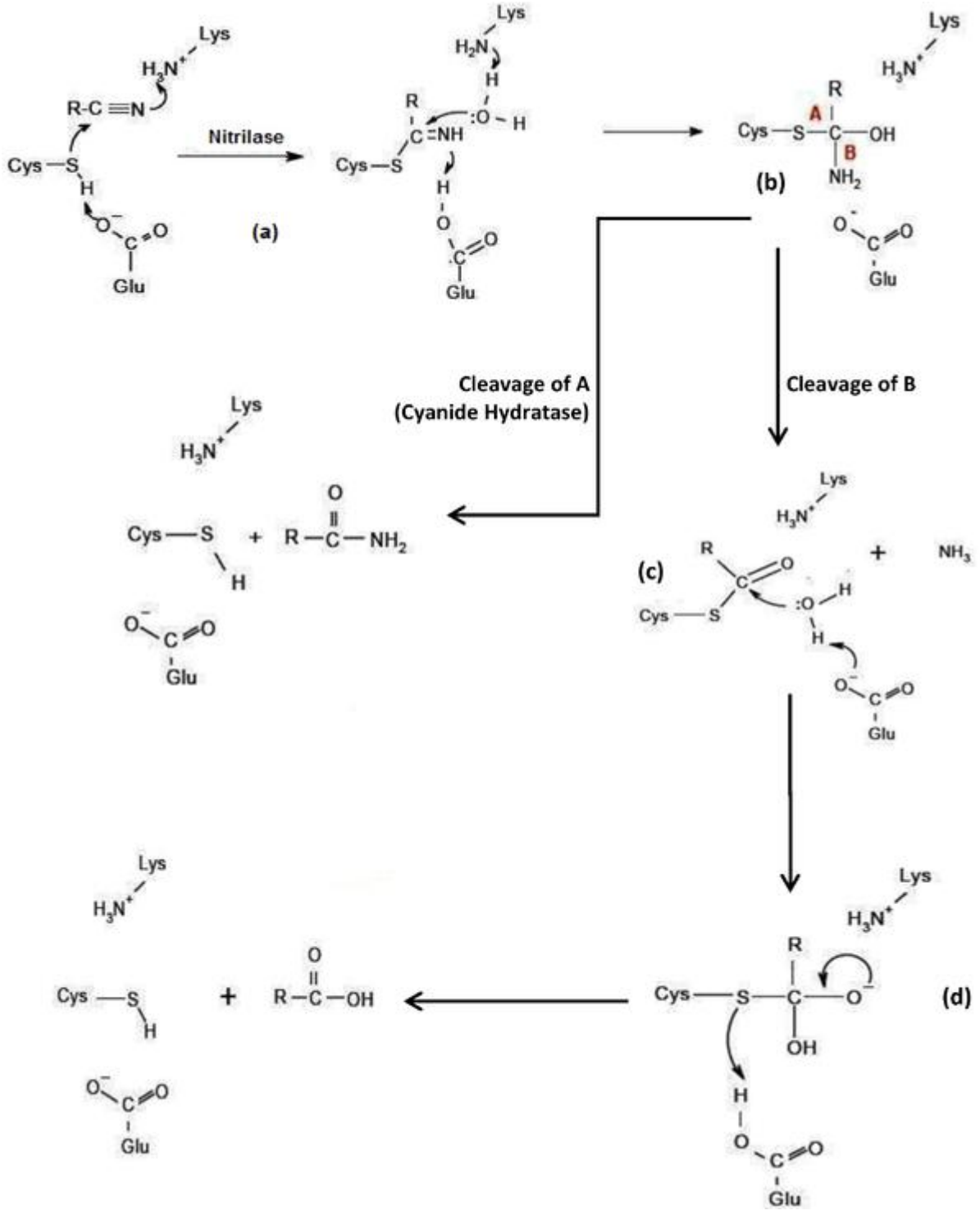


Figure 2.6b: Proposed reaction mechanism for nitrilase and cyanide hydratase enzymes (reproduced from Ramteke *et al.* 2013).

The general base amino acid glutamate undertakes a nucleophilic attack on a nitrile substrate which leads to the formation of a thioimidate intermediate. Lysine acts as the general base and activates a water molecule by increasing the nucleophilicity of the oxygen lone pair. The resulting thioimidate then undergoes hydrolysis to produce an acid product.

2.2.5.1 The Nitrilase Superfamily of Enzymes

Enzymes belonging to the nitrilase superfamily are found in both prokaryotic and eukaryotic organisms and are classified into 13 distinct branches based on their amino acid sequence data (Pace and Brenner, 2001). Enzymes in this superfamily function by hydrolyzing and condensing non-protein amide bonds.

Branch 1 enzymes (EC 3.5.5.1) include nitrilase, CH and CDH enzymes that have been isolated from plants, animals, fungi and many prokaryotes. The remaining 12 branches primarily exhibit amidase activity, with branches 2, 3, 4 and 5 showing aliphatic amidase, amino-terminal amidase, β-ureidopropionase and biotinidase activity. Branch 6 enzymes are known as carbamylase enzymes and function to decarbamylate *D*-amino acids. Branch 7 and 8 enzymes consist of prokaryotic and eukaryotic NAD synthetase enzymes that use glutamine and ammonia, to catalyze the transfer of amide *N* to a range of different substrates. Branch 9 enzymes termed *N*-acyltransferases, catalyze amide condensation reactions, while branches 11, 12 and 13 have yet to be characterised (Pace and Brenner, 2001) (Fig. 2.8).

All of these branches share a common fold with a Cys-Glu-Lys catalytic site (Brenner 2002, Novo *et al.* 2002) flanked by distinctive signature sequences which are conserved within the branch, but vary from members of other branches.

Sequence variations observed at the amino acid level result in the formation of proteins with conserved protein elements. Most maintain the distinctive αββα fold with protein dimerization noted in many together with the absence of any metal co-factors or prosthetic groups (Fig. 2.7).

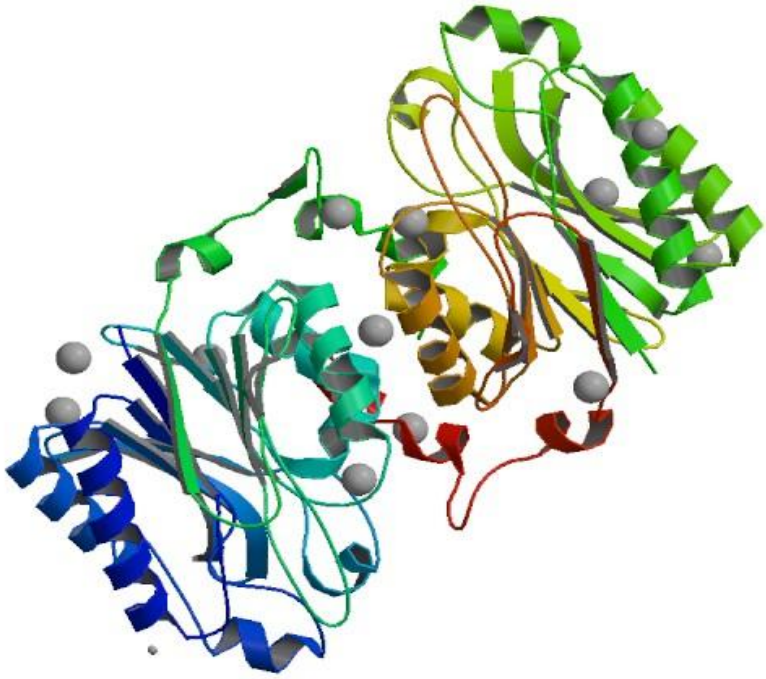


Figure 2.7: Crystal structure of a hyperthermophilic nitrilase from *Pyrococcus abyssi* – Protein Data Bank Code **3KLC**

The image above of a nitrilase homodimer was modelled on a protein sequence derived from *Pyrococcus abyssi* which was deposited by Raczynska and colleagues (Raczynska *et al.* 2010) and can be located on the PDB website - accession code **3KLC** (DOI: 10.2210/pdb3KLC/pdb).

Nitrilase enzymes play a diverse role in anabolism and catabolism, generating important hormones (such as 5-indole 3- acetic acid from 5-indole 3-acetonitrile) and signaling molecules needed by plants (Piotrowski 2008). Research by Kobayashi and his colleagues (Kobayashi *et al.*1997; 1998) have also shown the important role that this enzymes play in detoxification of small molecules.

Nitrilase enzymes typically form large aggregates of between 2- 26 subunits, with most enzymes showing substrate dependent activation. However, the presence of elevated concentrations of salt, organic solvents, temperature, pH and even enzyme concentration can result in the triggering of subunit associations resulting in subsequent activation. This is largely due to the hydrophobic effects which result in a conformational change in the protein and exposure of buried hydrophobic residues (Nagasawa *et al.* 2000).

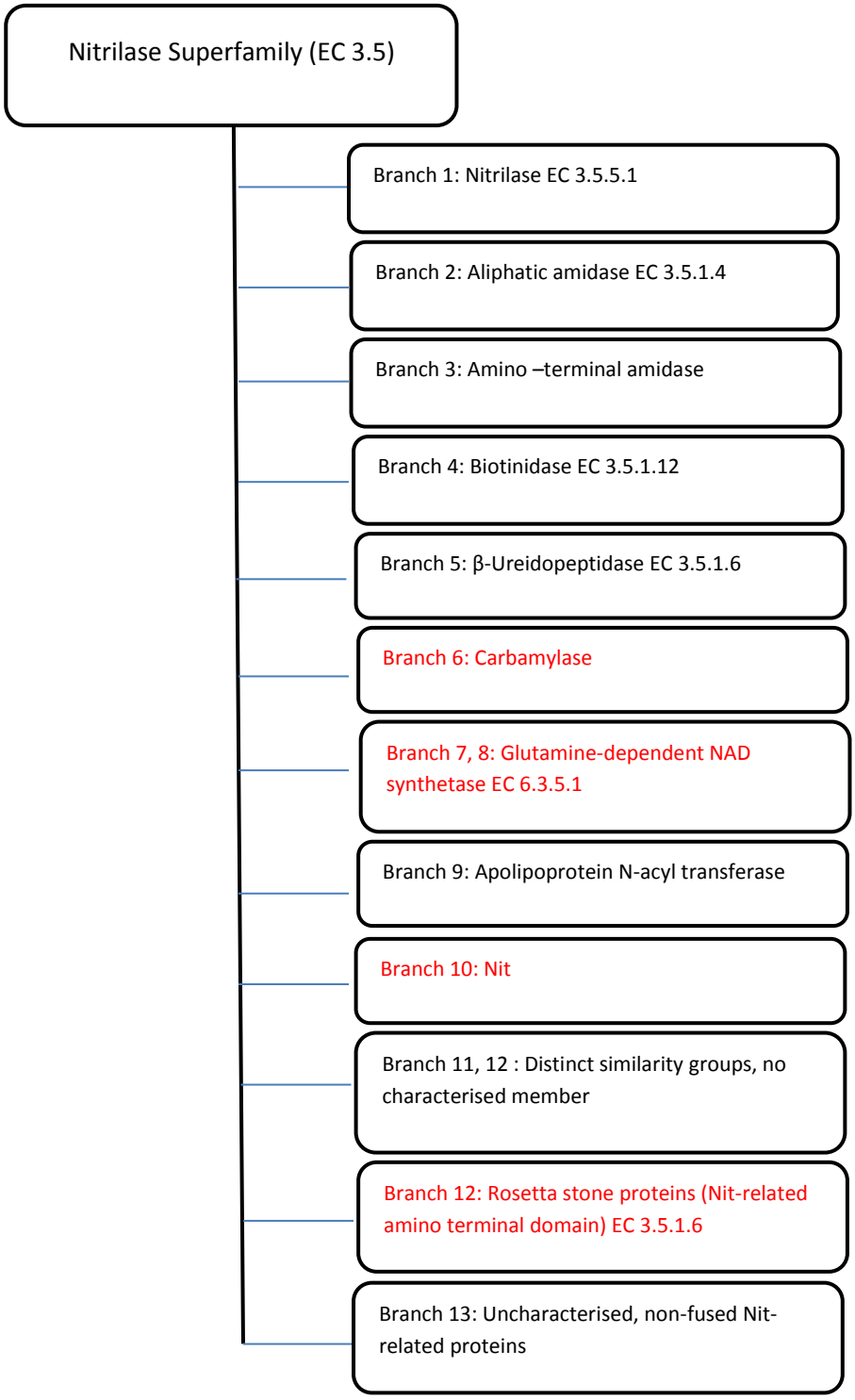


Figure 2.8: Branches of the Nitrilase superfamily (adapted from an image generated by J. Frederick, PhD Dissertation 2013).

Regions highlighted in red show family branches with protein crystal data available.

2.2.5.2 Nitrilase Mechanism of Action

Nitrilase enzymes occupy the first branch in the “Nitrilase” superfamily and catalyse the hydrolysis of nitriles to form a carboxylic acid product with the concomitant release of ammonia. The process involves a nucleophilic attack on the nitrile carbon by a sulfhydryl group on a cysteine residue which is present in the active site of the enzyme (Fig. 2.9). This results in the formation of a tetrahedral intermediate which undergoes subsequent hydrolysis to produce a thio-ester. Protonation of the nitrogen atom then results in the release of ammonia. The thio-ester intermediate is finally hydrolyzed by a water molecule with both the carboxylic acid as well as the enzyme being released (Pace and Brenner 2001; Martinkova and Kren, 2010).

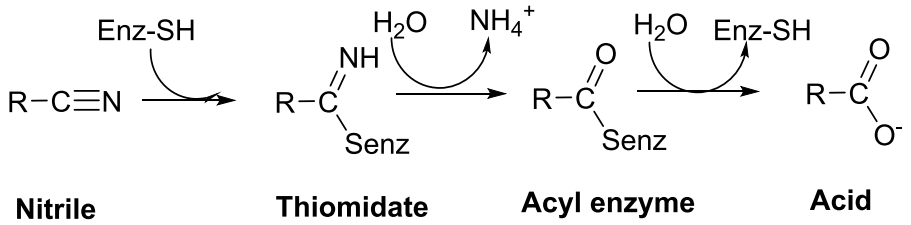


Figure 2.9: Schematic diagram showing the mechanism of action of nitrilase enzymes.

2.2.5.3 Substrate Specificity

Nitrilase enzymes have been broadly characterized into three groups based on their substrate specificity namely: aliphatic, aromatic, and arylacetonitrile nitrilases. This conventional method of classification may be irrelevant since many enzymes are capable of hydrolyzing both aliphatic and aromatic nitriles.

Aromatic nitrilases such as those produced by *R. rhodochrous* ATCC 39484, *R. rhodochrous* J1, *Nocardia* sp NCIB11215 and NCIB11216, *Fusarium solani* IMI196840, *F. oxysporum* f.sp. *Melonis* and *Bacillus pallidus* DAC521 have shown greater activity against substituted aromatic nitriles when compared to activity profiles against benzonitrile (BNZ) (Table 2.1). As a general rule most of these nitrilases prefered *meta* and *para* substitutions with little or no activity observed in the presence of *ortho*-substituted nitriles. This may be the result of steric hinderance effects.

Nitrilase enzymes produced by *Alcaligenes faecalis* Strain JM3 and ATCC 8750, as well *as P. fluorescens* DSM 7155 are all arylacetonitrilases. The relative activity levels of these enzymes vary considerably with JM3 showing highest activity with acrylonitrile, *m*-chlorobenzylcyanide, 2-thiophenacetonitrile, 3-pyridineacetonitrile and 2-phenoxypropionitriles, and showing no activity against benzonitrile (BNZ).

Table 2.1: Biological characteristics of purified nitrilases

Enzyme Substrate class	Organism	Expression	pH optimum/ Temp stability (°C)	Subunit size (kDa)	Biologically active molecular weight (kDa)	Substrate profile	Inducers	Reference
Aromatic nitrilase	*Arthrobacter* sp. Strain J1		8.5 / 45	30	30	Benzonitrile p-Tolunitrile	-	Bandyopadhyay *et al.* 1986
	Bacillus pallidus DAC 521		7.6 / 65	41	600	Benzonitrile Crotonitrile	-	Almatawah *et al.* 1999
	Fusarium solani IMI196840		7.8/-	76	620	Benzonitrile Acetonitrile 1,4-Benzodinitrile	-	Harper 1977
	Fusarium oxysporum f.sp. Melonis		6-11 / 40	37	550	Benzonitrile Acrylonitrile Crotonitrile	-	Goldlust and Bohak, 1989
	Nocardia (Rhodococcus) NCIMB 11215		7-9.5 / 30	45	560	Benzonitrile *m*-bromobenzonitrile *m*- nitrobenzonitrile	-	Harper 1985
	R. rhodochrous NCIMB 11216		8 / 30	45.8	560	Benzonitrile *m*-bromobenzonitrile	Propionitrile	Harper 1977, Hoyle *et al.* 1998 Brenner. 2002
	Rhodococcus ATCC 39484		7.5 / 40	40-40.3	560	Benzonitrile 2-furancarbonitrile	Isovaleronitrile	Stevenson *et al.* 1992 Bork and Koonin. 1994
	R. rhodochrous Strain PA-34	Inducible	7.5 / 35	45	45	Benzonitrile Acrylonitrile		Bhalla *et al.* 1992
	R. rhodochrous Strain J1	Inducible	7.6 / 45	40	410	Benzonitrile Acrylonitrile	Isovaleronitrile	Kobayashi *et al.* 1990

							Urea Cyclohexane carboxamide	Hann *et al.* 2004 Kobayashi *et al.* 1989 Nagasawa *et al.* 2000 Thuku *et al.* 2007
	Nocardia globerula NHB-2	Inducible	-		-	Aromatic and unsaturates nitriles	-	
Aliphatic nitrilase	*Acidovorax facilis* 72W		8-9 / 65	40	570	Fumaronitrile Benzonitrile	-	Gavagan *et al.* 1999 Chauhan. 2003
	Acinetobacter sp. AK226		8, 50	41, 43	580	Acrylonitrile Racemic Ibu-CN Benzonitrile	-	Yamamoto and Komatsu. 1991
	Pyrococcus abyssi	Constitutive	7.4 / 100	29.8	60	Malononitrile	-	Mueller *et al.* 2006
	Comomonas testosteroni sp.		7 / 30	-	354	Adiponitrile Benzonitrile	-	Lévy- Schil *et al.* 1998
	Pseudomonas sp. S1			41	41	Acrylonitrile Acetonitrile Benzonitrile	-	Dhillon *et al.* 1999
	R. rhodochrous K22	Inducible	5.5 / 55	41	650	Benzonitrile Acrylonitrile	Isovaleronitrile	Kobayashi *et al.* (1990, 1992) Pace and Brenner. 2001
	Synechocystis sp. Strain PCC8603		7 / 50	~40	390	Acrylonitrile Benzonitrile	-	Heinemann *et al.* 2003
Bromoxynil specific nitrilase	*Klebsiella pneumoniae* ssp. Ozaenae		9.2 / 35	74	349	Bromoxynil Benzonitrile	-	Stalker *et al.* 1988
Aryl-aceto nitrilase	*Alcaligenes faecalis* ATCC 8750		7.5 / 45	32	460	Mandelonitrile p-aminobenzyl cyanide Benzonitrile	-	Yamamoto *et al.* 1992

	Alcaligenes faecalis JM3		7.5/ 45	44	260	Mandelonitrile p-aminobenzyl cyanide 2-thiopenacetonitrile	Isovaleronitrile	Nagasawa *et al.* 1990 Meyers *et al.* 1993 Kobayashi *et al*. 1993
	Arabidopsis thaliana		9/ 35	38	450	3-phenylpropionitrile Benzonitrile	-	Osswald *et al.* 2002
	Pseudomonas fluorescens DSM7155		38, 40	130	-	Phenylacetonitrile 2-(Methoxy)-mandelonitrile	-	Layh *et al.* 1998
	Pseudomonas fluorescens EBC191		6.5/ 50	37.7	-	2-phenylvaleronitrile Benzonitrile	=	Kiziak *et al.* 2005

Finally, a number of nitrilases showing increasing activity against aliphatic nitriles were identified in *R. rhodochrous* K22, *Comamonas testosteroni* and *Arabidopsis thaliana*. The enzyme produced *by R. rhodochrous* K22 is the best characterised of these enzymes with maximum activity observed in the presence of unsaturated aliphatic nitrile acrylonitrile.

2.2.5.4 Nitrilase Activity Towards Amides

Studies done on the nitrilase produced by *R. rhodochrous* Strain J1 showed that the enzyme hydrolysed benzamide and BNZ with a K_m of 2.94 mM and 2.10 mM, respectively (Kobayashi *et al.* 1998). The similarities in the K_m values were not mirrored in the enzymes V_{max} values, with benzamide reactions showing a 6 fold lowered V_{max} value. The change in the V_{max} was attributed to nitrilase inhibition by benzamide which was found to function in a reversible, competitive manner. A common intermediate was proposed in the conversion of both nitrile and amide substrates (Fig. 2.10).

Mutational studies resulting in the replacement of the Cys165 residue showed that the observed amidase activity was lost, highlighting the importance of the Cys165 residue (Kobayashi *et al.* 1998).

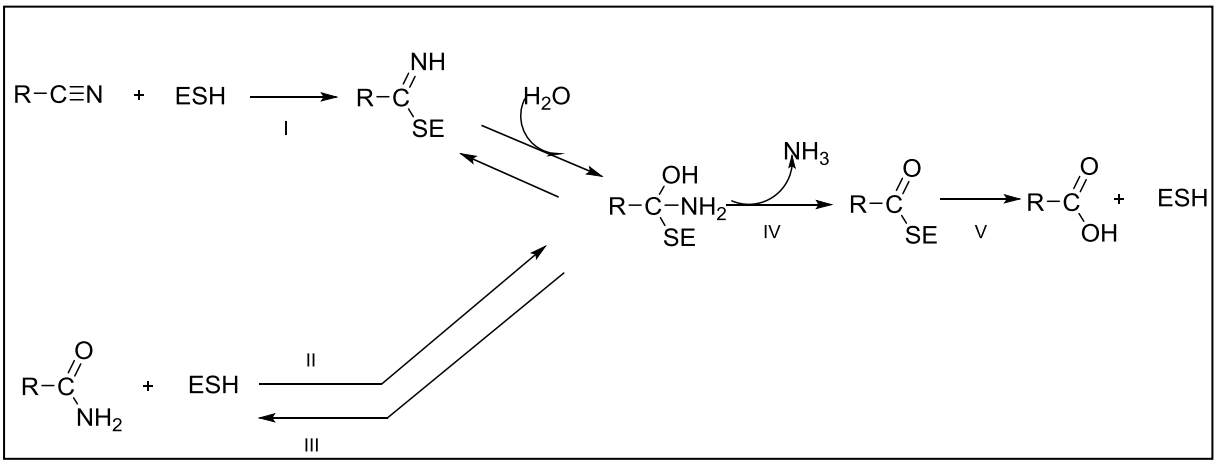


Figure 2.10: Schematic diagram showing the proposed nitrilase catalytic mechanism for hydrolysing BNZ and benzamide (after Kobayashi *et al.* 1998)

i-Nucleophilic attack in CN carbon by sulfhydryl group of the nitrilase enzyme resulting in the formation of a tetrahedral intermediate; **ii** and **iii**- proposed amidase activity ; **iv**- Ammonia is removed from the tetrahedral intermediate to yield formation of an acyl-enzyme intermediate; **v**- Hydrolysis of the intermediate from step ivresulting in the formation of an acid product.

2.2.5.5 Nitrilase Can Act as a Nitrile Hydratase

Fernandes *et al.* (2006) demonstrated that appreciable amounts of the amide intermediate could be formed in reactions using an arylacetonitrilase nitrilase produced by *Pseudomonas fluorescens* EBC

191. The amount of amide produced was found to be influenced by the nature of the α-substituent on the substrate molecule, and the reaction conditions used.

Characterization work on a recombinantly expressed nitrilase from *Arabidopsis thaliana* (AtNIT4) showed that >60% amide was produced in reactions using 3-cyano-L-alanine (Piotrowski *et al.* 2001) while a recombinant nitrilase isolated from *A. thaliana* (AtNIT1) showed that the electron-withdrawing group on the α-substituent played a crucial role in amide formation (Effenberger and Osswald. 2002). In this particular case the hydrolysis of 2-crotonitrile resulted in the formation of 99% crotonic acid, while reactions run in the presence of an electron-deficient substrate such as 3-nitroacrylonitrile, resulted in 95% amide formation (Fig. 2.11).

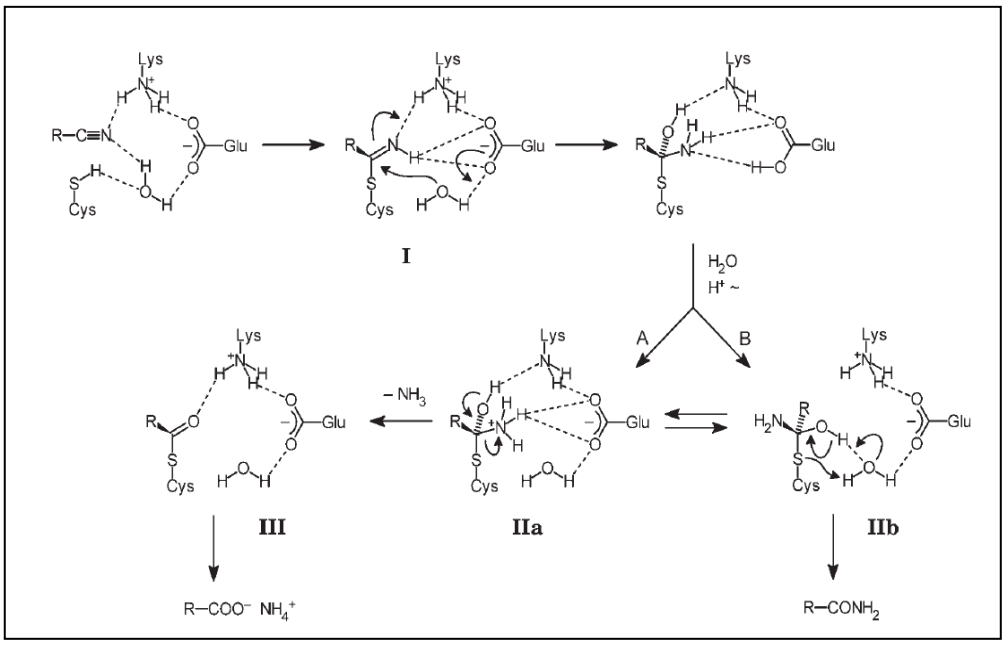


Figure 2.11: Proposed nitrilase mechanism generating both acid (A) and amide (B) products (image reproduced from Fernandes *et al.* 2006).

2.2.5.6 Nitrilase Enzyme Dimerization and 3-D Protein Modelling

Most nitrilase enzymes exist as inactive dimers which undergo substrate activation to generate larger active oligomers. Nagasawa *et al.* (2000), and Stevenson *et al*. (1992) demonstrated this phenomenon in *R. rhodochrous* J1, and *Rhodococus* ATCC 39484. However, exceptions to this rule include the nitrilase enzymes produced by *R. rhodochrous* PA-34 and *Arthrobacte*r sp. J1, which exist as monomers (Bhalla *et al.* 1992), and the dimeric and trimeric enzymes produced by *Pseudomonas fluorescens* DSM 7155 (Layh *et al.* 1998), and *Klebsiella pneumoniae* ssp. *Ozanenae* (Stalker *et al.* 1998) (Table 2.1).

The lack of crystal protein structure data for branch 1 nitrilase enzymes means that most tertiary structure predictions are based on data obtained from comparative models created using related crystal structure data. These studies are necessary since tertiary structure determination is crucial for identifying proposed catalytic residues, thus enabling observation of the substrate binding pocket and any related amino acid residues.

In an attempt to generate a protein structure model for the nitrilase produced by *R. rhodochrous* J1, target-template sequence alignment studies was undertaken by Ndorio Thuku (unpublished data, MSc dissertation 2006.) A 3-D homology model of *the R. rhodochrous* Strain J1 nitrilase enzyme was created using protein cystal structure data available for **1ERZ** (*N*-carbamyl-D-amino acid amidohydrolase from *Agrobacterium* sp KNK712); **1EMS** (Nit domain of Nit Fhit from *C. elegans*); **1F89** (Yeast Nit 3 protein); and **1J31** (Ph 0642 from *P. horikoshii*), (Fig. 2.12).

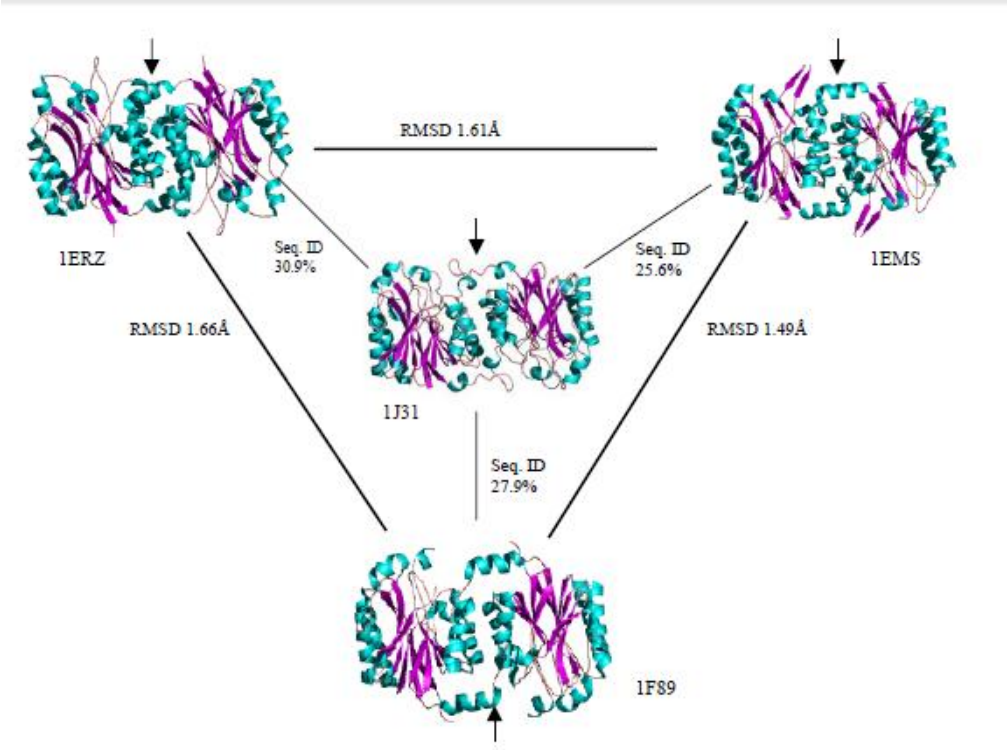


Figure 2.12: Dimeric structures of 1ERZ, 1EMS, 1F89 and 1J31 showing the signature αββα-αββα fold (Thuku -unpublished data, MSc dissertation 2006).

The modelled nitrilase from *R. rhodochrous* J1 was 366 amino acids in length and demonstrated a αββα- αββα sandwich fold. Three long insertions were located on the protein, between residues 54-73; 193-202 and; 234-249 (Thuku, unpublished data, MSc dissertation). One of these long insertions, 54-73 was found to extend the NH_3 terminal of the α-helix. A second insertion at residues 234-249 resulted in the formation of an extended loop of 14 residues between two β-sheets and was predicted to play a role in symmetric interaction between dimer subunits at the "C" surface (Jandhyala *et al.* 2003; Sewell *et al.* 2003; Sewell *et al.* 2005). Loops created by amino acid residues 234-249 and 193-

202 were found above the active site and were suggested to play a role in the oligomerization of the enzyme, restricting substrate access into the active site (see Fig. 2.13a for the full amino acid sequence of the nitrilase enzyme, and Fig. 2.13b for the molecular representation of the enzyme).

A number of hydrophobic amino acids located in the enzymes active site were found to control substrate accomodation by limiting substrate acceptance thus playing a determinant role in the enzyme's selectivity profile.

```
    10         20         30         40         50
MVEYTNTFKV AAVQAQPVWF DAAKTVDKTV SIIAEAARNG CELVAFPEVF
        60         70         80         90        100
IPGYPYHIWV DSPLAGMAKF AVRYHENSLT MDSPHVQRLL DAARDHNIAV
       110        120        130        140        150
VVGISERDGG SLYMTQLVID ADGQLVARRR KLKPTHVERS VYGEGNGSDI
       160        170        180        190        200
SVYDMPFARL GALNCWEHFQ TLTKYAMYSM HEQVHVASWP GMSLYQPEVP
       210        220        230        240        250
AFGVDAQLTA TRMYALEGQT FVVCTTQVVT PEAHEFFCDN DEQRKLIGRG
       260        270        280        290        300
GGFARIIGPD GRDLATPLAE DEEGILYADI DLSAITLAKQ AADPVGHYSR
       310        320        330        340        350
PDVLSLNFNQ RHTTPVNTAI STIHATHTLV PQSGALDGVR ELNGADEQRA
                                360
                  LPSTHSDETD RATASI
```

Figure 2.13a: UNIProt-Q03217 protein sequence (*R. rhodochrous* aliphatic nitrilase).

Amino acid residues highighted in blue extend the NH_2 terminal of the α-helix; residues highlighted in green are found between the dimer interface at the "C" surface; residues highlighted in red are found above the enzymes active site; while those in yellow highlight crucial catalytic residues.

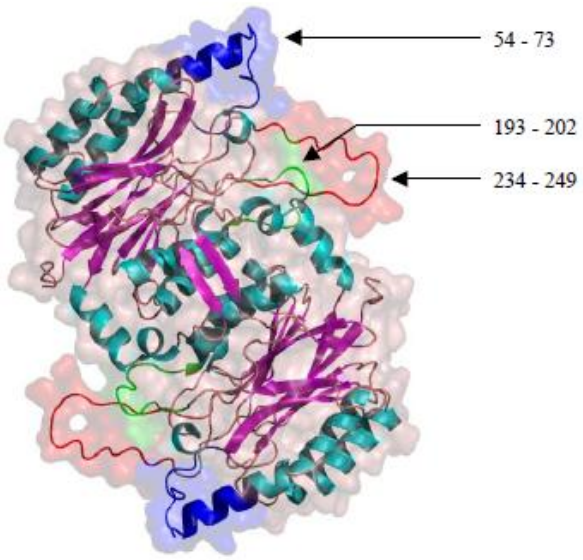


Figure 2.13b: Molecular representation of *R. rhodochorous* J1 nitrilase.

Insertion residues are highlighted by the arrows with residues 54-73 being shown in blue; residues 193-202 shown in green; and residues 234-249 shown in red (reproduced from Thuku *et al.* 2007)

2.2.5.7 Nitrilase Predicted Active Site Environment (*R. rhodochrous* J1)

Nitrilases are capable of hydrolyzing a variety of nitrile substrates, with the enzymes active site volume dictating the size of the substrate that can be accomodated. Crucial catalytic amino acid residues include Glu 48, Lys 131 and Cys 165, all located deep inside the enzyme cleft (Brenner, 2002; Nakai *et al*. 2000).

Structure predictions based on amino acid sequence alignments from related proteins such as 1F89 (Kuamaran *et al.* 2013), 1ERZ (Nakai *et al.* 2000), and 1FO6 (Chen *et al.* 2003) (Ndorio Thuku- MSc dissertation, unpublished) highlighted crucial amino acid residues found to line the binding pocket cleft These included amino acid residues Tyr 54, His 57, Phe 70, Tyr 74, Ser 105, Met 114, Thr 135, His 136, Glu 138, Tyr 142, Asn 164, Trp 166, His 168, Trp 189 and Met 192. These, the authors postulated, played an important role in substrate acceptance by the enzyme (see Table 2.2 for individual amino acid location and function information, and Fig. 2.14 for *Rhodococcal* nitrilase sequence alignment).

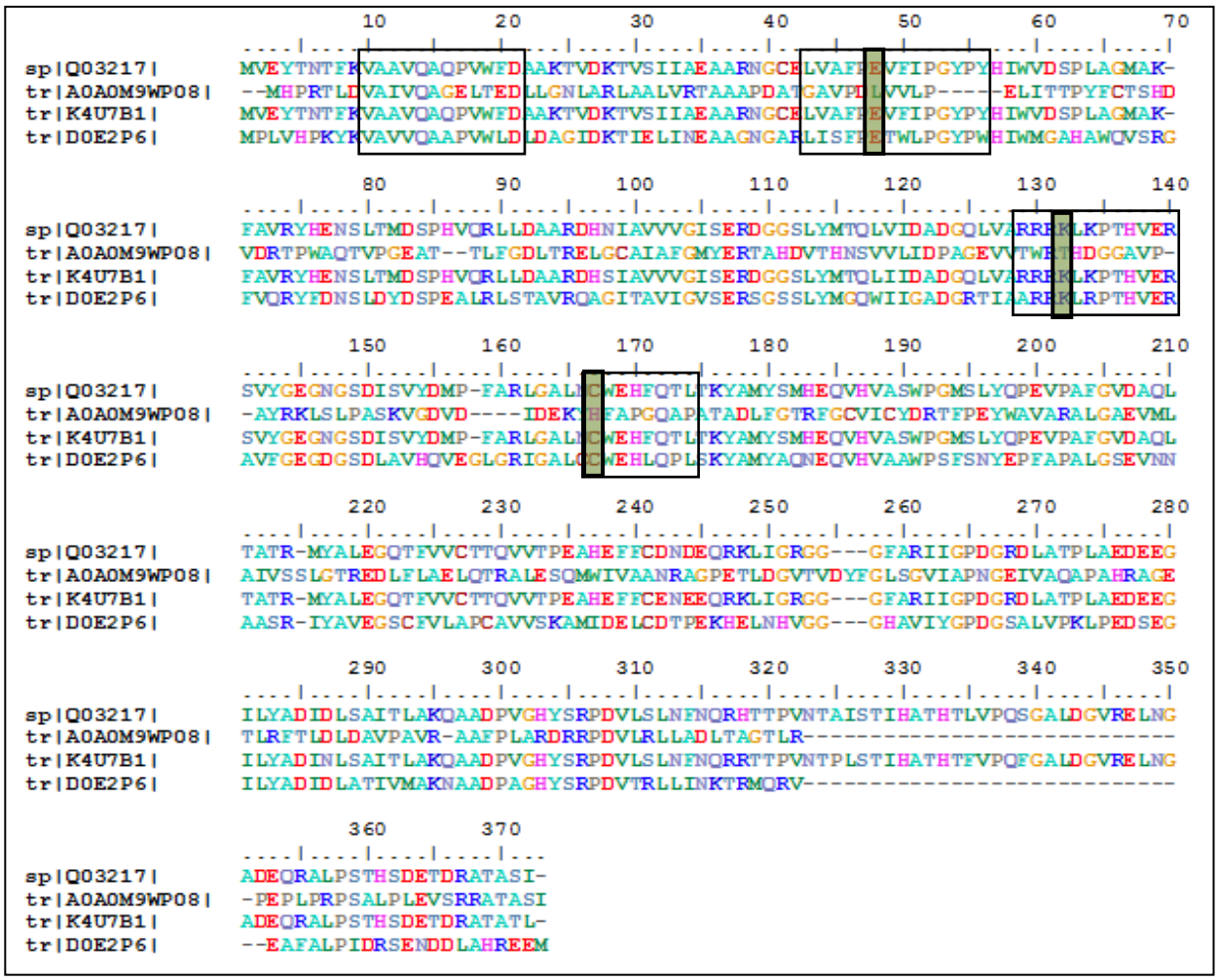


Figure 2.14: MAFFT protein sequence alignment of *Rhodococcal* nitrilase enzyme sequences.

Q03217- Aliphatic nitrilase protein from *R. rhodochrous* (NitA); **A0A0M9WP08**- nitrilase from *R. rhodochrous* KG-21 (Z051_11215); **K4U7B1**- nitrilase from *Rhodococcus rhodochrous* (NitA); **D0E2P6**- nitrilase from *R. erythropolis* (Nit1). Regions highlighted green within the alignment above show the core catalytic residues involved in nitrile hydrolysis. The consensus motifs have been boxed in in the alignment above. Alignment performed for the current study using MAFFT with iterative processing of these sequences done using Bioedit.

Table 2.2: *R. rhodochrous* J1 nitrilase catalytic residues.

Amino acid residue	Characteristic	Structural element/ Location	Position
Gln 48	Acidic Residue	NS2	Catalytic site
Tyr 54	Aromatic Residue	External loop	Hydrophobic pocket
His 57	Basic	External loop	Hydrophobic pocket
Phe 70	Aromatic	External loop (α2)	Hydrophobic pocket
Tyr 74	Aromatic	NH_2 (α2)	Hydrophobic pocket
Ser 105	Nuclephilic	Structurally conserved residue-NS3	Hydrophobic pocket
Met 114	Hydrophobic	Structurally conserved residue-NS4 (β4)	Hydrophobic pocket
Lys 131	Amide	NS5α	Catalytic residue
Thr 135	Nucleophilic	Structurally conserved region-NS5 (β5)	Hydrophobic pocket
His 136	Basic	External loop-NS5b	Hydrophobic pocket
Glu 138	Amide	External loop- NS6a (α4)	Hydrophobic pocket
Tyr 142	Aromatic	Solvent inaccessible region	Hydrophobic pocket
Asn 164	Amide	Structurally conserved region	Hydrophobic pocket
Cys 165	Nucleophilic	Structurally conserved region-NS7 (β7)	Catalytic residue
Trp 166	Aromatic	Structurally conserved region- NS7 (β7)	Hydrophobic pocket
His 168	Basic	Structurally conserved region	Hydrophobic pocket
Trp 189	Aromatic	Structurally conserved region-NS8 (β8)	Hydrophobic pocket
Met 192	Hydrophobic	External loop	Hydrophobic pocket

2.2.5.8 Nitrilase Gene Location and Regulation of Expression

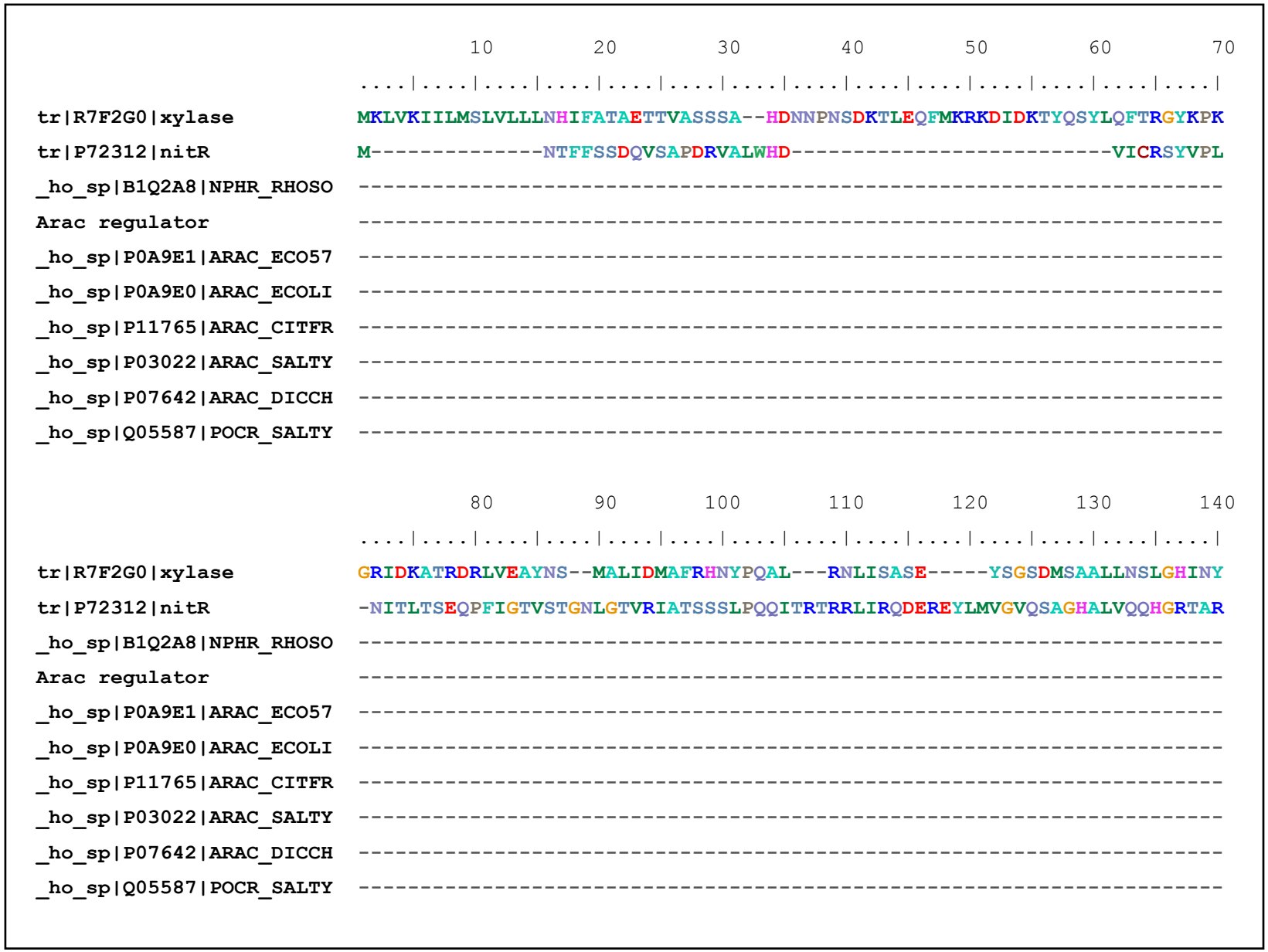
Transcription studies carried out on the *nitA* gene from *R. rhodochrous* J1 showed that a 1.4 bp region downstream to the *nitA* gene was required for isovaleronitrile induction (Komeda *et al.* 1996). Further analysis of the gene sequence showed that an open reading frame (ORF) encoded a *nitR* gene sequence, 975 base pairs in length, and encoded a protein of approximately 35.1 kilodalton (kDa) in size. This was found to play a crucial role in the isovaleronitrile induction of *nitA*.

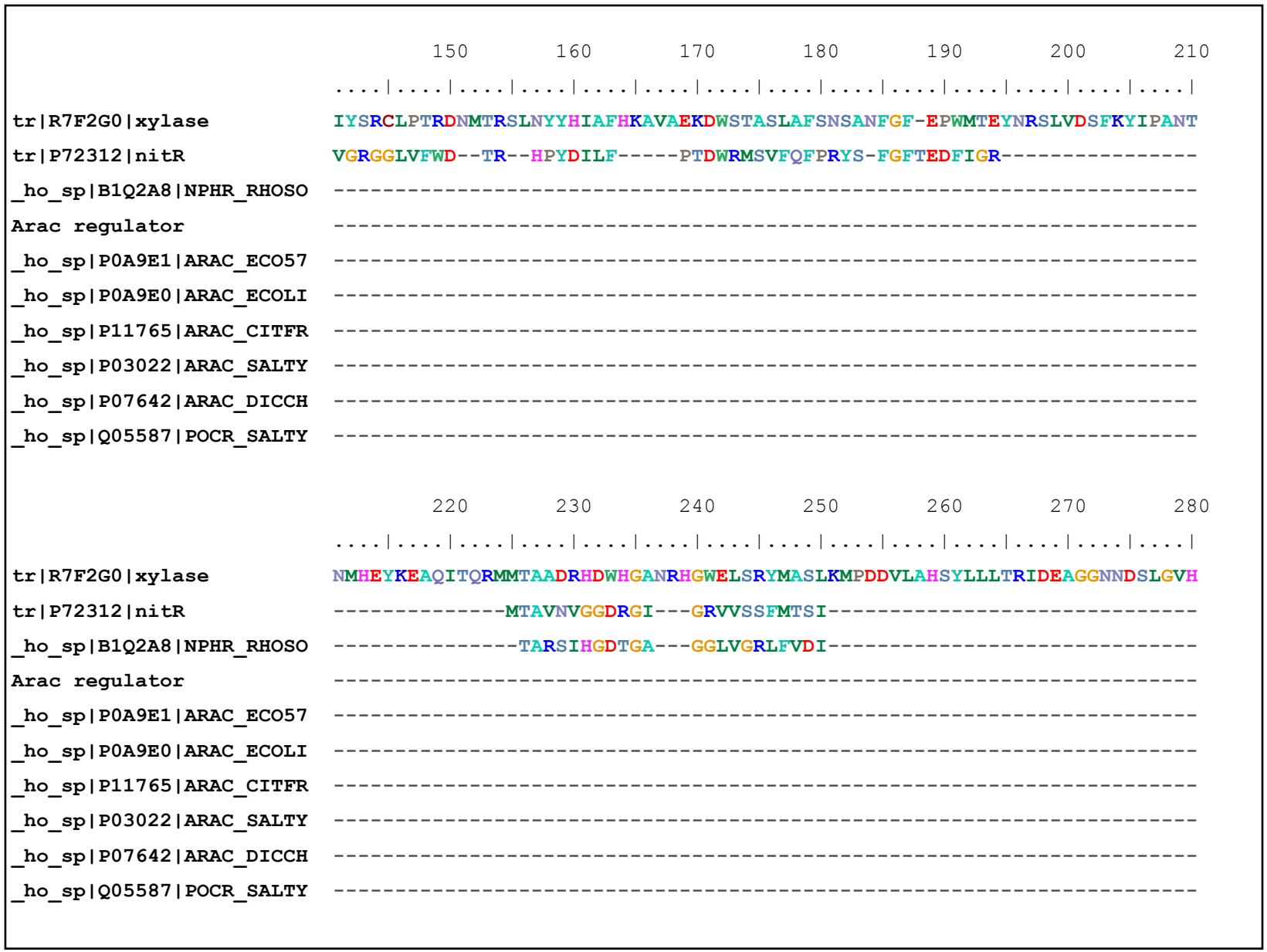
The gene product of the aliphatic nitrilase positive regulator sequence (NitR) was found to be related to other bacterial transcription regulators belonging to the AraC / XylS family, with most of these regulators involved in carbon metabolism and pathogenesis (Komeda *et al.* 1996) (see Table 2.3 for comparison against XylS and AraC regulator proteins, and Fig. 2.15 for protein sequence alignment data for NitR, XylS, AraC and other homologs generated).

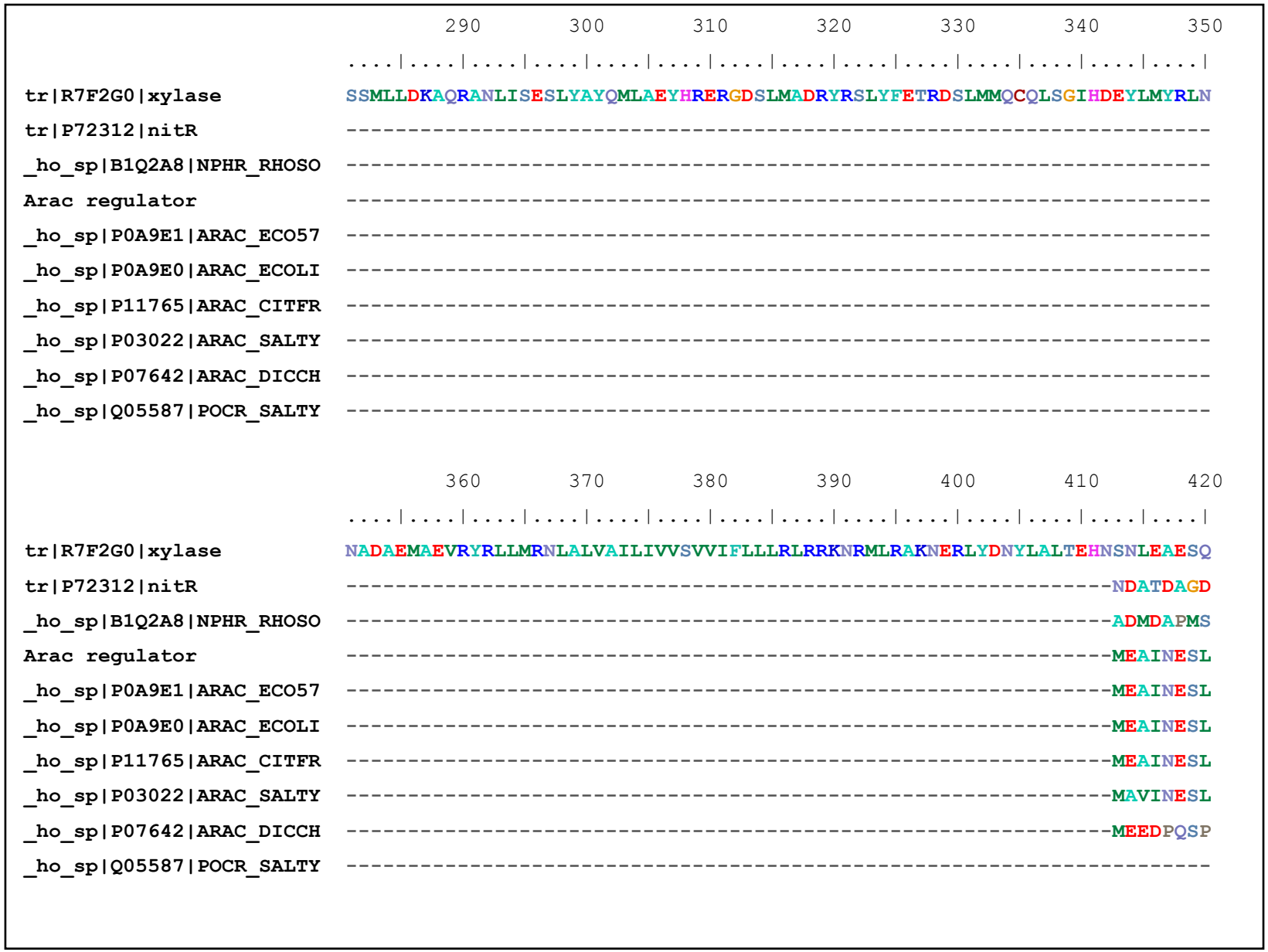
Sequence similarity at the carboxyl terminus was noted in these regulator proteins where a conserved helix-turn-helix deoxyribonucleic acid (DNA) binding motif was located (Fig. 2.15). The non-conserved *N*-terminal domain was presumed to play a role in binding of the activator molecule.

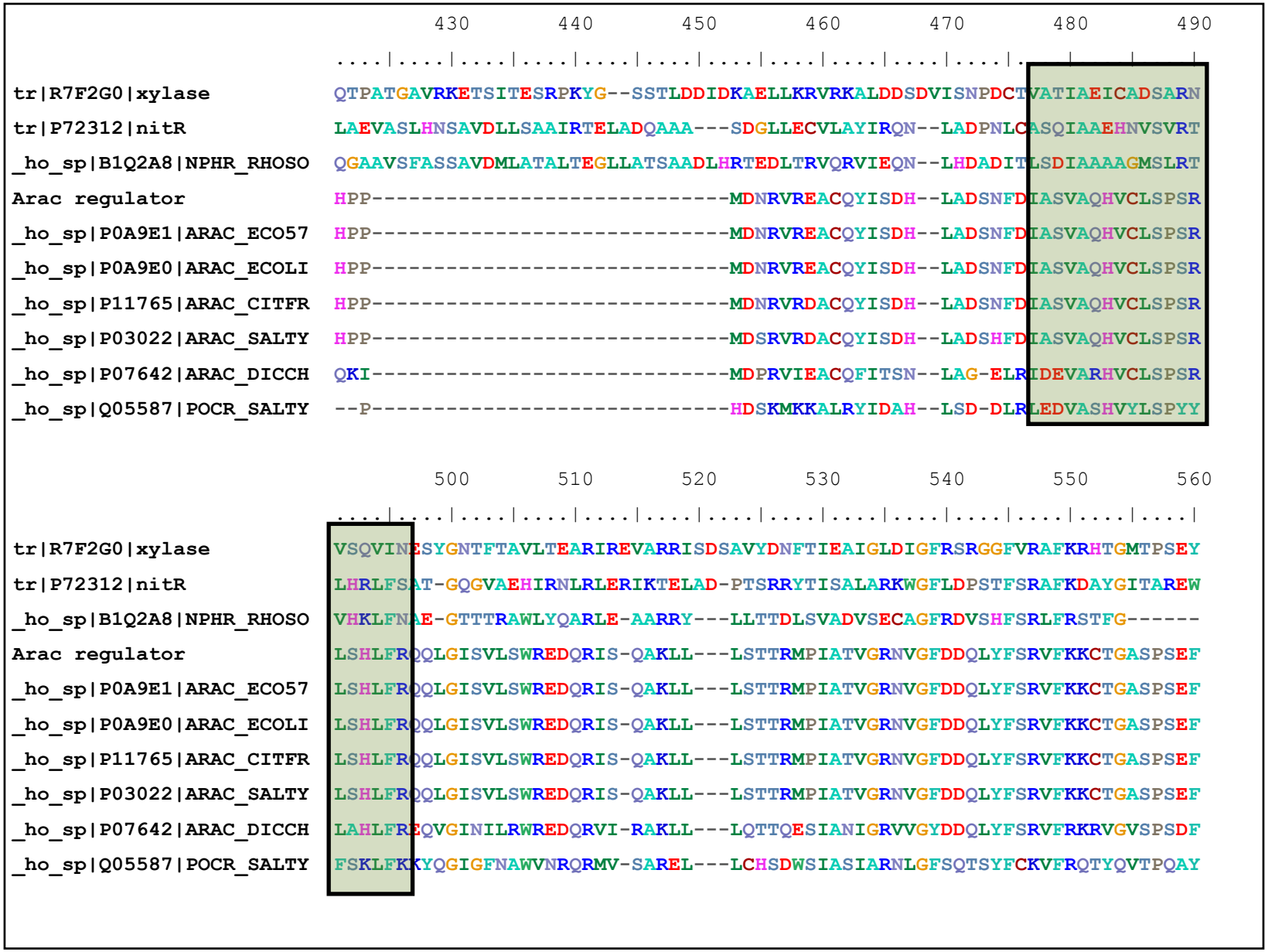
Table 2.3: Comparison of NitR versus XylS and AraC

	Determinant	**Compared to XylS**	**Compared to AraC**
NitR protein	**% Identity**	20.3	17.1
	No of overlapping residues	310	282
	Region of similarity	Carboxy terminus	Carboxy terminus


10 20 30 40 50 60 70
tr|R7F2G0|xylase MKLVKIILMSLVLLLNHIFATAETTVASSSA--HDNNPNSDKTLEQFMKRKDIDKTYQSYLQFTRGYKPK
tr|P72312|nitR M--------------NTFFSSDQVSAPDRVALWHD------------------------VICRSYVPL
_ho_sp|B1Q2A8|NPHR_RHOSO
Arac regulator
_ho_sp|P0A9E1|ARAC_ECO57
_ho_sp|P0A9E0|ARAC_ECOLI
_ho_sp|P11765|ARAC_CITFR
_ho_sp|P03022|ARAC_SALTY
_ho_sp|P07642|ARAC_DICCH
_ho_sp|Q05587|POCR_SALTY
80 90 100 110 120 130 140
tr|R7F2G0|xylase GRIDKATRDRLVEAYNS--MALIDMAFRHNYPQAL---RNLISASE-----YSGSDMSAALLNSLGHINY
tr|P72312|nitR -NITLTSEQPFIGTVSTGNLGTVRIATSSSLPQQITRTRRLIRQDEREYLMVGVQSAGHALVQQHGRTAR
_ho_sp|B1Q2A8|NPHR_RHOSO
Arac regulator
_ho_sp|P0A9E1|ARAC_ECO57
_ho_sp|P0A9E0|ARAC_ECOLI
_ho_sp|P11765|ARAC_CITFR
_ho_sp|P03022|ARAC_SALTY
_ho_sp|P07642|ARAC_DICCH
_ho_sp|Q05587|POCR_SALTY


150 160 170 180 190 200 210
tr|R7F2G0|xylase IYSRCLPTRDNMTRSLNYYHIAFHKAVAEKDWSTASLAFSNSANFGF-EPWMTEYNRSLVDSFKYIPANT
tr|P72312|nitR VGRGGLVFWD--TR--HPYDILF-----PTDWRMSVFQFPRYS-FGFTEDFIGR----------
_ho_sp|B1Q2A8|NPHR_RHOSO
Arac regulator
_ho_sp|P0A9E1|ARAC_ECO57
_ho_sp|P0A9E0|ARAC_ECOLI
_ho_sp|P11765|ARAC_CITFR
_ho_sp|P03022|ARAC_SALTY
_ho_sp|P07642|ARAC_DICCH
_ho_sp|Q05587|POCR_SALTY
220 230 240 250 260 270 280
tr|R7F2G0|xylase NMHEYKEAQITQRMMTAADRHDWHGANRHGWELSRYMASLKMPDDVLAHSYLLLTRIDEAGGNNDSLGVH
tr|P72312|nitR ----------MTAVNVGGDRGI---GRVVSSFMTSI----------
_ho_sp|B1Q2A8|NPHR_RHOSO ----------TARSIHGDTGA---GGLVGRLFVDI----------
Arac regulator
_ho_sp|P0A9E1|ARAC_ECO57
_ho_sp|P0A9E0|ARAC_ECOLI
_ho_sp|P11765|ARAC_CITFR
_ho_sp|P03022|ARAC_SALTY
_ho_sp|P07642|ARAC_DICCH
_ho_sp|Q05587|POCR_SALTY


290 300 310 320 330 340 350
tr|R7F2G0|xylase SSMLLDKAQRANLISESLYAYQMLAEYHRERGDSLMADRYRSLYFETRDSLMMQCQLSGIHDEYLMYRLN
tr|P72312|nitR
_ho_sp|B1Q2A8|NPHR_RHOSO
Arac regulator
_ho_sp|P0A9E1|ARAC_ECO57
_ho_sp|P0A9E0|ARAC_ECOLI
_ho_sp|P11765|ARAC_CITFR
_ho_sp|P03022|ARAC_SALTY
_ho_sp|P07642|ARAC_DICCH
_ho_sp|Q05587|POCR_SALTY
360 370 380 390 400 410 420
tr|R7F2G0|xylase NADAEMAEVRYRLLMRNLALVAILIVVSVVIFLLLRLRRKNRMLRAKNERLYDNYLALTEHNSNLEAESQ
tr|P72312|nitR NDATDAGD
_ho_sp|B1Q2A8|NPHR_RHOSO ADMDAPMS
Arac regulator MEAINESL
_ho_sp|P0A9E1|ARAC_ECO57 MEAINESL
_ho_sp|P0A9E0|ARAC_ECOLI MEAINESL
_ho_sp|P11765|ARAC_CITFR MEAINESL
_ho_sp|P03022|ARAC_SALTY MAVINESL
_ho_sp|P07642|ARAC_DICCH MEEDPQSP
_ho_sp|Q05587|POCR_SALTY


430 440 450 460 470 480 490
tr|R7F2G0|xylase QTPATGAVRKETSITESRPKYG--SSTLDDIDKAELLKRVRKALDDSDVISNPDCTVATIAEICADSARN
tr|P72312|nitR LAEVASLHNSAVDLLSAAIRTELADQAAA---SDGLLECVLAYIRQN--LADPNLCASQIAAEHNVSVRT
_ho_sp|B1Q2A8|NPHR_RHOSO QGAAVSFASSAVDMLATALTEGLLATSAADLHRTEDLTRVQRVIEQN--LHDADITLSDIAAAAGMSLRT
Arac regulator HPP----------MDNRVREACQYISDH--LADSNFDIASVAQHVCLSPSR
_ho_sp|P0A9E1|ARAC_ECO57 HPP----------MDNRVREACQYISDH--LADSNFDIASVAQHVCLSPSR
_ho_sp|P0A9E0|ARAC_ECOLI HPP----------MDNRVREACQYISDH--LADSNFDIASVAQHVCLSPSR
_ho_sp|P11765|ARAC_CITFR HPP----------MDNRVRDACQYISDH--LADSNFDIASVAQHVCLSPSR
_ho_sp|P03022|ARAC_SALTY HPP----------MDSRVRDACQYISDH--LADSHFDIASVAQHVCLSPSR
_ho_sp|P07642|ARAC_DICCH QKI----------MDPRVIEACQFITSN--LAG-ELRIDEVARHVCLSPSR
_ho_sp|Q05587|POCR_SALTY --P----------HDSKMKKALRYIDAH--LSD-DLRLEDVASHVYLSPYY
500 510 520 530 540 550 560
tr|R7F2G0|xylase VSQVINESYGNTFTAVLTEARIREVARRISDSAVYDNFTIEAIGLDIGFRSRGGFVRAFKRHTGMTPSEY
tr|P72312|nitR LHRLFSAT-GQGVAEHIRNLRLERIKTELAD-PTSRRYTISALARKWGFLDPSTFSRAFKDAYGITAREW
_ho_sp|B1Q2A8|NPHR_RHOSO VHKLFNAE-GTTTRAWLYQARLE-AARRY---LLTTDLSVADVSECAGFRDVSHFSRLFRSTFG------
Arac regulator LSHLFRQQLGISVLSWREDQRIS-QAKLL---LSTTRMPIATVGRNVGFDDQLYFSRVFKKCTGASPSEF
_ho_sp|P0A9E1|ARAC_ECO57 LSHLFRQQLGISVLSWREDQRIS-QAKLL---LSTTRMPIATVGRNVGFDDQLYFSRVFKKCTGASPSEF
_ho_sp|P0A9E0|ARAC_ECOLI LSHLFRQQLGISVLSWREDQRIS-QAKLL---LSTTRMPIATVGRNVGFDDQLYFSRVFKKCTGASPSEF
_ho_sp|P11765|ARAC_CITFR LSHLFRQQLGISVLSWREDQRIS-QAKLL---LSTTRMPIATVGRNVGFDDQLYFSRVFKKCTGASPSEF
_ho_sp|P03022|ARAC_SALTY LSHLFRQQLGISVLSWREDQRIS-QAKLL---LSTTRMPIATVGRNVGFDDQLYFSRVFKKCTGASPSEF
_ho_sp|P07642|ARAC_DICCH LAHLFREQVGINILRWREDQRVI-RAKLL---LQTTQESIANIGRVVGYDDQLYFSRVFRKRVGVSPSDF
_ho_sp|Q05587|POCR_SALTY FSKLFKKYQGIGFNAWVNRQRMV-SAREL---LCHSDWSIASIARNLGFSQTSYFCKVFRQTYQVTPQAY

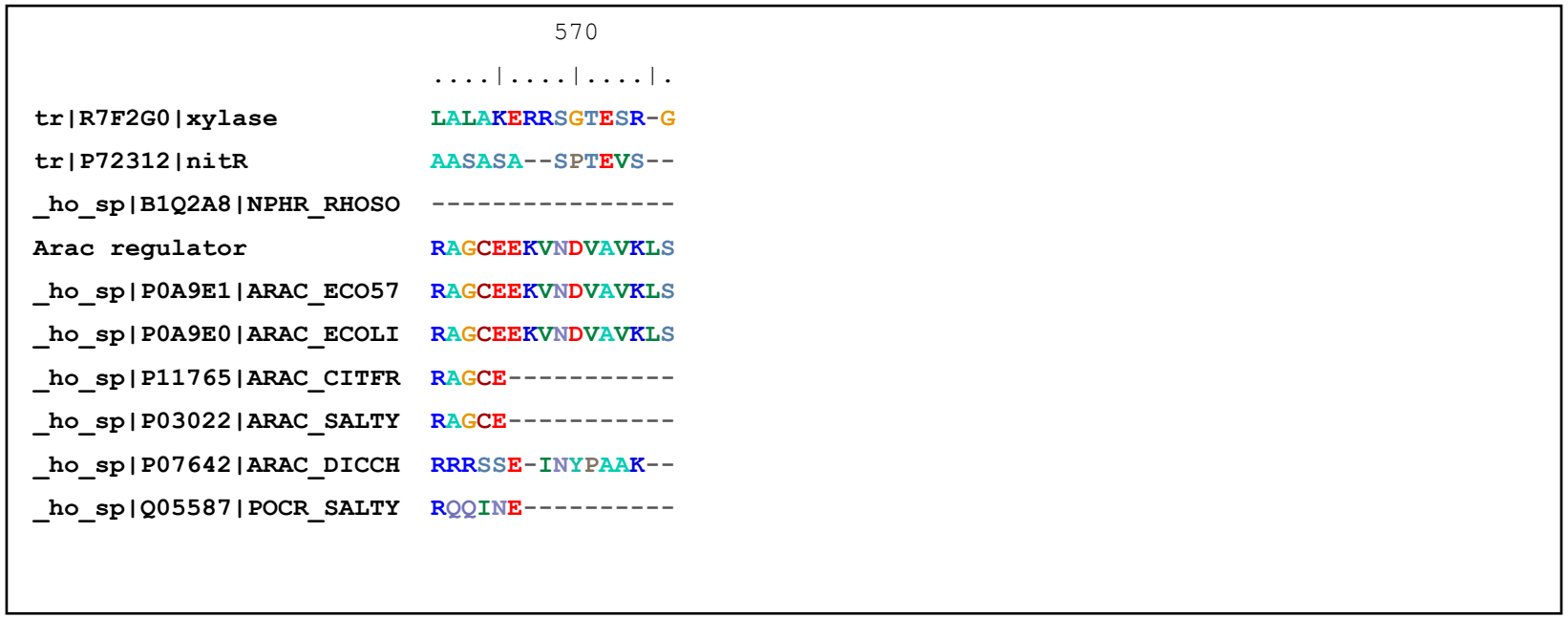


Figure 2.15: A comparison of the amino acid sequences of various transcription regulators.

R7F2G0- XylS transcription regulator AraC/ XylS (gene BN677)- *Prevotella sp*. CAG:485; **P72312**- Nitrilase regulator NitR (gene *nitR*)- *R. rhodochrous* J1; **B1Q2A8**- transcriptional activator NphR (gene *nphR*)- *Rhodococcus* sp.; **P0A9E1**-arabinose operon regulatory protein AraC (gene *araC*)- *Escherichia coli* 0157; **P0A9E0**- arabinose operon regulatory protein AraC (gene *araC*)- *Escherichia coli* K12 ; **P11765**- arabinose operon regulatory protein AraC (gene *araC*)- *Salmonella typhimurium*; **P03022**- arabinose operon regulatory protein AraC (gene *araC*)- *Dickeya chrysanthemi*; **P07642**- arabinose operon regulatory protein AraC (gene *araC*)- *Dickeya chrysanthemi*; **Q05587**- regulatory protein PocR (gene *pocR*)- *Salmonella typhimurium*. MAFFT online was used to complete sequence alignments with iterative processing of these sequences done using Bioedit. Resides highlighted show residues located in the conserved helix-turn-helix region of the protein

2.2.5.9 Nitrilase Post translational Modification-The Role of Chaperone Proteins

Protein folding is required for the basic functions of life to occur. Yet the aqueous cell environment is problematic for the efficient folding of a variety of proteins with constraints relating to protein size, function and topology resulting in misfolding and aggregation.

Larger topologically complex proteins often possess slower and more complicated folding reactions (Garel, 1992; Dobson, 2001; Grantcharova *et al.* 2001). Smaller proteins demonstrate two-state folding behaviour, while larger proteins can generate a myriad of unwanted meta-stable intermediate states, some showing low energy, non-native contacts. The journey towards productive native protein formation from these denatured proteins is often fraught with kinetic traps and conformational wells that prevent thermal motion processes from producing functional proteins. The result is the formation of non-functional protein aggregates.

Chaperone proteins are specialised proteins that use their unique molecular structures to help facilitate proper protein folding. Located within this group are large barrel shaped proteins called chaperonins that utilize ATP hydrolysis to facilitate proper folding of proteins (Fig. 2.16 for electron microscopy image of GroEL proteins). An archetypal member of this family is the GroEL protein which was initially isolated from *Escherichia coli*.

Characterisation studies have shown that GroEL and its co-chaperonin GroES are involved in driving protein folding when adverse cellular conditions prevent spontaneous native protein folding from occurring. GroES is made up of seven identical 10 kDa subunits, which arrange themselves in a domed disk structure that is ~80 Å in diameter (Hunt *et al.* 1996; Mande *et al.* 1996). GroEL on the other hand is a much larger complex that consists of fourteen identical 57 kDa subunits, that when arranged back to back, result in the formation of two seven membered ring structure. Each GroEL structure is ~147 Å in length and 137Å in diameter.

Characterisation of the inducible nitrilase from *Bacillus pallidus* Dac521 by Almatawah and Cowan (1999) showed that the nitrilase enzyme purified as a complex together with a putative GroEL protein that had a similar amino acid sequence to that produced by *Bacillus subtilis* Marburg (Tozawa *et al.* 1995). In the preceeding year, Layh *et al.* (1998) suggested that a chaperonin protein (CPN60) could play a role in the assembly of the basic nitrilase heterodimers into a larger molecular weight native protein in *Pseudomonas fluorescens* DSM 7155.

Cloning of the nitrilase gene from *C. testosteroni* into *E. coli* (Lévi-Schil *et al.* 1995) resulted in high level of expression of the nitrilase protein (30% of total cellular protein), however only 10% of this was found in the soluble fraction. Subsequent co-expression of a GroEL chaperonin protein resulted in an increase in the solublity of the protein with a five-fold increase in enzyme activity. This confirmed the crucial role played by GroEL proteins in the formation of a functional nitrilase enzyme.

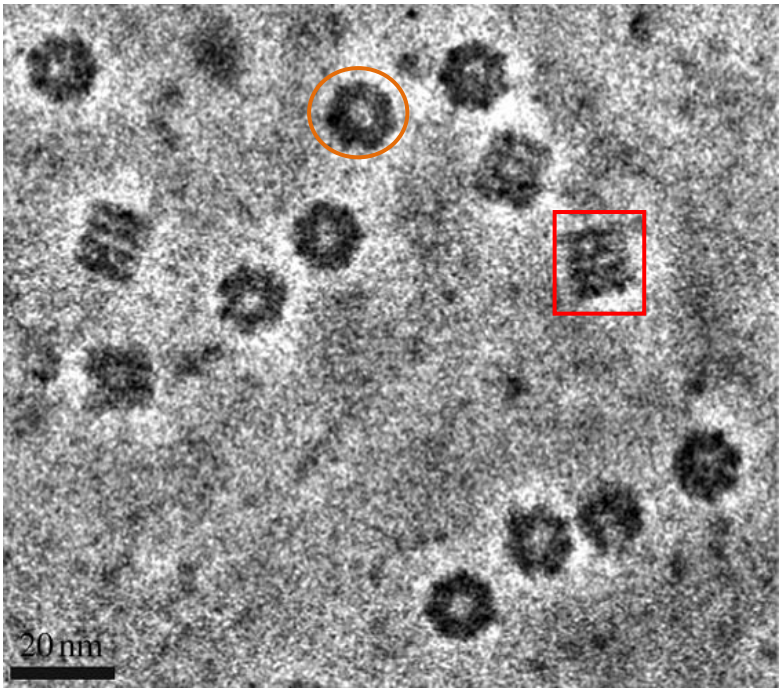


Figure 2.16: Zernike Phase Contrast-TEM image showing GroEL and GroES proteins.

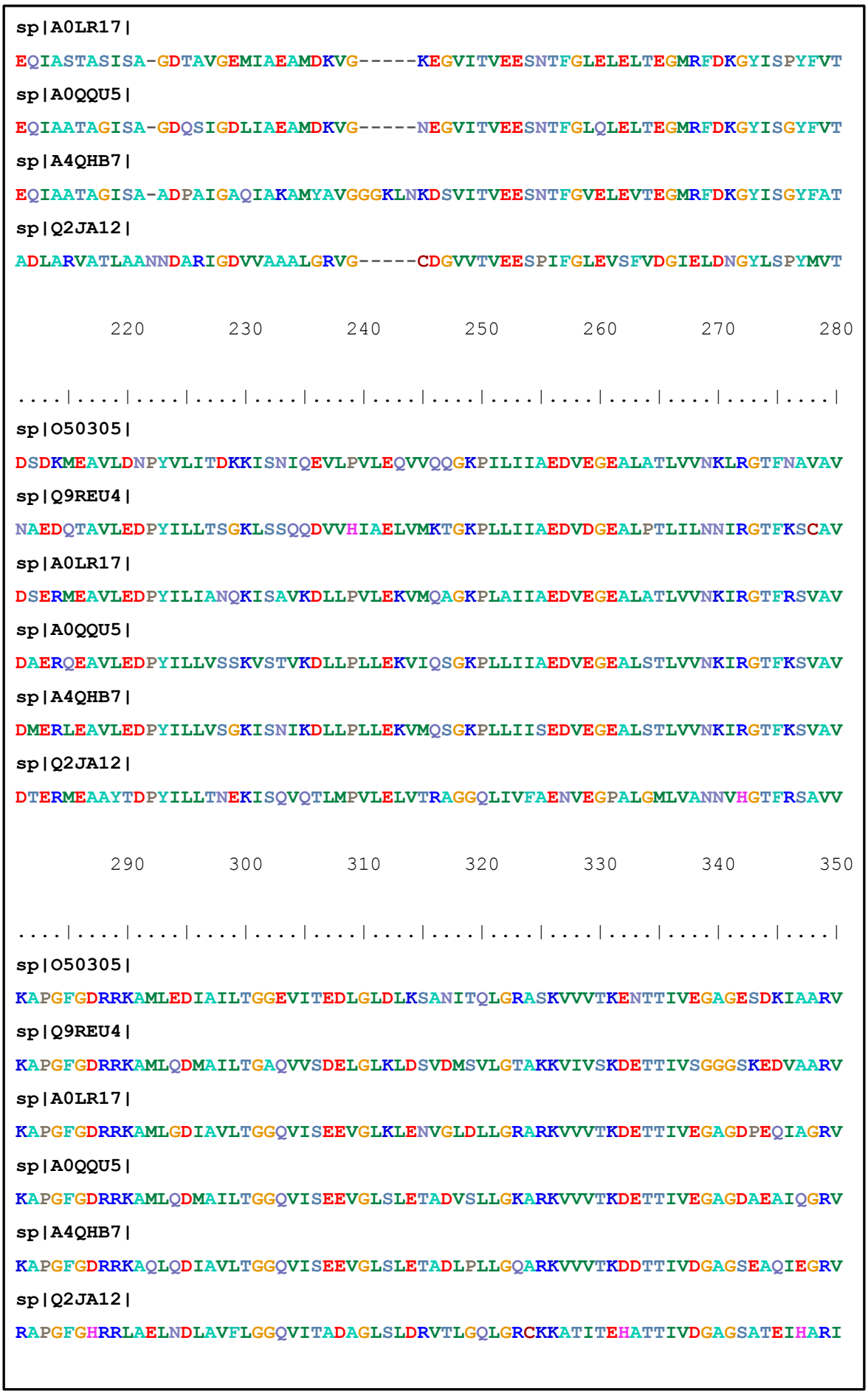
Transmission Electron Microscopy Images (ZPC-TEM) showing a vitrified GroEL protein samples (red rectangle) as well as GroES protein (orange circle) (reproduced from Nagayama and Danev. 2008).

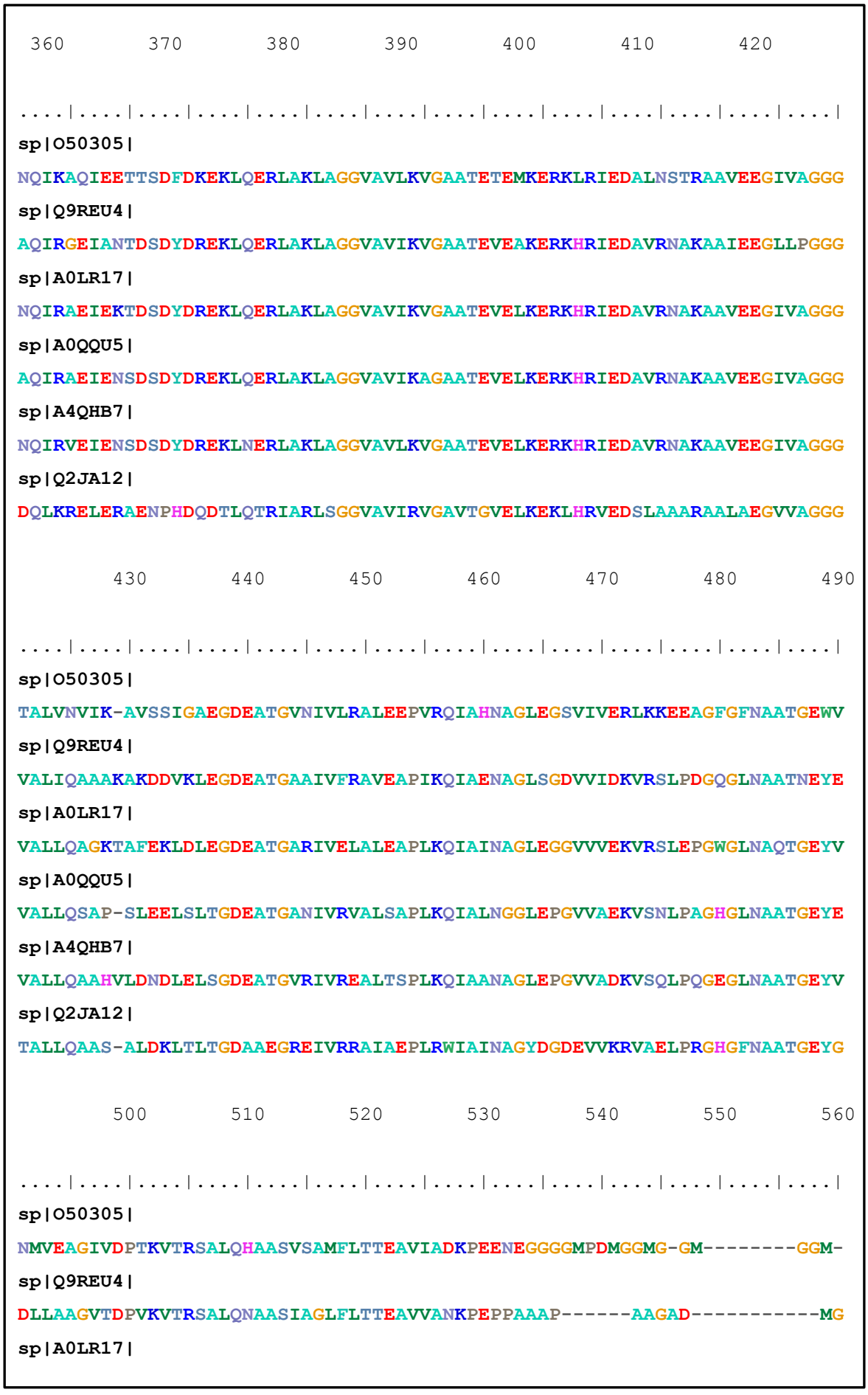
As can be seen in a sequence alignment peformed in this study, Fig. 2.16 shows a highly conserved sequence for all of the Chaperonin 60 proteins located in the selected *Rhodococca*l and *Pimelobacter* strains.

```
        10         20         30         40         50         60         70
....|....|....|....|....|....|....|....|....|....|....|....|....|....|
sp|O50305|
MAKDIKFSEDARRSMLRGVDKLADAVKVTLGPKGRNVVLEKKFGSPLITNDGVTIAKEIELEDAFENMGA
sp|Q9REU4|
MAKMIAYDDEARQGMLAGLDKLADTVKVTLGPKGRNVVLDKTYGAPTITNDGVSIAKEIDLDDPYERIGA
sp|A0LR17|  ----------------------------------------------------------
LEDPYEKIGA
sp|A0QQU5|
MAKTIAYDEEARRGLERGLNSLADAVKVTLGPKGRNVVLEKKWGAPTITNDGVSIAKEIELEDPYEKIGA
sp|A4QHB7|
MAKIIAFDEEARRGLEKGLNTLADAVKVTLGPKGRNVVLEKAWGAPTITNDGVTIAREIELEDPYEKIGA
sp|Q2JA12|
MAKDLRFNVEARRLLEAGVNALADAVKVTLGPKGRNAVIEKLTGPPTITNDGVTIAREIQLRNPFANMGA

         80         90        100        110        120        130        140
....|....|....|....|....|....|....|....|....|....|....|....|....|....|
sp|O50305|
KLVAEVASKTNDIAGDGTTTATVLAQAMIREGLKNVTSGANPMVIRKGIEKATQVAVEELSKISKPIEGK
sp|Q9REU4|
ELVKEVAKKTDDVAGDGTTTATVLAQSLVHEGLKNVTAGSNPIALRRGIEKAADAIVKELVAAAKDVETK
sp|A0LR17|
ELVKEVAKKTDDVAGDGTTTATVLAQTLVREGLRNVAAGANPMALKRGIEAATERVCQALLEIAKDVETR
sp|A0QQU5|
ELVKEVAKKTDDVAGDGTTTATVLAQALVREGLRNVAAGANPLGLKRGIEKAVEKVTETLLKSAKEVETK
sp|A4QHB7|
ELVKEVAKKTDDVAGDGTTTATVLAQALVREGLRNVAAGSNPMGIKRGIEKAVAQVTEKLLEAAKEVETE
sp|Q2JA12|
QLVKEVATKTNGTAGDGTTTATVLAQALVREGLHAVDGGANPMFLKNGIEAAVAALLEEFEKYRGEVEGE

        150        160        170        180        190        200        210
....|....|....|....|....|....|....|....|....|....|....|....|....|....|
sp|O50305|
DSIAQVAAISS-ADDEVGKIIAEAMERVG-----NDGVITIEESKGFSTELEVVEGMQFDRGYASPYMVT
sp|Q9REU4|
DQIAATATISA-ADPEVGEKIAEALDKVG-----QDGVVTVEDNNRFGLDLDFTEGMRFDKGYIAPYFVT
```


sp|A0LR17|
EQIASTASISA-GDTAVGEMIAEAMDKVG-----KEGVITVEESNTFGLELELTEGMRFDKGYISPYFVT
sp|A0QQU5|
EQIAATAGISA-GDQSIGDLIAEAMDKVG-----NEGVITVEESNTFGLQLELTEGMRFDKGYISGYFVT
sp|A4QHB7|
EQIAATAGISA-ADPAIGAQIAKAMYAVGGGKLNKDSVITVEESNTFGVELEVTEGMRFDKGYISGYFAT
sp|Q2JA12|
ADLARVATLAANNDARIGDVVAAALGRVG-----CDGVVTVEESPIFGLEVSFVDGIELDNGYLSPYMVT
220 230 240 250 260 270 280
sp|O50305|
DSDKMEAVLDNPYVLITDKKISNIQEVLPVLEQVVQQGKPILIIAEDVEGEALATLVVNKLRGTFNAVAV
sp|Q9REU4|
NAEDQTAVLEDPYILLTSGKLSSQQDVVHIAELVMKTGKPLLIIAEDVDGEALPTLILNNIRGTFKSCAV
sp|A0LR17|
DSERMEAVLEDPYILIANQKISAVKDLLPVLEKVMQAGKPLAIIAEDVEGEALATLVVNKIRGTFRSVAV
sp|A0QQU5|
DAERQEAVLEDPYILLVSSKVSTVKDLLPLLEKVIQSGKPLLIIAEDVEGEALSTLVVNKIRGTFKSVAV
sp|A4QHB7|
DMERLEAVLEDPYILLVSGKISNIKDLLPLLEKVMQSGKPLLIISEDVEGEALSTLVVNKIRGTFKSVAV
sp|Q2JA12|
DTERMEAAYTDPYILLTNEKISQVQTLMPVLELVTRAGGQLIVFAENVEGPALGMLVANNVHGTFRSAVV
290 300 310 320 330 340 350
sp|O50305|
KAPGFGDRRKAMLEDIAILTGGEVITEDLGLDLKSANITQLGRASKVVVTKENTTIVEGAGESDKIAARV
sp|Q9REU4|
KAPGFGDRRKAMLQDMAILTGAQVVSDELGLKLDSVDMSVLGTAKKVIVSKDETTIVSGGGSKEDVAARV
sp|A0LR17|
KAPGFGDRRKAMLGDIAVLTGGQVISEEVGLKLENVGLDLLGRARKVVVTKDETTIVEGAGDPEQIAGRV
sp|A0QQU5|
KAPGFGDRRKAMLQDMAILTGGQVISEEVGLSLETADVSLLGKARKVVVTKDETTIVEGAGDAEAIQGRV
sp|A4QHB7|
KAPGFGDRRKAQLQDIAVLTGGQVISEEVGLSLETADLPLLGQARKVVVTKDDTTIVDGAGSEAQIEGRV
sp|Q2JA12|
RAPGFGHRRLAELNDLAVFLGGQVITADAGLSLDRVTLGQLGRCKKATITEHATTIVDGAGSATEIHARI


360 370 380 390 400 410 420
sp|O50305|
NQIKAQIEETTSDFDKEKLQERLAKLAGGVAVLKVGAATETEMKERKLRIEDALNSTRAAVEEGIVAGGG
sp|Q9REU4|
AQIRGEIANTDSDYDREKLQERLAKLAGGVAVIKVGAATEVEAKERKHRIEDAVRNAKAAIEEGLLPGGG
sp|A0LR17|
NQIRAEIEKTDSDYDREKLQERLAKLAGGVAVIKVGAATEVELKERKHRIEDAVRNAKAAVEEGIVAGGG
sp|A0QQU5|
AQIRAEIENSDSDYDREKLQERLAKLAGGVAVIKAGAATEVELKERKHRIEDAVRNAKAAVEEGIVAGGG
sp|A4QHB7|
NQIRVEIENSDSDYDREKLNERLAKLAGGVAVLKVGAATEVELKERKHRIEDAVRNAKAAVEEGIVAGGG
sp|Q2JA12|
DQLKRELERAENPHDQDTLQTRIARLSGGVAVIRVGAVTGVELKEKLHRVEDSLAAARAALAEGVVAGGG
430 440 450 460 470 480 490
sp|O50305|
TALVNVIK-AVSSIGAEGDEATGVNIVLRALEEPVRQIAHNAGLEGSVIVERLKKEEAGFGFNAATGEWV
sp|Q9REU4|
VALIQAAAKAKDDVKLEGDEATGAAIVFRAVEAPIKQIAENAGLSGDVVIDKVRSLPDGQGLNAATNEYE
sp|A0LR17|
VALLQAGKTAFEKLDLEGDEATGARIVELALEAPLKQIAINAGLEGGVVVEKVRSLEPGWGLNAQTGEYV
sp|A0QQU5|
VALLQSAP-SLEELSLTGDEATGANIVRVALSAPLKQIALNGGLEPGVVAEKVSNLPAGHGLNAATGEYE
sp|A4QHB7|
VALLQAAHVLDNDLELSGDEATGVRIVREALTSPLKQIAANAGLEPGVVADKVSQLPQGEGLNAATGEYV
sp|Q2JA12|
TALLQAAS-ALDKLTLTGDAAEGREIVRRAIAEPLRWIAINAGYDGDEVVKRVAELPRGHGFNAATGEYG
500 510 520 530 540 550 560
sp|O50305|
NMVEAGIVDPTKVTRSALQHAASVSAMFLTTEAVIADKPEENEGGGGMPDMGGMG-GM--------GGM-
sp|Q9REU4|
DLLAAGVTDPVKVTRSALQNAASIAGLFLTTEAVVANKPEPPAAAP------AAGAD----------MG
sp|A0LR17|

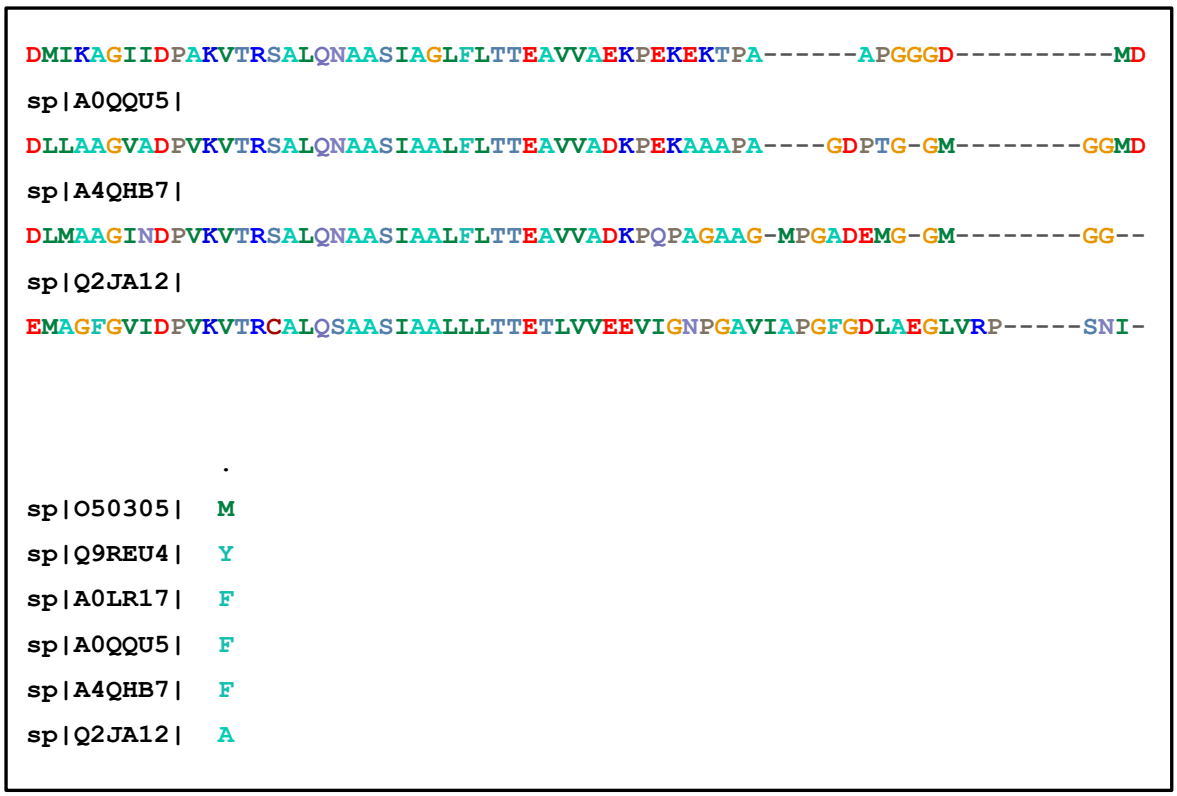


Figure 2.17: 60 kDa Chaperonin protein sequence alignment

SPO50305- 60 kDa chaperonin protein from *Bacillus halodurans* (gene *groL*); **Q9REU4**- 60 kDa chaperonin protein from *Bifidobacterium adolescentis* (gene *groL*); **A0LR17**- 60 kDa chaperonin from *Acidothermus cellulolyticus* (gene *groL1*); **A0QQU5**- 60 kDa chaperonin from *Mycobacterium smegmatis* (gene *groL1*); **A4QHB7**- 60 kDa chaperonin 2 from *Corynebacetrium glutamicum Strain* R (gene *groL2*); **Q2JA12**- 60 kDa chaperonin 3 from *Frankia casuarinae* (gene *groL3*). MAFFT online was used to complete sequence alignments with iterative processing of these sequences done using Bioedit.

2.2.6 Nitrile Hydratase (EC 4.2.1.84)

Nitrile hydratase enzymes are metalloenzymes that catalyse the hydration of nitriles to their structurally related carboxamide products. They contain a low-spin non-corrinoid cobalt (Kobayashi *et al.* 1991; Payne *et al.* 1997; Yamaki *et al.* 1997) or a mononuclear non-heme iron (Ikehata *et al.* 1989; Nishiyama *et al.* 1991) in their respective catalytic sites. Both genetic and biochemical profiling has revealed the presence of a $(\alpha\beta)_2$ dimer structure for both Co-type and Fe-type nitrile hydratases (Fig. 2.18).

Many metalloproteins have been studied over decades with recent investigations into the process of metal sequestration into protein structures shedding light on the role played by various activator proteins (Okhamoto and Eltis, 2011). Activator protein dependence in the production of functional Fe-containing nitrile hydratases have been demonstrated in *Rhodococcus* sp. N-771 (Nojiri *et al.* 1999), *Pseudomonas chloroaphis* B23 (Nishiyama *et al.* 1991), as well as *Rhodococcus* sp. N-774 (Hashimoto *et al.* 1994).

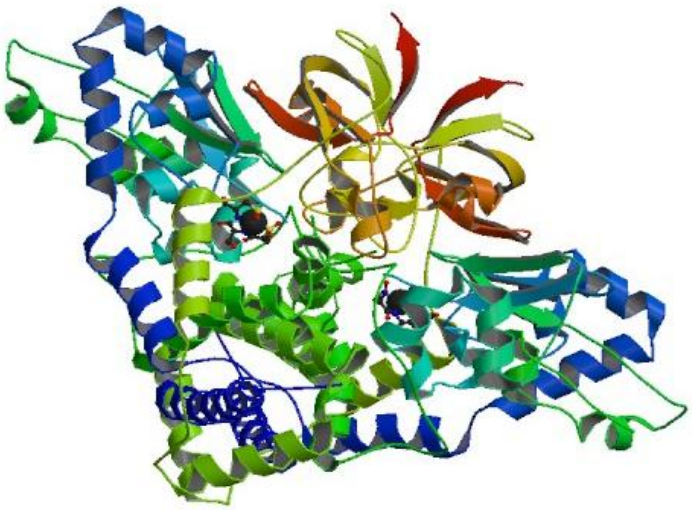


Figure 2.18: Crystal structure of a Co-type nitrile hydratase from *Pseudonocadia thermophilia*-Protein Data Bank Code **1IRE**)

The nitrile hydratase image above (heterodimer) was modelled on a protein sequence derived from *Pseudonocardia thermophilia* and deposited by Miyanaga *et al.* (2001). The image can be located on the PDB website - accession code **1IRE** (DOI: 10.2210/pdb1ire/pdb).

Both cobalt and iron type nitrile hydratase enzymes have metal ions that are located on the enzymes α-subunit, and share a common characteristic metal-binding motif [CXLC (SO_2H) SC (SOH)] which have two modified cysteine residues, namely cysteine-sulfinic acid (α-Cys-SO_2H) and cysteine-sulfenic acid (α-Cys-SOH) present. The structures of both ezymes are very similar except for the

presence of a water molecule in the sixth site of Co (III) instead of NO in the case of Fe (III) nitrile hydratases.

Co-type nitrile hydratase enzymes have one cobalt ion present on each paired α-β subunit, where the metal ion is involved in water activation, nitrile bond hydration, and protein folding. Co-type nitrile hydratase models synthesized using a vacant coordination site and the ligand $PyPSH_4$, demonstrated that the low-spin diamagnetic cobalt center occupied a distorted octahedral field; with *cis*-thiolato-S donors present (Harrop and Mascharak. 2004). The red-brown complex generated exhibited a maximum absorbance band (λ_{max}) at 410 nm .(Harrop and Mascharak. 2004).

Fe-type nitrile hydratase enzymes have one non-heme iron present on each paired α-βsubunit which is once again coordinated in a distorted octahedral geometry. Fe (III) complexes synthesized by Schiff's base condensation reactions using ethylenediamine, an appropriate ketone or mercaptoaldehyde, and $FeCl_3$, exhibited a low-energy thiolate to Fe (III) charge transfer band at 850 nm, which underwent a blue-shift to 690 nm in the sulfinato complex. This gave rise to the deep blue colour observed in these enzymes (Harrop and Mascharak. 2004). Furthermore, Fe (III) centers bound to caboxamido-*N* show resistance to hydrolytic decomposition, with some sulphur moeities positioned *cis* to each other (Harrop and Mascharak. 2004).

Recent characterisation studies into the low molecular weight (LMW)-nitrile hydratase enzyme produced by *R. rhodochrous* J1 showed that a novel mode of post-translational modification results in swapping of the metal-free α-subunit with a cobalt containing α-subunit from the LMW-nitrile hydratase mediator, Nh1AE (Liu *et al.* 2012). This process was coined "self-subunit swapping" and was found to be involved in the maturation of a number of Co-nitrile hydratase and thiocyanate hydrolase enzymes (Fig. 2.19).

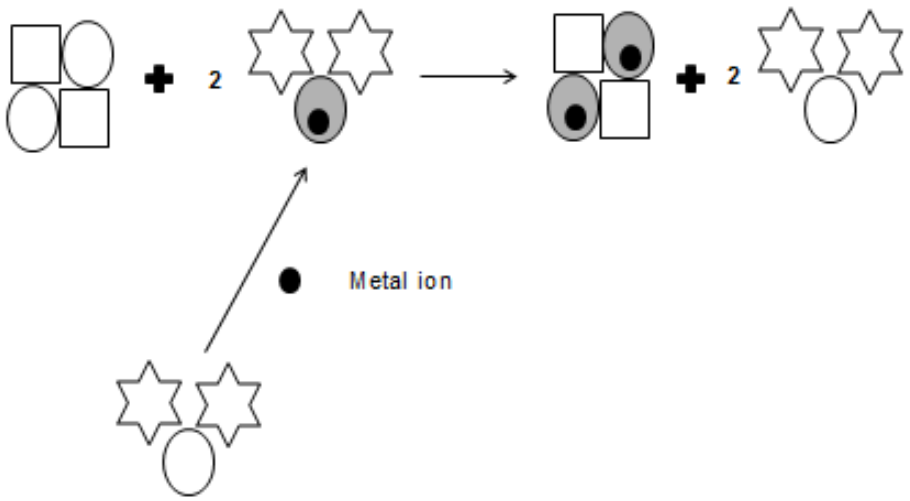


Figure 2.19: Self-subunit swapping of LMW-nitrile hydratase enzymes (Liu *et al.* 2012).

Insertion of a cobalt ion onto the apo NH1AE (represented as a black dot in the image) results in activation of the LMW nitrile hydratase. The holo-α subunit is shown highlighted in grey in the image above. Image adapted from Liu *et al.* 2012.

2.2.6.1 Cobalt versus Iron Containing Nitrile hydratase

Nitrile hydratase enzymes are divided into two classes based on the type of metal located in the metal coordination sphere namely, Co (III) or Fe (III) enzymes. The basic units of the enzyme include α and β subunits which are typically 22 870 kDa and 23 850 kDa in size. Both subunits have little sequence similarity to each other, but are boadly similar to α and β subunits found in other species.

Nitrile hydratase enzymes demonstrate the following unique characteristic profiles:

I) All contain deprotonated carboxamido nitrogens in combination with Cys-S bound to a metal center;
II) All exhibit asymmetric post-translational oxidation at Cys-S residues to generate cysteine-sulfenato ($Cys\text{-}SO^-$) and cysteine- sulfinito ($Cys\text{-}SO^{2-}$) moieties;
III) Fe-type Nitrile hydratase enzymes are photoregulated by reversible binding of nitric oxide (NO) at the sixth site which is replaced by water upon illumination;
IV) Are fully active despite being in the presence of a low spin Co (III) center which was previously considered kinetically inert.

Crystallographic studies have shown that the M (III) coordination centers in these enzymes are ligated to two deprotonated carboxamido nitrogens from the peptide backbone, and three cysteine sulfurs located in the highly conserved –C-S-L-C-S-C-motif (Huang *et al.* 1997: Miyanaga *et al.* 2001; Nagashima *et al.* 1998). Furthermore, a sixth site is occupied by a water / hydroxide molecule in the native form of the enzyme.

The claw setting observed in a Co-type nitrile hydratase enzyme produced by *Pseudonocardia thermophilia,* demonstrates two modified cysteine residues (αCys 111 and αCys 113), both coordinated to a cobalt ion (Miyanaga *et al.* 2001). The oxygen atoms of the Cys-sulfinic acid and Cys-sulfenic acid form hydrogen bonds with two Arg residues, namely βArg 52 and βArg 157, both highly conserved and located in the beta subunit of the enzyme.

The Fe-type nitrile hydratase enzyme from *Rhodococcus* sp. N771 is one of the best characterised enzymes in the nitrile hydratase family, exhibiting unique photoreactivity profile. Enzyme activation is achieved by photo-driven NO release, with nitrosylation (inactivation) of the iron center occuring when cells were cultivated in the dark (Nigashima *et al.* 1998: Noguchi *et al.* 1995: Odaka *et al.* 1997). This photoreactivity appears to be common among Fe-nitrile hydratases with the enzyme produced by *Comomonas testosteroni* N1 showing considerable amino acid sequence variation to *Rhodococcus sp*. N771 but displaying the same photoreactivity profile (Bonnet *et al.* 1997). Three oxygen atoms of αCys 112-SO_2H, αCys 114-SOH and αSer 113 form a novel claw setting that stabilizes a NO

molecule at the top of the iron center. Unlike other non-heme iron centered enzymes in biology, the Fe-center of nitrile hydratase does not participate in redox reactions but acts as a Lewis acid instead.

Structural evaluation of the various subunit structures show that the α subunit displays a Cys-Thr/ Ser-Leu-Cys-Tyr/ Thr-Cys sequence motif, with the cobalt-containing nitrile hydratase containing threonine and tyrosine amino acids in the 3rd and 8th position respectively. The Fe-centered enzyme on the other hand has a serine and threonine in the same postions while the active site is buried deep in the core protein with the distance from the enzyme surface to the cobalt centre being about ~15Å.

2.2.6.2 Zinc Centre Containing Nitrile Hydratases

Nitrile hydratase enzymes typically contain a metal ion active site which accomodates a Fe $(III)^{+}$ and or Co $(III)^{+}$ ion. However, a Zn2+ metal center was identified in the enzyme produced by *Myrrothecium verrucaria* (Maier-Greiner *et al.* 1991). The nitrile hydratase from *Rhodococcus* sp. N-774 when characterised was also found to have an iron-containing metallocenter that displays a $(\alpha\beta)_2$ structure configuration. Both the alpha and beta subunits produced by the organism were calculated to be ~ 28 500 kDa and 29 000 kDa respectively (Endo and Watanabe. 1989).

2.2.6.3 Low versus High Molecular Weight Nitrile hydratase Enzymes

Two cobalt-containing nitrile hydratase enzymes were identified in the Nocardiaform *R. rhodochrous* J1, namely a low molecular weight-nitrile hydratase (LMW), and a high molecular weight nitrile hydratase (HMW) enzyme. The LMW enzyme is a heterodimer consisting of both alpha and beta subunit chains that are approximately 130 kDa in size. The HMW enzyme is a multimeric, heterodimer of approximately 520 kDa in size, consisting of 9-10 groups of alpha and beta subunits.

Nitrile hydratase enzymes typically form αβ or $\alpha_2\beta_2$ functional proteins with the catalytic activity located at the center of the α-β subunit interface. Expression of the LMW nitrile hydratase enzyme was found to be selectively induced by cyclohexanecarboxamide addition during cultivation (requiring supplementation with low levels of Co^{2+} ions), while the HMW nitrile hydratase was induced by supplementation with urea (Weiser *et al.* 1998).

2.2.6.4 Nitrile Hydratase Mechanism of Action

Nitrile hydratase enzymes catalyse the hydration of nitriles, generating an amide product which is then converted to the corresponding acid by a coupled amidase enzyme (Fig. 2.20).

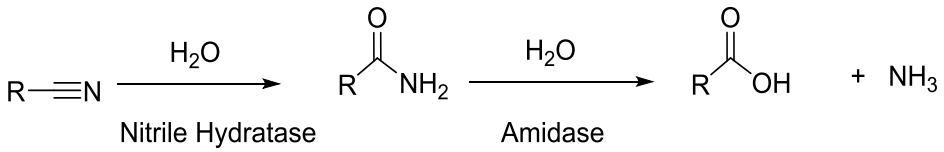


Figure 2.20: Schematic diagram showing nitrile hydratase and amidase cascade reactions

The exact mechanism by which nitrile hydratase enzymes convert nitriles to their corresponding amide products is still uncertain. Three different mechanisms have been proposed to explain the formation of the amide product namely; i) inner-sphere mechanism; ii) outer-sphere mechanism; and iii) second-outer sphere mechanism (Fig. 2.21) (Huang *et al.* 1997).

In the inner-sphere mechanism, a nitrile substrate displaces a hydroxide ligand found within the metal coordination sphere. The resulting metal-bound imminol intermediate is hydrolysed to generate the amide product. Mitra and Holz (2007) showed that the enzyme produced by *Pseudomonas thermophilia* JCM 3095 was stabilized by βTyr 68 which when deprotonated, hydrogen bonded with βTrp 72 and Ser 112. The abstraction of a proton from a nucleophilic water molecule then resulted in activation of the metal-bound nitrile for attack. Hydration of nitriles using platinum (II), rhodium (II), rhuthenium (II), cobalt (II) as well as nickel (0) supports the inner-sphere mechanism.

In the outer-sphere mechanism, a metal-bound hydroxide molecule participates in a nucleophilic attack on the nitrile, thus resulting in the formation of a transient immonilate species which is O-bonded to the metal. This undergoes rearrangement to generate the resulting amide.

Finally, in the second-outer-sphere mechanism, the metal-bound hydroxide causes deprotonation of a water molecule which carries out hydrolysis of the nitrile substrate.

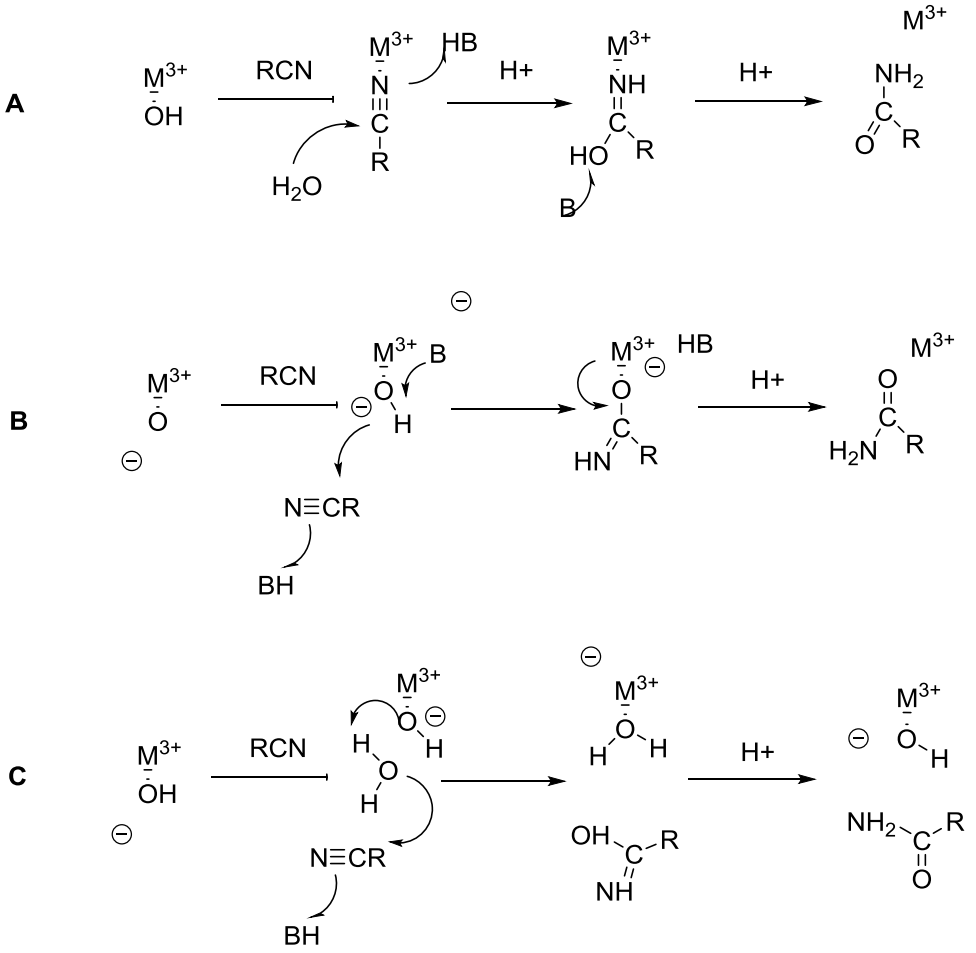


Figure 2.21: Nitrile hydratase reaction mechanisms

(A)- inner-sphere; (B)- outer-sphere; (C)- second outer-sphere mechanism. The image above was adapted from the image generated by Huang *et al.* (1997) and is adapted from Mascharak (2001).

2.2.6.5 Nitrile Hydratase Substrate, Inducers and Operational Parameters

Nitrile hydratase enzymes can be classified on the basis of their substrate specificity profiles. Some show preference for aromatic, aliphatic and indoleacetonitriles, while others catalyse the hydration of alkyl nitrile substrates. Most of these enzymes are inducible by nature with the reaction product rather than the substrate initiating gene expression. As shown in Table 2.4, methacrylamide addition was found to induce nitrile hydratase activity in *Pseudomonas chlororaphis* B23, *Pseudonocardia thermophilia* JCM3095 and *Rhodococcus equi* A4 as well.

Constitutive nitrile hydratase expression systems include those produced by *Rhodococcus* sp. N771, *Rhodococcus* N774, *Bacillus pallidus* Dac521, and *Brevibacterium* sp. R312 (Table 2.4).

Finally, as mentioned previously, *R. rhodochous* strain J1 has been found to generate two different nitrile hydratase enzymes with both enzymes showing considerable differences in their pH, temperature as well as induction profiles.

Table 2.4: Characteristics of purified nitrile hydratase enzymes.

Substrate class	Organism	Expression	Inducer	pH optimum/ Temp stability (°C)	Reference
Aromatic	*R. rhodochrous J1* -LMW Nitrile hydratase	Induced	cyclohexanecarboxamide	8.8 / 40	Wieser *et al.* 1998
Aromatic and Aliphatic	*Rhodococcus sp. YH3-3*	Induced	Nitrile/ amide/ aldoxime	-	Kato *et al.* 1999
	R. erythropolis JCM6823	Induced	ε- caprolactum	-	Duran *et al.* 1993
Aliphatic	*Arthrobacter* sp. Strain J1	Induced	Acetamide	7.0-7.2 / 35	Asano *et al.* 1982
	Brevibacterium sp. R312	Constitutive	-	7.8 / 25	Nagasawa *et al.* 1989
	Corynebacterium sp. C5	Induced	Isobutyronitrile	8.0- 8.5 / -	Tani *et al.* 1989
	Pseudomonas chloroaphis B23	Induced	Methacrylamide	7.5 / 20	Nagasawa *et al.* 1987; Nishiyama *et al.* 1991
	Pseudomonas putida NRRL 18668	Induced	Butyronitrile	7.2-7.8 / -	Payne *et al.* 1997
	Pseudonocardia thermophila JCM3095	Induced	Methacrylamide	- / 60	Yamaki *et al.* 1997
	Rhodococcus sp. N771	Constitutive	-	7.8 / 30	Yamada and Kobayashi. 1996
	Rhodococcus sp. N774	Constitutive	-	7.7 / 35	Endo and Watanabe, 1989
	R. rhodochrous J1 HMW Nitrile hydratase	Induced	Urea	6.5-6.8 / 35	Nagasawa *et al.* 1991
	Bacillus pallidus Dac521	Constitutive	-	/ 55	Cramp and Cowan. 1999
Chiral	*Agrobacterium tumefaciens* d3	Induced	Phenylacetonitrile	7.0/ 40	Bauer *et al.*1994
	Rhodococcus equi A4	Induced	Methacylamide	7.5 / 32-35	Prepechalova *et al.* 2001
Indoleaceto nitrile	*Agrobacterium tumefaciens* IAMB-261	Induced	Pivalamide	7.5 / -	Kobayashi *et al.* 1995

Alkylnitrile	*Bacillus pallidus* RAPc8	-	-	7.0 / 60	Pereira *et al.* 1998

2.2.6.6 Nitrile Hydratase Active Site Residues

Nitrile hydratase active site residues are located on the α-subunit of the enzyme with the amino acid sequence often highly conserved (Fig. 2.22). Experimental X-ray crystallography studies done on the enzyme from *Pseudonocardia thermophilia* JCM3095 suggested that both substrate and product transport takes place through a channel located along α and β subunit interface (Huang *et al.* 1997). A number of hydrophobic amino acid residues line the walls of this channel. These include Phe 37, Pro 38, Phe 41, Leu 48, Phe 51, Arg 52, Ile 55, Tyr 68, Trp 72, Phe 118, Ala 122, and Leu 127 (present on the β subunit) and Leu 88, Gln 89 and Trp 116 (present on the α subunit) (Huang *et al.* 1997; Song *et al.* 2007; Tastin-Bishop and Sewell. 2006; Peplowski *et al.* 2008).

The architecture of the channel was found to play a vital role in fine tuning the stereoselectivity of the catalyst while determining the enzymes substrate affinity profile (see Table 2.5 for the list of contributing amino acids). The β-subunit sequence was found to be more variable.

2.2.6.7 Nitrile Hydratase Gene Location and Regulation of Expression

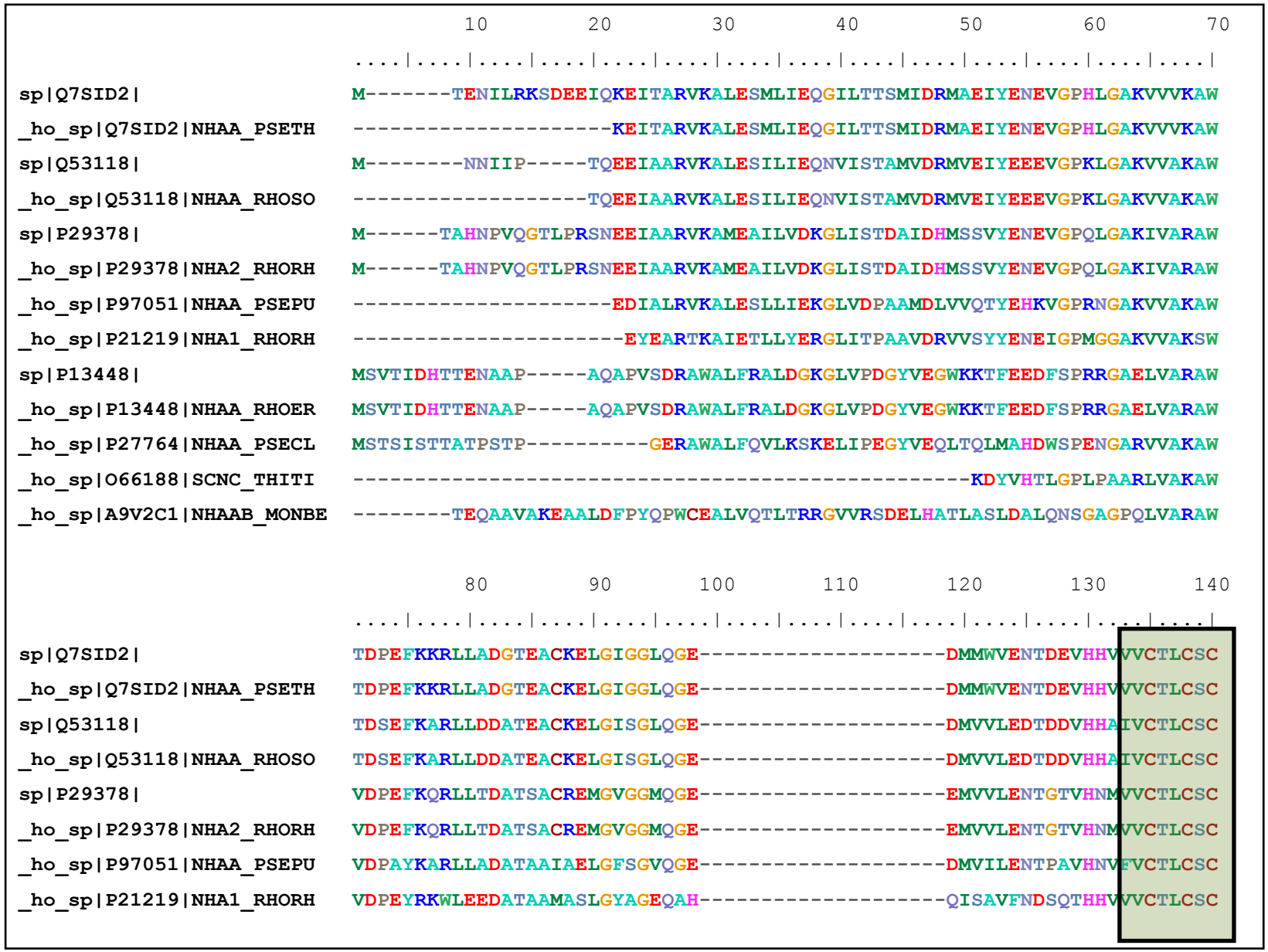
Both nitrile hydratase and amidase enzyme genes are often located in close proximity to each other suggesting that these enzymes may exist in the same operon (Mayaux *et al.* 1990). Structural genes are found adjacent on the same operon and are under the control of the same activator protein.

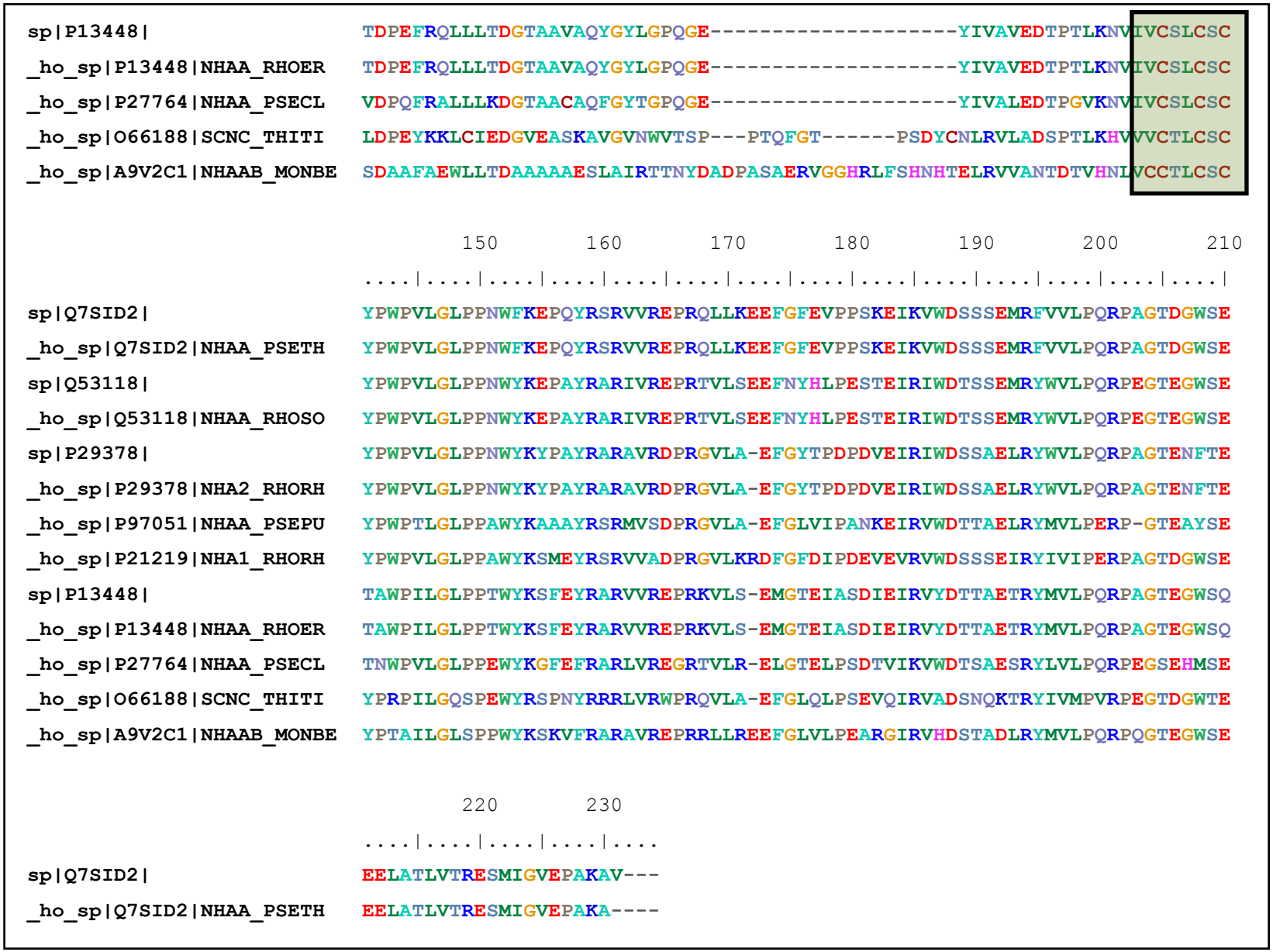
Nitrile hydratase genes consist of both the alpha and the beta subunit which are coded on two adjacent but separate open reading frames (ORFs). These ORFs are usually separated by a few base pairs and are characteristically similar in arrangement with most α-subunit ORFs located downstream to the β-subunit ORF (Komeda *et al.* 1996; Kim and Oriel. 2000). Exceptions have been located in the nitrile hydratase operon sequenced from *Pseudomonas putida* 5B, *Rhodococcus* sp. N771, and *Pseudomonas chlororaphis* B23, where the α-subunit ORF is upstream to the β-subunit (Wu *et al.* 1997; Nojiri, *et al.* 1999; Nishiyama *et al.* 1991).

Nitrile hydratase operons often consist of five to seven genes, with the number and variety of genes depending on the species being investigated. Typical genes located include nhr2 (nitrile hydratase regulator 2); *nhr*1 (nitrile hydratase regulator 1); *ami* (amidase); *nha*1 (nitrile hydratase α-subunit); *nha*2 (nitrile hydratase β-subunit); and *nh*3 (nitrile hydratase regulator) (Fig. 2.23)

However, the operon in *Bacillus pallidus* RAPC8 also includes a cobalamin biosynthesis gene implicated in cobalt ion transportation into the cell (cbiM, cbiN, cbiQ, cbiO). This has been shown to be crucial, since incorporation of the low-spin metal ion and formation of the metal coordination sphere, is necessary for activation of the nitrile hydratase enzyme (Fig. 2.23) (Cameron *et al.* 2005).

Finally, nitrile hydratase gene induction can be achieved by amide and nitrile addition during cell cultivation (Gradley *et al.* 1994).


10 20 30 40 50 60 70
sp|Q7SID2|
_ho_sp|Q7SID2|NHAA_PSETH
sp|Q53118|
_ho_sp|Q53118|NHAA_RHOSO
sp|P29378|
_ho_sp|P29378|NHA2_RHORH
_ho_sp|P97051|NHAA_PSEPU
_ho_sp|P21219|NHA1_RHORH
sp|P13448|
_ho_sp|P13448|NHAA_RHOER
_ho_sp|P27764|NHAA_PSECL
_ho_sp|O66188|SCNC_THITI
_ho_sp|A9V2C1|NHAAB_MONBE
80 90 100 110 120 130 140
sp|Q7SID2|
_ho_sp|Q7SID2|NHAA_PSETH
sp|Q53118|
_ho_sp|Q53118|NHAA_RHOSO
sp|P29378|
_ho_sp|P29378|NHA2_RHORH
_ho_sp|P97051|NHAA_PSEPU
_ho_sp|P21219|NHA1_RHORH


sp|P13448|
_ho_sp|P13448|NHAA_RHOER
_ho_sp|P27764|NHAA_PSECL
_ho_sp|O66188|SCNC_THITI
_ho_sp|A9V2C1|NHAAB_MONBE
150
160
170
180
190
200
210
sp|Q7SID2|
_ho_sp|Q7SID2|NHAA_PSETH
sp|Q53118|
_ho_sp|Q53118|NHAA_RHOSO
sp|P29378|
_ho_sp|P29378|NHA2_RHORH
_ho_sp|P97051|NHAA_PSEPU
_ho_sp|P21219|NHA1_RHORH
sp|P13448|
_ho_sp|P13448|NHAA_RHOER
_ho_sp|P27764|NHAA_PSECL
_ho_sp|O66188|SCNC_THITI
_ho_sp|A9V2C1|NHAAB_MONBE
220
230
sp|Q7SID2|
_ho_sp|Q7SID2|NHAA_PSETH

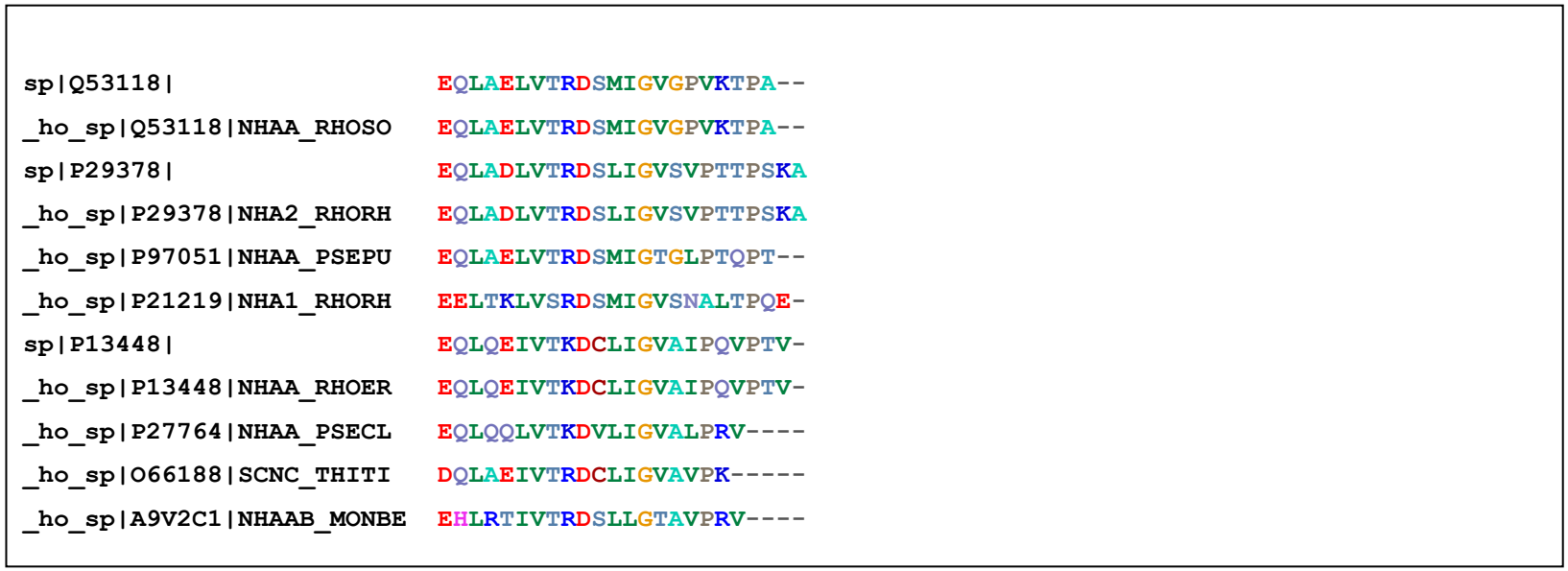


Figure 2.22: Nitrile hydratase α-subunit amino acid sequence alignment.

Highlighted region shows the highly conserved region involved in the binding of the metal-ion. **Q7SID2**- nitrile hydratase α-subunit from *Pseudomonas thermophilia* (Co centered); **Q531181** nitrile hydratase α-subunit- *Rhodococcus* sp. (Fe centered) ; **P29378**-nitrile hydratase α-subunit from *R. rhodochrous* ; **P97051**- nitrile hydratase α-subunit from *Pseudomonas putida* (Co centered); **P21219**- HMW nitrile hydratase (Co centered) from *R. rhodochrous*; **P13448**-nitrile hydratase α-subunit from *R. erythropolis* (Fe centered); **P27764**- nitrile hydratase α-subunit from *Pseudomonas chloroaphis* ; **O66188**- Uncharacterised protein ; **A9V2C1**- probable nitrile hydratase from *Monosiya brevicolis* (possibly Fe centered). MAFFT online was used to complete sequence alignments with iterative processing of the completed sequences done using Bioedit.

.

Table 2.5: Amino acid residues located at the α and β interface of nitrile hydratase produced by *Pseudonocardia thermophila* JCM3095

Amino acid residue (position)	Amino acid characteristic	Subunit location	Residue Location and/or Function	Reference
Phe 37	Aromatic/ Hydrophobic	β	Formation of hydrophobic pocket. Affects substrate acceptance. Plays a role in stereoselectivity.	Miyanaga *et al.* 2004: Peplowski *et al.* 2008
Pro 38	Hydrophobic	β	Substrate channel amino acid	Huang *et al.* 1997
Phe 41	Aromatic/ Hydrophobic	β	Substrate channel amino acid	Huang *et al.* 1997
Leu 48	Aromatic/ Hydrophobic		Formation of hydrophobic pocket	Miyanaga *et al.* 2001
Phe 51	Aromatic/ Hydrophobic	β	Formation of hydrophobic pocket	Miyanaga *et al.* 2001
Arg 52	Basic/ Hydrophilic	β	Forms $^{+}$H bond with the oxygen atoms of Cys-SO_2H111 and Cys-SOH113	Piersma *et al.* 2000; Endo *et .l*. 2001
Ile 55	Hydrophobic	β	Substrate channel amino acid	Huang *et al.* 1997
Tyr 68	Aromatic/ Hydrophilic	β	Responsible for catalytic activity and substrate binding	Takarada *et al*. 2006; Mitra and Holz. 2007
Trp 72	Aromatic/ Hydrophobic	β	Formation of hydrophobic pocket	Miyanaga *et al.* 2001
Ser 112	Nucleophilic/ Hydrophilic	α	Part of the proposed catalytic triad, functioning as a general base	Mitra and Holz, 2007
Phe 118	Aromatic/ Hydrophobic	β	Substrate channel amino acid	Huang *et al.* 1997
Ala 122	Small/ Hydrophobic	β	Substrate channel amino acids	Huang *et al.* 1997
Leu 127	Hydrophobic	β	Substrate channel amino acids	Huang *et al.* 1997
Arg 157	Basic/ Hydrophilic		Forms +H bond with the oxygen atoms of Cys-SO_2H 111 and Cys-SOH 113	Piersma *et al.* 2000; Endo *et al.* 2001
Leu 88	Hydrophobic	α	Substrate channel amino acids	Huang *et al.* 1997
Gln 89	Amide/ Hydrophobic	α	Responsible for catalytic activity, and $^{+}$H bonding with metal	Takarada *et al*. 2006; Mitra and Holz. 2007

Trp 116	Aromatic/ Hydrophobic	α	Substrate channel amino acids	Huang *et al.* 1997

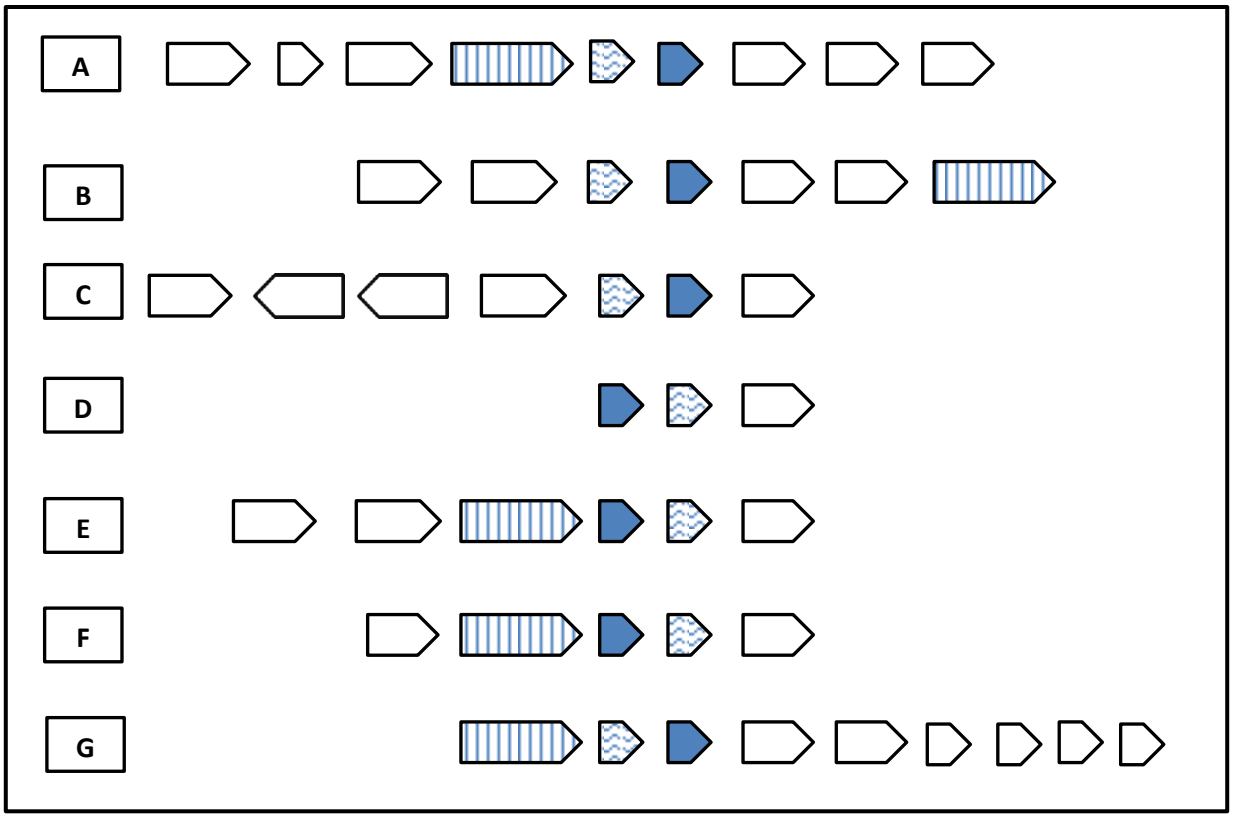


Figure 2.23: Nitrile hydratase genetic cluster organisation in varied microorganisms.

The direction of gene transcription is indicated by the direction of the arrow. The amidase gene in the image is represented by verticle blue lines; those showing the α-subunit have been shaded as a solid fill in blue; while the β-subunit is shown as a wavy line. Those not shaded show the presence of ORFs as well as regulatory genes. **A-** *R. erythropolis* strain AJ 270, **B-** *R. rhodochrous* J1 HMW-nitrile hydratase; **C-** *R. rhodochrous J1* LMW-nitrile hydratase; **D-** *Pseudomonas putida* 5B; **E-** *Rhodococcus* sp-N771; **F**-*Pseudomonas chlororaphis* B23; and **G-** *Bacillus pallidus* RAPc8.

2.3 References

Almatawah, Q. A., and Cowan, D. A. Thermostable nitrilase catalyzed production of nicotinic acid from 3-cyanopyridine. (1999). Enzyme. Microb. Technol. 25: 718-724.

Asano, Y., Fujishiro, K., Tany, Y. and Yamada, H. Aliphatic nitrile hydratase from *Arthrobacter* sp. J-1: purification and characterization. (1982). Agric. Biol. Chem. **46**: 1165-1174.

Bandyopadhyay, A. K., Nagasawa, T., Asano, Y., Fujishiro, K., Tani, Y. and Yamada, H. Purification and characterisation of benzonitrilases from *Arthrobacter* sp. Strain J-1. (1986). Appl. Environ. Microbiol. **51**: 302-306.

Banerjee, A., Sharma, R. and Banerjee, U. C. The nitrile-degrading enzymes: current status and future prospects. (2002). Appl. Microbiol. Biotechnol. **60**: 33-44.

Bartling, D., Seedorf, M., Mithofer, A., and Weiser, E. W. Cloning and expression of an *Arabidopsis* nitrilase which can convert indole-3-acetonitrile to the plant hormone, indole-3-acetic acid. (1992). Eur. J. Biochem. **205:** 417-424.

Bauer, R., Knackmuss, H-J. and Stolz, A. Enantioselective hydration of 2-arylpropionitriles by a nitrile hydratase from *Agrobacterium tumefaciens* strain d3. (1997). Appl. Microbiol. Biotechnol. **49**: 89-95.

Bhalla, T. C., Miura, A., Wakamoto, A., Ohba, Y., Furuhashi, K. *(1992).* Asymmetric hydrolysis of alpha-aminonitriles to optically active amino acids by a nitrilase of *R. rhodochrous PA-34.* (1992). Microbiol.Biotechnol. **37***:* 184-190.

Bonnet, D., Artaud, I., Moali, C., Petre, D. amd Mansuy, D. Highly efficient control of iron-containing nitrile hydratases by stoichiometric amounts of nitric oxide and light. (1997). FEBS Lett. **409**: 216-220.

Brenner, C. Catalysis in the nitrilase superfamily (2002). Curr. Opin. Struct .Biol. **12**: 775-782.

Cameron, R. A., Sayed, M and Cowan, D. A. Molecular analysis of the nitrile catabolism operon of the thermophile *Bacillus pallidus* RAPc8. (2005). Biochim. Biophys. Acta. **30**: 35-46.

Chauhan, S., Wu, S., Blumerman, W. S., Fallon, R. D., Gavagan, J. E., DiCosimo, R. and Payne, M. S. Purification, cloning, sequencing and over-expression in *Escherichia coli* of a regioselective aliphatic nitrilase from *Acidovorax facilis* 72W. (2003). Appl. Microbiol. Biotechnol. **61**:118-122.

Chen, C., Chiu, W., Liu, J., Hsu, W. and Wang, W. Structural basis for catalysis and substrate specificity of *Agrobacterium radiobacter* N-carbamoyl-D-amino acid amidohydrolase. (2003). J. Biol.Chem. **278**: 16194-26201.

Cramp, R. A. and Cowan, D. A.. Molecular characterisation of a novel thermophilic nitrile hydratase (1999). BBA-Proteins Proteom. **1431**: 249-260.

Dobson, C. M. The structural basis of protein folding and its link with human disease. (2001). Philos. Trans. R. Soc. Lond. B. Biol. Sci. **356**: 133-145.

Dorr, P and Knowles, C.. Cyanide oxygenase and cyanase activities of *Pseudomonas fluorescens* NCIMB 11764. (1989). FEMS Microbiol. Lett. **60**: 289-294.

Dhillon, J. K. and Shivaraman, N.. Biodegradation of canide compounds by a *Pseudomonas* species S1. (1999). Microbiol. **45**: 201-208.

Duran, R., Nishiyama, M., Horinouchi, S. and Beppu, T. Characterization of nitrile hydratase genes cloned by DNA screening from *Rhodococcus erythropolis*. (1993). Biosci. Biotech. Bioch. **57** : 1323-1328.

Endo, T. and Watanabe, I. Nitrile hydratase of *Rhodococcus* sp. N-774- Purification and amino acid sequences. (1989). FEBS Letters. **243** : 61-64.

Endo, I., Nojiri, M., Tsujishima, M., Nakasako, M., Nagashima, S., Yohda, M...Fe-type nitrile hydratase. (2001). J. Inorg. Biochem. **83**: 247-253.

Fernandes, B. C. M., Mateo, C., Kiziak, C., Chmura, A., Wacker, J., Rantwijk, F-van, Stolz, A. and Sheldon, R. A. Nitrile hydratase activity of a recombinant nitrilase. (2006). Adv. Synth. Catal. **348**: 2597-2603.

Fischer, K., Dilworth, M. J., Kim, C-H. and Newton, W. E. *Azotobacter vinelandii* nitrogenases containing altered MoFe proteins with substitutions in the FeMo-Cofactor environments: Effects on the catalysed reduction of acetylene and ethylene. (2000). Biochemistry. **39**: 2970-2979.

Frederick J. (2013). *Genetic characterization of Rhodococcus rhodochrous ATCC BAA-870 with emphasis on nitrile degrading enzymes*. PhD thesis. UCT Libraries (www.lib.uct.ac.za).

Garel, J. Folding of large proteins: multidomain and multisubunit proteins. In: Creishton. T. E., editor. Protein Folding. New York. W. H. Freeman and Company; 1992. 405-454.

Gavagan, J. E., DiCosimo, R., Eisenberg, A., Fager, S. K., Folsom, P. W., Hahn, E. C., Shneider, K. J., and Fallon, R. D. A gram-negative bacterium producing a heat-stable nitrilase highly active on aliphatic dinitriles. (1999). Appl. Microbiol. Biotechnol. **52**: 654-659.

Goldlust, A., and Bohak, Z. Induction, purification, and characterization of the nitrilase of *Fusarium oxysporum* f.sp *melonis*. (1989). Biotechnol. Appl. Biochem. **11**: 58-601.

Gradley, M. L., Deverson, C. J. F., and Knowles, C. J. Asymmetric hydrolysis of R-(-)-S (+)-2-methylbutyronitrile by *Rhodococcus rhodochrous* NCIMB 11216. (1994). Arch. Microbiol. **161**; 246-251.

Grantcharova, V., Alm, E. J., Baker, D. and Horwich, A. L. Mechanisms of protein folding (2001). Curr. Opin. Struct. Biol. **1**: 70-82.

Hagel, P., Gerding, J. J. T., Fieggen, W., and Bloemendal, H. Cyanate formation in solutions of urea. (1971). Biochem. Biophys. Acta. **243**: 366-373.

Hardy, R. W. F., and Knight, E. ATP-dependent reduction of azide and HCN by N_2 fixing enzymes of *Azotobacter vinelandii* and *Clostridium pasteurianum.* (1967). Biochim. Biophys. Acta. **139**: 69-90.

Harper D. B. Fungal degradation of aromatic nitriles: enzymology of C-N cleavage by *Fusarium solani*. (1977). Biochem. J. **167**: 685-692.

Harper, D. B. Characterization of a nitrilase from *Nocardia sp.* (*Rhodococcus* group) NCIB 11215, using p-hydroxybenzonitrile as sole carbon source. (1985). Int. J. Biochem. **17**: 677-683.

Harrop, T. C. and Mascharak, P. K. Fe(III) and Co(III) centers with carboxamido nitrogen and modified sulfur coordination: Lessons learned from nitrile hydratase. (2004). Acc. Chem. Res. **37**: 253-260.

Hashimoto, Y., Nishiyama, M., Horinouchi, S. and Beppu, T. Nitrile hydratase gene from *Rhodococcus* sp. N-774 requirement for its downstream region for efficient expression. (1994). Biosci. Biotech. and Bioch. **58**: 1859-1865.

Heinemann, U., Engels, D., Burger, S., Kiziak, C., Mattes, R., and Stolz, A. Cloning of a nitrilase gene from the cyanobacterium *Synchocystis* sp. Strain PCC6803 and heterologous expression and characterization of the encoded protein. (2003). Appl. Environ. Microbiol. **69**: 4359-4366.

Hoyle, A. J., Bunch, A. W., and Knowles, C. J. The nitrilases of *Rhodococcus rhodochrous* NCIMB 11216. (1998). Enzyme. Microb. Technol. **23**: 475-482.

Huang, W., Jia, J., Cummings, J., Nelson, M., Schneider, G. and Lindqvist, Y. Crystal structures nitrile hydratase reveals a novel iron centre in a novel fold. (1997). Structure. **5**: pp 691-699.

Hunt, J. F., Weaver, A. J., Landry, S. J., Gierasch, L. and Deisenhofer, J. The crystal structure of the GroES co-chaperonin at 2.8A resolution. (1996). Nature. **379**: 37-45.

Ikehata, O., Nishiyama, M., Horinouchi, S. and Beppu, T. Primary structure of nitrile hydratase deduced from the nucleotide sequence of a *Rhodococcus* species and its expression in *Escherichia coli*. (1989). Eur. J. Biochem. **181**: 563-570.

Ingvorsen, K., Hijer-Pedersen, B. and Godtfredsen, S. Novel cyanide hydrolysing enzyme from *Alcaligenes xyloxidans* subsp. denitrificans (1991). Appl. Environ. Microbiol. **57**: 1783-1789.

Kato, Y., Tsuda, T. and Asano, Y. Nitrile hydratase involved in aldoxime metabolism from *Rhodococcus* sp. Strain YH3-3 purification and characterization. (1999). Eur. J. Biochem. **263** : 662-670.

Kato, Y, Nakamura, K., Sakiyama, H., Mayhew, S. G., and Asano, Y. Novel heme-containing lyase, phenacetaldoxime dehydratase from *Bacillus* sp. Strain OxB-1 purification, characterization, and molecular cloning of the gene. (2000). Biochemistry-US. **39**: 800-809.

Kato, Y., Ooi, R and Asano, Y. Distribution of aldoxime dehydratase in microorganisms. (2000). Appl. Environ. Microbiol. **66** : 2290-2296.

Kato, Y., Yoshida, S., Xie, S.-X., and Asano, Y. Aldoxime dehydratase co-existing with nitrile hydratase and amidase in the iron-type nitrile hydratase-producer *Rhodococcus* sp. N-771. (2004). J. Biosci. Bioeng. **97**: 250-259.

Kato, Y. and Asano, Y. Molecular and enzymatic analysis of the'aldoxime and nitrile pathway' in the glutaronitrile degrader *Pseudomonas* sp K-9. (2006). Appl. Microbiol. Biotechnol. **70** : 92-101.

Kiziak, C., Conradt, D., Stolz, A., Mattes, R., and Klein, J. Nitrilase from *Pseudomonas fluorescens* EBC191: cloning and heterologous expression of the gene and bio-chemical characterization of the recombinant enzyme. (2005). Microbiol. **151**: 3639- 3648.

Kobayashi, M., Nagasawa, T., and Yamada, H. Nitrilase of *Rhodococcus rhodochrous* J1: Purification and characterization. (1989). Eur. J. Biochem. **182**: 349-356.

Kobayashi, M., Yanaka, N., Nagasawa, T. and Yamada, H. Purification and characterization of a novel nitrilase of *Rhodococcus rhodochrous* K22 that acts on aliphatic nitriles. (1990). J. Bacteriol. **172**: 4807-4815.

Kobayashi, M., Nishiyama, M., Nagasawa, T., Horinouchi, S., Beppu, T. and Yamada, H. Cloning, nucleotide sequence and expression in *Escherichia coli* of two cobalt-containing nitrile hydratase genes from *Rhodococcus rhodochrous* J1. (1991). BBA-Proteins Proteom . **1129**: 23-33.

Kobayashi, M., Yanaka, N., Nagasawa, T. and Yamada, H. Primary structure of an aliphatic nitrile-degrading enzyme, aliphatic nitrilase, from *Rhodococcus rhodochrous* K22 and expression of its gene and identification of the active site residue. (1992a). Biochem. **31**: 9000-9007.

Kobayashi, M., Nagasawa, T. and Yamada, H. Enzymatic synthesis of acrylamide: a success story not yet over. (1992b). Trends Biotechnol. **10**: 402-408.

Kobayashi, M., Izui, H., Nagasawa, T. and Yamada, H. Nitrilase in biosynthesis of the plant hormone indole-3-acetic acid from indole-3-acetonitrile: cloning of the *Alcaligenes* gene and site-directed mutagenesis of cysteine residues. (1993). Proc. Nat. Acad. Sci. USA. **90**:247-251.

Kobayashi, M., Goda, M. and Shimizu, S. Nitrilase catalyzes amide hydrolysis as well as nitrile hydrolysis. (1998). Biochem. Biophys. Res. Commun. **30**: 662-666.

Kobayashi, K., Yoshioka, S., Kato. Y. and Asano, S. Regulation of aldoxime dehydratase activity by redox-dependent change in the coordination structure of the aldoxime-heme complex (2005). J. Biol. Chem. **280**: 5486-5490.

Kumaran, D., Eswaramoorthy, S., Gerchman, S. E., Kycia, H., Studier, F. W. and Swaminathan, S. Crystal structure of a putative CN hydrolase from yeast. (2003). Struct. Func, Genet. **52**: 283-291.

Kunz, D. A., Wang, C-S. and Chen, J-L. Alternative routes of enzymic cyanide metabolism in *Pseudomonas fluorescens* NCIMB 11764. (1994). Microbiology. **140**: 1705-1712.

Layh, N., Paratt, J. and A. Willets. Characterization and partial purification of an enantioselective arylacetonitrilase from *Pseudomonas fluorescens* DSM 7155. (1998). J. Mol. Catal. B. Enzym. **5**: 467-474.

Lévi-Schil, S., Soubrier, F., Crutz-le Coq, A. M., Faucher, D., Crouzet, J. and Petre, D. Aliphatic nitrilase from a soil-isolated *Comomonas testosteroni* sp: gene cloning and over expression, purification and primary structure. (1995). Gene. **161**: 15-20.

Li, J-G., Burgess, B. K. and Corbin, J. L. (1982). Nitrogenase reactivity: cyanide as substrate and inhibitor. Biochemistry-US. **21**: 4393-4402.

Liu, Y., Cui, W., Xia, Y., Cui, Y., Kobayashi, M. and Zhou, Z. Self-subunit swapping occurs in another gene type of cobalt nitrile hydratase. (2012). PLOS ONE. **7** (11): e50829 pp 1-9.

Maier-Greiner, H., Obermaier-Skrobranek, B. M., Estermaier, L. M., Kammerloher, W., Freund, C., Wülfing, C., Burkert, U. I., Matern, H., Breuer, M. and Eulitz, M. Isolation and properties of a nitrile hydratase from the soil fungus *Myrothecium verrucaria* that is highly specific for the fertilizer cyanamide and cloning of its gene. (1991). Proc. Natl. Acad. Sci. USA. **88** (10): pp 4260-4264.

Mande, S. C., Mehra, V., Bloom, B. R. and Hol, W. G. Structure of the heat shock protein chaperonin-10 of *Mycobacterium leprae*. (1996). Science. **271**: pp 203-207.

Martinkova, L., and Kren, V. Biotransformations with nitrilases. (2010). V. Curr. Opin. Chem. Biol. **14**: pp 130-137.

Massey, V. and Palmer, G. On the existence of spectrally distinct classes of flavoprotein semiquinones. A new method for the quantitative production of flavoproten semiquinones. (1966) Biochemistry-US. **5**: 3181-3189.

Matthews, C. N., and Minard, R. D. Hydrogen cyanide polymers, comets and the origin of life. (2006). Faraday Discuss.**133**: 393-401.

Mayaux, J. F., Cerebelaud, E., Soubrier, F., Faucher, D. and Pétré, D. Purification, cloning, and primary structure of an enantiomer-selective amidase from Brevibacterium sp. Strain R312: structural evidence for genetic coupling with nitrile hydratase. (1990). J. Bacteriol. **172**: 6764-6773

Meyers, P. R., Rawlings, D. E., Woods, D. R. and Lindsey, G. G. Isolation and characterization of a cyanide dihydratase from *Bacillus pumilus* C1. (1993). J. Bacteriol. **175**: 6105-6112.

Miller, A. G., and Espie, G. S. The photosynthetic metabolism of cyanate by the cyanobacteriums *Synechococcus* TEX625. Arch. Microbiol. (1994). **162**: 151-159.

Mitra, S., Holz, R. C. Unraveliing the catalytic mechanism of nitrile hydratase. (2007). J. Biol. Chem. **282**: 7397-7404.

Miyanaga, A., Fushinobu, S., Ito, K. and Wakagi, T. Crystal structure of Co-type nitrile hydratase from *Pseudonocardia thermophilia*. (2001). Biochem. Biophys. Res. Commun. **288**: 1169-1174.

Mueller, P., Egarova, K., Vorgais, E. C., Boutou, E., Trauthwein, H., Verseck, S. and Atranikian, G. Cloning, expression and characterisation of a thermoactive nitrilase from the hyperthermophilic archaeon *Pyrococcus abysii*. (2006). Protein Expres. Purif. **47**: 672-681.

Nagasawa, T., Ryuno, K. and Yamada, H. Nitrile hydratase of *Brevibacterium* R312-purification and characterization. (1986). Biochem. Biophys. Res. Commun. **139**: 1305-1312.

Nagasawa, T., Nanba, H., Ryuno, K., Takeuchi, K. and Yamada, H. Nitrile hydratase of *Pseudomonas chloroaphis* B23. Purification and characterization. (1987). Eur. J. Biochem. **162**: 691-698.

Nagasawa, T., Mathew, C. D., Mauger, J. and Yamada, H. Nitrile hydratase-catalyzed production of nicotinamide from 3-cyanopyridine in *Rhodococcus rhodochrous* J1. (1988). Appl. Environ. Microbiol. **54** : 1766-1769.

Nagasawa, T., Mauger, J., and Yamada, H. A novel nitrilase, arylacetonitrilase, of *Alcaligenes faecalis* JM3: Purification and characterization. (1990). Eur. J. Biochem. **194**: 765-772.

Nagasawa, T., Takeuchi, K. and Yamada, H. Characterization of a new cobalt-containing nitrile hydratase purified from urea-induced cells of *Rhodococcus rhodochrous* J1. (1991). FEBS Journal. **196**: 581-589.

Nagasawa, T., Wieser, M., Nakamura, T., Iwahara, H., Yoshida, T and Gekko, K. Nitrilase of *Rhodococcus rhodochrous* J1: Conversion into active form by subunit association. (2000). Eur. J. Biochem. **267**: 138-144.

Nagashima, S., Nakasako, M., Dohmae, N., Tsujimura, M., Takio, K., Odaka, M., Yohda, M., Kamiya, N. and Endo, I. Novel non-heme iron center of nitrile hydratase with a claw setting of oxygen atoms. (1998). Nat. Struct. and Mol. Biol. **5**: 347-351.

Nagayama K. and Danev, R. Phase contract electron microscopy: development of thin-film phase plates and biological applicatons. (2008). Phil. Trans. R. Soc. B. **363**: 2153-2162.

Nakai, T., Hasegawa, T., Yamashita, E., Yamamoto, M., Kumasaka, T., Ueki, T., Nanba, H., Ikenaka, Y., Takahashi, Sato, M. and Tsukihara, T. Crystal structure of *N*-carbamyl-D-amino acid amidohydrolase with a novel catalytic framework common to amidohydrolases. (2000). Structure. **8**: 729-737

Nishiyama, M., Horinouchi, S., Kobayashi, M., Nagasawa, T., Yamada, H. and Beppu, T. Cloning and characterization of genes responsible for metabolism of nitrile compouds from *Pseudomonas chloroaphis* B23. (1991). J. Bacteriol. **173** : 2465-2472.

Noguchi, T., Honda, J., Nagamune, T., Sasabe, H., Inoue, Y. and Endo, I. Photosensitive nitrile hydratase intrinsically possesses nitric oxide bound to the non-heme iron center: evidence by Fourier transform infrared spectroscopy. (1995). FEBS Lett. 358 (**1**): 9-12.

Nojiri, M., Yohda, M., Odaka, M., Matsushita, Y., Tsujimura, M., Yoshida, T., Dohmae, N., Takio, K., and Endo, I. Functional expression of nitrile hydratase in *Escherichia coli*: requirement of a Nitrile hydratase activator and post translational modification of a ligand cysteine. (1999). J. Biochem. **125**: 696-704.

Novo, C., Farnaud, S., Tat, R., Clemente, A and Brown, P. R. Support for the three-dimensional structure predicting a Cys-Glu-Lys catalytic triad for *Pseudomonas aeruginosa* amidase comes from site-directed mutagenesis and mutations altering substrate specificity (2002). Biochem. J. **365**: 731-738.

Odaka, M., Fujii, K., Hoshino, M., Noguchi, T., Tsujimura, M., Nagashima, S., Yohda, M., Nagamune, T., Inoue. and Endo, I. Activity regulation of photoreactive nitrile hydratase by nitric oxide (1997). J. Am. Chem. Soc. **119** : 3785-3791.

Oro, J. Mechanism of synthesis of adenine from hydrogen cyanide under possible primitive Earth conditions. (1980). Nature. **191:** 1193–1194.

Osswald, S., Wajant, H. and Effenberger, F. Characterization and synthetic applications of recombinant AtNIT1 from *Arabidopsis thaliana*. (2002). Eur. J. Biochem. **269**: 680-687.

Pace, H. C., and C. Brenner. The nitrilase superfamily: classification structure and function. (2001). Genome Biol. **2**: reviews 0001.1-0001.9.

Payne, M. S., Wu, S., Fallon, R. P. and Tudor, G. A stereoselective cobalt-containing nitrile hydratase. (1997). Biochem. **36**: 5447-5454.

Peplowski, L., Kubiak, K. and Nowak, W. Mechanical aspects of nitrile hydratase enzymatic activity. Steered molecular dynamics simulations of *Pseudonocardia thermophila* JCM 3095. (2008). Chem. Phys. Lett. **467**: 144-149.

Pereira R. A., Graham. D., Rainey, F. A. and Cowan, D. A novel nitrile hydratase and amidase from a thermophilic *Bacillus* isolate. (1998). Extremophiles. **2**: 347-357.

Piersma, S. R., Nojiri, M., Tsujimura, M., Noguchi, T., Okada, M., Yohda, M. Arginine 56 mutation in the beta subunit of nitrile hydratase: importance of hydrogen bonding to the non-heme iron center. (2000). J. Inorg. Biochem. **80**: 283-288.

Piotrowski. M., Schönfelder, S. and Weiler, E. W. The *Arabidopsis thaliana* isogene NIT4 and its orthologs in tabacco encode β-cyano-L-alanine hydratase/ nitrilase. (2001). The Journal of Biological Chemistry. **26:** 2616-2621.

Piotrowski M. Primary or secondary? Versatile nitrilases in plant metabolism. (2008). Phytochemistry **69**: 2655-2667.

Pollock, R. J., and Hersh, L. B. N-methylglutamate synthetase. The use of flavin monomucleotide in oxidative catalysis. (1973), J. Biol. Chem. **248**. 6724-6733.

Prepechalová, I., Martinkova, L., Stolz, A., Ovesná, M., Bezouska, K., Kopecký, J and Kren, V. Purification and characterization of the enantioselective nitrile hydratase from *Rhodococcus equi* A4. (2001). Appl. Microbiol. Biotech. **55**: 156-159.

Raczynska, J., Vorgias, C., Antranikian, G. and Rypniewski, W. Crystallographic structure of a thermoactive nitrilase. (2010). J. Struc. Biol. **173**: 294-302.

Ramteke, P., Maurice, N. G., Joseph, B. and Wadher, B. J. Nitrile-converting enzymes: An eco-friendly tool for industrial biocatalysis (2013). Biotechnol. Appl. Bioc. **60** : 459-481.

Riviera-Ortiz, J. M. and R. H. Burris, R. H. Interactions among substrates and inhibitors of nitrogenase. (1975). J. Bacteriol. **123** : 537-545.

Sawai, H., Sugimoto H., Kato, Y., Asano, Y., Shiro, Y. and Aono, S. (2009). X-ray crystal structure of Michaelis complex of aldoxime dehydratase. J. Biol. Chem. **284**: 32089- 32096.

Stalker, D. M., Malyj, L. D., and McBride, K. E. Purification and properties of a nitrilase specific for the herbicide bromoxynil and corresponding nucleotide sequence analysis of the bxn gene. (1988). J. Biol. Chem. **263**: 6310-6314.

Stevenson, D. E., Feng, R., Dumas, F., Groleau, D., Mihoc, A. and Storer, A. C. (1992). Mechanistic and structural studies on *Rhodococcus* ATCC 39484 nitrilase. Biotechnol. Appl. Biochem. **15**: 283-302.

Takarada, H., Kawano, Y., Hashimoto, K., Nakayama, H., Ueda, S. and Yohda, M...Mutational study on αGln90 of Fe-type nitrile hydratase from *Rhododcoccus* sp. N771. (2006). Biosci. Biotechnol. Biochem. **70**: 881-889.

Tani, Y., Kurihara, M. and Nishise, H. Characterization of nitrile hydratase and amidase, which are responsible for the conversion of dinitriles to mononitriles, from *Corynebacterium* sp (1989). Agric. Biol. Chem. **53** : 3151-3158.

Thuku, R.N. (2006). *The structure of the nitrilase from Rhodococcus rhodochrous J:1 Homology modelling and three-dimensional reconctruction.* Masters dissertation UCT Libraries (www.lib.uct.ac.za).

Thuku, R. N., Weber, B. W., Varsani, A., and Sewell, B. T. Post-translational cleavage of recombinantly expressed nitrilase from *Rhodococcus rhodochrous* J1 yields a stable, active helical form. (2007). FEBS J. **274**:2099-2018.

Wang, P., Matthews, D. and Van Etten, H. Purification and characterization of cyanide hydratase from phytopathogenic fungus *Gloeocercospora sorghi*. (1992). Arch. Biochem. Biophys. **298**: 569-575.

Watanabe, A., Yano, K., Ikebukuro, K. and Karube, I. Cyanide hydrolysis in a cyanide-degrading bacterium, *Pseudomonas stutzeri* AK61, by cyanidase. (1998). Microbiology. **144**: 1677-1682.

Weiser, M., Takeuchi, K., Wada, Y., Yamada, H. and Nagasawa, T. Low-molecular-mass nitrile hydratase from *Rhodococcus rhodochrous* J1: purification, substrate selectivity and comparison with the analogous high-molecular-mass enzyme. (1998). FEMS Microbiol. Lett. **169**: 17-22.

Wu, S., Fallon, R. D. and Payne, M. S. Over-production of stereoselective nitrile hydratase from Pseudomonas putida 5B in Escherichia coli: activity requires a novel downstream potein. (1997). Appl. Microbial Biotechnol. **48:** 704-708.

Yamada, H and Kobayashi, M. Nitrile hydratase and its application to industrial production of acrylamide. (1996). Biosci. Biotechnol. Biochem. **60**: 1391-1400.

Yamaki, T., Oikawa, T., Ito, K. and Nakamura, T. Cloning and sequencing of a nitrile hydratase gene from *Pseudonocardia thermophilia* JCM3095. (1997). J. Ferm. Bioeng. **83**: 474-477.

Yamamoto, H. K. and Komatsu, K. Purification and characterization of nitrilase responsible for the enantioselective hydrolysis from *Acinetobacter* sp. AK 226. (1991). Agric. Biol. Chem. **55**: 1459-1466.

Yamamoto, F., Fijimatsu, I. and Komatsu, K. Purification and characterization of the nitrilase from *Alcaligenes faecalis* ATCC 8750 responsible for enantioselective hydrolysis of mandelonitrile. (1992). J. Ferment. Bioeng. **73**: 725-430.

Websites:

Protein Data Bank, accessed 15th February 2017, <https://www.rcsb.org/pdb/explore/emplore.do?structureId=3KLC>

Protein Data Bank, accessed 17th February 2017, https://www.rcsb.org/pdb/explore/emplore.do?structureId=1IRE

Chapter Three: PAPER I

Enantioselective hydrolysis of β-hydroxy nitriles using the whole cell biocatalyst *Rhodococcus rhodochrous* ATCC BAA-870

Henok Kinfe, **Varsha Chhiba**, Joni Frederick, M. L. Bode, K. Mathiba, Paul. A. Steenkamp and Dean Brady

(Journal of Molecular Catalysis B: Enzymatic, 2008)

(Appendix 2: Amidase substratedocking study- 2017).

Journal of Molecular Catalysis B: Enzymatic 59 (2009) 231–236

Contents lists available at ScienceDirect

Journal of Molecular Catalysis B: Enzymatic

journal homepage: www.elsevier.com/locate/molcatb

Enantioselective hydrolysis of β-hydroxy nitriles using the whole cell biocatalyst *Rhodococcus rhodochrous* ATCC BAA-870

H.H. Kinfe, V. Chhiba, J. Frederick, M.L. Bode, K. Mathiba, P.A. Steenkamp, D. Brady*

CSIR Biosciences, Pinelands, Ardeer Road, Modderfontein 1645, South Africa

ARTICLE INFO

Article history:
Received 31 January 2008
Received in revised form 13 May 2008
Accepted 4 June 2008
Available online 12 June 2008

Keywords:
Nitrile hydratase
Amidase
β-Hydroxy nitrile
Biocatalysis
Rhodococcus
Kinetic resolution

ABSTRACT

The kinetic resolution of 3-hydroxy-4-aryloxybutanenitriles and 3-hydroxy-3-arylpropanenitriles by the nitrile biocatalyst *Rhodococcus rhodochrous* ATCC BAA-870 was attempted. The nitriles were converted to the corresponding carboxyamides and carboxyacids with enantiomeric excesses (ee) of 0.55 to >99% depending on the substrate. The organism expressed nitrile hydratase and amidase activities responsible for these biotransformations.

© 2008 Elsevier B.V. All rights reserved.

1. Introduction

The resolution of β-hydroxy nitriles in the stereoselective synthesis of β-adrenergic blocking agents continues to attract attention [1–5]. β-Adrenergic agents (Fig. 1) are important pharmaceutical agents for the treatment of cardiovascular and psychiatric disorders. However, most of the β-adrenergic blocking agents are currently marketed as racemates due to the difficulty of separating the enantiomers. This has led many researchers to explore the preparation of optically active precursors for β-adrenergic blocking agents.

Unlike the explored chemistry of α-hydroxy nitriles [6], there are relatively few reports of biocatalytic asymmetric hydrolysis of β-hydroxy nitriles, besides that of 3-substituted glutaronitrile derivatives [7–9]. Li and Wu reported the hydrolysis of 3-hydroxy-4-aryloxybutanenitriles using *Rhodococcus* sp. CGMCC 0497 [10]. Unlike the hydrolysis of α-hydroxy nitriles, they did not obtain an excellent enantiomeric excess (ee), but they demonstrated that β-hydroxy nitriles can be hydrolysed to their corresponding amides and acids with moderate to high ee.

In view of the limited number of efficient approaches to the resolution of β-hydroxy nitriles using nitrile degrading enzymes, we felt there was scope for exploring alternative biocatalysts which can provide superior enantioselectivity. Whether via a direct nitrilase-catalysed conversion to a carboxylic acid, or through a nitrile hydratase-catalysed hydration followed by hydrolysis of the amide by an amidase, nitrile biotransformations have been successfully applied as environmentally safe, selective reactions for the production of optically active carboxylic acids and their amide derivatives [11–13]. Brady et al. have previously shown that *Rhodococcus rhodochrous* ATCC BAA-870, a species isolated from soil, possesses a nitrile hydratase/amidase biocatalytic system which is capable of metabolising a wide range of aliphatic and aromatic nitriles and amides [14]. The structurally diverse biocatalytic array of this organism affords potential in the fine chemicals and pharmaceuticals industry. Herein, we report our results on the asymmetric hydrolysis of chiral 3-hydroxy-3-arylpropanenitriles and 3-hydroxy-4-aryloxybutanenitriles using *R. rhodochrous* ATCC BAA-870 with excellent enantiomeric excess.

2. Experimental

2.1. General

The racemic β-hydroxy nitrile substrates were prepared from their corresponding epoxides following the literature procedure of Kamal et al. [3], except for 3-hydroxy-3-(4-methylphenyl)

* Corresponding author at: CSIR Biosciences, Private bag X2, Modderfontein 1645, South Africa. Tel.: +27 11 605 2711; fax: +27 11 608 3020.
E-mail addresses: hkinfe@csir.co.za (H.H. Kinfe), vchhiba@csir.co.za (V. Chhiba), jfrederick@csir.co.za (J. Frederick), mbode@csir.co.za (M.L. Bode), kmathiba@csir.co.za (K. Mathiba), psteenkamp@csir.co.za (P.A. Steenkamp), dbrady@csir.co.za (D. Brady).

1381-1177/$ – see front matter © 2008 Elsevier B.V. All rights reserved.
doi:10.1016/j.molcatb.2008.06.004

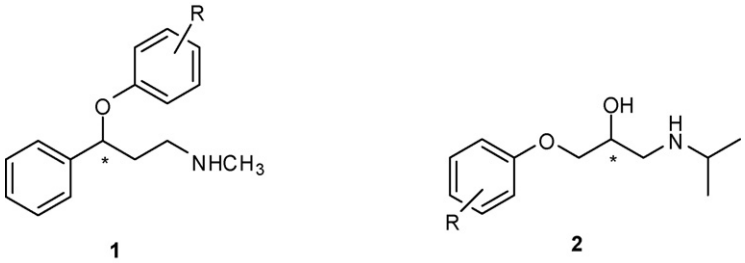


Fig. 1. General structure of β-adrenergic blocking agents.

propanenitrile which was synthesised from 4-methylstyrene [3]. Commercial reagents were used without further purification. Reactions were monitored by thin layer chromatography (TLC) on aluminium-backed Merck silica gel 60 F_{254} plates using an ascending technique. The plates were visualized by spraying with a 1:1 solution of 5% *p*-anisaldehyde in ethanol and 10% sulphuric acid in ethanol, baking at 150 °C. Gravity column chromatography was done on Merck silica gel 60 (70–230 mesh). Uncorrected melting points were determined using a Reichert–Jung Thermovar hot-stage microscope. Optical rotations were determined on a PerkinElmer 141 polarimeter as chloroform solutions. The concentration *c* refers to g/100 mL. Proton nuclear magnetic resonance (^{1}H NMR) spectra were recorded as deuteriochloroform solutions using tetramethylsilane as an internal standard on a Varian Gemini 200 MHz or a Varian Unity 400 MHz spectrometer. Carbon-13 nuclear magnetic resonance (^{13}C NMR) spectra were recorded on the same instruments at 50 MHz or 100 MHz using tetramethylsilane as an internal standard. Chemical shifts are reported in ppm.

Enantiomeric excess values of esters derived from the corresponding amides and acids (see below, Section 2.3) were determined by chiral HPLC analysis using chiracel HPLC columns (Daicel Chemical Industries Ltd.) OB-H, AD-H, and OD-H on a Waters Alliance HPLC system (2690 Separation Module, 996 PDA detector) with a dimension of 0.46 cm i.d. × 25 cm length at a flow rate of 1.00 mL/min with 9:1 hexane/isopropanol as eluent unless otherwise indicated. The column temperature was maintained at 25 °C using a Phenomenex ThermaSphere TS-430 temperature control unit. The detection wave length was set at 254 nm.

Initial compound identification was done on a Waters Thermabeam (TMD) system comprising of a 2695 Solvent Delivery System, a 2996 PDA detector, column heater and Thermabeam EI MS detector. Chromatographic separation of nitriles, amides and acids was done on a Phenomenex Aqua C18 column, 250 mm × 2 mm 125 A maintained at 40 °C. The starting eluent consisted of a water (containing 10 mM formic acid) and acetonitrile ratio of 9:1 at 0.2 mL/min. The initial starting eluent was maintained for 1 min and thereafter gradually changed through a linear gradient to a water:acetonitrile ratio of 10:90 and maintained for 3 min. The eluent ratio was thereafter returned to initial conditions and the column was allowed to equilibrate for 5 min.

The TMD was operated in positive scan mode (50–250 amu or 50–450 amu) with a gain of 10 and collecting 2 spectra per second, the nebuliser temperature set at 70 °C, the expansion region temperature at 80 °C and the source temperature at 225 °C. The total volume of post-column eluent was sent to the TMD detector. The TMD detector was tuned every day prior to starting an analysis run and caffeine was injected as test compound to ensure functionality of the total system. The photodiode array (PDA) detector was operated in scan mode (200–600 nm) with a resolution of 1.2 nm.

Data processing was done utilising Empower Version 1 software. Mass spectral data was compared with a NIST 2005 mass spectral library.

2.2. Microorganism and cultivation

The bacterial nitrile biocatalyst, *R. rhodochrous* ATCC BAA-870 was cultured and nitrile hydrolysis activity induced using a substrate-based growth enrichment protocol described by Brady et al. [14], based on that by Layh et al. [15,16]. The defined medium consisted of a sterile salt solution (4.97 g/L $NaHPO_4$, 0.2 g/L KH_2PO_4, 0.05 g/L $CaCl_2{\cdot}2H_2O$, 0.09 g/L $FeSO_4{\cdot}7H_2O$ and 0.02 g/L $MgSO_4$) and 1 mL/L trace element solution (0.2 g/L $ZnSO_4{\cdot}5H_2O$, 0.4 g/L $CuSO_4{\cdot}5H_2O$, 0.004 g/L $CoSO_4{\cdot}7H_2O$, 50 g/L trisodium citric acid and 0.4 g/L $MnSO_4{\cdot}H_2O$) that had been autoclaved separately. A glucose solution (sterilised by filtration) was added to bring the final glucose concentration to 1.2 g/L. Benzamide was added to the medium to a final concentration of 20 mM as the sole source of nitrogen and as an inducer of enzyme activity. The induced cells were cultured at 25 °C with shaking and harvested after 72 h by centrifugation. The cellular material was then water washed and re-suspended in 100 mM phosphate buffer, pH 7.2. The nitrile hydratase and amidase activities of the whole cell biocatalyst were determined using benzonitrile and benzamide with approximately 0.075 mg/mL reaction volume of biomass.

2.3. General procedure with whole cells

Wet cells (1.5 g) were added to a solution of 100 mg 3-hydroxy-4-aryloxybutanenitrile or 3-hydroxy-3-arylpropanenitrile in methanol (2 mL) and 100 mM potassium phosphate buffer, pH 7.2 (to a final volume of 20 mL), and the resulting mixture was stirred at 30 °C until TLC showed conversion of the nitrile substrate to the corresponding amide and acid. The reaction was quenched by centrifugation at 15000 rpm and 4 °C for 20 min and decantation of the supernatant from the biomass. The supernatant was basified with 2N NaOH and extracted with ethyl acetate (5 × 10 mL). The combined organic phases were washed successively with water and brine; dried over anhydrous $MgSO_4$ and then concentrated under reduced pressure. The crude product was purified by column chromatography on silica gel using a mixture of ethyl acetate and petroleum ether as eluent to give the amide derivative. The aqueous phase was then acidified using 3N HCl and extracted with ethyl acetate several times. The combined organic phases were washed with water, dried over $MgSO_4$, and then concentrated to yield the acid derivative. The yields of the corresponding acids and amides are given in Table 1.

To determine the ee values, the amides and acids produced by the biotransformation were esterified using Fischer esterification. A catalytic amount of concentrated sulphuric acid was added to the amide or acid in excess methanol, and the reaction mixture

Table 1
Biotransformation of racemic aromatic β-hydroxy nitriles[a]

Entry	Substrate	R	Time	Amide-**a**		Acid-**b**	
				Isolated yield (%)	ee (%)	Isolated yield (%)	ee (%)
1	**3**	Ph	1.5 h	32	>99	32	57
2	**4**	Bn	45 min	14	>99	37	60
3	**5**	*p*-OMe Ph	45 min	14	96	34	70
4	**6**	*p*-Cl Ph	45 min	24	82	37	72
5	**7**	H	3 h	8	3	46	0.5
6	**8**	Me	1.5 h	39	65	25	78

[a] The substrate nitrile had been completely converted in each case.

was refluxed at 70 °C until TLC showed completion of the reaction. After completion of the reaction, the reaction mixture was allowed to cool down to room temperature and then extracted with diethyl ether. The combined organic layers were washed successively with water, 5% aq Na_2CO_3, and brine; dried over anhydrous $MgSO_4$; and then concentrated to dryness to afford the corresponding esters. The esters were submitted for chiral HPLC and characterized fully. The absolute configuration of the products was assigned on the basis of optical rotation and elution order in chiral HPLC as compared to that reported in the literature [17–21]. The physical data of the esters are shown below:

2.3.1. Methyl (R)-(+)-3-hydroxy-4-phenoxybutanoate 3c [17]

Obtained after esterification of (*R*)-(+)-3-hydroxy-4-phenoxybutanamide **3a**; white solid, m.p. 40–44 °C (no m.p. reported in literature); >99% ee (Column: Chiralpak OD-H, retention time = 13.0 min); $[\alpha]_D^{29} + 0.32$ (*c* 0.31, $CHCl_3$); ^{1}H NMR (200 MHz, $CDCl_3$): δ 7.39–7.24 (m, 2H, ArH), 7.05–6.88 (m, 3H, ArH), 4.55–4.34 (m, 1H, H-3), 4.03 (d, 2H, *J* = 5.2 Hz, H-4), 3.76 (s, 3H, OMe), 3.06 (bs, 1H, OH), 2.76–2.66 (m, 2H, H-2); ^{13}C NMR (50 MHz, $CDCl_3$): δ 172.6, 158.6, 129.7 (x2), 121.5, 114.8 (x2), 70.9, 67.0, 52.1, 38.2.

2.3.2. Methyl (S)-(−)-3-hydroxy-4-phenoxybutanoate 3d [17]

Obtained after esterification of (*S*)-(−)-3-hydroxy-4-phenoxybutanoic acid **3b**; white solid, m.p. 41–44 °C (no m.p. reported in the literature); 57% ee (Column: Chiralpak OD-H, retention time = 14.7 min); $[\alpha]_D^{29} - 0.36$ (*c* 0.83, $CHCl_3$); ^{1}H NMR and ^{13}C NMR spectra identical to **3c**.

2.3.3. Methyl (S)-(+)-3-hydroxy-4-benzyloxybutanoate 4c [17]

Obtained from the esterification of (*S*)-(+)-3-hydroxy-4-benzyloxybutanamide **4a**; Colourless oil; >99% ee (Column: Chiralpak OD-H, retention time = 15.4 min); $[\alpha]_D^{29} + 0.42$ (*c* 0.48, $CHCl_3$); [lit.[13] $[\alpha]_D^{25} + 8.20$ (*c* 0.85, $CHCl_3$)]; ^{1}H NMR (200 MHz, $CDCl_3$): δ 7.35 (s, 5H, ArH), 4.59 (s, 2H, H-4), 4.36–4.16 (m, 1H, H-3), 3.72 (s, 3H, OMe), 3.57–3.48 (m, 2H, CH_2Ph), 2.94 (bs, 1H, OH), 2.58 (d, 2H, *J* = 6.2 Hz, H-2); ^{13}C NMR (50 MHz, $CDCl_3$): δ 172.7, 138.1, 128.7 (x2), 128.0, 127.9 (x2), 73.7, 73.4, 67.5, 52.0, 38.3.

2.3.4. Methyl (R)-(−)-3-hydroxy-4-benzyloxybutanoate 4d [17]

Obtained from the esterification of (*R*)-(−)-3-hydroxy-4-benzyloxybutanoic acid **4b**; Colourless oil; 60% ee (Column: Chiralpak OD-H, retention time = 12.4 min); $[\alpha]_D^{29} - 2.76$ (*c* 2.54, $CHCl_3$); ^{1}H and ^{13}C NMR spectra are identical to **4c**.

2.3.5. Methyl (R)-(+)-3-hydroxy-4-(4-methoxyphenoxy)butanoate 5c [18]

Obtained from the esterification of (*R*)-(+)-3-hydroxy-4-(4-methoxyphenoxy)butanamide **5a**; white solid, m.p. 52–55 °C (no m.p. reported in the literature); 96% ee (Column: Chiralpak AD-H, retention time = 16.7 min); $[\alpha]_D^{29} + 0.42$ (*c* 0.47, $CHCl_3$); ^{1}H NMR (200 MHz, $CDCl_3$): δ 6.87 (s, 4H, ArH), 4.49–4.33 (m, 1H, H-3), 3.98 (d, 2H, *J* = 5.4 Hz, H-4), 3.79 (s, 3H, OMe), 3.76 (s, 3H, OMe), 3.03 (d, 1H, *J* = 4.4 Hz, OH), 2.75–2.64 (m, 2H, H-2); ^{13}C NMR (50 MHz, $CDCl_3$): δ 172.6, 154.5, 115.9 (x2), 115.0 (x2), 71.8, 67.1, 56.0, 52.1, 38.2.

2.3.6. Methyl (S)-(−)-3-hydroxy-4-(4-methoxyphenoxy)butanoate 5d [1]

Obtained from the esterification of (*S*)-(−)-3-hydroxy-4-(4-methoxyphenoxy)butanoic acid **5b**; white solid, m.p. 68–72 °C (lit.[1] m.p. 81 °C for 97% ee); 70% ee (Column: Chiralpak AD-H, retention time = 19.4 min); $[\alpha]_D^{29} - 0.43$ (*c* 0.94, $CHCl_3$); [lit.[1] $[\alpha]_D^{20} - 3.30$ (*c* 0.93, MeOH) for 97% ee]; ^{1}H and ^{13}C NMR spectra are identical to **5c**.

2.3.7. Methyl (R)-(+)-3-hydroxy-4-(4-chlorophenoxy)butanoate 6c

Obtained from the esterification of (*R*)-3-hydroxy-4-(4-chlorophenoxy)butanamide **6a**; Colourless oil; 82% ee (Column: Chiralpak OD-H, retention time = 13.0 min); $[\alpha]_D^{29} + 0.38$ (*c* 1.57, $CHCl_3$); ^{1}H NMR (200 MHz, $CDCl_3$): δ 7.25 (d, 2H, *J* = 8.8 Hz, ArH), 6.86 (d, 2H, *J* = 9.0 Hz, ArH), 4.60–4.24 (m, 1H, H-3), 3.99 (d, 2H, *J* = 5.2 Hz, H-4), 3.75 (s, 3H, OMe), 3.11 (d, 1H, *J* = 3.8 Hz, OH), 2.73–2.65 (m, 2H, H-2); ^{13}C NMR (50 MHz, $CDCl_3$): δ 172.6, 157.3, 129.6 (x2), 126.4, 116.1 (x2), 71.4, 66.9, 52.1, 38.1.

2.3.8. Methyl (S)-(−)-3-hydroxy-4-(4-chlorophenoxy)butanoate 6d

Obtained from the esterification of (*R*)-3-hydroxy-4-(4-chlorophenoxy)butanoic acid **6b**; Colourless oil; 72% ee (Column: Chiralpak OD-H, retention time = 11.0 min); $[\alpha]_D^{29} - 0.45$ (*c* 1.54, $CHCl_3$); ^{1}H and ^{13}C NMR are identical to **6c**.

2.3.9. Methyl (R)-(−)-3-hydroxy-3-phenylpropanoate 7c [19]

Obtained after esterification of (*R*)-(+)-3-hydroxy-3-phenylpropanamide **7a**; Colourless oil; 3% ee (Column: Chiralpak OD-H, retention time = 10.7 min); $[\alpha]_D^{29} - 1.11$ (*c* 0.18, $CHCl_3$); ^{1}H NMR (200 MHz, $CDCl_3$): δ 7.60–7.20 (m, 5H, ArH), 5.17 (dd, 1H, *J* = 5.3 and 7.5 Hz, H-3), 3.75 (s, 3H, OMe), 3.22 (bs, 1H, OH), 2.90–2.70 (m, 2H, H-2); ^{13}C NMR (50 MHz, $CDCl_3$): δ 172.9, 142.7, 128.8 (x2), 128.1, 125.9 (x2), 70.6, 52.1, 43.4.

2.3.10. Methyl (S)-(−)-3-hydroxy-3-phenylpropanoate 7d [20]

Obtained after esterification of (*R*)-(+)-3-hydroxy-3-phenylpropanoic acid **7b**; Colourless oil; 0.5% ee (Column: Chiralpak OD-H, retention time = 12.6 min); $[\alpha]_D^{29} - 0.10$ (*c* 1.00, $CHCl_3$); [lit.[16] $[\alpha]_D^{23} - 21.5$ (*c* 1.00, EtOH)]; ^{1}H NMR and ^{13}C NMR spectra are identical to **7c**.

2.3.11. Methyl (R)-(+)-3-hydroxy-3-(4-methylphenyl)propanoate 8c [21]

Obtained from the esterification of (*R*)-(+)-3-hydroxy-3-(4-methylphenyl)propanamide **8a**; Colourless oil; 65% ee (Column: Chiralpak OB-H, hexane/isopropanol 95:5, retention time = 15.0 min); $[\alpha]_D^{29} + 0.93$ (*c* 1.29, $CHCl_3$); ^{1}H NMR (400 MHz, $CDCl_3$): δ 7.26 (d, 2H, *J* = 8.4 Hz, ArH), 7.16 (d, 2H, *J* = 7.6 Hz, ArH), 5.11 (d, 1H, *J* = 8.4 Hz, H-3), 3.72 (s, 3H, OMe), 3.08 (bs, 1H, OH), 2.78–2.68 (m, 2H, H-2), 2.34 (s, 3H, Me); ^{13}C NMR (50 MHz, $CDCl_3$): δ 172.9, 139.8, 137.8, 129.5 (x2), 125.8 (x2), 70.5, 52.1, 43.4, 21.4.

2.3.12. Methyl (S)-(−)-3-hydroxy-3-(4-methylphenyl)propanoate 8d [21]

Obtained from the esterification of (*S*)-(−)-3-hydroxy-3-(4-methylphenyl)propanoic acid **8b**; Colourless oil; 78% ee (Column: Chiralpak OB-H, hexane/isopropanol 95:5, retention time = 18.7 min); $[\alpha]_D^{29} - 2.31$ (*c* 0.65, $CHCl_3$); [lit.[17] $[\alpha]_D - 22.00$ (*c* 1.00, $CHCl_3$) and no temperature was reported]; ^{1}H and ^{13}C NMR spectra are identical to **8c**.

3. Results and discussion

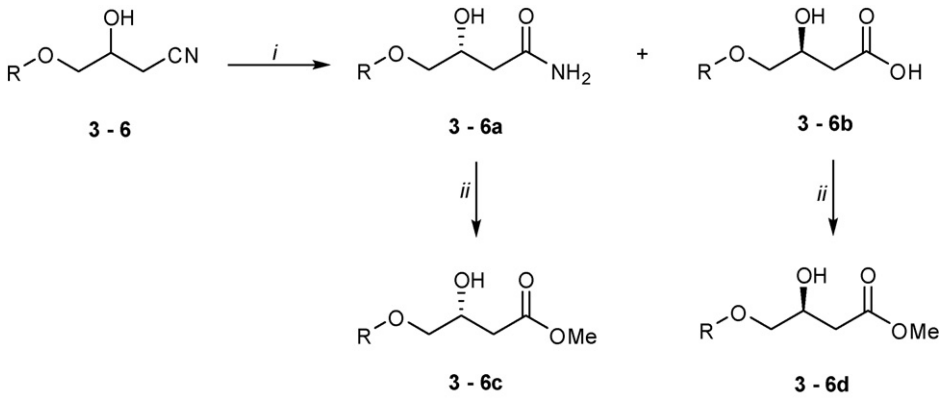
(*S*)-3-Hydroxy-4-phenoxybutanamides are of interest as they are potential intermediates for the synthesis of β-adrenergic blockers [4]. Li and Wu [10] demonstrated that β-hydroxy nitriles could be hydrolysed using *R. rhodochrous* sp. CGMCC 0497 at 20 °C in a 100 mM phosphate buffer of pH 7.0, and accordingly in our first attempt at nitrile hydrolysis we incubated a solution of 3-hydroxy-4-phenoxybutanenitrile **3** in methanol with *R. rhodochrous* ATCC BAA-870 under the reported biocatalytic reaction conditions for optimal ee of amide and acid. Unfortunately, conversion of the nitrile to either an amide or an acid was not observed even after overnight incubation. However, increasing the reaction temperature to 30 °C resulted in the disappearance of the starting material to untraceable products. The improved conversion may be due to improved cell membrane porosity for the larger substrates at the higher temperature. Lowering of the cell load to 1.5 g wet weight per 100 mg of the substrate and subsequent incubation at 30 °C allowed a smooth conversion of the nitrile to its corresponding amide and acid within 1.5 h (Scheme 1 and entry 1). The result was contrary to that reported by Li and Wu [10]. In their case, the conversion was incomplete at 30 °C showing the dependence of the biocatalysts on temperature.

An investigation was undertaken to confirm whether the biotransformation of the nitrile was via the nitrilase or the nitrile hydratase–amidase route. This was done by reducing the cell load from 1.5 g to 0.5 g in order to slow the reaction down and hence permit monitoring of amide production. Analysis of the products at time intervals showed exclusive formation of the corresponding amide, thus indicating the involvement of the nitrile hydratase–amidase enzymatic pathway. In accordance with previous reports and the general literature [14,22], we found the nitrile hydratase to be non-stereoselective, as samples of the unreacted nitrile taken at different time intervals showed <1% ee after analysis by chiral HPLC.

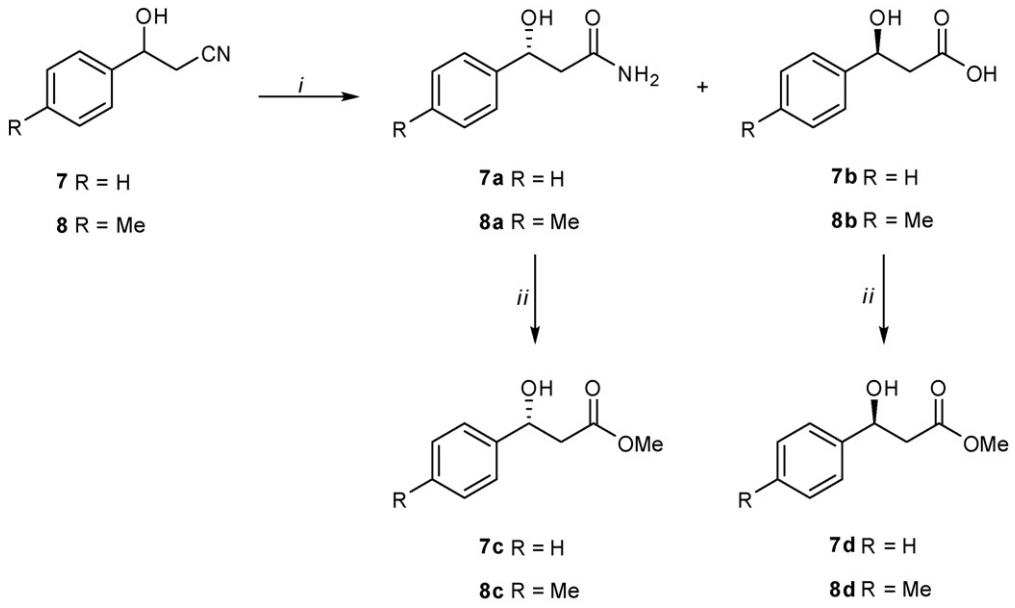
Incubation of various 3-hydroxy-4-aryloxybutanenitriles (Scheme 1) provided efficient and selective access to (*R*)-amide and (*S*)-acid (Table 1) except in the case of the benzyloxy substrate **4** where (*S*)-amide and (*R*)-acid were obtained (entry 2 in Table 1). In all cases complete conversion of the starting nitrile was achieved. The products were identified using ^{1}H and ^{13}C NMR spectroscopy after chromatographic separation and the ee of the products was determined by chiral HPLC after esterification. The enantioselectivities obtained with unsubstituted aromatic rings are the best yet reported. Interestingly, hydrolysis of 3-hydroxy-4-phenoxybutanenitrile using the *Rhodococcus* sp. CGMCC 0497 required incubation at 20 °C for 3.5 h with 5 g cell load to yield 76% ee [10], whereas the reaction proceeds at 30 °C within 1.5 h with a cell load of 1.5 g to yield >99% ee using our biocatalyst, indicating higher specific activity.

Substrates with electron donating and withdrawing substituents on the aromatic ring were transformed into their corresponding amides and acids (entry 3 and 4). Although the rate of the reaction was not affected by the electron withdrawing group (–Cl), the selectivity decreased in accordance with previous results by Wu and Li [10]. The electron donating substituent (–O–CH_3) did not have a significant effect on the rate of the enzyme or enantioselectivity. The reaction rates of *ortho*-substituted β-hydroxy aryloxy substrates were unacceptably slow and are therefore not reported here.

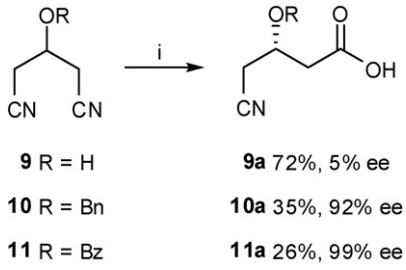
To evaluate the generality of the method, 3-hydroxy-3-phenylpropanenitrile (Scheme 2) was incubated with the bacterium. Hydrolysis proceeded at a lower rate and with poor stereoselectivity relative to the corresponding aryloxy β-hydroxy nitriles (entry 5). However, adding a substituent on the aromatic ring of the 3-hydroxy-3-phenylpropanenitrile resulted in better selectivity. This result could be attributed to the size dependency of the active site of the amidase. Substrate preference studies by Wang and Feng suggest that an amidase from a *Rhodococcus* strain was more stereoselective for larger molecules [23–25]. The size dependence of the enzyme was further investigated using 3-hydroxy-, 3-benzyloxy-, and 3-benzoyloxypentanedinitriles (**9**, **10**, and **11**, respectively) as shown in Scheme 3. The ee for the formation of the corresponding acids increased from 5% ee to 99% ee in proportion to the size of the substrate. The physical data of the products were in agreement with the literature values [7–9]. Similarly, other



Scheme 1. (i) *R. rhodochrous* sp., MeOH/potassium phosphate buffer (1:10), 30 °C, 45 min–1.5 h and (ii) conc. H_2SO_4, MeOH, 70 °C, 1 h–overnight.



Scheme 2. (i) *R. rhodochrous* sp., MeOH/potassium phosphate buffer (1:10), 30 °C, 1.5 h–3 h and (ii) conc. H_2SO_4, MeOH, 70 °C, 1 h–overnight.



Scheme 3. (i) *R. rhodochrous* sp., MeOH/potassium phosphate buffer (1:10), 30 °C, 48 h.

Rhodococcus species show enantioselectivity for these substrates. *R. rhodochrous* SP 361 (Novozymes), showed 22%, 84–88%, and 83% ee, for the (*S*)-acids **9a**, **10a** and **11a**, respectively [8,9]; while *R. erythropolis* NCIMB 11540 displayed 13%, 96% and 63% ee, respectively [26]. *R. butanica* yielded **10a** and **11a** at 90% and 99% ee, respectively [22], and similarly, 90% and 99% ee was obtained using *R. rhodochrous* IFO 15564 [13]. This type of reaction is interesting as the (*R*)-3-hydroxy-4-cyanobutanoic acid can be used as a chiral intermediate in a synthetic route to the lipitor (Atorvastatin), a HMG-CoA reductase inhibitor. This reaction was achieved using a nitrilase that had been obtained through metagenomics and directed evolution [27–29]. Similarly, the (*S*)-enantiomer can be used in the synthesis of 4-hydroxypiperidines [26]. However, the application of a stereoselective nitrilase allows for complete conversion of the pro-chiral substrate, whereas the use of a non-stereoselective nitrile hydratase and stereoselective amidase would only provide 50% yield of the desired enantiomer.

4. Conclusion

In summary, we have shown that asymmetric hydrolysis of aromatic β-hydroxy nitriles can be achieved with excellent ee and moderate to high yield using *R. rhodochrous* ATCC BAA-870. To the best of our knowledge, this is the first report to demonstrate the achievement of excellent ee for the hydrolysis of β-hydroxy nitriles using nitrile degrading enzymes. The organism is, therefore, a potentially useful tool in the synthesis of enantiomerically pure β-adrenergic agents and possibly in the production of non-proteinogenic amino acids, which are precursors for a range of biologically active compounds [30].

Acknowledgements

We would like to thank Professor B.T. Sewell of UCT, Dr L. Martínková, Czech Academy of Sciences and COST D25-02 (Nitrile Biocatalysis) group leader, and Dr F. van Rantwijk, TU Delft, for discussions.

References

[1] K. Wünsche, U. Schwaneberg, U.T. Bornscheuer, H.H. Meyer, Tetrahedron: Asymmetry 7 (1996) 2017–2022.
[2] A. Kamal, G.B. Ramesh Khanna, Tetrahedron: Asymmetry 12 (2001) 405–410.
[3] A. Kamal, G.B. Ramesh Khanna, R. Ramu, Tetrahedron: Asymmetry 13 (2002) 2039–2051.
[4] A. Kamal, G.B. Ramesh Khanna, T. Krishnaji, V. Tekumalla, R. Ramu, Tetrahedron: Asymmetry 16 (2005) 1485–1494.
[5] R.J. Hammond, B.W. Poston, I. Ghiviriga, B.D. Feske, Tetrahedron Lett. 48 (2007) 1217–1219.
[6] L. Martinková, V. Křen, Biocat. Biotrans. 20 (2002) 73–93.
[7] H. Kakeya, N. Sakai, A. Sano, M. Yokoyama, T. Sugai, H. Ohta, Chem. Lett. 20 (1991) 1823–1824.
[8] J. Crosby, J.S. Parratt, N.J. Turner, Tetrahedron: Asymmetry 3 (1992) 1547–1550.
[9] S.J. Maddrell, N.J. Turner, A. Kerridge, A.J. Willetts, J. Crosby, Tetrahedron Lett. 37 (1996) 6001–6004.
[10] Z.-L. Wu, Z.-Y. Li, J. Mol. Catal. B: Enzym. 22 (2003) 105–112.
[11] T. Beard, M.A. Cohen, J.S. Parratt, N.J. Turner, J. Crosby, J. Moilliet, Tetrahedron: Asymmetry 4 (1993) 1085–1105.
[12] T. Sugai, T. Yamazaki, M. Yokohama, H. Ohta, Biosci. Biotech. Biochem. 61 (1997) 1419–1427.
[13] M. Wieser, T. Nagasawa, in: R.N. Patel (Ed.), Stereoselective Biocatalysis, Marcel Dekker, New York-Basel, 2000, p. 461 (and references therein).
[14] D. Brady, A. Beeton, C. Kgaje, J. Zeevaart, F. van Rantwijk, R.A. Sheldon, Appl. Microbiol. Biotechnol. 64 (2004) 76–85.
[15] N. Layh, A. Stolz, S. Förster, F. Effenberger, H.-J. Knackmuss, Arch. Microbiol. 158 (1992) 405–411.
[16] N. Layh, B. Hirrlinger, A. Stolz, H.-J. Knackmuss, J. Appl. Microbiol. Biotechnol. 47 (1997) 668–674.
[17] N.A. Abood, Synth. Commun. 23 (1993) 811–815.
[18] L. Banfi, G. Cascio, C. Ghiron, G. Guanti, E. Manghisi, E. Narisano, R. Riva, Tetrahedron 50 (1994) 11983–11994.
[19] H.-X. Wei, K. Li, Q. Zhang, R.L. Jasoni, J. Hu, P.W. Paré, Helv. Chim. Acta 87 (2004) 2354–2358.
[20] T. Yakura, T. Tanaka, M. Ikeda, J. Uenishi, Chem. Pharm. Bull. 51 (2003) 471–473.
[21] V. Ratovelomanana-Vidal, C. Girard, R. Touati, J.P. Tranchier, B. Ben Hassine, J.P. Genêt, Adv. Synth. Catal. 345 (2003) 261–274.

[22] B. Schulze, in: K. Drauz, H. Waldmann (Eds.), Enzyme Catalysis in Organic Synthesis, vol. 2, second ed., Wiley-VCH, 2002, pp. 699–715 (and references therein).
[23] M.-X. Wang, G.-Q. Feng, New J. Chem. 26 (2002) 1575–1583.
[24] M.-X. Wang, G.-Q. Feng, J. Mol. Catal. B: Enzym. 18 (2002) 267–272.
[25] M.-X. Wang, G.-Q. Feng, J. Org. Chem. 68 (2003) 621–624.
[26] M.K.S. Vink, C.A. Schortinghuis, J. Luten, J.H. van Maarseveen, H.E. Schoemaker, H. Hiemstra, F.P.J.T. Rutjes, J. Org. Chem. 67 (2002) 7869–7871.
[27] D.E. Robertson, J.A. Chaplin, G. DeSantis, M. Podar, M. Madden, E. Chi, T. Richardson, A. Milan, M. Miller, D.P. Weiner, K. Wong, J. McQuaid, B. Farwell, L.A. Preston, X. Tan, M.A. Snead, M. Keller, E. Mathur, P.L. Kretz, M.J. Burk, J.M. Short, Appl. Environ. Microbiol. 70 (2004) 2429–2436.
[28] G. DeSantis, Z. Zhu, W.A. Greenberg, K. Wong, J. Chaplin, S.R. Hanson, B. Farwell, L.W. Nicholson, C.L. Rand, D.P. Weiner, D.E. Robertson, M.J. Burk, J. Am. Chem. Soc. 124 (2002) 9024–9025.
[29] G. DeSantis, K. Wong, B. Farwell, K. Chatman, Z. Zhu, G. Tomlinson, H. Huang, X. Tan, L. Bibbs, P. Chen, K. Kretz, M.J. Burk, J. Am. Chem. Soc. 125 (2003) 11476–11477.
[30] E. Eichhorn, J.P. Roduit, N. Shaw, K. Heinzmann, A. Kiener, Tetrahedron: Asymmetry 8 (1997) 2533–2536.

Chapter Four: PAPER II

Enantioselective biocatalytic hydrolysis of β-aminonitriles to β-amino-amides using *Rhodococcus rhodochrous* ATCC BAA-870

Varsha Chhiba, Moira, L. Bode, Kgama Mathiba, Wendy Kwezi, Dean Brady

(Journal of Molecular Catalysis B: Enzymatic, 2012)

Journal of Molecular Catalysis B: Enzymatic 76 (2012) 68–74

Contents lists available at SciVerse ScienceDirect

Journal of Molecular Catalysis B: Enzymatic

journal homepage: www.elsevier.com/locate/molcatb

Enantioselective biocatalytic hydrolysis of β-aminonitriles to β-amino-amides using *Rhodococcus rhodochrous* ATCC BAA-870

Varsha Chhiba[a], Moira L. Bode[a,b], Kgama Mathiba[a], Wendy Kwezi[a], Dean Brady[a,*]

[a] *Enzyme Technologies, CSIR Biosciences, Pinelands, Ardeer Road, Modderfontein 1645, South Africa*
[b] *Molecular Sciences Institute, School of Chemistry, University of the Witwatersrand, Private Bag 3, PO WITS, 2050, South Africa*

ARTICLE INFO

Article history:
Received 30 October 2011
Received in revised form 9 December 2011
Accepted 9 December 2011
Available online 17 December 2011

Keywords:
Nitrile hydratase
Amidase
β-Aminonitrile
Biocatalysis
Biotransformation
Rhodococcus
Kinetic resolution

ABSTRACT

A range of β-aminonitriles (3-amino-3-phenylpropanenitrile and derivatives) were synthesised by reaction of various benzonitriles with acetonitrile and subsequent reduction of the resulting acrylonitrile products. These compounds were hydrolysed to the corresponding amides using the nitrile biocatalytic activity of *Rhodococccus rhodochrous* ATCC BAA-870. Results showed that the nitrile hydratase enzyme was enantioselective for these compounds, in particular 3-amino-3-*p*-tolylpropanenitrile and 3-amino-3-(4-methoxyphenyl)propanenitrile and the corresponding amides (up to 85% in one case). The reactions were performed at pH 9.0 after initial attempts at pH 7.0 were unsuccessful, most likely as a result of protonation of the 3-amino group at the lower pH.

© 2012 Elsevier B.V. All rights reserved.

1. Introduction

β-Amino-amides and acids can be used as building blocks for the synthesis of pharmaceutical intermediates. This includes biologically active peptides and small molecule pharmaceuticals [1]. β-Amino acids are constituents of compounds such as the antitumour drug Taxol [2], the antifungal antibiotic Cispentacin [3], and the antidiabetic drug Sitagliptin [4]. Another pharmaceutical application is for inclusion in peptidomimetics that may be of use as protease inhibitors against retroviruses such as HIV [5–7].

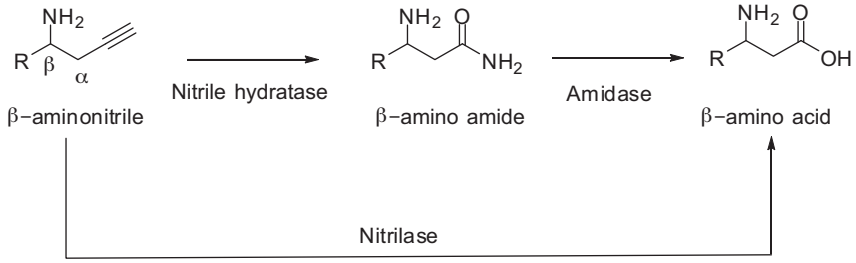
New potential applications for these compounds are being discovered continually. Wolin et al. [8] found that β-amino acid derivatives act as glycine transport inhibitors, while Zhu et al. [9] have discovered that others are proteasome inhibitors. Armour et al. [10] incorporated them into oxytocin inhibitors, Angelaud et al. [11] synthesised peptidase inhibitors and Imbriglio et al. included them in niacin receptor agonists for treatment of atherosclerosis and dyslipidemias [12].

There are a number of chemical synthesis methods for the preparation of racemic β^3-amino acids [13,14]. However, many applications require the β-amino substituted compounds as single enantiomers [1], and racemates thus need to be resolved. The classical method of resolving amino acids is through transformation of the racemate into a mixture of diastereomeric salts *via* complexation of the carboxylic acids with a chiral base, usually followed by multistep fractional recrystallisation.

Resolution may be achieved more simply through the application of biocatalysts, such as enzymatic resolution of β-amino esters and *N*-acyl derivatives [13] using lipases like CAL-B and the protease α-chymotrypsin; or by transesterification using lipase or acylase I [13]. Pousset et al. [15] demonstrated the application of *Burkholderia cepacia* lipase for hydrolytic resolution of heterocyclic β-amino acids, achieving greater than 99% ee. Tasnádi et al. [16–18] achieved ee values of 98–99% for both enantiomers of β-aryl-β-amino, β-arylalkyl-β-amino and β-heteroaryl-β-amino esters by enantioselective hydrolysis of the carboxylic acid ester using *B. cepacia* lipase (Amano PS) to hydrolyse the *S*-enantiomer. Li and Kanerva [19] used the lipase CAL-A to selectively acylate 3-amino-4-indolin-3-yl-butanenitrile, providing a 99% ee. A second option is to resolve the enantiomers through modification of the β-amine. *N*-acylation or deacylation can be performed by Acylase I and other enzymes [13]. Alternatively Forró et al. [20] and Tasnádi et al. [21] demonstrated enantioselective ring opening of β-lactams to provide β-amino acids with ee values of 99% using the lipase CAL-B. Aspartase can form β-amino acids through Michael addition. Hydantoinase hydrolysis of hydantoins, reductive amination by aminotransferase, and isomerisation by 2,3-aminomutase add

* Corresponding author at: CSIR Biosciences, Private bag X2, Modderfontein 1645, South Africa. Tel.: +27 82 467 6209.
E-mail address: dbrady@csir.co.za (D. Brady).

1381-1177/$ – see front matter © 2012 Elsevier B.V. All rights reserved.
doi:10.1016/j.molcatb.2011.12.005



Scheme 1. Biocatalytic conversion of β-aminonitriles to β-amino amides and acids.

yet more options [13]. Recently phenylalanine aminomutase (PAM) has been applied in the enzymatic synthesis of (*R*)-β-arylalanines with high ee (>99%) [22].

Single enantiomer β-amino-amides and acids can also be obtained through the enzymatic hydrolysis of the related nitrile (Scheme 1). Nitrile hydrolysing enzymes (nitrilase or a combination of nitrile hydratase and amidase) provide a mild approach for the synthesis of carboxylic acids from nitriles [23]. β-Alanine, the only naturally occurring beta amino acid, can be derived from β-aminopropanenitrile using whole cell biocatalysts *Alcaligenes* sp. OMT-MY14, *Aminobacter* sp ATCC 23314 [24] and *Rhodococcus* sp [25]. β-Alanine is an achiral substrate, however nitrile and amide biocatalysts may act enantioselectively on chiral substrates, and this has been successfully applied to the resolution of *N*-protected cyclic β-amino acids [26–28]. Veitía et al. [29] demonstrated synthesis of *N*-protected β^3-amino acids using the Codexis range of nitrilases to hydrolyse the single enantiomer nitrile precursors. Biotransformation of alicyclic *N*-*p*-toluenesulfonyl- and *N*-butyloxycarbonyl protected β-aminonitriles to the *trans* amides and carboxylic acids using two strains of *Rhodococcus* (*Rhodococcus* sp. R312 and *R. erythropolis* NCIMB 11540) has been demonstrated [27]. With *Rhodococcus erythropolis* AJ270 cells 96.4% ee was achieved where the *N*-protected β-amino acid β-substituent was a c-Pr group [30].

β-Aminonitriles themselves can be prepared by a number of methods. Preiml et al. [26] used cyanide mediated ring opening of aziridines. González et al. [31] used a Mannich-type reaction to synthesise enantio-enriched (*R*)-unsubstituted β-aminonitriles through the organocatalytic addition of β-phenylsulfonylacetonitrile to either *N*-Boc-protected (*R*)-amido sulfones or imines.

Herein we synthesise various aryl substituted unprotected 3-amino-3-phenylpropanenitriles and demonstrate the enantioselective hydrolysis of these β-aminonitriles to the corresponding amides using *Rhodococcus rhodochrous* ATCC BAA-870, a nitrile hydrolysing organism isolated from soil [32,33], that expresses a benzamide induced cobalt type nitrile hydratase.

2. Experimental

2.1. General

Reactions were monitored by thin layer chromatography (TLC) on aluminium-backed Merck silica gel 60 F_{254} plates using an ascending technique. The plates were visualized both by UV at λ = 254 nm and then visually by colour development after treatment with ninhydrin spray. Gravity column chromatography was carried out on Merck silica gel 60 (70–230 mesh) and a mixture of ethyl acetate and hexane (or DCM and methanol) was used as eluent unless otherwise specified. Organic layers were dried over anhydrous $MgSO_4$ or anhydrous Na_2SO_4 before evaporation on a Büchi rotary evaporator RE 111 with a bath temperature of 40 °C or below, as required.

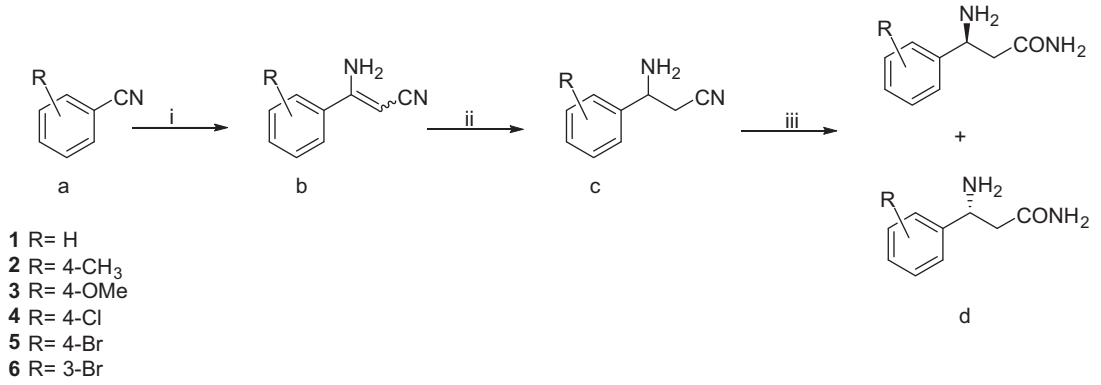
Nitrile and amide analysis was performed using a liquid chomatography (HPLC) system composed of a Waters 2690 separation module coupled with Waters diode array detector 996 (210–400 nm), a Waters X-Terra MS18 3.5 μm, 3.0 mm × 50 mm (ID × L) column (25 °C), with the isocratic eluent of 0.1% (v/v) trifluoroacetic acid in ultrapure water combined with acetonitrile (composition was varied according to the compound analysed) at a flow rate of 0.3–0.5 ml/min. The run time was 15–20.0 min, and all data handling was by Empower 2 Software.

Chiral nitrile analysis was performed using a liquid chromatography system composed of a Waters 600-MS Separation Module equipped with Waters 717 Autosampler, Waters 2486 UV/Visible Detector (210 nm) and Empower 2 software. Columns used were a Chiralpack AD-H, 250 mm × 4.6 mm, 5 μm and a Chiracel OD-H, 250 mm × 4.6 mm, 5 μm (Daicel Chemical Industries Ltd.). The eluent was n-hexane: isopropanol (both HPLC Grade) 90:10, % v/v and an isocratic flow rate of 1.00 ml/min at 25 °C with a run time of 35 min. The chromatographic system was conditioned for 1 h before the injection of samples. 3-Amino-3-phenylpropanenitrile (**1c**) enantiomers were eluted under these conditions at 12 and 13.6 min; 3-amino-3-*p*-tolylpropanenitrile (**2c**) at 11.0 and 12.7 min; 3-amino-3-(4-methoxyphenyl)propanenitrile (**3c**) at 19.0 and 23.0 min; 3-amino-3-(4-chlorophenyl)propanenitrile (**4c**) at 9.0 and 12.5 min; 3-amino-3-(4-bromophenyl)propanenitrile (**5c**) at 19.0 and 29.0 min; and 3-amino-3-(3-bromophenyl)propanenitrile (**6c**) at 19.0 and 29.8 min.

Chiral amide analysis was performed using a liquid chromatography system composed of a Waters 2690 Separation Module equipped with Photodiode Array Detector 996, and Empower 2 software. The column was a Crownpak CR (+), 150 mm × 4 mm (10 °C). The eluent used was 16.3 g/l perchloric acid, pH 2.00 in nano-pure water (MilliQ) at a flow rate of 0.25 ml/min over a run time of 20.0–60.0 min. The chromatographic system was conditioned for at least 1 h in advance with a column flow rate of 0.25 ml/min before the injection of samples. 3-Amino-3-phenylpropanamide (**1d**) enantiomers eluted at 10.9 and 12.9 min (210 nm); 3-amino-3-*p*-tolylpropanamide (**2d**) at 24.5 and 30.6 min (210 nm); 3-amino-3-(4-methoxy)phenylpropanamide (**3d**) at 20.0 and 23.4 min (225 nm), 3-amino-3-(4-bromophenyl)propanamide (**5d**) at 22.9 and 28.5 min (230 nm); and 3-amino-3-(3-bromophenyl)propanamide (**6d**) at 13.8 and 28.1 min (230 nm).

Uncorrected melting points were determined using a Reichert-Jung Thermovar hot-stage microscope or a Mettler FP62 capillary melting point apparatus.

Proton nuclear magnetic resonance (^{1}H NMR) spectra were recorded as either $CDCl_3$ or CD_3OD solutions with tetramethylsilane as an internal standard. Both a 400 MHz Varian Unity spectrometer as well as a 200 MHz spectrometer were used for all substrate and product analysis. The ^{13}C NMR spectra were recorded on the same instruments using tetramethylsilane as an internal standard. All chemical shifts were reported in ppm.



Scheme 2. Synthesis of β-amino amides. Reagents *i*. 2 equiv. CH_3CN, 4 equiv. KO^tBu, 24 h. *ii*. $NaBH_3CN$, HCl, EtOH, 2 h. *iii*. *R. rhodochrous* sp., MeOH in Tris buffer, pH 9.0 (1:10, v/v), at 5 °C or 30 °C.

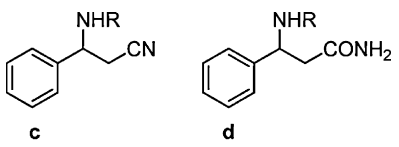
2.2. Overall synthetic route for preparation of β-amino compounds

The preparation of unprotected β-amino-amides (Scheme 2) was achieved by reacting benzonitrile (**1a**), or substituted derivatives (**2a**–**6a**) with acetonitrile and potassium *tert*-butoxide (KO^tBu) as described by de Paulis et al. [34]. The resulting 3-amino-3-phenylacrylonitrile (**1b)** or substituted derivatives (**2b**–**6b**) were then reduced with $NaBH_3CN$ [35] to yield the corresponding 3-amino-3-phenylpropanenitriles (**1c**–**6c**). These β-aminonitriles were subsequently hydrolysed to the amides (**1d**–**6d**) by the *R. rhodochrous* ATCC BAA-870 biocatalyst. Reaction progression was monitored by TLC and HPLC. After purification compounds were analysed by ^1H and ^{13}C NMR to confirm the structure. Chiral HPLC was used to determine the enantiomeric ratio of the purified products. For analytical purposes some material was *N*-Boc protected prior to analysis using the method of Kumar et al. [36].

The *N*-Boc and *N*-tosyl derivatives of **1c** were also prepared by standard methods in order to compare their activity with that of the unprotected substrate towards the biocatalyst (Fig. 1).

2.3. Microorganism and cell cultivation

Strain ATCC BAA-870 was first cultured in a rich medium (TSB) prior to nitrile hydratase induction by transfer into a defined media. The composition of the defined media was as follows: K_2HPO_4 4.97 g/l, KH_2PO_4 0.05 g/l, $CaCl_2{\cdot}2H_2O$ 0.05 g/l, $FeSO_4.7H_2O$ 0.09 g/l, $MgSO_4$ 0.02 g/l and 1 ml trace element solution, as previously described [32]. Glucose (1.8 g/l) and inducer (30 mM benzamide) addition into the defined media was done after autoclaving. The cellular pellet was water washed twice prior to it being re-suspended in 100 mM phosphate buffer, pH 7.0 (average cell wet weight was 1.0 mg/ml).



7 R=acetyl
8 R= *p*-toluensulfonyl
9 R= Boc

Fig. 1. *N*-protected β-aminonitriles.

2.4. Biotransformation using whole cells

Wet weight cells (1.0 g) were added to a solution containing 100 mg of the respective 3-amino-3-phenylpropanenitrile substrate (solubilised in 1 ml methanol) in 100 mM Tris buffer (either at pH 7 or at pH 9) to make the reaction volume up to 10 ml. The resulting mixture was then stirred at either 5 °C or 30 °C with amide generation being monitored by TLC analysis. The reactions were stopped by centrifugation at 10 000 rpm × 15 min with the supernatant being decanted and extracted using three volumes of ethyl acetate. The cell pellet was also washed with 5 ml of ethyl acetate. The extracted supernatant fraction as well as the cellular pellet extract were combined and then water and brine washed before drying over anhydrous magnesium sulphate. Concentration was performed under reduced pressure. Product purification was done by column chromatography using varied ratios of hexane/ethyl acetate or methanol/DCM solvent systems. Sample analysis was by HPLC.

2.5. General synthetic procedures

2.5.1. General method for synthesis of 3-amino-3-phenylacrylonitriles (compounds ***1b–6b***) exemplified by compound ***1b***

Benzonitrile **1a** (4.00 g, 38.8 mmol) was dissolved in dry toluene (100 ml) and acetonitrile (3.20 g, 78.0 mmol) was added. Potassium *tert*-butoxide (10.00 g, 89.2 mmol) was added in portions. The reaction was allowed to stir at room temperature overnight. Water (100 ml) and diethyl ether (100 ml) were added to the reaction mixture and the organic layer was separated. The aqueous layer was extracted again with diethyl ether (100 ml) and the combined organic layers were washed with brine and dried over $MgSO_4$. Solvent was removed *in vacuo* and to the brown oil was added a small volume of ether and sufficient hexane to make the mixture cloudy. After overnight cooling, crystals were collected and washed with ice-cold hexane to yield 3-amino-3-phenylacrylonitrile (3.68 g, 66%) as white crystals.

*2.5.1.1. 3-Amino-3-phenylacrylonitrile **1b** (66% yield).* White crystals, m.p. 82.9 °C (lit m.p. 81–84 °C [37]); ^1H NMR (400 MHz, $CDCl_3$) δ 7.54–7.40 (m, 5H), 4.97 (s, 2H), 4.25 (t, J = 0.8, 1H). ^{13}C NMR (101 MHz, $CDCl_3$) δ 161.48, 135.27, 130.91, 128.95, 125.94, 119.49, 63.61 (lit [38]). HRMS (ESI): m/z 145.0785 $(M+H)^+$; calc. for $C_9H_{19}N_2$: 145.0766.

*2.5.1.2. 3-Amino-3-p-tolylacrylonitrile **2b** (50% yield).* Yellow crystals, m.p. 103.5 °C (lit m.p. 107–110 °C [39]); ^1H NMR (400 MHz, $CDCl_3$) δ 7.39 (dd, J = 1.1, 7.3, 2H), 7.25–7.20 (m, 2H), 4.96 (s, 2H),

4.22 (t, J = 0.8, 1H), 2.39 (s, 3H). ^{13}C NMR (101 MHz, $CDCl_3$) δ 161.48, 141.31, 132.35, 129.58, 125.79, 119.73, 62.89, 21.29 (lit [38]). HRMS (ESI): m/z 159.0896 $(M+H)^+$; calc. for $C_{10}H_{11}N_2$: 159.0922.

2.5.1.3. 3-Amino-3-(4-methoxyphenyl)acrylonitrile 3b. (36% yield). Yellow–brown crystals, m.p. 119.4 °C (lit m.p. 117–118 °C [39]); ^{1}H NMR (400 MHz, $CDCl_3$) δ 7.47–7.42 (*m*, 2H), 6.95–6.90 (*m*, 2H), 4.98 (s, 2H), 4.17 (s, 1H), 3.83 (s, 3H). ^{13}C NMR (101 MHz, $CDCl_3$) δ 161.60, 161.17, 133.87, 127.36, 119.94, 114.12, 62.07, 55.34 (lit [38,40]). HRMS (ESI): m/z 175.0880 $(M+H)^+$; calc. for $C_{10}H_{11}N_2O$: 175.0871.

2.5.1.4. 3-Amino-3-(4-chlorophenyl)acrylonitrile 4b (56% yield). Beige powder, m.p. 124.8 °C (lit m.p. 140–144 °C [40]); ^{1}H NMR (400 MHz, $CDCl_3$) δ 7.48–7.39 (*m*, 5H), 4.89 (s, 2H), 4.24 (t, J = 0.9, 1H). ^{13}C NMR (101 MHz, $CDCl_3$) δ 160.26, 136.97, 133.70, 129.22, 127.33, 119.13, 64.27 (lit [38]). HRMS (ESI): m/z 179.0357 $(M+H)^+$; calc. for $C_9H_8N_2Cl$: 179.0376.

2.5.1.5. 3-Amino-3-(4-bromophenyl)acrylonitrile 5b (42% yield). Yellow powder, m.p. 135 °C (lit m.p.147–148 °C [37]); ^{1}H NMR (400 MHz, $CDCl_3$) δ 7.60–7.54 (*m*, 2H), 7.41–7.35 (*m*, 2H), 4.90 (s, 2H), 4.25 (d, J = 0.8, 1H). ^{13}C NMR (101 MHz, $CDCl_3$) δ 160.35, 134.17, 132.17, 127.54, 125.23, 119.13, 64.21 (lit [38]). HRMS (ESI): m/z 222.9867 $(M+H)^+$; calc. for $C_9H_8N_2Br$: 222.9871.

2.5.1.6. 3-Amino-3-(3-bromophenyl)acrylonitrile 6b (33% yield). Yellow powder; ^{1}H NMR (400 MHz, $CDCl_3$) δ 7.65 (t, J = 1.8, 1H), 7.59 (ddd, J = 1.0, 2.0, 8.0, 1H), 7.44 (ddd, J = 1.1, 1.8, 7.8, 1H), 7.30 (t, J = 7.9, 1H), 5.05 (s, 2H), 4.22 (t, J = 0.9, 1H). ^{13}C NMR (101 MHz, $CDCl_3$) δ 159.99, 137.24, 133.74, 130.44, 129.07, 124.66, 122.91, 119.02, 64.30. HRMS (ESI): m/z 222.9822 $(M+H)^+$; calc. for $C_9H_8N_2Br$: 222.9871.

*2.5.2. General method for preparation of 3-amino-3-phenylpropanenitriles (compounds **1c–6c**) exemplified by **1c***

3-Amino-3-phenylacrylonitrile (**1b**) (3.00 g, 20.8 mmol) was dissolved in absolute ethanol (50 ml). Sodium cyanoborohydride (1.44 g, 22.9 mmol) was added, followed by bromocresol green (1 drop of a 0.5% solution in ethanol). Concentrated HCl (32%) was added dropwise until a permanent yellow colour was obtained. The reaction was stirred at room temperature for 3 h. Water was added, followed by concentrated aqueous ammonia (25%) to about pH 11. The aqueous layer was extracted with diethyl ether (×3) and the combined organic layers were washed with brine, dried over $MgSO_4$ and the solvent removed *in vacuo*. The resulting brown oil was purified by column chromatography (elution ethyl acetate) to yield 3-amino-3-phenylpropanenitrile (1.79 g, 59%) as a colourless oil.

*2.5.2.1. 3-Amino-3-phenylpropanenitrile **1c** (59% yield).* Clear oil; ^{1}H NMR (400 MHz, $CDCl_3$) δ 7.35 (*m*, 4H), 7.31–7.25 (*m*, 1H), 4.27 (dd, J = 5.8, 7.1, 1H), 2.68–2.55 (*m*, 2H), 1.73 (s, 2H). ^{13}C NMR (101 MHz, $CDCl_3$) δ 142.17, 128.55, 127.85, 125.65, 117.80, 52.25, 28.06. ^{13}C NMR (101 MHz, $CDCl_3$) δ 143.92, 129.89, 129.13, 127.46, 119.31, 53.82, 28.29. HRMS (ESI): m/z 147.0909 $(M+H)^+$; calc. for $C_9H_{11}N_2$: 147.0922.

*2.5.2.2. 3-Amino-3-p-tolylpropanenitrile **2c** (53% yield).* Clear oil; ^{1}H NMR (400 MHz, $CDCl_3$) δ 7.29–7.24 (*m*, 2H), 7.21–7.15 (*m*, 2H), 4.30 (dd, J = 5.8, 7.1, 1H), 2.71–2.58 (*m*, 1H), 2.35 (s, 3H), 1.73 (s, 2H). ^{13}C NMR (101 MHz, $CDCl_3$) δ 139.37, 137.93, 129.48, 125.72, 117.96, 52.33, 28.45, 21.03. HRMS (ESI): m/z 161.1083 $(M+H)^+$; calc. for $C_{10}H_{13}N_2$: 161.1079.

*2.5.2.3. 3-Amino-3-(4-methoxyphenyl)propanenitrile **3c** (53% yield).* Clear oil; ^{1}H NMR (400 MHz, $CDCl_3$) δ 7.32–7.27 (*m*, 2H), 6.92–6.87 (*m*, 2H), 4.32–4.25 (*m*, 1H), 3.79 (s, 3H), 2.63 (dd, J = 5.5, 6.4, 2H), 1.74 (s, 2H). ^{13}C NMR (101 MHz, $CDCl_3$) δ 159.21, 134.33, 126.94, 117.96, 114.02, 55.16, 51.93, 28.42. HRMS (ESI): m/z 177.1027 $(M+H)^+$; calc. for $C_{10}H_{13}N_2O$: 177.1028.

*2.5.2.4. 3-Amino-3-(4-chlorophenyl)propanenitrile **4c** (52% yield).* Clear oil; ^{1}H NMR (400 MHz, $CDCl_3$) δ 7.40–7.30 (*m*, 4H), 4.37–4.29 (*m*, 1H), 2.73–2.58 (*m*, 2H), 1.99 (s, 2H). ^{13}C NMR (101 MHz, $CDCl_3$) δ 140.45, 133.92, 128.98, 127.36, 117.56, 51.94, 28.23. HRMS (ESI): m/z 181.0522 $(M+H)^+$; calc. for $C_9H_{10}N_2Cl$: 181.0533.

2.5.2.5. 3-Amino-3-(4-bromophenyl)propanenitrile 5c. (26% yield). Yellow oil; ^{1}H NMR (400 MHz, $CDCl_3$) δ 7.46 (d, J = 8.5, 2H), 7.25 (d, J = 8.5, 2H), 4.25 (t, J = 6.3, 1H), 2.70–2.53 (*m*, 2H), 1.80 (s, 2H). ^{13}C NMR (101 MHz, $CDCl_3$) δ 141.07, 131.37, 127.44, 121.33, 117.48, 51.48, 27.74. HRMS (ESI): m/z 225.0027 $(M+H)^+$; calc. for $C_9H_{10}N_2Br$: 225.0027.

*2.5.2.6. 3-Amino-3-(3-bromophenyl)propanenitrile **6c** (40% yield).* Yellow oil; ^{1}H NMR (400 MHz, $CDCl_3$) δ 7.55 (t, J = 1.8, 1H), 7.45 (ddd, J = 1.2, 1.9, 7.8, 1H), 7.35–7.29 (*m*, 1H), 7.29–7.21 (*m*, 1H), 4.31 (dd, J = 5.7, 7.1, 1H), 2.67 (*m*, 2H), 1.85 (s, 2H). ^{13}C NMR (101 MHz, $CDCl_3$) δ 144.45, 131.26, 130.40, 129.03, 124.65, 122.81, 117.50, 52.05, 28.20. HRMS (ESI): m/z 225.0007 $(M+H)^+$; calc. for $C_9H_{10}N_2Br$: 225.0027.

*2.5.3. General method for biotransformation of β-aminonitriles to β-amino-amides (compounds **1d–6d**)*

3-Amino-3-phenylpropanenitrile (100 mg) was incubated with resting cells of *R. rhodochrous* ATCC BAA-870 in a 100 mM Tris buffer, pH 9.0. Incubation was at 5 °C or 30 °C with agitation and reaction sampling/termination being done at varying time periods (0 min – 25 h).

*2.5.3.1. 3-Amino-3-phenylpropanamide **1d** (23% yield).* White powder; m.p. 110.1 °C; ^{1}H NMR (400 MHz, $CDCl_3$) δ 7.37–7.30 (*m*, 5H), 6.94 (s, 1H), 5.54 (s, 1H), 4.37 (t, J = 6.7, 1H), 2.59–2.54 (*m*, 2H), 2.04 (s, 2H). ^{13}C NMR (101 MHz, $CDCl_3$) δ 174.38, 143.53, 128.65, 127.52, 125.97, 52.38, 43.90. HRMS (ESI): m/z 165.1042 $(M+H)^+$; calc. for $C_9H_{13}N_2O$: 165.1028.

*2.5.3.2. 3-Amino-3-p-tolylpropanamide **2d** (22% yield).* Yellow powder; ^{1}H NMR (400 MHz, $CDCl_3$) δ 7.22 (d, J = 8.1, 2H), 7.18–7.12 (*m*, 2H), 7.02 (s, 1H), 5.73 (s, 1H), 4.32 (t, J = 6.7, 1H), 2.53 (d, J = 6.5, 2H), 2.34 (s, 3H), 1.96 (s, 2H). ^{13}C NMR (101 MHz, $CDCl_3$) δ 174.02, 141.98, 137.07, 129.38, 125.68, 52.54, 44.82, 21.02. HRMS (ESI): m/z 179.1287 $(M+H)^+$; calc. for $C_{10}H_{14}N_2O_2Na$: 179.1284.

*2.5.3.3. 3-Amino-3-(4-methoxyphenyl)propanamide **3d** (16% yield).* White powder; ^{1}H NMR (400 MHz, CD_3OD) δ 7.63 (br s, 1H), 7.53 (br s, 1H), 7.35–7.27 (*m*, 2H), 6.92–6.85 (*m*, 2H), 4.55–4.49 (*m*, 1H), 3.71 (s, 3H), 2.83 (qd, J = 7.2, 15.8, 2H). ^{13}C NMR (101 MHz, $CDCl_3$) δ 174.21, 158.89, 127.23, 127.20, 114.02, 55.21, 51.88, 43.85. HRMS (ESI): m/z 217.0926 $(M+H)^+$; calc. for $C_{10}H_{14}N_2O_2Na$: 217.0953.

*2.5.3.4. 3-Amino-3-(4-bromophenyl)propanamide **5d** (28% yield).* Yellow powder; ^{1}H NMR (400 MHz, $CDCl_3$) δ 7.48 (d, J = 8.4, 2H), 7.25 (d, J = 8.4, 2H), 4.43–4.35 (*m*, 1H), 2.75–2.39 (*m*, 2H), 1.26 (s, 4H). ^{13}C NMR (101 MHz, $CDCl_3$) δ 173.83, 141.80, 131.72, 127.92, 121.41, 51.85, 43.24. HRMS (ESI): m/z 243.0150 $(M+H)^+$; calc. for $C_9H_{12}N_2OBr$: 243.0133.

2.5.3.5. 3-Amino-3-(3-bromophenyl)propanamide ***6d*** *(6% yield).* Yellow oil; ^{13}C NMR (101 MHz, $CDCl_3$) δ 173.69, 145.30, 130.76, 130.33, 129.31, 124.90, 122.69, 51.97, 43.28. HRMS (ESI): m/*z* 243.0140 $(M+H)^+$; calc. for $C_9H_{12}N_2OBr$: 243.0133.

2.5.4. Procedure for N-acetylation of β-amino compounds

To the 3-amino substituted compound (1.23 mmol solubilised in 5 ml DCM), was added 5 equiv. acetic anhydride (6.13 mmol), 4 equiv. of pyridine (4.9 mmol) and a catalytic quantity of DMAP (~1 mg). This was stirred at room temperature and monitored by TLC. After conversion, as evidenced by TLC, the reaction mixture was washed with 1 M HCl, followed by 1 M NaOH. The organic layer was washed with brine and dried over $MgSO_4$ and the solvent removed *in vacuo*. The product was purified by column chromatography.

2.5.4.1. N*-(2-cyano-1-phenylethyl)acetamide* ***7c*** *(60% yield) cream crystals.* ^{1}H NMR (200 MHz, $CDCl_3$) δ 7.55–7.06 (*m*, 5H), 6.98 (s, 1H), 5.30–4.87 (*m*, 1H), 2.98–2.58 (*m*, 2H), 1.85 (s, 3H). ^{13}C NMR (50 MHz, $CDCl_3$) δ 171.122, 149.15, 131.33, 129.23, 127.53, 118.84, 63.92, 24.14, 20.94. HRMS (ESI): m/*z* 187.0871 $(M+H)^+$; calc. for $C_{11}H_{11}N_2O$: 187.0871.

2.5.4.2. 3-Acetamido-3-phenylpropanamide ***7d*** *(60% yield) white crystals.* ^{1}H NMR (400 MHz, $CDCl_3$) δ 7.43–7.27 (*m*, 6H), 6.17 (dd, *J* = 5.1, 8.7, 1H), 5.53 (s, 1H), 5.46 (s, 1H), 2.87 (dd, *J* = 8.7, 14.9, 1H), 2.68 (dd, *J* = 5.1, 14.9, 1H), 2.08 (s, 3H). ^{13}C NMR (101 MHz, $CDCl_3$) δ 171.02, 169.84, 139.33, 128.69, 128.36, 126.25, 72.53, 43.05, 21.13. HRMS (ESI): m/*z* 229.0895 $(M+H)^+$; calc. for $C_{11}H_{14}N_2O_2Na$: 229.0953.

2.5.5. N*-(2-cyano-1-phenylethyl)-4-methylbenzenesulfonamide* ***8c***

3-Amino-3-phenylpropanenitrile (**1c**) (1.62 g, 0.011 mol) was dissolved in dichloromethane (50 ml) and 4-dimethylaminopyridine (1.3 equiv., 1.76 g, 0.014 mol) and *p*-toluenesulfonyl chloride (1.2 equiv., 2. 53 g, 0.013 mol) were added. The reaction was allowed to stir at room temperature for 2 days. The organic layer was then washed with 1 M HCl (50 ml), dried over $MgSO_4$ and the solvent removed *in vacuo*. The crude product was purified by silica gel column chromatography, elution hexane: ethyl acetate (from 7:3 to 5:5) to yield **8c** (1.66 g, 50%). White powder, ^{1}H NMR (400 MHz, $CDCl_3$) δ 7.61 (d, *J* = 8.3, 2H), 7.33–7.12 (*m*, 5H), 7.12–7.04 (*m*, 2H), 5.56 (d, *J* = 7.3, 1H), 4.53 (td, *J* = 5.6, 7.2, 1H), 2.87 (dd, *J* = 3.9, 6.4, 2H), 2.35 (s, 3H); ^{13}C NMR (101 MHz, $CDCl_3$) δ 143.95, 137.09, 136.41, 129.73, 129.09, 128.86, 127.07, 126.20, 116.47, 54.13, 26.29, 21.51. HRMS (ESI): m/*z* 323.0811 $(M+H)^+$; calc. for $C_{16}H_{16}N_2O_2$: 323.0830.

2.5.6. General procedure for preparation of N-Boc derivatives

The β-amino compound (~1.20 mmol) was dissolved in dioxane (2.5 ml), water (1.2 ml) and 1 M NaOH (1.2 ml). This reaction was cooled in an ice-bath and di-*tert*-butyl dicarbonate (1.1 equiv., 0.29 g, 1.33 mmol) was added. The reaction was stirred at room temperature for 2 –6 h. Half of the solvent was removed *in vacuo*. Ethyl acetate (10 ml) was added, forming two layers. The aqueous layer was acidified to pH 2–3 using a solution of $KHSO_4$. The aqueous layer was extracted with ethyl acetate (×4) and the combined organic layer was washed with brine, dried over $MgSO_4$, and the solvent removed *in vacuo* to yield product.

2.5.6.1. tert-Butyl N*-(2-cyano-1-phenylethyl)-carbamate* ***9c*** *(92% yield).* White powder, ^{1}H NMR (200 MHz, $CDCl_3$) δ 7.50–7.23 (*m*, 5H), 5.22–5.03 (*m*, 1H), 5.03–4.83 (*m*, 1H), 3.12–2.75 (*m*, 2H), 1.45 (s, 9H). ^{13}C NMR (50 MHz, $CDCl_3$) δ 154.73, 138.44, 129.13, 128.64, 126.17, 117.01, 80.56, 51.23, 28.28, 25.22. HRMS (ESI): m/*z* 269.1261 $(M+H)^+$; calc. for $C_{14}H_{18}N_2O_2Na$: 269.1266.

2.5.6.2. tert-Butyl N*-(3-amino-3-oxo-1-phenyl-propyl)carbamate* ***9d*** *(45% yield).* White crystals; ^{1}H NMR (400 MHz, DMSO) δ 7.41–7.34 (*m*, 1H), 7.31–7.23 (*m*, 5H), 7.23–7.15 (*m*, 1H), 6.80 (s, 1H), 4.88 (q, *J* = 7.5, 1H), 2.48–2.37 (*m*, 2H), 1.35 (s, 9H). ^{13}C NMR (101 MHz, DMSO) δ 171.68, 154.76, 143.70, 128.15, 126.71, 126.35, 77.84, 51.45, 42.43, 28.32. HRMS (ESI): m/*z* 287.1349 $(M+H)^+$; calc. for $C_{14}H_{20}N_2O_3Na$: 287.1372.

3. Results and discussion

Previous studies with unprotected β-hydroxynitriles showed that these compounds were hydrolysed by *R. rhodochrous* ATCC BAA-870 to the corresponding amides and acids [41]. The first reaction, catalysed by nitrile hydratase, was relatively rapid, but not enantioselective. The subsequent hydrolysis of the amide to the corresponding carboxylic acid was slower, but yielded β-substituted phenoxy compounds with high enantiomeric excess (up to 99% ee).

In the current study we attempted to enantioselectively hydrolyse the nitrile group of β-amino substituted nitrile compounds. Surprisingly initial biocatalytic studies using *R. rhodochrous* failed to produce any hydrolysis products using the unprotected 3-amino-3-phenylpropanenitrile. Hence we investigated the use of *N*-protected β-substituted amino derivatives, specifically *N*-acetyl (**7c**), *N*-tosyl (**8c**) and *N*-Boc (**9c**) 3-amino-3-phenylpropanenitrile (Fig. 1). The conversion of the tosyl and Boc compounds was negligible, an observation also made by Preiml et al. [26] when investigating the hydrolysis of **8c** using other *Rhodococcus* strains as nitrile biocatalysts.

However, the acetyl compound yielded a modest 19% of the corresponding amide (reaction conditions 30 °C, pH 7.0, whole cell reaction, 7 days, high cell load) showing that this class of compound may be amenable to nitrile hydratase catalysed hydrolysis. It is possible that the *N*-tosyl and *N*-Boc protected compounds were not hydrolysed because they were too large for the nitrile hydratase active site, while the smaller *N*-acetyl compound was a better fit. However, based on this assumption (and previous results with the structurally similar β-hydroxynitriles [41]) the unprotected 3-amino-3-phenylpropanenitrile should fit into the active site. Therefore it was hypothesised that the lack of hydrolysis could be ascribed to protonation of the amino group at pH 7, resulting in a positive charge. Amino groups are protonated at pH below 9–10, but a pH > 10 could result in enzyme inactivation [42]. Hence we repeated the reactions at the intermediate pH 9.0 (Tris buffer) where there is a significant proportion of the unprotonated species. Under these conditions hydrolysis was indeed observed, and eventually **1c** was completely converted to **1d**. Confirmation that the reaction was catalysed by nitrile hydratase was obtained by use of purified enzyme in the reaction instead of whole cells.

Although we had previously seen conversion of β-hydroxynitriles to the corresponding carboxylic acids [41], in the current study of unprotected aliphatic β-aminonitriles the amides were predominantly generated and the carboxylic acid yield was low (as determined by HPLC-MS analysis). The same result was observed by Preiml et al. for *N*-protected six-membered carbocyclic β-aminonitriles which were accumulated during *Rhodococcus* catalysed hydrolysis [27], even though the structurally related five-membered carbocyclic nitriles were converted mainly to the respective acids. This implies a difference in the substrate profiles of the nitrile hydratase and the amidase.

Table 1
Biotransformation of racemic aromatic β-aminonitriles.

Entry	Substrate	Aryl substitution	Reaction temperature (°C)	Conversion (%)	(*R*)-Nitrile % ee	(*S*)-Amide %ee	Enantiomeric ratio (E) nitrile amide	
1	**1c**	4-H	30	46	8	7	1.3	1.2
2	**2c**	4-Me	30	39	21	3	2.4	1.1
3	**2c**	4-Me	5	61	19	48	1.5	6.1
4	**3c**	4-OMe	30	62	39	24	2.3	2.3
5	**3c**	4-OMe	5[a]	33	15	62	2.2	5.7
6	**3c**	4-OMe	5[a]	68	85	37	5.8	4.8
7	**4c**	4-Cl	30	0	0	0	–	–
8	**5c**	4-Br	30	55	32	43	2.3	4.1
9	**6c**	3-Br	30	33	4	22	1.2	1.7

[a] At 2 and 24 h, entries 5 and 6, respectively.

In the current study of the parent compound **1c** there was relatively insignificant enantioselectivity (Table 1), however enantioselectivity was observed for the derivatives with substitution on the aromatic moiety, an exception being the chloro-substituted nitrile (**4c**) that did not yield the expected amide product. Compounds **2d**, **3d**, **5d** and **6d** were all generated with an enantiomeric excess (Table 1). In particular the amide **3d** and the nitrile **3c** could be obtained with relatively high enantiometic excess. This was more evident when the reactions were run at 5 °C than at 30 °C. This improved enantioselectivity based on decreased temperature is opposite to that of some other enzymatic reactions [43,44]. The (*S*)-enantiomer of the β-amino-amide was preferentially generated, according to assignment based on the elution times of the 3-amino-3-phenylpropanamide enantiomer standards. This observation was supported by the positive optical rotation value demonstrated by *N*-Boc derivatised 3-amino-3-*p*-tolylpropanenitrile remaining after biocatalytic conversion of 3-amino-3-*p*-tolylpropanenitrile, which according to González et al. [31] corresponds to the (*R*)-enantiomer. Although these enantiomeric excesses are not as high as observed with the β-hydroxyl compounds [41] it is interesting that, contrary to the case of β-hydroxynitrile compounds here the β-aminonitriles were enantioselectively hydrolysed to amides, and hence the enantioselectivity resided in the nitrile hydratase and not the amidase. Cobalt containing nitrile hydratases, such as the enzyme expressed by this organism, have previously been demonstrated to have enantioselectively towards α-aminonitriles, while the iron containing nitrile hydratases do not show any enantioselectivity [45].

Enzyme enantioselectivity was not absolute, and eventually complete conversion of the starting nitrile occurred with time, defining this reaction as a kinetic resolution. The *p*-tolyl (**2**) and the 4-methoxy derivatives (**3**) had the highest enantiomeric ratios (*E*) at 5 °C (Table 1). It also appears that *para* substitution of the bromine (**5c**) on the aromatic ring provided better enantioselectivity when compared to the *meta* position (**6c**) (Table 1). The stereoselective biocatalytic conversion of unprotected chiral aliphatic β-aminonitriles to the corresponding amides demonstrated here seems to be unprecedented.

4. Conclusion

We have shown that asymmetric hydrolysis of unprotected β-aminonitriles to the corresponding amides can be achieved with ee values of product and substrate above 50% using *R. rhodochrous* ATCC BAA-870. This was achieved by the nitrile hydratase, which demonstrated enantioselective activity for substrates where there was substitution on the β-aromatic moiety. Higher enantiomeric excesses may be achievable through enzyme engineering, reaction engineering, use of different substrates, or combination of the nitrile hydratase with an amidase with complementary enantioselectivity.

N-protection of the β-aminonitriles with Boc, tosyl, and acetyl groups provided insights into the selectivity of the nitrile hydratase active site. Both steric hindrance from bulky groups (Boc or tosyl) and an inability to convert compounds with a charged primary amine are suggested as no reaction was observed in any of these examples, while the smaller acetylated amine and unprotonated amine were both accepted.

Acknowledgements

We would like to thank the DST and the CSIR Thematic Programme for Funding. This research was presented in part at the 5th International Congress on Biocatalysis (Hamburg, Germany, August 29–September 2, 2010) and at a European Science Foundation COST Action CM0701 (Cascade Biocatalysis) workshop (Vilnius, Lithuania, 8–11 September 2010). We would like to thank, Dr Ludmila Martínková and Prof Andreas Stolz (working group leaders), Prof Paul Steenkamp for additional analysis, Dr Henok Kinfe and Jonathan Pantshwa (CSIR) and Prof N Klempier and Dr M Winkler (University of Graz) for technical inputs and discussions. We would also like to thank Dr Daniel Visser, Dr Petrus van Zyl and Joni Frederick for fermentation to bulk up the biocatalytic biomass and enzyme purification. Chemical structures were created using Chem Draw.

References

[1] Y. Hsiao, N.R. Rivera, T. Rosner, S.W. Krska, E. Njolito, F. Wang, Y. Sun, J.D. Armstrong, E.J.J. Grabowski, R.D. Tillyer, F. Spindler, C. Malan, J. Am. Chem. Soc. 126 (2004) 9918–9919.
[2] R.A. Holton, C. Somoza, H.-B. Kim, F. Liang, R.J. Biediger, P.D. Boatman, M. Shindo, C.C. Smith, S. Kim, H. Nadizadeh, Y. Suzuki, C. Tao, P. Vu, S. Tang, P. Zhang, K.K. Murthi, L.N. Gentile, J.H. Liu, J. Am. Chem. Soc. 116 (1994) 1597–1598.
[3] S.G. Davies, O. Ichihara, I. Lenoir, I.A.S. Walters, J. Chem. Soc. Perkin Trans. 1. (1994) 1411–1415.
[4] D. Steinhuebel, Y. Sun, K. Matsumura, N. Sayo, T. Saito, J. Am. Chem. Soc. 131 (2009) 11316–11317.
[5] M.-I. Aguilar, A.W. Purcell, R. Devi, R. Lew, J. Rossjohn, A.I. Smith, P. Perlmutter, Org. Biomol. Chem. 5 (2007) 2884–2890.
[6] D.L. Steer, R.A. Lew, P. Perlmutter, A.I. Smith, M.-I. Aguilar, Curr. Med. Chem. 9 (2002) 811–822.
[7] K. Gademann, T. Hintermann, J.V. Schreiber, Curr. Med. Chem. 6 (1999) 905–925.
[8] R.L. Wolin, A. Santillán Jr., T. Barclay, L. Tang, H. Venkatesan, S. Wilson, D.H. Lee, T.W. Lovenberg, Bioorg. Med. Chem. 12 (2004) 4493–4509.
[9] Y. Zhu, G. Wu, X. Zhu, Y. Ma, X. Zhao, Y. Li, Y. Yuan, J. Yang, S. Yu, F. Shao, M. Lei, J. Med. Chem. 53 (2010) 8619–8626.
[10] D.R. Armour, A.S. Bell, P.J. Edwards, D. Ellis, D. Hepworth, M.L. Lewis, C.R. Smith, PCT Pat WO2004/020414 (2004).
[11] R. Angelaud, J.D. Armstrong, D. Askin, J. Balsells, K. Hansen, J. Lee, P.E. Maligres, N.R. Rivera, Y. Xiao, Y.L. Zhong, PCT Pat WO2004087650 (2004).
[12] J. Imbriglio, S.L. Colletti, J.R. Tata, R.T. Beresis, D. Marley, S. Raghavan, D.R. Schmidt, A.R. Lins, A.L. Smenton, W. Chen, H. Shen, F.X. Ding, R. Bodner, PCT Pat. WO2007075749 (2007).
[13] A. Liljeblad, L.T. Kanerva, Tetrahedron 62 (2006) 5831–5854.
[14] B. Weiner, W. Szymański, D.B. Janssen, A.J. Minnaard, B.L. Feringa, Chem. Soc. Rev. 39 (2010) 1656–1691.
[15] C. Pousset, R. Callens, M. Haddad, M. Larchevêque, Tetrahedron Asymm. 15 (2004) 3407–3412.

[16] G. Tasnádi, E. Forró, F. Fülöp, Tetrahedron Asymm. 19 (2008) 2072–2077.
[17] G. Tasnádi, E. Forró, F. Fülöp, Tetrahedron Asymm. 20 (2009) 1771–1777.
[18] G. Tasnádi, E. Forró, F. Fülöp, Org. Biomol. Chem. 8 (2010) 793–799.
[19] X.-G. Li, L.T. Kanerva, Tetrahedron Asymm. 16 (2005) 1709–1714.
[20] E. Forró, T. Paál, G. Tasnádi, F. Fülöp, Adv. Synth. Catal. 348 (2006) 917–923.
[21] G. Tasnádi, E. Forró, F. Fülöp, Tetrahedron Asymm. 18 (2007) 2841–2844.
[22] B. Wu, W. Szymański, S. De Wildeman, G.J. Poelarends, B.L. Feringa, D.B. Janssen, Adv. Synth. Catal. 352 (2010) 1409–1412.
[23] L. Martínková, V. Křen, Biocatal. Biotrans. 20 (2002) 73–93.
[24] O. Toshihiro, M. Yasuko, S. Akio, Pat. JP10042886 (1998).
[25] L.-Y. Liang, Y.-G. Zheng, Y.-C. Shen, Process Biochem. 43 (2008) 758–764.
[26] M. Preiml, K. Hillmayer, N. Klempier, Tetrahedron Lett. 44 (2003) 5057–5059.
[27] M. Preiml, H. Honig, N. Klempier, J. Mol. Catal. B: Enz. 29 (2004) 115–121.
[28] M. Winkler, L. Martínková, A.C. Knall, S. Krahulec, N. Klempier, Tetrahedron 61 (2005) 4249–4260.
[29] M.S.-I. Veitía, P.L. Brun, P. Jorda, A. Falguières, C. Ferroud, Tetrahedron Asymm. 20 (2009) 2077–2089.
[30] D.-Y. Ma, D.-X. Wang, J. Pan, Z.-T. Huang, M.-X. Wang, J. Org. Chem. 73 (2008) 4087–4091.
[31] P.B. González, R. Lopez, C.J. Palomo, J. Org. Chem. 75 (2010) 3920–3922.
[32] D. Brady, A. Beeton, C. Kgaje, J. Zeevaart, F. van Rantwijk, R.A. Sheldon, Appl. Microbiol. Biotechnol. 64 (2004) 76–85.
[33] D. Brady, N. Dube, R. Petersen, S. Afr. J. Sci. 102 (2006) 339–344.
[34] T. de Paulis, K. Hemstapat, Y. Chen, Y. Zhang, S. Saleh, D. Alagille, R.M. Baldwin, G.D. Tamagnan, P.J. Conn, J. Med. Chem. 49 (2006) 3332–3344.
[35] J.P. Michael, C.M. Jungmann, Tetrahedron 48 (1992) 10211–10220.
[36] A. Kumar, D. Banerjee, M.G.B. Drew, S. Ray, D. Haldar, A. Banerjee, Tetrahedron 61 (2005) 5027–5036.
[37] D.N. Ridge, J.W. Hanifin, L.A. Harten, B.D. Johnson, J. Menschik, G. Nicolau, A.E. Sloboda, D.E. Watt, J. Med. Chem. 22 (1979) 1385–1389.
[38] U. Chiacchio, A. Corsaro, G. Musumarra, G. Perrini, G. Purrello, J. Chem. Soc. Perkin Trans. 2. (1986) 1847–1849.
[39] J.K. Coward, T.C. Bruice, J. Am. Chem. Soc. 91 (1969) 5329–5339.
[40] Y. Gao, H. Wang, M. Xu, H. Lian, Y. Pan, Y. Shi, Org. Prep. Proc. Int. 33 (2001) 351–356.
[41] H.H. Kinfe, V. Chhiba, J. Frederick, M.L. Bode, K. Mathiba, P.A. Steenkamp, D. Brady, J. Mol. Catal. B: Enzym. 59 (2009) 231–236.
[42] L. Martínková, B. Uhnáková, M. Pátek, J. Nešvera, V. Křen, Environ. Int. 35 (2009) 162–177.
[43] C. Ewert, S. Lutz-Wahl, L. Fischer, Tetrahedron Asymm. 19 (2008) 2573–2578.
[44] R. Bauer, H.-J. Knackmuss, A. Stolz, Appl. Microbiol. Biotechnol. 49 (1998) 89–95.
[45] S. van Pelt, M. Zhang, L.G. Otten, J. Holt, D.Y. Sorokin, F. van Rantwijk, G.W. Black, J.J. Perry, R.A. Sheldon, Org. Biomol. Chem. 9 (2011) 3011–3019.

Chapter Five: PAPER III

Enzymatic stereoselective synthesis of β-amino acids

Varsha Chhiba, Moira Bode, Dean Brady and Kgama Mathiba

Cascade Biocatalysis, Chapter 14, pp 297-313

14
Enzymatic Stereoselective Synthesis of β-Amino Acids

Varsha Chhiba, Moira Bode, Kgama Mathiba, and Dean Brady

14.1
Introduction

The β-hydroxy and β-amino acid structural motif occurs commonly in compounds of pharmaceutical importance [1]. Examples include the β-substituted β-adrenergic agents, used in the treatment of cardiovascular and psychiatric disorders [2–4], and the biologically active molecules cispentacin [5], sitagliptin [6] (Figure 14.1), taxol [7], and otamixaban [8].

Although in the past many of these compounds have been used in racemic form, the current trend in the pharmaceutical industry is toward enantiomerically pure drugs. The enantioselective synthesis or the chiral separation of racemic mixtures is often difficult, and synthetic chemistry is increasingly looking toward the use of enzymes for the preparation of single enantiomer compounds to be used for the generation of β-substituted pharmaceutical intermediates [9, 10], an area that our group has also focused on [11, 12].

The traditional use of peptides as therapeutic compounds has often been problematic for a number of reasons. Small peptides often display a great degree of flexibility, which enables changes in conformation that adversely affect the activity of the peptide *in vivo*. Similarly, susceptibility to protease activity, aggregation of the peptides, poor absorption through the cell membrane, as well as poor solubility contribute to poor efficacy of peptide based therapeutics [13, 14].

Of particular interest in medicinal chemistry is the inclusion of non-standard amino acids in therapeutic peptides or peptidomimetics [15] to overcome these problems. Peptidomimetic approaches employing β-amino acids (Figure 14.2) have shown potential in recent years since β-amino acids are similar enough to their α-analogs to function as required while reducing the rate of peptide hydrolysis by proteases and consequently improving the pharmacokinetic properties of these compounds [16].

Peptidomimetics typically function as antimicrobial compounds [15, 17], but new functions are being discovered. Wolin *et al.* [18] found that β-amino acid derivatives act as glycine transport inhibitors, whereas Zhu *et al.* [19] have identified others that function as proteasome inhibitors. Armour *et al.* [20] incorporated them into

Cascade Biocatalysis: Integrating Stereoselective and Environmentally Friendly Reactions, First Edition.
Edited by Sergio Riva and Wolf-Dieter Fessner.
© 2014 Wiley-VCH Verlag GmbH & Co. KGaA. Published 2014 by Wiley-VCH Verlag GmbH & Co. KGaA.

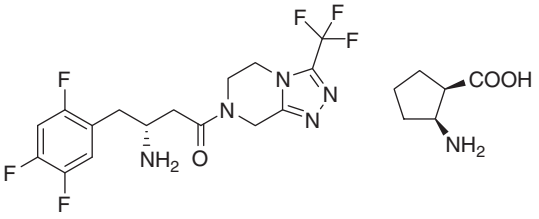


Figure 14.1 Sitagliptin, an antidiabetic drug (a) and cispentacin (b), an antifungal antibiotic.

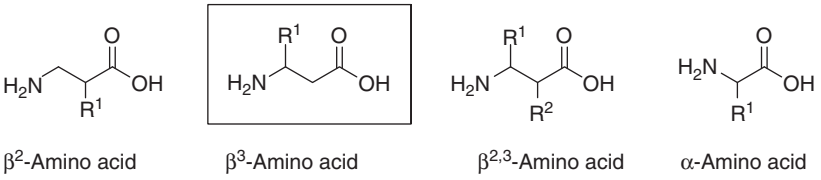


Figure 14.2 General structure of α- and β-amino acids.

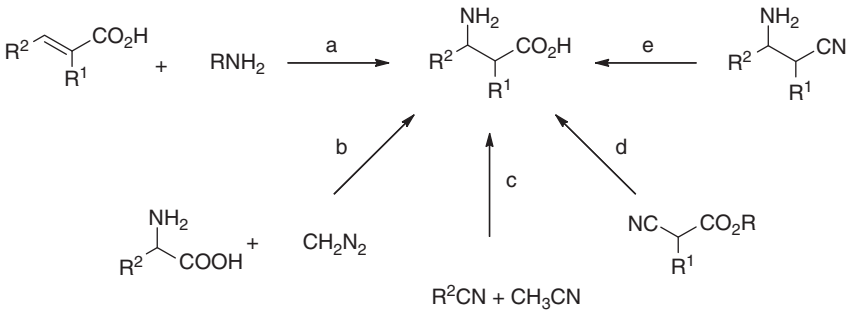
oxytocin inhibitors, whereas Angelaud *et al.* [21] synthesized peptidase inhibitors. Imbriglio *et al.* [22] studied the effect of peptidomimetic compounds as niacin receptor agonists for treating atherosclerosis and dyslipidemias, and other novel applications for peptidomimetic compounds incorporating β-amino acids are being investigated [23].

14.2
Preparation of β-Amino Acids

14.2.1
Chemical Methods for Generating β-Amino Acids

There are a number of chemical methods for the preparation of racemic β^3-amino acids. Selected methods are shown in Scheme 14.1, and include Michael addition to unsaturated carboxylic acids (a), homologation of α-amino acids (b), Thorpe reaction followed by reduction (c), nitrile reduction (d), and nitrile hydrolysis (e), among many others. Strategies for the stereoselective synthesis of β-amino acids are emerging, but there is not as yet a method that is generally applicable [24, 25].

Currently, resolution of racemates is a valuable strategy for the production of enantiopure β-amino acids [26]. The classical method of resolving amino acids is through transformation of the racemate into diastereomeric salts via complexation of the carboxylic acids with a chiral base, usually followed by multistep fractional recrystallization [25]. An alternative method is to resolve the enantiomers by applying the high stereoselectivity of enzymes, and there are a number of suitable biocatalysts available.

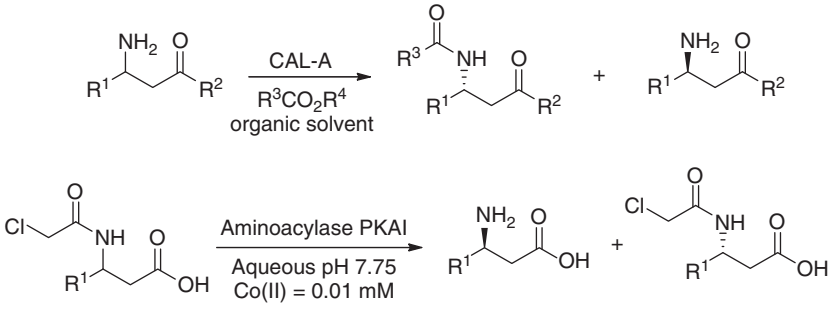


Scheme 14.1 Selected methods for the synthesis of racemic β-amino acids.

14.2.2
Biocatalytic Preparation of Enantiopure β-Amino Acids

14.2.2.1 Lipases and Aminoacylases

A method that has been successfully applied to the resolution of β-amino acids is N-acylation or *N*-acyl hydrolysis. Enantioselective N-acylation of β-amino esters in an organic solvent has been carried out using *Candida antarctica* lipase A (CAL-A) lipase, while enantioselective hydrolysis of *N*-acyl β-amino acids in aqueous medium has been catalyzed by aminoacylase (Scheme 14.2).



Scheme 14.2 N-acylation and hydrolysis as a kinetic resolution tool.

The application of lipases in the resolution of racemic β-amino acids and their derivatives has been comprehensively reviewed by Liljeblad and Kanerva [27]. The N-acylation method has been commonly employed in the resolution of β^3 as well as $\beta^{2,3}$-amino esters [28–34] (Scheme 14.2). Suitable organic solvents for this reaction have proven to be, among others, diisopropylether, *tert*-butyl methyl ether, and diethyl ether, whereas the commonly employed acyl donors are butyl butanoate and 2,2,2-trifluoroethyl butanoate.

The catalytic conversion of *N*-chloroacetylated derivatives of β-amino acids using porcine kidney acylase type I showed significant activity, with the (*S*)-enantiomer of the acid being formed [35]. A 96% ee together with a 46% conversion was obtained when using a racemic *p*-methoxyphenyl-substituted substrate, whereas a 95% ee

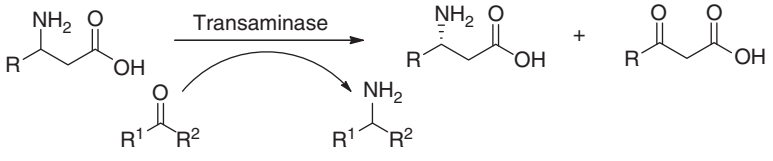
and a 45% conversion was achieved when using a *p*-fluorophenyl-substituted substrate.

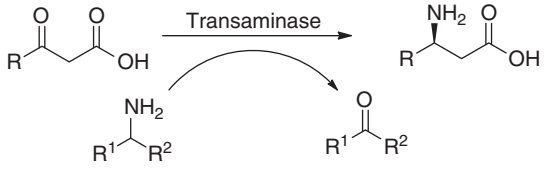
CAL-B lipase has been applied to the resolution of some β-amino esters, by means of *N*-acylation or transesterification [27]. Resolution using CAL-B is complicated by the tendency of the enzyme to catalyze competing reactions at the amino and ester functional groups. However, CAL-B has proved very useful for resolution by means of β-lactam hydrolysis.

Lipase PS has also demonstrated excellent biocatalytic potential for use in the *O*-acylation of hydroxymethylated β-lactam compounds. Lipase PS, much like CAL-B, is capable of catalyzing *N*-acylation as well as reactions at the carboxylic group of the β-amino ester [27].

14.2.2.2 **Transaminases**

Transaminases have been used to generate β-amino acids from racemic β-amino acids (Scheme 14.3a) or prochiral β-keto acids (Scheme 14.3b) [36]. The latter method has the benefit of potentially converting all the starting material into a single enantiomer, but because it is still relatively early in its development, it suffers from disadvantages such as the propensity for the starting β-keto acids to undergo decarboxylation under very mild conditions.

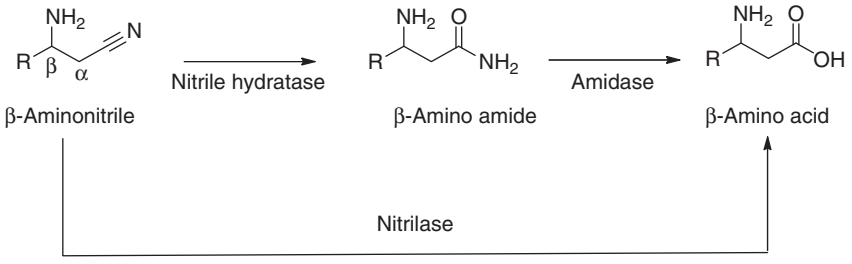




Scheme 14.3 Resolution (a) and synthesis (b) of β-amino acids using transaminase.

14.2.2.3 **Nitrile Converting Biocatalysts**

Another biocatalytic option is the hydrolysis of β-aminonitriles, compounds that are relatively easily synthesized. There are two hydrolytic routes for the enzymatic conversion of nitriles to the corresponding carboxylic acids. These transformations can be achieved either through a two-step cascade reaction involving a nitrile hydratase followed by an amidase that hydrolyzes the intermediate amide, or through use of a nitrilase, an enzyme able to perform the two sequential transformations (Scheme 14.4). The focus of this chapter is on nitrile hydrolysis enzymes.



Scheme 14.4 Biocatalytic conversion of β-aminonitriles to β-amino acids by nitrile hydrolyzing enzymes.

14.3 Nitrile Hydrolysis Enzymes

14.3.1 Nitrilase

Nitrilases (EC 3.5.5.1, α, β hydrolase enzymes) are thiol enzymes capable of hydrolyzing nitriles to their corresponding acids with the concomitant release of ammonia. They belong to the first branch of the nitrilase superfamily and are found in a variety of plants, animals, as well as prokaryotes [37]. The nitrilase superfamily consists of 13 different enzyme classes with considerable structural homology, despite demonstrating significant sequence variation. Members included in this listing are (i) nitrilase, (ii) aliphatic amidase, (iii) amino-terminal amidase, (iv) biotinidase, (v) β-ureidopropionate, (vi) carbamylase, (vii) prokaryote nicotinamide adenine dinucleotide (NAD) synthetase, (viii) eukaryote NAD synthetase, (ix) apolipoprotein *N*-acyltransferase, (x) Nit and NitFhit, (xi) NB11, and finally (xii) NB 12 [37].

Nitrilases can be used on a commercial scale as demonstrated by the production of acrylic acid, (*R*)-(−)-mandelic acid (Mitsubishi Rayon-Japan, BASF-Germany) as well as nicotinic acid (Lonza-China), thus proving the economic potential of this class of enzyme [38–40].

14.3.1.1 Nitrilase Structure and Mechanism

Brenner [41] showed that a nitrilase folded protein consisted of a polypeptide of α-helices and β-sheets that formed a novel α-β-β-α sandwich fold, with a triad of residues in the active site (Glu-Lys-Cys) essential for the covalent catalysis. Structural elucidation of a nitrilase produced by *Rhodococcus rhodochrous* J1 showed that it formed a multimeric extended helix [42].

Mahadevan and Thimann [43] postulated the first nitrilase reaction mechanism, suggesting that the nitrile carbon present in the substrate displays a partial positive charge that is subject to nucleophilic attack by one of the two SH groups in the nitrilase active site. The resulting thioimidate is then hydrolyzed to a thioester, with the release of ammonia as a by-product. Hydrolysis of the acyl-enzyme then results in the release of the final acid product.

14.3.1.2 Nitrilase Substrate Selectivity

Many nitrilases have been screened for their ability to catalyze enantioselective production of valuable carboxylic acid analogs with substitution in the α, β, or γ position. For instance, nitrilase selectivity profiles identified a catalyst capable of resolution of racemic mandelonitrile (an α-hydroxynitrile). Strains such as an *Alcaligenes* sp. [44], *Pseudomonas putida*, and *Microbacterium paraoxydans* [45] showed >93% ee when hydrolyzing mandelonitrile to (*R*)-mandelic acid (Table 14.1). In another example, researchers at Diversa reported on the enantioselective conversion of aromatic aminonitrile compounds for the production of α-amino acids [46]. The authors were successful in achieving a 79.5% yield of the (*R*)-acid product at an enantiomeric excess of 96.3% from the substrate 4-fluorophenylglycinonitrile.

Recently we determined that two *R. rhodochrous* strains (A29 and A99) expressed nitrilase activity after induction. These strains were capable of enantioselectively hydrolyzing racemic 3-amino-3-phenylpropanenitrile directly to the corresponding (*R*)-3-amino-3-phenylpropanoic acid with >95% ee (Table 14.1) in a kinetic resolution. Various inhibitors were used, that indicated the observed hydrolytic activity was due to the presence of a nitrilase rather than a nitrile hydratase and amidase pair [47].

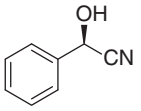
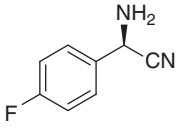
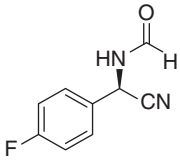
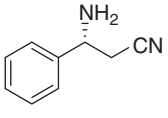
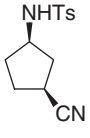
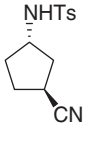
Enantioselectivity at the γ position of alicyclic substrates has also been observed. Winkler and colleagues [48] used commercial nitrilases (NIT 106 and NIT 107, from Codexis, USA) to enantioselectively hydrolyze, conformationally constrained γ-aminonitriles. Racemic five- and six-membered carbocylic γ-amino nitriles (both *cis* and *trans*) were hydrolyzed enantioselectively to the corresponding amino acid using the nitrilases. *Cis* isomers gave excellent enantiomeric excesses up to 99%, while the reaction was less enantioselective for *trans* isomers (86% ee) (Table 14.1).

14.3.2 Nitrile Hydratase

Nitrile hydratases (EC 4.2.1.84) are metallo-enzymes that catalyze the hydration of nitriles to their corresponding amides. From a structural viewpoint, nitrile hydratases consist of two non-identical subunits (α and β), with similar molecular masses of approximately 23 kDa. Nitrile hydratases exist as αβ dimers or $\alpha_2\beta_2$ tetramers, with each αβ dimer binding a single metal atom. The amino acid sequence of each subunit is unrelated, with the structural genes normally adjacent to each other on the same operon [49]. Nitrile hydratases are classified into two groups on the basis of their catalytic metal ion center: a nonheme iron atom [50] or a noncorrinoid cobalt atom [51].

The distribution of nitrile hydratases in microorganisms is diverse, with bacteria collected from shallow marine environments, varied geothermal locations, as well as in numerous soil samples demonstrating this activity. Nitrile hydratases are used as whole cell biocatalysts in industry to produce nicotinamide and acrylamide [52].

Table 14.1 Enantioselective conversion of racemic amino- and hydroxynitriles by nitrilases.

Substrate	Reaction catalyzed	Selectivity	Organism
	Enantioselective conversion of mandelonitrile to (*R*)-(−) mandelic acid	93% to >99% ee	*Alcaligenes* sp. *nitrilase* [44], *Pseudomonas putida*, *Microbacterium paraoxydans*, and *M. liquefaciens* [45]
	Enantioselective conversion of 2-amino-2-(4-fluorophenyl)acetonitrile to the corresponding acid	96.3% ee (*R*-acid)	Nitrilase 5275 [46]
	Enantioselective conversion of *N*-formyl 4-fluorophenylglycinonitrile to the corresponding acid	98–99% ee (*R*-acid)	Nitrilase 5086 [46]
	Stereoselective conversion of 3-amino-3-phenylpropanenitrile to the corresponding acid	>95% ee (*R*)-acid	*Rhodococcus rhodochrous* A29, A99 [47]
	Enantioselective conversion of γ-substituted nitriles to the corresponding γ-amino acids from *cis*-substrates	>99% ee (acid)	Commercial nitrilase NIT 106 [48]
		97% ee (acid)	Commercial nitrilase NIT 106 [48]
	Enantioselective conversion of γ-substituted nitriles to the corresponding γ-amino acids from *trans*-substrates	86% ee (acid)	Commercial nitrilase NIT 107 [48]

14.3.2.1 Nitrile Hydratase Structure and Mechanism

The metal active site in nitrile hydratase enzymes displays a distorted octahedral geometry, with most nitrile hydratases exhibiting significant protein sequence homology especially at the metal binding domain present in the α subunit of the enzyme (Cys^1-Ser-Leu-Cys^2-Ser-Cys^3 motif) [53]. Consensus exists among researchers that most nitrile hydratases must function in a similar manner, with the two amide nitrogens of Ser and Cys^3 and the three Cys sulfur atoms being coordinated to the metal. Both Cys^2 and Cys^3 undergo posttranslational modification to generate cysteine-sulfinic acid and cysteine-sulfenic acid respectively, which exist in a deprotonated form at the metal site.

Fe-(III) Nitrile Hydratases Nitrile hydratases function as Lewis acids, in contrast to the mode of action of most nonheme iron center enzymes, which catalyze redox type reactions. The nitrile hydratase activity found in *Rhodococcus* N-771 [54–56] was found to be photoregulated, with light reversing the *in vivo* inhibitory nitric oxide (NO) binding and thereby activating the nitrile hydratase [56].

Co-(III) Nitrile Hydratases Results obtained from X-ray absorption studies identified sequence homology at the metal binding region of both the Fe and the Co nitrile hydratases. This strongly suggests that the active site structure is similar in both types of enzymes. The precise nitrile hydratase mode of action remains unknown, but Huang and coworkers [57] suggested three possible mechanisms for hydration of nitrile substrates to their corresponding amides.

14.3.3 Amidases

Amidase enzymes (EC 3.5.1.4) belong to the hydrolase family of enzymes and catalyze the hydrolysis of monocarboxylic amides to their corresponding acid products. Conventional amidase classification is done according to substrate profile or is based on their amino acid sequence homology [58].

Amidases play a significant role in both prokaryotes and eukaryotes, functioning in the production of growth regulators such as auxin and biotin in plants [59], in nutrient metabolism, in the degradation of toxic cyanogenic compounds, and finally in posttranslational modification of amino acids and proteins.

14.3.3.1 Amidase Structure and Mechanism

Amidase enzymes catalyze the hydrolysis of amide bonds with considerable divergence noted within the family with respect to substrate specificity. All amidase enzymes, however, maintain the core α,β,α structure, where the topologies of the C and N terminal halves are similar.

Aliphatic amidase enzymes demonstrate sequence similarity to the nitrilase superfamily thus indicating some form of evolutionary relationship. These amidases contain a Glu-Lys-Cys catalytic triad and exist as homotetrameric or homohexameric structures that function via a ping-pong (bi-bi) reaction mechanism [60, 61].

14.3.4 Nitrile Hydratase and Amidase Cascade Substrate Selectivity

Winkler and coworkers tested the substrate specificity of three different *Rhodococcus* sp. strains on five- and six-membered *cis*- or *trans*-alicyclic β-aminonitriles. They found that the five-membered substrates were hydrolyzed significantly faster than their corresponding six-membered counterparts, and the reaction products from the *trans*-aminonitriles were formed considerably faster than for the cis-substrates [62]. In addition, the *Rhodococci* exhibited far greater enantioselectivity for the

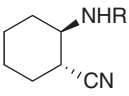
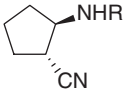
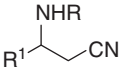
trans-isomers (Table 14.2). Reactions performed using benzyl protected *trans*-aminocyclohexanenitriles gave rise to the corresponding carboxylic acids with a high enantiomeric excess (95–99%) for all three strains tested (*Rhodococcus equi* A4, *Rhodococcus erythropolis* NCIMB 11540, and *Rhodococcus* sp. R312). The enantiomeric excess of the remaining nitrile was found to be particularly high in the case of *R. equi* A4, whereas the intermediate amide products exhibited poor enantiomeric excess values [62]. This implies that a selective nitrile hydratase was acting in *R. equi* A4, leaving the unreacted nitrile with a high enantiomeric excess, and that an amidase with matching enantioselectivity was converting the intermediate amide to enantiopure acid (Table 14.2). The high enantiomeric excess values seen for the acid produced by all three strains, regardless of nitrile hydratase selectivity, supports the presence of a highly enantioselective amidase in the three organisms. When using a tosyl protecting group, good enantioselectivity was also measured in the conversion of the amide to the acid, whereas nitrile hydratase enantioselectivity was much poorer when using *R. equi* cells but enhanced for *R. erythropolis* cells.

In contrast to these results, the five-membered *trans*-aminonitriles yielded *trans*-amides of high enantiopurity, whereas the respective acid products had poor enantiomeric excess values. The results support an enantioselective amidase and a nonselective nitrile hydratase, particularly for the benzyl protected substrate, where all the nitrile was converted [62].

Ma *et al*. [1] examined the effect of an *N*-protecting group on the conversion of β-aminoalkanenitriles by a strain of *Rhodococcus eryrthropolis* AJ 270. Whole cell reactions were performed using resting cells expressing both nitrile hydratase and amidase activity. The nitrile in each case was converted to the intermediate amide and the corresponding acid with opposite stereochemistry in >99.5% ee when employing an *N*-benzyl protecting group (Table 14.2). In the absence of the protecting group, the enantiomeric excess of the acid product fell to 20.8% [1]. Thus, the presence of the *N*-benzyl group resulted in a dramatic improvement in enantioselectivity. Variation of the R^1 group resulted in minor changes to the observed selectivity (Table 14.2). The presence of an ethyl or an isopropyl group at R^1 resulted in improved enantioselectivity (>99.5% ee) compared to a methyl substituent. A cyclopropyl group proved slightly inferior to the ethyl and isopropyl groups (Table 14.2). Interestingly, the same improvement in enantioselectivity was observed for *O*-benzylated β-hydroxynitriles. The excellent enantioselectivities observed for the amide and acid products were attributed by the authors to a slightly selective nitrile hydratase in combination with a highly enantioselective matching amidase.

Our original studies with unprotected β-hydroxynitriles showed that these compounds were hydrolyzed by *R. rhodochrous* ATCC BAA-870, expressing a benzamide-induced cobalt type nitrile hydratase, to the corresponding amides and acids [11]. The formation of the amide implies a nitrile hydratase and amidase system (although sometimes nitrilases can release partially hydrolyzed substrates as amides [63]). Further studies in our laboratories demonstrated that the system was indeed a nitrile hydratase and amidase cascade reaction functioning via a two

Table 14.2 Enantioselective conversion of racemic β-aminonitriles.

Substrate	Functional groups	Reaction catalyzed	Selectivity	Organism
	R-C_6H_5CO-	Hydrolysis of cyclic β-aminonitriles	99% ee (nitrile) >95% ee (acid)	*Rhodococcus equi* A4 [62]
			44% ee (nitrile) >95% ee (acid)	*R. erythropolis* NCIMB 11540 [62]
			82% ee (nitrile) >95% ee (acid)	*Rhodococcus* sp. R312 [62]
	R-*p*-$CH_3C_6H_4SO_2$-	Hydrolysis of cyclic β-aminonitriles	78% ee (nitrile) >99% ee (acid)	*Rhodococcus equi* A4 [62]
			98% ee (nitrile) 97% ee (acid)	*R. erythropolis* NCIMB 11540 [62]
			47% ee (nitrile) 87% ee (acid)	*Rhodococcus* sp. R312 [62]
	R=C_6H_5CO-	Hydrolysis of cyclic β-aminonitriles	94% ee (amide)	*Rhodococcus equi* A4 [62]
			>99% ee (amide)	*Rhodococcus erythropolis* NCIMB 11540 [62]
			>99% ee (amide)	*Rhodococcus* sp. R312 [62]
	R=*p*-$CH_3C_6H_4SO_2$-	Hydrolysis of cyclic β-aminonitriles	>99% ee (amide)	*Rhodococcus equi* A4 [62]
			>99% ee (amide)	*Rhodococcus erythropolis* NCIMB 11540 [62]
			>99% ee (amide)	*Rhodococcus* sp. R312 [62]
	R-benzyl R^1-ethyl	Hydrolysis of aliphatic β-aminonitriles	>99.5% ee (amide) >99.5% ee (acid)	*Rhodococcus erythropolis* AJ 270 [1]
	R-benzyl R^1-isopropyl	Hydrolysis of aliphatic β-aminonitriles	>99.5% ee (amide) 90.2% ee (acid)	*Rhodococcus erythropolis* AJ 270 [1]
	R-benzyl R^1-cyclopropyl	Hydrolysis of aliphatic β-aminonitriles	92.4% ee (amide) 96.4% ee (acid)	*Rhodococcus erythropolis* AJ 270 [1]
	R-benzyl R^1-methyl	Hydrolysis of aliphatic β-aminonitriles	74.2% (amide) 86.6% ee (acid)	*Rhodococcus erythropolis* AJ 270 [1]
	R-H R^1-4-methoxy phenyl	Hydrolysis of aliphatic β-aminonitriles	85% ee ((*S*)-nitrile) 62% ee ((*R*)-amide)	*Rhodococcus rhodochrous* BAA-870 [12]

enzyme system. The first reaction step, as catalyzed by nitrile hydratase, was rapid but not enantioselective for β-hydroxy substituted phenoxy compounds. The subsequent hydrolysis of the resultant amide to the corresponding carboxylic acid by the amidase was considerably slower, but enantioselective (99% ee). The amidase enantioselectivity was reduced when other β-substituted substrates were used, such as 3-hydroxy-3-phenylpropanenitrile or 3-hydroxy-3-arylpropanenitrile [11].

In a subsequent study, we turned our attention to β-aminonitriles. Various aryl substituted unprotected β-aminonitriles (3-amino-3-arylpropanenitriles) were synthesized and enantioselective hydrolysis of these compounds to the corresponding amides was achieved using *R. rhodochrous* ATCC BAA-870 [12]. Interestingly, initial biocatalytic experiments did not result in the formation of hydrolysis products of 3-amino-3-phenylpropanenitrile. Further investigations proved that the charge on the amine in the β-position made this compound a less suitable substrate than the corresponding β-hydroxy compounds [11, 12]. This problem was overcome by shifting the reaction pH higher, where a higher percentage of the amino groups would be unprotonated. In order to avoid rapid denaturation of the enzyme at high pH, a functional balance was achieved at pH 9 [12].

Unlike the results obtained for the β-hydroxy compounds, the main product from the β-aminonitriles was determined to be the amide, rather than the acid (Table 14.2). In fact, acid formation was only detected after extended incubation times, indicating that the amidase responsible required some form of induction or derepression that was not observed in the β-hydroxy studies. At this point, we cannot be sure that the amidases responsible are the same for the β-hydroxy- and the β-hydroxynitrile compounds. The accumulation of amide may indicate that there is a mismatch between the optimal substrate profiles of the nitrile hydratases and the amidases available in *Rhodococci*. Suitably matching amidases may, however, be available from other microorganisms. Heck and coworkers [64] discovered β-aminopeptidases from *Sphingosinicella* sp. capable of enantioselectively hydrolyzing β^3-amino amides to the corresponding L-β^3-amino acids in greater than 99% ee.

Another difference between the catalysis of the β-amino and the β-hydroxynitrile compounds is that the nitrile hydratase appears to have been partially enantioselective toward the β-aminonitriles, resulting in moderate enantiomeric excess values for both the residual (*R*)-enantiomer of the parent nitrile and for the (*S*)-enantiomer of the amide product, while the nitrile hydratase seemed non-enantioselective when acting on β-hydroxynitrile compounds [11, 12]. Based on the results of genome sequencing it appears that there is only one nitrile hydratase present in *R. rhodochrous* ATCC BAA-870, and although a gene coding for a nitrilase enzyme is present on the genome, no nitrilase activity was detected [65]. Hence, the observed enantioselectivity seems to be substrate dependent.

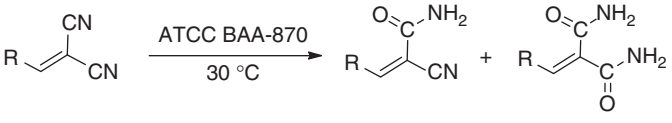
Of interest is the fact that β-lactamases from *Rhodococcus globerulus* could be used by Lloyd [66] to hydrolyze enantiomers of β-lactams to yield cyclic β-amino acids with greater than 90% ee. β-Lactamases belong to the β-lactam-recognizing enzymes (BLREs) superfamily. Their active site is characterized by a Ser-Ser-Lys catalytic triad and an oxyanion hole [67], similar to amidase signature enzymes.

Table 14.3 Biotransformation of malononitriles.

R	Time (h)	Yield of amido-nitrile (%)
Furanyl	3	82
Ph	0.75	22
p-OH Ph	0.75	25

Most research has been focused on the preparation of β^3-amino acids, but the nitrile hydratase–amidase cascade system has also been investigated for the preparation of β^2-amino acids. Malononitriles contain two nitrile groups separated by a single carbon, and the regioselective hydrolysis of one of the two nitriles to the corresponding acid, with subsequent reduction of the carbon–carbon double bond and of the other nitrile to an amino group would yield β^2-amino acids. This approach has been described using a *Rhodococcus* sp. acting on α,α-disubstituted saturated malononitriles [68], however multiple acid and amide products were formed.

More recently, three malononitriles were reacted at 30 °C with cell pastes of *R. rhodochrous* ATCC BAA-870 and the reactions resulted in successful conversion to the corresponding amido-nitrile products (Scheme 14.5 and Table 14.3). The configuration of the furanyl amido-nitriles was determined to be *Z*, by comparison of our NMR data with that previously described for the *E* product [69].



R = furanyl, Ph, *p*-OH Ph

Scheme 14.5 Conversion of malononitrile derivatives.

Longer reaction times led to the diamide product only, with no acid being formed. Further conversion of 2-cyano-3-furan-2-yl-but-2-enamide was attempted using both whole cells of *R. rhodochrous* ATCC BAA-870 as well as a commercial amidase enzyme preparation (*Pseudomonas aeruginosa*, Sigma–Aldrich), but neither showed conversion of the substrate (unpublished results).

14.4 Conclusion

Nitriles may be converted to amino acids by nitrilases, which catalyze a two-step nitrile hydrolysis reaction, and can provide β^3-amino acids in high enantiopurity. The same reaction can be catalyzed by a combination of nitrile hydratase and

amidase. However, the matching of the substrate profile and enantioselectivity for this two enzyme combination may require the use of selected enzymes from more than one microbial strain, necessitating heterologous expression in a host organism. A possible advantage of a two enzyme system is that the enantioselectivity of the enzymes can be synergistic.

Another possible cascade reaction would be the combination of nitrilases and transaminases, in principle again exploiting enantioselective synergy. Similarly the combined use of nitrilases with acylases or lipases is conceivable, when working with *N*-acylated substrates. However, the size of the acyl group should be compatible with the nitrilase active site.

Acknowledgments

We would like to thank the European Science Foundation as well as the working group leaders Dr. Ludmila Martmková and Prof. Andreas Stolz for the opportunity to participate in COST Action CM0701 (Cascade Biocatalysis). Many thanks to L. Rapheeha and Profs M.P. Roux-van der Merwe and J. Bezuidenhout of Tshwane University of Technology for microbial strains, and Prof. N. Klempier and Dr. M. Winkler of the University of Graz for technical inputs and discussions. This work was supported financially by the Department of Science and Technology and the CSIR.

References

1. Ma, D.-Y., Wang, D.-X., Pan, J., Huang, Z.-T., and Wang, M.-X. (2008) Nitrile biotransformations for the synthesis of highly enantioenriched β-hydroxy and β-amino acid and amide derivatives: a general and simple but powerful and efficient benzyl protection strategy to increase enantioselectivity of the amidase. *J. Org. Chem.*, **73**, 4087–4091.
2. Wünsche, K., Schwaneberg, U., Bornscheuer, U.T., and Meyer, H.H. (1996) Chemoenzymatic route to β-blockers via 3-hydroxy esters. *Tetrahedron: Asymmetry*, **7**, 2017–2022.
3. Kamal, A., Ramesh Khanna, G.B., Krishnaji, T., Tekumalla, V., and Ramu, R. (2005) New chemoenzymatic pathway for β-adrenergic blocking agents. *Tetrahedron: Asymmetry*, **16**, 1485–1494.
4. Hammond, R.J., Poston, B.W., Ghiviriga, I., and Feske, B.D. (2007) Biocatalytic synthesis towards both antipodes of 3-hydroxy-3-phenylpropanitrile a precursor to fluoxetine, atomoxetine and nisoxetine. *Tetrahedron Lett.*, **48**, 1217–1219.
5. Davies, S.G., Ichihara, O., Lenoir, I., and Walters, I.A.S. (1994) Asymmetric synthesis of (−)-(1*R*,2*S*)-cispentacin and related *cis*- and *trans*-2-amino cyclopentane- and cyclohexane-1-carboxylic acids. *J. Chem. Soc., Perkin Trans. 1*, 1411–1415.
6. Steinhuebel, D., Sun, Y., Matsumura, K., Sayo, N., and Saito, T. (2009) Direct asymmetric reductive amination. *J. Am. Chem. Soc.*, **131**, 11316–11317.
7. Holton, R.A., Somoza, C., Kim, H.-B., Liang, F., Biediger, R.J., Boatman, P.D., Shindo, M., Smith, C.C., Kim, S., Nadizadeh, H., Suzuki, Y., Tao, C., Vu, P., Tang, S., Zhang, P., Murthi, K.K., Gentile, L.N., and Liu, J.H. (1994) First total synthesis of taxol. 1. Functionalization of the B-ring. *J. Am. Chem. Soc.*, **116**, 1597–1598.

8. Gerfaud, T., Chiang, Y.-L., Kreituss, I., Russak, J.A., and Bode, J.W. (2012) Enantioselective, chromatography-free synthesis of β^3-amino acids with natural and unnatural side chains. *Org. Process Res. Dev.*, **16**, 687–696.
9. Kamal, A. and Ramesh Khanna, G.B. (2001) A facile preparation of (±)-β-hydroxy nitriles and their enzymatic resolution with lipases. *Tetrahedron: Asymmetry*, **12**, 405–410.
10. Kamal, A., Ramesh Khanna, G.B., and Ramu, R. (2002) Chemoenzymatic synthesis of both enantiomers of fluoxetine, tomoxetine and nisoxetine: lipase-catalyzed resolution of 3-aryl-3-hydroxypropanenitriles. *Tetrahedron: Asymmetry*, **13**, 2039–2051.
11. Kinfe, H.H., Chhiba, V., Frederick, J., Bode, M.L., Mathiba, K., Steenkamp, P.A., and Brady, D. (2009) Enantioselective hydrolysis of β-hydroxy nitriles using the whole cell biocatalyst *Rhodococcus rhodochrous* ATCC BAA-870. *J. Mol. Catal. B: Enzym.*, **59**, 231–236.
12. Chhiba, V.P., Bode, M.L., Mathiba, K., Kwezi, W., and Brady, D. (2012) Enantioselective biocatalytic hydrolysis of β-aminonitriles to β-amino-amides using *Rhodococcus rhodochrous* ATCC BAA-870. *J. Mol. Catal. B: Enzym.*, **76**, 68–74.
13. Fix, J.A. (1996) Oral controlled release technology for peptides: status and future prospects. *Pharm. Res.*, **13**, 1760–1764.
14. Olson, G.L., Bolin, D.R., Bonner, M.P., Bös, M., Cook, C.M., Fry, D.C., Graves, B.J., Hatada, M., Hill, D.E., Khan, M., Madison, V.S., Rusiecki, V.K., Sarabu, R., Sepinwall, J., Vincent, G.P., and Voss, M.E. (1993) Concepts and progress in the development of peptide mimetics. *J. Med. Chem.*, **36**, 3039–3049.
15. Godballe, T., Nilsson, L.L., Petersen, P.D., and Jenssen, H. (2011) Antimicrobial β-peptides and α-peptoids. *Chem. Biol. Drug Des.*, **77**, 107–116.
16. Vagner, J., Qu, H., and Hruby, V.J. (2008) Peptidomimetics, a synthetic tool of drug discovery. *Curr. Opin. Chem. Biol.*, **12**, 292–296.
17. Mittendorf, J., Kunisch, F., Matzke, M., Militzer, H.-C., Schmidt, A., and Schönfeld, W. (2003) Novel antifungal β-amino acids: synthesis and activity against *Candida albicans*. *Bioorg. Med. Chem. Lett.*, **13**, 433–436.
18. Wolin, R.L., Santillán, A. Jr.,, Barclay, T., Tang, L., Venkatesan, H., Wilson, S., Lee, D.H., and Lovenberg, T.W. (2004) Novel glycine transporter type-2 reuptake inhibitors. Part 2: β- and γ-amino acid derivatives. *Bioorg. Med. Chem.*, **12**, 4493–4509.
19. Zhu, Y., Wu, G., Zhu, X., Ma, Y., Zhao, X., Li, Y., Yuan, Y., Yang, J., Yu, S., Shao, F., and Lei, M. (2010) Synthesis, *in vitro* and *in vivo* biological evaluation, and comprehensive understanding of structure-activity relationships of dipeptidyl boronic acid proteasome inhibitors constructed from β-amino Acids. *J. Med. Chem.*, **53**, 8619–8626.
20. Armour, D.R., Bell, A.S., Edwards, P.J., Ellis, D., Hepworth, D., Lewis, M.L., and Smith, C.R. (2004) Preparation of heterocyclylcarboxamides as oxytocin inhibitors. PCT Patent WO2004/020414.
21. Angelaud, R., Armstrong, J.D., Askin, D., Balsells, J., Hansen, K., Lee, J., Maligres, P.E., Rivera, N.R., Xiao, Y., and Zhong, Y.L. (2004) Process for the preparation of β-amino acid amide dipeptidyl peptidase-IV inhibitors. PCT Patent WO2004/087650.
22. Imbriglio, J., Colletti, S.L., Tata, J.R., Beresis, R.T., Marley, D., Raghavan, S., Schmidt, D.R., Lins, A.R., Smenton, A.L., Chen, W., Shen, H., Ding, F.-X., and Bodner, R. (2006) Preparation of (hetero) aryl amino acid amides as niacin receptor agonists for treatment of atherosclerosis, dyslipidemia, diabetes, and metabolic syndrome. PCT Patent WO2007/075749.
23. Aguilar, M.-I., Purcell, A.W., Devi, R., Lew, R., Rossjohn, J., Smith, A.I., and Perlmutter, P. (2007) β-Amino acid-containing hybrid peptides -new opportunities in peptidomimetics. *Org. Biomol. Chem.*, **5**, 2884–2890.
24. Weiner, B., Szymański, W., Janssen, D.B., Minnaard, A.J., and Feringa, B.L. (2010) Recent advances in the catalytic asymmetric synthesis of beta-amino acids. *Chem. Soc. Rev.*, **39**, 1656–1691.

25. Liu, M. and Sibi, M.P. (2002) Recent advances in the stereoselective synthesis of β-amino acids. *Tetrahedron*, **58**, 7991–8035.
26. Grayson, J.I., Roos, J., and Osswald, S. (2011) Development of a commercial process for (S)- β-phenylalanine. *Org. Process Res. Dev.*, **15**, 1201–1206.
27. Liljeblad, A. and Kanerva, L.T. (2006) Biocatalysis as a profound tool in the preparation of highly enantiopure β-amino acids. *Tetrahedron*, **62**, 5831–5854.
28. Gyarmati, Z.C., Liljeblad, A., Argay, G., Kálmán, A., Bernáth, G., and Kanerva, L.T. (2004) Chemoenzymatic preparation of enantiopure homoadamantyl β-amino acid and β-lactam derivatives. *Adv. Synth. Catal.*, **346**, 566–572.
29. Liljeblad, A. and Kanerva, L.T. (1999) Enzymatic methods for the preparation of enantiopure malic and aspartic acid derivatives in organic solvents. *Tetrahedron: Asymmetry*, **10**, 4405–4415.
30. Gedey, S., Liljeblad, A., Lázár, L., Fülöp, F., and Kanerva, L.T. (2001) Preparation of highly enantiopure β-amino esters by *Candida antarctica* lipase A. *Tetrahedron: Asymmetry*, **12**, 105–110.
31. Solymár, M., Fülöp, F., and Kanerva, L.T. (2002) *Candida Antarctica* lipase a – a powerful catalyst for the resolution of heteroaromatic β-amino esters. *Tetrahedron: Asymmetry*, **13**, 2383–2388.
32. Solymár, M., Liljeblad, A., Lázár, L., Fülöp, F., and Kanerva, L.T. (2002) Lipase-catalysed kinetic resolution in organic solvents: an approach to enantiopure α-methyl-β-alanine esters. *Tetrahedron: Asymmetry*, **13**, 1923–1928.
33. Solymár, M., Kanerva, L.T., and Fülöp, F. (2004) Synthesis of the enantiomers and *N*-protected derivatives of 3-amino-3-(4-cyanophenyl)propanoic acid. *Tetrahedron: Asymmetry*, **15**, 1893–1897.
34. Kanerva, L.T., Csomós, P., Sundholm, O., Bernáth, G., and Fülöp, F. (1996) Approach to highly enantiopure β-amino acid esters by using lipase catalysis in organic media. *Tetrahedron: Asymmetry*, **7**, 1705–1716.
35. Gröger, H., Trauthwein, H., Buchholz, S., Drauz, K., Sacherer, C., Godfrin, S., and Werner, H. (2004) The first aminoacylase-catalyzed enantioselective synthesis of aromatic β-amino acids. *Org. Biomol. Chem.*, **2**, 1977–1978.
36. Rudat, J., Brucher, B.R., and Syldatk, C. (2012) Transaminases for the synthesis of enantiopure beta-amino acids. *AMB Express*, **2**, 1–10.
37. Pace, H.C. and Brenner, C. (2001) The nitrilase superfamily: classification, structure and function. *Genome Biol.*, **2**, 1–9.
38. Schmid, A., Dordick, J.S., Hauer, B., Kiener, A., Wubbolts, M., and Witholt, B. (2001) Industrial biocatalysis today and tomorrow. *Nature*, **409**, 258–268.
39. Gong, J.-S., Lu, Z.-M., Li, H., Shi, J.-S., Zhou, Z.-M., and Xu, Z.-H. (2012) Nitrilases in nitrile biocatalysis: recent progress and forthcoming research. *Microb. Cell Fact.*, **11**, 142–159.
40. Kaul, P., Banerjee, A., and Banerjee, U.C. (2007) in *Industrial Enzymes* (eds J. Polaina and A.P. MacCabe), Springer, India, pp. 531–547.
41. Brenner, C. (2002) Catalysis in the nitrilase superfamily. *Curr. Opin. Struct. Biol.*, **12**, 775–782.
42. Thuku, R.N., Weber, B.W., Varsani, A., and Sewell, B.T. (2007) Post-translational cleavage of recombinantly expressed nitrilase from *Rhodococcus rhodochrous* J1 yields a stable, active helical form. *FEBS J.*, **274**, 2099–2108.
43. Mahadevan, S. and Thimann, K.V. (1964) Nitrilase. II. Substrate specificity and possible mode of action. *Arch. Biochem. Biophys.*, **107**, 62–68.
44. Zhang, Z.-J., Xu, J.-H., He, Y.-C., Ouyang, L.-M., and Liu, Y.-Y. (2011) Cloning and biochemical properties of a highly thermostable and enantioselective nitrilase from *Alcaligenes* sp. ECU0401 and its potential for (*R*)-(−)-mandelic acid production. *Bioprocess Biosyst. Eng.*, **34**, 315–322.
45. Kaul, P., Banerjee, A., Mayilraj, S., and Banerjee, U.C. (2004) Screening for enantioselective nitrilases: kinetic resolution of racemic mandelonitrile to (*R*)-(−)-mandelic acid by new bacterial isolates. *Tetrahedron: Asymmetry*, **15**, 207–211.
46. Chaplin, J.A., Levin, M.D., Morgan, B., Farid, N., Li, J., Zhu, Z., McQuaid, J.,

Nicholson, L.W., Rand, C.A., and Burk, M.J. (2004) Chemoenzymatic approaches to the dynamic kinetic asymmetric synthesis of aromatic amino acids. *Tetrahedron: Asymmetry*, **15**, 2793–2796.

47. Rapheeha, O.K.L. (2013) The enzyme conversion of nitriles by bacterial strains isolated from soil. MSc dissertation. Tshwane University of Technology.
48. Winkler, M., Knall, A.C., Kulterer, M.R., and Klempier, N. (2007) Nitrilases catalyze key step to conformationally constrained GABA analogous γ-amino acids in high optical purity. *J. Org. Chem.*, **72**, 7423–7426.
49. Kobayashi, M., Nagasawa, T., and Yamada, H. (1992) Enzymatic synthesis of acrylamide: a success story not yet over. *Trends Biotechnol.*, **10**, 402–408.
50. Sugiura, Y., Kuwahara, J., Nagasawa, T., and Yamada, H. (1987) Nitrile hydratase: the first non-heme iron enzyme with a typical low spin Fe (III)-active center. *J. Am. Chem. Soc.*, **109**, 5848–5850.
51. Brennan, B.A., Alms, G., Nelson, M.J., Durney, L.T., and Scarrow, R.C. (1996) Nitrile hydratase from *Rhodococcus rhodochrous* J1 contains a non-corrin cobalt ion with two sulfur ligands. *J. Am. Chem. Soc.*, **118**, 9194–9195.
52. Brady, D., Beeton, A., Zeevart, J., Kgaje, C., van Rantwijk, F., and Sheldon, R.A. (2004) Characterisation of nitrilase and nitrile hydratase biocatalytic systems. *Appl. Microbiol. Biotechnol.*, **64**, 76–85.
53. Mascharak, P.K. (2002) Structural and functional models of nitrile hydratase. *Coord. Chem. Rev.*, **225**, 201–214.
54. Nagamune, T., Honda, J., Cho, W.-D., Kamiya, N., Teratani, Y., Hirata, A., Sasabe, H., and Endo, I. (1991) Crystallization of a photosensitive nitrile hydratase from *Rhodococcus* sp. N-771. *J. Mol. Biol.*, **220**, 221–222.
55. Endo, I., Odaka, M., and Yohda, M. (1999) An enzyme controlled by light: the molecular mechanism of photoreactivity in nitrile hydratase. *Trends Biotechnol.*, **17**, 244–249.
56. Endo, I. and Odaka, M. (2000) What evidences were elucidated about photoreactive nitrile hydratase? *J. Mol. Catal. B: Enzym.*, **10**, 81–86.
57. Huang, W., Jia, J., Cummings, J., Nelson, M., Schneider, G., and Lindqvist, Y. (1997) Crystal structure of nitrile hydratase reveals a novel iron centre in a novel fold. *Structure*, **5**, 691–699.
58. Mayaux, J.F., Cerbelaud, E., Soubrier, F., Yeh, P., Blanche, F., and Pétré, D. (1991) Purification, cloning and primary structure of a new enantiomer-selective amidase from a *Rhodococcus* strain: structural evidence for a conserved genetic coupling with nitrile hydratase. *J. Bacteriol.*, **173**, 6694–6704.
59. Piotrowski, M., Schönfelder, S., and Weiler, E.W. (2001) The *Arabidopsis thaliana* isogene NIT4 and its orthologs in tobacco encode β-cyano-L-alanine hydratase/ nitrilase. *J. Biol. Chem.*, **276**, 2616–2621.
60. Fournand, D., Bigey, F., and Arnaud, A. (1998) Acyl transfer activity of an amidase from *Rhodococcus* sp. Strain R312: formation of a wide range of hydroxamic acids. *Appl. Environ. Microbiol.*, **64**, 2844–2852.
61. Sharma, M., Sharma, N.N., and Bhalla, T.C. (2009) Amidases: versatile enzymes in nature. *Rev. Environ. Sci. Biotechnol.*, **8**, 343–366.
62. Winkler, M., Martmková, L., Knall, A.C., Krahulec, S., and Klempier, N. (2005) Synthesis and microbial transformation of β-amino nitriles. *Tetrahedron*, **61**, 4249–4260.
63. Fernandes, B.C.M., Mateo, C., Kiziak, C., Chmura, A., Wacker, J., Van Rantwijk, F., Stolz, A., and Sheldon, R.A. (2006) Nitrile hydratase activity of a recombinant nitrilase. *Adv. Synth. Catal.*, **348**, 2597–2603.
64. Heck, T., Seebach, D., Osswald, S., ter Wiel, M.K.J., Kohler, H.-P.E., and Geueke, B. (2009) Kinetic resolution of aliphatic β-amino acid amides by β-aminopeptidases. *ChemBioChem*, **10**, 1558–1561.
65. Frederick, J. (2013) Genetic characterization of Rhodococcus rhodochrous ATTCC BAA-870 with emphasis on nitrile hydrolysing enzymes. PhD thesis. University of Cape Town.

66. Lloyd, M., Lloyd, R., Keene, P., and Osborne, A. (2007) A concise synthesis of single-enantiomer β-lactams and β-amino acids using *Rhodococcus globerulus*. *J. Chem. Technol. Biotechnol.*, **82**, 1099–1106.
67. Pratt, R.F. and McLeish, M.J. (2010) Structural relationship between the active sites of β-lactam- recognizing and amidase signature enzymes: convergent evolution? *Biochemistry*, **49**, 9688–9697.
68. Wu, Z.-L. and Li, Z.-Y. (2003) Enantioselective biotransformation of α,α-disubstituted dinitriles to the corresponding 2-cyanoacetamides using *Rhodococcus* sp. CGMCC 0497. *Tetrahedron: Asymmetry*, **14**, 2133–2142.
69. Dotsenko, V.V., Frolov, K.A., and Krivokolysko, S.G. (2012) Mannich reaction in the synthesis of N,S-containing heterocycles. 13. One-pot method for preparing pyrimido[4,3-*b*][1,3,5]thiadiazines by reaction of aldehydes, cyanothioacetamide, formaldehyde, and primary amines. *Chem. Heterocycl. Compd.*, **48**, 642–649.

Chapter Six: PAPER IV

Hydrolysis of nitriles by soil bacteria: variation with soil origin.

O. K. L. Rapeeha, M. P. Roux-van der Merwe, J. Badenhorst, **V. Chhiba**, M. L. Bode, D. Brady

Journal of Applied Microbiology (2017)

Journal of Applied Microbiology

Journal of Applied Microbiology ISSN 1364-5072

ORIGINAL ARTICLE

Hydrolysis of nitriles by soil bacteria: variation with soil origin

O.K.L. Rapheeha[1], M.P. Roux-van der Merwe[1], J. Badenhorst[1], V. Chhiba[2,3], M.L. Bode[3], K. Mathiba[2] and D. Brady[1,2,3]

1 Department of Biotechnology and Food Technology, Tshwane University of Technology, Pretoria, South Africa
2 CSIR Biosciences, Pretoria, South Africa
3 Molecular Sciences Institute, School of Chemistry, University of the Witwatersrand, Johannesburg, South Africa

Keywords
biocatalysis, nitrile hydratase, nitriles, peptidomimetics, *Rhodococcus*.

Correspondence
Dean Brady, Molecular Sciences Institute, School of Chemistry, University of the Witwatersrand, PO Wits 2050, Johannesburg, South Africa.
E-mail: dean.brady@wits.ac.za

2016/1967: received 7 September 2016, revised 9 November 2016 and accepted 28 November 2016

doi:10.1111/jam.13367

Abstract

Aims: The aim of this study was to explore bacterial soil diversity for nitrile biocatalysts, in particular, those for hydrolysis of β-substituted nitriles, to the corresponding carboxamides and acids that may be incorporated into peptidomimetics. To achieve this, we needed to compare the efficiency of isolation methods and determine the influence of land use and geographical origin of the soil sample.

Methods and Results: Nitrile-utilizing bacteria were isolated from various soil environments across a 1000 km long transect of South Africa, including agricultural soil, a gold mine tailing dam and uncultivated soil. The substrate profile of these isolates was determined through element-limited growth studies on seven different aliphatic or aromatic nitriles. A subset of these organisms expressing broad substrate ranges was evaluated for their ability to hydrolyse β-substituted nitriles (3-amino-3-phenylpropionitrile and 3-hydroxy-4-phenoxybutyronitrile) and the active organisms were found to be *Rhodococcus erythropolis* from uncultivated soil and *Rhodococcus rhodochrous* from agricultural soils.

Conclusions: The capacity for hydrolysis of β-substituted nitriles appears to reside almost exclusively in Rhodococci. Land use has a much greater effect on the biocatalysis substrate profile than geographical location.

Significance and Impact of the Study: Enzymes are typically substrate specific in their catalytic reactions, and this means that a wide diversity of enzymes is required to provide a comprehensive biocatalysis toolbox. This paper shows that the microbial diversity of nitrile hydrolysis activity can be targeted according to land utilization. Nitrile biocatalysis is a green chemical method for the enzymatic production of amides and carboxylic acids that has industrial applications, such as in the synthesis of acrylamide and nicotinamide. The biocatalysts discovered in this study may be applied to the synthesis of peptidomimetics which are an important class of therapeutic compounds.

Introduction

Nitriles are important products or intermediates in the pharmaceutical, agricultural and chemical industries (Rezende *et al.* 2003; Zheng *et al.* 2008; Zhang *et al.* 2009), as well as waste products generated from industrial processes that require subsequent remedial treatment (Nyska and Ghanayem 2003; Cantarella *et al.* 2006; Zhang *et al.* 2009). Nitriles can provide synthetic routes to synthesise enantiomerically pure β-hydroxy and β-amino acids, which form common structural motifs in many compounds of pharmaceutical importance (Ma *et al.* 2008), including antimicrobial peptidomimetics (Godballe *et al.* 2011).

Microbial biocatalysts have been shown to effectively hydrolyse a wide range of nitriles (Martínková and Mylerová 2003; Bhalla and Kumar 2005; Brady *et al.* 2006; Ramteke *et al.* 2013). This hydrolysis is achieved by either nitrilase enzymes, which hydrolyse nitriles to their corresponding carboxylic acid products, through the addition of two water molecules, or nitrile hydratases, which convert them to the carboxamides through the addition of a single water molecule (Martínková *et al.* 2009) (Fig. 1). This capability has made nitrile biocatalysts broadly applicable in industrial chemistry, such as in the commercial synthesis of acrylamide, nicotinamide, (*R*)-(−)-mandelic acid and azafenidin (via 5-cyanovaleramide) (Thomas *et al.* 2002; Gong *et al.* 2012; Ramteke *et al.* 2013).

Bacterial isolates capable of nitrile hydrolysis have been found in a wide variety of taxonomic groups (Demakov *et al.* 2007) with cells belonging to the genera *Rhodococcus* often being isolated (Langdahl *et al.* 1996; Brady *et al.* 2006; Zhang *et al.* 2009). Other well known nitrile-hydrolysing isolates include *Bacillus* (Zheng *et al.* 2008), *Agrobacterium*, *Arthrobacter*, *Microbacterium* (Demakov *et al.* 2007) and *Klebsiella* (Kao *et al.* 2006) among others. Many of these micro-organisms have been isolated from industrial and mining sites in which the micro-organisms have been exposed to nitriles or cyanide (Akcil 2003; Demakov *et al.* 2007; Tang *et al.* 2008; Dash *et al.* 2009; Feng and Lee 2009) as well as soil and lake samples (Bhalla and Kumar 2005; Brady *et al.* 2006; Chmura *et al.* 2008).

Information regarding the distribution and specificity of nitrile-hydrolysing micro-organisms, and the environment in which they are found, is limited. The aim of this study was therefore to isolate soil bacteria in which nitrile-producing plants were cultivated, as well as from uncultivated soil and industrial land from various regions of South Africa and evaluate their reactivity against various nitrile substrates.

Materials and methods

Soil sampling

A total of 11 sites were sampled over a transect of approximately 1000 km stretching from central South Africa to the South African south-west coast (Bultfontein, Christiana, Kroonstad, Yzerfontein, Constantia Nek, Somerset West, Calvinia, Brandvlei, Upington, Ladismith and Montagu; Fig. S1). This covers a range of climates (arid, semi-arid, winter and summer rainfall) and the associated ecosystems. A soil sample of 1 kg, comprising of at least 10 subsamples, was taken at a depth of 10 cm over an area of 10 m^2, and sealed in paper bags.

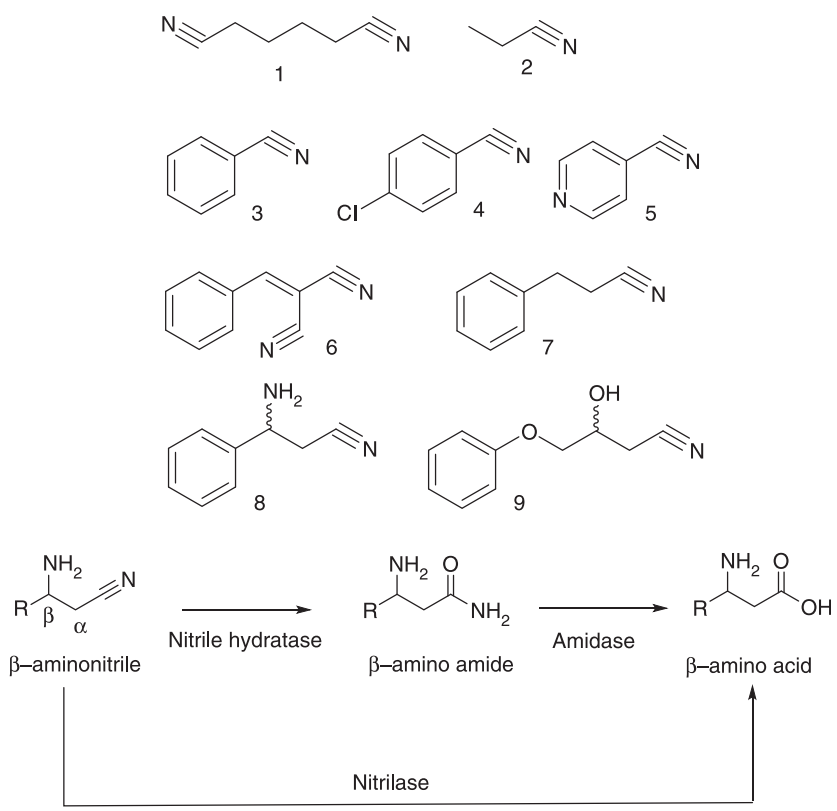


Figure 1 Nitrile compounds involved in this study: **1** adiponitrile; **2** propionitrile; **3** benzonitrile; **4** 4-chlorobenzonitrile; **5** 4-cyanopyridine; **6** benzylidenemalononitrile; **7** hydrocinnamonitrile; **8** 3-amino-3-phenylpropionitrile **9** 3-hydroxy-4-phenoxybutyronitrile; and biocatalytic hydrolysis of the *β*-amino nitrile.

Ten grams of soil sample was suspended in 250 ml sterile Ringer's solution and, after settling, 0·1 ml of the solution was spread-plated onto solid minimal media containing a particular nitrile. The plates were subsequently incubated for 7–14 days at 30°C, and pure cultures were obtained by repeated streaking on the same minimal medium and finally plating on tryptone soy agar for culture maintenance.

Isolates were described according to the site of origin, Gram stain, acid fast test, oxidative fermentation test, oxidase or catalase activity, bacterial morphology under light microscopy (size, rod or cocci), endospore formation, motility, pigmentation and colony surface appearance.

Gold mine waters typically contain the inorganic nitrile cyanide ion (Khamar *et al.* 2015). A culture collection (Tshwane University of Technology) of 219 isolates obtained from the sediment, soil and water of a refractory gold mine tailings dam was screened.

Nitriles used for isolation

For each nutrient limitation-based isolation procedure, one of the seven following nitriles was used as a sole carbon and/or nitrogen source: adiponitrile **1**, propionitrile **2**, benzonitrile **3**, 4-chlorobenzonitrile **4**, 4-cyanopyridine **5**, benzylidenemalononitrile **6** and hydrocinnamonitrile **7**. Three isolation methods were compared for optimal strain discovery:

- **i** Solid minimal medium with a nitrile as both the carbon and nitrogen source: This consisted of (g l^{-1}): NaCl, 9·6; NaH_2PO_4, 0·002; Na_2HPO_4, 0·008 and bacteriological agar, 15. The medium was autoclaved and cooled to 50°C whereupon the nitrile was added to a final concentration of 20 mmol l^{-1}.
- **ii** Solid minimal medium with nitriles as only the nitrogen source: The carbon supplemented minimal medium, was prepared according to Kinfe *et al.* (2009), modified from the medium of Layh *et al.* (1997) containing (g l^{-1}): sodium succinate, 1·6 (carbon source); $MgSO_4.7H_2O$, 0·02; $FeSO_4.7H_2O$, 0·05; $CaCl_2.2H_2O$, 0·05; KH_2PO_4, 0·2; Na_2HPO_4, 4·97 and trace element solution (1 ml) consisting of (g l^{-1}): $ZnSO_4.5H_2O$, 0·2; $CuSO_4.5H_2O$, 0·4; $CoNO_3$, 0·004; citric acid, 50 and $MnSO_4$, 0·4. The medium was then autoclaved and left to cool to 50°C, whereupon the nitrile was added to a final concentration of 0·5 mmol l^{-1}.
- **iii** Liquid culture enrichment medium with nitriles as the nitrogen source: 1 g of the soil sample was inoculated into carbon supplemented minimal medium (30 ml) in triplicate Erlenmeyer flasks and incubated for 7 days at 30°C at 180 rev min^{-1}. Thereafter, 10% of the volume was transferred into fresh minimal medium and incubated for a further 7 days. The cultures were then transferred onto plates of the same medium containing 15 g bacteriological agar and incubated at 30°C.

Isolate substrate profiling

The screening method was based on the ability of the isolates to grow on carbon supplemented minimal medium agar plates containing nitriles (5 and 20 mmol l^{-1} respectively), as a sole source of nitrogen. The solid carbon supplemented minimal medium (modified so that sodium succinate was replaced by filter sterilized 1·2 g l^{-1} glucose), was poured into OmniTrays (Nalge Nunc International, ThermoFisher Scientific, Johannesburg) and left to solidify. Nutrient agar plates served as a control to confirm the viability of the cells.

Colonies were subsequently suspended in 500 μl phosphate buffer and 100 μl of this liquid culture was transferred into microtitre plates. *Escherichia coli* acted as a negative control, while a nitrile-hydrolysing *Rhodococcus* (*R. rhodochrous* ATCC BAA-870) was the positive control. Using a robotic colony picker (QPix2; Genetix, New Milton, UK), the cells in the microtitre plates were inoculated onto the solid minimal media and incubated at 30°C for up to 14 days.

Biocatalytic hydrolysis of β-substituted nitriles

In order to determine the biocatalytic activity of the isolates on 3-amino-3-phenylpropionitrile **8** and 3-hydroxy-4-phenoxybutyronitrile **9**, a reaction mixture consisting of 1·125 ml Tris (pH 9) or phosphate buffer (pH 7), 75 μl of a 100 mmol l^{-1} stock solution of the respective nitrile substrates and 300 μl of the cells was prepared (to a final volume of 1·5 ml). These were incubated at 30°C with shaking at 160 rev min^{-1}. Aliquots of 100 μl were collected at 0·5, 2, 4 and 24 h. After centrifugation to remove the cells the supernatants were extracted with ethyl acetate and then analysed by thin layer chromatography on aluminium backed Merck silica gel 60 F_{254} plates. The mobile phases were 30% ethyl acetate in hexane, followed by 100% ethyl acetate (for 3-hydroxy-4-phenoxybutyronitrile **9** and its corresponding hydrolysis products) or 100% ethyl acetate followed by 80% dichloromethane in methanol (for 3-amino-3-phenylpropionitrile **8** and its corresponding hydrolysis products) and the plates observed under UV light and by ninhydrin or anisaldehyde staining.

Analysis by HPLC

The collected supernatants (270 μl) from the reaction studies were transferred into vials containing vial inserts.

Benzonitrile **4** or benzamide (30 μl of 100 mmol l^{-1} stock) was added as an internal standard for the 3-amino-3-phenylpropionitrile **8** or 3-hydroxy-4-phenoxybutyronitrile **9** reaction mixtures respectively. Analyses of nitrile transformations were performed with the use of a Waters 2690 separation module, coupled with a Waters Diode Array Detector 996 using a 3·0 × 5·0 mm Waters X-Terra MS18 3·5 μm column (Microsep, Johannesburg, South Africa) with acetonitrile and trifluoroacetic acid (0·1%) as the eluent (0·3–0·5 ml min^{-1}). The wavelength of the detector was set at 215 nm. Acid and amide standards were used to confirm formation of biocatalysis hydrolysis products.

Statistical analysis

The statistical analyses were performed using the Stata V11 statistical software package. The interpretation was performed at the 95% confidence limit. To test for association, the exact test was employed. Logistic regression models, both adjusted and unadjusted models, were fitted to compare the sites.

Identification of bacterial isolates using 16S rRNA

DNA isolation

Pure colonies of the isolates were cultured in liquid lysogeny broth medium for 18 h in a 30°C shaking incubator at 160 rev min^{-1}. Procedures of DNA isolation from bacteria were performed according to manufacturer's instructions prescribed in the QIAamp DNA mini kit (Southern Cross Biotechnology, Cape Town, South Africa) and visualized by gel electrophoresis.

PCR amplification and purification of the 16S rRNA gene

For the PCR amplification of the 16S rRNA gene fragments from the isolates, the universal primer pair, 27F (5′-AGAGTTTGATCCTGGCTCAG-3′) and 1492R (5′-GGTTACCTTGTTACGACTT-3′), was used. The PCR reaction was performed in 50 μl reaction volumes consisting of 50–100 ng of DNA, 200 mmol l^{-1} of each deoxynucleoside phosphate (ThermoFisher, Johanneburg, South Africa), 25 pmol of each primer, 1× reaction buffer, 1·5 mmol l^{-1} $MgCl_2$ and 1 U of *Taq* DNA polymerase (Super Therm, Fermentas, Vilnius, Lithuania). The PCR reaction was carried out using a gradient thermal cycler (Eppendorf AG 22331 thermal cycler) with initial melting at 94°C for 5 min, followed by 30 cycles of denaturation at 94°C for 30 s, annealing at 55°C for 30 s, extension at 72°C for 1 min, a final extension at 72°C for 10 min and a holding temperature of 4°C. The PCR products were analysed on a 1% agarose electrophoresis gel. DNA purification was performed using the QIAquick purification kit (Southern Cross Biotechnology) according to manufacturer's instructions.

Sequencing of the 16S rRNA fragment

The nucleotide sequencing of the 16S rRNA gene was performed using the Sanger-sequencing method provided by the services of Inqaba Biotechnology (Pretoria, South Africa) using the primer set: 27F (5′-AGAGTTTGATCCTGGCTCAG-3′), 1492R (5′-GGTTACCTTGTTACGACTT-3′), as well as 907R (5′-CCGTCAATTCCTTTAAGTTT-3′).

Computational analysis and construction of a phylogenetic tree

The 16S rRNA sequences were analysed using the Bioedit ver. 5·0·6 software program (Hall 2001). The common overlapping Forward and Reverse sequences were assembled with the help of the GenBank database (http://ncbi.nlm.nih.gov) and a continuous stretch of approximately 1·4 kb was constructed by joining and editing the Forward and Reverse sequences using Bioedit. The query sequences were subjected to BLAST (Basic Local Alignment Sequence Tool) in order to search for homologous sequences of identified strains available in the GenBank database.

The 16S rRNA gene sequence used as a reference for phylogenetic analysis was downloaded from the National Centre for Biotechnology Information website (http://ncbi.nlm.nih.gov). Multiple sequence alignments were processed using the CLUSTAL W algorithm and these aligned sequences were studied using Molecular Evolutionary Genetics Analysis, ver. 4 (MEGA4) software program (Tamura *et al.* 2007) for phylogenetic inference (neighbour joining). The confidence value for the aligned sequence data set was obtained by performing 1000 bootstrap replications. A phylogenetic tree was constructed using the Neighbour-Joining method with pair-wise substitution of gaps (gap penalty of 10%).

Results

Isolation method

The use of nitriles as a source of both carbon and nitrogen resulted in fewer isolates (60) compared to media supplemented with an exogenous carbon source (123), which was statistically highly significant ($P = 0·001$) (Table 1). Based on the number of isolates, it appears that the residual carboxylic acids formed by hydrolysis of adiponitrile **1**, propionitrile **2**, benzonitrile **3**, 4-chlorobenzonitrile **4** and 4-cyanopyridine **5** (yielding propionic acid, adipic acid, benzoic acid, 4-chlorobenzoic acid and isonicotinic acid

Table 1 Number of isolates obtained from samples of uncultivated soil

Substrate	Direct plating method		Liquid enrichment method
	Carbon and Nitrogen (20 mmol l^{-1})	Nitrogen only (0·5 mmol l^{-1})	Nitrogen only (0·5 mmol l^{-1})
Adiponitrile **1**	11	23	13
Propionitrile **2**	9	12	18
Benzonitrile **3**	16	19	12
4-Chlorobenzonitrile 4	13	17	13
4-Cyanopyridine **5**	11	23	16
Benzylidenemalononitrile 6	0	17	14
Hydrocinnamonitrile **7**	0	12	14
Total isolates	60	123	100

respectively) were relatively easily metabolised, thereby providing both a carbon and a nitrogen source. Conversely, the products of benzylidenemalononitrile **6** and hydrocinnamonitrile **7**, being benzylidenemalonic acid and hydrocinnamic acid, seem to be very poor carbon sources.

Compared to direct plating, the classical liquid medium enrichment approach resulted in fewer isolates (100), although the difference was not significant ($P = 0{\cdot}494$). The isolates were re-plated onto solid media, this time with a carbon source and increased nitrile concentrations of 5 and 20 mmol l^{-1} (Table 2). From this, it was evident that not all of the isolates would grow at these nitrile concentrations, and that the agricultural isolates had the broadest substrate range, while those from the mine soil the least (growth of agricultural soil isolates was 1·305 (odds ratio) more likely than uncultivated soil isolates ($P < 0{\cdot}001$), while growth of the mine-derived isolates was 0·563 (odds ratio) less likely than the uncultivated soil-derived isolates ($P < 0{\cdot}001$)).

Sampling sites

For uncultivated soil sampling, the geographical location had a minor influence, with samples across all 11 sites yielding 17–43 isolates, and a total of 266 isolates. Cultivated soil samples were collected from agricultural land, specifically radish and cabbage fields, as well as from potato fields (Table 3). Surprisingly, the crop type had negligible influence on the isolate numbers of 42–43 in each case ($P = 0{\cdot}963$–$1{\cdot}000$) in spite of the fact that potatoes are not nitrile producers. However, the selected organisms (as described below) that hydrolysed two β-substituted nitrile compounds were either from radish or cabbage fields (Table S1).

Substrate profiling

Through nitrile substrate profiling of the 223 isolates from uncultivated soil that could be re-cultured (group G), 171 from agricultural soil (group A), and 219 from mine-derived isolates (group M), it was evident that in each environment there were organisms that could grow on a range of aliphatic (adiponitrile **1** and propionitrile **2**), aromatic (benzonitrile **3**, 4-chlorobenzonitrile **4** and 4-cyanopyridine **5**) and aryl-aliphatic (hydrocinnamonitrile **6** and benzylidenemalononitrile **7**) nitriles (Fig. 1; Table 4). The isolates from uncultivated soil failed to grow on benzylidenemalononitrile, while conversely the mine isolates grew exceptionally well on this substrate. The results also showed that increased concentrations of up to 20 mmol l^{-1} of hydrocinnamonitrile **7** and the dinitrile benzylidenemalononitrile **6** had a toxic or inhibitory effect on many isolates.

From the 613 isolates, a subset of 73 isolates were selected based on their broad nitrile substrate ranges and tested on two β-substituted nitrile compounds, 3-amino-3-phenylpropionitrile **8** and 3-hydroxy-4-phenoxybutyronitrile **9**. Of these isolates, 14 were able to convert one or both of the substrates, and were subsequently identified using 16S RNA. It was observed that 11 isolates showed the ability to utilize 3-amino-3-phenylbutyronitrile, while eight isolates showed the ability to utilize 3-hydroxy-4-

Table 2 Substrate range of isolates: percentages of agricultural, mine and uncultivated soil isolates with the ability to grow on the nitriles (combined results on all nitriles)

Sampling site	5 mmol l^{-1}			20 mmol l^{-1}			
	Day 2	Day 7	Day 14	Day 2	Day 4	Day 7	Day 14
Agricultural	13	46	58	0	30	44	54
Uncultivated	13	39	49	0	16	31	37
Mine	1	29	39	0	7	21	37

Table 3 Number of isolates obtained from the different agricultural samples by a combination of enrichment and nonenrichment methods

Nitrile	Cabbage field 1	Cabbage field 2	Radish field	Potato field
Adiponitrile **1**	6	4	6	5
Propionitrile **2**	6	6	5	7
Benzonitrile **3**	6	5	7	5
4-Chlorobenzonitrile **4**	8	7	7	7
4-Cyanopyridine **5**	5	6	4	6
Benzylidenemalononitrile 6	6	7	8	6
Hydrocinnamonitrile **7**	6	7	6	7
Total isolates	43	42	43	43

phenoxybutyronitrile (Table S1). For both compounds, representative isolates from both agricultural and uncultivated soils were active, but interestingly no isolates were derived from the mine soil. Perhaps, this is not surprising due to the low growth of the mine-derived isolates observed on the structurally similar hydrocinnamonitrile **7** at 20 mmol l^{-1} (Table 4). These isolates were then used in biocatalysis reactions in aqueous buffer. Prior to running the reactions, we confirmed our earlier observation (Chhiba *et al.* 2012) that 3-amino-3-phenylpropionitrile was only hydrolysed at pH 9 where the amine tends to be in the uncharged state, rather than the protonated form which dominates at lower pH (Fig. 2) and thereby defined the higher-than-usual reaction medium pH for that substrate. HPLC analysis of reactions indicated that both amide and acid were generated (Table 5), suggesting that nitrile hydratase and the corresponding amidase activity was involved. This was subsequently confirmed using a higher substrate concentration (Fig. 3). Some of the organisms that grew on plates containing β-substituted nitrile compounds demonstrated low or negligible conversions in the biocatalysis reactions (isolates A98, G58 and G140), possibly due to substrate toxicity.

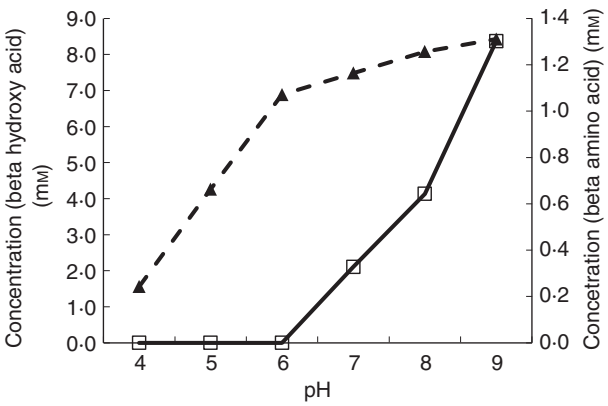


Figure 2 The hydrolysis of 3-amino-3-propionitrile **8** (-□-) and 3-hydroxy-4-phenoxybutyronitrile **9** (-▲-) in 1 h by isolate *Rhodococcus erythropolis* G117 at pH (4–9).

Microbial identification using 16S rRNA

Twenty four isolates were selected for 16S rRNA identification, of which 14 isolates were those with the ability to convert beta substituted nitriles as listed in Table 5, while another nine isolates were randomly selected from those cultures without the ability to convert the β-substituted nitriles and were included for comparison. These were G150, G151, G196, G208 and G257 from uncultivated soil, A85 from agricultural soil, and M148, M195 and M208 from mine-derived soil (Table S2).

Out of 24 isolates, a total of 23 could be identified using 16S rRNA using the standard 27F and 1492R primers, as well as the internal primer 907R. Isolate A16a

Table 4 Substrate profiling: percentage of isolates with the ability to grow on nitriles

	Agricultural (%)	Uncultivated (%)	Mine (%)	Agricultural (%)	Uncultivated (%)	Mine (%)
Substrate	5 mmol l^{-1}			20 mmol l^{-1}		
Adiponitrile **1**	72	56	69	85	59	88
Propionitrile **2**	64	56	41	66	55	27
Benzonitrile **3**	68	52	35	53	37	40
4-Chlorobenzonitrile **4**	61	52	27	78	42	63
4-Cyanopyridine **5**	58	55	12	65	59	18
Benzylidenemalononitrile **6**	45	0	60	21	0	25
Hydrocinnamonitrile **7**	32	33	28	3	12	1

Growth after 14 days of incubation.

Table 5 Biocatalytic activity towards β-substituted nitriles

Organism		% 3-amino-3-phenylpropionitrile and products			% 3-hydroxy-4-phenoxybutyronitrile and products		
		Nitrile	Amide	Acid	Nitrile	Amide	Acid
A12	*Rhodococcus rhodochrous*	98	0	2	41	50	9
A16a	Not identified	98	2	0	–	–	–
A19	*R. rhodochrous*	54	46	0	3	95	2
A29	*R. rhodochrous*	–	–	–	75	22	3
A73	*R. rhodochrous*	94	6	0	–	–	–
A98	*R. rhodochrous*	–	–	–	100	0	0
A99	*Pimelobacter simplex*	35	65	0	–	–	–
G1	*Rhodococcus erythropolis*	91	7	2	96	2	2
G58	*R. erythropolis*	100	0	0	100	0	0
G65	*R. erythropolis*	0	49	51	–	–	–
G117	*R. erythropolis*	34	5	61	67	0	33
G126	*R. erythropolis*	79	2	19	–	–	–
G132	*R. erythropolis*	12	4	84	–	–	–
G140	*R. erythropolis*	100	0	0	–	–	–
G180	*R. erythropolis*	–	–	–	3	0	97

A dash (–) = not determined (as activity was not observed in the initial 5 mmol l^{-1} screening).
Reaction conditions 100 mg substrate in 20 ml buffer (34·2 mmol l^{-1} 3-amino-3-phenylpropionitrile and 28·5 mmol l^{-1} 3-hydroxy-4-phenoxybutyronitrile) at a reaction time of 24 h.

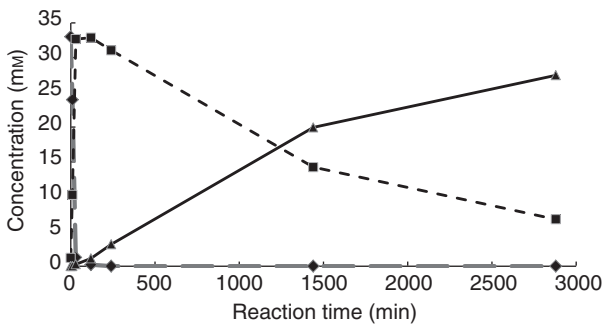


Figure 3 The hydrolysis of 3-amino-3-phenylpropionitrile **8** (♦) to 3-amino-3-phenylpropionamide (■) and 3-amino-3-phenylpropanoic acid **9** (▲) by *Rhodococcus erythropolis* G65.

could not be identified. The gene sequences were compared with the sequences of the identified strains existing in the GenBank database. An outlier, namely *Cenarchaeum symbiosum* was selected in order to compile a phylogenetic tree (Fig. 4).

The 16S rRNA gene sequences revealed that most of the β-nitrile-hydrolysing isolates clustered (with 99–100% similarity) to *Rhodococcus erythropolis* or *Rhodococcus* sp. The latter cluster was subsequently determined to be *R. rhodochrous*, based on comparison to *R. rhodochrous* ATCC BAA-870. These colonies also exhibited the pink colour characteristic of *R. rhodochrous* associated with the cobalt-based nitrile hydratases they express. Conversely, the *R. erythropolis* colonies had a distinctive brown colour associated with the iron-based nitrile hydratases they express (Brandão *et al.* 2003). Therefore, the isolates from the two groups were designated as *R. rhodochrous* and *R. erythropolis* respectively. The only exception was A99, identified as *Pimelobacter simplex* (also known as *Nocardiodes simplex*); however, taxonomically this species clusters closely to *Rhodococcus*.

Discussion

It is of interest to synthetic organic chemists to have access to suitable biocatalysts to synthesise β-substituted amides and acids (Chhiba *et al.* 2012, 2014; Rudat *et al.* 2012; Coady *et al.* 2013), which can be used as precursors for the synthesis of peptidomimetics and other pharmaceuticals. However, in our search the chiral compound 3-amino-3-phenylpropionitrile **8** was only hydrolysed at pH 9 or above by a strain of *R. rhodochrous* (Chhiba *et al.* 2012), and hence this compound could not be used in a growth-based primary screen to discover new biocatalysts. Moreover, the possible release of the amino group at the beta position through alternative enzyme reactions would have made the nitrogen dependent screen results ambiguous. Hence, we performed a preliminary growth-based selection based on a variety of substrates, including the structurally similar hydrocinnamonitrile **7**.

Although some organisms can utilize nitrile compounds as both sole carbon and nitrogen source (Demakov *et al.* 2007; Chmura *et al.* 2008), others require a supplementary carbon source (Wang *et al.*

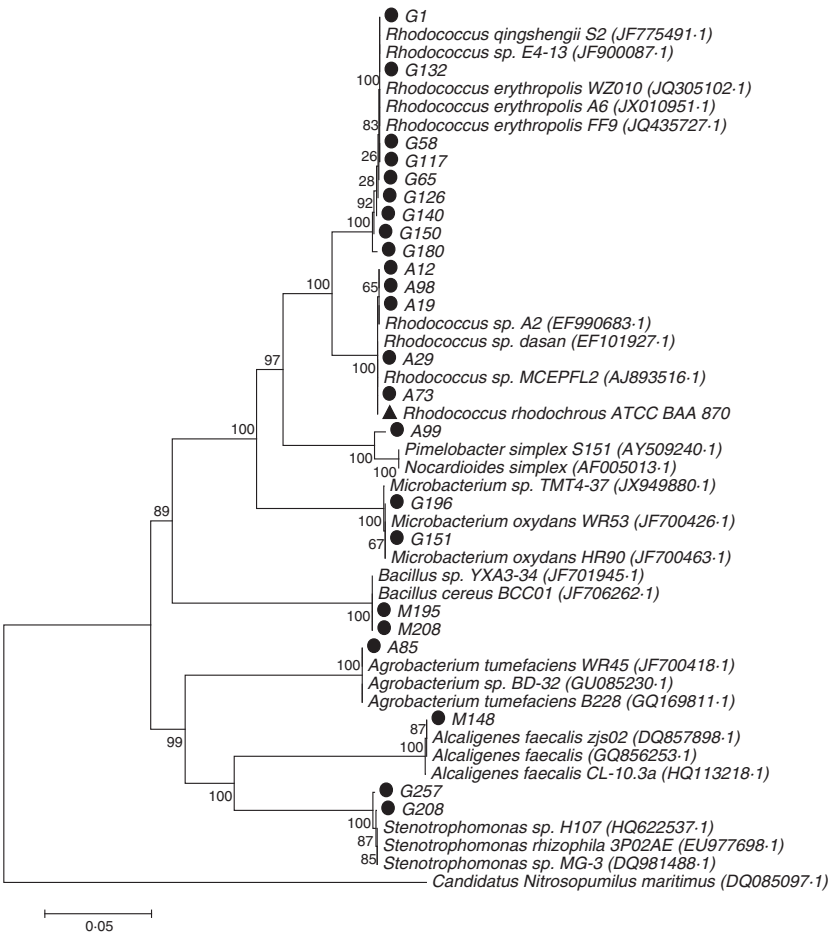


Figure 4 Neighbour-joining phylogenetic tree showing the position of nitrile-hydrolysing isolates from agricultural, uncultivated as well as mine sampling sites. The tree was drawn using a 1000 replicates using the Neighbour-Joining method from 6053 sites, with pair-wise substitution of gaps. Isolates from this study are marked with symbol (●). *Rhodococcus rhodochrous* ATCC BAA 870 (marked with symbol ▲) was used as a reference strain.

2001; Rezende *et al.* 2003; Huertas *et al.* 2006) as they may be unable to utilise the carboxylic acids generated from the substrate by the nitrile-hydrolysing enzymes (Park *et al.* 2004). The structure of substrates will obviously play a role due to the constraints of enzyme active sites. Adiponitrile **1** and propionitrile **2** are both aliphatic, and both were suitable as a carbon source. Three of the aromatic compounds (benzonitrile **3**, 4-chlorobenzonitrile **4** and 4-cyanopyridine **5**) were also suitable as a carbon source, but not those with bulkier substituents (benzylidenemalononitrile **6** and hydrocinnamonitrile **7**). The poor growth on hydrocinnamonitrile as both a carbon and nitrogen source implies that the organisms suitable for hydrolysis of β-amino nitrile compounds may not have been discovered using this screen. While adiponitrile **1** and benzylidenemalononitrile **6** are both dinitriles, only adiponitrile was a suitable carbon source.

The classical liquid medium enrichment approach (Demakov *et al.* 2007; Martĺnková *et al.* 2008; Zheng *et al.* 2008; Zhang *et al.* 2009) yielded fewer isolates when compared to direct plating, which indicates some loss of bacterial diversity due to competition for resources. Hence, directly plating may be the optimal method for isolation of nitrile-hydrolysing organisms. The concentration of the nitrile also appears to be an important factor, as many of the isolates obtained on 0·5 mmol l^{-1} nitrile plates would not subsequently grow on 5 mmol l^{-1} nitrile plates. Similarly Li *et al.* (2007) observed maximum growth of adapted mixed cultures occurring at concentrations of 12–24 mmol l^{-1} of acetonitrile, with inhibition taking place at 170 mmol l^{-1}, while Wang *et al.* (2001) found that *Comamonas testosteroni* and an *Acidovorax* sp. could hydrolyse benzonitrile only up to 4 mmol l^{-1}, and 24 mmol l^{-1} propionitrile was too high for the *Acidovorax* strain. Fumaronitrile (not used in this study) was found to be toxic even at concentrations as low as 0·05 mmol l^{-1} (Wyatt and Knowles 1995).

Previously, we reported on microbial isolation of nitrile-hydrolysing organisms from land used by the chemical industry and other soils near Johannesburg (Brady *et al.* 2006). In the current research we performed a much wider study on soils from agricultural, uncultivated and mine tailings dams. The geographical location of the uncultivated soil did not seem to have a large

impact on the presence of nitrile-hydrolysing organisms, with these organisms being found at all 11 sampling sites, and the β-amino nitrile-hydrolysing organisms being isolated from five of the sites.

Nitrile-hydrolysing organisms were also discovered in cultivated soil. Many commercial crops produce cyanide and nitriles as a defence mechanism. The cyanogenic glucoside dhurrin is found in sorghum (Tattersall *et al.* 2001), while glucosinolates are found as secondary metabolites in almost all plants of the Brassicaceae family (which includes cabbage, radish, cauliflower and mustard) (Lambrix *et al.* 2001; Blažević and Mastelić 2009). Upon hydrolysis, these compounds release defence molecules such as isothiocyanates, nitriles, epithionitriles and thiocyanates (Al-Turki and Dick 2003). It was therefore not surprising that nitrile-hydrolysing bacteria were isolated from radish and cabbage fields. However, agricultural land for potato farming yielded just as many isolates, although potatoes do not use nitriles as a defence mechanism. However, common nitrile containing agricultural chemicals (e.g. fungicides such as chloronil (tetrachloroisophthalonitrile), pesticides and herbicides) are applied to a broad spectrum of crops, including cabbage, potato and radish, and these may contribute to the microbial profile of the soil. Interestingly, the four isolates from agricultural land that hydrolysed 3-amino-3-phenylpropionitrile were all obtained from cabbage fields. This suggests that the soils associated with this crop may be an ideal source for this type of biocatalyst.

The mine tailings isolates were of no value in the hydrolysis of β-substituted nitriles, but these grew exceptionally well on benzylidenemalononitrile **6**, which is commonly used in organic synthesis of various products (Elinson *et al.* 2008), and may therefore be useful in other reactions. It is noteworthy that the Rhodococci were unusually poor at converting this substrate. M195 and M208 were similar to *Bacillus cereus*, which is a known nitrile converter (Saroja *et al.* 2000), while M148 was closely clustered to *Alcaligenes faecalis,* which is also known to convert nitriles (Yamamoto *et al.* 1991). Species of *Bacillus* and *Alcaligenes* have been isolated from cyanide containing mine tailings previously (Ingvorsen *et al.* 1991; Meyers *et al.* 1991, 1993).

The β-substituted nitrile-hydrolysing organisms were identified as either *R. erythropolis* or *R. rhodochrous*, as well as one strain of that was identified as *P. simplex*, a closely related species. Rhodococci are a widespread and persistent soil organism (Bell *et al.* 1999; Wu and Li 2003; Brady *et al.* 2006; Zhang *et al.* 2009) and strains are frequently associated with the hydrolysis of nitriles (Brandão *et al.* 2003), such as *R. erythropolis* MP50 (Effenberger *et al.* 1997), *R. erythropolis* AJ270 (Snell and Crosby 1999; Song *et al.* 2007), *Rhodococcus rhodochrous* ATCC BAA-870 (Brady *et al.* 2006; Kinfe *et al.* 2009) and *R. rhodochrous* PA-34 (Bhalla *et al.* 1995). There appears to be some variation between the activity profiles within species in the present study, possibly due to regional evolution (Brandão *et al.* 2003).

Other comparatively good nitrile-hydrolysing isolates could not hydrolyse the β-substituted nitriles **8**, **9** or hydrocinnamonitrile **7**. These included isolates G151 and G196, which were similar to *Microbacterium oxydans* while G257 showed closest similarities to *Stenotrophomonas* species. Isolate A85 showed similarity to *Agrobacterium tumefaciens*, which expresses a nitrile hydratase (Kobayashi *et al.* 1995). Although mainly nitrile hydratases appear to be involved in the nitrile hydrolysis observed in the current study, the contribution of nitrilases cannot be discounted as these are also expressed by Rhodococci (Thuku *et al.* 2009). Recently Vergne-Vaxelaire *et al.* (2013) generated an extensive library of heterologously expressed diverse nitrilases derived from genomic sequences. Interestingly, the nitrilase from *Syntrophobacter fumaroxidans* was the only one out of 125 to hydrolyse 3-amino-3-phenylpropionitrile **8**.

In conclusion, the genus *Rhodococcus* and a closely related genus were exclusively represented in the subset of the β-substituted nitrile-hydrolysing strains, in which the isolates phylogenetically related to *R. erythropolis* predominated in the uncultivated soil-derived isolates, while those identified as *R. rhodochrous* predominated in isolates derived from the agricultural (cultivated) sites. This study indicates that the enzymes from Rhodococci are possibly uniquely suitable for these substrates. Further work will explore the enantioselectivity of the enzymes and the associated variation in the gene sequences.

Acknowledgements

We thank the NRF, DST Biocatalysis Initiative, the CSIR, Tshwane University of Technology and the European Cooperation in Science and Technology COST programme for financial support, and Drs D Visser and Walter Sanyika for technical assistance.

Conflict of Interest

There are no conflicts of interest associated with this work.

References

Akcil, A. (2003) Destruction of cyanide in gold mill effluents: biological versus chemical treatments. *Biotechnol Adv* **21**, 501–511.

Al-Turki, A.I. and Dick, W.A. (2003) Myrosinase activity in soil. *Soil Sci Soc Am J* **67**, 139–145.

Bell, K.S., Kuyukina, M.S., Heidbrink, S., Philp, J.C., Aw, D.W., Ivshina, I.B. and Christofi, N. (1999) Identification and environmental detection of *Rhodococcus* species by 16S rDNA-targeted PCR. *J Appl Microbiol* **87**, 472–480.

Bhalla, T.C. and Kumar, H. (2005) *Nocardia globerula* NHB-2: a versatile nitrile-degrading organism. *Can J Microbiol* **51**, 705–708.

Bhalla, T.C., Aoshima, M., Misawa, S., Muramatsu, R. and Furuhashi, K. (1995) The molecular cloning and sequencing of the nitrilase gene of *Rhodococcus rhodochrous* PA-34. *Acta Biotechnol* **15**, 297–306.

Blažević, I. and Mastelić, J. (2009) Glucosinolate degradation products and other bound and free volatiles in the leaves and roots of radish (*Raphanus sativus L*). *Food Chem* **113**, 96–102.

Brady, D., Dube, N. and Petersen, R. (2006) Green chemistry: highly selective biocatalytic hydrolysis of nitrile compounds. *S Afr J Sci* **102**, 339–344.

Brandão, P.F.B., Clapp, J.P. and Bull, A.T. (2003) Diversity of nitrile hydratase and amidase enzyme genes in *Rhodococcus erythropolis* recovered from geographically distinct habitats. *Appl Environ Microb* **69**, 5754–5766.

Cantarella, M., Cantarella, L., Gallifouco, A. and Spera, A. (2006) Nitrile conversion by *Microbacterium imperiale* CBS 498-74 resting cells in batch and ultrafiltration membrane bioreactors. *J Ind Microbiol Biot* **33**, 208–241.

Chhiba, V.P., Bode, M.L., Mathiba, K., Kwezi, W. and Brady, D. (2012) Enantiomeric biocatalytic hydrolysis of β-aminonitriles to β-aminoamides using *Rhodococcus rhodochrous* ATCC BAA-870. *J Mol Cat B Enz* **76**, 68–74.

Chhiba, V., Bode, M., Mathiba, K. and Brady, D. (2014) Enzymatic stereoselective synthesis of beta amino acids. In *Cascade Biocatalysis: Integrating Stereoselective and Environmentally Friendly Reactions*. Chapter 14 ed. Riva, S.A. and Fessner, W.-D. pp. 297–314. Wiley-VCH Verlag GmbH & Co. KGaA, Weinheim, Germany. ISBN: 978-3-527-33522-0.

Chmura, A., Shapovalova, A.A., Van Pelt, S., Van Rantwijk, F., Tourova, T.P., Muyzer, G. and Sorokin, D.Y. (2008) Utilization of arylaliphatic nitriles by haloaliphilic *Halomonas nitrilicus* sp. nov. isolated from soda soils. *Appl Microbial Cell Physiol* **81**, 371–378.

Coady, T.M., Coffey, L.V., O'Reilly, C., Owens, E.B. and Lennon, C.M. (2013) A high throughput screening strategy for the assessment of nitrile-hydrolyzing activity towards the production of enantiopure ß-hydroxy acids. *J Mol Cat B Enz* **97**, 150–155.

Dash, R.R., Gaur, A. and Balomajumder, C. (2009) Cyanide in industrial wastewaters and its removal: a review on biotreatment. *J Hazard Mater* **163**, 1–11.

Demakov, V.A., Maksimov, A.Y., Kuznetsova, M.V., Ovechkina, G.V., Remezovskaya, N.B. and Maksimova, Y.-G. (2007) Biological diversity of nitrile-metabolizing bacteria in soil of the Perm region affected by human activities. *Russ J Ecol* **38**, 168–173.

Effenberger, F., Graef, B.W. and Osswald, S. (1997) Preparation of (*S*)-naproxen by enantioselective hydrolysis of racemic naproxen amide with resting cells of *Rhodococcus erythropolis* MP50 in organic solvents. *Tetrahedron Asymm* **8**, 2749–2755.

Elinson, M.N., Feducovich, S.K., Stepanov, N.O., Vereshchagin, A.N. and Nikishin, G. (2008) A new strategy of the chemical route to the cyclopropane structure: direct transformation of benzylidenemalononitriles and malononitriles into 1,1,2,2-tetracyanocyclopropanes. *Tetrahedron* **64**, 708–713.

Feng, Y.-S. and Lee, C.-M. (2009) The potential of the acetonitrile biodegradation by *Mesorhizobium* sp. F28. *J Hazard Mater* **164**, 646–650.

Godballe, T., Nilsson, L.L., Petersen, P.D. and Jenssen, H. (2011) Antimicrobial β-peptides and α-peptoids. *Chem Biol Drug Des* **77**, 107–116.

Gong, J.-S., Lu, Z.-M., Li, H., Shi, J.-S., Zhou, Z.-M. and Xu, Z.-H. (2012) Nitrilases in nitrile biocatalysis: recent progress and forthcoming research. *Microb Cell Fact* **11**, 142.

Hall, T. (2001) *Bioedit version 5.0.6*. North Carolina State University: Department of Microbiology. Available at: http://www.mbio.ncsu.edu/BioEdit/bioedit.html Accessed 26 October 2010.

Huertas, M.J., Luque-Almagro, V.M., Martinez-Luque, M., Blasco, R., Moreno-Vivian, C., Castillo, F. and Roldan, M.D. (2006) Cyanide metabolism of *Pseudomonas pseudoalcaligenes* CECT5344: role of siderophores. *Biochem Soc Trans* **34**, 152–155.

Ingvorsen, K., Højer-Pedersen, B. and Godtfredsen, S.E. (1991) Novel cyanide-hydrolyzing enzyme from *Alcaligenes xylosoxidans* subsp. *denitrificans*. *Appl Microbiol Biotechnol* **57**, 1783–1789.

Kao, C.M., Chen, K.F., Liu, J.K., Chou, S.M. and Chen, S.C. (2006) Enzymatic degradation of nitriles by *Klebsiella oxytoca*. *Appl Microbial Cell Physiol* **71**, 228–233.

Khamar, Z., Makhdoumi-Kakhki, A. and Mahmudy Gharaie, M.H. (2015) Remediation of cyanide from the gold mine tailing pond by a novel bacterial co-culture. *Int Biodeterior Biodegradation* **99**, 123–128.

Kinfe, H.H., Chhiba, V., Frederick, J., Bode, M.L., Mathiba, K., Steenkamp, P.A. and Brady, D. (2009) Enantioselective hydrolysis of β-hydroxy nitriles using the whole cell biocatalyst *Rhodococcus rhodochrous* ATCC BAA-870. *J Mol Catal B Enzym* **59**, 231–236.

Kobayashi, M., Suzuki, T., Fujita, T., Masuda, M. and Shimizu, M. (1995) Occurrence of enzymes involved in biosynthesis of indole—3-acetic acid from indole-3-acetonitrile in plant-associated bacteria, *Agrobacterium and Rhizobium*. *Proc Natl Acad Sci USA* **92**, 714–718.

Lambrix, V., Reichelt, M., Mitchell-Olds, T., Kliebenstein, D.J. and Gershenzon, J. (2001) The *Arabidopsis* epithiospecifier

protein promotes the hydrolysis of glucosinolates to nitriles and influences *Trichoplusia ni* herbivory. *Plant Cell* **13**, 2793–2807.

Langdahl, B.R., Bisp, P. and Ingvorsen, K. (1996) Nitrile hydrolysis by *Rhodococcus erythropolis* BL1, an acetonitrile-tolerant strain isolated from marine sediment. *Microbiology* **142**, 145–154.

Layh, N., Hirrlinger, B., Stoltz, A. and Knackmuss, H.-J. (1997) Enrichment strategies for nitrile-hydrolysing bacteria. *Appl Microbiol Biot* **47**, 668–674.

Li, T., Liu, J., Bai, R., Ohandja, D.-G. and Wong, F.-S. (2007) Biodegradation of organonitriles by adapted activated sludge consortium with acetonitrile-degrading microorganisms. *Water Res* **41**, 3465–3473.

Ma, D.-Y., Wang, D.-X., Pan, J., Huang, Z.-T. and Wang, M.-X. (2008) Nitrile biotransformations for the synthesis of highly enantioenriched β-hydroxy and β-amino acid and amide derivatives: a general and simple but powerful and efficient benzyl protection strategy to increase enantioselectivity of the amidase. *J Org Chem* **73**, 4087–4091.

Martínková, L. and Mylerová, V. (2003) Synthetic applications of nitrile-converting enzymes. *Curr Org Chem* **7**, 1279–1295.

Martínková, L., Uhnáková, B., Pátek, M., Nešvera, J. and Křen, V. (2009) Biodegradation potential of the genus *Rhodococcus*. *Environ Int* **35**, 162–177.

Martĺnková, L., Vejvoda, V. and Kren, V. (2008) Selection and screening for enzymes of nitrile metabolism. *J Biotechnol* **133**, 318–326.

Meyers, P.R., Gokool, P., Rawlings, D.E. and Woods, D.R. (1991) An efficient cyanide degrading *Bacillus pumilus* strain. *J Gen Microbiol* **137**, 1397–1400.

Meyers, P.R., Rawlings, D.E., Woods, D.R. and Lindsey, G.G. (1993) Isolation and characterization of a cyanide dihydratase from *Bacillus pumilus* Cl. *J Bacteriol* **175**, 6105–6112.

Nyska, A. and Ghanayem, B.I. (2003) Characterization of the toxicity, mutagenicity, and carcinogenicity of methacrylonitrile in F344 Rats and B6C3F1 mice. *Arch Toxicol* **77**, 233–242.

Park, D.W., Lee, K., Chae, J.-C., Kudo, T. and Kim, C.-K. (2004) Genetic structure of *xyl* gene cluster responsible for complete degradation of (4-chloro)benzoate from *Pseudomonas* sp. S-47. *J Microbiol Biotechnol* **14**, 483–489.

Ramteke, P.W., Maurice, N.G., Joseph, B. and Wadher, B.J. (2013) Nitrile-converting enzymes: an eco-friendly tool for industrial biocatalysis. *Biotechnol Appl Biochem* **60**, 459–481.

Rezende, R.P., Dias, J.C.T., Monteiro, A.S., Carraza, F. and Linardi, V.R. (2003) The use of acetonitrile as the sole nitrogen and carbon source by *Geotrichum* sp. JR1. *Braz J Microbiol* **34**, 117–120.

Rudat, J., Brucher, B.R. and Syldatk, C. (2012) Transaminases for the synthesis of enantiopure beta-amino acids. *AMB Express* **2**, 1–10.

Saroja, N., Shamala, T.R. and Tharanathan, R.N. (2000) Biodegradation of starch-g-polyacrylonitrile, a packaging material by *Bacillus cereus*. *Process Biochem* **36**, 119–125.

Snell, D. and Crosby, J. (1999) Enantioselective hydrolysis of racemic ibuprofen amide to s-(+)-ibuprofen by *Rhodococcus* AJ270. *Enzyme Microb Tech* **24**, 160–163.

Song, L., Wang, M., Shi, J., Xue, Z., Wang, M.-X. and Qian, S. (2007) High resolution X-ray molecular structure of the nitrile hydratase from *Rhodococcus erythropolis* AJ270 reveals posttranslational oxidation of two cysteines into sulfinic acids and a novel biocatalytic nitrile hydration mechanism. *Biochem Biophys Res Commun* **362**, 319–324.

Tamura, K., Dudley, J., Nei, M. and Kumar, S. (2007) MEGA4: molecular evolutionary genetics analysis (MEGA) software version 4.0. *Mol Biol Evol* **24**, 1596–1599.

Tang, P., Liu, J.-K., Chou, S.-M., Hor, L.-I., Chen, W.-J. and Chen, S.C. (2008) A proteomic analysis of *Klebsiella oxytoca* after exposure to succinonitrile. *Process Biochem* **43**, 753–757.

Tattersall, D.B., Bak, S., Jones, P.R., Olsen, C.E., Nielsen, J.K., Hansen, M.L., Høj, P.B. and Møller, B.L. (2001) Resistance to an herbivore through engineered cyanogenic glucoside synthesis. *Science* **293**, 1826–1828.

Thomas, S.M., DiCosimo, R. and Nagarajan, V. (2002) Biocatalysis: applications and potentials for the chemical industry. *Trends Biotechnol* **20**, 2s38–242.

Thuku, R.N., Brady, D., Benedik, M.J. and Sewel, B.T. (2009) Microbial nitrilases: versatile, spiral forming enzymes. *J Appl Microbiol* **106**, 703–727.

Vergne-Vaxelaire, C., Bordier, F., Fossey, A., Besnard-Gonnet, M., Debard, A., Mariage, A., Pellouin, V., Perret, A. *et al.* (2013) Nitrilase activity screening on structurally diverse substrates: providing biocatalytic tools for organic synthesis. *Adv Synth Catal* **355**, 1763–1779.

Wang, C.-C., Lee, C.-M. and Chen, P.W. (2001) Acrylonitrile removal from synthetic wastewater and actual industrial wastewater with high-strength nitrogen using a pure bacterial culture. *Water Sci Technol* **43**, 349–354.

Wu, Z.-L. and Li, Z.-Y. (2003) Biocatalytic asymmetric hydrolysis of ($\pm$)-β-hydroxy nitriles by *Rhodococcus* sp. CGMCC 0497. *J Mol Catal B Enzym* **22**, 105–112.

Wyatt, J.M. and Knowles, C.J. (1995) Microbial degradation of acrylonitrile waste effluents: the degradation of effluents and condensates from the manufacture of acrylonitrile. *Int Biodeterior Biodegradation* **35**, 227–248.

Yamamoto, K., Oishi, K., Fujimatsu, I. and Komatsu, K.-I. (1991) Production of *R*-(—)-mandelic acid from mandelonitrile by *Alcaligenes faecalis* ATCC 8750. *Appl Environ Microb* **57**, 3028–3032.

Zhang, J.-L., Wang, M., Sun, H., Li, X.-D. and Zhong, L.-P. (2009) Isolation and characterization of *Rhodococcus ruber* CGMCC3090 that hydrolyzes aliphatic, aromatic and heterocyclic nitriles. *Afr J Biotechnol* **8**, 5467–5486.

Zheng, Y.-G., Chen, J., Liu, Z.-Q., Wu, M.-H., Xing, L.-Y. and Shen, Y.-C. (2008) Isolation, identification and characterization of *Bacillus subtilis* ZJB-063, a versatile nitrile-converting bacterium. *Appl Microbiol Biot* **77**, 985–993.

Supporting Information

Additional Supporting Information may be found in the online version of this article:

Figure S1 Uncultivated soil sampling points, transect across South Africa.

Table S1 Substrate profiling: isolates with the ability to grow on nitriles.

Table S2 Comparison of nitrile-hydrolysing isolates to those identified strains obtained from GenBank using BLAST search for homologous sequences.

Chapter Seven

PAPER V

Dimethylformamide – a novel inducer of nitrilase in *Rhodococcus rhodochrous* and *Pimelobacter simplex*

V. P. Chhiba-Govindjee[1], K. Mathiba[1], C. W. van der Westhuyzen[1], P. Steenkamp, J[1]. K. Rashamuse[2,] S. Stoychev[1], M. L. Bode[3] and D. Brady[3]

[1] CSIR Biosciences, PO Box 395, Pretoria, 0001, South Africa

[2] Department of Science and Technology (DST), Meiring Naude Road, Brummeria, Pretoria, 0001, South Africa

[3]Molecular Sciences Institute, School of Chemistry, University of the Witwatersrand, PO Wits 2050, South Africa

Corresponding author email address: dean.brady@wits.co.za

Primary author email address: vchhiba@csir.co.za

Abstract

Successful nitrilase induction was achieved through the incorporation of a previously untested inducer, dimethylformamide, during cell cultivation in two species belonging to the species *Rhodococcus rhodochrous*, namely ATCC BAA-870 and strain A99, as well as in a closely related organism *Pimelobacter simplex* strain A99. A ~40 kDa protein was observed during SDS-PAGE profiling of the cell lysate. Further inspection of the expressed peptide fragments by LC-MSMS sequencing revealed that the protein showed high sequence similarity to a documented nitrilase protein Uniprot Q-03217. Biocatalytic and inhibition studies of the enzyme activity of A29 and A99 demonstrated that the enzyme was indeed a nitrilase enzyme.

The expressed nitrilase enzyme hydrolyzed 3-cyanopyridine to produce nicotinic acid exclusively in strains A29 and A99, while ATCC BAA-870 showed a mixed amide and acid product; the result of competitive nitrile conversion by a constitutively produced nitrile hydratase enzyme in this organism.

1 Introduction

Nitrilase enzymes (EC 3.5.5.1) belong to a large super family of enzymes that are found widely distributed in nature (Brenner 2002). Nitrilases catalyse the hydrolysis of aliphatic, aromatic as well as aryl-aliphatic nitriles generating an acid product with the concomitant release of ammonia (**Fig. 1**). The Nitrilase Superfamily is often known to consist of proteins constituted of homo-dimeric building blocks with αββα-αββα sandwich folds that contain an active site which displays conserved cysteine, glutamic acid and lysine residues. C-Site interactions between adjacent homodimers generate a spiral polymer structure which is then in a catalytically active state (Thuku *et al.* 2009).

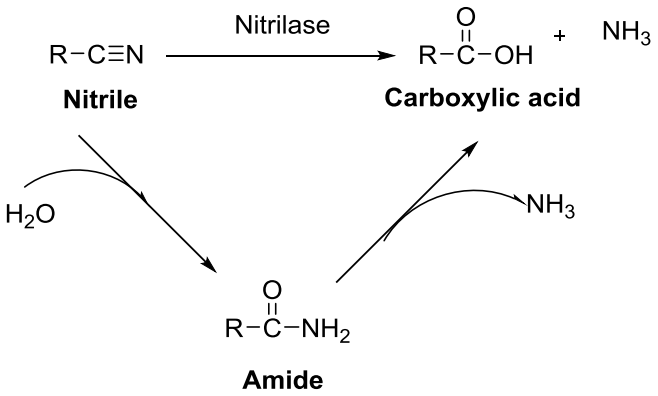


Figure 1: Schematic diagram showing nitrilase activity in comparison to nitrile hydratase/ amidase coupled reactions.

Unlike other nitrile degrading biocatalysts such as nitrile hydratases (EC 4.2.1.84), which is known to be constitutively expressed [Cramp and Cowan. 1999; Nagasawa *et al.* 1986; Yamada and Kobayashi, 1996; Endo and Watanabe. 1989] nitrilase often requires induction [Robinson and Hook. 1964; Harper. 1977; Lévi-Schil *et al.* 1995] with only a handful of species demonstrating constitutive

nitrilase enzyme production [Zheng *et al.* 2008; Zhang *et al.* 2011; Gradley *et al.* 1994; Stalker *et al.* 1988]. A number of nitrile-containing nitrilase inducers have been discovered. These include the substrate benzonitrile which was found to be an effective nitrilase enzyme inducer in *Alcaligenes faecalis* MTCC 10757 [Nageshwar *et al.* 2011]; 2-cyanopyridine in *Fusarium solani* Strain IMI96840 [Vejvoda *et al.* 2010]; as well as isovaleronitrile in *Rhodococcus rhodochrous* Strain J1 [Kobayashi *et al.* 1989]. Nitrilase expression in these organisms enables nitrile hydrolysis, thus eliminating potential toxins and providing an avenue to utilize these as a nitrogen source. However, the function of the inductive properties of non-nitrile compounds is less obvious.

As a means of increasing whole cell biocatalyst activity, an alternative to induction is the activation of previously expressed enzymes. Work done by Stevenson *et al.* (1992), Nagasawa *et al.* (2000) and Kaul and Banerjee (2008) demonstrated that nitrilase enzyme activation occurred in organic solvents, including in the presence of dimethylformamide (DMF), where the solvent appeared to have an effect on increasing nitrilase activity in *Alcaligenes faecalis* MTCC 126 [Kaul and Banerjee. 2008]. However, neither study looked into the possibility of using DMF to induce expression of nitrile-degrading enzymes.

In previous work [Chhiba *et al.* 2014], initial results indicated that isolates A29 and A99 provided high enantioselectivity in the conversion of 3-amino-3-propionitrile to 3-amino-3-propionic acid. In this work we explore the basis of this activity.

Our study commenced with an assessment of a range of known nitrile hydratase activator molecules to help identify a biological process that could be used to "tailor" a biotransformation process towards accumulation of an industrially relevant amide product. Dimethylformamide seemed analogous in structure to natural nitrile hydratase inducers and was therefore included in the screen undertaken. However, as will be seen, the function of the DMF was unexpected.

2 Materials and Methods

2.1 Isolates

Three bacterial strains, namely *Rhodococcus rhodochrous* (*R. rhodochrous*) ATCC BAA-870 and strain A29 as well as *Pimelobacter simplex* (*P. simplex*) A99 were assessed in the current study. *R. rhodochrous* ATCC BAA-870 was isolated from an industrial soil sample collected in Modderfontein, Johannesburg [Brady *et al.* 2004], while strains A29 and A99 were isolated from agricultural soil samples isolated in the Gauteng province [Rapheeha *et al.* 2017]. All cells were cryopreserved in phosphate buffer (100 mM, pH 7.2) containing a 20% (v/v) final glycerol concentration.

2.2 Cell Cultivation and Induction

All three strains were inoculated into tryptone soy broth (TSB) media for 72 h at 28^{o}C to allow for biomass production (0.5% inoculum volume, agitation at 180 rpm). Aseptic cell harvesting was done by centrifugation (10 000 rpm, 15 min) prior to biomass transfer into minimal media containing 5 mM

benzonitrile (BNZ), DMF (0.5 % v/v), or minimal media without any chemical modulators (control) (Kinfe *et al.* 2009). All induction flasks were incubated for a further 72 h at 28°C, prior to cell harvesting by centrifugation (10 000 rpm, 15 min) and subsequent storage of the pellet at -20°C.

2.3 3-CP Biotransformation Reactions

3- Cyanopyridine (3-CP) biotransformation reactions involved reacting ~100 - 200 mg (wet weight) of each of the induced or non-induced resting cell preparations with 40 mM 3-CP in a TTRIS buffer system (100 mM, pH 9.0) (cell load size was dependent on the reaction scale and nature of the experiment undertaken). Reaction quenching was done by sample acidification with 1 N HCl.

2.4 Nicotinamide and Nicotinic Acid Product Recovery

Residual 3-CP was isolated from the reaction mixture by solvent extraction using ethyl acetate (3 x sample volume). Extraction of the two reaction products was done by acid-base extraction. To extract nicotinamide, the reaction mixture was basified using a 1.0 M sodium hydroxide solution, to a pH of 10.0 and then extracted (3 x sample volume of ethyl acetate). The combined organic phase was dried over anhydrous magnesium sulfate prior to rotary evaporation and product concentration. Flash column purification allowed for the separation of the nitrile and the amide product.

Reactions generating nicotinic acid as a possible product required additional sample acidification. This was done using a 1M hydrochloric acid solution to obtain a final pH of 3.5-4. This allowed for protonation of the carboxylic acid. The resulting sample was then subjected to multiple solvent extractions (3 x sample volume of *n*-butanol) using a water miscible solvent. Product concentration was achieved by *n*-butanol evaporation *in vacuo*.

2.5 Sample Preparation for NMR Analysis

Nicotinamide and nicotinic acid samples were solubilised in ~200 µL of deuterated methanol prior to the addition of ~400 µL of deuterated chloroform. All samples were analysed using a 400 MHz Varian Innova NMR spectrometer operating at 399.939 MHz (^{1}H) and 100.574 MHz (^{13}C). Spectra were referenced against tetramethylsilane (TMS, δ 0.00 ppm) in the proton spectra, and against residual protonated methanol (δ 49.1 ppm) in the carbon spectra. Spectra were obtained at 30 °C.

2.5.1 Nicotinamide- ATCC BAA-870- Using the general procedure: 75 mg of 3-CP, 1 mL methanol, 4 mL TRIS buffer, (pH 9.0), and 200 mg of DMF-induced resting cells were reacted, with agitation at 28°C for 15 minutes. The pure product, a white solid, was extractable using ethyl acetate, after the aqueous phase had been basified to a pH of 10 using a 1M sodium hydroxide solution.

R_f (EtOAc) 0.40

^{1}H NMR (400 MHz- $CDCl_3$/ CD_3OD) δ 9.03 (dd, J=2.2, 0.7 Hz, 1H, H-2), 8.69 (dd, J=4.9, 1.7 Hz, 1H, H-6), 8.27-8.22 (m, 1H, H-4), 7.44 (ddd, J=8.0, 4.9, 0.9Hz, 1H, H-5).

^{13}C NMR (100 MHz, $CDCl_3$,/ CD_3OD) δ 170.60 (CO_2NH_2), 154.53 (C2), 150.77 (C6), 138.68 (C4), 132.15 (C3), 126.32 (C5).

UPLC-MS: t_R= 1.78- 1.79 min

2.5.2 Nicotinic acid- ATCC BAA-870, strain A29 and A99- Using the general procedure: 75 mg of 3-CP, 1 mL methanol, 4 mL TRIS buffer, pH 9.0, and 200 mg of DMF-induced resting cells were reacted, with agitation at 28°C for 15 minutes. The pure product, a fine white powder product was isolated after acidification of the aqueous phase mentioned in 2.5.1 to a pH of 3.5- 4 using a 1M HCl solution.

R_f (EtOAc) 0.04.

^{1}H NMR (400 MHz- $CDCl_3$, CD_3OD) δ 9.20 (d, J=1.0 Hz, 1H, H-2), 8.73 (dd, J=5.0, 1.4 Hz, 1H, H-6), 8.38 (dt, J=8.0, 2.0Hz, 1H, H-4), 7.47 (ddd, J=8.0, 4.9, 0.7 Hz, 1H, H-5).

^{13}C NMR (100 MHz- $CDCl_3$/ CD_3OD) δ 167.24 (CO_2H), 152.64 (C2), 150.75 (C6), 138.19 (C4), 127.45 (C3) and 123.89 (C5).

UPLC-MS: t_R= 1.61-1.62 min

(See **Appendix 1A – 1C** for NMR Spectra data)

2.6 HPLC Method Development

Nicotinic acid, nicotinamide and 3-CP present in the reaction mixtures were quantified by HPLC using a Waters Agilent 1100 (USA) equipped with a binary pump, auto sampler and column thermostat. Data processing was done using Chemstation chromatography management data software. Separation was achieved using a Waters Spherisorb 5 cm ODS2 column (250 mm x 4.6 mm), temperature controlled at 30°C. The volume injected onto the column was 10 µl. The mobile phase was a binary gradient prepared from aqueous KH_2PO_4 solution (10 mM, pH 2.8) against acetonitrile solution (HPLC grade). An initial ratio of 90:10 (% v/v) was run for 6.0 min. Then the gradient was ramped to a 30:70 (% v/v) aqueous: organic gradient for 5 min. The flow rate used was 1.0 mL/min [Binfeng *et al.* 2011]. Ultra violet detection was performed at a wavelength of 230 nm [Sharma *et al.* 2006].

Calibration curves were constructed for nicotinic acid (1-20 mM), nicotinamide (1-10 mM) and 3-CP (1-5 mM). The calibration curves gave correlation coefficients (R^2) of 0.990, 0.998, and 0.995 for

nicotinic acid, nicotinamide and 3-CP, respectively. The retention times for nicotinic acid, nicotinamide and 3-CP and were 3.541, 3.955 and 10.660 minutes, respectively.

2.7 Enantioselective Biotransformation of β-Amino Nitriles:

DMF-induced cells (wet weight-0.1 g) were resuspended in a 100 mM TRIS buffer solution (pH 9) prior to the addition of 10 mM of 3-amino-3-phenylpropanenitrile and 3-amino-3-(4-methoxyphenyl) propanenitrile, respectively. The reaction mixture was stirred at 28°C with amide generation monitored by TLC analysis. Biocatalytic reactions were terminated by acidification of the reaction (1M HCl) prior to cell centrifugation (10 000 rpm, 5 min). The supernatant fraction was analyzed by chiral HPLC.

Chiral nitrile analysis was performed using a Hewlett Packard 1100 series High Performance Liquid Chromatography system consisting of a binary pump, autosampler, column thermostat compartment, diode array detector and Chemstation chromatograph data management software, version B.03.02. The analytical column used for separation was a Chiralpak AD-H, 250 mm x 4.6 mm, 5 µm (Chiral Technologies Europe, France). The mobile phase used was a mixture of n-hexane and isopropanol (both analytical grade) in the volumetric ratio of 90: 10. The flow rate used was 1.00 mL/ min, column temperature was set at 25°C. Detection was monitored at 210 nm wavelength for 30 min. Column conditioning was done for 1 h.

2.8 Mass Spectrometric Analysis

2.8.1 Ultra Performance Liquid Chromatography- Mass Spectrometry Sample Analysis (UPLC-MS)

A Waters UPLC coupled in tandem to a Waters SYNAPT G1 HDMS mass spectrometer was used to generate accurate mass data. Optimisation of the chromatographic separation was done utilising a Waters HSS T3 C18 column (150 mm x 2.1 mm, 1.7 µm) with the column temperature controlled at 60 °C. A binary solvent mixture was used consisting of water (Eluent A) containing 10 mM formic acid (natural pH of 2.3) and methanol (Eluent B) containing 10 mM formic acid. The initial conditions were: 98% A at a flow rate of 0.4 mL/min which was maintained for 5 minutes, followed by a linear gradient to 5% A at 6 min. The conditions were kept constant for 1 min and then changed to the initial conditions. The run time was 10 min and the sample injection volume was 1 µL.

2.8.2 Time-of -Flight Mass Spectrometry analysis (Tof-MS)

The SYNAPT G1 mass spectrometer was used in V-optics and operated in electrospray mode to enable detection of phenolic and other ESI-compatible compounds. Leucine enkephalin (50pg/mL) was used as reference calibrant to obtain typical mass accuracies between 1 and 5 mDalton (mDa). The mass spectrometer was operated in ESI positive and negative mode with a capillary voltage of 4.0 kV, the sampling cone at 10 V and the extraction cone at 3.0 V. The scan time was 0.2 sec covering the 50 to 650 Dalton (Da) mass ranges. The source temperature was 120°C and the desolvation temperature was set at 450°C. Nitrogen gas was used as the nebulisation gas at a flow rate of 550 L/hand cone gas was added at 50 L/h. The software used to control the hyphenated system and do all data manipulation was MassLynx 4.1 (SCN 872).

2.9 Nitrile Degrading Activity Modulation Studies

A range of nitrile hydratase, nitrilase as well as amidase enzyme inhibitors were evaluated to ascertain the nature of the activity observed in the DMF-induced cells. Reactions were carried out using 100 mg of DMF-induced cells (wet weight) with nitrile degrading activity quantification performed using 20 mM 3-CP as substrate. All reactions were incubated at 28°C for 60 min.

2.9.1 Nitrile Hydratase Inhibition Studies

A coupled nitrile hydratase/ amidase cascade enzyme system or a nitrilase enzyme could result in the formation of the observed acid product. It was therefore crucial to determine which of these enzymes was behind the nitrile hydrolysis to production of the acid product.

Work done by Precigou *et al.* (2004) and Yamada and Kobayashi (1996) showed that 5 % urea functioned as a high molecular weight nitrile hydratase activator in both *R. pyridinovorans* MW3 and *R. rhodochrous* Strain J1. This however appeared to be the result of activity induction during cell cultivation. Urea was also found to function as an aliphatic amidase inhibitor in studies using *Pseudomonas aeruginosa* and *Bacillus* sp. [Gregoriou and Brown, 1979; Thalenfeld and Grossowicz, 1975]. It was in keeping with the outcome of the latter study that urea was assessed in reactions employing the DMF-induced cells to determine whether amide accumulation would occur.

Chemicals such as hydroxylamine (10 mM) (Prasad *et al.* 2009), nickel chloride (5 mM) and ascorbic acid (10 mM) have been found to inhibit some nitrile hydratase enzymes produced by *R. rhodochrous* PA-34, *R. rhodochrous* Strain J1 and *Corynebacterium* sp. C5) respectively (Prasad *et al.* 2009; Nagasawa *et al.* 1991; Tani *et al.* 1989). Incorporation of these compounds into metal-coordinating enzyme systems has been shown to have the effect of destabilizing the metal-coordination sphere and possibly abstracting the catalytic water in the enzyme's active site required for nitrile hydrolysis. A destabilization or disruption of the metal-ion complex present in nitrile hydratase would reduce acid formation or result in total loss of 3-CP hydrolysis.

Furthermore, both ascorbic acid and hydroxylamine have been previously tested against the nitrilase enzymes produced by *R. rhodochrous* PA-34 (Prasad *et al.* 2009) and *Pseudomonas putida* MTCC 5110. No inhibition was noted in these cells (Mueller *et al.* 2006).

2.9.2 Amidase Inhibition Studies

Bauer *et al.* (1998), in research utilizing *Agrobacterium tumefaciens* D3, showed that diethylphosphoramidate (DEPA) addition into biocatalytic reactions resulted in the accumulation of 2-aryl propionamide when using 2-aryl propionitrile as a substrate. Additional work done by Brady *et al.* (2004) confirmed this result. To eliminate the possibility that the activity in our current work was from a coupled nitrile hydratase/ amidase reaction, DEPA (7 mM) was added into reactions to determine whether amide accumulation would occur.

2.9.3 Nitrilase Inhibition Studies

The incorporation of nitrilase competitive inhibitors such as benzylamine as well as benzaldehyde (10 mM) was used to confirm the presence of nitrilase activity in the current systems [Stevenson *et al.* 1992]. Both compounds resemble nitrilase reaction intermediates, with benzylamine similar to the thio-imidate intermediate and benzaldehyde analogous to the thio-ester intermediate. Substrate occupancy in the nitrilase enzyme active site pocket should result in a drop in conversion rate to the acid product.

2. 10 Protein Isolation and SDS-PAGE Analysis

2.10.1 Cell Disruption

All control and induced cells were disrupted using a modified cell lysis method based on the protocol by Goncalves *et al*. (2006). Approximately 200 mg (wet weight) of the control, BNZ and DMF-induced resting cells (72 hold induced cells) were re-suspended in 2 mL TRIS buffer (0.1 M, pH 8.8). Sodium dodecyl sulfate was added to the samples to a final concentration of 2.5 % (v/v), prior to the addition of a protease inhibitor cocktail tablet into each sample [cOmplete ULTRA tablets, mini EDTA-free, Cat No: 05892791001]. Glass beads (0.5 mm glass beads, BioSpec Products, Cat No: 11079105) were added into each tube to a final volume of 5 mL, with each subjected to 5 cycles of vortexing for 1 min followed by sample storage on ice for an additional minute. Samples were finally subjected to vortexing and heating at 64°C for 10 cycles of 1 min each. The cell lysate was centrifuged (13 000 rpm, 5 min) prior to storage of the samples at -20°C. Further characterization of the cell lysate was then done by sodium dodecyl sulfate polyacrylamide gel electrophoresis (SDS-PAGE).

2.10.2 Protein Sample Denaturation

Protein samples were incubated at 70°C for 10 min in the presence of a 1 x reducing agent (Bolt ™ sample reducing buffer, Cat No: 1772696) and a 1 x loading sample buffer (Bolt ™ LDS sample loading buffer, Cat No:1772823) prior to protein separation on a commercially prepared denaturing SDS-PAGE gel.

2.10.3 SDS-PAGE Gel Profiling

Denaturing SDS-PAGE gel electrophoresis was done using the method of Laemmli (1970). All samples were loaded onto a pre-cast 4-12% PAGE gel [Bolt ™, 4-12% Bis-TRIS Plus, Cat No: NW04125] and run under constant voltage conditions (200 V) using a commercial morpholinoethanesulfonic acid buffer [Bolt™ MES buffer, Cat No: 1771547]. Electrophoresis was performed at room temperature until the loading dye had migrated to the bottom of the gel. Gel staining was done using a Coomassie B-250 stain solution. Molecular weight determination was done using the Fermentas Pst1 molecular weight marker [Thermofischer, PageRuler Plus Pre-stained Protein ladder-Thermoscientific, Cat No: 26634]. Bands of interest were excised from each of the protein gels and submitted for in-gel digestion prior to LC-MSMS sequence analysis.

2.11 Sample Preparation for Peptide Sequence Characterisation by LC-MSMS Analysis

2.11.1 In-gel Digestions

SDS-PAGE excised gel slices were diced into ~1 mm^2 fragments, with 200 µL of 50 mM NH_4HCO_3 in 50% methanol being added into each sample. The protein mix was vortexed for 20 min before discarding the supernatant. A repeat of the previous step was done to allow for adequate gel de-staining prior to the addition of 100 µL of 75% acetonitrile. The resulting sample was then vortexed for 20 min with the supernatant being discarded and the gel pieces dried under vacuum. Protein plugs were stored at -20°C prior to sample denaturation and alkylation.

Alkylation and reduction of each sample was done by following the steps described below: Approximately 25 µL of freshly prepared 10 mM dithiothreitol (DTT) prepared in 25 mM NH_4HCO_3 was added to each gel slice prior to vortexing. The protein sample was then incubated at 60°C for 1h to allow for sample denaturation and reduction before being cooled down to room temperature. Approximately 500 µL of MS grade acrylonitrile (ACN) was added to the samples, which were incubated at room temperature for a further 10 min with the supernatant being discarded. Approximately 25 µL of a 55 mM iodoacetamide solution prepared in 25 mM NH_4HCO_3 was added to the protein gel pieces before being vortexed and incubated at room temperature for another 20 min. The supernatant was discarded and the gel pieces were washed with 100 µL NH_4HCO_3 prepared in milliQ-water. The supernatant was once again discarded and the individual gel pieces dehydrated by the addition of 100 µL of a 50% ACN in 25 mM NH_4HCO_3 solution. Protein plugs were dried under vacuum and stored at -20°C until trypsin digestion was done.

Trypsin digestion of the plugs was done by incubating each protein plug with 1- 5 ng/ µL MS grade trypsin. Approximately 50 µL of 25 mM NH_4HCO_3 was added to each sample prior to incubation overnight at 37°C to facilitate protein cleavage.

Peptide extraction was carried out in protein Lo-Bind tubes [Eppendorf, Cat No: 0030108035]. Approximately 30 µL of 50% ACN/ 5% formic acid in milli-Q deionised water was added to the protein plugs with the samples being vortexed for 30 min at room temperature. All samples were centrifuged and then sonicated for 5 min prior to collection of the digest solution and vacuum drying before analysing by LCMS-MS.

2.11.2 LCMS-MS Analysis

Digests were resuspended in 20 µL, 2% acetonitrile/ 0.2% formic acid and analysed using a Dionex Ultimate 3000 RSLC system coupled to a Sciex 6600 TripleTOF mass spectrometer. Peptides were first de-salted on an Acclaim PepMap C18 trap column (100 µm x 2 cm) for 2 min at 15 µL/ min using 2% acetonitrile/ 0.2% formic acid, than separated on Acclain Pepmap C18 RSLC column (300 µm x 15 cm, 2 µm particle size). Peptide elution was achieved using a flow-rate of 8 µL/ min with a gradient of 4-60% B in 15 min (A: 0.1% formic acid; B: 80% acetonitrile/ 0.1% formic acid). An electrospray

voltage of 5.5 kV was applied to the emitter. The 6600 TripleTOF mass spectrometer was operated in Data Dependant Acquisition mode. Precursor MS scans were acquired from *m/z* 400- 1500 using an accumulation time of 250 ms followed by 30 MSMS scans, acquired from *m/z* 100- 1800 at 100 ms each, for a total scan of 3.3 sec. Multiply charged ions (2+, 5+, 400- 1500 *m/z*) were automatically fragmented in Q2 collision cells using nitrogen as the collision gas. Collision energies were chosen automatically as a function of *m/z* and charge.

Protein pilot v5.01.10 using Paragom search engine (Sciex) was used for comparison of the obtained MS/MS spectra against protein sequences in a Uniprot Swissprot 2016 database. Proteins with threshold above ≥ 99.9% confidence were reported. Peptides with ≥95% confidence were used to report sequence coverage.

3 Results

This study explored the induction and characterization of nitrile hydrolysing enzymes belonging to the species *Rhodococcus rhodochrous*, namely ATCC BAA-870 and strain A99, as well as to a closely related organism *Pimelobacter simplex* strain A99. This was achieved using peptide sequencing, molecular analysis, biocatalytic profiling, and inhibition studies.

3.1 ATCC BAA-870, strain A29 and A99 Induction Time Studies

Biotransformation reactions using resting cells of the control and induced cells of ATCC BAA-870, strain A29, and strain A99 when reacted with 3-CP showed the following reaction profiles (**Fig. 2**):

1) The control cells of strain ATCC BAA-870 showed both amide and acid formation (green bars) in the reaction sample, with nitrile persistence in all day one samples (blue bars). Control cells of both strain A29 and A99 showed no nicotinic acid production, with low levels of amide detected (red bars).
2) The BNZ-induced cells of ATCC BAA-870 mirrored the effects noted in the control cells, with a mixed amide and acid product observed. Meanwhile, BNZ-induced resting cells of strain A29 and A99 showed slight nicotinamide accumulation when compared to the control cells (24h old induced cells). This is likely to be the result of BNZ inclusion during cultivation. This transient effect on nitrile hydratase activity was lost in the later samples, as determined by LC-MSMS analysis.
3) All DMF-induced resting cells harvested after 24, 48 and 72 h induction in minimal media showed complete hydrolysis of 3-CP, with only nicotinic acid having been formed.

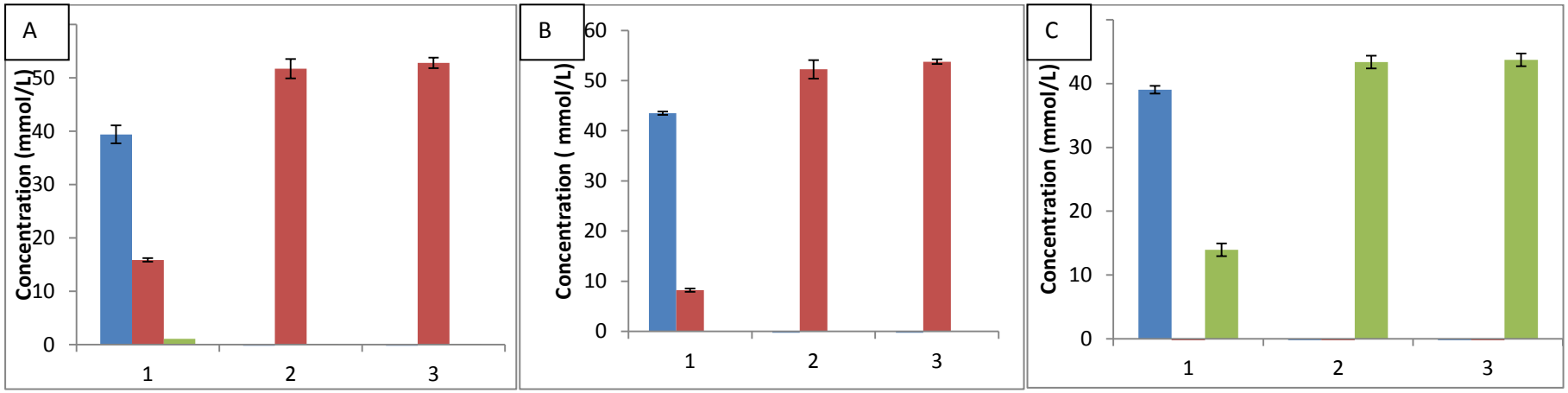


Figure 2: Strain ATCC BAA-870; 3-CP Bio-catalytic reaction data.

A- Control; B- BNZ-induced cells; C- DMF-induced cells.

A29 Cells induced in mmol/L were harvested at 0 h (sample 1), 48 h (sample 2), and 72 h (sample 3) respectively with 100 mg of cells used in each reaction performed. All biotransformation reactions were carried out in the presence of 40 mmol/L 3-CP with incubation at 28°C with agitation. 3-CP levels in the samples are shown in blue; nicotinamide levels are in red; while nicotinic acid levels are shown in green.

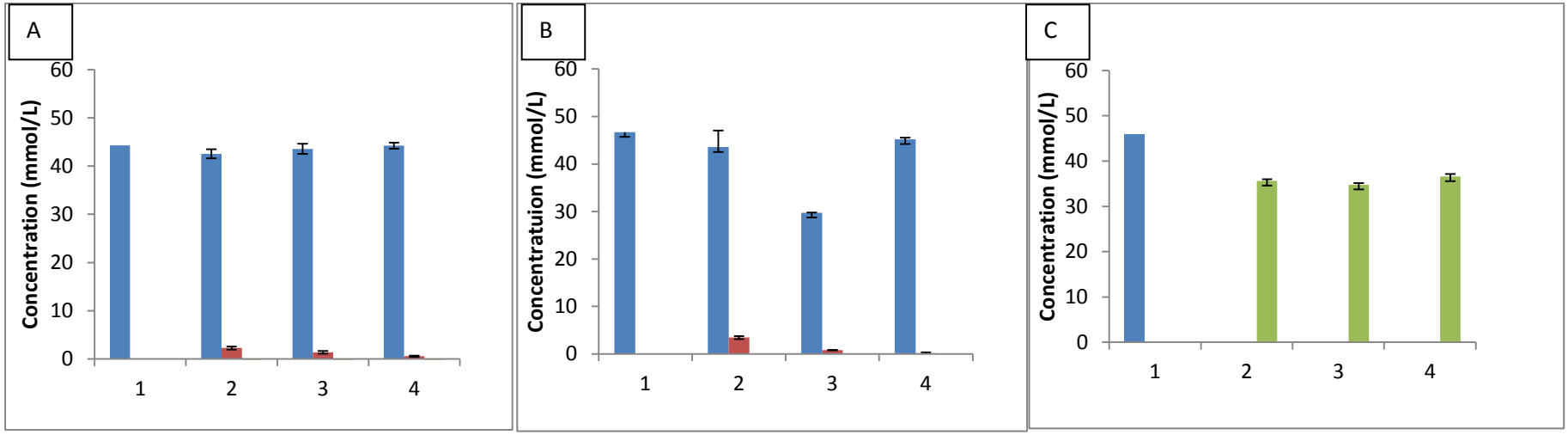


Figure 3: Strain A29; 3-CP Bio-catalytic reaction data.

A- Control; B- BNZ-induced cells; C- DMF induced cells.

A29 Cells induced in mmol/L were harvested at 0 h (sample 1), 24 h (sample 2), 48 h (sample 3), and 72 h (sample 4) respectively with 100 mg of cells used in each reaction performed. All biotransformation reactions were carried out in the presence of 40 mmol/L 3-CP with incubation at 28°C with agitation. 3-CP levels in the samples are shown in blue; nicotinamide levels are in red; while nicotinic acid levels are shown in green.

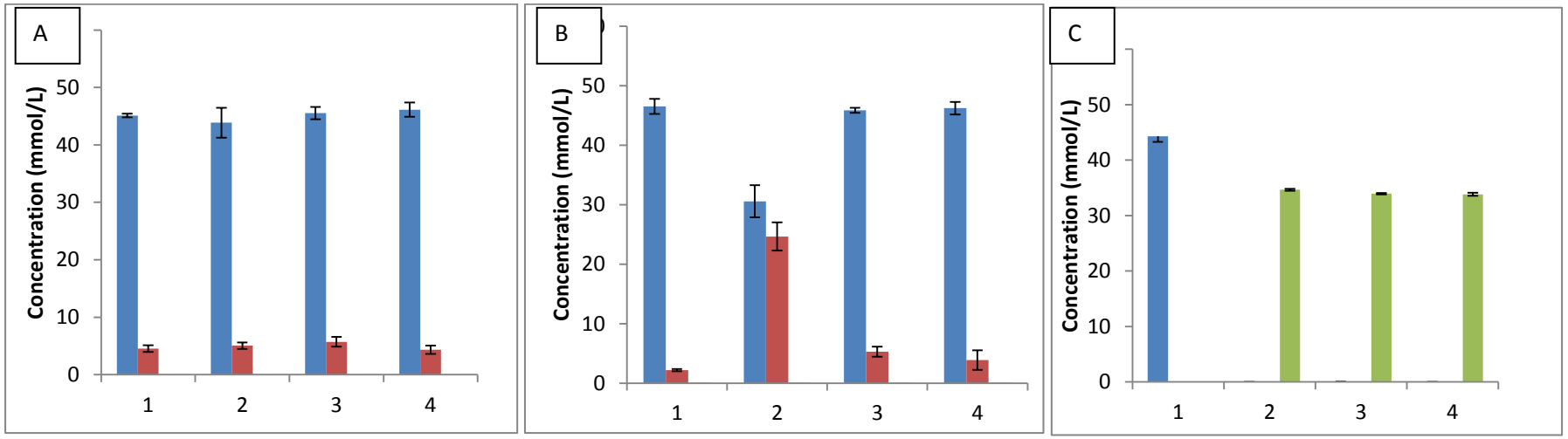


Figure 4: Strain A99; 3-CP Bio-catalytic reaction data.

A- Control; B- BNZ-induced cells; C- DMF-induced cells.

A99 Cells induced in mmol/L were harvested at 0 minutes (sample 1); 24 h (sample 2); 48 h (sample 3); and 72 h respectively (sample 4) with 100 mg of cells used in each reaction. 3-CP levels in the samples are shown in blue; nicotinamide levels are in red; while nicotinic acid levels are shown in green. All the biotransformation reactions were carried out in the presence of 40 mmol/L 3-CP with incubation at 28°C with agitation.

3.2 Ultra Performance Liquid Chromatography- Mass Spectrometry Data (UPLC-MS)

UPLC-MS data evaluation of the DMF-induced cells of strain A29 and A99 showed complete conversion of 3-CP (elution time 6.47 min- peak highlighted in blue) to nicotinic acid (elution time 1.61-1.62 min- peak highlighted in green) when samples were analyzed in ESI^+ mode. The same strains when cultured in the presence of 5 mmol/L BNZ or in the absence of any chemical activators were found to be less reactive, with 3-CP persistence observed in these samples (**Fig. 5**).

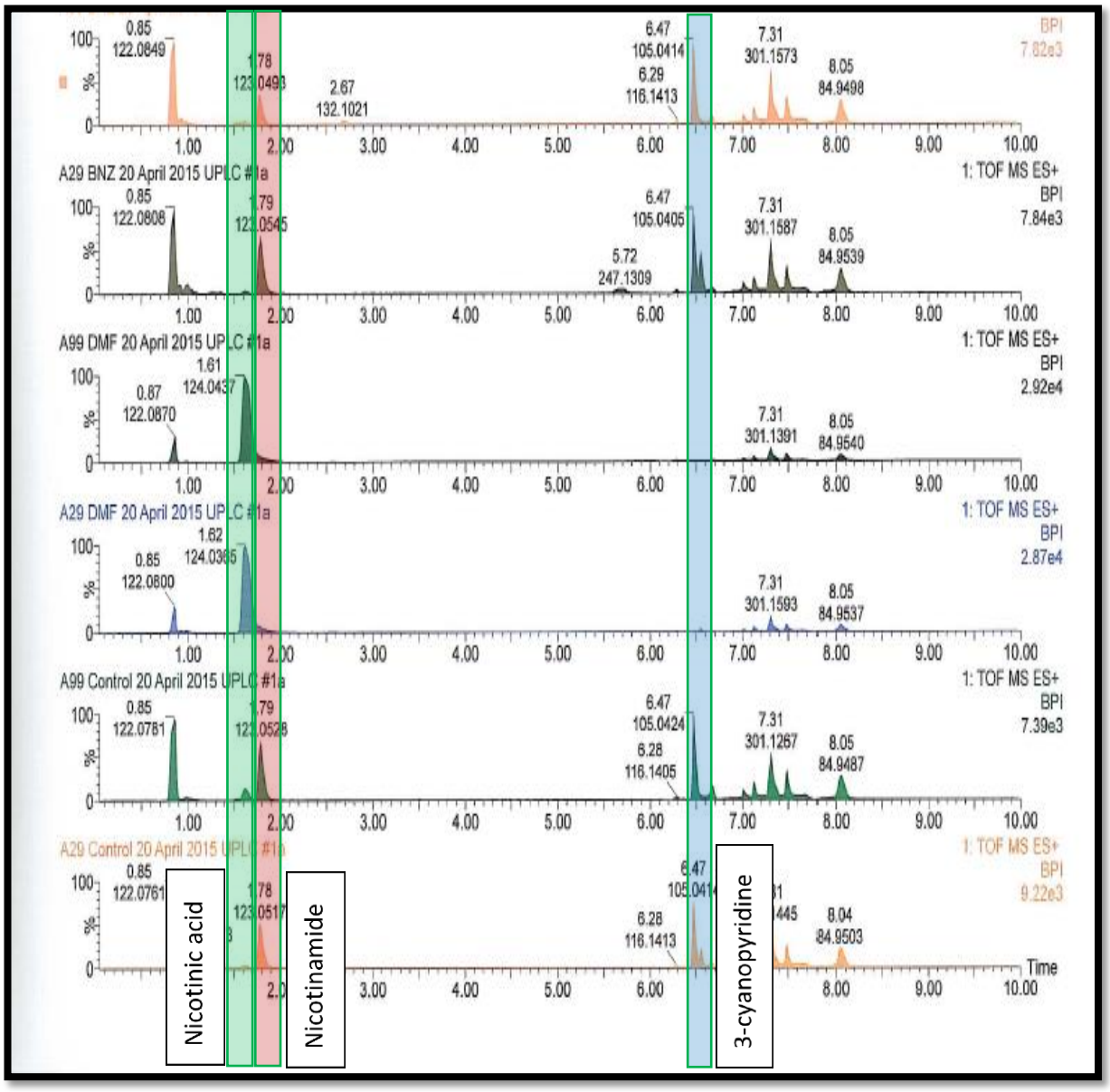


Figure 5: UPLC-MS data (in ESI^{+ve} mode) showing complete conversion of 3-CP to nicotinic acid (elution time 1.61-1.62 min) by DMF-induced cells of strain A29 and A99.

Chromatogram 1: A99 BNZ-induced cell reactions; chromatogram 2: A29 BNZ-induced cell reaction; chromatogram 3: A99 DMF-induced cell reaction; chromatogram 4: A29 DMF-induced cell reaction: chromatogram 5: A99 non-induced cell reaction; and chromatogram 6: A29 non-induced cell reaction. Both cell lines when cultured in the absence of any inducer or when induced in the presence of 5 mmol/L BNZ showed nitrile persistence (3-CP eluted at 6.47 min) as well as slight amide production (nicotinamide eluted at 1.78-1.79 min). Negligible acid levels were noted in these reactions. Regions highlighted in blue serve to highlight the 3-cyanopyridine present in the sample: those highlighted in red indicate nicotinamide presence; while those highlighted in green show nicotinic acid.

3.3 Biocatalytic Synthesis of Nicotinic Acid

Aqueous samples prepared from the individual scaled-up biocatalytic experiments were subjected to ethyl acetate extraction to remove residual 3-CP and nicotinamide present in the sample. Nicotinic acid recovery was then carried out on the remaining aqueous phase. **Table 1** shows the isolated nitrile, amide and acid yields for each reaction.

The DMF-induced cell pastes of ATCC BAA-870, strain A29 and A99 showed complete conversion of 3-CP to generate: I) nicotinamide and nicotinic acid in the ATCC BAA-870 reactions; and II) nicotinic acid as a sole product in strains A29 and A99. The high variability in the overall nicotinic acid yields observed in strains A29 and A99 (58- 79.8%) are the result of high product loss incurred during *n*-butanol extractions.

Both the control and the BNZ-induced cells of strain A29 and A99 showed nitrile persistence (70-80%) with no amide or acid production observed, while strain ATCC BAA-870 control and BNZ-induced cells showed nitrile persistence and amide formation (product verification can be done by correlating data to the ^{1}H and ^{13}C NMR data obtained for these strains- see **Section 2.5**).

Table 1: 3-Cyanopyridine Control versus Induced cell reaction yields

Reactions were carried out using 200 mg (wet weight) of the 72 h old induced resting cells. Reaction samples contained 75 mg 3-CP solubilized in methanol with reactions performed in a TRIS buffer system (50 mM, pH 9.0). All samples were incubated for 15 min at 28°C with agitation.

Sample Description	(% Isolated yield)			% Conversion (based on residual nitrile levels)	Implied enzyme system responsible
	Residual 3-CP	Amide	Acid		
ATCC BAA-870 control cells	13.3	68.2	0	~87	Nitrile hydratase
A29 Control cells	75	0	0	0	None
A99 Control cells	80	0	0	0	None
ATCC BAA-870 BNZ-induced cells	32	49	0	~70	Nitrile hydratase
A29 BNZ-induced cells	74	0	0	0	None
A99 BNZ-induced cells	82	0	0	0	None
ATCC BAA-870 DMF-induced cells	0	22	38	100	Nitrile hydratase/ amidase Nitrilase
A29 DMF-induced cells	0	0	80	100	Nitrilase
A99 DMF-induced cells	0	0	58	100	Nitrilase

3.4 Nitrilase Stereoselective Conversion of β-Aminonitriles

Enantioselectivity data obtained using DMF induced cells of strain A29 and A99 reacted in the presence of 3-amino-3-phenylpropanenitrile and 3-amino-3-(4-methoxyphenyl) propanenitrile showed kinetic resolution of these substrates. Excellent selectivity was observed when cells were reacted with the former substrate (>99% *ee*), while moderate selectivity was found in the case of the latter substrate (**Table 2**).

Table 2: Enantioselectivity of nitrilase on β-amino substrates

Strain	Experimental condition	Nitrile Substrate*	Reaction time (hrs)	Peak area Nitrile enantiomer 1	Elution time	Peak area Nitrile enantiomer 2	Elution time	Nitrile Conversion	(S)-Nitrile[#] % ee(s)	E
A29	Control	PAN	0	36988.00	12.98	36325.20	14.80	44.17	0.90	0
A29	Control	PAN	4	32682.20	12.94	32221.90	14.77	49.46	0.71	1.13
A29	Control	PAN	24	31681.80	12.93	29196.70	14.75	45.42	4.08	1.60
A29	DMF induced	PAN	0	30748.40	12.95	25496.00	14.78	40.34	9.34	2.12
A29	DMF induced	PAN	4	30088.90	12.94	13287.50	14.79	51.85	38.73	5.34
A29	DMF induced	PAN	24	5239.00	12.98	0.00	14.79	31.07	>99	4.92
A29	Control	Methoxy	0	9172.00	17.37	8620.76	21.49	39.08	3.10	1.05
A29	Control	Methoxy	4	7590.46	17.35	7429.18	21.47	41.48	1.07	1.01
A29	Control	Methoxy	24	6210.87	17.34	6523.31	21.49	37.00	-2.45	0.97
A29	DMF induced	Methoxy	0	7574.57	17.44	7287.01	21.54	23.69	1.94	1.02
A29	DMF induced	Methoxy	4	7188.35	17.36	6696.25	25.36	27.23	3.54	1.04
A29	DMF induced	Methoxy	24	5978.07	17.34	2929.98	21.52	28.04	34.22	1.40
A99	Control	PAN	0	43075.30	12.95	42931.10	14.77	47.29	0.17	0.98
A99	Control	PAN	4	36461.60	12.94	36672.90	14.75	48.48	-0.29	2.53
A99	Control	PAN	24	35096.10	12.93	34376.70	14.75	48.73	1.04	1.60
A99	DMF induced	PAN	0	32678.80	12.92	30340.90	14.74	40.59	3.71	1.70
A99	DMF induced	PAN	4	29463.30	12.91	20868.90	14.73	47.72	17.08	2.65
A99	DMF induced	PAN	24	12127.00	12.94	0.00	14.73	52.60	>99	7.92
A99	Control	Methoxy	0	7391.26	17.27	7659.00	21.47	40.37	-1.78	0.98
A99	Control	Methoxy	4	7549.75	17.22	7223.00	21.46	43.47	2.21	1.03
A99	Control	Methoxy	24	5523.11	17.34	6199.23	21.52	29.76	-5.77	0.94
A99	DMF induced	Methoxy	0	5423.41	17.37	5367.92	21.51	23.20	0.51	1.01
A99	DMF induced	Methoxy	4	13090.50	17.26	12175.00	21.45	24.28	3.62	1.07
A99	DMF induced	Methoxy	24	2598.35	17.48	1092.50	21.57	15.26	40.80	1.33

*PAN: 3-amino-3-phenylpropanenitrile; Methoxy: 3-amino-3-(4-methoxyphenyl)propanenitrile. # Assigned according to the previously determined (*R*)-acid generated from this substrate by the same strains.

3.5 Nitrile Degrading Enzyme Inhibitor Studies

The enzyme system responsible for the observed activity profiles noted could not be definitively determined by the reaction product profile observed. In an attempt to further characterize the responsible enzymes, a number of nitrilase, nitrile hydratase as well as amidase inhibitors were tested to determine the nature of the activity driving acid formation in the DMF-induced cells (**Table 3**).

Urea inclusion into the individual cell reactions showed low levels of activity reduction in strain A29, A99 (11.2 and 3.1% respectively) and ATCC BAA-870 (4.9%). The loss in activity observed could be the result of an increased solubilization of non-polar side chains on the enzyme; resulting from the weakening of hydrophobic interactions present on the enzyme (Zangi *et al.* 2009).

Cobalt containing nitrile hydratase enzymes all demonstrate a conserved catalytic motif, "**C**TL**C**S**C**" which contains an oxidised thiol group- Cys111 sulfinic acid [Cys-SO_2H]; Cys113 (sulfenic group [Cys-SOH]) and a native Cys108 thiol group (amino acid residue annotation based on crystal structure sequence obtained from *Pseudonocardia thermophilia*, 1IRE) (Miyanaga *et al.* 2001). These sulfur containing residues are all necessary for stabilizing a non-corrinoid low-spin cobalt ion crucial for substrate hydrolysis.

Nickel incorporation into metal-mediated enzyme complexes such as those found in nitrile hydratase enzymes could result in displacement of the cobalt ion present in the metal-coordination sphere. This in turn would affect the overall energy reaction profile of the metal-coordinated enzyme. Cobalt (III) ion replacement by nickel (II) ions may alter activity by changing the substrate conversion activation barrier required. An important observation in this study was that the most significant loss in activity was observed in ATCC BAA-870 induced cells when they were incubated in the presence of nickel chloride (12%).

The addition of hydroxylamine, a strong nucleophile, resulted in activity loss once again in ATCC BAA-870 induced cells (12%), but showed little to no effect on the remaining two induced cell lines.

Ascorbic acid can take up the equivalent of at least 3 atoms of oxygen through the course of its oxidation. This is done via three steps yielding dehydroascorbic acid and 2,3-diketo-[-gluonic acid as products (Borsook *et al.* 1937). Incorporation of ascorbic acid into reaction samples resulted in an 18% loss in enzyme activity in ATCC BAA-870, and a 4-5% loss in activity in strain A99 and A29 respectively. This could be the result of the abstraction of a catalytic water molecule located in the active site of the enzyme, or the result of the reduction of crucial cysteine residues required for catalytic activity.

Nicotinic acid levels in DMF-induced cell reactions of strain A29 and A99 were considerably reduced when reactions were carried out in the presence of benzaldehyde and benzylamine. This concurred with the data documented by Stevenson *et al*. (1992) who noted a 65% loss of nitrilase activity in the

presence of 10 mM benzylamine and nearly complete inhibition in the presence of 10 mM benzaldehyde in reactions using *Rhodococcus* ATCC-39484. In our studies we observed a 61.4% - 79.5% loss in nitrile degrading activity in the presence of benzylamine, and an 88.4% - 87.5% loss in activity in the presence of benzaldehyde in strain A29 and A99 cells, respectively (**Fig. 6**).

Table 3: Residual nitrilase activity levels of DMF-induced ATCC BAA-870, strain A29 and A99 cells in the presence of various inhibitor molecules.

Reactions were carried out using 20 mM 3-CP as substrate with 100 mg of the DMF-induced resting cells of ATCC BAA-870, strain A29 and A99 used in each reaction. Relative percentages shown below are based on HPLC data demonstrating 3-CP conversion to nicotinic acid in control versus treated samples. Control data was set at 100%.

Organism	**Control* (% activity)**	**Nitrile hydratase inhibitors (% activity)**			**Amidase inhibitor (% activity)**		**Nitrilase inhibitors (% activity)**	
		Ascorbic Acid	**Hydroxyl-amine**	**$NiCl_2$**	**Urea**	**DEPA**	**Benzamine**	**Benzaldehyde**
ATCC BAA-870	100	**84.0**	**88.0**	**88.0**	95.1	100	98.5	100
Strain A29	100	94.7	94.0	96.7	**88.8**	96.8	**38.6**	**11.6**
Strain A99	100	96.9	100	96.9	96.9	100	**20.5**	**12.5**

- Control cells are DMF cells in the absence of any inhibitor molecule

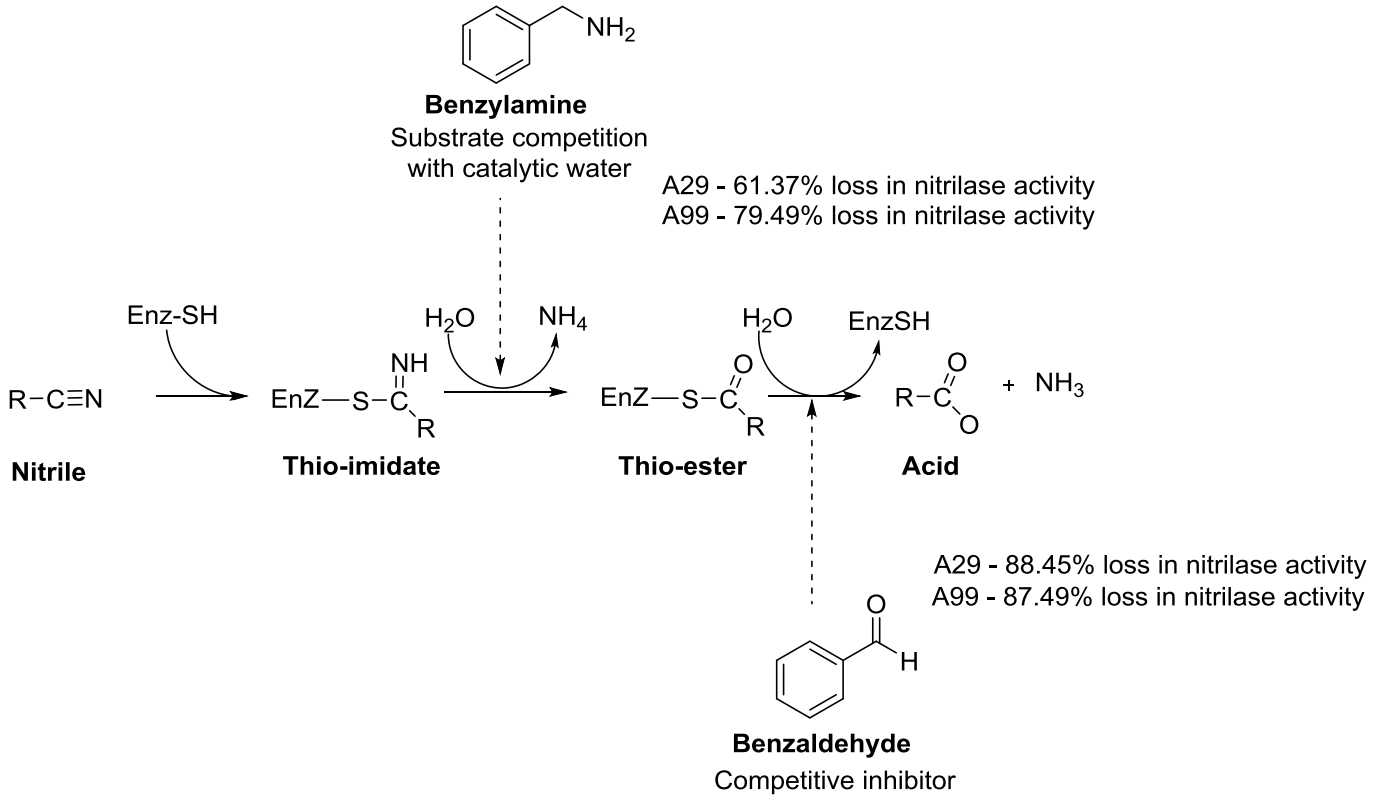


Figure 6: Benzaldehyde and benzylamine competitive inhibition of nitrilase activity in strain A29 and A99.

The Need for Additional Enzyme Characterization Studies

Inhibition studies undertaken on the DMF-induced cells suggests that the nitrile degrading activity of strain A29 and A99 is most likely the result of an induced nitrilase enzyme. However, ATCC BAA-870 showed conflicting results, with the highest loss in nitrile activity observed in the presence of ascorbic acid, hydroxylamine and nickel chloride. In addition little or no effect was noted when the resting cells were exposed to benzylamine and benzaldehyde, contrary to accepted theory on nitrilase enzymatic mechanisms. This when coupled with the isolation of a mixed amide and acid product from the DMF-induced cells of strain ATCC BAA-870, suggested that the nicotinic acid observed could be the result of the interplay of multiple nitrile degrading enzyme systems.

Additional profiling of each of the protein fractions was therefore undertaken to confirm this with LC-MSMS peptide characterisation studies.

3.6 SDS-PAGE electrophoresis and LCMS-MS Analysis

SDS-PAGE protein profiling studies were done on strains ATCC BAA-870, A29 and A99 for control, BNZ and DMF-induced cells. **Fig. 7A** shows strain ATCC BAA-870 control (lane 7-8), BNZ-induced (lane 9-10) and DMF-induced cells (lane 11-12). A BSA standard curve (100 ng- 800 ng/10 µL: lane 2-6) was used for quantification purposes. A dominant ~40 kDa size protein was visible in the DMF-induced cells, which when quantified contributed to 12% of the total soluble protein present in the sample.

SDS-PAGE protein profiling of strain A29 control (lane 2-3), BNZ-induced (lane 4-5) and DMF-induced cells (lane 6-7) are shown in Fig.**7B**. Once again a distinct difference in the protein banding pattern was observed in the DMF-induced cell sample. A dominant protein band corresponding to ~40 kDa was found in the DMF-induced protein sample (lane 6 and 7) which contributed to 12% of the total soluble protein in the sample. The control and BNZ-induced cells showed similar banding characteristics to each other with dominant bands noted at ~65 kDa, ~55 kDa, ~35 kDa, and ~25 kDa, but nothing at ~40 kDa.

Meanwhile, SDS-PAGE protein profiles for *P. simplex* strain A99 cells showed a significant ~40 kDa protein band in the DMF-induced cells, corresponding to 11% of the total soluble protein in the sample (**Fig. 7C**). Samples prepared showed considerable protein degradation with only faint bands discernible even after cell lysis in the presence of a protease inhibitor cocktail sample. Further inspection on the MEROPS website showed that *P. simplex* cells produce an array of proteases with ~82 varied known and putative proteolytic enzymes identified in this one strain (MEROPS the Peptidase Database – EMBL-EBI 2017). Protein bands correlating to ~100 kDa, ~ 70 kDa, 55 kDa and ~25 kDa (based on previous protein sample data obtained from strains A29 and ATCC BAA-870) were excised and submitted for LC-MSMS analysis.

Nitrilase peptide fragments corresponding to Uniprot Q-03217 were found in the DMF-induced cells of all three strains evaluated, with no nitrilase fragments being found in any of the control or BNZ-

induced cells (MS-derived proteomics analysis done using Peptide shaker- Compomics) (Vaudel *et al.* 2015) . The nitrilase protein size determined for *R. rhodochrous* was ~40 kDa and corresponded well with the nitrilase protein fragment data identified by LC-MSMS amino acid sequencing. The protein fragment data showed 100% sequence identity to an aliphatic nitrilase protein produced by *R. rhodochrous* J1 Q-03217 with 36.1% of protein coverage observed in ATCC BAA-870; 92.62% of the total sequence coverage located in the A29; and finally 35.3% sequence coverage identified in the strain A99 sample (maximum sequence coverage located in the ~40 kDa fragment in all DMF-induced samples analyzed) (**Fig. 8**). The core Cys-Lys-Glu catalytic residues in **Fig. 8** are highlighted in green, while all residues highlighted in blue serving to identify amino acids that line the surface of the catalytic cleft. Regions highlighted in magenta are located at the “D” surface interface; while those in yellow sit at the “A” interface, facilitating enzyme dimerization. Amino acid residues in black are fragments located by LC-MSMS analysis.

A constitutive low molecular weight nitrile hydratase, enzyme was observed in the control, BNZ-induced and DMF-induced protein samples prepared from ATCC BAA-870 cells (**Fig. 9**). A nitrile hydratase alpha subunit was identified showing maximum sequence coverage in the ~35 kDa fragment analyzed. Sequence analysis suggested that the fragments were 100% identical to Uniprot P-29378 with 24.15% of protein sequence coverage observed. The core cysteine residues located in the signature CTLCSC amino acid sequence of the protein are highlighted in green in **Fig. 9**, with all LC-MSMS residues fragments located shown in black.

An amidase enzyme was also identified in the control and BNZ-induced cells of ATCC BAA-870 (**Fig. 10**), with maximum coverage located in the 100 kDa fragment sample prepared (P-84650-enantioselective amidase from *R. rhodochrous*, 100% sequence similarity, 6% sequence coverage). Once again, all LC-MSMS identified fragments are shown in black in **Fig. 10**. Fragments of this enzyme were not found present in the DMF-induced cells of this strain.

No nitrile hydratase or amidase protein sequence fragments were located in any of the strain A29 and A99 samples, suggesting the inducible nature of this enzyme in these strains.

An array of transcription and translational proteins were found present in the DMF-induced cells. These include both the 30s and 50s ribosomal proteins crucial for protein translation; DNA-directed RNA polymerase; various elongation factors (EF-U, EF-G as well as EF-Ts); as well as numerous 60 kDa chaperonin proteins. One of the chaperonin peptides identified located in all three strains was Uniprot Q-2JA12 (**Fig. 11**) which showed high amino acid sequence similarity to Uniprot O50305 (GroEL 60 kDa chaperonin protein from *Bacillus halodurans*). In **Fig. 11,** the amino acid sequence highlighted draws to attention the highly conserved helix-turn helix region on the protein.

The energy requirements of the cell appear to be provided for by an array of enzymes producing Krebs cycle intermediates. Tight cellular control may be provided by the adenylate kinase located within these samples (**COZW47-** *R. erythropolis***)** that plays an important regulatory role in cells, catalyzing the transfer of terminal phosphates between ATP and AMP.

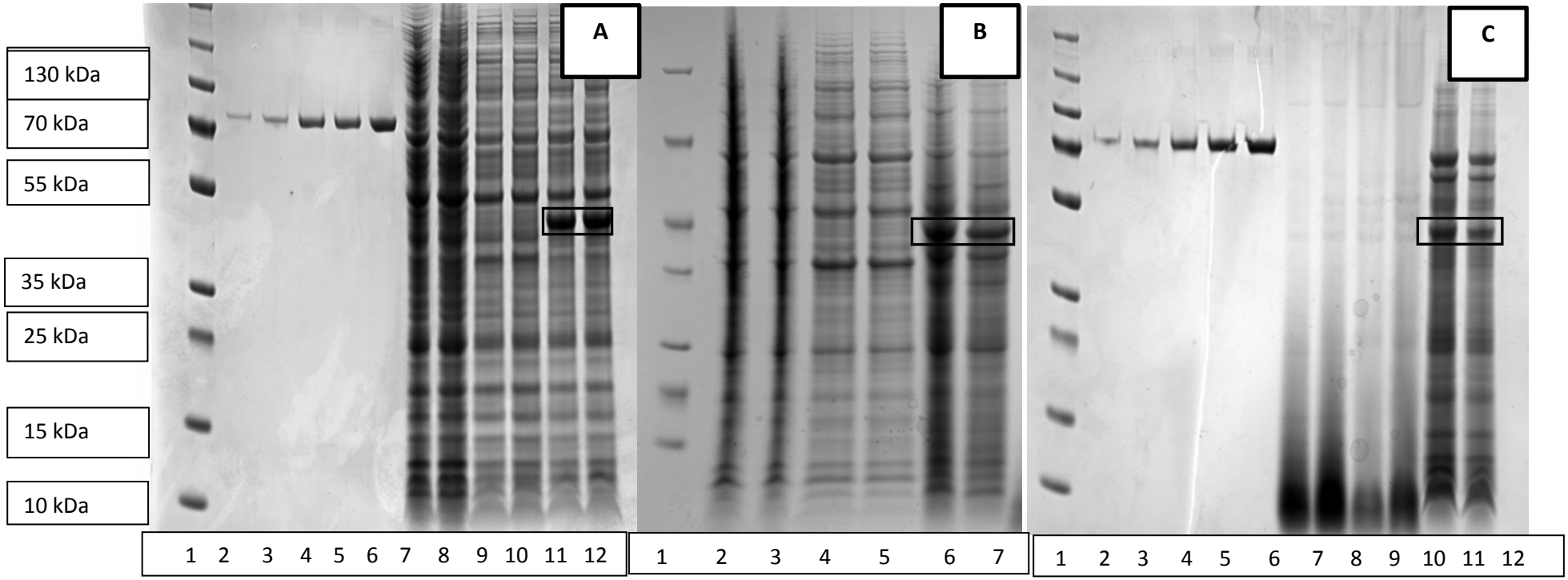


Figure 7: SDS-PAGE gel of protein soluble fraction from induced and non-induced cells.

ATCC BAA-870 (A): Lane 1- PageRuler Plus Prestained Protein ladder- Thermoscientific, Cat No- 26634; lane 3-6, BSA standard curve 100 - 500 ng protein. Lane 7-8, ATCC BAA-870 control cell sample; lane 9-10, ATCC BAA-870 BNZ-nduced cell sample; lane 11-12, ATCC BAA-870 DMF-induced cell sample. Strain A29 (B): Lane 2 -3, A29 control cell sample; lane 4 - 5, A29 BNZ-induced cell sample; lane 6 - 7, DMF-induced cell sample. Strain A99 (C): Lane 1: PageRuler Plus Prestained Protein ladder- Thermoscientific, Cat No: 26634 ; Lane 2-6, BSA standard cuve, 100 µg/ 10 µL -800 µg/ µL); Lane 7-8, A99 control cell sample; lane 9-10, A99 BNZ-induced cell sample; lane 11-12, DMF-induced cell sample. Samples were run on a 4-12% gradient SDS gel (LTC scientific, Bolt^{TM}) with each sample undergoing denaturation in the presence of a reducing agent at 70°C for 10 min prior to loading onto the gel. SDS gels were run under constant voltage at 200 V with gel staining being done using Coomassie blue stain (method of Laemmli).

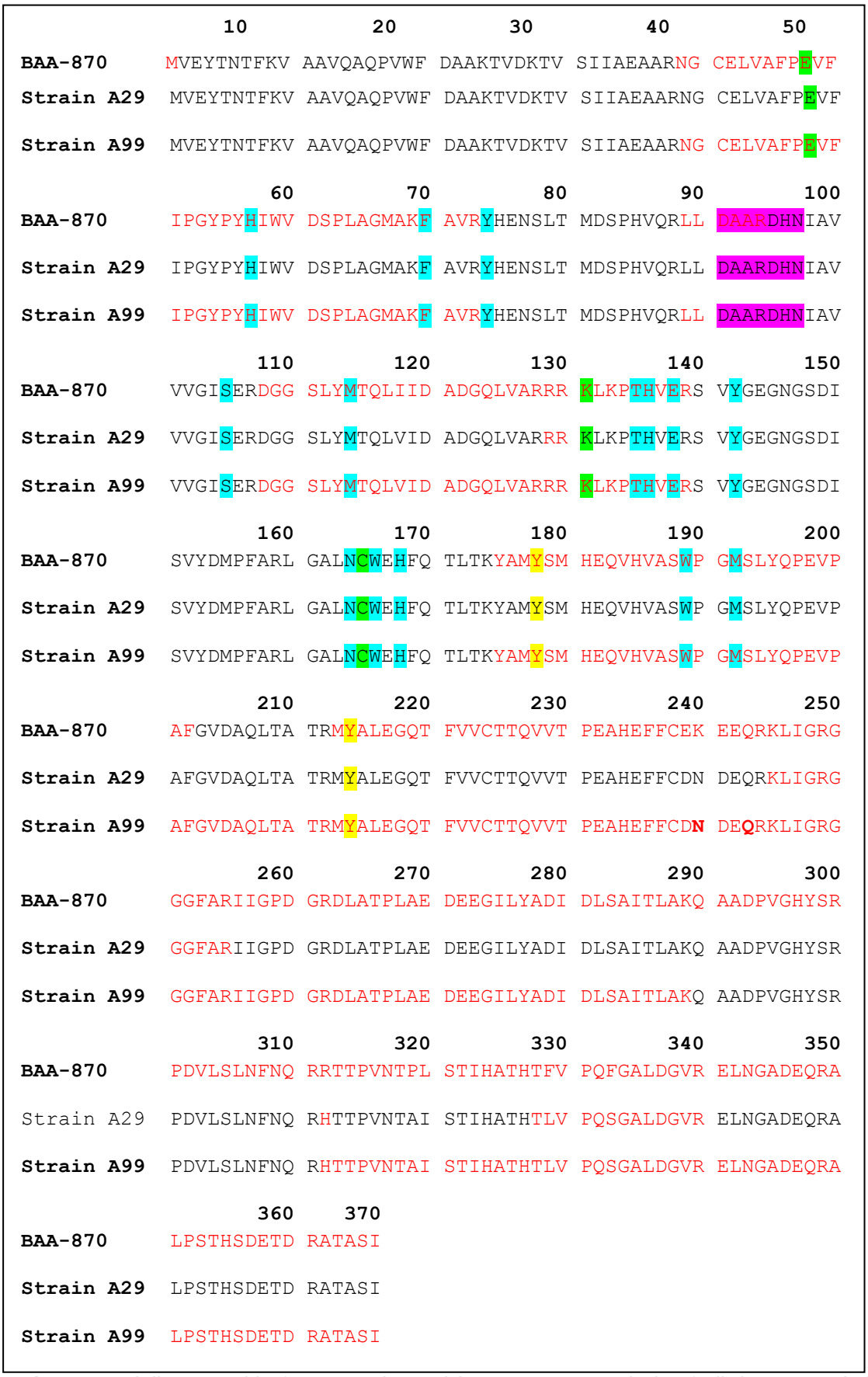


Figure 8: Nitrilase peptide fragments located by LCMS-MS analysis of all three DMF-induced cell samples.

ATCC BAA-870, A29 and A99 matched to Q03217 with 35.9%, 93% and 35.3% sequence coverage respectively, obtained using peptides with ≥ 95% confidence. Residues highlighted in green make up the core catalytic triad; residues highlighted in blue line the surface of the catalytic cleft; residues highlighted in magenta correlate to residues found at the "D" surface interface; residues highlighted in yellow are located at the "A" interface and are involved in enzyme dimerization. Finally residues highlighted in black show all amino acid fragments located through LC-MSMS analysis studies undertaken.

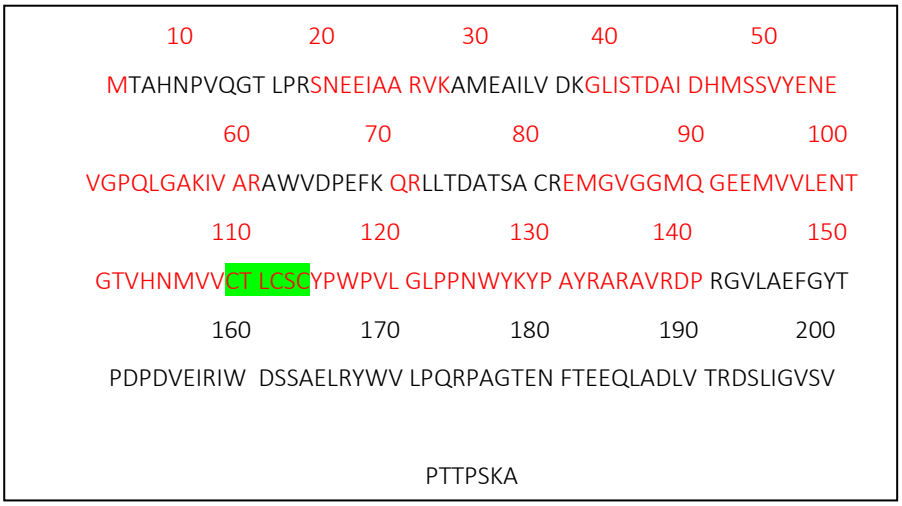


Figure 9: ATCC BAA-870 low molecular weight nitrile hydratase α-subunit peptide fragments identified from LCMS-MS studies undertaken (Uniprot P-29378)

Residues in black show fragments located in LC-MSMS studies done (106/207 amino acid residues located)- 100% sequence identity with a 51.2% amino acid sequence coverage). The area highlighted in green shows Cys109, Cys112, and Cys 114; the three cysteine residues involved in the formation and maintenance of the metal (III) coordination sphere.

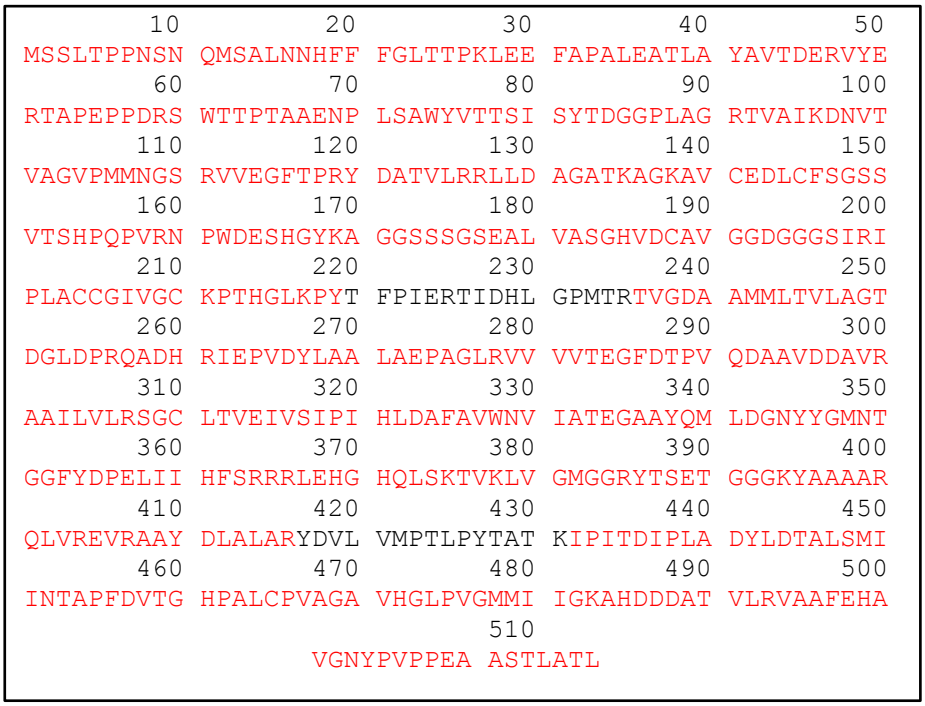


Figure 10: ATCC BAA-870 Amidase peptide fragments located from LC-MSMS analysis.

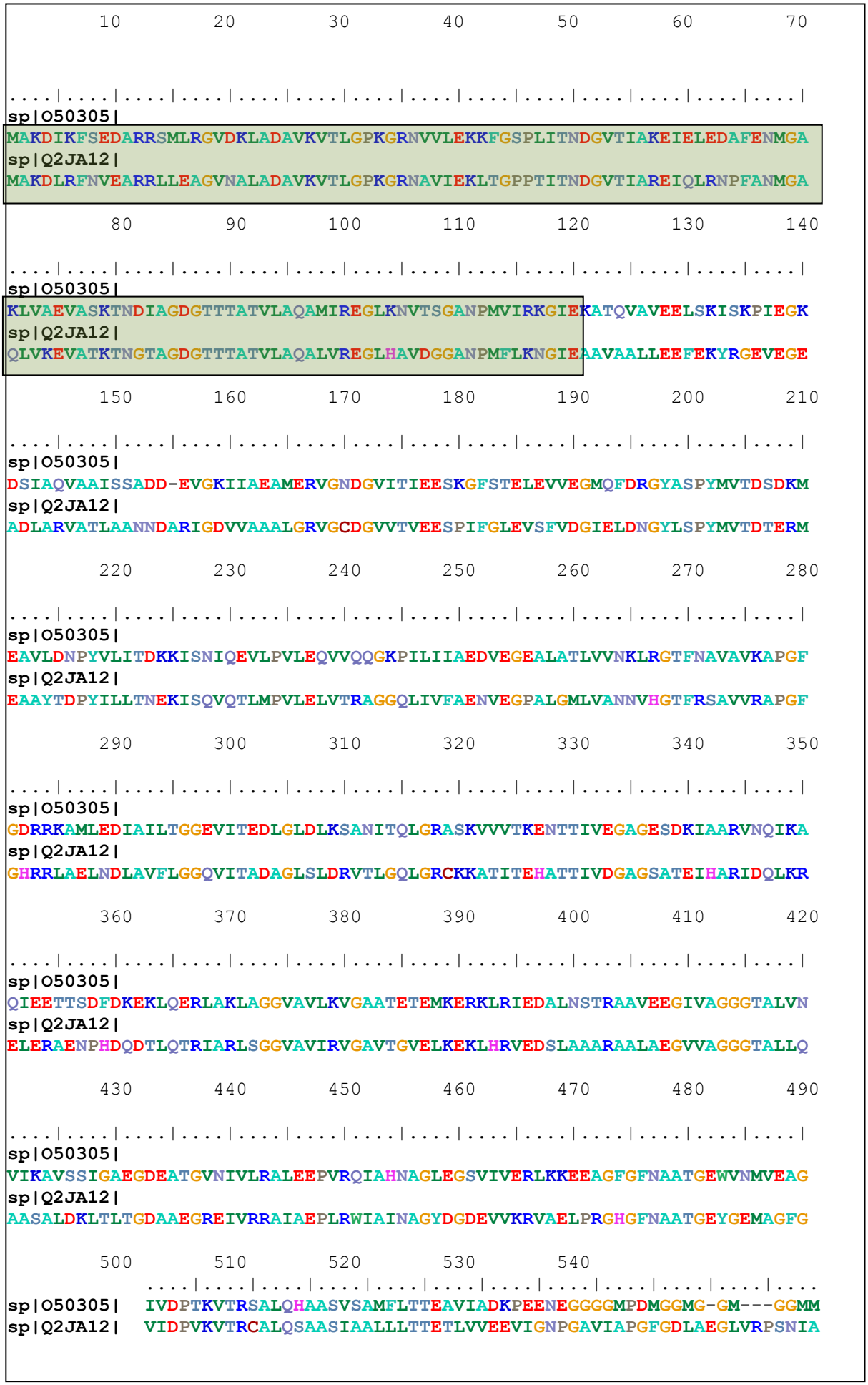

10 20 30 40 50 60 70
sp|O50305|
MAKDIKFSEDARRSMLRGVDKLADAVKVTLGPKGRNVVLEKKFGSPLITNDGVTIAKEIELEDAFENMGA
sp|Q2JA12|
MAKDLRFNVEAARRLLEAGVNALADAVKVTLGPKGRNAVIEKLTGPPTITNDGVTIAREIQLRNPFANMGA
80 90 100 110 120 130 140
sp|O50305|
KLVAEVASKTNDIAGDGTTTATVLAQAMIREGLKNVTSGANPMVIRKGIEKATQVAVEELSKISKPIEGK
sp|Q2JA12|
QLVKEVATKTNGTAGDGTTTATVLAQALVREGLHAVDGGANPMFLKNGIEAAVAALLEEFEKYRGEVEGE
150 160 170 180 190 200 210
sp|O50305|
DSIAQVAAISSADD-EVGKIIAEAMERVGNDGVITIEESKGFSTELEVVEGMQFDRGYASPYMVTDSDKM
sp|Q2JA12|
ADLARVATLAANNDARIGDVVAAALGRVGCDGVVTVEESPIFGLEVSFVDGIELDNGYLSPYMVTDTERM
220 230 240 250 260 270 280
sp|O50305|
EAVLDNPYVLITDKKISNIQEVLPVLEQVVQQGKPILIIAEDVEGEALATLVVNKLRGTFNAVAVKAPGF
sp|Q2JA12|
EAAYTDPYILLTNEKISQVQTLMPVLELVTRAGGQLIVFAENVEGPALGMLVANNVHGTFRSAVVRAPGF
290 300 310 320 330 340 350
sp|O50305|
GDRRKAMLEDIAILTGGEVITEDLGLDLKSANITQLGRASKVVVTKENTTIVEGAGESDKIAARVNQIKA
sp|Q2JA12|
GHRRLAELNDLAVFLGGQVITADAGLSLDRVTLGQLGRCKKATITEHATTIVDGAGSATEIHARIDQLKR
360 370 380 390 400 410 420
sp|O50305|
QIEETTSDFDKEKLQERLAKLAGGVAVLKVGAATETEMKERKLRIEDALNSTRAAVEEGIVAGGGTALVN
sp|Q2JA12|
ELERAENPHDQDTLQTRIARLSGGVAVIRVGAVTGVELKEKLHRVEDSLAAARAALAEGVVAGGGTALLQ
430 440 450 460 470 480 490
sp|O50305|
VIKAVSSIGAEGDEATGVNIVLRALEEPVRQIAHNAGLEGSVIVERLKKEEAGFGFNAATGEWVNMVEAG
sp|Q2JA12|
AASALDKLTLTGDAAEGREIVRRAIAEPLRWIAINAGYDGDEVVKRVAELPRGHGFNAATGEYGEMAGFG
500 510 520 530 540
sp|O50305| IVDPTKVTRSALQHAASVSAMFLTTEAVIADKPEENEGGGGMPDMGGMG-GM---GGMM
sp|Q2JA12| VIDPVKVTRCALQSAASIAALLLTTETLVVEEVIGNPGAVIAPGFGDLAEGLVRPSNIA

Figure 11: 60 kDa Chaperonin protein sequence alignment

O50305- 60 kDa chaperonin protein from *Bacillus halodurans* (gene *groL*); **Q2JA12**- 60 kDa chaperonin 3 from *Frankia casuarinae* (gene *groL3*) identified peptides located in ATCC BAA-870, strain A29, and strain A99. MAFFT online was used to complete sequence alignments with iterative processing of these sequences done using Bioedit. Resides highlighted show residues located in the conserved helix-turn-helix region of the protein

Table 4: Result Summary

Strain Information	Small scale reaction data	Large scale reaction data	UPLC-MS data	$^{+}$H NMR, ^{13}C NMR Verification	Inhibitor Studies	SDS-PAGE verification	LC-MSMS verification of DMF induced cells
ATCC BAA-870- DMF induced cells	3-CP conversion complete. Single product, Nicotinic acid characterised by HPLC	Nicotinic acid and Nicotinamide peaks located by HPLC	Not determined	Nicotinic Acid and Nicotinamide isolated. Peaks verified	Hydroxylamine, ascorbic acid, and nickel chloride addition resulted in a slower 3-CP conversion to nicotinic acid (12-16% loss in activity noted)	A ~40 kDa dominant protein band was observed which was similar in size to other documented nitrilase enzymes from *R. rhodochrous* (accounting for 12% of total soluble protein in the sample)	Nitrilase (Q03217) and α-subunit LMW Nitrile hydratase (P29378) located in the DMF-induced cells
A29- DMF-induced cells	3-CP conversion complete. Single product, Nicotinic acid characterised by HPLC	Single product, Nicotinic acid characterised by HPLC	Single product, Nicotinic acid formed (Mol. mass 124.04)	Nicotinic Acid peaks identified	Nitrilase inhibitors benzylamine and benzaldehyde showed slower 3-CP conversion to nicotinic acid (61.3 and 88.4% loss in activity respectively)	A ~40 kDa band verified similar in size to *R. rhodochrous* nitrilase enzymes (accounting for 12% of the total soluble protein in the sample)	Nitrilase enzyme only located in the DMF-induced A29 cells (Q03217)
A99- DMF induced cells	3-CP conversion complete. Single product, Nicotinic acid characterised by HPLC	Single product, Nicotinic acid characterised by HPLC	Single product, Nicotinic acid formed (Mol. mass 124.03)	Nicotinic Acid peaks identified	Nitrilase inhibitors benzylamine and benzaldehyde showed reaction slow down (79.5 and 87.5% respectively)	A ~40 kDa band verified similar in size to *R. rhodochrous* nitrilase enzymes (accounting for 11% of the total soluble protein in the sample)	Nitrilase enzyme only located in the DM- induced A99 cells (Q03217)
Report Section	**3.1**	**3.3**	**3.2**	**2.5**	**3.5**	**3.6**	

4. Discussion

Tauber *et al.* (2000) studied the effect DMF addition had on the overall nitrile degrading enzyme activity in treatment reactions studied using poly acrylonitrile substrates and found that DMF increased the accessibility of the nitrile groups thus aiding catalysis. However, DMF addition as a nitrilase enzyme inducer was not assessed by the authors in their study.

Rhodococcal strains ATCC BAA-870, strain A29 and the closely related *P. simplex* strain A99 showed varied biochemical profiles when exposed to different chemical modulators during cultivation. However all three bacterial strains showed increased nitrilase production levels when cultured in the presence of DMF, with rapid biocatalytic conversion of 3-CP to nicotinic acid noted. Reactions containing 40 mM 3-CP showed complete conversion to nicotinic acid within an hour, while the control and BNZ-induced cells showed no acid formation under the same reaction conditions.

BNZ-induced cells of A29 and A99 harvested 24 hours after the onset of induction showed a distinctive nicotinamide peak that could be the result of induction of the nitrile hydratase enzyme in these strains. This transient effect was lost in the 48h sample analyzed, with no nicotinamide production noted thereafter. This could be the result of BNZ hydrolysis during induction, or could be the result of benzonitrile loss by volatilization.

Larger scale reactions that were carried out using control and induced cells of all three strains revealed that the DMF-induced resting cell reactions of strain A29 and A99 generated nicotinic acid only as confirmed by NMR post extraction (complete conversion observed for both A29 as well as A99), whereas the DMF-induced cells prepared from ATCC BAA-870 generated both nicotinamide and nicotinic acid products (22% and 38% respectively).

UPLC-MS data generated from the biotransformation of 3-CP using DMF-induced cells showed that A29 and A99 converted 3-CP to nicotinic acid. The same cells when cultured in the absence of any inducer or when induced in the presence of 5 mM BNZ showed nitrile persistence and limited amide production.

Amidase, nitrile hydratase and nitrilase inhibition studies done with the DMF-induced cells of strain A29 and A99 once again suggested that the activity observed was most likely a nitrilase enzyme. As a first proof, the addition of hydroxylamine and ascorbic acid showed no amide accumulation in both the A29 and A99 cells tested. Furthermore, inclusion of the amidase inhibitor compound DEPA did not result in any amide accumulation in the samples. However, addition of the nitrilase inhibitor molecules benzaldehyde and benzylamine showed a slow-down in the conversion of 3-CP to nicotinic acid. This is in agreement with data published by Stevenson *et al.* (1992) that showed that both benzaldehyde and benzylamine competitively inhibited nitrilase activity in resting cells of *Rhodococcus* ATCC 39484.

SDS-PAGE analysis of the cell lysates showed that all of the DMF-induced cells produced elevated nitrilase enzyme levels, visible as a dominant protein band of ~40 kDa in size in the soluble fractions (11-15%). LC-MSMS amino acid sequence analysis confirmed the presence of Uniprot Q03217 exclusively in all three DMF-induced strains, while ATCC BAA-870 showed additional constitutive expression of nitrile hydratase activity.

The role that DMF addition plays in nitrilase activity induction in these cells is still not understood. It does seem likely though that nitrilase activity induction may be a mechanism by which cell detoxification is attempted.

Nitrilase enzyme production in plants is often used to facilitate cellular detoxification when the breakdown of glucosinolates yields toxic isothiocyanates and nitrile compounds (Miller and Conn, 1980). These are subsequently converted to less toxic acid product by nitrilase enzymes. DMF is toxic to most cells and its effective removal from the environment is crucial for cell survival and proliferation.

We therefore consider that DMF addition could function to elicit nitrilase expression in these strains by, i) directly functioning as a nit*R* gene regulator or; ii) through a DMF breakdown product such as dimethylamine. Work done by Nagasawa *et al*. (1990) showed that ε-Caprolactum and isovaleronitrile could function as nitrilase inducers in *R. rhodochrous* J1 cells by Kobayashi *et al.* (1989).

To the best of our knowledge neither DMF nor dimethylamine has ever been studied in its capacity to function as a nitrilase regulator.

5. Conclusion

The inclusion of DMF in the strains used in this study can be used to guide biocatalytic conversion of nitriles to their corresponding acid analogues. More importantly, in the case of strain A29 and A99 this can be done without product contamination from any amides generated via the presence of any constitutively produced nitrile hydratase enzyme.

The obvious benefit to employing a biocatalytically “directed” whole cell industrial process is the non-requirement for purification of the nitrilase enzyme produced by the cell. This not only improves the techno-economics of the process but also allows for quick cell cultivation to reaction times, without the need for specialised enzyme purification processes or equipment.

Finally, nitrilase enzyme activation by subunit dimerization and subsequent polymerization is often achieved through the action of specialized chaperone proteins. Nitrilase purification studies on *Bacillus pallidus* Dac521 and *Pseudomonas fluorescens* DSM 7155 showed that nitrilase enzymes are often co-purified with the chaperonin GroEL. Furthermore, recombinant expression of a nitrilase from *Clostridium testosteroni* in *Escherichia coli* showed high levels of protein expression (30%) but low soluble protein levels (10%). Co-expression of a GroEL protein in this case resulted in a five-fold increase in nitrilase activity levels. Thus, using a whole cell catalyst rather than a recombinantly expressed protein circumvents the need for co-expression of any additional chaperone proteins which can be problematic.

6. Acknowledgements

We would like to thank the following people at the University of the Witwatersrand: Prof. Joseph Michael; Prof Charles De Koning; and Dr Amanda Rousseau. At the CSIR, I would like to extend thanks to Mr Sipho Mamputhu (for assistance with LC-MSMS protein sequencing) as well as Dr Priyen Pillay, Dr Lusisiwe Kwezi, Dr Ofense Poe, Advaita, Sibongile, Ntombi, Dr Daria Rutkovska and Dr Kevin Wellington. Financial support from the DST Biocatalysis Initiative and Dr Tsepo Tsekoa was greatly appreciated.

7. References

Bauer, R., Knackmuss, H-J., and Stolz, A. Enantioselective hydration of 2-arylpropionitriles by a nitrile hydratase from *Agrobacterium tumefaciens* Strain d 3. (1998), Appl. Microbiol. Biotechnol. **49**: 89-95.

Borsook, H., Davenport, H. W., Jeffreys, C. E. P. and Warner, R. C. The oxidation of ascorbic acid and its reduction in vitro and in vivo. (1937). J. Biol. Chem. **117**: 237-279.

Binfeng, L., Jinhuan, S. Tao, J. Enzyme and process development for production of nicotinamide. (2011). Org. Process Res. Dev. **15**: 291-293.

Brady D, Beeton A, Kgaje C, Zeevaart J, van Rantwijk F, Sheldon R. A. Characterisation of Nitrilase and Nitrile Hydratase Biocatalytic Systems. (2004). Appl. Microbiol. Biotechnol. **64:** 76-85.

Brenner, C. Catalysis in the nitrilase superfamily. (2002). Curr. Opin. Struct .Biol. **12**: 775-782.

Chhiba, V. P., Bode, M., Mathiba, K. and Brady, D. Enzymatic Stereoselective Synthesis of β-amino Acids, (2014). in S. Riva & W. D. Fessner (eds), Cascade Biocatalysis: Integrating and Environmentally Friendly Reactions, Wiley-VCH, Germany, 297-313.

Cramp, R. A. amd Cowan, D. A. Molecular characterization of a novel thermophilic nitrile hydratase. (1999). Biochem. Biophys. Acta. **1431**; 249-260.

Endo, T., and Watanabe, I. Nitrile hydratase of *Rhodococcus* sp. N774 purification and amino acid sequences. (1989), FEBS Lett. **243:** 61-64.

Goncalves , E. R., Hara, H., Miyazawa, D., Davies, J. E., Eltis, L. P. and Mohn, W. W. Transcriptomic assesment of isozymes in the biphenyl pathway of *Rhodococcus* sp. Strain RHA1. (2006). Appl. Environ. Microbiol. **72**: 6183-6193.

Gregoriou, M. and Brown, P. R. Inhibition of the aliphatic amidase from *Pseudomonas aeruginosa* by urea and related compounds. (1979). Eur. J. Biochem. **96**: 101-108.

Gradley, M. L., Deverson, C. J. F. and Knowles, C. J. Asymmetric hydrolysis of *R*-(-)-*S* (+)-2-methylbutyronitrile by *Rhodococcus rhodochrous* NCIMB 11216 (1994). Arch. Microbiol. **161**: 246-251.

Harper D. B. (1977) Microbial metabolism of aromatic nitriles: enzymology of aromatic nitriles: enzymology of C-N cleavage by Nocardia sp. (*Rhodococcus* group) N. C. I. B. 11216. Biochem. J. **165**: 309-319.

Kaul P. and U. C. Banerjee. Predicting enzyme behaviour in nonconventional media: correlating nitrilase function with solvent properties. (2008). J. Ind. Microbiol. Biotechnol. **35:** 713-720.

Kinfe, H. H., Chhiba, V., Bode, M. L., Mathiba, K., Steenkamp, P. A. and Brady, D. Enantioselective hydrolysis of β- hydroxy nitriles using whole cell biocatalyst *Rhodococcus rhodochrous* ATCC BAA-870. (2009). J. Mol. Catal. B-Enzym. **59**: 231-236

Kobayashi, M., Nagasawa, T. and Yamada, H. Nitrilase of *Rhodococcus rhodochrous* J1. (1989). Eur. J. Biochem. **182**: 349-356.

Laemmli. Cleavage of structural proteins during the assembly of the head of bacteriophage T4. (1970). Nature. **227**: 680-685.

Lévi-Schil, S., Soubrier, F., Crutz-Le Coq, A-M., Faucher, D., Crouzet, J. and Pétré, D. Aliphatic nitrilase from a soil-isolated *Comomonas testosteroni* sp.: gene cloning and overexpression, purification and primary structure. (1995). Gene. **161**: 15-20.

Miller, J. M. and Conn, E. E. Metabolism of hydrogen cyanide by higher plants. (1980). Physiologica Plantarum. **65**: 1199-1202.

Miyanaga, A., Fushinobu, S., Ito, K. and Wakagi, T. Crystal structure of cobalt-containing nitrile hydratase. (2001). Biochem. Biophys. Res. Commun. **288**: 1169-1174.

Mueller, P., Egorova, K., Vorgias, C. E., Boutou, E., Trauthwein, H., Verseck, S and Antranikian, G. Cloning, overexpression, and characterization of a thermoactive nitrilase from the hyperthermophilic archaeon *Pyrococcus abyssi*. (2006). Protein. Expr. Purif. **47**: 672-681.

Nagasawa, T., Ryuno, K. Yamada, H. Nitrile hydratase of *Brevibacterium* R-312 purification and characterisation. (1986). Biochem. Biophy. Res. Commun. **139**: 1304-1312.

Nagasawa, T., Nakamura, T. and Yamada., H ε-Caprolactum, a new powerful inducer for the formation of *Rhodococcus rhodochrous* J1 nitrilase. (1990). Arch. Microbiol. **155**: 13-17.

Nagasawa, T., Takeuchi, K. and Yamada, H. Characterization of a new cobalt-containing nitrile hydratase purified from urea-induced cells of *Rhodococcus rhodochrous* J1. (1991). FEBS Journal. **196**: 581-589.

Nagasawa, T., Weiser, M., Nakamura, T., Iwahara, H., Yoshida, T. and Gekko, K. Nitrilase or *Rhodococcus rhodochrous* J1. Conversion into the active form by subunit association. (2000). Eur. J. Biochem. **267**: 138-144.

Nageshwar, Y. V. D., Sheelu, G., Shambu, R. R., Muluka, H., Mehdi, N., Malik, M. S. and Kamal, A. Optimization of nitrilase production from *Alcaligenes faecalis* MTCC 10757 (IICT-A3): Effect of inducers on substrate specificity. (2011). Bioproc. Biosys. Eng. **34**: 515-523.

Prasad, S., Raj, J. and Bhalla, T. C. Purification of a hyperactive nitrile hydratase from resting cells of *Rhodococus rhodochrous* PA-34. (2009). Indian J. Microbiol. **49**: 237-242.

Precigou, S., Wieser, M., Pommares, P., Goulas, P. and Duran, R. *Rhodococcus pyridinovorans* MW3, a bacterium producing a nitrile hydratase. (2004). Biotechnol.Lett. **26:** 1379-1384.

Rapheeha, O.K.; Roux- van der Merwe, MP; Badenhorst, J; Chhiba, V; Bode, ML; Mathiba, K. and Brady, D. Hydrolysis of nitriles by soil bacteria: variation with soil origin. (2017). J. Appl. Microbiol. **122**: 686-697.

Robinson, W. G. and Hook, R. H. Ricinine nitrilase: I. Reaction producer and substrate specificity. (1964). J. Biol. Chem. **239**: 4257-4262.

Stalker, D. M., Malyj, L. B., McBride, K. E. Properties of a nitrilase specific for the herbicide bromoxynil and corresponding nucleotide sequence analysis of the bxn gene. (1988). J. Biol. Chem. **263**: 6310-6314.

Stevenson, D. E., Feng, R., Dumas, F., Groleau, D., Mihoc, A. and Storer, A. C. Mechanistic and structural studies on *Rhodococcus* ATCC 39484 nitrilase. (1992). Biotechnol. Appl. Biochem. **15**: 283-302.

Tani, Y., Kurihara, M. and Nishise, H. Characterization of nitrile hydratase and amidase, which are responsible for the conversion of dinitriles to mononitriles, from *Corynebacterium* sp (1989). Agric. Biol. Chem. **53**: 3151-3158.

Tauber, M.M., Cavaco-Paulo, A., Robra, K., Gubitz, G.M. Nitrile hydratase and amidase from *Rhodococcus rhodochrous* hydrolyze acrylic fibers and granular polyacrylonitriles. (2000). Appl. Environ. Microbiol. **66**: 1634-1638.

Thalenfeld, B. and Grossowicz, N . Regulatory properties of an inducible aliphatic amidase in a thermophilic *Bacillus.* (1976). J. Gen. Microbiol. **94**: 131-141.

Thuku, R. N., Brady, D., Benedik, M. J., and Sewell, B. T. Microbial nitrilases: Versatile, spiral forming enzymes. (2009). J. Appl. Microbiol. **106**: 703–727.

Vaudel, M., Burkhart, J. M., Zahedi, R. P., Oveland, E., Berven, F. S., Sickmann, A., Martens, L. and Barsnes, H. PeptideShaker enables reanalysis of MS-derived proteomics data sets. (2015). Nat. Biotechnol. **33**: 22-24.

Vejvoda, V., Kubác, D., Davidová, A. Kaplan, O., Śulc, M., Śveda, O., Chaloupková, R. and Martínkova, L. Purification and characterization of nitrilase from *Fusarium solani* IMI96840. (2010). Process Biochem. **45**: 1115-1120.

Yamada, H. and Kobayashi, M. Nitrile hydratase and its application to industrial production of acrylamide. (1996). Biosci. Biotechnol. Biochem. **60**; 1391-1400.

Zhang, Z. J., Xu, J. H., He, Y. C., Ouyang, L. M. and Liu, Y. Y. Cloning and biochemical properties of a highly thermostable and enantioselective nitrilase from *Alcaligenes* sp. ECU0401 and its potential for (R)-(-)- mandelic acid production. (2011). Bioproc. Biosys. Eng. **34**; 315-322.

Zhangi, R., Zhou, R. and Berne, B. J. Urea's action on hydrophobic interaction. (2009). J. Am. Chem. Soc. **131**: 1535-1541.

Zheng, J. G., Chen, J., Liu, Z. Q., Wu, M. H., Xing, L. Y. and Shen, Y. C. Isolation, identification and characterization of *Bacillus subtilis* ZJB-063, a versatile nitrile-converting bacterium. (2008). Appl. Microbiol. Biotechnol. **77**: 985-993.

Websites:

Merops- the Peptidase database 2017, accessed 20th March 2017, <https://www.ebi.ac.uk/merops/cgi-bin/speccards?sp=sp034913;type=peptidase>

Chapter Eight: Conclusion

The genus *Rhodococcus* is versatile in being able to grow in a wide range of environments, as we also observed in our transect of South Africa. One of the important characteristics of this group of bacteria is their capacity for translocation of hydrophobic compounds due to their cell membrane plasticity, allowing them to proliferate on a broad diversity of organic and inorganic hydrocarbons and other compounds.

To achieve this feat *Rhodococcal* species need to be biocatalytically dynamic systems capable of oxidative metabolism of several organic compounds. This can be associated with the large genomic DNA component they house, which includes diverse plasmids acquired through numerous recombination events. Genome studies on *R. rhodochrous* ATCC BAA870 (Frederick *et al.* unpublished data[1]) showed that these cells house a 5.7 Mbp chromosome with a single plasmid of 453 000 nucleotides located in these cells (**Chapter 1**).

Because of their impressive biocatalytic arsenal *Rhodococcus* strains have found application in established industrial processes (**Chapter 2**). Their ability to convert highly recalcitrant compounds such as aliphatic, aromatic, and heterocyclic compounds make them suitable for use in both biocatalytic as well as bioremediation processes. Other commercially interesting products derived from nitriles include acrylamide, acrylic acid, niacin, nicotinamide, *para*-aminobenzoic acid, and isoniazid (**Chapter 1**). High yields and excellent selectivity profiles make these catalysts attractive for industrial applications. This potential should be exploited further.

Results from the study reported in **Chapter 6** showed that isolation of nitrile degrading organisms with broad microbial distribution patterns were observed from soil samples removed from varied geographical locations. An interesting observation from the study undertaken was that all 11 uncultivated soil environments yielded nitrile-degrading microorganisms, with the genus *Rhodococcus* and many other related genera selectively enriched in the presence of β-substituted nitrile compounds.

Isolates of *R. erythropolis* predominated in many of the uncultured soil samples, while *R. rhodochrous* was dominant in many cultivated site environments. This suggests that *R. rhodochrous* cells could possess interesting catabolic enzyme systems that could play a role in facilitating conversion of nitriles to intermediates capable of feeding into primary metabolism. However, the versatility of these enzymes required further investigation to determine the synthetic potential of these rich microbial resources. Furthermore, the nature of the expression systems needed to be studied since not all nitrile degrading enzymes are constitutively produced.

[1] 1. Joni Frederick, Fritha Hennessy, Uli Horn, Linda G. Otten, Marcel van den Broek, Ulrich Strych, Richard Willson Charles A. Hefer, Trevor Sewell, Dean Brady. The genome sequence of *Rhodococcus rhodochrous* ATCC BAA-870 and comparison to other Rhodococcal genomes. To be submitted.

Many novel nitrilase inducers have been identified recently, with significant improvements in nitrilase activity levels observed when bacterial cells were cultured in the presence of propionitrile, isovaleronitrile or ε-caprolactam. However the use of nitriles can be problematic since these compounds are toxic and their inclusion during cell cultivation often results in cell growth inhibition. Nitriles can also be metabolized by nitrile-assimilating bacteria thus decreasing the inducer concentration as cultivation continues.

Nitrilase induction in our study using *R. rhodochrous* ATCC BAA-870, A29 and *Pimelobacter simplex* A99 (**Chapter 7**) was achieved by incorporation of dimethylformamide (DMF) during cell cultivation. DMF is a non-nitrile chemical that is unlikely to undergo catalysis by nitrile degrading enzymes, unlike the nitrile-based inducers previously discovered. Nitrilase induction was confirmed by SDS-PAGE electrophoresis and protein sequencing by LC-MSMS analysis. A dominant ~40 kDa protein spot was found by SDS-PAGE analysis, with further inspection indicating that the protein showed no mutational changes when compared to the nitrilase protein produced by *Rhodococcus* sp. Uniprot entry Q03217. Biocatalytic activity was confirmed by biotransformation reactions using 3-cyanopyridine as substrate and inhibition studies which showed that the induced protein in strains A29 and A99 was inhibited by benzylamine and benzaldehyde.

From a cost perspective, DMF is considerably cheaper than any of the other documented chemical inducer molecules mentioned above and the low concentration used in this study means that the estimated cost required for induction is 6 times lower than the cost of isovaleronitrile required for induction; is equivalent in cost to benzonitrile (BNZ) but not as volatile or susceptible to nitrile assimilation; and is approximately 9 times cheaper than ε-caprolactam and propionitrile (based on Sigma Aldrich cost estimates).

From a viewpoint of determining the biocatalytic potential of these strains, a number of different nitrilase and nitrile hydratase / amidase enzyme systems were evaluated through the course of this study, with both BNZ and DMF-inductions evaluated. The selection of the inducer was found to determine the protein composition in each cell, thus determining overall catalytic selectivity.

BNZ-induced cells of strain ATCC BAA-870 showed that asymmetric hydrolysis of aromatic β-hydroxy nitriles could be achieved with excellent enantiomeric excess (*ee*) for the amide intermediates *S*-(+)-3-hydroxy-4-benzyloxybutanamide and *S*-(+)-3-hydroxy-4-phenoxybutanamide that were produced (>99% *ee*) (**Chapter 3**). This selectivity was attributed to the presence of a highly selective amidase enzyme which could be potentially useful in the synthesis of enantiomerically pure β-adrenergic agents. At the time of publication, selectivity was attributed to a perceived size dependency from the enzyme, however substrate docking studies subsequently undertaken have shed light on the quaternary structure of the enzyme, highlighting some crucial hydrophobic interactions with amino acid residues in the binding pocket, possibly playing a role in the observed selectivity (**Appendix 2**).

These same ATCC BAA-870 cells also showed asymmetric kinetic resolution of β-aminonitriles, with *ee* values of both the product and the substrate found to be ~50% (**Chapter 4**). Although enantioselectivity was not absolute, kinetic resolution was observed when 3-amino-3-(4-methoxyphenyl)propanenitrile and 3-amino-3-*p*-tolylpropanenitrile were used. In this particular study though, the selectivity was driven by the nitrile hydratase enzyme with nitrile substrates containing larger, electron-withdrawing substituents at the *para*-position of the aromatic ring structure, showing improved selectivity. Furthermore, *N*-protection by the addition of Boc and tosyl groups seemed to cause steric hindrance as no conversion was noted. The pH was also found to affect the reactivity of the substrates, possibly the result of the protonation state of the primary amine.

The nitrilase enzyme produced by the DMF-induced cells of strain A29 and A99, showed moderate to excellent enantioselectivity (~30-40% ee, and >99% ee respectively) when incubated with 3-amino-3-(4-methoxyphenyl)propanenitrile, and 3-amino-3-*p*-tolylacrylonitrile, respectively (**Chapter 5** and **Chapter 7**). This shows that the nitrilase enzyme can be used as a biological “vehicle” for generating stereoselective peptidomimetic compounds.

Finally, a class of malononitrile substrates reacted with BNZ-induced ATCC BAA-870 cells showed regioselective conversion of furanylmethylenemalononitrile, with the final product configuration determined to be in the *trans* configuration (Z) (obtained through NMR data comparison) (**Chapter 5**).

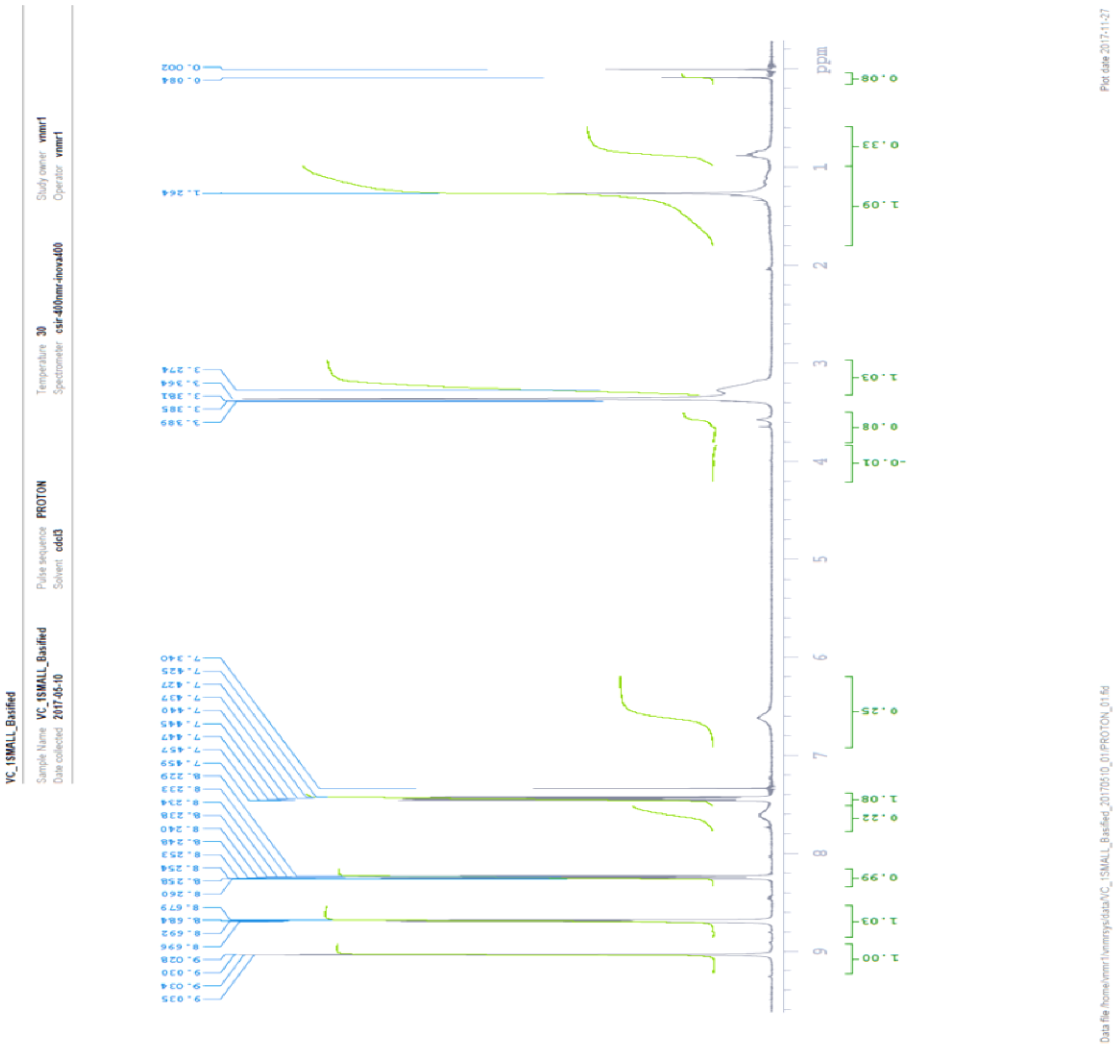
The *Rhodococcal* strains used in this study are extremely versatile biological catalysts, showing moderate to excellent stereoselectivity when reacted with a number of beta-subtituted nitrile compounds of pharmaceutical relevance. The biocatalytic activities provided by the selective induction of the nitrile degrading enzymes in these isolates could be used to engineer regio- and stereo-selective synthesis of amide and acid analogues.

Finally, biological processes for industrial production of nicotinamide and nicotinic acid are significantly “greener” than the chemical processes previously employed. Biological reactions eliminate the need for incorporation of corrosive acids and high temperatures which are often required for chemical hydrolysis. Subsequent alkali neutralization steps require addition of large quantities of caustic agents which are required for iterative processing of the material generated. Biological reactions also typically function at neutral pH conditions and under ambient incubation temperatures (28-30°C). However, a limitation arising from the strategy of using stereoselective hydrolysis of racemic β-subsituted nitriles to form single enantiomer compounds is the residual unreacted and unwanted opposite enantiomer. Subsequent racemization of this enantiomer may be required through dynamic kinetic resolution, possibly coupling with other enzymes such as transaminases.

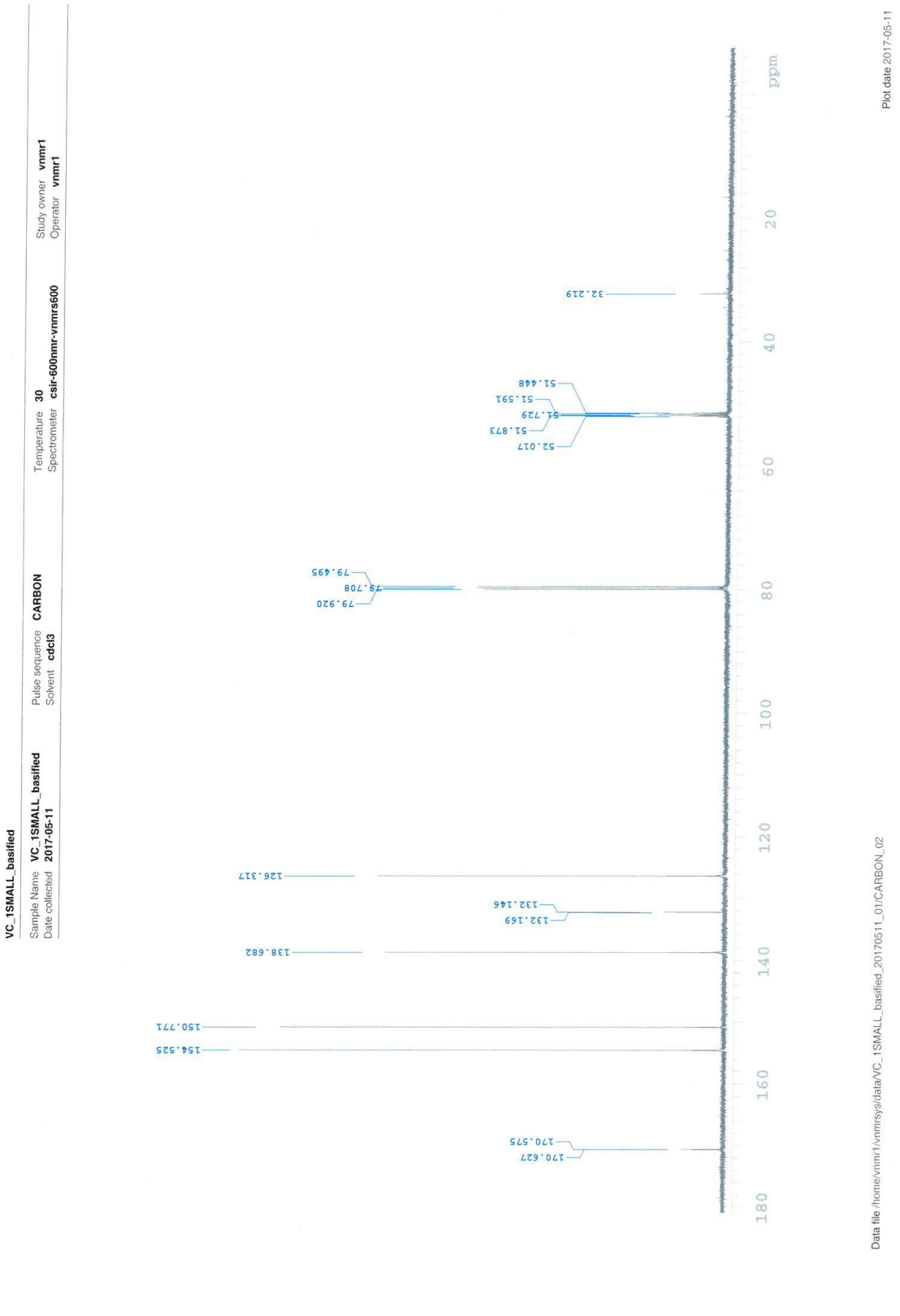
Appendix

Appendix 1A-1C: ATCC BAA-870 NMR Spectra (DMF induced cells)

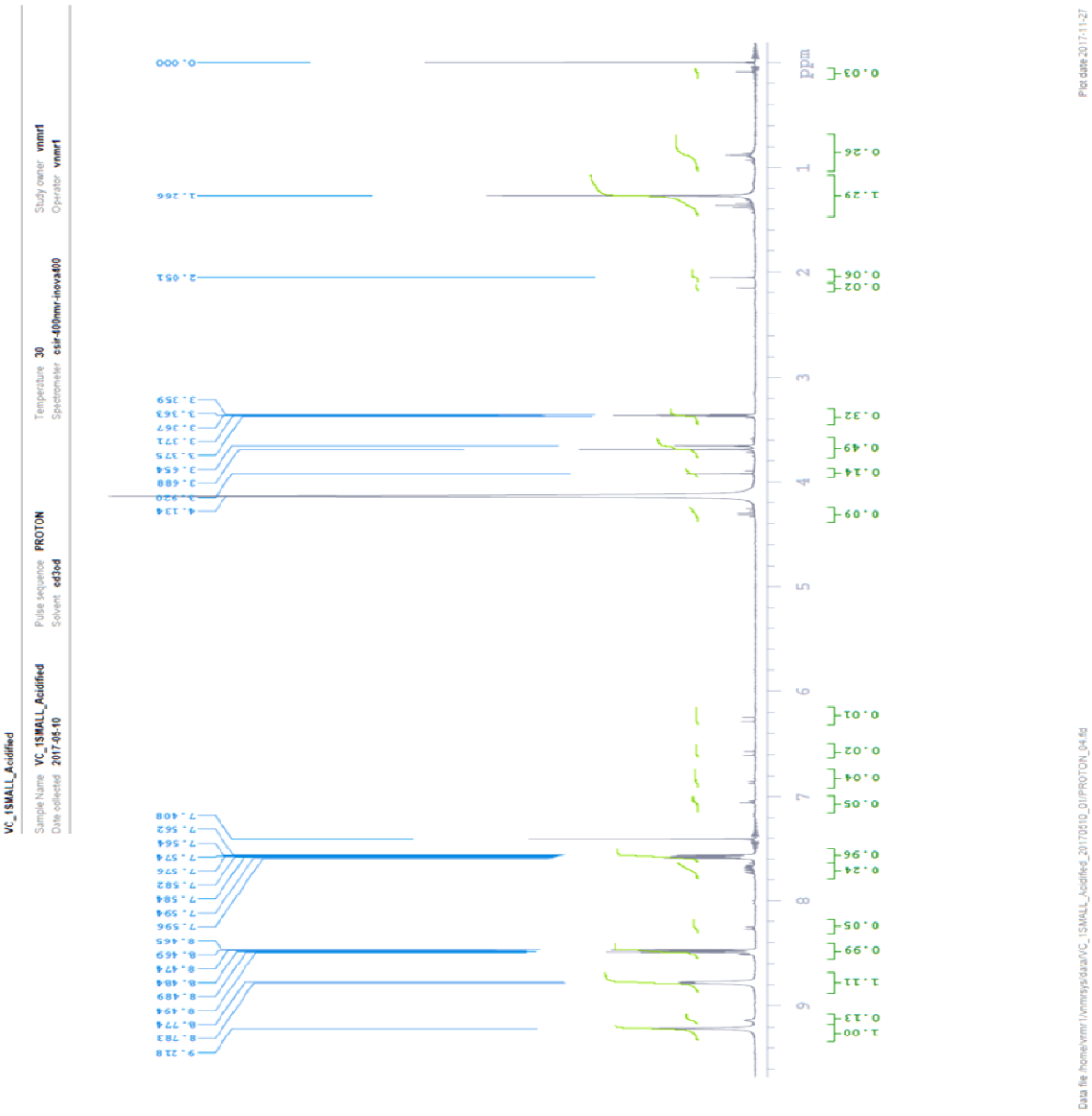
Appendix 1A: (^{1}H NMR) - Basified Sample Extraction



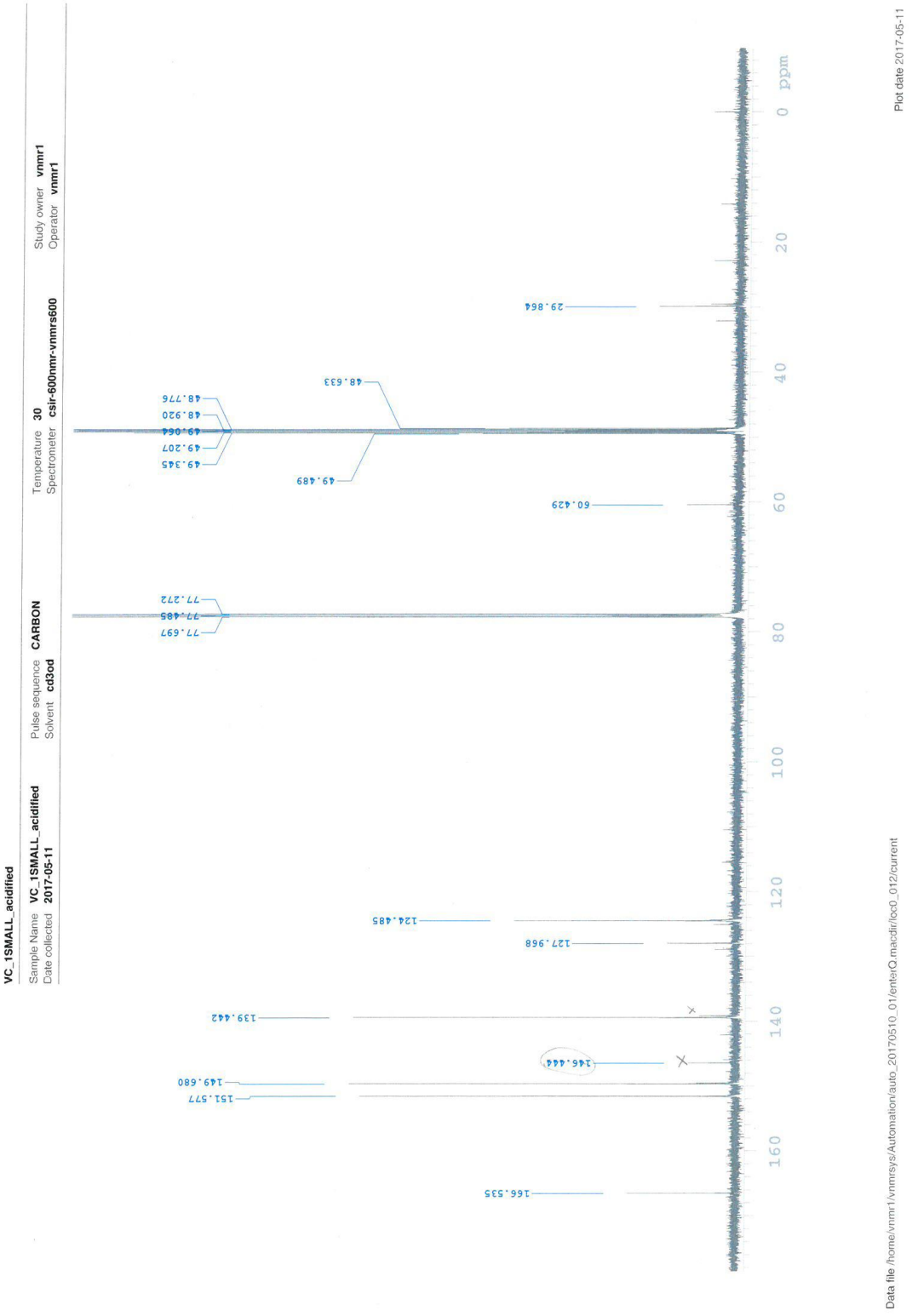
Appendix 1A (^{13}C NMR) - Basified Sample Extraction



Appendix 1A (^{1}H NMR) - Acidifed Sample Extraction

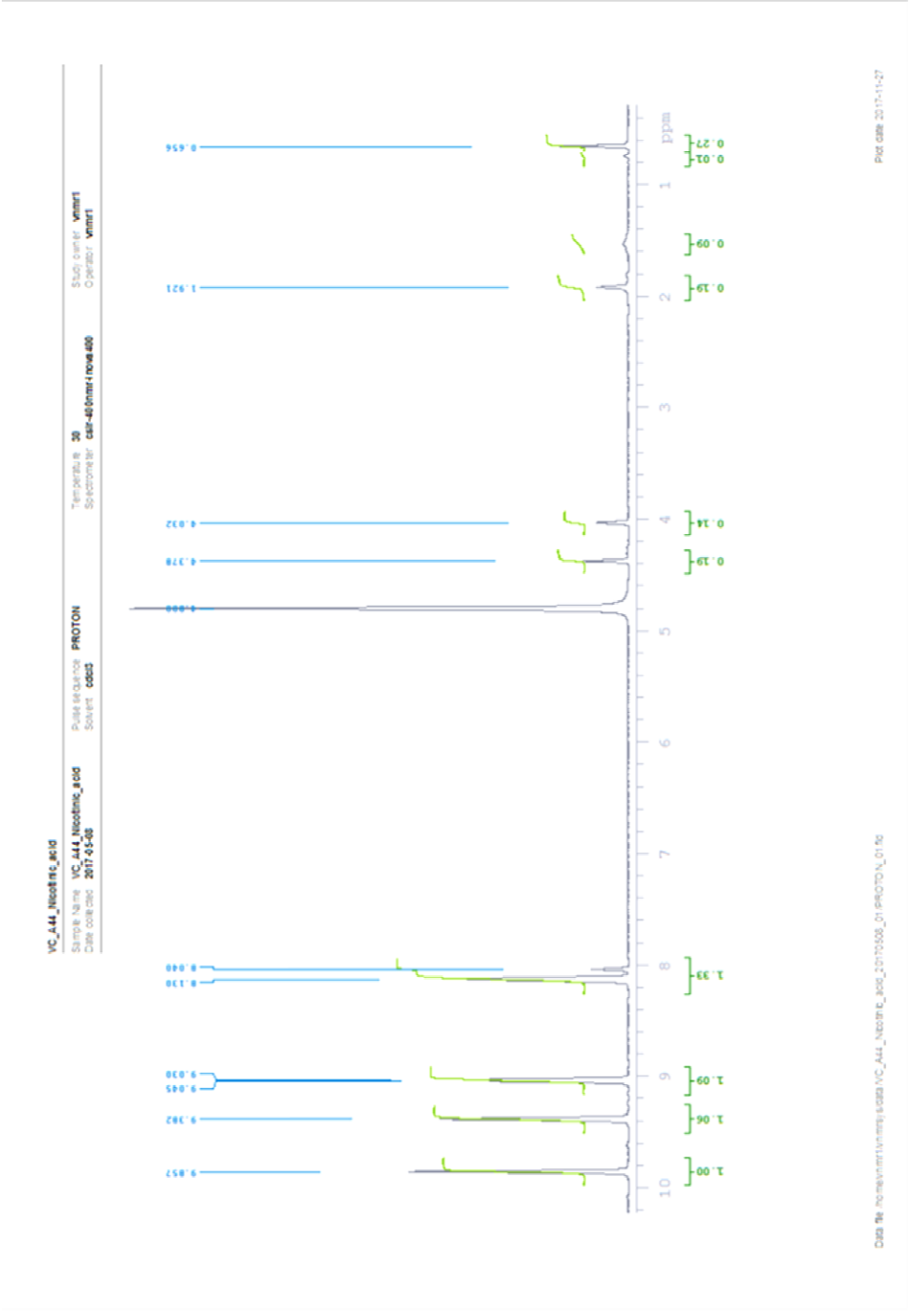


Appendix 1A- (^{13}C NMR) - Acidified Sample Extraction

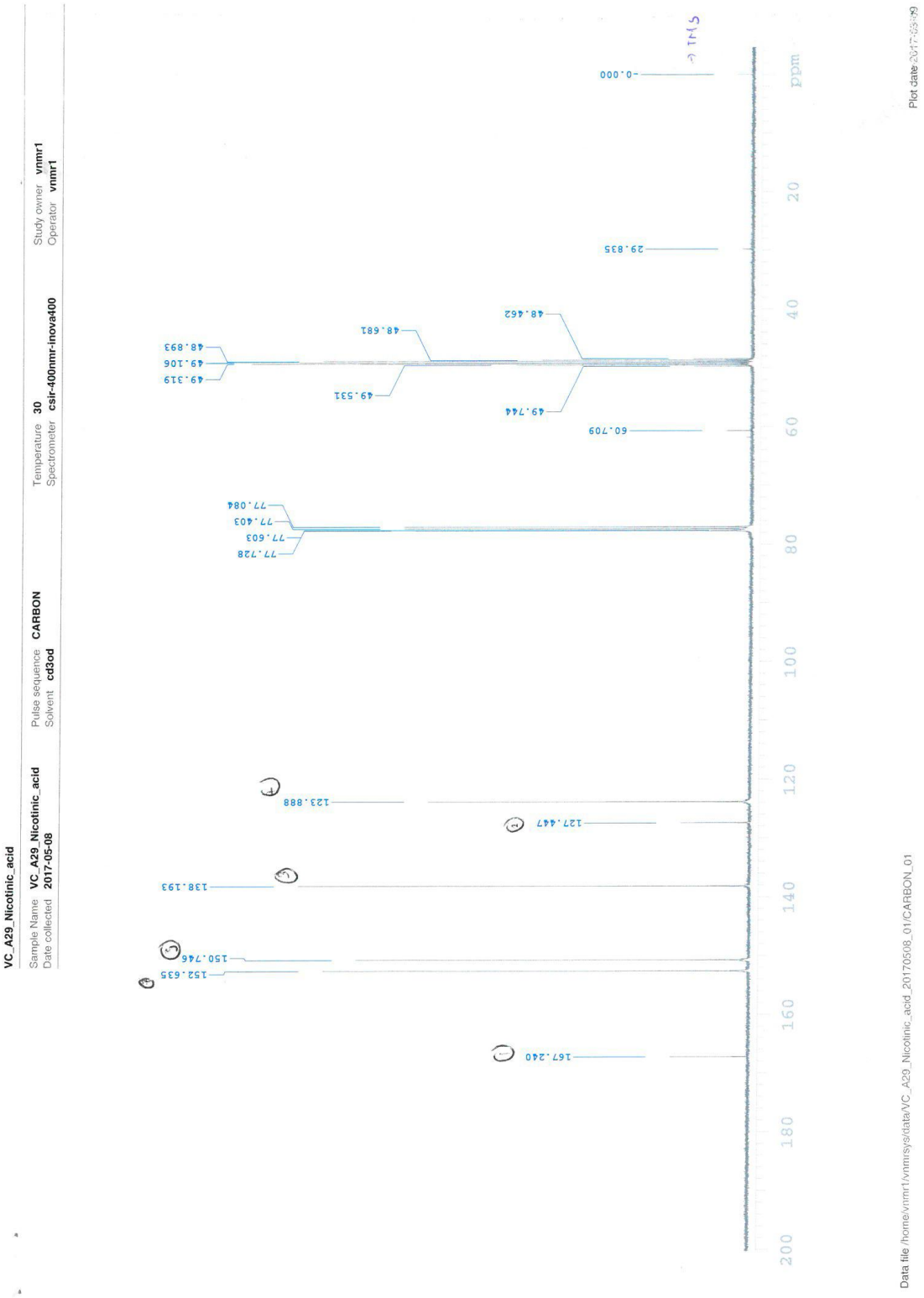


Appendix 1B - Strain A29 NMR Spectra (DMF-induced cells)

Appendix 1 (^{1}H NMR)

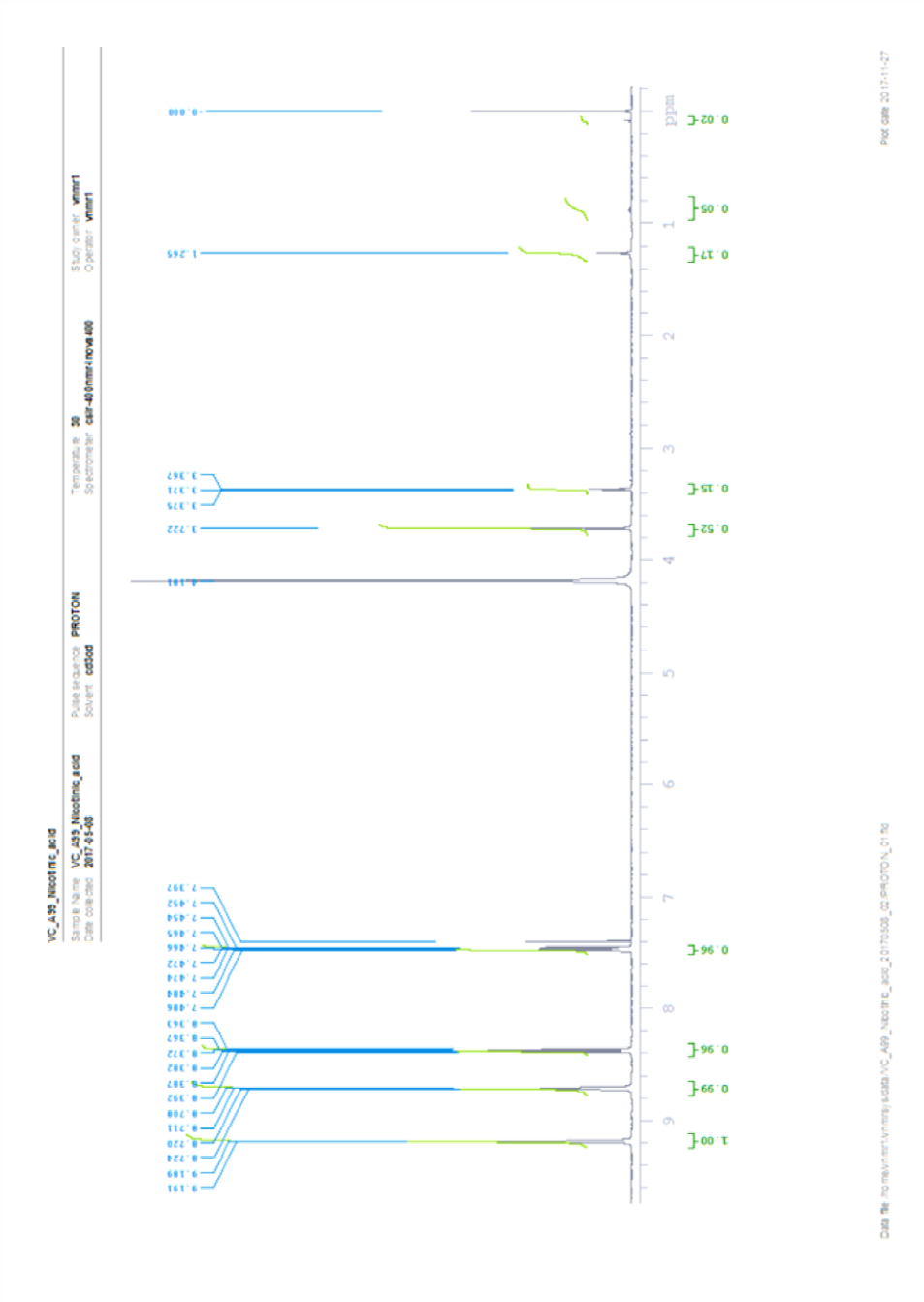


Appendix 1B (^{13}C NMR)

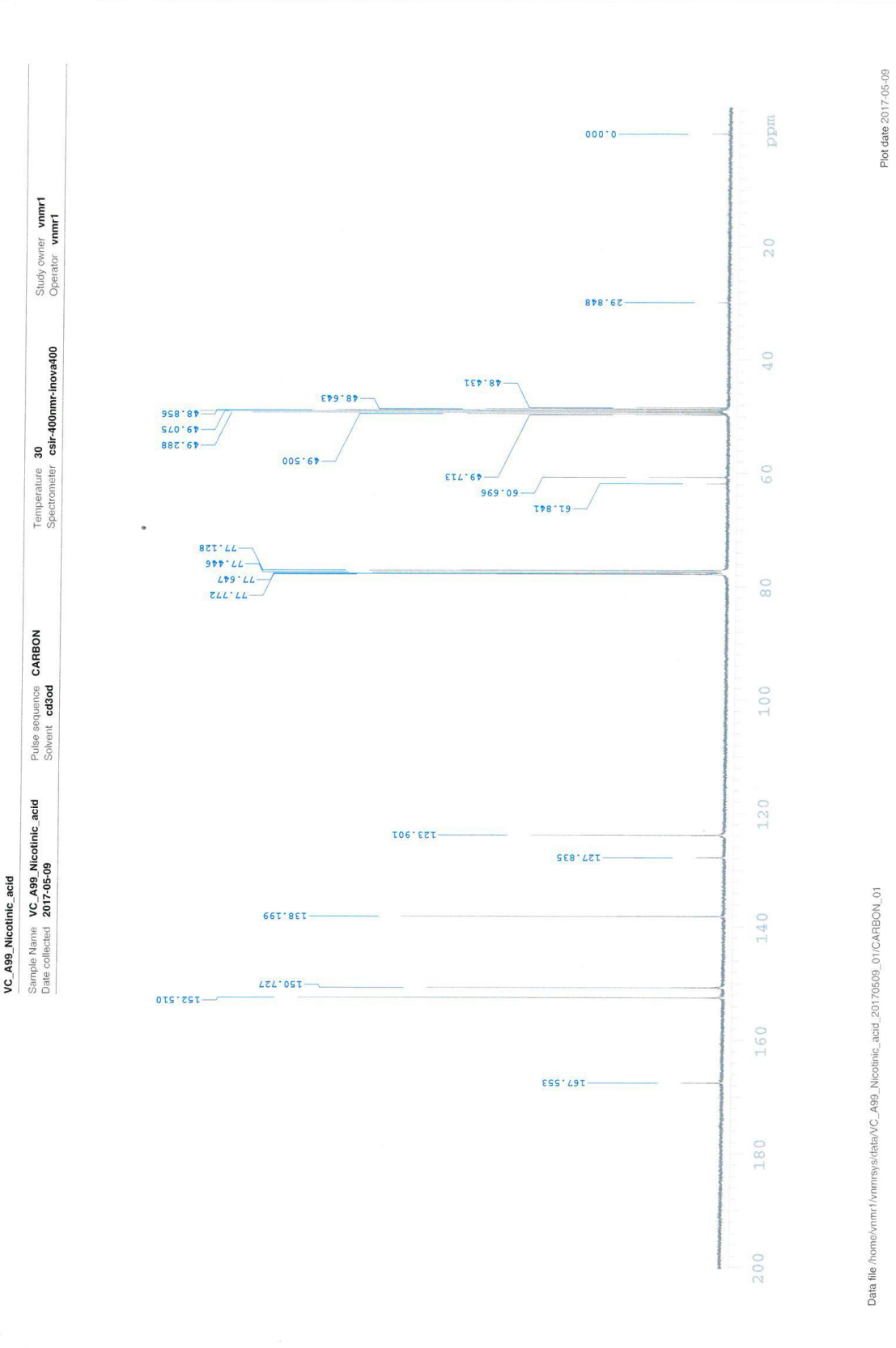


Appendix 1C - Strain A99 NMR Spectra (DMF-induced cells)

Appendix 1C (^{1}H NMR)



Appendix 1C (^{13}C NMR)



Appendix 2: Amidase Docking Studies

Amidase enzymes are typically classified into two separate groups based on their amino acid sequence and any structural similarities that they may possess. The first group is the nitrilase superfamily amidase enzymes which exist as homotetrameric or homooctameric complexes in solution. They have the typical nitrilase catalytic triad that includes Glu, Cys, and Lys.

Amidase signature enzymes (AS enzymes) form homodimeric or homooctameric complexes and contain a stretch of 130 amino acids that are highly conserved and have the AS sequence containing a Ser, Ser, Lys catalytic triad.

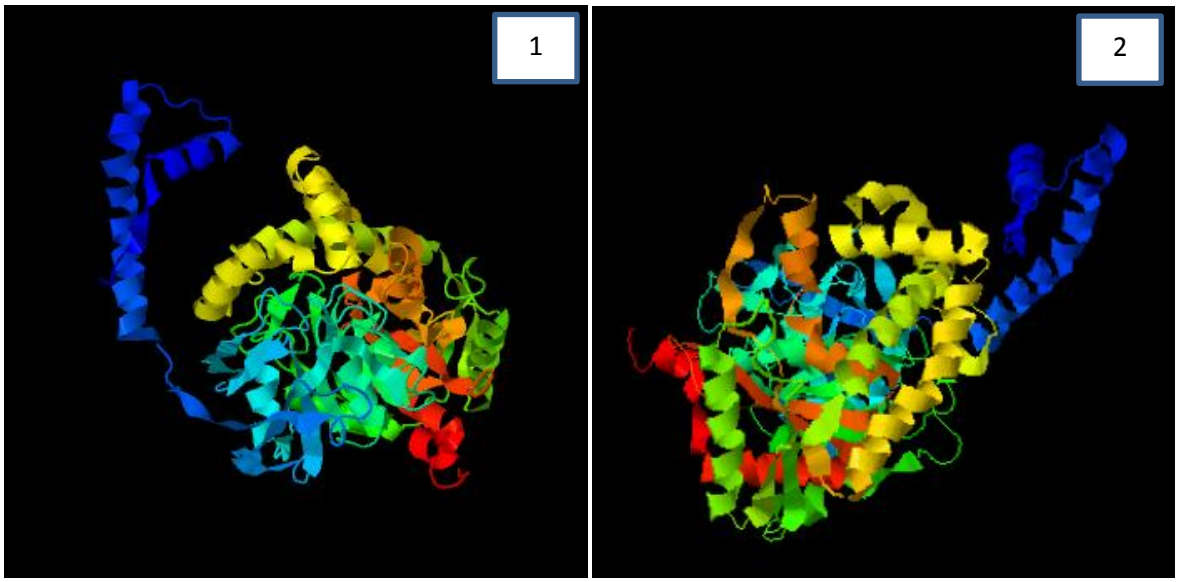


Figure A2-1and A2-2: Crystal structure of RhAmidase produced by *Rhodococcus* sp. N-771 (Image reproduced from Ohtaki *et al*. (2010)).

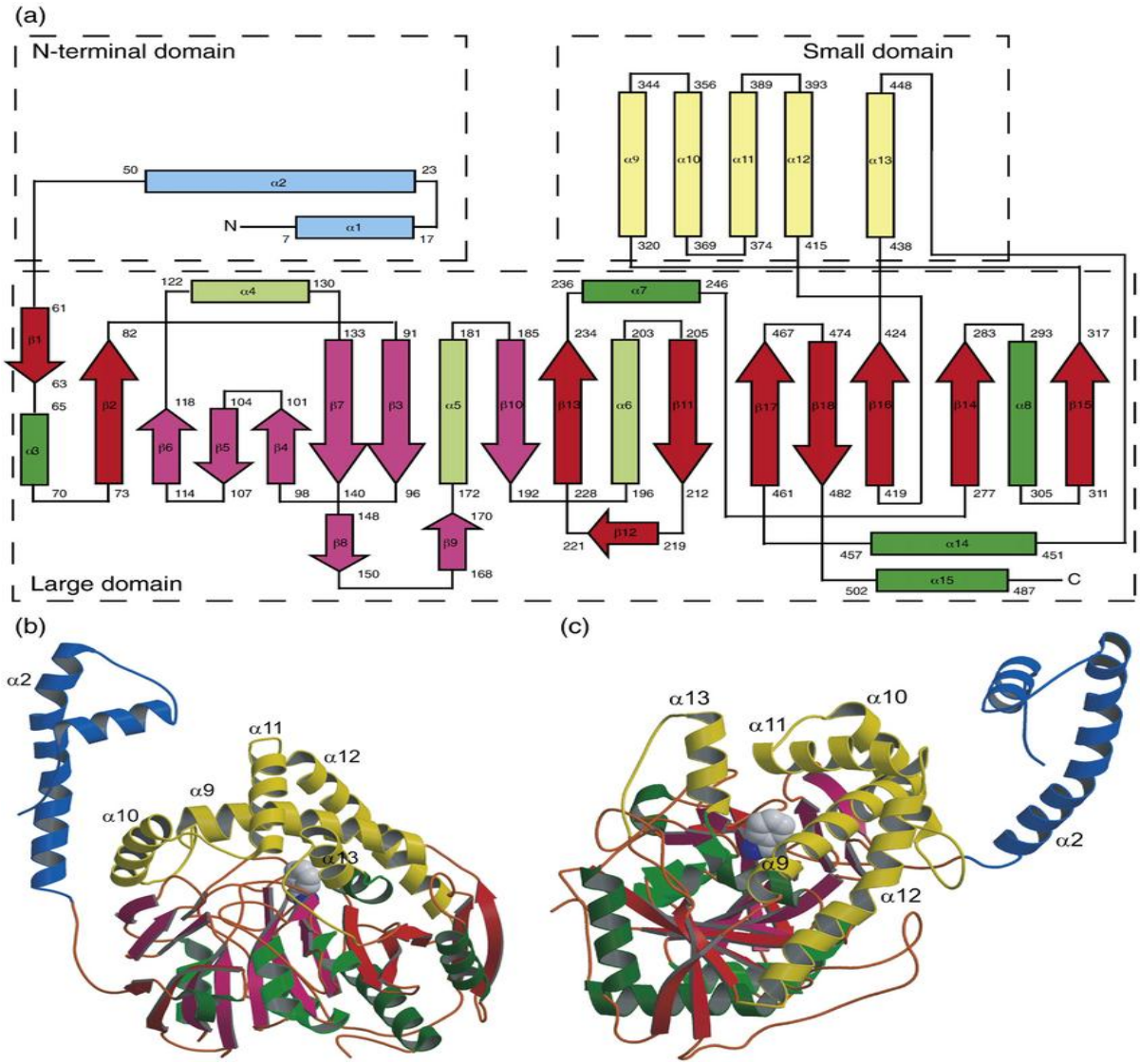


Figure A2-3: *Crystal structure of Rhodococcus* sp. N771 RhAmidase showing secondary structure unit arrangement (a), as well as side (b) and top views(c). Image reproduced from Ohtaki *et al.* (2010).

Structural elements noted in study done

The apoenzyme amidase produced by *R. rhodochrous* ATCC BAA-870 is an AS enzyme which showed high identity/ similarity against the *Rhodococcus* sp. Strain 771 S195A mutant- Q9ZBD4 (60.6-71.2%).

Within the active site of the two superimposed protein structures, the RMS deviation of both amidase enzymes is 0.2 square Angstroms, suggesting that they are spatially identical.

The catalytic waters which are associated with the amidase from ATCC BAA-870 were unknown, therefore homology modelling with the mutant enzyme allowed for prediction of ligand positions within the enzymes catalytic site.

Lys 96 shows hydrogen bond interactions with the Oγ atom of Ser171, as well as the Oγ atom of Ser172. A third hydrogen bond was noted between Lys96 and a catalytic water molecule in the enzymes active site, thus potentially playing a crucial role in maintaining the orientation of the *cis*-Ser171.

Looking at the enzymes hydrophobic pocket, we observed pi-pi (face on) interaction between the aromatic amide substrate and amino acid residue Phe146. The hydrophobic substrate pocket was also found to contain the following amino acid residues:

Ile223 and Ile227 (hydrophobic amino acid residues), Ala332 (small amino acid), and Trp326 (aromatic/ hydrophobic amino acid.)

Additional hydrogen bonding was observed between the β-OH group substituent on the alkyl chain and Gly 148.

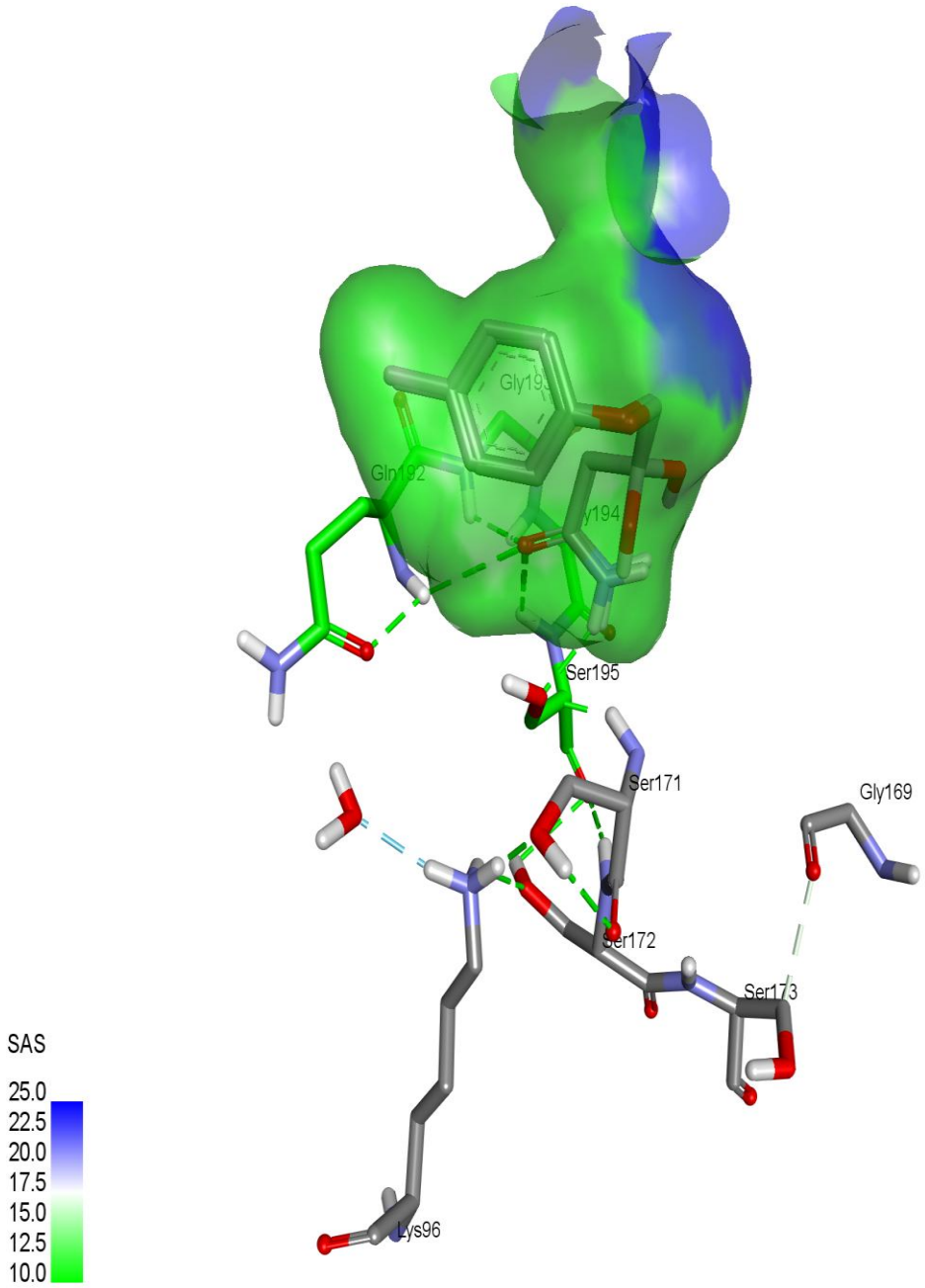


Figure A2-4: Lys 96, Ser171, Ser172, Ser173, Gly169 and catalytic water interactions.

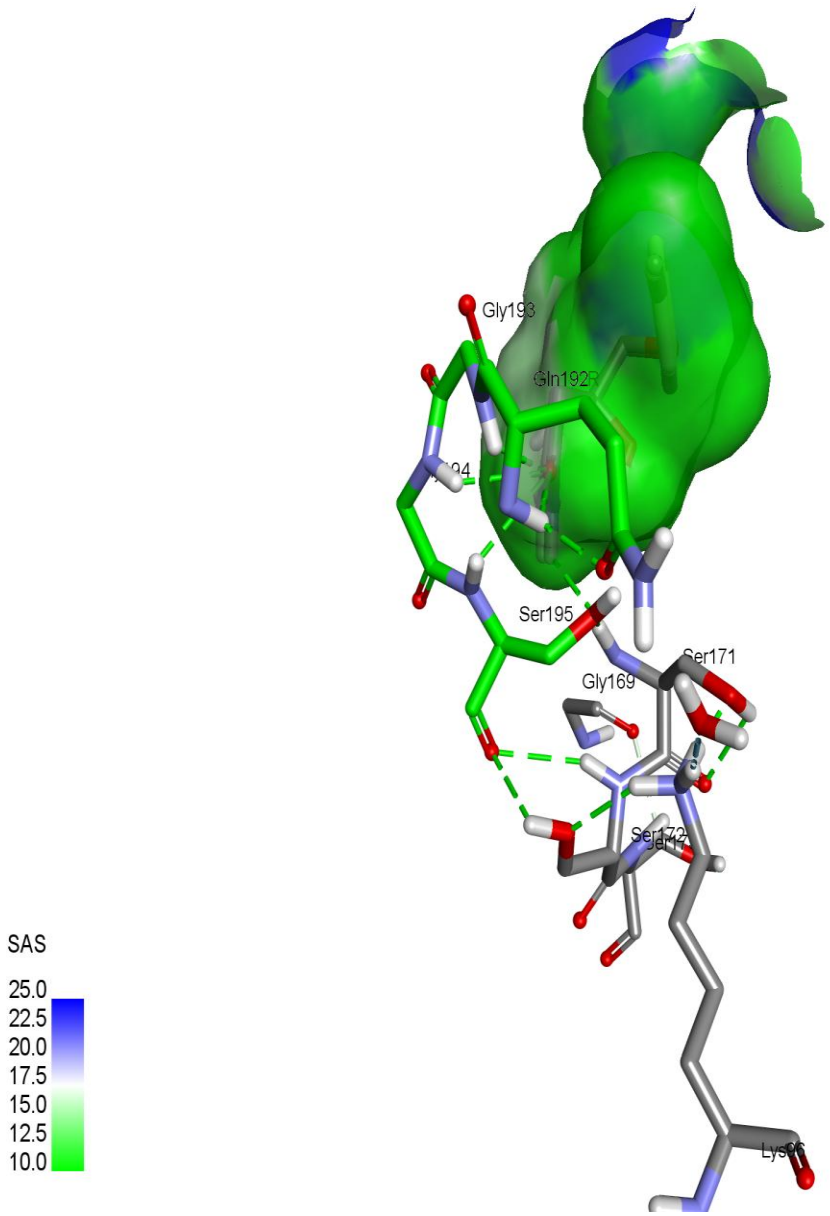


Figure A2-5: Side view, catalytic residues, Lys96, Ser171, Ser172, Ser173, Gly169, and catalytic water interactions.

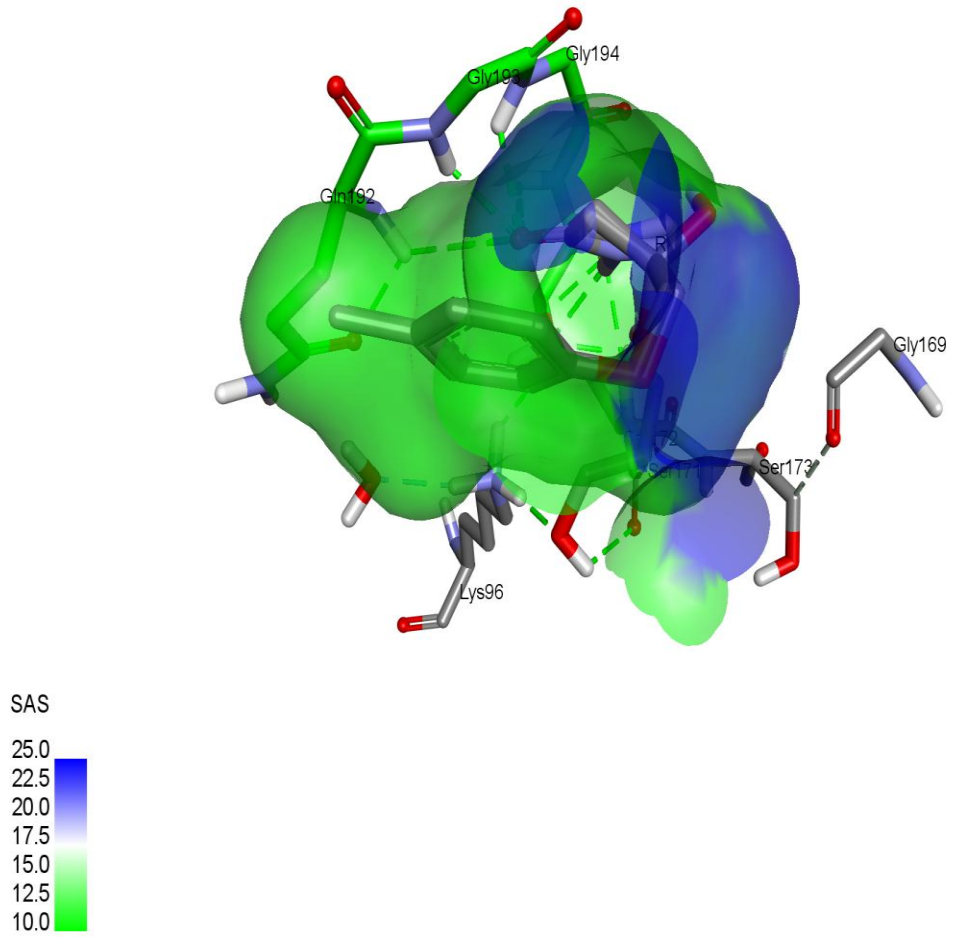


Figure A2-6: Channel view, showing substrate entrance point. Green area indicates hydrophobic binding pocket region while with the blue zone identifies more polar region in the catalytic site. Interaction with Ser 171, Ser172, Ser173, Gly169, Lys96 as well as the catalytic water are visible.

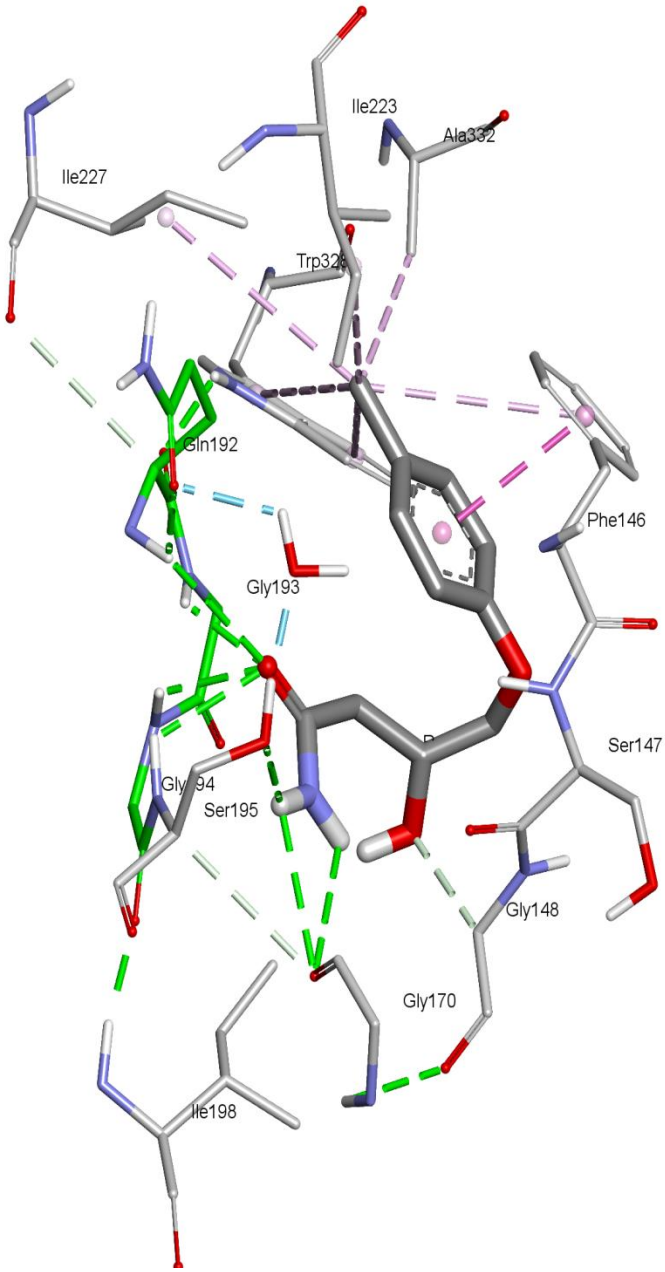


Figure A2-7: Face on pi-pi stacking between the aromatic substrate (3-hydroxy-4-benzyloxybutanamide) and Phe146 noted. Ionic interaction noted between the para-substituted functional group on the aromatic ring and Trp326, Ile227, Ala332, Ile223.

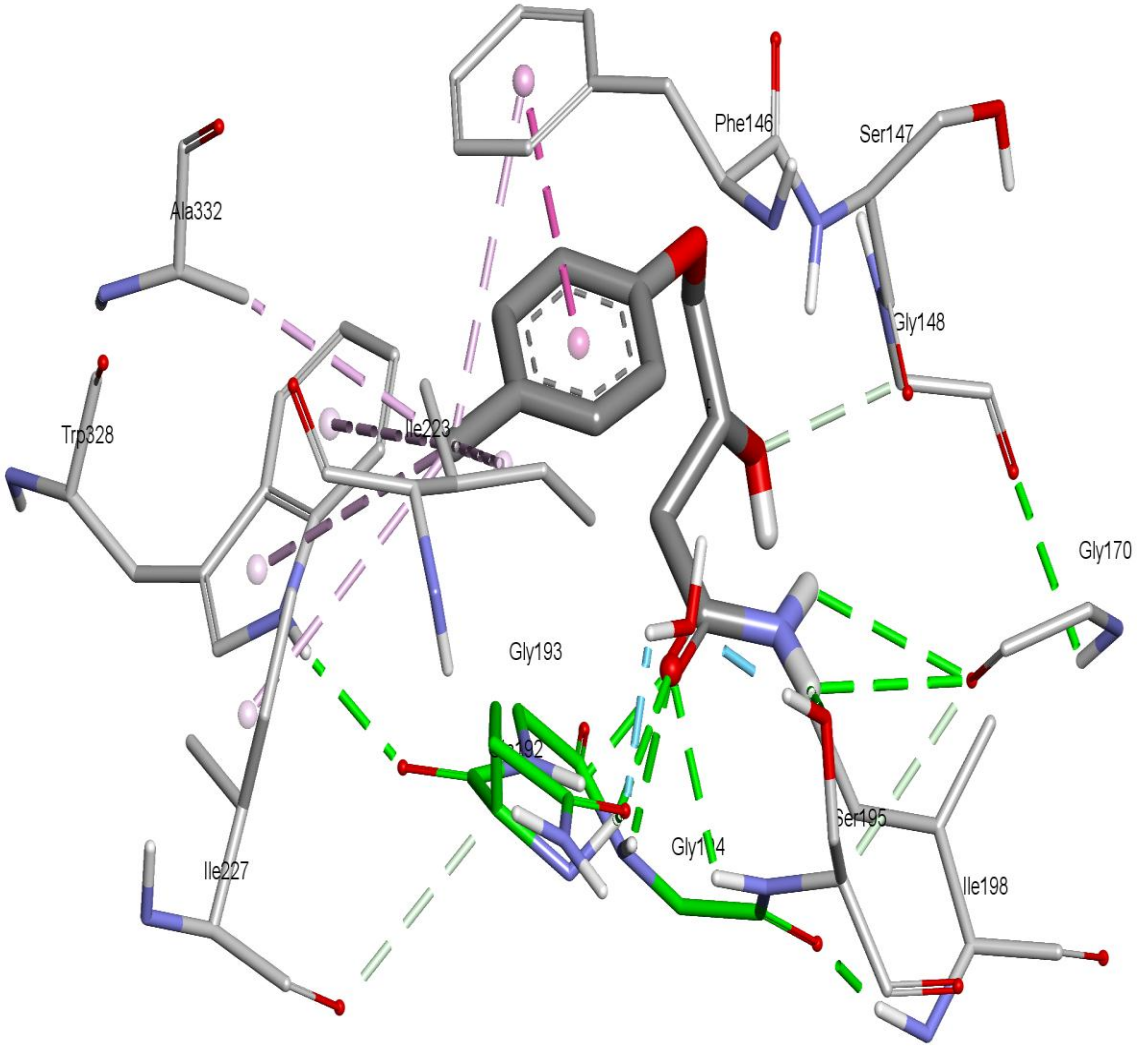


Figure A2-8: Pi-pi stacking of Phe146 and aromatic amide substrate. Covalent bonding observed between hydrophobic amino acids found present in substrate binding pocket.

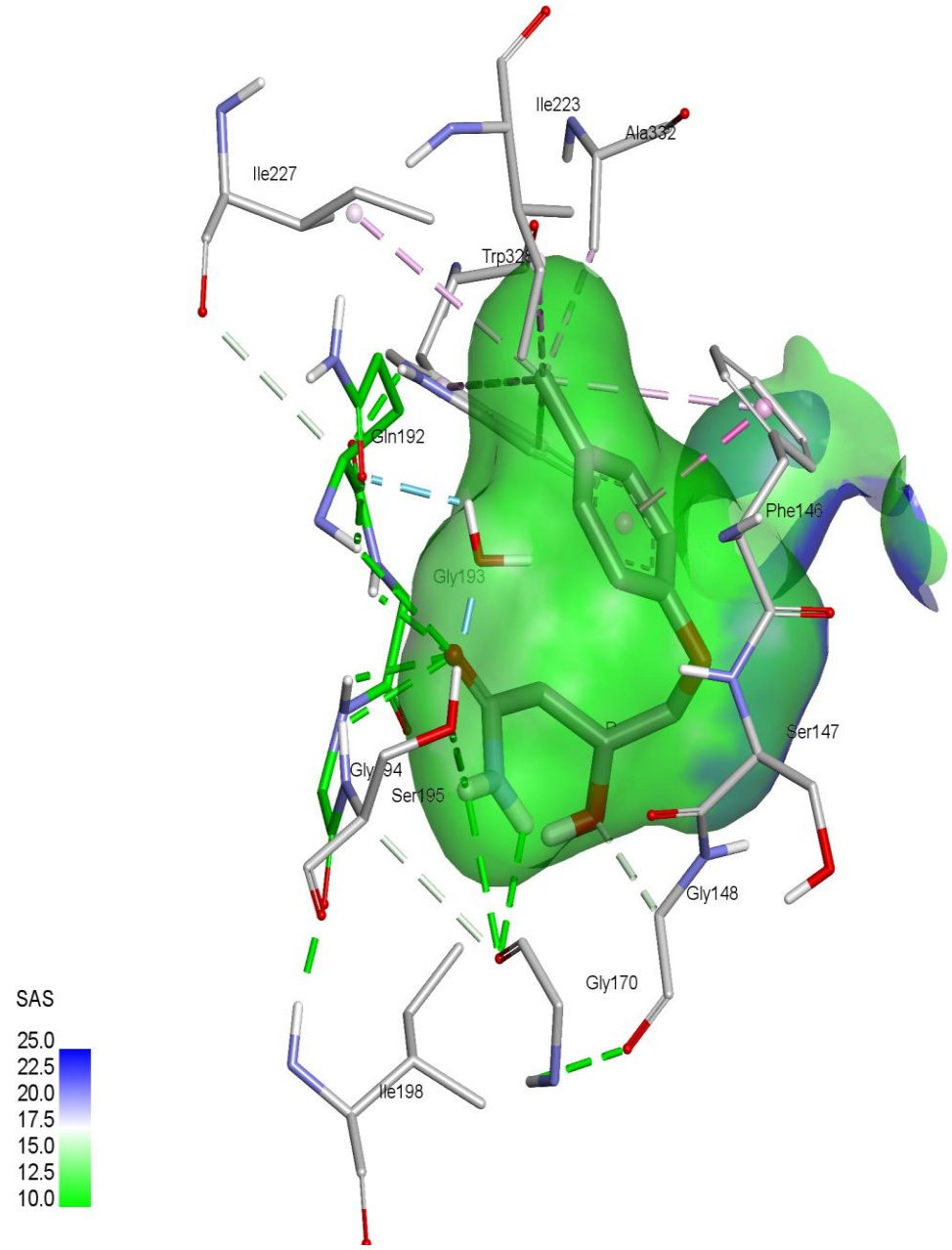


Figure A2-9: Crystal structure additional image 1.

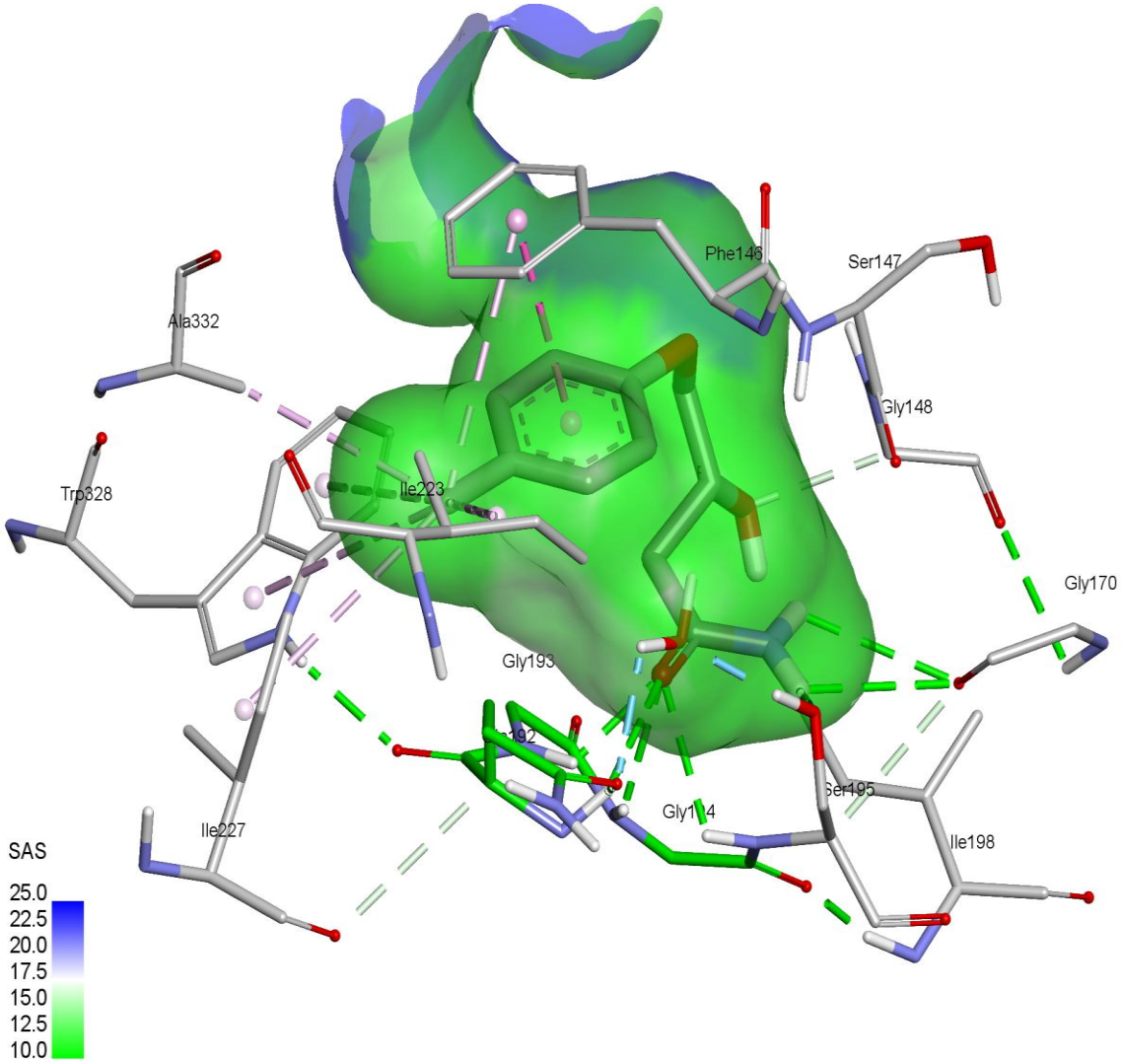


Figure A2-10: Crystal structure additional image 2.

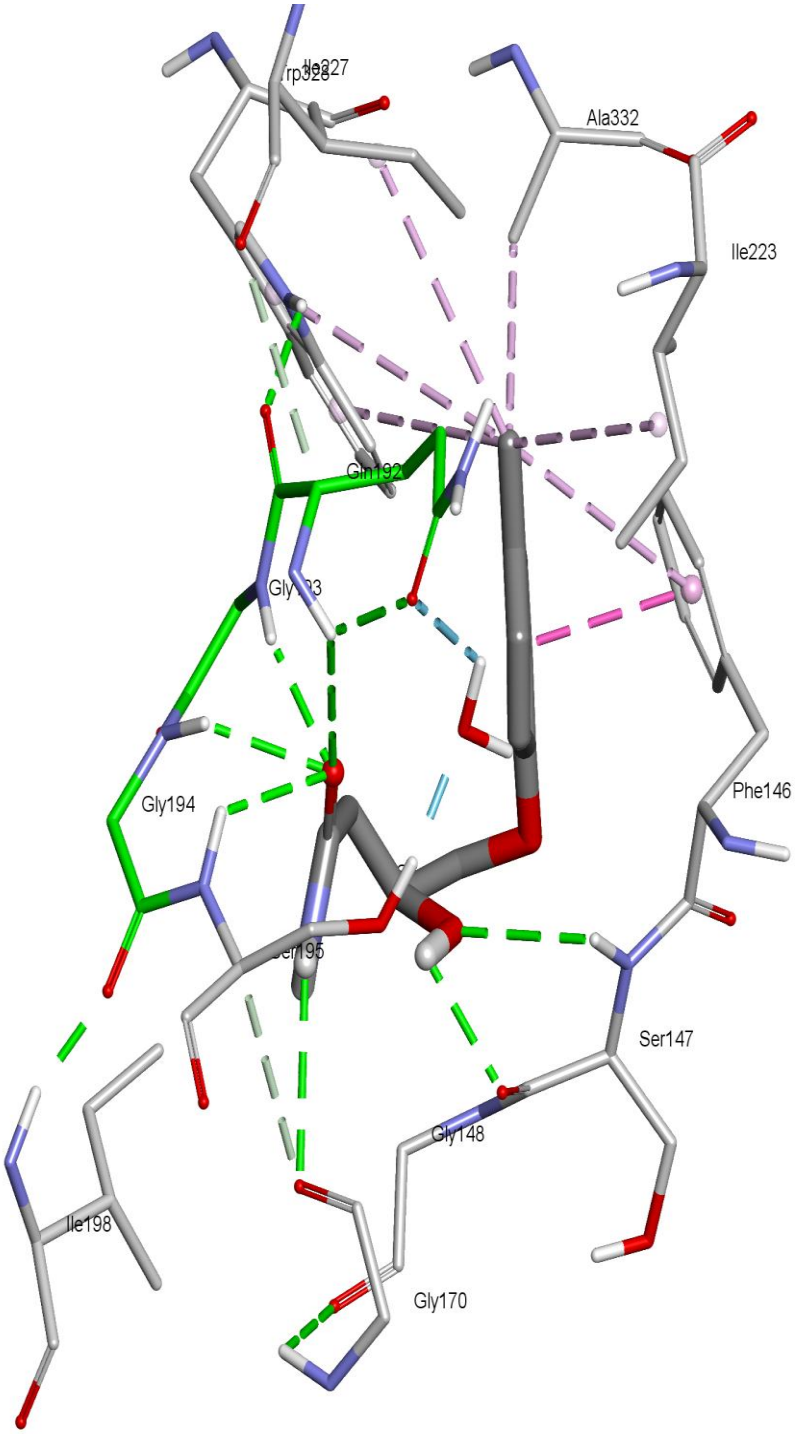


Figure A2-11: Crystal structure additional image 3.

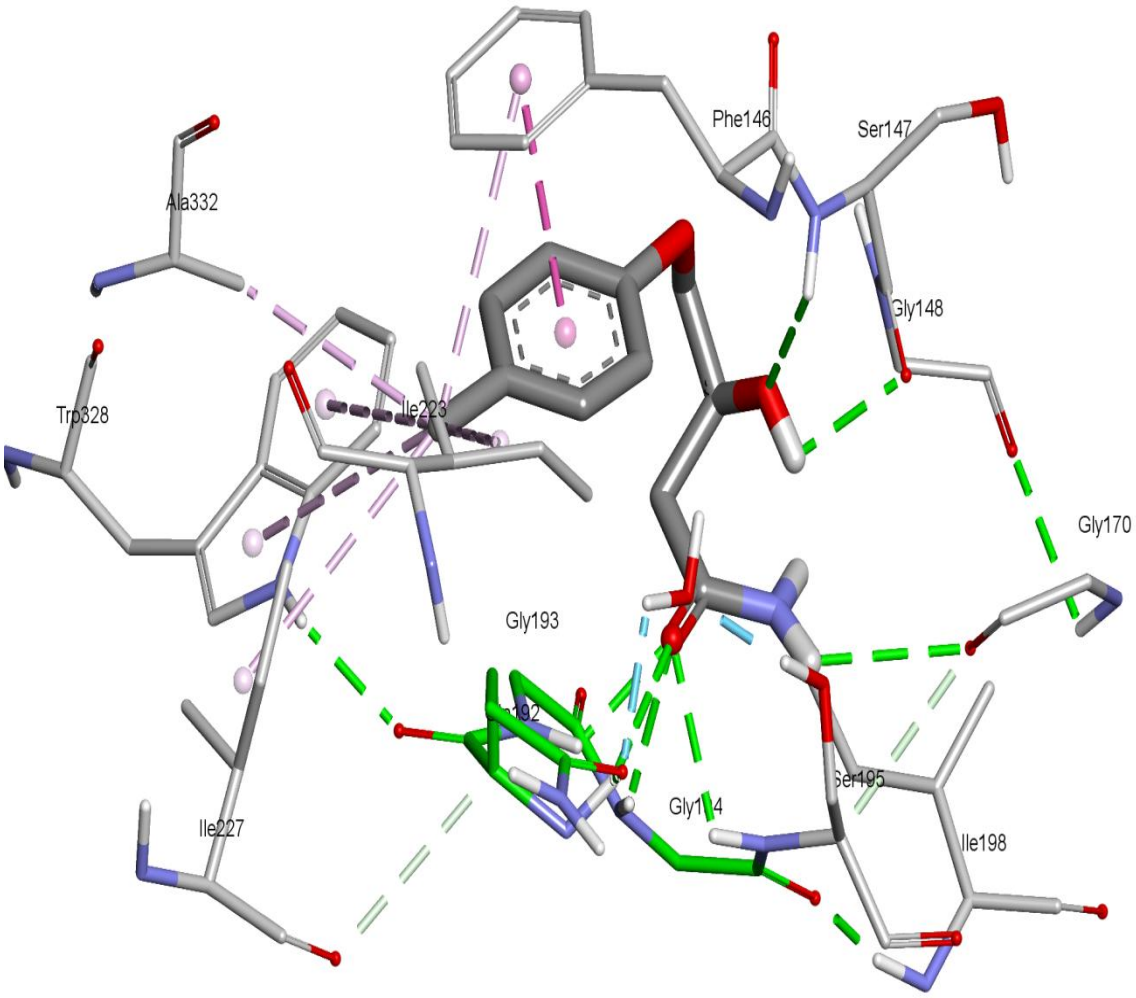


Figure A2-12: Crystal structure additional image 4.

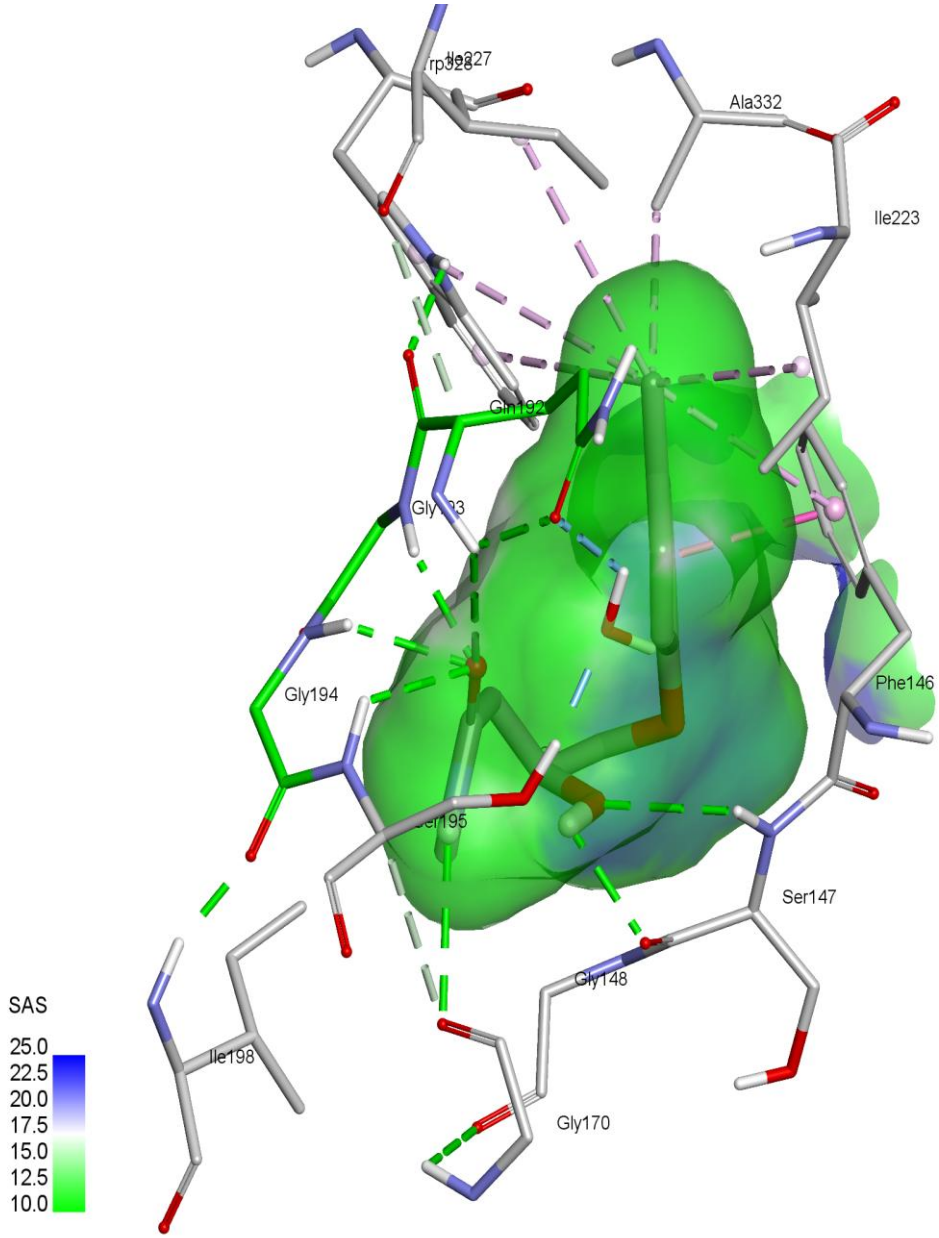


Figure A2-13: Crystal structure additional image 5.

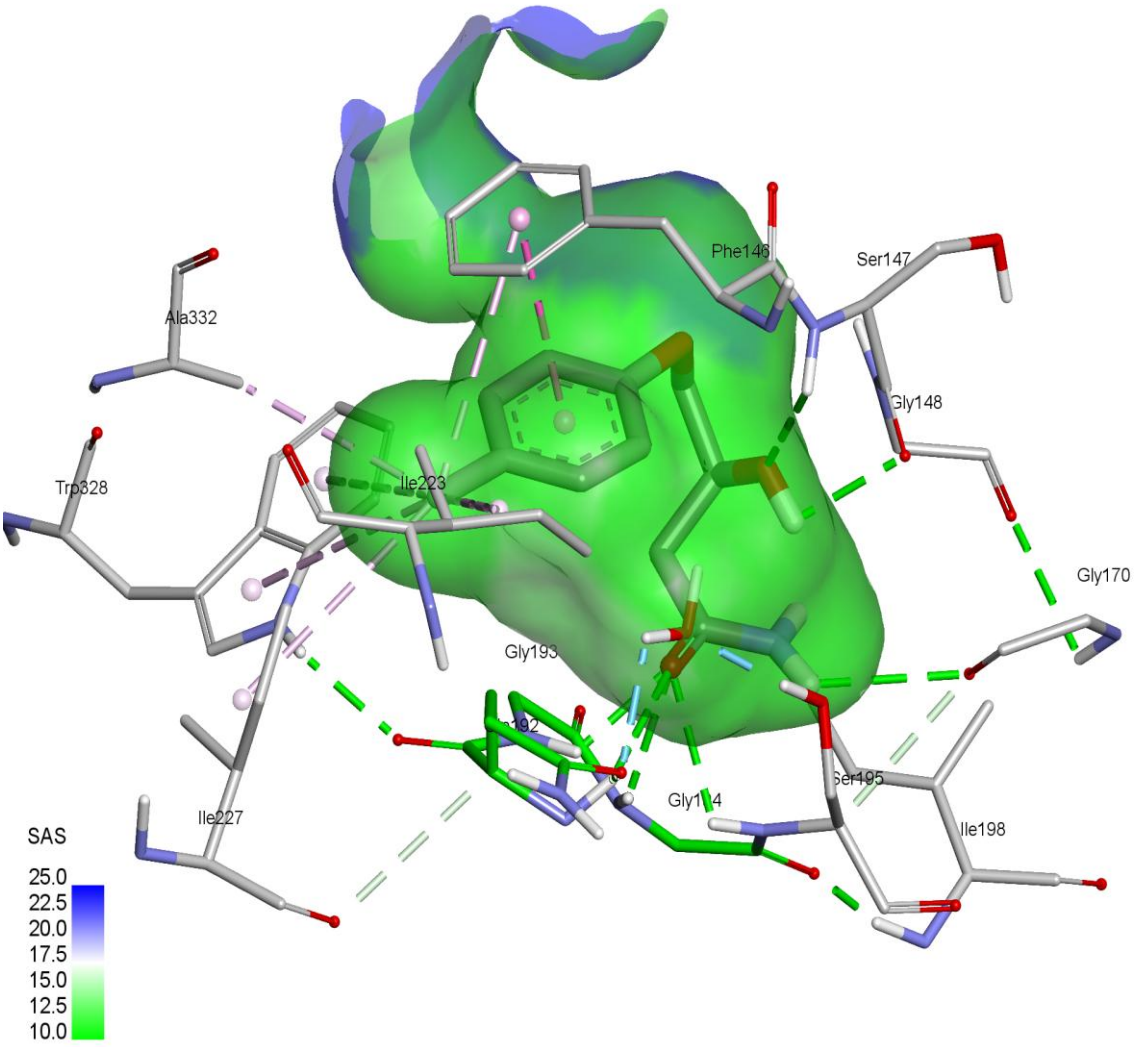
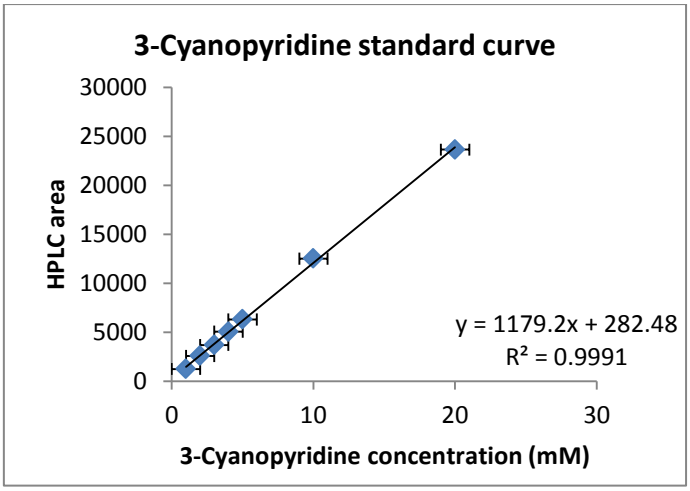
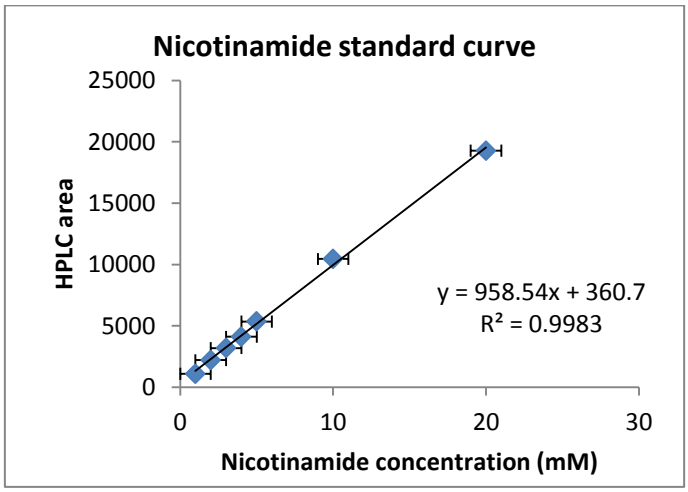
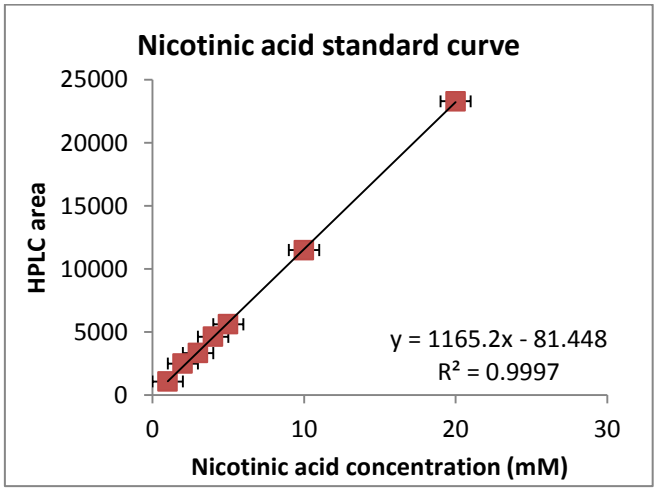


Figure A2-14: Crystal structure additional image 6.

Appendix 3: 3-CP, Nicotinamide and Nicotinic Acid Standard Curves.







Appendix 4: SDS-PAGE Report

ATCC BAA-870-SDS-PAGE Report

Lane 1- Molecular weight Marker (Thermofischer, PageRuler Plus Prestained Protein ladder- Thermoscientific, Cat No: 26634).

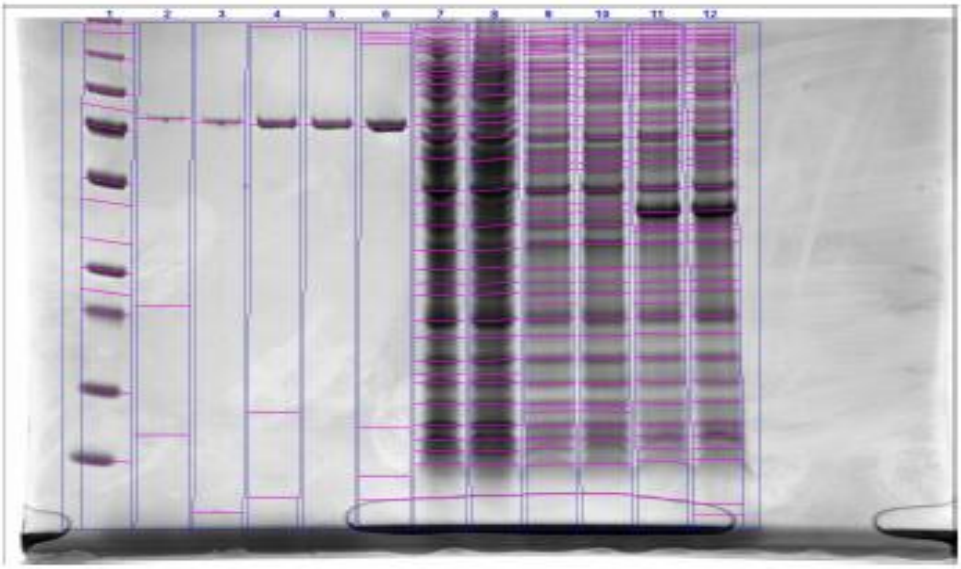
Lane2-6: BSA standard curve (100ng -800 ng).

Lane 7- Control cell proteins.

Lane 9- BNZ-induced cell proteins.

Lane 11- DMF-induced cell proteins.

Image Report: Varsha Chhiba 2017-03-02 08hr 43min



Acquisition Information

Imager	ChemiDoc™ MP
Exposure Time (sec)	0.088 (Auto - Intense Bands)
Serial Number	731BR01206
Software Version	4.1
Application	Coomassie Blue
Excitation Source	White Trans Illumination
Emission Filter	Standard Filter

Image Information

Acquisition Date	02/03/2017 08:43
User Name	Varsha Chhiba
Image Area (mm)	X: 90.0 Y: 67.2
Pixel Size (um)	X: 84.7 Y: 84.7
Data Range (Int)	0 - 51771

Analysis Settings

Detection	Lane detection: Automatically detected lanes Band detection: Automatically detected bands with sensitivity: High Lane Background Subtraction: Lane background subtracted with disk size: 10

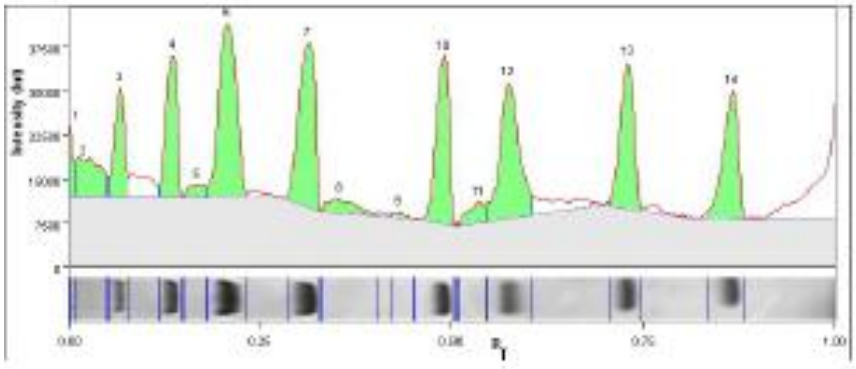
1

Lane 2-6: BSA Standard Curve

Quantity Analysis	Quantity Standard Bands: Lane 2 Band 1 Quantity 100.0 Lane 3 Band 1 Quantity 200.0 Lane 4 Band 2 Quantity 400.0 Lane 5 Band 2 Quantity 600.0 Lane 6 Band 4 Quantity 800.0 Quantity regression method: Linear Regression equation: y = 1.8E-005 * x - 24.7 R-squared value: R^2 = 0.952183

Lane And Band Analysis

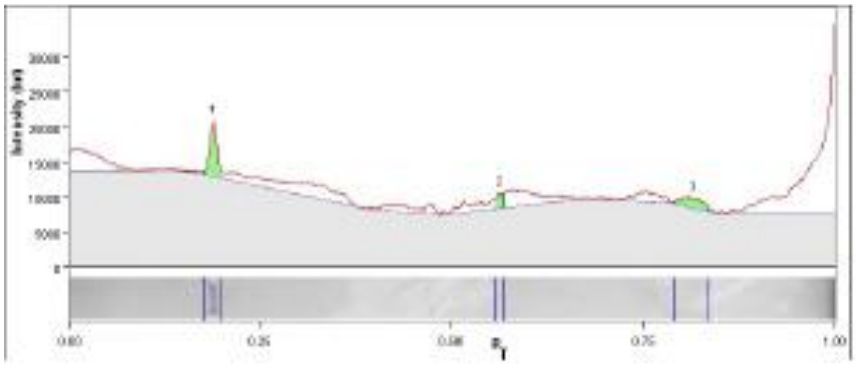
Lane 1



Band No.	Band Label	Mol. Wt. (KDa)	Relative Front	Volume (Int)	Abs. Quant.	Rel. Quant.	Band %	Lane %
1		N/A	0.001	3 842 225	33.5	N/A	1.0	0.9
2		N/A	0.019	18 102 300	264.6	N/A	5.0	4.3
3		N/A	0.087	19 815 425	288.7	N/A	5.4	4.6
4		N/A	0.135	30 479 175	462.3	N/A	8.4	7.2
5		N/A	0.168	3 698 625	34.4	N/A	1.0	0.9
6		N/A	0.207	58 182 600	904.9	N/A	15.9	13.7
7		N/A	0.313	51 354 225	795.8	N/A	14.1	12.1
8		N/A	0.355	7 584 525	98.5	N/A	2.1	1.8
9		N/A	0.432	1 269 825	N/A	N/A	0.3	0.3
10		N/A	0.490	39 867 225	612.3	N/A	10.9	9.4
11		N/A	0.533	6 606 250	80.7	N/A	1.8	1.6
12		N/A	0.572	49 877 775	772.2	N/A	13.7	11.8
13		N/A	0.728	38 602 975	590.5	N/A	10.6	9.1
14		N/A	0.888	36 041 850	551.2	N/A	9.9	8.5

Band Detection	Automatically detected bands with sensitivity: High
Lane Background	Lane background subtracted with disk size: 10

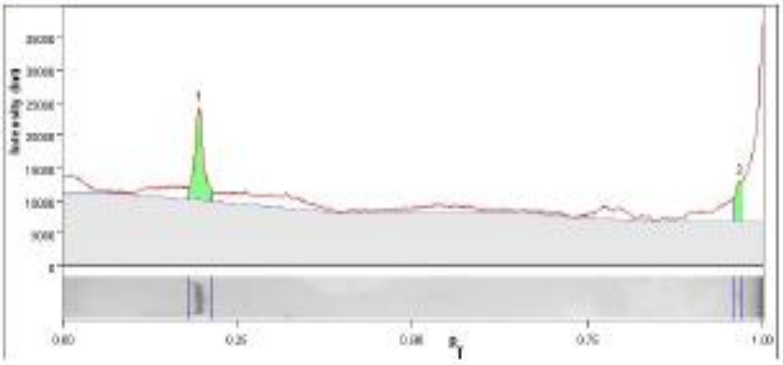
Lane 2



Band No.	Band Label	Mol. Wt. (KDa)	Relative Front	Volume (Int)	Abs. Quant.	Rel. Quant.	Band %	Lane %
1		N/A	0.189	5 915 100	100.0	N/A	51.9	5.3
2		N/A	0.560	1 789 950	3.9	N/A	15.7	1.6
3		N/A	0.815	3 690 300	34.3	N/A	32.4	3.3

Band Detection	Automatically detected bands with sensitivity: High
Lane Background	Lane background subtracted with disk size: 10

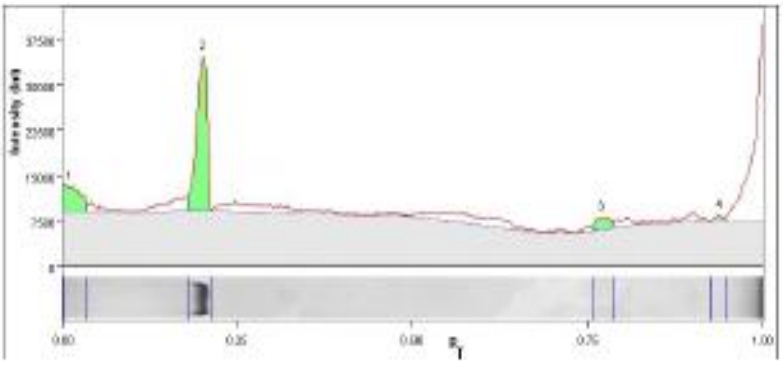
Lane 3



Band No.	Band Label	Mol. Wt. (KDa)	Relative Front	Volume (Int)	Abs. Quant.	Rel. Quant.	Band %	Lane %
1		N/A	0.198	15 060 450	200.0	N/A	74.1	13.3
2		N/A	0.968	5 261 475	69.4	N/A	25.9	4.6

Band Detection	Automatically detected bands with sensitivity: High
Lane Background	Lane background subtracted with disk size: 10

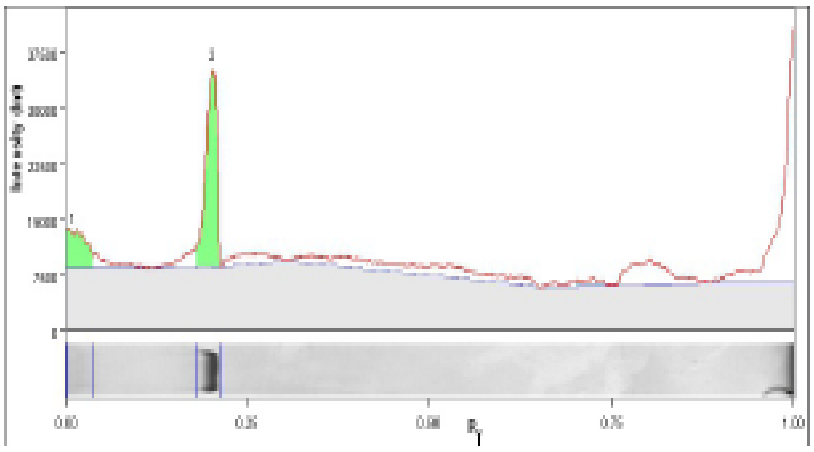
Lane 4



Band No.	Band Label	Mol. Wt. (KDa)	Relative Front	Volume (Int)	Abs. Quant.	Rel. Quant.	Band %	Lane %
1		N/A	0.008	8 807 475	116.0	N/A	19.1	7.0
2		N/A	0.201	32 832 750	400.0	N/A	71.0	26.1
3		N/A	0.769	3 582 075	32.6	N/A	7.8	2.9
4		N/A	0.938	990 450	N/A	N/A	2.1	0.8

Band Detection	Automatically detected bands with sensitivity: High
Lane Background	Lane background subtracted with disk size: 10

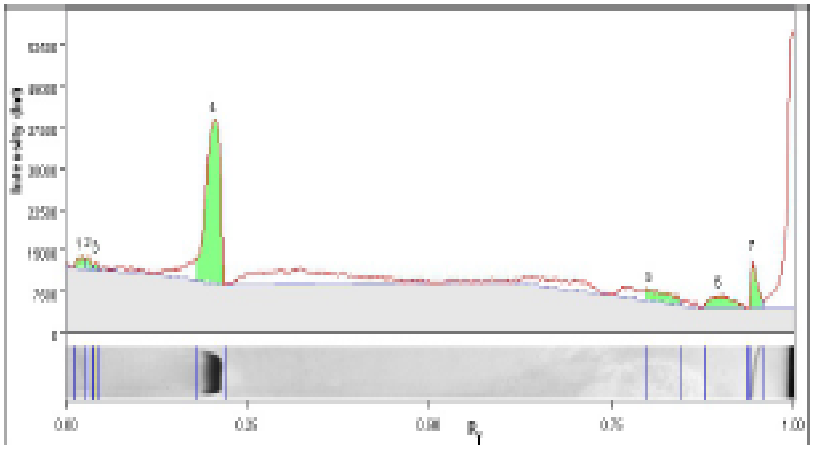
Lane 5



Band No.	Band Label	Mol. Wt. (KDa)	Relative Front	Volume (Int)	Abs. Quant.	Rel. Quant.	Band %	Lane %
1		N/A	0.011	11 297 775	155.8	N/A	24.3	7.5
2		N/A	0.202	35 112 450	600.0	N/A	75.7	23.2

Band Detection	Automatically detected bands with sensitivity: High
Lane Background	Lane background subtracted with disk size: 10

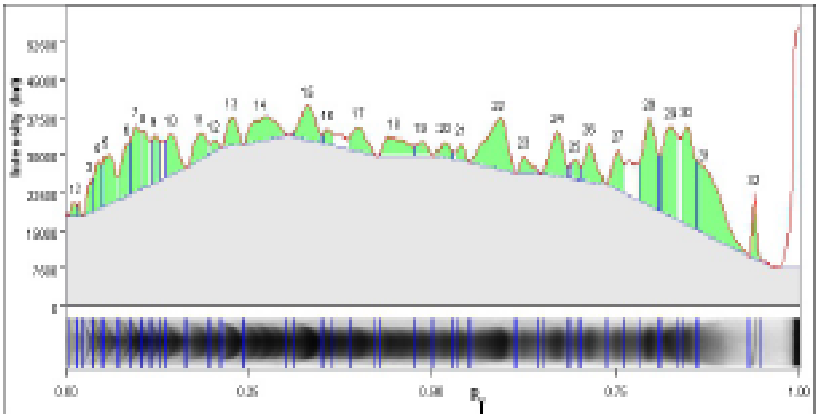
Lane 6



Band No.	Band Label	Mol. Wt. (KDa)	Relative Front	Volume (Int)	Abs. Quant.	Rel. Quant.	Band %	Lane %
1		N/A	0.020	2 017 850	7.8	N/A	2.8	1.2
2		N/A	0.030	1 038 000	N/A	N/A	1.4	0.6
3		N/A	0.042	725 550	N/A	N/A	1.0	0.4
4		N/A	0.204	50 237 625	800.0	N/A	69.7	29.1
5		N/A	0.801	5 998 425	71.2	N/A	8.3	3.5
6		N/A	0.898	5 877 900	69.2	N/A	8.1	3.4
7		N/A	0.943	6 229 500	74.9	N/A	8.6	3.6

Band Detection	Automatically detected bands with sensitivity: High
Lane Background	Lane background subtracted with disk size: 10

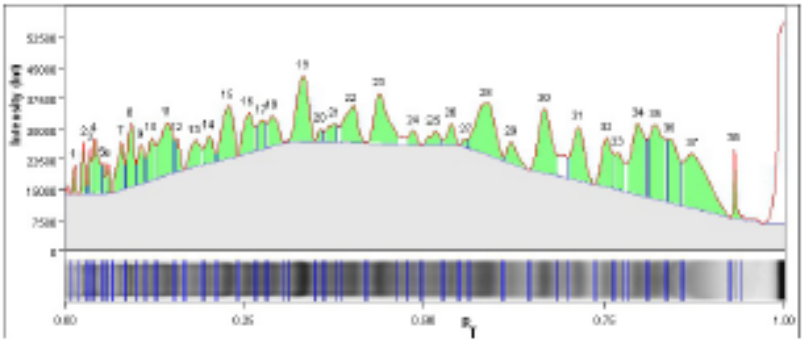
Lane 7: ATCC BAA-870 control cells.



Band No.	Band Label	Mol. Wt. (KDa)	Relative Front	Volume (Int)	Abs. Quant.	Rel. Quant.	Band %	Lane %
1		N/A	0.010	1 788 125	3.9	N/A	0.5	0.4
2		N/A	0.018	906 825	N/A	N/A	0.3	0.2
3		N/A	0.033	4 111 875	41.0	N/A	1.2	1.0
4		N/A	0.045	8 425 050	109.9	N/A	2.5	2.1
5		N/A	0.056	12 322 350	172.2	N/A	3.7	3.1
6		N/A	0.084	10 340 475	140.5	N/A	3.1	2.6
7		N/A	0.096	12 773 025	179.4	N/A	3.9	3.2
8		N/A	0.106	7 803 450	101.4	N/A	2.4	2.0
9		N/A	0.122	6 679 500	82.1	N/A	2.0	1.7
10		N/A	0.144	10 092 750	136.6	N/A	3.1	2.5
11		N/A	0.183	7 549 200	95.9	N/A	2.3	1.9
12		N/A	0.202	1 695 075	2.4	N/A	0.5	0.4
13		N/A	0.228	6 610 950	81.0	N/A	2.0	1.7
14		N/A	0.267	13 232 325	186.7	N/A	4.0	3.3
15		N/A	0.331	11 388 275	157.0	N/A	3.4	2.8
16		N/A	0.359	2 520 300	15.6	N/A	0.8	0.6
17		N/A	0.401	7 773 225	99.5	N/A	2.4	1.9
18		N/A	0.451	9 668 175	129.8	N/A	2.9	2.4
19		N/A	0.487	3 063 675	24.3	N/A	0.9	0.8
20		N/A	0.516	3 374 100	29.2	N/A	1.0	0.8
21		N/A	0.538	2 701 575	18.5	N/A	0.8	0.7
22		N/A	0.589	24 184 350	361.7	N/A	7.3	6.0
23		N/A	0.623	4 060 575	40.2	N/A	1.2	1.0
24		N/A	0.669	12 885 900	181.2	N/A	3.9	3.2
25		N/A	0.694	3 101 175	24.9	N/A	0.9	0.8
26		N/A	0.713	9 514 725	127.3	N/A	2.9	2.4
27		N/A	0.752	8 689 425	114.2	N/A	2.6	2.2
28		N/A	0.795	27 013 200	406.9	N/A	8.2	6.7
29		N/A	0.825	27 841 025	417.0	N/A	8.4	6.9
30		N/A	0.848	27 314 325	411.7	N/A	8.3	6.8
31		N/A	0.872	35 976 750	550.1	N/A	10.9	9.0
32		N/A	0.939	5 296 500	80.0	N/A	1.6	1.3

Band Detection	Automatically detected bands with sensitivity: High
Lane Background	Lane background subtracted with disk size: 10

Lane 9: ATCC BAA-870 BNZ-induced cells.

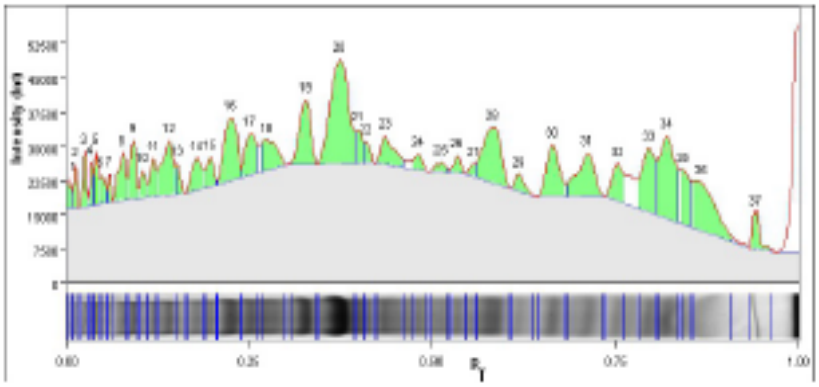


Band No.	Band Label	Mol. Wt. (KDa)	Relative Front	Volume (Int)	Abs. Quant.	Rel. Quant.	Band %	Lane %
1		N/A	0.014	2 052 975	8.1	N/A	0.5	0.4
2		N/A	0.027	4 859 300	49.8	N/A	1.1	0.9
3		N/A	0.035	4 082 850	40.6	N/A	0.9	0.8
4		N/A	0.042	9 108 450	120.9	N/A	2.1	1.8
5		N/A	0.053	2 487 750	15.1	N/A	0.6	0.5
6		N/A	0.060	2 562 900	18.3	N/A	0.6	0.5
7		N/A	0.079	9 283 575	123.7	N/A	2.1	1.8
8		N/A	0.093	12 461 175	174.4	N/A	2.9	2.5
9		N/A	0.106	6 662 175	81.8	N/A	1.5	1.3
10		N/A	0.121	8 503 425	111.2	N/A	2.0	1.7
11		N/A	0.143	19 144 875	281.2	N/A	4.4	3.8
12		N/A	0.156	4 487 325	47.0	N/A	1.0	0.9
13		N/A	0.182	7 492 350	95.0	N/A	1.7	1.5
14		N/A	0.201	6 408 900	77.7	N/A	1.5	1.3
15		N/A	0.228	17 095 650	248.5	N/A	3.9	3.4
16		N/A	0.256	11 298 975	155.9	N/A	2.6	2.2
17		N/A	0.276	5 566 500	64.3	N/A	1.3	1.1
18		N/A	0.289	8 179 800	106.0	N/A	1.9	1.6
19		N/A	0.332	22 414 125	333.4	N/A	5.2	4.4
20		N/A	0.357	1 628 775	1.4	N/A	0.4	0.3
21		N/A	0.377	5 104 875	56.9	N/A	1.2	1.0
22		N/A	0.400	14 087 250	200.4	N/A	3.2	2.8
23		N/A	0.439	20 059 050	295.8	N/A	4.6	4.0
24		N/A	0.486	3 197 475	26.4	N/A	0.7	0.6
25		N/A	0.513	3 544 950	32.0	N/A	0.8	0.7
26		N/A	0.535	4 498 650	47.2	N/A	1.0	0.9
27		N/A	0.557	1 319 550	N/A	N/A	0.3	0.3
28		N/A	0.584	27 882 425	420.5	N/A	6.4	5.5
29		N/A	0.619	6 555 900	80.1	N/A	1.5	1.3
30		N/A	0.666	24 341 700	364.2	N/A	5.6	4.8
31		N/A	0.713	18 320 775	268.0	N/A	4.2	3.6
32		N/A	0.752	14 050 800	199.8	N/A	3.2	2.8
33		N/A	0.788	8 792 025	115.8	N/A	2.0	1.7
34		N/A	0.797	26 315 925	395.8	N/A	6.1	5.2
35		N/A	0.820	28 824 525	435.9	N/A	6.6	5.7
36		N/A	0.841	20 028 675	295.3	N/A	4.6	4.0
37		N/A	0.873	38 505 275	558.6	N/A	8.4	7.2
38		N/A	0.930	5 524 500	83.6	N/A	1.3	1.1

Band Detection	Automatically detected bands with sensitivity: High
Lane Background	Lane background subtracted with disk size: 10

Lane 10

Lane 11: ATCC BAA-870 DMF-induced cells.



Band No.	Band Label	Mol. Wt. (KDa)	Relative Front	Volume (Int)	Abs. Quant.	Rel. Quant.	Band %	Lane %
1		N/A	0.002	2 448 500	14.4	N/A	0.8	0.5
2		N/A	0.012	3 006 600	23.4	N/A	0.8	0.7
3		N/A	0.025	5 144 700	57.5	N/A	1.3	1.1
4		N/A	0.033	3 023 925	23.6	N/A	0.8	0.7
5		N/A	0.041	5 193 900	58.3	N/A	1.3	1.1
6		N/A	0.048	3 221 475	26.8	N/A	0.8	0.7
7		N/A	0.058	2 103 600	8.9	N/A	0.5	0.5
8		N/A	0.077	9 087 375	120.5	N/A	2.3	2.0
9		N/A	0.092	9 660 675	129.7	N/A	2.4	2.1
10		N/A	0.104	3 503 625	32.7	N/A	0.9	0.8
11		N/A	0.119	5 569 425	64.3	N/A	1.4	1.2
12		N/A	0.140	15 757 575	227.1	N/A	4.0	3.4
13		N/A	0.152	3 532 875	31.8	N/A	0.9	0.8
14		N/A	0.179	8 348 325	108.7	N/A	2.1	1.8
15		N/A	0.197	5 507 475	63.3	N/A	1.4	1.2
16		N/A	0.225	20 907 150	309.4	N/A	5.3	4.6
17		N/A	0.252	11 182 725	154.0	N/A	2.8	2.4
18		N/A	0.276	11 200 050	154.3	N/A	2.8	2.4
19		N/A	0.328	18 295 050	267.6	N/A	4.6	4.0
20		N/A	0.375	48 290 775	748.9	N/A	12.2	10.5
21		N/A	0.400	5 322 975	80.4	N/A	1.3	1.2
22		N/A	0.411	2 738 025	19.1	N/A	0.7	0.6
23		N/A	0.437	9 815 475	132.2	N/A	2.5	2.1
24		N/A	0.462	3 335 175	28.6	N/A	0.8	0.7
25		N/A	0.511	2 099 475	8.9	N/A	0.5	0.5
26		N/A	0.532	3 150 075	25.7	N/A	0.8	0.7
27		N/A	0.555	1 841 550	4.8	N/A	0.5	0.4
28		N/A	0.581	25 718 250	386.2	N/A	6.5	5.6
29		N/A	0.616	4 252 275	43.3	N/A	1.1	0.9
30		N/A	0.663	17 050 200	247.7	N/A	4.3	3.7
31		N/A	0.711	19 303 575	283.7	N/A	4.9	4.2
32		N/A	0.752	9 712 650	130.5	N/A	2.5	2.1
33		N/A	0.796	20 600 025	304.5	N/A	5.2	4.5
34		N/A	0.819	31 606 950	481.8	N/A	8.0	6.9
35		N/A	0.842	11 173 425	153.8	N/A	2.8	2.4
36		N/A	0.867	26 661 675	401.3	N/A	6.7	5.8
37		N/A	0.941	6 808 950	84.1	N/A	1.7	1.5

Band Detection	Automatically detected bands with sensitivity: High
Lane Background	Lane background subtracted with disk size: 10

Strain A29-SDS-PAGE Report

Lane 12- Molecular weight Marker (Thermofischer, PageRuler Plus Prestained Protein ladder-Thermoscientific, Cat No: 26634).

Lane 12: Molecular weight marker

Lane 7-11: BSA standard curve (100ng -800 ng).

Lane 1-2- A29 Control cell proteins.

Lane 3-4- A29 BNZ-induced cell proteins.

Lane 5-6- A29 DMF-induced cell proteins.

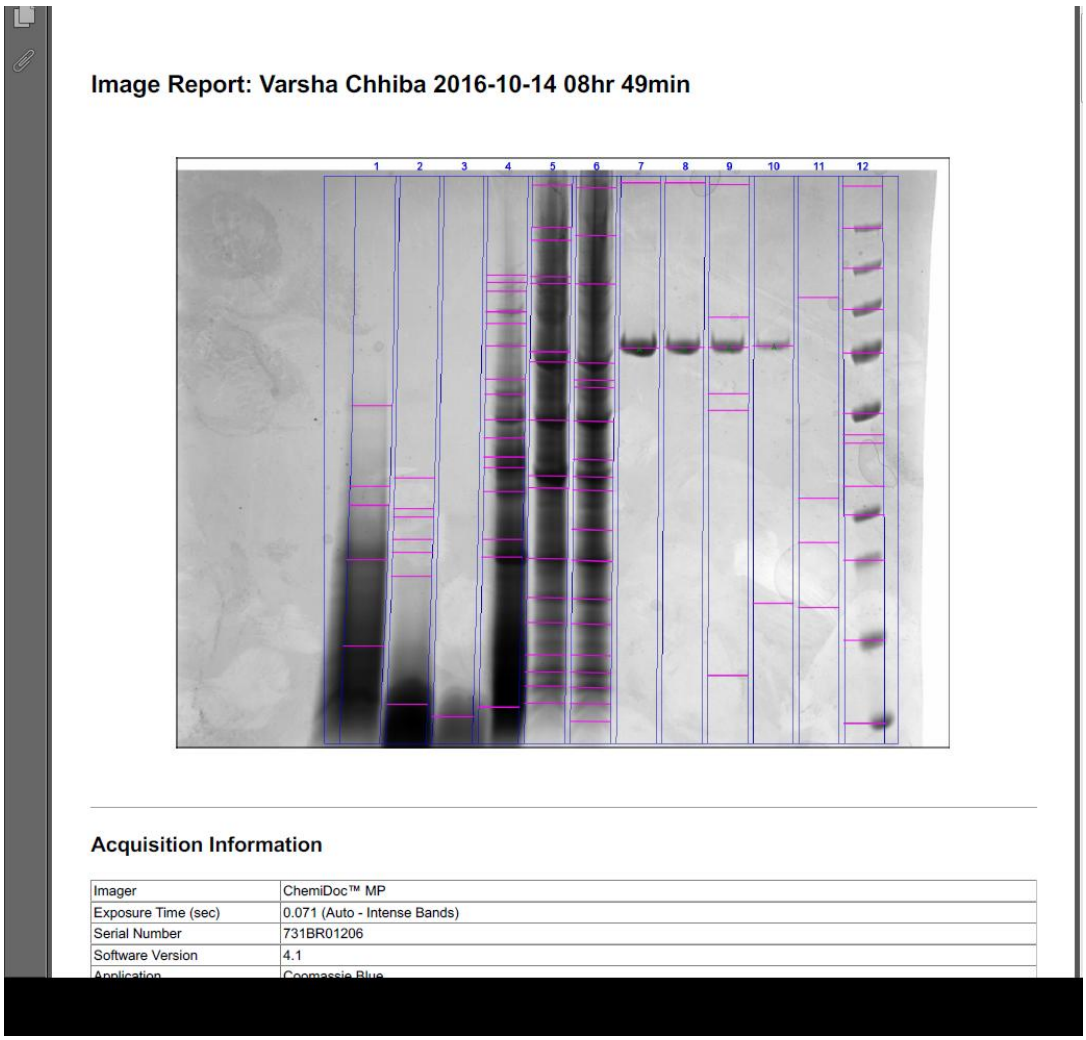


Image Report: Varsha Chhiba 2016-10-14 08hr 49min

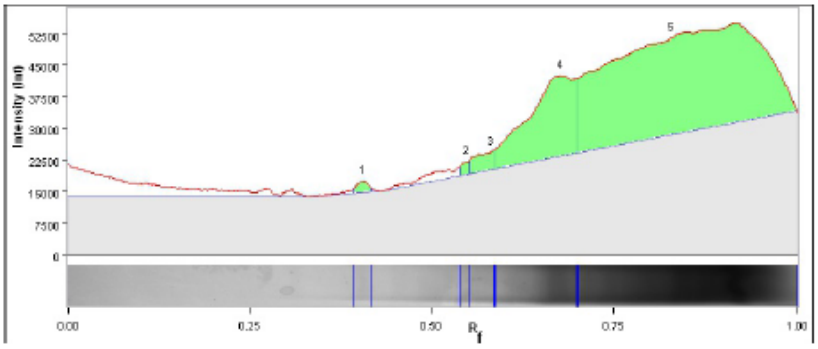
Acquisition Information

Imager	ChemiDoc™ MP
Exposure Time (sec)	0.071 (Auto - Intense Bands)
Serial Number	731BR01206
Software Version	4.1
Application	Coomassie Blue

Lane 1-2: A29 Control cells.

Lane And Band Analysis

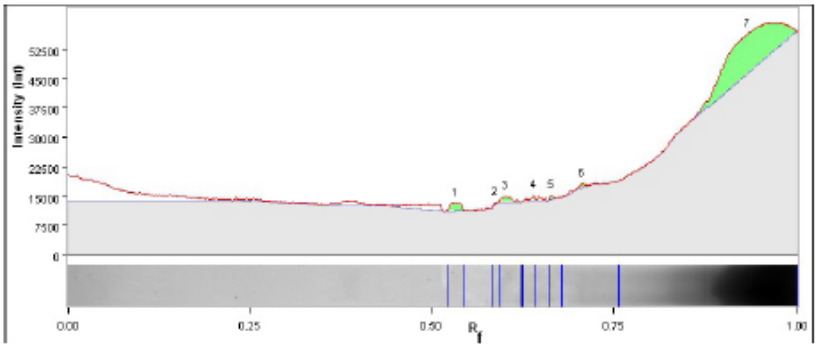
Lane 1



Band No.	Band Label	Mol. Wt. (KDa)	Relative Front	Volume (Int)	Abs. Quant.	Rel. Quant.	Band %	Lane %
1		N/A	0.405	3 706 575	16.7	N/A	0.7	0.6
2		N/A	0.548	2 858 534	6.2	N/A	0.5	0.4
3		N/A	0.581	10 377 899	98.8	N/A	1.8	1.6
4		N/A	0.677	109 435 687	1 317.8	N/A	19.3	17.0
5		N/A	0.829	440 086 486	5 386.8	N/A	77.7	68.4

Band Detection	Automatically detected bands with sensitivity: High
Lane Background	Lane background subtracted with disk size: 10

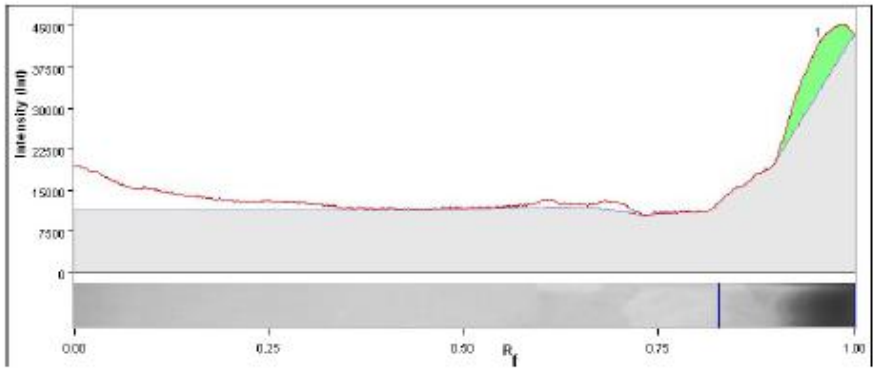
Lane 2



Band No.	Band Label	Mol. Wt. (KDa)	Relative Front	Volume (Int)	Abs. Quant.	Rel. Quant.	Band %	Lane %
1		N/A	0.533	2 755 239	4.9	N/A	3.7	2.3
2		N/A	0.587	200 823	N/A	N/A	0.3	0.2
3		N/A	0.601	1 822 737	N/A	N/A	2.5	1.5
4		N/A	0.641	532 754	N/A	N/A	0.7	0.4
5		N/A	0.664	455 374	N/A	N/A	0.6	0.4
6		N/A	0.706	1 286 041	N/A	N/A	1.7	1.1
7		N/A	0.931	66 697 034	791.8	N/A	90.4	54.5

Lane 3-4: A29 BNZ induced cells

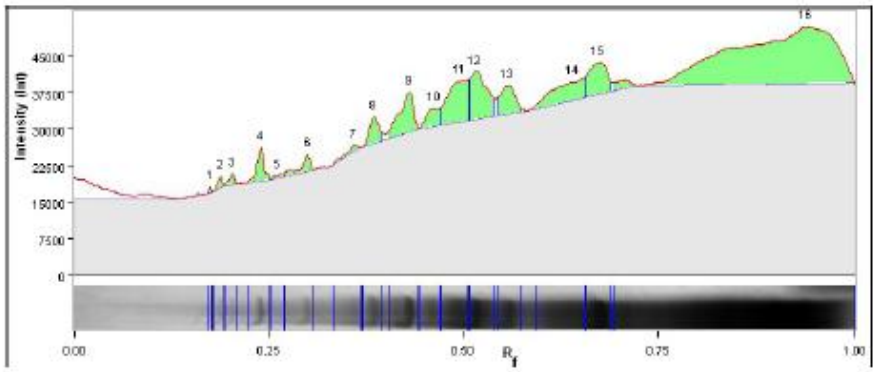
Lane 3



Band No.	Band Label	Mol. Wt. (KDa)	Relative Front	Volume (Int)	Abs. Quant.	Rel. Quant.	Band %	Lane %
1		N/A	0.953	43 290 825	503.8	N/A	100.0	32.4

Band Detection	Automatically detected bands with sensitivity: High
Lane Background	Lane background subtracted with disk size: 10

Lane 4

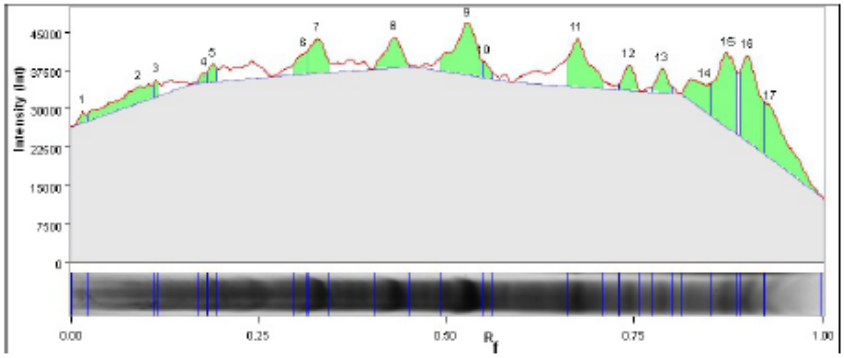


Band No.	Band Label	Mol. Wt. (KDa)	Relative Front	Volume (Int)	Abs. Quant.	Rel. Quant.	Band %	Lane %
1		N/A	0.175	322 733	N/A	N/A	0.1	0.1
2		N/A	0.188	1 076 677	N/A	N/A	0.4	0.4
3		N/A	0.204	1 264 360	N/A	N/A	0.5	0.5
4		N/A	0.240	5 513 033	38.9	N/A	2.3	2.1
5		N/A	0.261	625 683	N/A	N/A	0.3	0.2
6		N/A	0.300	3 647 664	15.9	N/A	1.5	1.4
7		N/A	0.358	1 558 258	N/A	N/A	0.6	0.6
8		N/A	0.385	5 462 006	38.3	N/A	2.2	2.1
9		N/A	0.430	13 107 515	132.3	N/A	5.3	5.0
10		N/A	0.462	5 516 610	38.9	N/A	2.3	2.1
11		N/A	0.496	19 172 282	207.0	N/A	7.8	7.3
12		N/A	0.514	17 753 527	189.5	N/A	7.2	6.7
13		N/A	0.556	9 275 161	85.2	N/A	3.8	3.5
14		N/A	0.641	14 726 874	152.3	N/A	6.0	5.6
15		N/A	0.672	13 004 147	131.1	N/A	5.3	4.9
16		N/A	0.936	132 981 910	1 607.5	N/A	54.3	50.4

Band Detection	Automatically detected bands with sensitivity: High

Lane 5-6: A29 DMF induced cells.

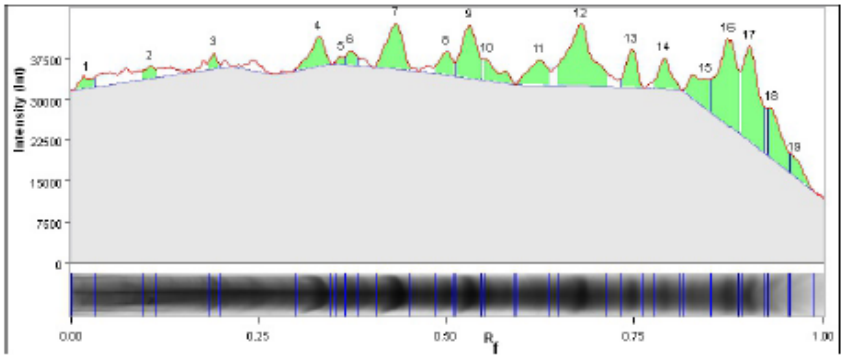
Lane 5



Band No.	Band Label	Mol. Wt. (KDa)	Relative Front	Volume (Int)	Abs. Quant.	Rel. Quant.	Band %	Lane %
1		N/A	0.017	1 585 341	N/A	N/A	0.7	0.6
2		N/A	0.091	14 837 542	153.6	N/A	6.9	5.6
3		N/A	0.114	1 714 697	N/A	N/A	0.8	0.6
4		N/A	0.178	1 521 904	N/A	N/A	0.7	0.6
5		N/A	0.190	3 134 255	9.6	N/A	1.5	1.2
6		N/A	0.310	5 103 430	33.8	N/A	2.4	1.9
7		N/A	0.328	11 620 432	114.0	N/A	5.4	4.4
8		N/A	0.431	11 948 348	118.1	N/A	5.6	4.5
9		N/A	0.529	26 160 499	293.0	N/A	12.2	9.9
10		N/A	0.550	2 469 444	1.4	N/A	1.1	0.9
11		N/A	0.675	20 713 823	225.9	N/A	9.6	7.8
12		N/A	0.743	6 343 335	49.1	N/A	3.0	2.4
13		N/A	0.787	5 738 749	41.7	N/A	2.7	2.2
14		N/A	0.844	12 618 342	126.3	N/A	5.9	4.8
15		N/A	0.875	26 936 489	302.5	N/A	12.5	10.2
16		N/A	0.899	33 516 782	383.5	N/A	15.6	12.7
17		N/A	0.929	28 912 161	326.8	N/A	13.5	10.9

Band Detection	Automatically detected bands with sensitivity: High
Lane Background	Lane background subtracted with disk size: 10

Lane 6

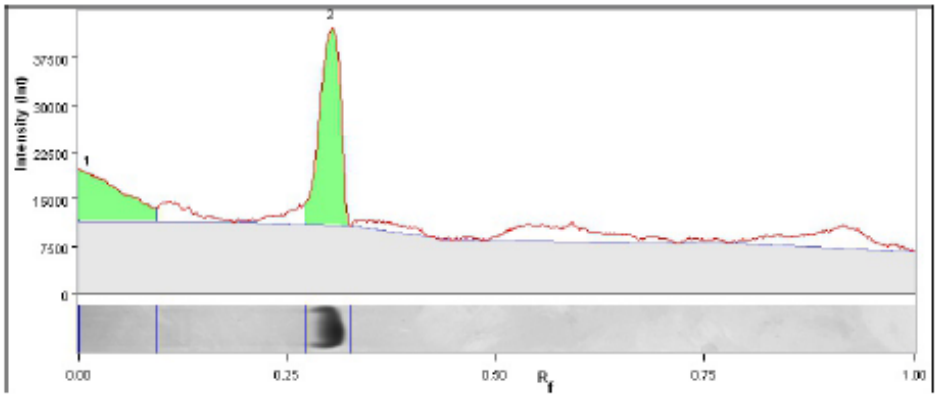


Band No.	Band Label	Mol. Wt. (KDa)	Relative Front	Volume (Int)	Abs. Quant.	Rel. Quant.	Band %	Lane %
1		N/A	0.022	3 222 147	10.7	N/A	1.5	1.3
2		N/A	0.106	2 747 428	4.9	N/A	1.2	1.1
3		N/A	0.191	2 282 418	N/A	N/A	1.0	0.9

4		N/A	0.330	9 603 442	89.2	N/A	4.3	3.7
5		N/A	0.360	1 274 507	N/A	N/A	0.6	0.5
6		N/A	0.373	2 672 530	3.9	N/A	1.2	1.0
7		N/A	0.433	16 265 130	171.2	N/A	7.4	6.3
8		N/A	0.500	6 065 278	45.7	N/A	2.7	2.4
9		N/A	0.531	17 240 775	183.2	N/A	7.8	6.7
10		N/A	0.554	6 958 068	56.7	N/A	3.1	2.7
11		N/A	0.624	9 968 223	93.7	N/A	4.5	3.9
12		N/A	0.679	32 500 695	371.0	N/A	14.7	12.7
13		N/A	0.746	9 105 509	83.1	N/A	4.1	3.6
14		N/A	0.790	8 381 787	74.2	N/A	3.8	3.3
15		N/A	0.845	11 035 264	106.8	N/A	5.0	4.3
16		N/A	0.876	30 247 623	343.3	N/A	13.7	11.8
17		N/A	0.902	31 333 498	356.6	N/A	14.2	12.2
18		N/A	0.930	14 826 957	153.5	N/A	6.7	5.8
19		N/A	0.962	5 502 375	38.8	N/A	2.5	2.1

Band Detection	Automatically detected bands with sensitivity: High
Lane Background	Lane background subtracted with disk size: 10

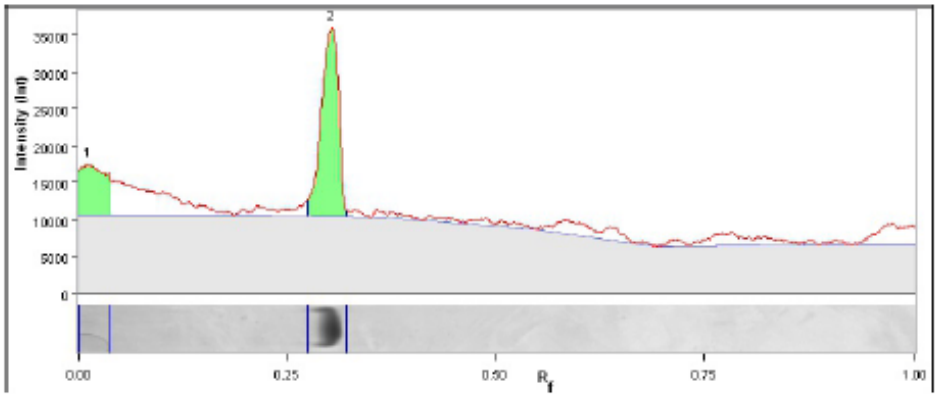
Lane 7



Band No.	Band Label	Mol. Wt. (KDa)	Relative Front	Volume (Int)	Abs. Quant.	Rel. Quant.	Band %	Lane %
1		N/A	0.013	36 772 509	423.6	N/A	35.0	19.6
2		N/A	0.304	68 171 999	800.0	N/A	65.0	36.4

Band Detection	Automatically detected bands with sensitivity: High
Lane Background	Lane background subtracted with disk size: 10

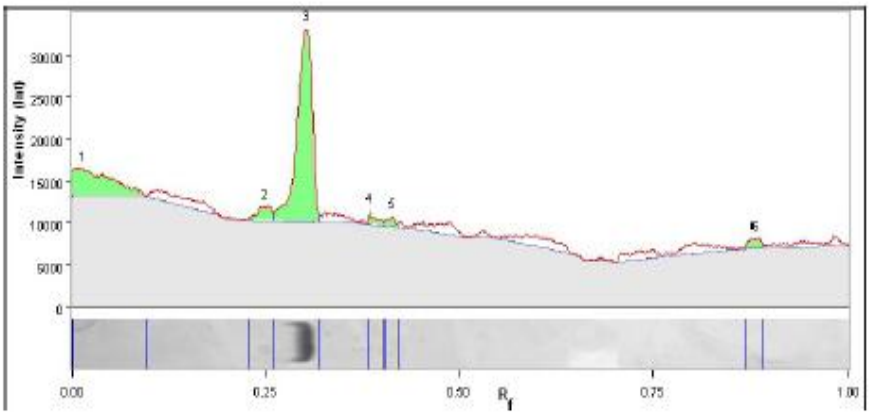
Lane 8



1		N/A	0.013	17 843 974	190.6	N/A	27.9	13.0
2		N/A	0.303	46 103 807	600.0	N/A	72.1	33.7

Band Detection	Automatically detected bands with sensitivity: High
Lane Background	Lane background subtracted with disk size: 10

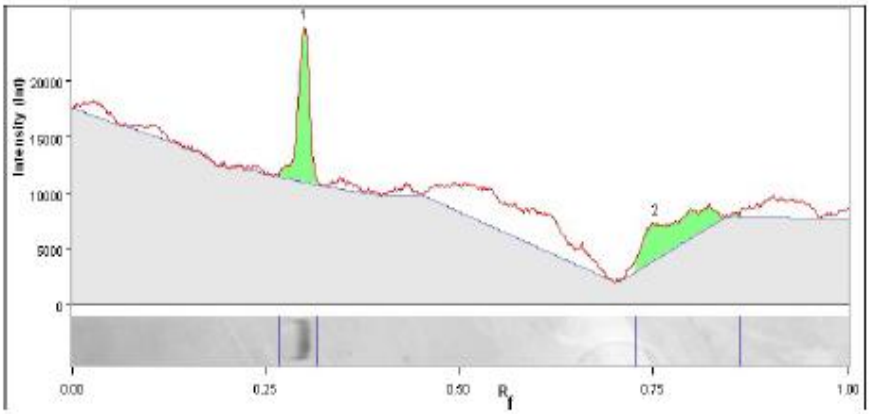
Lane 9



Band No.	Band Label	Mol. Wt. (KDa)	Relative Front	Volume (Int)	Abs. Quant.	Rel. Quant.	Band %	Lane %
1		N/A	0.016	14 480 572	149.2	N/A	23.8	15.3
2		N/A	0.250	2 931 096	7.1	N/A	4.8	3.1
3		N/A	0.303	39 511 542	400.0	N/A	65.0	41.8
4		N/A	0.384	1 212 165	N/A	N/A	2.0	1.3
5		N/A	0.413	1 200 996	N/A	N/A	2.0	1.3
6		N/A	0.881	1 450 729	N/A	N/A	2.4	1.5

Band Detection	Automatically detected bands with sensitivity: High
Lane Background	Lane background subtracted with disk size: 10

Lane 10



Band No.	Band Label	Mol. Wt. (KDa)	Relative Front	Volume (Int)	Abs. Quant.	Rel. Quant.	Band %	Lane %
1		N/A	0.300	18 147 435	200.0	N/A	48.6	18.0
2		N/A	0.753	19 177 757	207.0	N/A	51.4	19.0

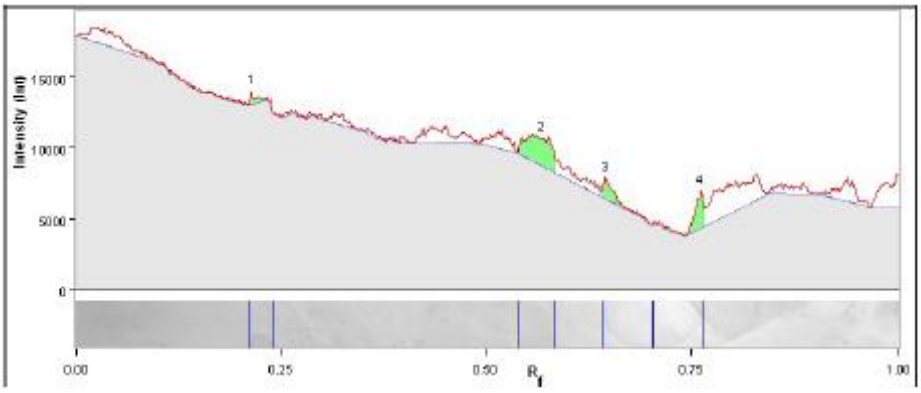
Band Detection	Automatically detected bands with sensitivity: High
Lane Background	Lane background subtracted with disk size: 10

Lane 11

2		N/A	0.753	19 177 757	207.0	N/A	51.4	19.0

Band Detection	Automatically detected bands with sensitivity: High
Lane Background	Lane background subtracted with disk size: 10

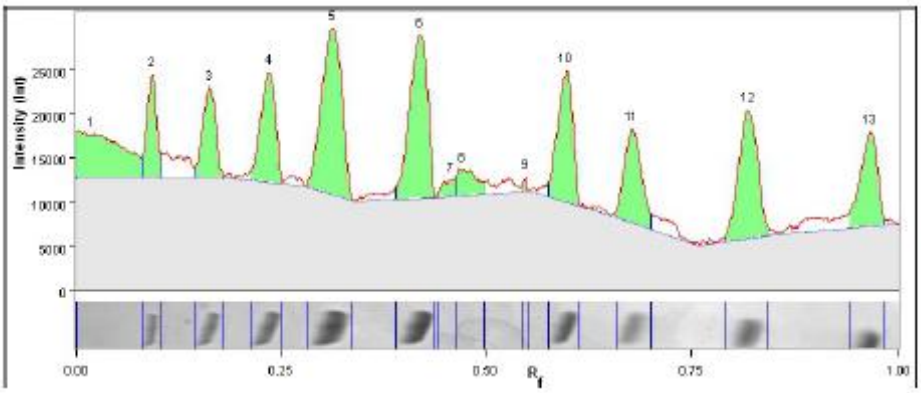
Lane 11



Band No.	Band Label	Mol. Wt. (KDa)	Relative Front	Volume (Int)	Abs. Quant.	Rel. Quant.	Band %	Lane %
1		N/A	0.214	605 097	N/A	N/A	5.8	1.4
2		N/A	0.568	5 688 598	41.0	N/A	54.9	12.8
3		N/A	0.646	1 642 792	N/A	N/A	15.9	3.7
4		N/A	0.761	2 422 724	0.9	N/A	23.4	5.5

Band Detection	Automatically detected bands with sensitivity: High
Lane Background	Lane background subtracted with disk size: 10

Lane 12



Band No.	Band Label	Mol. Wt. (KDa)	Relative Front	Volume (Int)	Abs. Quant.	Rel. Quant.	Band %	Lane %
1		N/A	0.019	24 926 872	277.8	N/A	10.0	8.9
2		N/A	0.093	11 991 637	118.6	N/A	4.8	4.3
3		N/A	0.164	14 205 654	145.9	N/A	5.7	5.1
4		N/A	0.236	19 512 754	211.2	N/A	7.8	7.0
5		N/A	0.312	40 613 696	470.8	N/A	16.3	14.5
6		N/A	0.419	35 760 583	411.1	N/A	14.4	12.8
7		N/A	0.456	2 839 116	6.0	N/A	1.1	1.0
8		N/A	0.471	6 079 659	45.9	N/A	2.4	2.2
9		N/A	0.548	484 574	N/A	N/A	0.2	0.2
10		N/A	0.597	23 960 425	265.9	N/A	9.6	8.5

Strain A99-SDS-PAGE Report

Lane 2- Molecular weight Marker (Thermofischer, PageRuler Plus Prestained Protein ladder-Thermoscientific, Cat No: 26634).

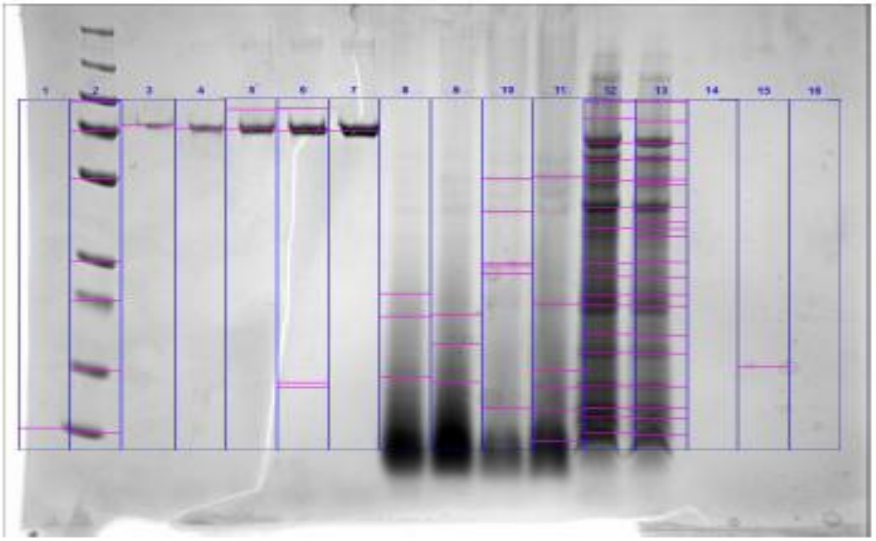
Lane2-7: BSA standard curve (100ng -800 ng).

Lane 8- Control cell proteins.

Lane 10- BNZ-induced cell proteins.

Lane 12- DMF-induced cell proteins.

Image Report: Varsha Chhiba 2017-02-16 08hr 34min



Acquisition Information

Imager	ChemiDoc™ MP
Exposure Time (sec)	0.071 (Auto - Intense Bands)
Serial Number	731BR01206
Software Version	4.1
Application	Coomassie Blue
Excitation Source	White Trans Illumination
Emission Filter	Standard Filter

Image Information

Acquisition Date	16/02/2017 08:34
User Name	Varsha Chhiba
Image Area (mm)	X: 90.0 Y: 67.2
Pixel Size (um)	X: 84.7 Y: 84.7
Data Range (Int)	0 - 57943

Analysis Settings

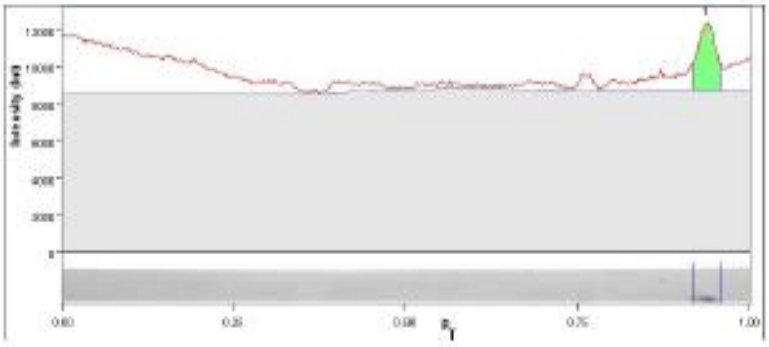
Detection	Lane detection: Manually created lanes Band detection: Automatically detected bands with sensitivity: High Lane Background Subtraction: Lane background subtracted with disk size: 10
Quantity Analysis	Quantity Standard Bands:

1

	Lane 3 Band 1 Quantity 100.0 ng Lane 4 Band 1 Quantity 200.0 ng Lane 5 Band 2 Quantity 400.0 ng Lane 6 Band 2 Quantity 600.0 ng Lane 7 Band 1 Quantity 800.0 ng Quantity regression method: Linear Regression equation: y = 1.34E-005 * x - 87.7 R-squared value: R^2 = 0.958077

Lane And Band Analysis

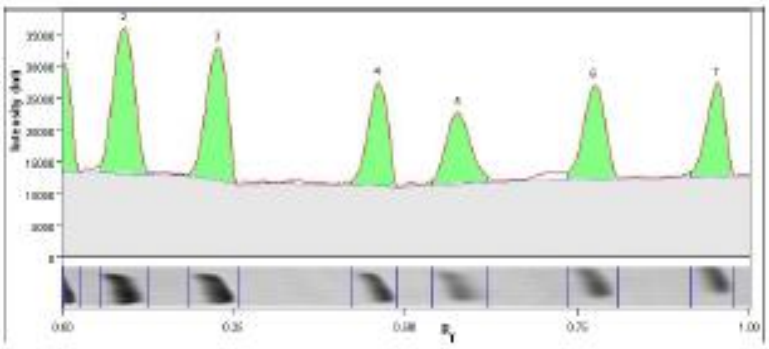
Lane 1



Band No.	Band Label	Mol. Wt. (KDa)	Relative Front	Volume (Int)	Abs. Quant. (ng)	Rel. Quant.	Band %	Lane %
1		N/A	0.939	6 239 100	N/A	N/A	100.0	11.2

Band Detection	Automatically detected bands with sensitivity: High
Lane Background	Lane background subtracted with disk size: 10

Lane 2

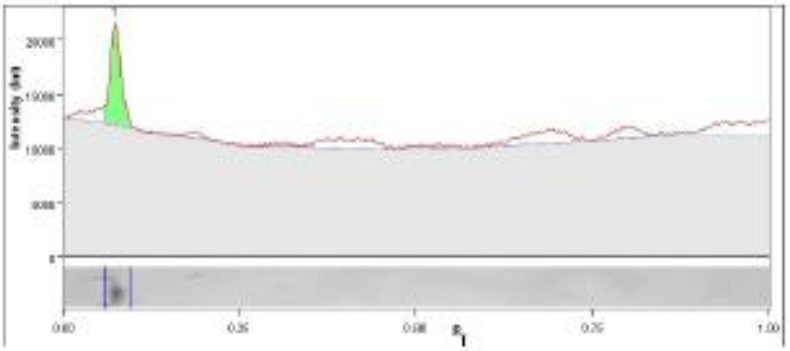


Band No.	Band Label	Mol. Wt. (KDa)	Relative Front	Volume (Int)	Abs. Quant. (ng)	Rel. Quant.	Band %	Lane %
1		N/A	0.006	14 225 820	102.3	N/A	6.4	6.1
2		N/A	0.090	48 353 760	568.3	N/A	21.7	20.8
3		N/A	0.227	43 352 904	491.5	N/A	19.4	18.5
4		N/A	0.462	31 396 176	331.8	N/A	14.1	13.4
5		N/A	0.574	27 287 064	276.9	N/A	12.2	11.6
6		N/A	0.774	31 764 264	336.7	N/A	14.2	13.5
7		N/A	0.952	26 682 600	268.8	N/A	12.0	11.4

Band Detection	Automatically detected bands with sensitivity: High
Lane Background	Lane background subtracted with disk size: 10

Lane 3-7: BSA Standard Curve

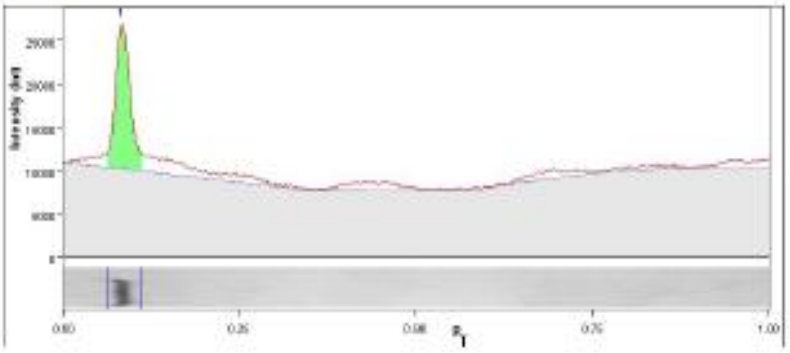
Lane 3



Band No.	Band Label	Mol. Wt. (KDa)	Relative Front	Volume (Int)	Abs. Quant. (ng)	Rel. Quant.	Band %	Lane %
1		N/A	0.074	10 340 232	100.0	N/A	100.0	27.7

Band Detection	Automatically detected bands with sensitivity: High
Lane Background	Lane background subtracted with disk size: 10

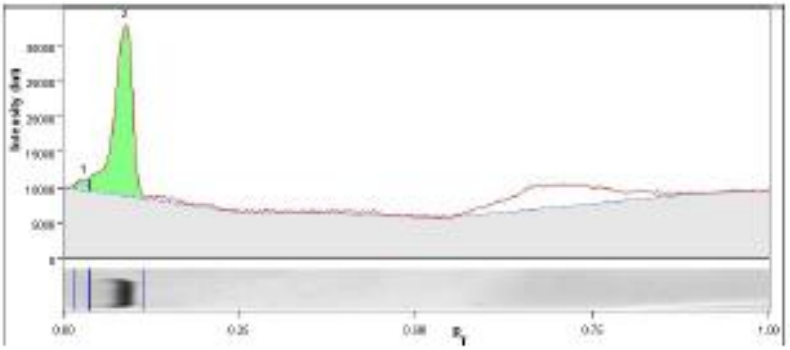
Lane 4



Band No.	Band Label	Mol. Wt. (KDa)	Relative Front	Volume (Int)	Abs. Quant. (ng)	Rel. Quant.	Band %	Lane %
1		N/A	0.084	23 336 376	200.0	N/A	100.0	42.9

Band Detection	Automatically detected bands with sensitivity: High
Lane Background	Lane background subtracted with disk size: 10

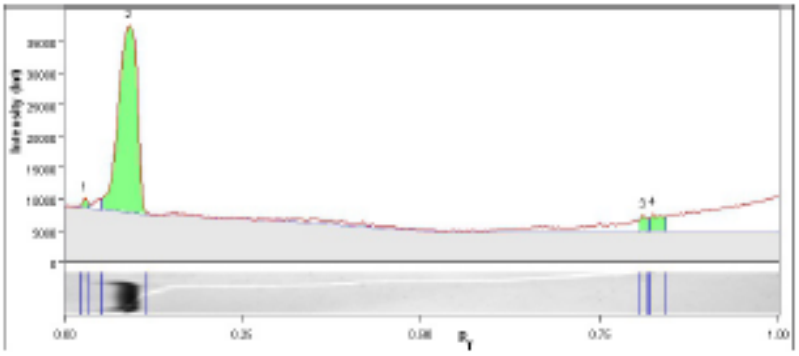
Lane 5



Band No.	Band Label	Mol. Wt. (KDa)	Relative Front	Volume (Int)	Abs. Quant. (ng)	Rel. Quant.	Band %	Lane %
1		N/A	0.031	1 486 800	N/A	N/A	3.4	1.8
2		N/A	0.089	42 320 460	400.0	N/A	96.6	50.3

Band Detection	Automatically detected bands with sensitivity: High
Lane Background	Lane background subtracted with disk size: 10

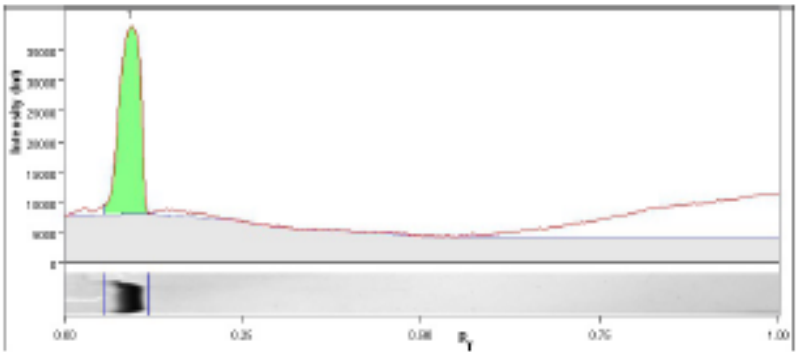
Lane 6



Band No.	Band Label	Mol. Wt. (KDa)	Relative Front	Volume (Int)	Abs. Quant. (ng)	Rel. Quant.	Band %	Lane %
1		N/A	0.029	789 012	N/A	N/A	1.3	0.7
2		N/A	0.092	52 569 556	600.0	N/A	89.6	47.4
3		N/A	0.810	1 847 916	N/A	N/A	3.1	1.7
4		N/A	0.824	3 483 984	N/A	N/A	5.9	3.1

Band Detection	Automatically detected bands with sensitivity: High
Lane Background	Lane background subtracted with disk size: 10

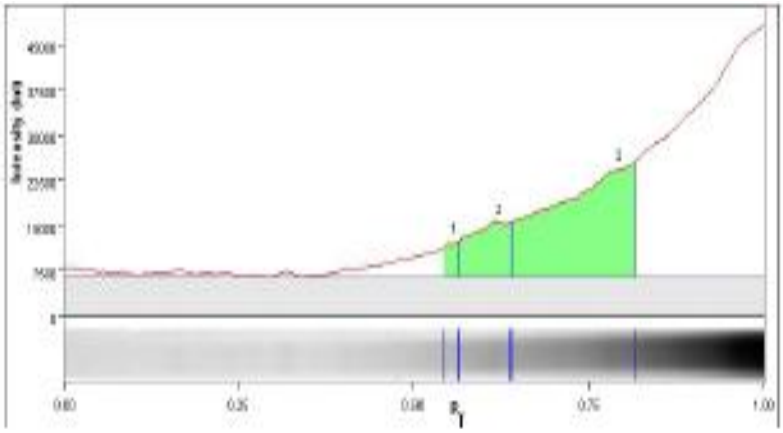
Lane 7



Band No.	Band Label	Mol. Wt. (KDa)	Relative Front	Volume (Int)	Abs. Quant. (ng)	Rel. Quant.	Band %	Lane %
1		N/A	0.094	61 441 464	800.0	N/A	100.0	38.2

Band Detection	Automatically detected bands with sensitivity: High
Lane Background	Lane background subtracted with disk size: 10

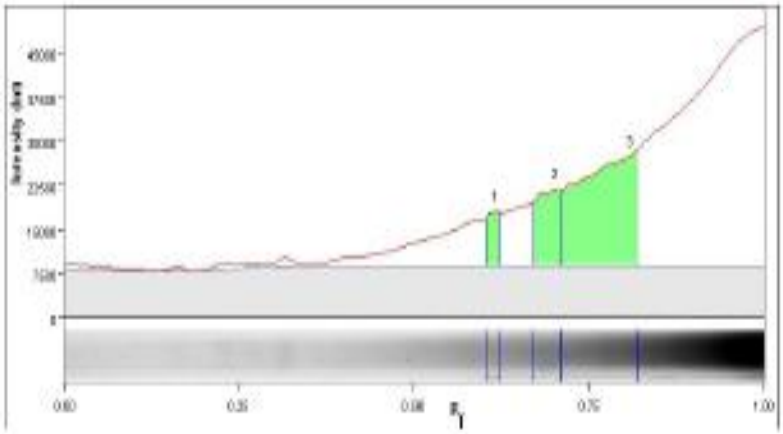
Lane 8-9: A99 Control cells



Band No.	Band Label	Mol. Wt. (KDa)	Relative Front	Volume (Int)	Abs. Quant. (ng)	Rel. Quant.	Band %	Lane %
1		N/A	0.557	6 880 188	4.2	N/A	3.7	1.3
2		N/A	0.621	34 885 872	378.4	N/A	19.0	6.5
3		N/A	0.794	141 729 336	1 808.0	N/A	77.2	26.5

Band Detection	Automatically detected bands with sensitivity: High
Lane Background	Lane background subtracted with disk size: 10

Lane 9

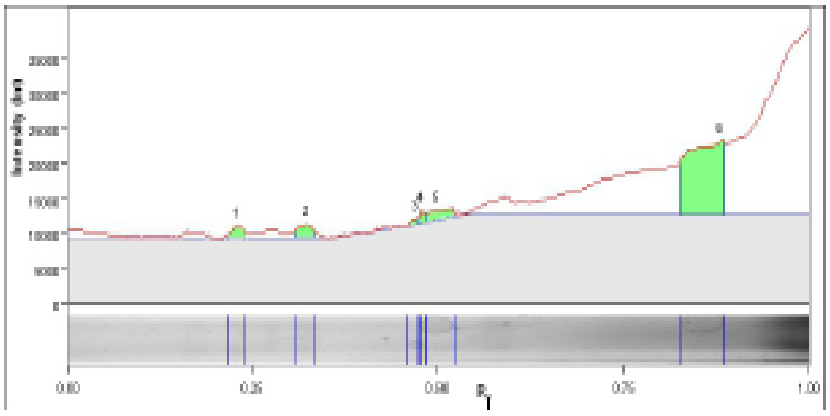


Band No.	Band Label	Mol. Wt. (KDa)	Relative Front	Volume (Int)	Abs. Quant. (ng)	Rel. Quant.	Band %	Lane %
1		N/A	0.615	10 628 688	54.3	N/A	7.5	1.9
2		N/A	0.701	28 142 520	288.3	N/A	19.7	5.1
3		N/A	0.808	103 727 484	1 298.2	N/A	72.8	18.8

Band Detection	Automatically detected bands with sensitivity: High
Lane Background	Lane background subtracted with disk size: 10

Lane 10

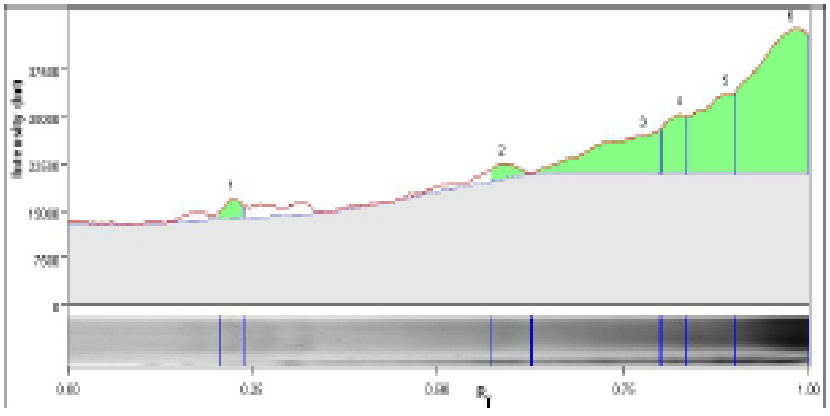
Lane 10-11: A99 BNZ-induced cells



Band No.	Band Label	Mol. Wt. (kDa)	Relative Front	Volume (Int)	Abs. Quant. (ng)	Rel. Quant.	Band %	Lane %
1		N/A	0.230	1 809 024	N/A	N/A	4.3	0.8
2		N/A	0.323	2 405 508	N/A	N/A	5.7	1.0
3		N/A	0.471	591 864	N/A	N/A	1.4	0.3
4		N/A	0.478	797 832	N/A	N/A	1.9	0.3
5		N/A	0.500	2 463 804	N/A	N/A	5.9	1.1
6		N/A	0.879	33 795 888	365.8	N/A	80.7	14.6

Band Detection	Automatically detected bands with sensitivity: High
Lane Background	Lane background subtracted with disk size: 10

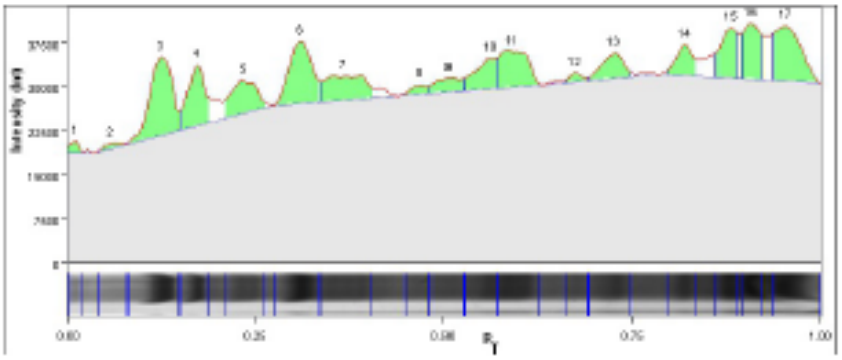
Lane 11



Band No.	Band Label	Mol. Wt. (kDa)	Relative Front	Volume (Int)	Abs. Quant. (ng)	Rel. Quant.	Band %	Lane %
1		N/A	0.224	4 659 564	N/A	N/A	2.1	1.9
2		N/A	0.585	5 072 760	N/A	N/A	2.3	2.1
3		N/A	0.776	39 589 784	441.4	N/A	18.0	16.3
4		N/A	0.825	17 737 272	140.3	N/A	8.1	7.3
5		N/A	0.888	42 511 308	480.3	N/A	19.3	17.5
6		N/A	0.977	110 749 548	1 392.0	N/A	50.3	45.5

Band Detection	Automatically detected bands with sensitivity: High
Lane Background	Lane background subtracted with disk size: 10

Lane 12-13: A99 DMF-induced cells

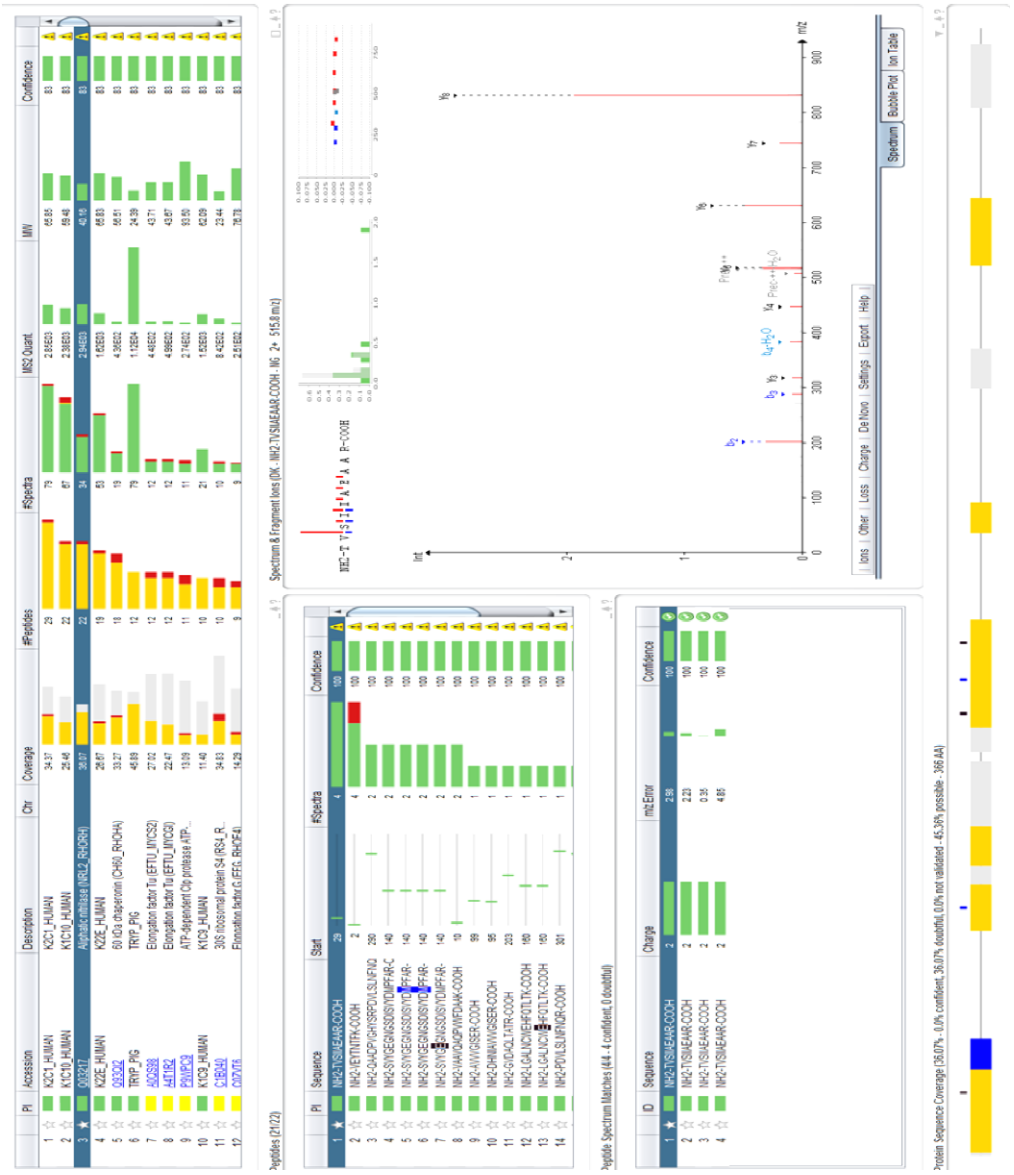


Band No.	Band Label	Mol. Wt. (KDa)	Relative Front	Volume (Int.)	Abs. Quant. (ng)	Rel. Quant.	Band %	Lane %
1		N/A	0.010	1 764 924	N/A	N/A	0.9	0.8
2		N/A	0.057	1 376 592	N/A	N/A	0.7	0.6
3		N/A	0.125	27 045 060	273.6	N/A	13.9	12.4
4		N/A	0.173	15 675 828	121.7	N/A	8.0	7.2
5		N/A	0.234	12 943 560	85.2	N/A	6.6	5.9
6		N/A	0.310	21 684 936	202.0	N/A	11.1	9.9
7		N/A	0.368	15 021 384	113.0	N/A	7.7	6.9
8		N/A	0.470	2 317 308	N/A	N/A	1.2	1.1
9		N/A	0.507	5 065 536	N/A	N/A	2.6	2.3
10		N/A	0.560	10 296 132	49.8	N/A	5.3	4.7
11		N/A	0.590	15 829 632	123.8	N/A	8.1	7.3
12		N/A	0.672	1 737 456	N/A	N/A	0.9	0.8
13		N/A	0.725	8 664 684	28.0	N/A	4.4	4.0
14		N/A	0.820	7 786 044	16.3	N/A	4.0	3.6
15		N/A	0.881	11 657 520	88.0	N/A	6.0	5.3
16		N/A	0.908	13 990 536	99.2	N/A	7.2	6.4
17		N/A	0.953	22 012 284	206.4	N/A	11.3	10.1

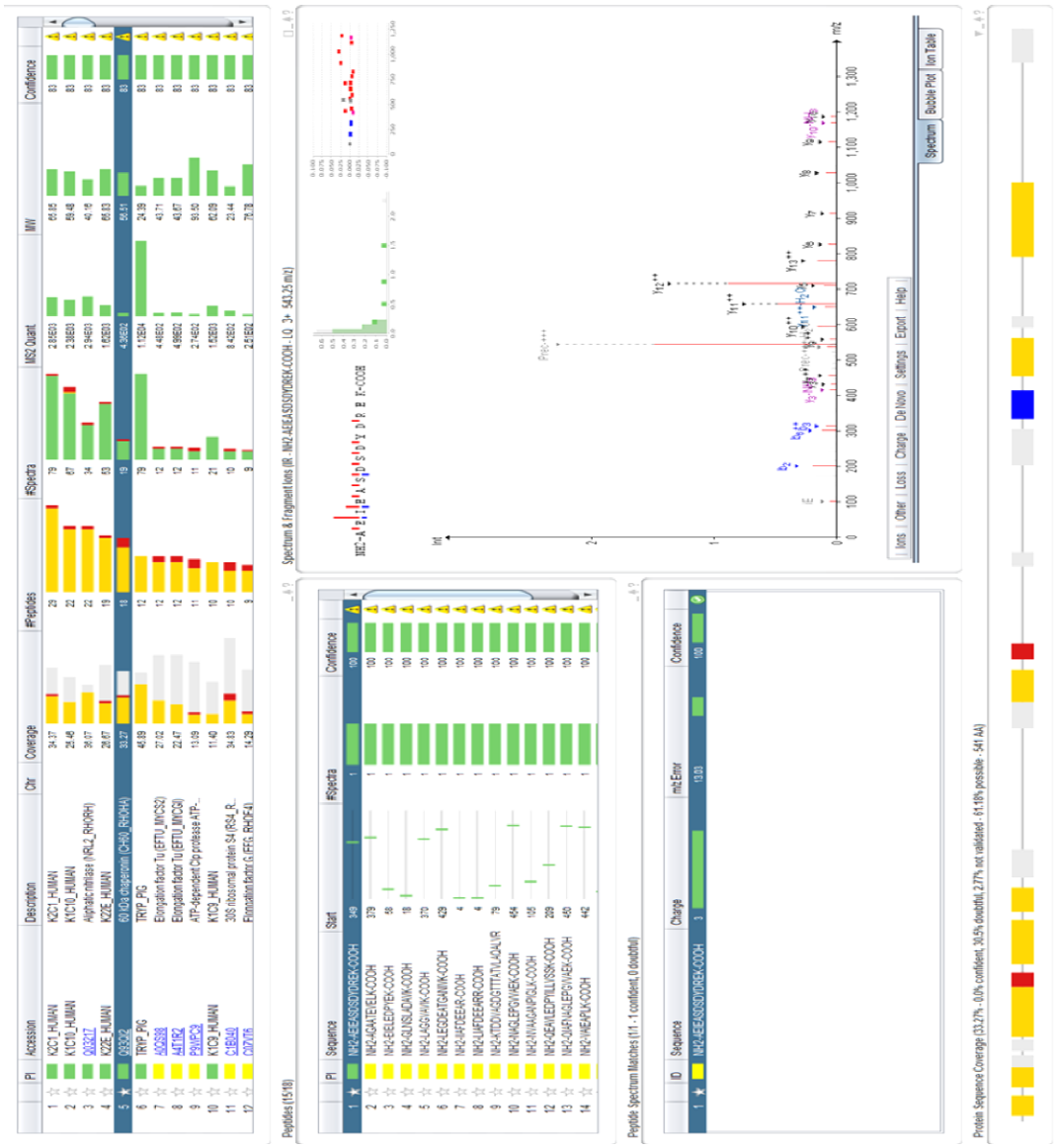
Appendix 5A-5C: LCMS-MS Data

ATCC BAA 870- LCMS-MS Peptide Data

Nitrilase peptide fragments



Chaperonin peptide fragment



Strain A29- LCMS-MS Peptide Data

Nitrilase Peptide Fragments

Accessions	Names	Conf	Sequence
Nitrilase_Rhodococcus_rhodochrous_strain_J1	_UniProt_KB_Q_03217	99	ALPSTHSDETDR
Nitrilase_Rhodococcus_rhodochrous_strain_J1	_UniProt_KB_Q_03217	99	AVQAQPVWFDAAK
Nitrilase_Rhodococcus_rhodochrous_strain_J1	_UniProt_KB_Q_03217	99	DGGSLYMTQLVIDADGQLVAR
Nitrilase_Rhodococcus_rhodochrous_strain_J1	_UniProt_KB_Q_03217	99	DHNIAVVVGISER
Nitrilase_Rhodococcus_rhodochrous_strain_J1	_UniProt_KB_Q_03217	99	DLATPLAEDEEGILYADIDLSAITLAK
Nitrilase_Rhodococcus_rhodochrous_strain_J1	_UniProt_KB_Q_03217	99	ELNGADEQR
Nitrilase_Rhodococcus_rhodochrous_strain_J1	_UniProt_KB_Q_03217	99	GCELVAFPEVFIPGYPYHIWVDSPLAGMAK
Nitrilase_Rhodococcus_rhodochrous_strain_J1	_UniProt_KB_Q_03217	99	GSDISVYDMPFAR
Nitrilase_Rhodococcus_rhodochrous_strain_J1	_UniProt_KB_Q_03217	99	HIWVDSPLAGMAK
Nitrilase_Rhodococcus_rhodochrous_strain_J1	_UniProt_KB_Q_03217	99	IIGPDGR
Nitrilase_Rhodococcus_rhodochrous_strain_J1	_UniProt_KB_Q_03217	99	IWVDSPLAGMAK
Nitrilase_Rhodococcus_rhodochrous_strain_J1	_UniProt_KB_Q_03217	99	KLKPTHVER
Nitrilase_Rhodococcus_rhodochrous_strain_J1	_UniProt_KB_Q_03217	99	KVAAVQAQPVWFDAAK
Nitrilase_Rhodococcus_rhodochrous_strain_J1	_UniProt_KB_Q_03217	99	LGALNCWEHFQTL
Nitrilase_Rhodococcus_rhodochrous_strain_J1	_UniProt_KB_Q_03217	99	LGALNCWEHFQTLTK
Nitrilase_Rhodococcus_rhodochrous_strain_	_UniProt_KB_Q_0321	99	MVEYTNTFK

J1	7		
Nitrilase_Rhodococcus_rhodochrous_strain_J1	_UniProt_KB_Q_03217	99	MYALEGQTFVVC
Nitrilase_Rhodococcus_rhodochrous_strain_J1	_UniProt_KB_Q_03217	99	MYALEGQTFVVCTTQVVTPEAHEFFCDNDEQR
Nitrilase_Rhodococcus_rhodochrous_strain_J1	_UniProt_KB_Q_03217	99	MYALEGQTFVVCTTQVVTPEAHEFFCDNDEQRK
Nitrilase_Rhodococcus_rhodochrous_strain_J1	_UniProt_KB_Q_03217	99	NGCELVAFPEVFIPGYPYHIWVDSPLAGMAK
Nitrilase_Rhodococcus_rhodochrous_strain_J1	_UniProt_KB_Q_03217	99	PDVLSLNFNQR
Nitrilase_Rhodococcus_rhodochrous_strain_J1	_UniProt_KB_Q_03217	99	PSTHSDETDR
Nitrilase_Rhodococcus_rhodochrous_strain_J1	_UniProt_KB_Q_03217	99	QAADPVGHYSR
Nitrilase_Rhodococcus_rhodochrous_strain_J1	_UniProt_KB_Q_03217	99	QAADPVGHYSRPDVL
Nitrilase_Rhodococcus_rhodochrous_strain_J1	_UniProt_KB_Q_03217	99	QAADPVGHYSRPDVLSL
Nitrilase_Rhodococcus_rhodochrous_strain_J1	_UniProt_KB_Q_03217	99	QAADPVGHYSRPDVLSLNFNQR
Nitrilase_Rhodococcus_rhodochrous_strain_J1	_UniProt_KB_Q_03217	99	SMHEQVHVASWPGMSLYQPEVPAFGVDAQLTATR
Nitrilase_Rhodococcus_rhodochrous_strain_J1	_UniProt_KB_Q_03217	99	SRPDVLSLNFNQR
Nitrilase_Rhodococcus_rhodochrous_strain_J1	_UniProt_KB_Q_03217	99	SVYGEGNGSDISVYDMPFAR
Nitrilase_Rhodococcus_rhodochrous_strain_J1	_UniProt_KB_Q_03217	99	TMDSPHVQR
Nitrilase_Rhodococcus_rhodochrous_strain_J1	_UniProt_KB_Q_03217	99	TTQVVTPEAHEFFCDNDEQR
Nitrilase_Rhodococcus_rhodochrous_strain_J1	_UniProt_KB_Q_03217	99	TVDKTVSIIAEAAR
Nitrilase_Rhodococcus_rhodochrous_strain_J1	_UniProt_KB_Q_03217	99	TVSIIAEAAR
Nitrilase_Rhodococcus_rhodochrous_strain_J1	_UniProt_KB_Q_03217	99	VAAVQAQPVWFDAAK

Nitrilase_Rhodococcus_rhodochrous_strain_J1	_UniProt_KB_Q_03217	99	VEYTNTFK
Nitrilase_Rhodococcus_rhodochrous_strain_J1	_UniProt_KB_Q_03217	99	VIDADGQLVAR
Nitrilase_Rhodococcus_rhodochrous_strain_J1	_UniProt_KB_Q_03217	99	YAMYSMHEQVHVASWPGMSLYQPEVPAFGVDAQLTATR
Nitrilase_Rhodococcus_rhodochrous_strain_J1	_UniProt_KB_Q_03217	99	YHENSLTMDSPHVQR
Nitrilase_Rhodococcus_rhodochrous_strain_J1	_UniProt_KB_Q_03217	99	YSRPDVLSLNFNQR
Nitrilase_Rhodococcus_rhodochrous_strain_J1	_UniProt_KB_Q_03217	99	SLTMDSPHVQR
Nitrilase_Rhodococcus_rhodochrous_strain_J1	_UniProt_KB_Q_03217	99	YAMYSMHEQVHVASWPGM
Nitrilase_Rhodococcus_rhodochrous_strain_J1	_UniProt_KB_Q_03217	99	VASWPGMSLYQPEVPAFGVDAQLTATR
Nitrilase_Rhodococcus_rhodochrous_strain_J1	_UniProt_KB_Q_03217	99	EFFCDNDEQR
Nitrilase_Rhodococcus_rhodochrous_strain_J1	_UniProt_KB_Q_03217	99	NGCELVAFPEVFIPGYPY
Nitrilase_Rhodococcus_rhodochrous_strain_J1	_UniProt_KB_Q_03217	99	SLNFNQR
Nitrilase_Rhodococcus_rhodochrous_strain_J1	_UniProt_KB_Q_03217	99	MDSPHVQR
Nitrilase_Rhodococcus_rhodochrous_strain_J1	_UniProt_KB_Q_03217	99	YAMYSMHEQVH
Nitrilase_Rhodococcus_rhodochrous_strain_J1	_UniProt_KB_Q_03217	98.65	DLATPLAEDEEGILYADIDLSAITL
Nitrilase_Rhodococcus_rhodochrous_strain_J1	_UniProt_KB_Q_03217	99	AQPVWFDAAK
Nitrilase_Rhodococcus_rhodochrous_strain_J1	_UniProt_KB_Q_03217	96.64	QAADPVGHY
Nitrilase_Rhodococcus_rhodochrous_strain_J1	_UniProt_KB_Q_03217	80.91	IAVVVGISER
Nitrilase_Rhodococcus_rhodochrous_strain_J1	_UniProt_KB_Q_03217	58.84	GALNCWEHFQTLTK
Nitrilase_Rhodococcus_rhodochrous_strain_J1	_UniProt_KB_Q_03217	99	ALPSTHSDETDR

Nitrilase_Rhodococcus_rhodochrous_strain_J1	_UniProt_KB_Q_03217	99	ALPSTHSDETDR
Nitrilase_Rhodococcus_rhodochrous_strain_J1	_UniProt_KB_Q_03217	99	AVQAQPVWFDAAK
Nitrilase_Rhodococcus_rhodochrous_strain_J1	_UniProt_KB_Q_03217	99	DGGSLYMTQLVIDADGQLVAR
Nitrilase_Rhodococcus_rhodochrous_strain_J1	_UniProt_KB_Q_03217	99	DGGSLYMTQLVIDADGQLVAR
Nitrilase_Rhodococcus_rhodochrous_strain_J1	_UniProt_KB_Q_03217	99	DGGSLYMTQLVIDADGQLVAR
Nitrilase_Rhodococcus_rhodochrous_strain_J1	_UniProt_KB_Q_03217	99	DGGSLYMTQLVIDADGQLVAR
Nitrilase_Rhodococcus_rhodochrous_strain_J1	_UniProt_KB_Q_03217	99	DGGSLYMTQLVIDADGQLVAR
Nitrilase_Rhodococcus_rhodochrous_strain_J1	_UniProt_KB_Q_03217	99	DGGSLYMTQLVIDADGQLVAR
Nitrilase_Rhodococcus_rhodochrous_strain_J1	_UniProt_KB_Q_03217	99	DGGSLYMTQLVIDADGQLVAR
Nitrilase_Rhodococcus_rhodochrous_strain_J1	_UniProt_KB_Q_03217	99	DGGSLYMTQLVIDADGQLVAR
Nitrilase_Rhodococcus_rhodochrous_strain_J1	_UniProt_KB_Q_03217	99	DGGSLYMTQLVIDADGQLVAR
Nitrilase_Rhodococcus_rhodochrous_strain_J1	_UniProt_KB_Q_03217	99	DGGSLYMTQLVIDADGQLVAR
Nitrilase_Rhodococcus_rhodochrous_strain_J1	_UniProt_KB_Q_03217	99	DGGSLYMTQLVIDADGQLVAR
Nitrilase_Rhodococcus_rhodochrous_strain_J1	_UniProt_KB_Q_03217	99	DGGSLYMTQLVIDADGQLVAR
Nitrilase_Rhodococcus_rhodochrous_strain_J1	_UniProt_KB_Q_03217	99	DGGSLYMTQLVIDADGQLVAR
Nitrilase_Rhodococcus_rhodochrous_strain_J1	_UniProt_KB_Q_03217	99	DGGSLYMTQLVIDADGQLVAR
Nitrilase_Rhodococcus_rhodochrous_strain_J1	_UniProt_KB_Q_03217	99	DGGSLYMTQLVIDADGQLVAR
Nitrilase_Rhodococcus_rhodochrous_strain_J1	_UniProt_KB_Q_03217	99	DGGSLYMTQLVIDADGQLVAR
Nitrilase_Rhodococcus_rhodochrous_strain_J1	_UniProt_KB_Q_03217	99	DGGSLYMTQLVIDADGQLVAR
Nitrilase_Rhodococcus_rhodochrous_strain_J1	_UniProt_KB_Q_03217	99	DGGSLYMTQLVIDADGQLVAR

Nitrilase_Rhodococcus_rhodochrous_strain_J1	_UniProt_KB_Q_03217	99	DGGSLYMTQLVIDADGQLVAR
Nitrilase_Rhodococcus_rhodochrous_strain_J1	_UniProt_KB_Q_03217	99	DGGSLYMTQLVIDADGQLVAR
Nitrilase_Rhodococcus_rhodochrous_strain_J1	_UniProt_KB_Q_03217	99	DGGSLYMTQLVIDADGQLVAR
Nitrilase_Rhodococcus_rhodochrous_strain_J1	_UniProt_KB_Q_03217	99	DGGSLYMTQLVIDADGQLVAR
Nitrilase_Rhodococcus_rhodochrous_strain_J1	_UniProt_KB_Q_03217	99	DGGSLYMTQLVIDADGQLVAR
Nitrilase_Rhodococcus_rhodochrous_strain_J1	_UniProt_KB_Q_03217	99	DGGSLYMTQLVIDADGQLVAR
Nitrilase_Rhodococcus_rhodochrous_strain_J1	_UniProt_KB_Q_03217	99	DGGSLYMTQLVIDADGQLVAR
Nitrilase_Rhodococcus_rhodochrous_strain_J1	_UniProt_KB_Q_03217	99	DGGSLYMTQLVIDADGQLVAR
Nitrilase_Rhodococcus_rhodochrous_strain_J1	_UniProt_KB_Q_03217	99	DGGSLYMTQLVIDADGQLVAR
Nitrilase_Rhodococcus_rhodochrous_strain_J1	_UniProt_KB_Q_03217	99	DGGSLYMTQLVIDADGQLVAR
Nitrilase_Rhodococcus_rhodochrous_strain_J1	_UniProt_KB_Q_03217	99	DGGSLYMTQLVIDADGQLVAR
Nitrilase_Rhodococcus_rhodochrous_strain_J1	_UniProt_KB_Q_03217	99	DGGSLYMTQLVIDADGQLVAR
Nitrilase_Rhodococcus_rhodochrous_strain_J1	_UniProt_KB_Q_03217	99	DGGSLYMTQLVIDADGQLVAR
Nitrilase_Rhodococcus_rhodochrous_strain_J1	_UniProt_KB_Q_03217	99	DGGSLYMTQLVIDADGQLVAR
Nitrilase_Rhodococcus_rhodochrous_strain_J1	_UniProt_KB_Q_03217	99	DGGSLYMTQLVIDADGQLVAR
Nitrilase_Rhodococcus_rhodochrous_strain_J1	_UniProt_KB_Q_03217	99	DGGSLYMTQLVIDADGQLVAR
Nitrilase_Rhodococcus_rhodochrous_strain_J1	_UniProt_KB_Q_03217	99	DGGSLYMTQLVIDADGQLVAR
Nitrilase_Rhodococcus_rhodochrous_strain_J1	_UniProt_KB_Q_03217	99	DGGSLYMTQLVIDADGQLVAR
Nitrilase_Rhodococcus_rhodochrous_strain_J1	_UniProt_KB_Q_03217	99	DGGSLYMTQLVIDADGQLVAR
Nitrilase_Rhodococcus_rhodochrous_strain_J1	_UniProt_KB_Q_03217	99	DGGSLYMTQLVIDADGQLVAR

Nitrilase_Rhodococcus_rhodochrous_strain_J1	_UniProt_KB_Q_03217	99	DGGSLYMTQLVIDADGQLVAR
Nitrilase_Rhodococcus_rhodochrous_strain_J1	_UniProt_KB_Q_03217	99	DGGSLYMTQLVIDADGQLVAR
Nitrilase_Rhodococcus_rhodochrous_strain_J1	_UniProt_KB_Q_03217	99	DGGSLYMTQLVIDADGQLVAR
Nitrilase_Rhodococcus_rhodochrous_strain_J1	_UniProt_KB_Q_03217	99	DGGSLYMTQLVIDADGQLVAR
Nitrilase_Rhodococcus_rhodochrous_strain_J1	_UniProt_KB_Q_03217	99	DGGSLYMTQLVIDADGQLVAR
Nitrilase_Rhodococcus_rhodochrous_strain_J1	_UniProt_KB_Q_03217	99	DGGSLYMTQLVIDADGQLVAR
Nitrilase_Rhodococcus_rhodochrous_strain_J1	_UniProt_KB_Q_03217	99	DGGSLYMTQLVIDADGQLVAR
Nitrilase_Rhodococcus_rhodochrous_strain_J1	_UniProt_KB_Q_03217	99	DGGSLYMTQLVIDADGQLVAR
Nitrilase_Rhodococcus_rhodochrous_strain_J1	_UniProt_KB_Q_03217	99	DGGSLYMTQLVIDADGQLVAR
Nitrilase_Rhodococcus_rhodochrous_strain_J1	_UniProt_KB_Q_03217	99	DGGSLYMTQLVIDADGQLVAR
Nitrilase_Rhodococcus_rhodochrous_strain_J1	_UniProt_KB_Q_03217	99	DGGSLYMTQLVIDADGQLVAR
Nitrilase_Rhodococcus_rhodochrous_strain_J1	_UniProt_KB_Q_03217	99	DGGSLYMTQLVIDADGQLVAR
Nitrilase_Rhodococcus_rhodochrous_strain_J1	_UniProt_KB_Q_03217	99	DGGSLYMTQLVIDADGQLVAR
Nitrilase_Rhodococcus_rhodochrous_strain_J1	_UniProt_KB_Q_03217	99	DGGSLYMTQLVIDADGQLVAR
Nitrilase_Rhodococcus_rhodochrous_strain_J1	_UniProt_KB_Q_03217	99	DGGSLYMTQLVIDADGQLVAR
Nitrilase_Rhodococcus_rhodochrous_strain_J1	_UniProt_KB_Q_03217	99	DGGSLYMTQLVIDADGQLVAR
Nitrilase_Rhodococcus_rhodochrous_strain_J1	_UniProt_KB_Q_03217	99	DGGSLYMTQLVIDADGQLVAR
Nitrilase_Rhodococcus_rhodochrous_strain_J1	_UniProt_KB_Q_03217	99	DGGSLYMTQLVIDADGQLVAR
Nitrilase_Rhodococcus_rhodochrous_strain_J1	_UniProt_KB_Q_03217	99	DGGSLYMTQLVIDADGQLVAR
Nitrilase_Rhodococcus_rhodochrous_strain_J1	_UniProt_KB_Q_03217	99	DGGSLYMTQLVIDADGQLVAR

Nitrilase_Rhodococcus_rhodochrous_strain_J1	_UniProt_KB_Q_03217	99	DGGSLYMTQLVIDADGQLVAR
Nitrilase_Rhodococcus_rhodochrous_strain_J1	_UniProt_KB_Q_03217	99	DGGSLYMTQLVIDADGQLVAR
Nitrilase_Rhodococcus_rhodochrous_strain_J1	_UniProt_KB_Q_03217	99	DGGSLYMTQLVIDADGQLVAR
Nitrilase_Rhodococcus_rhodochrous_strain_J1	_UniProt_KB_Q_03217	99	DGGSLYMTQLVIDADGQLVAR
Nitrilase_Rhodococcus_rhodochrous_strain_J1	_UniProt_KB_Q_03217	99	DGGSLYMTQLVIDADGQLVAR
Nitrilase_Rhodococcus_rhodochrous_strain_J1	_UniProt_KB_Q_03217	99	DGGSLYMTQLVIDADGQLVAR
Nitrilase_Rhodococcus_rhodochrous_strain_J1	_UniProt_KB_Q_03217	99	DGGSLYMTQLVIDADGQLVAR
Nitrilase_Rhodococcus_rhodochrous_strain_J1	_UniProt_KB_Q_03217	99	DGGSLYMTQLVIDADGQLVAR
Nitrilase_Rhodococcus_rhodochrous_strain_J1	_UniProt_KB_Q_03217	99	DGGSLYMTQLVIDADGQLVAR
Nitrilase_Rhodococcus_rhodochrous_strain_J1	_UniProt_KB_Q_03217	99	DGGSLYMTQLVIDADGQLVAR
Nitrilase_Rhodococcus_rhodochrous_strain_J1	_UniProt_KB_Q_03217	99	DGGSLYMTQLVIDADGQLVAR
Nitrilase_Rhodococcus_rhodochrous_strain_J1	_UniProt_KB_Q_03217	99	DGGSLYMTQLVIDADGQLVAR
Nitrilase_Rhodococcus_rhodochrous_strain_J1	_UniProt_KB_Q_03217	99	DGGSLYMTQLVIDADGQLVAR
Nitrilase_Rhodococcus_rhodochrous_strain_J1	_UniProt_KB_Q_03217	99	DGGSLYMTQLVIDADGQLVAR
Nitrilase_Rhodococcus_rhodochrous_strain_J1	_UniProt_KB_Q_03217	99	DGGSLYMTQLVIDADGQLVAR
Nitrilase_Rhodococcus_rhodochrous_strain_J1	_UniProt_KB_Q_03217	99	DGGSLYMTQLVIDADGQLVAR
Nitrilase_Rhodococcus_rhodochrous_strain_J1	_UniProt_KB_Q_03217	99	DGGSLYMTQLVIDADGQLVAR
Nitrilase_Rhodococcus_rhodochrous_strain_J1	_UniProt_KB_Q_03217	99	DGGSLYMTQLVIDADGQLVAR
Nitrilase_Rhodococcus_rhodochrous_strain_J1	_UniProt_KB_Q_03217	99	DGGSLYMTQLVIDADGQLVAR
Nitrilase_Rhodococcus_rhodochrous_strain_J1	_UniProt_KB_Q_03217	99	DGGSLYMTQLVIDADGQLVAR

Nitrilase_Rhodococcus_rhodochrous_strain_J1	_UniProt_KB_Q_03217	99	DGGSLYMTQLVIDADGQLVAR
Nitrilase_Rhodococcus_rhodochrous_strain_J1	_UniProt_KB_Q_03217	99	DGGSLYMTQLVIDADGQLVAR
Nitrilase_Rhodococcus_rhodochrous_strain_J1	_UniProt_KB_Q_03217	99	DGGSLYMTQLVIDADGQLVAR
Nitrilase_Rhodococcus_rhodochrous_strain_J1	_UniProt_KB_Q_03217	99	DGGSLYMTQLVIDADGQLVAR
Nitrilase_Rhodococcus_rhodochrous_strain_J1	_UniProt_KB_Q_03217	99	DGGSLYMTQLVIDADGQLVAR
Nitrilase_Rhodococcus_rhodochrous_strain_J1	_UniProt_KB_Q_03217	99	DGGSLYMTQLVIDADGQLVAR
Nitrilase_Rhodococcus_rhodochrous_strain_J1	_UniProt_KB_Q_03217	99	DGGSLYMTQLVIDADGQLVAR
Nitrilase_Rhodococcus_rhodochrous_strain_J1	_UniProt_KB_Q_03217	98.46	DGGSLYMTQLVIDADGQLVAR
Nitrilase_Rhodococcus_rhodochrous_strain_J1	_UniProt_KB_Q_03217	98.32	DGGSLYMTQLVIDADGQLVAR
Nitrilase_Rhodococcus_rhodochrous_strain_J1	_UniProt_KB_Q_03217	97.84	DGGSLYMTQLVIDADGQLVAR
Nitrilase_Rhodococcus_rhodochrous_strain_J1	_UniProt_KB_Q_03217	97.55	DGGSLYMTQLVIDADGQLVAR
Nitrilase_Rhodococcus_rhodochrous_strain_J1	_UniProt_KB_Q_03217	95.82	DGGSLYMTQLVIDADGQLVAR
Nitrilase_Rhodococcus_rhodochrous_strain_J1	_UniProt_KB_Q_03217	95.41	DGGSLYMTQLVIDADGQLVAR
Nitrilase_Rhodococcus_rhodochrous_strain_J1	_UniProt_KB_Q_03217	93.07	DGGSLYMTQLVIDADGQLVAR
Nitrilase_Rhodococcus_rhodochrous_strain_J1	_UniProt_KB_Q_03217	92.28	DGGSLYMTQLVIDADGQLVAR
Nitrilase_Rhodococcus_rhodochrous_strain_J1	_UniProt_KB_Q_03217	92.28	DGGSLYMTQLVIDADGQLVAR
Nitrilase_Rhodococcus_rhodochrous_strain_J1	_UniProt_KB_Q_03217	79.01	DGGSLYMTQLVIDADGQLVAR
Nitrilase_Rhodococcus_rhodochrous_strain_J1	_UniProt_KB_Q_03217	79.01	DGGSLYMTQLVIDADGQLVAR
Nitrilase_Rhodococcus_rhodochrous_strain_J1	_UniProt_KB_Q_03217	72.54	DGGSLYMTQLVIDADGQLVAR

Nitrilase_Rhodococcus_rhodochrous_strain_J1	_UniProt_KB_Q_03217	70.31	DGGSLYMTQLVIDADGQLVAR
Nitrilase_Rhodococcus_rhodochrous_strain_J1	_UniProt_KB_Q_03217	66.12	DGGSLYMTQLVIDADGQLVAR
Nitrilase_Rhodococcus_rhodochrous_strain_J1	_UniProt_KB_Q_03217	63.71	DGGSLYMTQLVIDADGQLVAR
Nitrilase_Rhodococcus_rhodochrous_strain_J1	_UniProt_KB_Q_03217	50.33	DGGSLYMTQLVIDADGQLVAR
Nitrilase_Rhodococcus_rhodochrous_strain_J1	_UniProt_KB_Q_03217	49.07	DGGSLYMTQLVIDADGQLVAR
Nitrilase_Rhodococcus_rhodochrous_strain_J1	_UniProt_KB_Q_03217	42.31	DGGSLYMTQLVIDADGQLVAR
Nitrilase_Rhodococcus_rhodochrous_strain_J1	_UniProt_KB_Q_03217	33.99	DGGSLYMTQLVIDADGQLVAR
Nitrilase_Rhodococcus_rhodochrous_strain_J1	_UniProt_KB_Q_03217	19.89	DGGSLYMTQLVIDADGQLVAR
Nitrilase_Rhodococcus_rhodochrous_strain_J1	_UniProt_KB_Q_03217	17.41	DGGSLYMTQLVIDADGQLVAR
Nitrilase_Rhodococcus_rhodochrous_strain_J1	_UniProt_KB_Q_03217	17.09	DGGSLYMTQLVIDADGQLVAR
Nitrilase_Rhodococcus_rhodochrous_strain_J1	_UniProt_KB_Q_03217	15.72	DGGSLYMTQLVIDADGQLVAR
Nitrilase_Rhodococcus_rhodochrous_strain_J1	_UniProt_KB_Q_03217	15.38	DGGSLYMTQLVIDADGQLVAR
Nitrilase_Rhodococcus_rhodochrous_strain_J1	_UniProt_KB_Q_03217	15.38	DGGSLYMTQLVIDADGQLVAR
Nitrilase_Rhodococcus_rhodochrous_strain_J1	_UniProt_KB_Q_03217	99	DHNIAVVVGISER
Nitrilase_Rhodococcus_rhodochrous_strain_J1	_UniProt_KB_Q_03217	99	DHNIAVVVGISER
Nitrilase_Rhodococcus_rhodochrous_strain_J1	_UniProt_KB_Q_03217	99	DHNIAVVVGISER
Nitrilase_Rhodococcus_rhodochrous_strain_J1	_UniProt_KB_Q_03217	99	DHNIAVVVGISER
Nitrilase_Rhodococcus_rhodochrous_strain_J1	_UniProt_KB_Q_03217	99	DHNIAVVVGISER
Nitrilase_Rhodococcus_rhodochrous_strain_J1	_UniProt_KB_Q_03217	99	DHNIAVVVGISER

Nitrilase_Rhodococcus_rhodochrous_strain_J1	_UniProt_KB_Q_03217	99	DHNIAVVVGISER
Nitrilase_Rhodococcus_rhodochrous_strain_J1	_UniProt_KB_Q_03217	99	DHNIAVVVGISER
Nitrilase_Rhodococcus_rhodochrous_strain_J1	_UniProt_KB_Q_03217	99	DHNIAVVVGISER
Nitrilase_Rhodococcus_rhodochrous_strain_J1	_UniProt_KB_Q_03217	99	DHNIAVVVGISER
Nitrilase_Rhodococcus_rhodochrous_strain_J1	_UniProt_KB_Q_03217	99	DHNIAVVVGISER
Nitrilase_Rhodococcus_rhodochrous_strain_J1	_UniProt_KB_Q_03217	99	DHNIAVVVGISER
Nitrilase_Rhodococcus_rhodochrous_strain_J1	_UniProt_KB_Q_03217	99	DHNIAVVVGISER
Nitrilase_Rhodococcus_rhodochrous_strain_J1	_UniProt_KB_Q_03217	99	DHNIAVVVGISER
Nitrilase_Rhodococcus_rhodochrous_strain_J1	_UniProt_KB_Q_03217	99	DHNIAVVVGISER
Nitrilase_Rhodococcus_rhodochrous_strain_J1	_UniProt_KB_Q_03217	99	DHNIAVVVGISER
Nitrilase_Rhodococcus_rhodochrous_strain_J1	_UniProt_KB_Q_03217	99	DHNIAVVVGISER
Nitrilase_Rhodococcus_rhodochrous_strain_J1	_UniProt_KB_Q_03217	99	DHNIAVVVGISER
Nitrilase_Rhodococcus_rhodochrous_strain_J1	_UniProt_KB_Q_03217	99	DHNIAVVVGISER
Nitrilase_Rhodococcus_rhodochrous_strain_J1	_UniProt_KB_Q_03217	99	DHNIAVVVGISER
Nitrilase_Rhodococcus_rhodochrous_strain_J1	_UniProt_KB_Q_03217	99	DHNIAVVVGISER
Nitrilase_Rhodococcus_rhodochrous_strain_J1	_UniProt_KB_Q_03217	99	DHNIAVVVGISER
Nitrilase_Rhodococcus_rhodochrous_strain_J1	_UniProt_KB_Q_03217	99	DHNIAVVVGISER
Nitrilase_Rhodococcus_rhodochrous_strain_J1	_UniProt_KB_Q_03217	99	DHNIAVVVGISER
Nitrilase_Rhodococcus_rhodochrous_strain_J1	_UniProt_KB_Q_03217	99	DHNIAVVVGISER
Nitrilase_Rhodococcus_rhodochrous_strain_J1	_UniProt_KB_Q_03217	99	DHNIAVVVGISER

Nitrilase_Rhodococcus_rhodochrous_strain_J1	_UniProt_KB_Q_03217	99	DHNIAVVVGISER
Nitrilase_Rhodococcus_rhodochrous_strain_J1	_UniProt_KB_Q_03217	99	DHNIAVVVGISER
Nitrilase_Rhodococcus_rhodochrous_strain_J1	_UniProt_KB_Q_03217	99	DHNIAVVVGISER
Nitrilase_Rhodococcus_rhodochrous_strain_J1	_UniProt_KB_Q_03217	99	DHNIAVVVGISER
Nitrilase_Rhodococcus_rhodochrous_strain_J1	_UniProt_KB_Q_03217	99	DHNIAVVVGISER
Nitrilase_Rhodococcus_rhodochrous_strain_J1	_UniProt_KB_Q_03217	99	DHNIAVVVGISER
Nitrilase_Rhodococcus_rhodochrous_strain_J1	_UniProt_KB_Q_03217	99	DHNIAVVVGISER
Nitrilase_Rhodococcus_rhodochrous_strain_J1	_UniProt_KB_Q_03217	99	DHNIAVVVGISER
Nitrilase_Rhodococcus_rhodochrous_strain_J1	_UniProt_KB_Q_03217	99	DHNIAVVVGISER
Nitrilase_Rhodococcus_rhodochrous_strain_J1	_UniProt_KB_Q_03217	99	DHNIAVVVGISER
Nitrilase_Rhodococcus_rhodochrous_strain_J1	_UniProt_KB_Q_03217	99	DHNIAVVVGISER
Nitrilase_Rhodococcus_rhodochrous_strain_J1	_UniProt_KB_Q_03217	99	DHNIAVVVGISER
Nitrilase_Rhodococcus_rhodochrous_strain_J1	_UniProt_KB_Q_03217	99	DHNIAVVVGISER
Nitrilase_Rhodococcus_rhodochrous_strain_J1	_UniProt_KB_Q_03217	99	DHNIAVVVGISER
Nitrilase_Rhodococcus_rhodochrous_strain_J1	_UniProt_KB_Q_03217	99	DHNIAVVVGISER
Nitrilase_Rhodococcus_rhodochrous_strain_J1	_UniProt_KB_Q_03217	99	DHNIAVVVGISER
Nitrilase_Rhodococcus_rhodochrous_strain_J1	_UniProt_KB_Q_03217	99	DHNIAVVVGISER
Nitrilase_Rhodococcus_rhodochrous_strain_J1	_UniProt_KB_Q_03217	99	DHNIAVVVGISER
Nitrilase_Rhodococcus_rhodochrous_strain_J1	_UniProt_KB_Q_03217	99	DHNIAVVVGISER
Nitrilase_Rhodococcus_rhodochrous_strain_J1	_UniProt_KB_Q_03217	99	DHNIAVVVGISER

Nitrilase_Rhodococcus_rhodochrous_strain_J1	_UniProt_KB_Q_03217	99	DHNIAVVVGISER
Nitrilase_Rhodococcus_rhodochrous_strain_J1	_UniProt_KB_Q_03217	99	DHNIAVVVGISER
Nitrilase_Rhodococcus_rhodochrous_strain_J1	_UniProt_KB_Q_03217	99	DHNIAVVVGISER
Nitrilase_Rhodococcus_rhodochrous_strain_J1	_UniProt_KB_Q_03217	99	DHNIAVVVGISER
Nitrilase_Rhodococcus_rhodochrous_strain_J1	_UniProt_KB_Q_03217	99	DHNIAVVVGISER
Nitrilase_Rhodococcus_rhodochrous_strain_J1	_UniProt_KB_Q_03217	99	DHNIAVVVGISER
Nitrilase_Rhodococcus_rhodochrous_strain_J1	_UniProt_KB_Q_03217	99	DHNIAVVVGISER
Nitrilase_Rhodococcus_rhodochrous_strain_J1	_UniProt_KB_Q_03217	99	DHNIAVVVGISER
Nitrilase_Rhodococcus_rhodochrous_strain_J1	_UniProt_KB_Q_03217	99	DHNIAVVVGISER
Nitrilase_Rhodococcus_rhodochrous_strain_J1	_UniProt_KB_Q_03217	99	DHNIAVVVGISER
Nitrilase_Rhodococcus_rhodochrous_strain_J1	_UniProt_KB_Q_03217	99	DHNIAVVVGISER
Nitrilase_Rhodococcus_rhodochrous_strain_J1	_UniProt_KB_Q_03217	99	DHNIAVVVGISER
Nitrilase_Rhodococcus_rhodochrous_strain_J1	_UniProt_KB_Q_03217	98.33	DHNIAVVVGISER
Nitrilase_Rhodococcus_rhodochrous_strain_J1	_UniProt_KB_Q_03217	96.84	DHNIAVVVGISER
Nitrilase_Rhodococcus_rhodochrous_strain_J1	_UniProt_KB_Q_03217	88.54	DHNIAVVVGISER
Nitrilase_Rhodococcus_rhodochrous_strain_J1	_UniProt_KB_Q_03217	87.6	DHNIAVVVGISER
Nitrilase_Rhodococcus_rhodochrous_strain_J1	_UniProt_KB_Q_03217	86.13	DLATPLAEDEEGILYADIDLSAITL
Nitrilase_Rhodococcus_rhodochrous_strain_J1	_UniProt_KB_Q_03217	99	DLATPLAEDEEGILYADIDLSAITLAK

Nitrilase_Rhodococcus_rhodochrous_strain_J1	_UniProt_KB_Q_03217	99	DLATPLAEDEEGILYADIDLSAITLAK
Nitrilase_Rhodococcus_rhodochrous_strain_J1	_UniProt_KB_Q_03217	99	DLATPLAEDEEGILYADIDLSAITLAK
Nitrilase_Rhodococcus_rhodochrous_strain_J1	_UniProt_KB_Q_03217	99	DLATPLAEDEEGILYADIDLSAITLAK
Nitrilase_Rhodococcus_rhodochrous_strain_J1	_UniProt_KB_Q_03217	99	DLATPLAEDEEGILYADIDLSAITLAK
Nitrilase_Rhodococcus_rhodochrous_strain_J1	_UniProt_KB_Q_03217	99	DLATPLAEDEEGILYADIDLSAITLAK
Nitrilase_Rhodococcus_rhodochrous_strain_J1	_UniProt_KB_Q_03217	99	DLATPLAEDEEGILYADIDLSAITLAK
Nitrilase_Rhodococcus_rhodochrous_strain_J1	_UniProt_KB_Q_03217	99	DLATPLAEDEEGILYADIDLSAITLAK
Nitrilase_Rhodococcus_rhodochrous_strain_J1	_UniProt_KB_Q_03217	99	DLATPLAEDEEGILYADIDLSAITLAK
Nitrilase_Rhodococcus_rhodochrous_strain_J1	_UniProt_KB_Q_03217	99	DLATPLAEDEEGILYADIDLSAITLAK
Nitrilase_Rhodococcus_rhodochrous_strain_J1	_UniProt_KB_Q_03217	99	DLATPLAEDEEGILYADIDLSAITLAK
Nitrilase_Rhodococcus_rhodochrous_strain_J1	_UniProt_KB_Q_03217	99	DLATPLAEDEEGILYADIDLSAITLAK
Nitrilase_Rhodococcus_rhodochrous_strain_J1	_UniProt_KB_Q_03217	99	DLATPLAEDEEGILYADIDLSAITLAK
Nitrilase_Rhodococcus_rhodochrous_strain_J1	_UniProt_KB_Q_03217	99	DLATPLAEDEEGILYADIDLSAITLAK
Nitrilase_Rhodococcus_rhodochrous_strain_J1	_UniProt_KB_Q_03217	99	DLATPLAEDEEGILYADIDLSAITLAK
Nitrilase_Rhodococcus_rhodochrous_strain_J1	_UniProt_KB_Q_03217	99	DLATPLAEDEEGILYADIDLSAITLAK
Nitrilase_Rhodococcus_rhodochrous_strain_J1	_UniProt_KB_Q_03217	99	DLATPLAEDEEGILYADIDLSAITLAK
Nitrilase_Rhodococcus_rhodochrous_strain_J1	_UniProt_KB_Q_03217	99	DLATPLAEDEEGILYADIDLSAITLAK
Nitrilase_Rhodococcus_rhodochrous_strain_J1	_UniProt_KB_Q_03217	99	DLATPLAEDEEGILYADIDLSAITLAK
Nitrilase_Rhodococcus_rhodochrous_strain_J1	_UniProt_KB_Q_03217	99	DLATPLAEDEEGILYADIDLSAITLAK
Nitrilase_Rhodococcus_rhodochrous_strain_J1	_UniProt_KB_Q_03217	99	DLATPLAEDEEGILYADIDLSAITLAK
Nitrilase_Rhodococcus_rhodochrous_strain_J1	_UniProt_KB_Q_03217	99	DLATPLAEDEEGILYADIDLSAITLAK

Nitrilase_Rhodococcus_rhodochrous_strain_J1	_UniProt_KB_Q_03217	99	DLATPLAEDEEGILYADIDLSAITLAK
Nitrilase_Rhodococcus_rhodochrous_strain_J1	_UniProt_KB_Q_03217	99	DLATPLAEDEEGILYADIDLSAITLAK
Nitrilase_Rhodococcus_rhodochrous_strain_J1	_UniProt_KB_Q_03217	99	DLATPLAEDEEGILYADIDLSAITLAK
Nitrilase_Rhodococcus_rhodochrous_strain_J1	_UniProt_KB_Q_03217	99	DLATPLAEDEEGILYADIDLSAITLAK
Nitrilase_Rhodococcus_rhodochrous_strain_J1	_UniProt_KB_Q_03217	99	DLATPLAEDEEGILYADIDLSAITLAK
Nitrilase_Rhodococcus_rhodochrous_strain_J1	_UniProt_KB_Q_03217	99	DLATPLAEDEEGILYADIDLSAITLAK
Nitrilase_Rhodococcus_rhodochrous_strain_J1	_UniProt_KB_Q_03217	99	DLATPLAEDEEGILYADIDLSAITLAK
Nitrilase_Rhodococcus_rhodochrous_strain_J1	_UniProt_KB_Q_03217	99	DLATPLAEDEEGILYADIDLSAITLAK
Nitrilase_Rhodococcus_rhodochrous_strain_J1	_UniProt_KB_Q_03217	99	DLATPLAEDEEGILYADIDLSAITLAK
Nitrilase_Rhodococcus_rhodochrous_strain_J1	_UniProt_KB_Q_03217	99	DLATPLAEDEEGILYADIDLSAITLAK
Nitrilase_Rhodococcus_rhodochrous_strain_J1	_UniProt_KB_Q_03217	99	DLATPLAEDEEGILYADIDLSAITLAK
Nitrilase_Rhodococcus_rhodochrous_strain_J1	_UniProt_KB_Q_03217	99	DLATPLAEDEEGILYADIDLSAITLAK
Nitrilase_Rhodococcus_rhodochrous_strain_J1	_UniProt_KB_Q_03217	99	DLATPLAEDEEGILYADIDLSAITLAK
Nitrilase_Rhodococcus_rhodochrous_strain_J1	_UniProt_KB_Q_03217	99	DLATPLAEDEEGILYADIDLSAITLAK
Nitrilase_Rhodococcus_rhodochrous_strain_J1	_UniProt_KB_Q_03217	99	DLATPLAEDEEGILYADIDLSAITLAK
Nitrilase_Rhodococcus_rhodochrous_strain_J1	_UniProt_KB_Q_03217	99	DLATPLAEDEEGILYADIDLSAITLAK
Nitrilase_Rhodococcus_rhodochrous_strain_J1	_UniProt_KB_Q_03217	99	DLATPLAEDEEGILYADIDLSAITLAK
Nitrilase_Rhodococcus_rhodochrous_strain_J1	_UniProt_KB_Q_03217	99	DLATPLAEDEEGILYADIDLSAITLAK
Nitrilase_Rhodococcus_rhodochrous_strain_J1	_UniProt_KB_Q_03217	99	DLATPLAEDEEGILYADIDLSAITLAK
Nitrilase_Rhodococcus_rhodochrous_strain_J1	_UniProt_KB_Q_03217	99	DLATPLAEDEEGILYADIDLSAITLAK

Nitrilase_Rhodococcus_rhodochrous_strain_J1	_UniProt_KB_Q_03217	99	DLATPLAEDEEGILYADIDLSAITLAK
Nitrilase_Rhodococcus_rhodochrous_strain_J1	_UniProt_KB_Q_03217	99	DLATPLAEDEEGILYADIDLSAITLAK
Nitrilase_Rhodococcus_rhodochrous_strain_J1	_UniProt_KB_Q_03217	99	DLATPLAEDEEGILYADIDLSAITLAK
Nitrilase_Rhodococcus_rhodochrous_strain_J1	_UniProt_KB_Q_03217	99	DLATPLAEDEEGILYADIDLSAITLAK
Nitrilase_Rhodococcus_rhodochrous_strain_J1	_UniProt_KB_Q_03217	99	DLATPLAEDEEGILYADIDLSAITLAK
Nitrilase_Rhodococcus_rhodochrous_strain_J1	_UniProt_KB_Q_03217	99	DLATPLAEDEEGILYADIDLSAITLAK
Nitrilase_Rhodococcus_rhodochrous_strain_J1	_UniProt_KB_Q_03217	99	DLATPLAEDEEGILYADIDLSAITLAK
Nitrilase_Rhodococcus_rhodochrous_strain_J1	_UniProt_KB_Q_03217	99	DLATPLAEDEEGILYADIDLSAITLAK
Nitrilase_Rhodococcus_rhodochrous_strain_J1	_UniProt_KB_Q_03217	99	DLATPLAEDEEGILYADIDLSAITLAK
Nitrilase_Rhodococcus_rhodochrous_strain_J1	_UniProt_KB_Q_03217	99	DLATPLAEDEEGILYADIDLSAITLAK
Nitrilase_Rhodococcus_rhodochrous_strain_J1	_UniProt_KB_Q_03217	99	DLATPLAEDEEGILYADIDLSAITLAK
Nitrilase_Rhodococcus_rhodochrous_strain_J1	_UniProt_KB_Q_03217	99	DLATPLAEDEEGILYADIDLSAITLAK
Nitrilase_Rhodococcus_rhodochrous_strain_J1	_UniProt_KB_Q_03217	99	DLATPLAEDEEGILYADIDLSAITLAK
Nitrilase_Rhodococcus_rhodochrous_strain_J1	_UniProt_KB_Q_03217	99	DLATPLAEDEEGILYADIDLSAITLAK
Nitrilase_Rhodococcus_rhodochrous_strain_J1	_UniProt_KB_Q_03217	99	DLATPLAEDEEGILYADIDLSAITLAK
Nitrilase_Rhodococcus_rhodochrous_strain_J1	_UniProt_KB_Q_03217	99	DLATPLAEDEEGILYADIDLSAITLAK
Nitrilase_Rhodococcus_rhodochrous_strain_J1	_UniProt_KB_Q_03217	99	DLATPLAEDEEGILYADIDLSAITLAK
Nitrilase_Rhodococcus_rhodochrous_strain_J1	_UniProt_KB_Q_03217	99	DLATPLAEDEEGILYADIDLSAITLAK
Nitrilase_Rhodococcus_rhodochrous_strain_J1	_UniProt_KB_Q_03217	99	DLATPLAEDEEGILYADIDLSAITLAK
Nitrilase_Rhodococcus_rhodochrous_strain_J1	_UniProt_KB_Q_03217	99	DLATPLAEDEEGILYADIDLSAITLAK

Nitrilase_Rhodococcus_rhodochrous_strain_J1	_UniProt_KB_Q_03217	99	DLATPLAEDEEGILYADIDLSAITLAK
Nitrilase_Rhodococcus_rhodochrous_strain_J1	_UniProt_KB_Q_03217	99	DLATPLAEDEEGILYADIDLSAITLAK
Nitrilase_Rhodococcus_rhodochrous_strain_J1	_UniProt_KB_Q_03217	99	DLATPLAEDEEGILYADIDLSAITLAK
Nitrilase_Rhodococcus_rhodochrous_strain_J1	_UniProt_KB_Q_03217	99	DLATPLAEDEEGILYADIDLSAITLAK
Nitrilase_Rhodococcus_rhodochrous_strain_J1	_UniProt_KB_Q_03217	99	DLATPLAEDEEGILYADIDLSAITLAK
Nitrilase_Rhodococcus_rhodochrous_strain_J1	_UniProt_KB_Q_03217	99	DLATPLAEDEEGILYADIDLSAITLAK
Nitrilase_Rhodococcus_rhodochrous_strain_J1	_UniProt_KB_Q_03217	99	DLATPLAEDEEGILYADIDLSAITLAK
Nitrilase_Rhodococcus_rhodochrous_strain_J1	_UniProt_KB_Q_03217	99	DLATPLAEDEEGILYADIDLSAITLAK
Nitrilase_Rhodococcus_rhodochrous_strain_J1	_UniProt_KB_Q_03217	99	DLATPLAEDEEGILYADIDLSAITLAK
Nitrilase_Rhodococcus_rhodochrous_strain_J1	_UniProt_KB_Q_03217	99	DLATPLAEDEEGILYADIDLSAITLAK
Nitrilase_Rhodococcus_rhodochrous_strain_J1	_UniProt_KB_Q_03217	99	DLATPLAEDEEGILYADIDLSAITLAK
Nitrilase_Rhodococcus_rhodochrous_strain_J1	_UniProt_KB_Q_03217	99	DLATPLAEDEEGILYADIDLSAITLAK
Nitrilase_Rhodococcus_rhodochrous_strain_J1	_UniProt_KB_Q_03217	99	DLATPLAEDEEGILYADIDLSAITLAK
Nitrilase_Rhodococcus_rhodochrous_strain_J1	_UniProt_KB_Q_03217	99	DLATPLAEDEEGILYADIDLSAITLAK
Nitrilase_Rhodococcus_rhodochrous_strain_J1	_UniProt_KB_Q_03217	99	DLATPLAEDEEGILYADIDLSAITLAK
Nitrilase_Rhodococcus_rhodochrous_strain_J1	_UniProt_KB_Q_03217	99	DLATPLAEDEEGILYADIDLSAITLAK
Nitrilase_Rhodococcus_rhodochrous_strain_J1	_UniProt_KB_Q_03217	93.12	DLATPLAEDEEGILYADIDLSAITLAK
Nitrilase_Rhodococcus_rhodochrous_strain_J1	_UniProt_KB_Q_03217	87.53	DLATPLAEDEEGILYADIDLSAITLAK
Nitrilase_Rhodococcus_rhodochrous_strain_J1	_UniProt_KB_Q_03217	85.25	DLATPLAEDEEGILYADIDLSAITLAK
Nitrilase_Rhodococcus_rhodochrous_strain_J1	_UniProt_KB_Q_03217	85.25	DLATPLAEDEEGILYADIDLSAITLAK

Nitrilase_Rhodococcus_rhodochrous_strain_J1	_UniProt_KB_Q_03217	85.25	DLATPLAEDEEGILYADIDLSAITLAK
Nitrilase_Rhodococcus_rhodochrous_strain_J1	_UniProt_KB_Q_03217	85.25	DLATPLAEDEEGILYADIDLSAITLAK
Nitrilase_Rhodococcus_rhodochrous_strain_J1	_UniProt_KB_Q_03217	85.25	DLATPLAEDEEGILYADIDLSAITLAK
Nitrilase_Rhodococcus_rhodochrous_strain_J1	_UniProt_KB_Q_03217	85.25	DLATPLAEDEEGILYADIDLSAITLAK
Nitrilase_Rhodococcus_rhodochrous_strain_J1	_UniProt_KB_Q_03217	85.25	DLATPLAEDEEGILYADIDLSAITLAK
Nitrilase_Rhodococcus_rhodochrous_strain_J1	_UniProt_KB_Q_03217	85.1	DLATPLAEDEEGILYADIDLSAITLAK
Nitrilase_Rhodococcus_rhodochrous_strain_J1	_UniProt_KB_Q_03217	83.71	DLATPLAEDEEGILYADIDLSAITLAK
Nitrilase_Rhodococcus_rhodochrous_strain_J1	_UniProt_KB_Q_03217	81.61	DLATPLAEDEEGILYADIDLSAITLAK
Nitrilase_Rhodococcus_rhodochrous_strain_J1	_UniProt_KB_Q_03217	81.61	DLATPLAEDEEGILYADIDLSAITLAK
Nitrilase_Rhodococcus_rhodochrous_strain_J1	_UniProt_KB_Q_03217	65.55	DLATPLAEDEEGILYADIDLSAITLAK
Nitrilase_Rhodococcus_rhodochrous_strain_J1	_UniProt_KB_Q_03217	65.55	DLATPLAEDEEGILYADIDLSAITLAK
Nitrilase_Rhodococcus_rhodochrous_strain_J1	_UniProt_KB_Q_03217	42.49	DLATPLAEDEEGILYADIDLSAITLAK
Nitrilase_Rhodococcus_rhodochrous_strain_J1	_UniProt_KB_Q_03217	42.49	DLATPLAEDEEGILYADIDLSAITLAK
Nitrilase_Rhodococcus_rhodochrous_strain_J1	_UniProt_KB_Q_03217	25.8	DLATPLAEDEEGILYADIDLSAITLAK
Nitrilase_Rhodococcus_rhodochrous_strain_J1	_UniProt_KB_Q_03217	25.8	DLATPLAEDEEGILYADIDLSAITLAK
Nitrilase_Rhodococcus_rhodochrous_strain_J1	_UniProt_KB_Q_03217	25.8	DLATPLAEDEEGILYADIDLSAITLAK
Nitrilase_Rhodococcus_rhodochrous_strain_J1	_UniProt_KB_Q_03217	25.8	DLATPLAEDEEGILYADIDLSAITLAK
Nitrilase_Rhodococcus_rhodochrous_strain_J1	_UniProt_KB_Q_03217	21.6	DLATPLAEDEEGILYADIDLSAITLAK
Nitrilase_Rhodococcus_rhodochrous_strain_J1	_UniProt_KB_Q_03217	19.32	DLATPLAEDEEGILYADIDLSAITLAK

Nitrilase_Rhodococcus_rhodochrous_strain_J1	_UniProt_KB_Q_03217	17.74	DLATPLAEDEEGILYADIDLSAITLAK
Nitrilase_Rhodococcus_rhodochrous_strain_J1	_UniProt_KB_Q_03217	17.74	DLATPLAEDEEGILYADIDLSAITLAK
Nitrilase_Rhodococcus_rhodochrous_strain_J1	_UniProt_KB_Q_03217	15.13	DLATPLAEDEEGILYADIDLSAITLAK
Nitrilase_Rhodococcus_rhodochrous_strain_J1	_UniProt_KB_Q_03217	15.13	DLATPLAEDEEGILYADIDLSAITLAK
Nitrilase_Rhodococcus_rhodochrous_strain_J1	_UniProt_KB_Q_03217	15.13	DLATPLAEDEEGILYADIDLSAITLAK
Nitrilase_Rhodococcus_rhodochrous_strain_J1	_UniProt_KB_Q_03217	15.13	DLATPLAEDEEGILYADIDLSAITLAK
Nitrilase_Rhodococcus_rhodochrous_strain_J1	_UniProt_KB_Q_03217	99	ELNGADEQR
Nitrilase_Rhodococcus_rhodochrous_strain_J1	_UniProt_KB_Q_03217	85.62	HENSLTMDSPHVQR
Nitrilase_Rhodococcus_rhodochrous_strain_J1	_UniProt_KB_Q_03217	20.86	HENSLTMDSPHVQR
Nitrilase_Rhodococcus_rhodochrous_strain_J1	_UniProt_KB_Q_03217	99	IIGPDGR
Nitrilase_Rhodococcus_rhodochrous_strain_J1	_UniProt_KB_Q_03217	98.14	IIGPDGR
Nitrilase_Rhodococcus_rhodochrous_strain_J1	_UniProt_KB_Q_03217	74.27	IIGPDGR
Nitrilase_Rhodococcus_rhodochrous_strain_J1	_UniProt_KB_Q_03217	99	KLKPTHVER
Nitrilase_Rhodococcus_rhodochrous_strain_J1	_UniProt_KB_Q_03217	99	KLKPTHVER
Nitrilase_Rhodococcus_rhodochrous_strain_J1	_UniProt_KB_Q_03217	99	KLKPTHVER
Nitrilase_Rhodococcus_rhodochrous_strain_J1	_UniProt_KB_Q_03217	99	KLKPTHVER
Nitrilase_Rhodococcus_rhodochrous_strain_J1	_UniProt_KB_Q_03217	99	KLKPTHVER
Nitrilase_Rhodococcus_rhodochrous_strain_J1	_UniProt_KB_Q_03217	98.16	KLKPTHVER
Nitrilase_Rhodococcus_rhodochrous_strain_J1	_UniProt_KB_Q_03217	99	LGALNCWEHFQTLTK

Nitrilase_Rhodococcus_rhodochrous_strain_J1	_UniProt_KB_Q_03217	99	LGALNCWEHFQTLTK
Nitrilase_Rhodococcus_rhodochrous_strain_J1	_UniProt_KB_Q_03217	99	LGALNCWEHFQTLTK
Nitrilase_Rhodococcus_rhodochrous_strain_J1	_UniProt_KB_Q_03217	99	LGALNCWEHFQTLTK
Nitrilase_Rhodococcus_rhodochrous_strain_J1	_UniProt_KB_Q_03217	99	LGALNCWEHFQTLTK
Nitrilase_Rhodococcus_rhodochrous_strain_J1	_UniProt_KB_Q_03217	99	LGALNCWEHFQTLTK
Nitrilase_Rhodococcus_rhodochrous_strain_J1	_UniProt_KB_Q_03217	99	LGALNCWEHFQTLTK
Nitrilase_Rhodococcus_rhodochrous_strain_J1	_UniProt_KB_Q_03217	99	LGALNCWEHFQTLTK
Nitrilase_Rhodococcus_rhodochrous_strain_J1	_UniProt_KB_Q_03217	99	LGALNCWEHFQTLTK
Nitrilase_Rhodococcus_rhodochrous_strain_J1	_UniProt_KB_Q_03217	99	LGALNCWEHFQTLTK
Nitrilase_Rhodococcus_rhodochrous_strain_J1	_UniProt_KB_Q_03217	99	LGALNCWEHFQTLTK
Nitrilase_Rhodococcus_rhodochrous_strain_J1	_UniProt_KB_Q_03217	99	LGALNCWEHFQTLTK
Nitrilase_Rhodococcus_rhodochrous_strain_J1	_UniProt_KB_Q_03217	99	LGALNCWEHFQTLTK
Nitrilase_Rhodococcus_rhodochrous_strain_J1	_UniProt_KB_Q_03217	99	LGALNCWEHFQTLTK
Nitrilase_Rhodococcus_rhodochrous_strain_J1	_UniProt_KB_Q_03217	99	LGALNCWEHFQTLTK
Nitrilase_Rhodococcus_rhodochrous_strain_J1	_UniProt_KB_Q_03217	99	LGALNCWEHFQTLTK
Nitrilase_Rhodococcus_rhodochrous_strain_J1	_UniProt_KB_Q_03217	97.84	LGALNCWEHFQTLTK
Nitrilase_Rhodococcus_rhodochrous_strain_J1	_UniProt_KB_Q_03217	96.7	LGALNCWEHFQTLTK
Nitrilase_Rhodococcus_rhodochrous_strain_J1	_UniProt_KB_Q_03217	96.47	LGALNCWEHFQTLTK
Nitrilase_Rhodococcus_rhodochrous_strain_J1	_UniProt_KB_Q_03217	96.43	LGALNCWEHFQTLTK

Nitrilase_Rhodococcus_rhodochrous_strain_J1	_UniProt_KB_Q_03217	96.32	LGALNCWEHFQTLTK
Nitrilase_Rhodococcus_rhodochrous_strain_J1	_UniProt_KB_Q_03217	93.21	LGALNCWEHFQTLTK
Nitrilase_Rhodococcus_rhodochrous_strain_J1	_UniProt_KB_Q_03217	74.51	LGALNCWEHFQTLTK
Nitrilase_Rhodococcus_rhodochrous_strain_J1	_UniProt_KB_Q_03217	71.42	LGALNCWEHFQTLTK
Nitrilase_Rhodococcus_rhodochrous_strain_J1	_UniProt_KB_Q_03217	62.63	LGALNCWEHFQTLTK
Nitrilase_Rhodococcus_rhodochrous_strain_J1	_UniProt_KB_Q_03217	48.49	LGALNCWEHFQTLTK
Nitrilase_Rhodococcus_rhodochrous_strain_J1	_UniProt_KB_Q_03217	44.05	LGALNCWEHFQTLTK
Nitrilase_Rhodococcus_rhodochrous_strain_J1	_UniProt_KB_Q_03217	39.38	LGALNCWEHFQTLTK
Nitrilase_Rhodococcus_rhodochrous_strain_J1	_UniProt_KB_Q_03217	23.32	LGALNCWEHFQTLTK
Nitrilase_Rhodococcus_rhodochrous_strain_J1	_UniProt_KB_Q_03217	18.32	LGALNCWEHFQTLTK
Nitrilase_Rhodococcus_rhodochrous_strain_J1	_UniProt_KB_Q_03217	17.26	LGALNCWEHFQTLTK
Nitrilase_Rhodococcus_rhodochrous_strain_J1	_UniProt_KB_Q_03217	75.68	MDSPHVQR
Nitrilase_Rhodococcus_rhodochrous_strain_J1	_UniProt_KB_Q_03217	99	MVEYTNTFK
Nitrilase_Rhodococcus_rhodochrous_strain_J1	_UniProt_KB_Q_03217	99	MVEYTNTFK
Nitrilase_Rhodococcus_rhodochrous_strain_J1	_UniProt_KB_Q_03217	99	MVEYTNTFK
Nitrilase_Rhodococcus_rhodochrous_strain_J1	_UniProt_KB_Q_03217	98.18	MVEYTNTFK
Nitrilase_Rhodococcus_rhodochrous_strain_J1	_UniProt_KB_Q_03217	99	MYALEGQTFVVC
Nitrilase_Rhodococcus_rhodochrous_strain_J1	_UniProt_KB_Q_03217	99	MYALEGQTFVVCTTQVVTPEAHEFFCDNDEQR
Nitrilase_Rhodococcus_rhodochrous_strain_J1	_UniProt_KB_Q_03217	99	MYALEGQTFVVCTTQVVTPEAHEFFCDNDEQR

Nitrilase_Rhodococcus_rhodochrous_strain_J1	_UniProt_KB_Q_03217	99	MYALEGQTFVVCTTQVVTPEAHEFFCDNDEQR
Nitrilase_Rhodococcus_rhodochrous_strain_J1	_UniProt_KB_Q_03217	99	MYALEGQTFVVCTTQVVTPEAHEFFCDNDEQR
Nitrilase_Rhodococcus_rhodochrous_strain_J1	_UniProt_KB_Q_03217	99	MYALEGQTFVVCTTQVVTPEAHEFFCDNDEQR
Nitrilase_Rhodococcus_rhodochrous_strain_J1	_UniProt_KB_Q_03217	99	MYALEGQTFVVCTTQVVTPEAHEFFCDNDEQR
Nitrilase_Rhodococcus_rhodochrous_strain_J1	_UniProt_KB_Q_03217	93.88	MYALEGQTFVVCTTQVVTPEAHEFFCDNDEQR
Nitrilase_Rhodococcus_rhodochrous_strain_J1	_UniProt_KB_Q_03217	91.93	MYALEGQTFVVCTTQVVTPEAHEFFCDNDEQR
Nitrilase_Rhodococcus_rhodochrous_strain_J1	_UniProt_KB_Q_03217	89.46	MYALEGQTFVVCTTQVVTPEAHEFFCDNDEQR
Nitrilase_Rhodococcus_rhodochrous_strain_J1	_UniProt_KB_Q_03217	99	NGCELVAFPEVFIPGYPYHIWVDSPLAGMAK
Nitrilase_Rhodococcus_rhodochrous_strain_J1	_UniProt_KB_Q_03217	99	NGCELVAFPEVFIPGYPYHIWVDSPLAGMAK
Nitrilase_Rhodococcus_rhodochrous_strain_J1	_UniProt_KB_Q_03217	99	NGCELVAFPEVFIPGYPYHIWVDSPLAGMAK
Nitrilase_Rhodococcus_rhodochrous_strain_J1	_UniProt_KB_Q_03217	99	NGCELVAFPEVFIPGYPYHIWVDSPLAGMAK
Nitrilase_Rhodococcus_rhodochrous_strain_J1	_UniProt_KB_Q_03217	99	NGCELVAFPEVFIPGYPYHIWVDSPLAGMAK
Nitrilase_Rhodococcus_rhodochrous_strain_J1	_UniProt_KB_Q_03217	99	NGCELVAFPEVFIPGYPYHIWVDSPLAGMAK
Nitrilase_Rhodococcus_rhodochrous_strain_J1	_UniProt_KB_Q_03217	99	NGCELVAFPEVFIPGYPYHIWVDSPLAGMAK
Nitrilase_Rhodococcus_rhodochrous_strain_J1	_UniProt_KB_Q_03217	99	NGCELVAFPEVFIPGYPYHIWVDSPLAGMAK
Nitrilase_Rhodococcus_rhodochrous_strain_J1	_UniProt_KB_Q_03217	99	NGCELVAFPEVFIPGYPYHIWVDSPLAGMAK
Nitrilase_Rhodococcus_rhodochrous_strain_J1	_UniProt_KB_Q_03217	99	NGCELVAFPEVFIPGYPYHIWVDSPLAGMAK
Nitrilase_Rhodococcus_rhodochrous_strain_J1	_UniProt_KB_Q_03217	99	NGCELVAFPEVFIPGYPYHIWVDSPLAGMAK
Nitrilase_Rhodococcus_rhodochrous_strain_J1	_UniProt_KB_Q_03217	99	NGCELVAFPEVFIPGYPYHIWVDSPLAGMAK

Nitrilase_Rhodococcus_rhodochrous_strain_J1	_UniProt_KB_Q_03217	99	NGCELVAFPEVFIPGYPYHIWVDSPLAGMAK
Nitrilase_Rhodococcus_rhodochrous_strain_J1	_UniProt_KB_Q_03217	99	NGCELVAFPEVFIPGYPYHIWVDSPLAGMAK
Nitrilase_Rhodococcus_rhodochrous_strain_J1	_UniProt_KB_Q_03217	99	NGCELVAFPEVFIPGYPYHIWVDSPLAGMAK
Nitrilase_Rhodococcus_rhodochrous_strain_J1	_UniProt_KB_Q_03217	99	NGCELVAFPEVFIPGYPYHIWVDSPLAGMAK
Nitrilase_Rhodococcus_rhodochrous_strain_J1	_UniProt_KB_Q_03217	99	NGCELVAFPEVFIPGYPYHIWVDSPLAGMAK
Nitrilase_Rhodococcus_rhodochrous_strain_J1	_UniProt_KB_Q_03217	93.09	NGCELVAFPEVFIPGYPYHIWVDSPLAGMAK
Nitrilase_Rhodococcus_rhodochrous_strain_J1	_UniProt_KB_Q_03217	93.09	NGCELVAFPEVFIPGYPYHIWVDSPLAGMAK
Nitrilase_Rhodococcus_rhodochrous_strain_J1	_UniProt_KB_Q_03217	80.41	NGCELVAFPEVFIPGYPYHIWVDSPLAGMAK
Nitrilase_Rhodococcus_rhodochrous_strain_J1	_UniProt_KB_Q_03217	78.44	NGCELVAFPEVFIPGYPYHIWVDSPLAGMAK
Nitrilase_Rhodococcus_rhodochrous_strain_J1	_UniProt_KB_Q_03217	57.48	NGCELVAFPEVFIPGYPYHIWVDSPLAGMAK
Nitrilase_Rhodococcus_rhodochrous_strain_J1	_UniProt_KB_Q_03217	57.48	NGCELVAFPEVFIPGYPYHIWVDSPLAGMAK
Nitrilase_Rhodococcus_rhodochrous_strain_J1	_UniProt_KB_Q_03217	57.48	NGCELVAFPEVFIPGYPYHIWVDSPLAGMAK
Nitrilase_Rhodococcus_rhodochrous_strain_J1	_UniProt_KB_Q_03217	57.48	NGCELVAFPEVFIPGYPYHIWVDSPLAGMAK
Nitrilase_Rhodococcus_rhodochrous_strain_J1	_UniProt_KB_Q_03217	45.62	NGCELVAFPEVFIPGYPYHIWVDSPLAGMAK
Nitrilase_Rhodococcus_rhodochrous_strain_J1	_UniProt_KB_Q_03217	30.32	NGCELVAFPEVFIPGYPYHIWVDSPLAGMAK
Nitrilase_Rhodococcus_rhodochrous_strain_J1	_UniProt_KB_Q_03217	30.32	NGCELVAFPEVFIPGYPYHIWVDSPLAGMAK
Nitrilase_Rhodococcus_rhodochrous_strain_J1	_UniProt_KB_Q_03217	18.2	NGCELVAFPEVFIPGYPYHIWVDSPLAGMAK
Nitrilase_Rhodococcus_rhodochrous_strain_J1	_UniProt_KB_Q_03217	17.94	NGCELVAFPEVFIPGYPYHIWVDSPLAGMAK
Nitrilase_Rhodococcus_rhodochrous_strain_J1	_UniProt_KB_Q_03217	17.39	NGCELVAFPEVFIPGYPYHIWVDSPLAGMAK

Nitrilase_Rhodococcus_rhodochrous_strain_J1	_UniProt_KB_Q_03217	16.36	NGCELVAFPEVFIPGYPYHIWVDSPLAGMAK
Nitrilase_Rhodococcus_rhodochrous_strain_J1	_UniProt_KB_Q_03217	16.23	NGCELVAFPEVFIPGYPYHIWVDSPLAGMAK
Nitrilase_Rhodococcus_rhodochrous_strain_J1	_UniProt_KB_Q_03217	16.23	NGCELVAFPEVFIPGYPYHIWVDSPLAGMAK
Nitrilase_Rhodococcus_rhodochrous_strain_J1	_UniProt_KB_Q_03217	99	PDVLSLNFNQR
Nitrilase_Rhodococcus_rhodochrous_strain_J1	_UniProt_KB_Q_03217	98.53	PDVLSLNFNQR
Nitrilase_Rhodococcus_rhodochrous_strain_J1	_UniProt_KB_Q_03217	23.66	PGYPYHIWVDSPLAGMAKFAVRYHENSLTMDSPHVQRLLDAAR
Nitrilase_Rhodococcus_rhodochrous_strain_J1	_UniProt_KB_Q_03217	99	QAADPVGHYSR
Nitrilase_Rhodococcus_rhodochrous_strain_J1	_UniProt_KB_Q_03217	78.53	QAADPVGHYSRPDVL
Nitrilase_Rhodococcus_rhodochrous_strain_J1	_UniProt_KB_Q_03217	97.33	QAADPVGHYSRPDVLSL
Nitrilase_Rhodococcus_rhodochrous_strain_J1	_UniProt_KB_Q_03217	99	QAADPVGHYSRPDVLSLNFNQR
Nitrilase_Rhodococcus_rhodochrous_strain_J1	_UniProt_KB_Q_03217	99	QAADPVGHYSRPDVLSLNFNQR
Nitrilase_Rhodococcus_rhodochrous_strain_J1	_UniProt_KB_Q_03217	99	QAADPVGHYSRPDVLSLNFNQR
Nitrilase_Rhodococcus_rhodochrous_strain_J1	_UniProt_KB_Q_03217	99	QAADPVGHYSRPDVLSLNFNQR
Nitrilase_Rhodococcus_rhodochrous_strain_J1	_UniProt_KB_Q_03217	99	QAADPVGHYSRPDVLSLNFNQR
Nitrilase_Rhodococcus_rhodochrous_strain_J1	_UniProt_KB_Q_03217	99	QAADPVGHYSRPDVLSLNFNQR
Nitrilase_Rhodococcus_rhodochrous_strain_J1	_UniProt_KB_Q_03217	99	QAADPVGHYSRPDVLSLNFNQR
Nitrilase_Rhodococcus_rhodochrous_strain_J1	_UniProt_KB_Q_03217	99	QAADPVGHYSRPDVLSLNFNQR
Nitrilase_Rhodococcus_rhodochrous_strain_J1	_UniProt_KB_Q_03217	99	QAADPVGHYSRPDVLSLNFNQR
Nitrilase_Rhodococcus_rhodochrous_strain_J1	_UniProt_KB_Q_03217	99	QAADPVGHYSRPDVLSLNFNQR

Nitrilase_Rhodococcus_rhodochrous_strain_J1	_UniProt_KB_Q_03217	99	QAADPVGHYSRPDVLSLNFNQR
Nitrilase_Rhodococcus_rhodochrous_strain_J1	_UniProt_KB_Q_03217	98.57	QAADPVGHYSRPDVLSLNFNQR
Nitrilase_Rhodococcus_rhodochrous_strain_J1	_UniProt_KB_Q_03217	96.39	QAADPVGHYSRPDVLSLNFNQR
Nitrilase_Rhodococcus_rhodochrous_strain_J1	_UniProt_KB_Q_03217	95.17	QAADPVGHYSRPDVLSLNFNQR
Nitrilase_Rhodococcus_rhodochrous_strain_J1	_UniProt_KB_Q_03217	92.39	QAADPVGHYSRPDVLSLNFNQR
Nitrilase_Rhodococcus_rhodochrous_strain_J1	_UniProt_KB_Q_03217	55.24	QAADPVGHYSRPDVLSLNFNQR
Nitrilase_Rhodococcus_rhodochrous_strain_J1	_UniProt_KB_Q_03217	55.24	QAADPVGHYSRPDVLSLNFNQR
Nitrilase_Rhodococcus_rhodochrous_strain_J1	_UniProt_KB_Q_03217	51.36	QAADPVGHYSRPDVLSLNFNQR
Nitrilase_Rhodococcus_rhodochrous_strain_J1	_UniProt_KB_Q_03217	51	QAADPVGHYSRPDVLSLNFNQR
Nitrilase_Rhodococcus_rhodochrous_strain_J1	_UniProt_KB_Q_03217	49.17	QAADPVGHYSRPDVLSLNFNQR
Nitrilase_Rhodococcus_rhodochrous_strain_J1	_UniProt_KB_Q_03217	18.15	QAADPVGHYSRPDVLSLNFNQR
Nitrilase_Rhodococcus_rhodochrous_strain_J1	_UniProt_KB_Q_03217	17.75	QAADPVGHYSRPDVLSLNFNQR
Nitrilase_Rhodococcus_rhodochrous_strain_J1	_UniProt_KB_Q_03217	16.15	QAADPVGHYSRPDVLSLNFNQR
Nitrilase_Rhodococcus_rhodochrous_strain_J1	_UniProt_KB_Q_03217	16.15	QAADPVGHYSRPDVLSLNFNQR
Nitrilase_Rhodococcus_rhodochrous_strain_J1	_UniProt_KB_Q_03217	33.26	SLNFNQR
Nitrilase_Rhodococcus_rhodochrous_strain_J1	_UniProt_KB_Q_03217	99	SLTMDSPHVQR
Nitrilase_Rhodococcus_rhodochrous_strain_J1	_UniProt_KB_Q_03217	48.01	SLTMDSPHVQR
Nitrilase_Rhodococcus_rhodochrous_strain_J1	_UniProt_KB_Q_03217	42.37	SLTMDSPHVQR
Nitrilase_Rhodococcus_rhodochrous_strain_J1	_UniProt_KB_Q_03217	39.27	SLTMDSPHVQRLLDAARDHNIAVVVGISERDGGSLYMTQLVIDADGQLVAR

Nitrilase_Rhodococcus_rhodochrous_strain_J1	_UniProt_KB_Q_03217	33.48	SLTMDSPHVQRLLDAARDHNIAVVVGISERDGGSLYMTQLVIDADGQLVAR
Nitrilase_Rhodococcus_rhodochrous_strain_J1	_UniProt_KB_Q_03217	33.48	SLTMDSPHVQRLLDAARDHNIAVVVGISERDGGSLYMTQLVIDADGQLVAR
Nitrilase_Rhodococcus_rhodochrous_strain_J1	_UniProt_KB_Q_03217	33.48	SLTMDSPHVQRLLDAARDHNIAVVVGISERDGGSLYMTQLVIDADGQLVAR
Nitrilase_Rhodococcus_rhodochrous_strain_J1	_UniProt_KB_Q_03217	43.41	SMHEQVHVASWPGMSLYQPEVPAFGVDAQLTATR
Nitrilase_Rhodococcus_rhodochrous_strain_J1	_UniProt_KB_Q_03217	43.41	SMHEQVHVASWPGMSLYQPEVPAFGVDAQLTATR
Nitrilase_Rhodococcus_rhodochrous_strain_J1	_UniProt_KB_Q_03217	36.2	SMHEQVHVASWPGMSLYQPEVPAFGVDAQLTATR
Nitrilase_Rhodococcus_rhodochrous_strain_J1	_UniProt_KB_Q_03217	32.34	SMHEQVHVASWPGMSLYQPEVPAFGVDAQLTATR
Nitrilase_Rhodococcus_rhodochrous_strain_J1	_UniProt_KB_Q_03217	32.34	SMHEQVHVASWPGMSLYQPEVPAFGVDAQLTATR
Nitrilase_Rhodococcus_rhodochrous_strain_J1	_UniProt_KB_Q_03217	32.34	SMHEQVHVASWPGMSLYQPEVPAFGVDAQLTATR
Nitrilase_Rhodococcus_rhodochrous_strain_J1	_UniProt_KB_Q_03217	32.34	SMHEQVHVASWPGMSLYQPEVPAFGVDAQLTATR
Nitrilase_Rhodococcus_rhodochrous_strain_J1	_UniProt_KB_Q_03217	99	SRPDVLSLNFNQR
Nitrilase_Rhodococcus_rhodochrous_strain_J1	_UniProt_KB_Q_03217	98.57	SRPDVLSLNFNQR
Nitrilase_Rhodococcus_rhodochrous_strain_J1	_UniProt_KB_Q_03217	99	SVYGEGNGSDISVYDMPFAR
Nitrilase_Rhodococcus_rhodochrous_strain_J1	_UniProt_KB_Q_03217	99	SVYGEGNGSDISVYDMPFAR
Nitrilase_Rhodococcus_rhodochrous_strain_J1	_UniProt_KB_Q_03217	99	SVYGEGNGSDISVYDMPFAR
Nitrilase_Rhodococcus_rhodochrous_strain_J1	_UniProt_KB_Q_03217	99	SVYGEGNGSDISVYDMPFAR
Nitrilase_Rhodococcus_rhodochrous_strain_J1	_UniProt_KB_Q_03217	99	SVYGEGNGSDISVYDMPFAR
Nitrilase_Rhodococcus_rhodochrous_strain_J1	_UniProt_KB_Q_03217	99	SVYGEGNGSDISVYDMPFAR
Nitrilase_Rhodococcus_rhodochrous_strain_J1	_UniProt_KB_Q_03217	99	SVYGEGNGSDISVYDMPFAR

Nitrilase_Rhodococcus_rhodochrous_strain_J1	_UniProt_KB_Q_03217	99	SVYGEGNGSDISVYDMPFAR
Nitrilase_Rhodococcus_rhodochrous_strain_J1	_UniProt_KB_Q_03217	99	SVYGEGNGSDISVYDMPFAR
Nitrilase_Rhodococcus_rhodochrous_strain_J1	_UniProt_KB_Q_03217	99	SVYGEGNGSDISVYDMPFAR
Nitrilase_Rhodococcus_rhodochrous_strain_J1	_UniProt_KB_Q_03217	99	SVYGEGNGSDISVYDMPFAR
Nitrilase_Rhodococcus_rhodochrous_strain_J1	_UniProt_KB_Q_03217	99	SVYGEGNGSDISVYDMPFAR
Nitrilase_Rhodococcus_rhodochrous_strain_J1	_UniProt_KB_Q_03217	99	SVYGEGNGSDISVYDMPFAR
Nitrilase_Rhodococcus_rhodochrous_strain_J1	_UniProt_KB_Q_03217	99	SVYGEGNGSDISVYDMPFAR
Nitrilase_Rhodococcus_rhodochrous_strain_J1	_UniProt_KB_Q_03217	99	SVYGEGNGSDISVYDMPFAR
Nitrilase_Rhodococcus_rhodochrous_strain_J1	_UniProt_KB_Q_03217	99	SVYGEGNGSDISVYDMPFAR
Nitrilase_Rhodococcus_rhodochrous_strain_J1	_UniProt_KB_Q_03217	98.27	SVYGEGNGSDISVYDMPFAR
Nitrilase_Rhodococcus_rhodochrous_strain_J1	_UniProt_KB_Q_03217	85.25	SVYGEGNGSDISVYDMPFAR
Nitrilase_Rhodococcus_rhodochrous_strain_J1	_UniProt_KB_Q_03217	74.28	SVYGEGNGSDISVYDMPFAR
Nitrilase_Rhodococcus_rhodochrous_strain_J1	_UniProt_KB_Q_03217	71.48	SVYGEGNGSDISVYDMPFAR
Nitrilase_Rhodococcus_rhodochrous_strain_J1	_UniProt_KB_Q_03217	70.43	SVYGEGNGSDISVYDMPFAR
Nitrilase_Rhodococcus_rhodochrous_strain_J1	_UniProt_KB_Q_03217	49.11	SVYGEGNGSDISVYDMPFAR
Nitrilase_Rhodococcus_rhodochrous_strain_J1	_UniProt_KB_Q_03217	25.8	SVYGEGNGSDISVYDMPFAR
Nitrilase_Rhodococcus_rhodochrous_strain_J1	_UniProt_KB_Q_03217	25.8	SVYGEGNGSDISVYDMPFAR
Nitrilase_Rhodococcus_rhodochrous_strain_J1	_UniProt_KB_Q_03217	23.16	SVYGEGNGSDISVYDMPFAR
Nitrilase_Rhodococcus_rhodochrous_strain_J1	_UniProt_KB_Q_03217	16.47	SVYGEGNGSDISVYDMPFAR

Nitrilase_Rhodococcus_rhodochrous_strain_J1	_UniProt_KB_Q_03217	99	TMDSPHVQR
Nitrilase_Rhodococcus_rhodochrous_strain_J1	_UniProt_KB_Q_03217	48.98	TMDSPHVQR
Nitrilase_Rhodococcus_rhodochrous_strain_J1	_UniProt_KB_Q_03217	62.4	TTPVNTAISTIHATH
Nitrilase_Rhodococcus_rhodochrous_strain_J1	_UniProt_KB_Q_03217	99	TVDKTVSIIAEAAR
Nitrilase_Rhodococcus_rhodochrous_strain_J1	_UniProt_KB_Q_03217	99	TVDKTVSIIAEAAR
Nitrilase_Rhodococcus_rhodochrous_strain_J1	_UniProt_KB_Q_03217	99	TVDKTVSIIAEAAR
Nitrilase_Rhodococcus_rhodochrous_strain_J1	_UniProt_KB_Q_03217	51.53	TVDKTVSIIAEAAR
Nitrilase_Rhodococcus_rhodochrous_strain_J1	_UniProt_KB_Q_03217	99	TVSIIAEAAR
Nitrilase_Rhodococcus_rhodochrous_strain_J1	_UniProt_KB_Q_03217	99	TVSIIAEAAR
Nitrilase_Rhodococcus_rhodochrous_strain_J1	_UniProt_KB_Q_03217	99	TVSIIAEAAR
Nitrilase_Rhodococcus_rhodochrous_strain_J1	_UniProt_KB_Q_03217	99	TVSIIAEAAR
Nitrilase_Rhodococcus_rhodochrous_strain_J1	_UniProt_KB_Q_03217	99	TVSIIAEAAR
Nitrilase_Rhodococcus_rhodochrous_strain_J1	_UniProt_KB_Q_03217	99	TVSIIAEAAR
Nitrilase_Rhodococcus_rhodochrous_strain_J1	_UniProt_KB_Q_03217	99	TVSIIAEAAR
Nitrilase_Rhodococcus_rhodochrous_strain_J1	_UniProt_KB_Q_03217	99	TVSIIAEAAR
Nitrilase_Rhodococcus_rhodochrous_strain_J1	_UniProt_KB_Q_03217	97.16	TVSIIAEAAR
Nitrilase_Rhodococcus_rhodochrous_strain_J1	_UniProt_KB_Q_03217	92.1	TVSIIAEAAR
Nitrilase_Rhodococcus_rhodochrous_strain_J1	_UniProt_KB_Q_03217	89.74	TVSIIAEAAR
Nitrilase_Rhodococcus_rhodochrous_strain_J1	_UniProt_KB_Q_03217	65.61	TVSIIAEAAR

Nitrilase_Rhodococcus_rhodochrous_strain_J1	_UniProt_KB_Q_03217	42.03	TVSIIAEAAR
Nitrilase_Rhodococcus_rhodochrous_strain_J1	_UniProt_KB_Q_03217	99	VAAVQAQPVWFDAAK
Nitrilase_Rhodococcus_rhodochrous_strain_J1	_UniProt_KB_Q_03217	99	VAAVQAQPVWFDAAK
Nitrilase_Rhodococcus_rhodochrous_strain_J1	_UniProt_KB_Q_03217	99	VAAVQAQPVWFDAAK
Nitrilase_Rhodococcus_rhodochrous_strain_J1	_UniProt_KB_Q_03217	99	VAAVQAQPVWFDAAK
Nitrilase_Rhodococcus_rhodochrous_strain_J1	_UniProt_KB_Q_03217	99	VAAVQAQPVWFDAAK
Nitrilase_Rhodococcus_rhodochrous_strain_J1	_UniProt_KB_Q_03217	99	VAAVQAQPVWFDAAK
Nitrilase_Rhodococcus_rhodochrous_strain_J1	_UniProt_KB_Q_03217	95.73	VAAVQAQPVWFDAAK
Nitrilase_Rhodococcus_rhodochrous_strain_J1	_UniProt_KB_Q_03217	41.1	VAAVQAQPVWFDAAK
Nitrilase_Rhodococcus_rhodochrous_strain_J1	_UniProt_KB_Q_03217	16.02	VAAVQAQPVWFDAAK
Nitrilase_Rhodococcus_rhodochrous_strain_J1	_UniProt_KB_Q_03217	99	VEYTNTFK
Nitrilase_Rhodococcus_rhodochrous_strain_J1	_UniProt_KB_Q_03217	99	VEYTNTFK
Nitrilase_Rhodococcus_rhodochrous_strain_J1	_UniProt_KB_Q_03217	97.41	VEYTNTFK
Nitrilase_Rhodococcus_rhodochrous_strain_J1	_UniProt_KB_Q_03217	89.97	VEYTNTFK
Nitrilase_Rhodococcus_rhodochrous_strain_J1	_UniProt_KB_Q_03217	39.73	VEYTNTFK
Nitrilase_Rhodococcus_rhodochrous_strain_J1	_UniProt_KB_Q_03217	99	YAMYSMHEQVHVASWPGMSLYQPEVPAFGVDAQLTATR
Nitrilase_Rhodococcus_rhodochrous_strain_J1	_UniProt_KB_Q_03217	99	YAMYSMHEQVHVASWPGMSLYQPEVPAFGVDAQLTATR
Nitrilase_Rhodococcus_rhodochrous_strain_J1	_UniProt_KB_Q_03217	99	YAMYSMHEQVHVASWPGMSLYQPEVPAFGVDAQLTATR
Nitrilase_Rhodococcus_rhodochrous_strain_J1	_UniProt_KB_Q_03217	99	YAMYSMHEQVHVASWPGMSLYQPEVPAFGVDAQLTATR

Nitrilase_Rhodococcus_rhodochrous_strain_J1	_UniProt_KB_Q_03217	99	YAMYSMHEQVHVASWPGMSLYQPEVPAFGVDAQLTATR
Nitrilase_Rhodococcus_rhodochrous_strain_J1	_UniProt_KB_Q_03217	99	YAMYSMHEQVHVASWPGMSLYQPEVPAFGVDAQLTATR
Nitrilase_Rhodococcus_rhodochrous_strain_J1	_UniProt_KB_Q_03217	99	YAMYSMHEQVHVASWPGMSLYQPEVPAFGVDAQLTATR
Nitrilase_Rhodococcus_rhodochrous_strain_J1	_UniProt_KB_Q_03217	99	YAMYSMHEQVHVASWPGMSLYQPEVPAFGVDAQLTATR
Nitrilase_Rhodococcus_rhodochrous_strain_J1	_UniProt_KB_Q_03217	99	YAMYSMHEQVHVASWPGMSLYQPEVPAFGVDAQLTATR
Nitrilase_Rhodococcus_rhodochrous_strain_J1	_UniProt_KB_Q_03217	99	YAMYSMHEQVHVASWPGMSLYQPEVPAFGVDAQLTATR
Nitrilase_Rhodococcus_rhodochrous_strain_J1	_UniProt_KB_Q_03217	99	YAMYSMHEQVHVASWPGMSLYQPEVPAFGVDAQLTATR
Nitrilase_Rhodococcus_rhodochrous_strain_J1	_UniProt_KB_Q_03217	99	YAMYSMHEQVHVASWPGMSLYQPEVPAFGVDAQLTATR
Nitrilase_Rhodococcus_rhodochrous_strain_J1	_UniProt_KB_Q_03217	99	YAMYSMHEQVHVASWPGMSLYQPEVPAFGVDAQLTATR
Nitrilase_Rhodococcus_rhodochrous_strain_J1	_UniProt_KB_Q_03217	99	YAMYSMHEQVHVASWPGMSLYQPEVPAFGVDAQLTATR
Nitrilase_Rhodococcus_rhodochrous_strain_J1	_UniProt_KB_Q_03217	99	YAMYSMHEQVHVASWPGMSLYQPEVPAFGVDAQLTATR
Nitrilase_Rhodococcus_rhodochrous_strain_J1	_UniProt_KB_Q_03217	99	YAMYSMHEQVHVASWPGMSLYQPEVPAFGVDAQLTATR
Nitrilase_Rhodococcus_rhodochrous_strain_J1	_UniProt_KB_Q_03217	99	YAMYSMHEQVHVASWPGMSLYQPEVPAFGVDAQLTATR
Nitrilase_Rhodococcus_rhodochrous_strain_J1	_UniProt_KB_Q_03217	99	YAMYSMHEQVHVASWPGMSLYQPEVPAFGVDAQLTATR
Nitrilase_Rhodococcus_rhodochrous_strain_J1	_UniProt_KB_Q_03217	99	YAMYSMHEQVHVASWPGMSLYQPEVPAFGVDAQLTATR
Nitrilase_Rhodococcus_rhodochrous_strain_J1	_UniProt_KB_Q_03217	99	YAMYSMHEQVHVASWPGMSLYQPEVPAFGVDAQLTATR
Nitrilase_Rhodococcus_rhodochrous_strain_J1	_UniProt_KB_Q_03217	99	YAMYSMHEQVHVASWPGMSLYQPEVPAFGVDAQLTATR
Nitrilase_Rhodococcus_rhodochrous_strain_J1	_UniProt_KB_Q_03217	99	YAMYSMHEQVHVASWPGMSLYQPEVPAFGVDAQLTATR
Nitrilase_Rhodococcus_rhodochrous_strain_J1	_UniProt_KB_Q_03217	99	YAMYSMHEQVHVASWPGMSLYQPEVPAFGVDAQLTATR
Nitrilase_Rhodococcus_rhodochrous_strain_J1	_UniProt_KB_Q_03217	99	YAMYSMHEQVHVASWPGMSLYQPEVPAFGVDAQLTATR

Nitrilase_Rhodococcus_rhodochrous_strain_J1	_UniProt_KB_Q_03217	99	YAMYSMHEQVHVASWPGMSLYQPEVPAFGVDAQLTATR
Nitrilase_Rhodococcus_rhodochrous_strain_J1	_UniProt_KB_Q_03217	99	YAMYSMHEQVHVASWPGMSLYQPEVPAFGVDAQLTATR
Nitrilase_Rhodococcus_rhodochrous_strain_J1	_UniProt_KB_Q_03217	99	YAMYSMHEQVHVASWPGMSLYQPEVPAFGVDAQLTATR
Nitrilase_Rhodococcus_rhodochrous_strain_J1	_UniProt_KB_Q_03217	98.2	YAMYSMHEQVHVASWPGMSLYQPEVPAFGVDAQLTATR
Nitrilase_Rhodococcus_rhodochrous_strain_J1	_UniProt_KB_Q_03217	96.12	YAMYSMHEQVHVASWPGMSLYQPEVPAFGVDAQLTATR
Nitrilase_Rhodococcus_rhodochrous_strain_J1	_UniProt_KB_Q_03217	96.12	YAMYSMHEQVHVASWPGMSLYQPEVPAFGVDAQLTATR
Nitrilase_Rhodococcus_rhodochrous_strain_J1	_UniProt_KB_Q_03217	96.12	YAMYSMHEQVHVASWPGMSLYQPEVPAFGVDAQLTATR
Nitrilase_Rhodococcus_rhodochrous_strain_J1	_UniProt_KB_Q_03217	95.19	YAMYSMHEQVHVASWPGMSLYQPEVPAFGVDAQLTATR
Nitrilase_Rhodococcus_rhodochrous_strain_J1	_UniProt_KB_Q_03217	95.19	YAMYSMHEQVHVASWPGMSLYQPEVPAFGVDAQLTATR
Nitrilase_Rhodococcus_rhodochrous_strain_J1	_UniProt_KB_Q_03217	83.14	YAMYSMHEQVHVASWPGMSLYQPEVPAFGVDAQLTATR
Nitrilase_Rhodococcus_rhodochrous_strain_J1	_UniProt_KB_Q_03217	82.39	YAMYSMHEQVHVASWPGMSLYQPEVPAFGVDAQLTATR
Nitrilase_Rhodococcus_rhodochrous_strain_J1	_UniProt_KB_Q_03217	75.62	YAMYSMHEQVHVASWPGMSLYQPEVPAFGVDAQLTATR
Nitrilase_Rhodococcus_rhodochrous_strain_J1	_UniProt_KB_Q_03217	75.62	YAMYSMHEQVHVASWPGMSLYQPEVPAFGVDAQLTATR
Nitrilase_Rhodococcus_rhodochrous_strain_J1	_UniProt_KB_Q_03217	75.62	YAMYSMHEQVHVASWPGMSLYQPEVPAFGVDAQLTATR
Nitrilase_Rhodococcus_rhodochrous_strain_J1	_UniProt_KB_Q_03217	74.51	YAMYSMHEQVHVASWPGMSLYQPEVPAFGVDAQLTATR
Nitrilase_Rhodococcus_rhodochrous_strain_J1	_UniProt_KB_Q_03217	74.51	YAMYSMHEQVHVASWPGMSLYQPEVPAFGVDAQLTATR
Nitrilase_Rhodococcus_rhodochrous_strain_J1	_UniProt_KB_Q_03217	74.51	YAMYSMHEQVHVASWPGMSLYQPEVPAFGVDAQLTATR
Nitrilase_Rhodococcus_rhodochrous_strain_J1	_UniProt_KB_Q_03217	74.51	YAMYSMHEQVHVASWPGMSLYQPEVPAFGVDAQLTATR
Nitrilase_Rhodococcus_rhodochrous_strain_J1	_UniProt_KB_Q_03217	74.51	YAMYSMHEQVHVASWPGMSLYQPEVPAFGVDAQLTATR

Nitrilase_Rhodococcus_rhodochrous_strain_J1	_UniProt_KB_Q_03217	73.37	YAMYSMHEQVHVASWPGMSLYQPEVPAFGVDAQLTATR
Nitrilase_Rhodococcus_rhodochrous_strain_J1	_UniProt_KB_Q_03217	73.16	YAMYSMHEQVHVASWPGMSLYQPEVPAFGVDAQLTATR
Nitrilase_Rhodococcus_rhodochrous_strain_J1	_UniProt_KB_Q_03217	73.16	YAMYSMHEQVHVASWPGMSLYQPEVPAFGVDAQLTATR
Nitrilase_Rhodococcus_rhodochrous_strain_J1	_UniProt_KB_Q_03217	73.16	YAMYSMHEQVHVASWPGMSLYQPEVPAFGVDAQLTATR
Nitrilase_Rhodococcus_rhodochrous_strain_J1	_UniProt_KB_Q_03217	73.16	YAMYSMHEQVHVASWPGMSLYQPEVPAFGVDAQLTATR
Nitrilase_Rhodococcus_rhodochrous_strain_J1	_UniProt_KB_Q_03217	66.85	YAMYSMHEQVHVASWPGMSLYQPEVPAFGVDAQLTATR
Nitrilase_Rhodococcus_rhodochrous_strain_J1	_UniProt_KB_Q_03217	61.94	YAMYSMHEQVHVASWPGMSLYQPEVPAFGVDAQLTATR
Nitrilase_Rhodococcus_rhodochrous_strain_J1	_UniProt_KB_Q_03217	61.94	YAMYSMHEQVHVASWPGMSLYQPEVPAFGVDAQLTATR
Nitrilase_Rhodococcus_rhodochrous_strain_J1	_UniProt_KB_Q_03217	57.74	YAMYSMHEQVHVASWPGMSLYQPEVPAFGVDAQLTATR
Nitrilase_Rhodococcus_rhodochrous_strain_J1	_UniProt_KB_Q_03217	54.67	YAMYSMHEQVHVASWPGMSLYQPEVPAFGVDAQLTATR
Nitrilase_Rhodococcus_rhodochrous_strain_J1	_UniProt_KB_Q_03217	54.67	YAMYSMHEQVHVASWPGMSLYQPEVPAFGVDAQLTATR
Nitrilase_Rhodococcus_rhodochrous_strain_J1	_UniProt_KB_Q_03217	54.67	YAMYSMHEQVHVASWPGMSLYQPEVPAFGVDAQLTATR
Nitrilase_Rhodococcus_rhodochrous_strain_J1	_UniProt_KB_Q_03217	52.2	YAMYSMHEQVHVASWPGMSLYQPEVPAFGVDAQLTATR
Nitrilase_Rhodococcus_rhodochrous_strain_J1	_UniProt_KB_Q_03217	43.02	YAMYSMHEQVHVASWPGMSLYQPEVPAFGVDAQLTATR
Nitrilase_Rhodococcus_rhodochrous_strain_J1	_UniProt_KB_Q_03217	43.02	YAMYSMHEQVHVASWPGMSLYQPEVPAFGVDAQLTATR
Nitrilase_Rhodococcus_rhodochrous_strain_J1	_UniProt_KB_Q_03217	43.02	YAMYSMHEQVHVASWPGMSLYQPEVPAFGVDAQLTATR
Nitrilase_Rhodococcus_rhodochrous_strain_J1	_UniProt_KB_Q_03217	43.02	YAMYSMHEQVHVASWPGMSLYQPEVPAFGVDAQLTATR
Nitrilase_Rhodococcus_rhodochrous_strain_J1	_UniProt_KB_Q_03217	43.02	YAMYSMHEQVHVASWPGMSLYQPEVPAFGVDAQLTATR
Nitrilase_Rhodococcus_rhodochrous_strain_J1	_UniProt_KB_Q_03217	42.38	YAMYSMHEQVHVASWPGMSLYQPEVPAFGVDAQLTATR

Nitrilase_Rhodococcus_rhodochrous_strain_J1	_UniProt_KB_Q_03217	42.38	YAMYSMHEQVHVASWPGMSLYQPEVPAFGVDAQLTATR
Nitrilase_Rhodococcus_rhodochrous_strain_J1	_UniProt_KB_Q_03217	42.38	YAMYSMHEQVHVASWPGMSLYQPEVPAFGVDAQLTATR
Nitrilase_Rhodococcus_rhodochrous_strain_J1	_UniProt_KB_Q_03217	38.89	YAMYSMHEQVHVASWPGMSLYQPEVPAFGVDAQLTATR
Nitrilase_Rhodococcus_rhodochrous_strain_J1	_UniProt_KB_Q_03217	38.89	YAMYSMHEQVHVASWPGMSLYQPEVPAFGVDAQLTATR
Nitrilase_Rhodococcus_rhodochrous_strain_J1	_UniProt_KB_Q_03217	32.61	YAMYSMHEQVHVASWPGMSLYQPEVPAFGVDAQLTATR
Nitrilase_Rhodococcus_rhodochrous_strain_J1	_UniProt_KB_Q_03217	22.17	YAMYSMHEQVHVASWPGMSLYQPEVPAFGVDAQLTATR
Nitrilase_Rhodococcus_rhodochrous_strain_J1	_UniProt_KB_Q_03217	19.45	YAMYSMHEQVHVASWPGMSLYQPEVPAFGVDAQLTATR
Nitrilase_Rhodococcus_rhodochrous_strain_J1	_UniProt_KB_Q_03217	17.25	YAMYSMHEQVHVASWPGMSLYQPEVPAFGVDAQLTATR
Nitrilase_Rhodococcus_rhodochrous_strain_J1	_UniProt_KB_Q_03217	99	YHENSLTMDSPHVQR
Nitrilase_Rhodococcus_rhodochrous_strain_J1	_UniProt_KB_Q_03217	99	YHENSLTMDSPHVQR
Nitrilase_Rhodococcus_rhodochrous_strain_J1	_UniProt_KB_Q_03217	99	YHENSLTMDSPHVQR
Nitrilase_Rhodococcus_rhodochrous_strain_J1	_UniProt_KB_Q_03217	99	YHENSLTMDSPHVQR
Nitrilase_Rhodococcus_rhodochrous_strain_J1	_UniProt_KB_Q_03217	99	YHENSLTMDSPHVQR
Nitrilase_Rhodococcus_rhodochrous_strain_J1	_UniProt_KB_Q_03217	99	YHENSLTMDSPHVQR
Nitrilase_Rhodococcus_rhodochrous_strain_J1	_UniProt_KB_Q_03217	99	YHENSLTMDSPHVQR
Nitrilase_Rhodococcus_rhodochrous_strain_J1	_UniProt_KB_Q_03217	99	YHENSLTMDSPHVQR
Nitrilase_Rhodococcus_rhodochrous_strain_J1	_UniProt_KB_Q_03217	99	YHENSLTMDSPHVQR
Nitrilase_Rhodococcus_rhodochrous_strain_J1	_UniProt_KB_Q_03217	99	YHENSLTMDSPHVQR

Nitrilase_Rhodococcus_rhodochrous_strain_J1	_UniProt_KB_Q_03217	99	YHENSLTMDSPHVQR
Nitrilase_Rhodococcus_rhodochrous_strain_J1	_UniProt_KB_Q_03217	99	YHENSLTMDSPHVQR
Nitrilase_Rhodococcus_rhodochrous_strain_J1	_UniProt_KB_Q_03217	99	YHENSLTMDSPHVQR
Nitrilase_Rhodococcus_rhodochrous_strain_J1	_UniProt_KB_Q_03217	99	YHENSLTMDSPHVQR
Nitrilase_Rhodococcus_rhodochrous_strain_J1	_UniProt_KB_Q_03217	99	YHENSLTMDSPHVQR
Nitrilase_Rhodococcus_rhodochrous_strain_J1	_UniProt_KB_Q_03217	99	YHENSLTMDSPHVQR
Nitrilase_Rhodococcus_rhodochrous_strain_J1	_UniProt_KB_Q_03217	99	YHENSLTMDSPHVQR
Nitrilase_Rhodococcus_rhodochrous_strain_J1	_UniProt_KB_Q_03217	99	YHENSLTMDSPHVQR
Nitrilase_Rhodococcus_rhodochrous_strain_J1	_UniProt_KB_Q_03217	99	YHENSLTMDSPHVQR
Nitrilase_Rhodococcus_rhodochrous_strain_J1	_UniProt_KB_Q_03217	99	YHENSLTMDSPHVQR
Nitrilase_Rhodococcus_rhodochrous_strain_J1	_UniProt_KB_Q_03217	99	YHENSLTMDSPHVQR
Nitrilase_Rhodococcus_rhodochrous_strain_J1	_UniProt_KB_Q_03217	99	YHENSLTMDSPHVQR
Nitrilase_Rhodococcus_rhodochrous_strain_J1	_UniProt_KB_Q_03217	99	YHENSLTMDSPHVQR
Nitrilase_Rhodococcus_rhodochrous_strain_J1	_UniProt_KB_Q_03217	99	YHENSLTMDSPHVQR
Nitrilase_Rhodococcus_rhodochrous_strain_J1	_UniProt_KB_Q_03217	99	YHENSLTMDSPHVQR
Nitrilase_Rhodococcus_rhodochrous_strain_J1	_UniProt_KB_Q_03217	99	YHENSLTMDSPHVQR
Nitrilase_Rhodococcus_rhodochrous_strain_J1	_UniProt_KB_Q_03217	99	YHENSLTMDSPHVQR
Nitrilase_Rhodococcus_rhodochrous_strain_J1	_UniProt_KB_Q_03217	99	YHENSLTMDSPHVQR
Nitrilase_Rhodococcus_rhodochrous_strain_J1	_UniProt_KB_Q_03217	99	YHENSLTMDSPHVQR
Nitrilase_Rhodococcus_rhodochrous_strain_J1	_UniProt_KB_Q_03217	99	YHENSLTMDSPHVQR
Nitrilase_Rhodococcus_rhodochrous_strain_J1	_UniProt_KB_Q_03217	99	YHENSLTMDSPHVQR

Nitrilase_Rhodococcus_rhodochrous_strain_J1	_UniProt_KB_Q_03217	99	YHENSLTMDSPHVQR
Nitrilase_Rhodococcus_rhodochrous_strain_J1	_UniProt_KB_Q_03217	99	YHENSLTMDSPHVQR
Nitrilase_Rhodococcus_rhodochrous_strain_J1	_UniProt_KB_Q_03217	95.97	YHENSLTMDSPHVQR
Nitrilase_Rhodococcus_rhodochrous_strain_J1	_UniProt_KB_Q_03217	92.89	YHENSLTMDSPHVQR
Nitrilase_Rhodococcus_rhodochrous_strain_J1	_UniProt_KB_Q_03217	92.43	YHENSLTMDSPHVQR
Nitrilase_Rhodococcus_rhodochrous_strain_J1	_UniProt_KB_Q_03217	91.56	YHENSLTMDSPHVQR
Nitrilase_Rhodococcus_rhodochrous_strain_J1	_UniProt_KB_Q_03217	86.22	YHENSLTMDSPHVQR
Nitrilase_Rhodococcus_rhodochrous_strain_J1	_UniProt_KB_Q_03217	82.27	YHENSLTMDSPHVQR
Nitrilase_Rhodococcus_rhodochrous_strain_J1	_UniProt_KB_Q_03217	80.02	YHENSLTMDSPHVQR
Nitrilase_Rhodococcus_rhodochrous_strain_J1	_UniProt_KB_Q_03217	78.87	YHENSLTMDSPHVQR
Nitrilase_Rhodococcus_rhodochrous_strain_J1	_UniProt_KB_Q_03217	77.47	YHENSLTMDSPHVQR
Nitrilase_Rhodococcus_rhodochrous_strain_J1	_UniProt_KB_Q_03217	51.02	YHENSLTMDSPHVQR
Nitrilase_Rhodococcus_rhodochrous_strain_J1	_UniProt_KB_Q_03217	49.58	YHENSLTMDSPHVQR
Nitrilase_Rhodococcus_rhodochrous_strain_J1	_UniProt_KB_Q_03217	42.71	YHENSLTMDSPHVQR
Nitrilase_Rhodococcus_rhodochrous_strain_J1	_UniProt_KB_Q_03217	36.85	YHENSLTMDSPHVQR
Nitrilase_Rhodococcus_rhodochrous_strain_J1	_UniProt_KB_Q_03217	31.75	YHENSLTMDSPHVQR
Nitrilase_Rhodococcus_rhodochrous_strain_J1	_UniProt_KB_Q_03217	27.31	YHENSLTMDSPHVQR
Nitrilase_Rhodococcus_rhodochrous_strain_J1	_UniProt_KB_Q_03217	23.68	YHENSLTMDSPHVQR
Nitrilase_Rhodococcus_rhodochrous_strain_J1	_UniProt_KB_Q_03217	22.46	YHENSLTMDSPHVQR

Nitrilase_Rhodococcus_rhodochrous_strain_J1	_UniProt_KB_Q_03217	21.17	YHENSLTMDSPHVQR
Nitrilase_Rhodococcus_rhodochrous_strain_J1	_UniProt_KB_Q_03217	19.04	YHENSLTMDSPHVQR
Nitrilase_Rhodococcus_rhodochrous_strain_J1	_UniProt_KB_Q_03217	17.3	YHENSLTMDSPHVQR
Nitrilase_Rhodococcus_rhodochrous_strain_J1	_UniProt_KB_Q_03217	16.86	YHENSLTMDSPHVQR
Nitrilase_Rhodococcus_rhodochrous_strain_J1	_UniProt_KB_Q_03217	16.74	YHENSLTMDSPHVQR
Nitrilase_Rhodococcus_rhodochrous_strain_J1	_UniProt_KB_Q_03217	16.74	YHENSLTMDSPHVQR
Nitrilase_Rhodococcus_rhodochrous_strain_J1	_UniProt_KB_Q_03217	16.74	YHENSLTMDSPHVQR
Nitrilase_Rhodococcus_rhodochrous_strain_J1	_UniProt_KB_Q_03217	16.74	YHENSLTMDSPHVQR
Nitrilase_Rhodococcus_rhodochrous_strain_J1	_UniProt_KB_Q_03217	16.74	YHENSLTMDSPHVQR
Nitrilase_Rhodococcus_rhodochrous_strain_J1	_UniProt_KB_Q_03217	16.31	YHENSLTMDSPHVQR
Nitrilase_Rhodococcus_rhodochrous_strain_J1	_UniProt_KB_Q_03217	15.05	YHENSLTMDSPHVQR

Strain A29- LCMS-MS Peptide Data

Chaperonin Peptide Fragments

Accessions	Names	Sequence
sp|Q93QI2|CH60_RHOHA	60 kDa chaperonin OS=Rhodococcus hoagii GN=groL PE=3 SV=1	AEIEASDSDYDR
sp|Q93QI2|CH60_RHOHA	60 kDa chaperonin OS=Rhodococcus hoagii GN=groL PE=3 SV=1	AEIEASDSDYDREK
sp|Q93QI2|CH60_RHOHA	60 kDa chaperonin OS=Rhodococcus hoagii GN=groL PE=3 SV=1	GYISLYFATDAER
sp|Q93QI2|CH60_RHOHA	60 kDa chaperonin OS=Rhodococcus hoagii GN=groL PE=3 SV=1	IIAFDEEAR
sp|Q93QI2|CH60_RHOHA	60 kDa chaperonin OS=Rhodococcus hoagii GN=groL PE=3 SV=1	KEIELEDPYEK
sp|Q93QI2|CH60_RHOHA	60 kDa chaperonin OS=Rhodococcus hoagii GN=groL PE=3 SV=1	KTDDVAGDGTTTATVLAQALVR
sp|Q93QI2|CH60_RHOHA	60 kDa chaperonin OS=Rhodococcus hoagii GN=groL PE=3 SV=1	KWGAPTITNDGVSIAK
sp|Q93QI2|CH60_RHOHA	60 kDa chaperonin OS=Rhodococcus hoagii GN=groL PE=3 SV=1	NVAAGANPLGLK
sp|Q93QI2|CH60_RHOHA	60 kDa chaperonin OS=Rhodococcus hoagii GN=groL PE=3 SV=1	QEAVLEDPYILLVSSK
sp|Q93QI2|CH60_RHOHA	60 kDa chaperonin OS=Rhodococcus hoagii GN=groL PE=3 SV=1	QIAFNAGLEPGVVAEK
sp|Q93QI2|CH60_RHOHA	60 kDa chaperonin OS=Rhodococcus hoagii GN=groL PE=3 SV=1	SALQNAASIAALFLTTEAVVADKPEK
sp|Q93QI2|CH60_RHOHA	60 kDa chaperonin OS=Rhodococcus hoagii GN=groL PE=3 SV=1	TDDVAGDGTTTATVLAQALVR
sp|Q93QI2|CH60_RHOHA	60 kDa chaperonin OS=Rhodococcus hoagii GN=groL PE=3 SV=1	VALEAPLK
sp|Q93QI2|CH60_RHOHA	60 kDa chaperonin OS=Rhodococcus hoagii GN=groL PE=3 SV=1	WGAPTITNDGVSIAK
sp|Q93QI2|CH60_RHOHA	60 kDa chaperonin OS=Rhodococcus hoagii GN=groL PE=3 SV=1	EIELEDPYEK
sp|Q93QI2|CH60_RHOHA	60 kDa chaperonin OS=Rhodococcus hoagii GN=groL PE=3 SV=1	LAGGVAVIK
sp|Q93QI2|CH60_RHOHA	60 kDa chaperonin OS=Rhodococcus hoagii GN=groL PE=3 SV=1	IIAFDEEARR
sp|Q93QI2|CH60_RHOHA	60 kDa chaperonin OS=Rhodococcus hoagii GN=groL PE=3 SV=1	DLLPLLEK
sp|Q93QI2|CH60_RHOHA	60 kDa chaperonin OS=Rhodococcus hoagii GN=groL PE=3 SV=1	IGAELVK
sp|Q93QI2|CH60_RHOHA	60 kDa chaperonin OS=Rhodococcus hoagii GN=groL PE=3 SV=1	AGAATEVELK
sp|Q93QI2|CH60_RHOHA	60 kDa chaperonin OS=Rhodococcus hoagii GN=groL PE=3 SV=1	KVVVTKDETTIVEGAGDADAIAGR
sp|Q93QI2|CH60_RHOHA	60 kDa chaperonin OS=Rhodococcus hoagii GN=groL PE=3 SV=1	DETTIVEGAGDADAIAGR
sp|Q93QI2|CH60_RHOHA	60 kDa chaperonin OS=Rhodococcus hoagii GN=groL PE=3 SV=1	GYISLYFATDAER
sp|Q93QI2|CH60_RHOHA	60 kDa chaperonin OS=Rhodococcus hoagii GN=groL PE=3 SV=1	KTDDVAGDGTTTATVLAQALVR

sp|Q93QI2|CH60_RHOHA	60 kDa chaperonin OS=Rhodococcus hoagii GN=groL PE=3 SV=1	QEAVLEDPYILLVSSK
sp|Q93QI2|CH60_RHOHA	60 kDa chaperonin OS=Rhodococcus hoagii GN=groL PE=3 SV=1	QEAVLEDPYILLVSSK
sp|Q93QI2|CH60_RHOHA	60 kDa chaperonin OS=Rhodococcus hoagii GN=groL PE=3 SV=1	QEAVLEDPYILLVSSK
sp|Q93QI2|CH60_RHOHA	60 kDa chaperonin OS=Rhodococcus hoagii GN=groL PE=3 SV=1	QEAVLEDPYILLVSSK
sp|Q93QI2|CH60_RHOHA	60 kDa chaperonin OS=Rhodococcus hoagii GN=groL PE=3 SV=1	QIAFNAGLEPGVVAEK
sp|Q93QI2|CH60_RHOHA	60 kDa chaperonin OS=Rhodococcus hoagii GN=groL PE=3 SV=1	SALQNAASIAALFLTTEAVVADKPEK
sp|Q93QI2|CH60_RHOHA	60 kDa chaperonin OS=Rhodococcus hoagii GN=groL PE=3 SV=1	SALQNAASIAALFLTTEAVVADKPEK

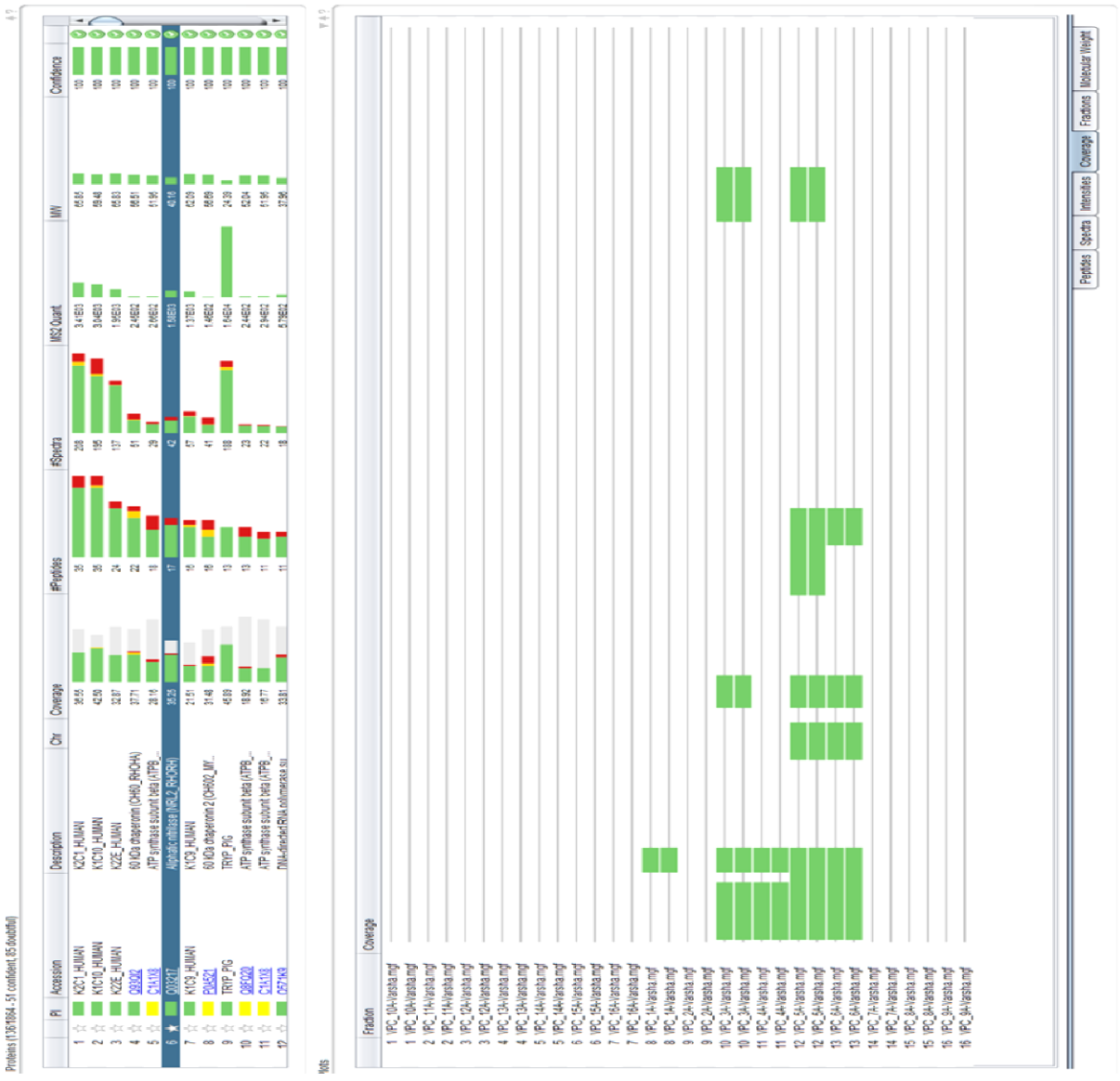
Strain A99 LCMS-MS Peptide Data

Nitrilase Fragment Sequence Coverage

VPC1 toVPC6 – DMF induced cell peptide fragments

VPC7 toVPC11- BNZ induced cell peptide fragments

VPC2 to VPC 16- Control cell peptide fragments



Chaperonin Fragment Sequence Coverage

VPC1 toVPC6 – DMF induced cell peptide fragments

VPC7 toVPC11- BNZ induced cell peptide fragments

VPC2 to VPC 16- Control cell peptide fragments

